

Federal Agency	Department of Energy, Office of Energy Efficiency and Renewable Energy		
Nature of Report	Final Technical Report		
Award Number	DE-EE0007883		
Award Type	Cooperative Agreement		
Recipient Name	Renewable Energy Wildlife Institute (formerly American Wind Wildlife Institute): Lauren Flinn		
Recipient Title	Director of Operations		
Recipient Email	lflinn@rewi.org		
Recipient Phone Number	(202) 448-8780		
Prime Recipient Type	Non-Profit		
Project Title	Evaluating the Effectiveness of a Detection and Deterrent System in Reducing Golden Eagle Fatalities at Operational Wind Facilities		
Principle Investigator	Shilo Felton, sfelton@rewi.org		
Recipient DUNS Number	015077939		
Date of Report	May 31 2024		
Period Covered by Report	June 1, 2017 - May 31, 2024		
Attachments	<ol> <li>Statement of Project Objectives (MOD 10)</li> <li>Budget Information (MOD 12)</li> <li>Milestone 8.2 Report: Goodnoe Hills Two-year Experiment</li> <li>Milestone 9.1 Report: Goodnoe Hills Eagle Behavioral Responses to Deterrents</li> <li>Milestone 10.1 Report: Multi-site Analysis of DTBird Detection and Deterrence Trigger Distances</li> <li>Milestone 10.2 Report: Multi-site Analysis of False Positive and False Negative DTBird Detection Rates</li> <li>Milestone 10.3 Report: Multi-site Analysis of Avian Behavioral Response to Deterrents</li> <li>Milestone 10.4 Report: Multi-site Estimate of Eagle Collision Risk Reduction</li> <li>Milestone 11.1 Report: DTBird Cost Analysis</li> </ol>		

Renewable Energy Wildlife Institute Final Technical Report DE-EE0007883.0012

Evaluating the Effectiveness of a Detection and Deterrent System in Reducing Golden Eagle Fatalities at Operational Wind Facilities

Award Number: DE-EE0007883

May 31, 2024

Renewable Energy Wildlife Institute (REWI)
700 12<sup>th</sup> Street, NW, Suite 700
Washington, DC 20005
www.rewi.org

### Prepared By

Shilo K. Felton, Ph.D., Senior Scientist, REWI

La' Portia J. Perkins, M.Sc., Project Manager, REWI

Jeff P. Smith, Ph.D., Associate Wildlife Ecologist, H. T. Harvey & Associates

Scott B. Terrell, Ph.D., Principal Wildlife Ecologist, H. T. Harvey & Associates

# Contents

Section 1. Executive Summary	7
Section 2. Acknowledgments	9
Section 3. Disclaimer	9
Section 4. Study Narrative	9
4.1 Introduction	9
4.2 Study Objectives	11
4.3 Field Methods and Data Processing	12
4.3.1 Study Sites	13
4.3.2 DTBird System Operation	14
4.3.3 Sampling Protocol	19
4.3.4 Controlled Experimental Design at Goodnoe Hills	23
4.3.5 UAV Flight Trials to Assess False Negative Detection Rates	25
4.4 Analytical Methods	27
4.4.1 Factors Influencing DTBird Detection Capabilities (Objective 1)	27
4.4.2 In Situ Behavioral Responses of Eagles and Raptors (Objective 2)	30
4.4.3 Factors Influencing False Positive Detection Rates (Objective 3)	32
4.4.4 In Situ Experimental Evaluation of Raptor Responses (Objective 4)	33
4.4.5 Multi-site Analysis of Collision Risk Reduction (Objective 5)	36
4.4.6 Performance Reliability and Cost Analysis (Objective 6)	36
4.5 Results	36
4.5.1 Factors Influencing Probability of Detection (Objective 1)	36
4.5.2 In Situ Behavioral Responses of Eagles and Raptors (Objective 2)	48
4.5.3 Factors Influencing False Positive Detection Rates (Objective 3)	59
4.5.4 In Situ Experimental Evaluation of Raptor Responses (Objective 4)	68
4.5.5 Multi-site Analysis of Collision Risk Reduction (Objective 5)	82
4.5.6 Performance Reliability and Cost Analysis (Objective 6)	84
Discussion	85
DTBird Detection Performance	85
Behavioral Differences at Treatment vs Control Turbines	92

Behavior Responses Across Both Sites	94
Eagle Collision Risk Reduction	96
Conclusion	97
Literature Cited	98
Section 5. Technical Scope and Objectives	102
5.1 Budget Period 1: Develop a detailed, peer-reviewed study design for expanded stud evaluate results of California pilot study (Tasks 1-4)	-
5.2 Budget Period 2: Expand evaluation of DTBird Detection and Deterrence Systems (7 4-8) 103	Гаsks
5.3 Budget Period 3: Complete primary or alternative controlled experiment & video	
evaluation at Washington Facility; Conduct multi-site analyses (Task 8-12)	105
Section 6. Award and Modifications to Prime Award and the Statement of Project	
Objectives (SOPO)	106
Section 7. Issues and Changes in Approach	108
Section 8. Task Accomplishments & Milestones	109
8.1 Task 1.0: Project Launch and Development of Peer-reviewed Study Design	109
8.1.1 Milestone 1.1.1: Completed peer-reviewed study design and quantitative	
performance targets (Q5:M15)	109
8.2 Task 2.0: Evaluate false positives using data collected during the pilot study at Cali	fornia
wind facility	109
8.2.1 Milestone 2.1 False positive rates quantified at California wind facility	
(Q5:Q15)	109
8.3 Task 3.0: Evaluation of pilot study	110
8.3.1 Milestone 3.1 Recommended updates to DTBird system delivered to	
technology vendor (Q6:M16)	110
8.3.2 Milestone 3.2 QTPs established based on analysis of pilot study (Q6:M18)	110
8.4 Task 4.0: Update DTBird system and revise study design for BP2 and BP3 as appro	Reduction
8.4.1 Milestone 4.1 Study design revised (Q7:M19)	111
8.4.2 Milestone 4.2 Updates to DTBird system completed (Q8:M22)	112
8.5 Task 5.0: Install DTBird systems at Washington wind facility	113

8.5.1 Milestone 5.1 DTBird systems installed and commissioned at Washington wind facility (Q13:M37)	113
8.6 Task 6.0: Expand evaluation of <i>in situ</i> bird video footage at California and Washington wind facilities, conduct UAV flight trials at Washington wind facility, and analyze site-	
specific results	113
8.6.1 Milestone 6.1: UAV flight trials completed at Washington wind facility (Q18:M53)	113
8.6.2 Milestone 6.2 DTBird video data collection and enhanced site-specific evaluation of <i>in situ</i> eagle responses to deterrents completed for California facility, with evaluation restricted to first year of data collection (Q10:M28)	114
8.6.3 Milestone 6.3 Preliminary site-specific estimates of rates of false positives and false negatives produced for Washington wind facility (Q20:M60)	115
8.6.4 Milestone 6.4 Initial site-specific models developed to quantify the spatial accuracy of the DTBird detection and deterrent-triggering system at Washington wind facility (Q20:M60)	116
8.7 Task 7.0: Conduct first year of controlled experiment at Washington Wind Facility	116
8.7.1 Milestone 7.1 First year data collection completed for controlled experiment (Q21:M63)	116
8.7.2 Milestone 7.2 A summary of progress and findings up to 10 months of data will be included in the Go/No Go report for BP2. This summary will include a power analysis performed on at least 6 months of data, as well as a recommendation of which objective (proximate effectiveness or habituation) to pursue in Year 2 of the experiment (Q21:M63)	117
8.8 Task 8.0: Complete controlled experiment and analyze results	
8.8.1 Milestone 8.1 First two months of controlled experiment's Year 2 DTBird data collected at Washington site (Q21:M65)	
8.8.2 Milestone 8.2 Controlled experiment completed, and results analyzed; an estimate of eagle collision risk reduction from DTBird calculated	117
(Q26:M78)	11/
8.9 Task 9.0: Evaluate behavioral responses of raptors exposed to deterrent signals at Washington wind facility	118

8.9.1 Milestone 9.1 All DTBird video evaluation and classification of in-situ raptor responses to deterrent signals completed. Target performance is ≥50% successful deterrence for eagles (Q27:M79)	118
8.10 Task 10.0: Complete combined multi-site analyses	
8.10.1 Milestone 10.1 Multi-site analyses of detection and deterrence triggering capabilities as a function of flight and landscape characteristics completed (Q24: M72)	119
8.10.2 Milestone 10.2 Complete multi-site analyses of false positives and false negatives (Q25:M73)	120
8.10.3 Milestone 10.3 Complete multi-site analyses of behavioral responses of in-situ raptors to deterrence signals (Q26:M76)	121
8.10.4 Milestone 10.4 Produce a multi-site estimate of collision risk reduction, estimate of eagle fatality reduction (# eagles/year) attributable to DTBird	
completed (Q27:M79)	
8.11 Task 11.0: Prepare systems cost analysis	
8.11.1 Milestone 11.1 System cost analysis completed (Q28:M84)	
Section 9. Project Output/STI	124
9.1 Publications	124
9.2 Technologies/Techniques	124
9.3 Status Reports	124
9.4 Media Reports	124
9.5 Invention Disclosures	124
9.6 Patent Applications	125
9.7 Licensed Technologies	125
9.8 Networks/Collaborations Fostered	125
9.9 Websites Featuring Project Work or Results	125
9.10 Other Products	125
9.11 Awards, Prizes, and Recognition	125
Section 10. Project Summary Table	125

## Section 1. Executive Summary

The Renewable Energy Wildlife Institute (REWI) was appointed as the prime awardee of DOE award number DE-EE0007883 to lead a team of scientists, wind developers, and technology manufacturers toward the overarching goal of evaluating the effectiveness of the current DTBird system in minimizing the risk of golden eagles (*Aquila chrysaetos*) and other large soaring raptors from approaching the rotor-swept zone (RSZ) of operating wind turbines. As part of this goal, the team set out to 1) quantify the expected reduction in collision risk for golden eagles from operation of the detection and deterrence modules in a manner that supports the approach used by the U.S. Fish and Wildlife Service (USFWS) to assess and credit facility operators for their efforts to minimize predicted collision fatalities and 2) provide information to help improve the technology to maximize its effectiveness.

DTBird is an automated detection and audio deterrent system created by the Spanish company Liquen, designed to discourage birds from entering the RSZ of spinning wind turbines. The system uses cameras to automatically detect airborne targets of interest, records each such event in an online database, and triggers a warning signal (loud sound) if the tracked object has moved close to the turbine. If the object moves even closer to the RSZ, a more aggressive dissuasion signal is broadcast.

To meet our objectives, the team conducted a two-year experiment at the Goodnoe Hills wind facility in Washington state, in which 14 turbines were outfitted with DTBird units. Daily, each DTBird-equipped turbine was randomly assigned to a control or treatment group. Treatment turbines operated with DTBird running as intended-broadcasting warning or deterrent signals when DTBird detected a target within range. On control turbines, no sound signals were broadcast if a moving target triggered the DTBird system. The team also flew unmanned aerial vehicles (UAVs) designed to coarsely mimic the general size, weight, and coloration of golden eagles in programmed flight transects across DTBird detection ranges to quantify DTBird's ability to detect intended targets and to evaluate factors that influence the probability of detection and DTBird's response distances. Additionally, the team evaluated the behavioral responses of in situ eagles exposed to spinning turbines alone (visual and sound influences) versus spinning turbines plus broadcasted DTBird audio deterrents, to estimate the effectiveness of deterrence by the DTBird system. The data and results from these investigations were combined with those from a pilot study conducted at the Manzana Wind Power Project in California to better evaluate DTBird's effectiveness across different landscapes.

Results of the controlled two-year experiment in Washington indicated that broadcasted deterrence signals significantly reduced the time eagles spent near DTBird-equipped turbines (aka dwell time). However, the initial warning signals did not significantly influence the rate at which eagles triggered more intense dissuasion signals, likely because eagles often entered the dissuasion signal zone without first being detected by DTBird within the warning signal zone. There was also a strong interactive effect of deterrence-signal and false-positive rates, meaning that if warning/dissuasion signals were triggered and broadcast more frequently at experimental turbines due to false positives (e.g., detection events triggered by birds other than

eagles, or by non-bird objects like rotor blades, airplanes, or clouds) eagles generally spent less time around those turbines. These results suggest that, despite our concerns that high false-positive rates could cause eagles to become less responsive to deterrent signals, negative habituation did not occur over this experiment. Additionally, although the video quality made it difficult to confidently classify events as successful, 53-100% of all probable golden and bald eagles exhibited a successful (or potentially successful) response to deterrent and warning signals, rates that matched or exceeded the established performance metric of  $\geq 50\%$  successful deterrence for eagles.

Overall, the behavioral results from both the California and Washington wind facilities indicated that operation of DTBird reduced the overall likelihood that an eagle passing through the expected detection range would approach the RSZ by 20–30%, and that value increased by at least 5–10% for birds classified as at moderate to high risk of approaching the RSZ prior to deterrent signaling (moderate risk: bird on a course taking it near but not directly toward the RSZ; high risk: bird on course to intersect with RSZ). Both multi-species and golden eagle analyses confirmed response differences at the two facilities and in relation to preexposure risk levels, and the multi-species model also emphasized that species responded differently to wind speed. The probability of effective deterrence was generally highest for birds classified as at moderate preexposure risk of approaching the RSZ, potentially because those birds had more time and space to effectively respond to the deterrents than birds making high-risk movements toward the RSZ.

Trials using eagle-like UAVs to evaluate DTBird's ability to detect golden eagles and other large raptors revealed an overall 65% probability of detection within 240 meters of the cameras, with the highest chance of detection when the target flew within 80–160 meters of the turbine versus closer or farther away. Cloudy skies, wind speed, different UAV models (potentially reflecting differences between eagle sexes and age classes), UAV speed, and pitch and roll angles all influenced the distance at which DTBird detected the UAVs.

Initially, DTBird registered non-bird objects (e.g., turbine blades, planes, shadows) relatively frequently, so Liquen adjusted the algorithms in January 2023 (5 months into Year 2 of the experiment) to lower the rate of these false positive events. Doing so lowered the false positive rate from 3.9 to 0.8 false-positive deterrence triggers/turbine/day to meet or fall under the established performance metric (1.6–2.8 triggers/turbine/day). Overall, results emphasized the value of running the detection algorithm for an additional three months prior to considering DTBird fully commissioned in the field and suited to operation with deterrents broadcasting.

The standard DTBird V4D8 model sale cost (with Falco cameras and Larus software) is around \$18-\$22K, and the yearly service sale cost is around \$2-3K. Additionally, installation costs \$4-6K/unit and maintenance runs \$0.6-2K/unit/year. This brings the total investment to purchase and operate a single DTBird unit for the first year to a minimum of \$24,600, based on the cost of installing, operating, and maintaining the 14 DTBird units at Goodnoe Hills.

While the cost per unit may be less than other commercially available risk-reduction systems, our study results revealed some areas in which the technology could be improved. We did not find that eagles showed negative habituation to the overactive triggers, however, we would need

further study to confirm this, and there may be other negative consequences of excessive deterrence signals. Given this better camera resolution and refined Al algorithms could greatly improve the functionality of the system and better enable target detections against various backdrops. Furthermore, we recommend users ensure regular replacement of camera lenses to avoid solar degradation which further affects target detection.

.

This report provides details on the study design and implementation as well as the tasks, milestones, costs, and challenges related to the evaluation of the DTBird system.

# Section 2. Acknowledgments

This material is based upon work supported by the U.S. Department of Energy's Office of Energy Efficiency and Renewable Energy (EERE) under the Wind Energy Technologies Office Award Number DE-EE0007883. Avangrid Renewables, Puget Sound Energy (PSE), Pacific Wind Lessee, Portland General Electric (PGE), PacifiCorp, Liquen, and H. T. Harvey & Associates provided additional support for this project. We also thank reviewers C. Hein, M. Huso, J. Garvin, and N. Lewandowski for their valuable feedback which greatly improved the study design, analyses, and this report as a whole.

## Section 3. Disclaimer

This report was prepared as an account of work sponsored by an agency of the United States Government. Neither the United States Government nor any agency thereof, nor any of their employees, makes any warranty, express or implied, or assumes any legal liability or responsibility for the accuracy, completeness, or usefulness of any information, apparatus, product, or process disclosed, or represents that its use would not infringe privately owned rights. Reference herein to any specific commercial product, process, or service by trade name, trademark, manufacturer, or otherwise does not necessarily constitute or imply its endorsement, recommendation, or favoring by the United States Government or any agency thereof. The views and opinions of authors expressed herein do not necessarily state or reflect those of the United States Government or any agency thereof.

# Section 4. Study Narrative

### 4.1 Introduction

The Renewable Energy Wildlife Institute (REWI) was appointed as the prime awardee of DOE award number DE-EE0007883 to lead a team of scientists, wind developers, and technology manufacturers toward the overarching goal of evaluating the effectiveness of the current DTBird system in minimizing the risk of golden eagles (*Aquila chrysaetos*) and other large soaring raptors from approaching the rotor-swept zone (RSZ) of operating wind turbines.

Eagle collisions with wind turbines (Hunt 2002, Erickson et al. 2005, de Lucas et al. 2008, Smallwood 2013) are well-documented. The Migratory Bird Treaty Act (16 U.S.C. §703), the California Department of Fish and Game Code (§3503 and §3511), and the Bald and Golden Eagle Protection Act (Eagle Act) (16 U.S.C. §668–668c) protect eagles from human-related mortality and disturbance sufficient to cause a decline in eagle survival or productivity. We propose to evaluate the effectiveness of DTBird detection and deterrence system in reducing golden eagle collisions at wind turbines.

The DTBird system to be evaluated includes a video-surveillance detection module and a collision-avoidance or deterrence module. Technical specifications for this project are based on the model DTBirdV4D8, with four HD wide-angle cameras located every 90° on the mast of the wind turbine below the blades, and eight speakers, four located by the cameras and four at 90° on the mast of the wind turbine below the nacelle. Overlapping detection areas and improvement in sound distribution will provide good performance in detection and collision avoidance.

Previous European evaluations of DTBird provided preliminary insight into its ability to detect and deter raptors and other birds from approaching turbines (May et al. 2012, Hanagasioglu et al. 2015). Those researchers accomplished this objective primarily by comparing the frequency and turbine-approach distances of *in situ* raptors that they visually observed flying near turbines with and without the DTBird warning and dissuasion signals muted.

May et al. (2012) evaluated the ability of DTBird to detect and deter raptors flying near and in the risk zone of wind turbines in Norway, with the DTBird system calibrated to detect and deter large raptors such as white-tailed sea eagles (*Haliaeetus albicilla*) and golden eagles. The authors of this study compared the detection rates of the DTBird camera and video surveillance system against detections documented by a radar system. Using this approach, they were able to quantify false positives (i.e., video recording stimulated by activity other than target birds) and false negatives (i.e., the detection system failed to trigger video surveillance when radar indicated a target passed by in detectable range) detection rates. This study, as well as Hanagasioglu et al. 2015, did not explicitly address the potential existence and importance of "blind spots" in the DTBird detection system, nor did it evaluate detectability as a function of covariates that can only be addressed by controlled experiments using flying objects manipulated to fly under specified conditions and in predefined patterns.

In alignment with the recommendations of May et al. (2012), we used unmanned aerial vehicles (UAVs) in experimental trials to further evaluate the performance of the DTBird detection and deterrence system at two operational wind-energy facilities in distinctly different landscape settings where golden eagles occur. We will combine insight gained from these trials with data on the detection and deterrence responses of *in situ* golden eagles and large buteos, such as red-tailed hawks, recorded by the DTBird system, as well as with insight derived from a controlled field experiment designed to quantify the degree to which operation of the DTBird detection and deterrence system reduces the probability of eagles and surrogate raptors entering the collision risk zone of equipped turbines.

The primary outcomes of the study will be:

- 1. Statistically robust understanding of the current DTBird detection and deterrence system's ability to successfully deter golden eagles and suitable surrogate raptors from entering the collision risk zone of turbines.
- 2. Statistically robust understanding of the limitations of the system and how various environmental and behavioral variables influence the system's effectiveness.
- Assistance to DTBird engineers with refining the system to maximize its performance and effectiveness in reducing conflict between eagles/raptors and operating wind turbines.
- 4. Effective, statistically robust projections concerning the ability of DTBird to reduce fatality rates for golden eagles and other raptors at wind facilities similar to those involved in the study, thereby assisting the USFWS, state regulatory agencies, and facility operators with projecting the anticipated risk-reduction benefits of deploying the DTBird system.

### 4.2 Study Objectives

To achieve the primary outcomes above and the overall goal of providing a rigorous multi-site evaluation of DTBird's ability to reduce the risk of eagles and other medium/large raptors entering the collision risk zone of operational wind turbines, we pursued the following primary objectives:

<u>Objective 1</u>: Quantify the probability of detection and evaluate the accuracy, precision, and limitations of the DTBird detection and deterrent-triggering functions using UAVs designed to resemble golden eagles at the California (pilot study) and Washington study sites.

<u>Objective 2:</u> Quantify the probability of deterrence and evaluate the effectiveness of the DTBird deterrent signals in reducing raptor activity within the RSZ of turbines by evaluating the behavioral responses of *in situ* eagles and other raptors exposed to the deterrent signals as revealed in DTBird video records from both study sites.

<u>Objective 3:</u> Quantify the prevalence and describe the nature of false positive detections (i.e., DTBird detections of birds and other objects that are not target raptors) at the two study sites.

<u>Objective 4:</u> Quantify DTBird's proximate and longer-term effectiveness in reducing eagle and surrogate raptor activity around equipped turbines by conducting a two-phase 2-year controlled experiment at the Washington study site to evaluate the comparative DTBird event triggering rates at turbines with and without muted deterrent signals.

<u>Objective 5:</u> Produce a multi-site estimate of the potential for DTBird to reduce the risk of eagles entering the collision risk zone of operational turbines at facilities similar to those involved in the study.

<u>Objective 6:</u> Evaluate the performance reliability and maintenance requirements of the DTBird systems installed at the study sites and prepare a detailed systems cost analysis.

## 4.3 Field Methods and Data Processing

To meet our objectives, the team conducted a two-year experiment at the Goodnoe Hills wind facility in Washington state, in which 14 turbines were outfitted with DTBird units. Daily, each DTBird-equipped turbine was randomly assigned to a control or treatment group. Treatment turbines operated with DTBird running as intended—broadcasting warning or deterrent signals when DTBird detected a target within range. On control turbines, no sound signals were broadcast if a moving target triggered the DTBird system. The team also flew UAVs designed to coarsely mimic the general size, weight, and coloration of golden eagles in programmed flight transects across DTBird detection ranges to quantify DTBird's ability to detect intended targets and to evaluate factors that influence the probability of detection and DTBird's response distances. Additionally, the team evaluated the behavioral responses of *in situ* eagles exposed to spinning turbines alone (visual and sound influences) versus spinning turbines plus broadcasted DTBird audio deterrents, to estimate the effectiveness of deterrence by the DTBird system. The data and results from these investigations were combined with those from a pilot study conducted at the Manzana Wind Power Project in California to better evaluate DTBird's effectiveness across different landscapes.

## 4.3.1 Study Sites

### 4.3.1.1 Manzana Wind Project, California

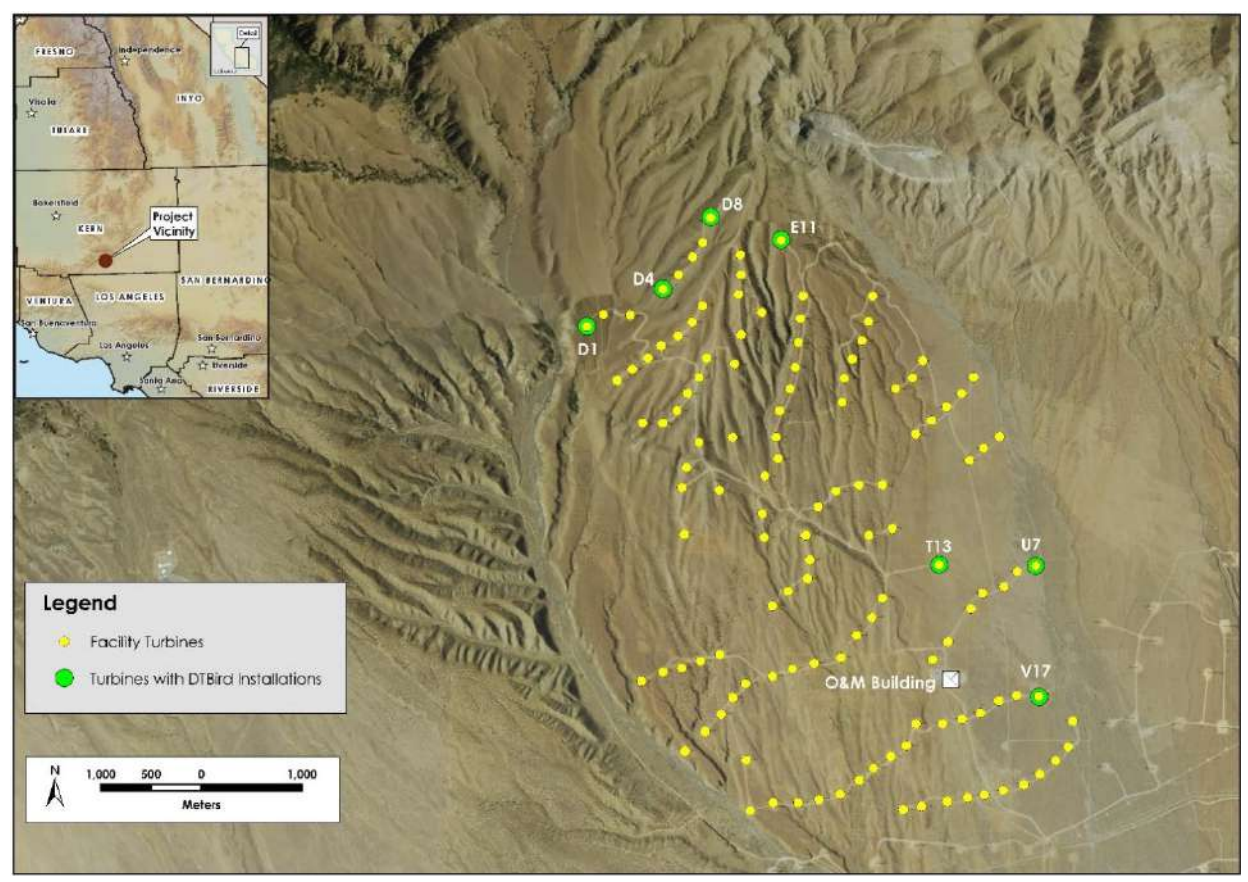


Figure 1. Layout of the Manzana Wind Power Project in southern California showing locations of installed DTBird systems.

The Manzana Wind Project has been in operation since 2012 and comprises 126 1.5 MW GE 1.5-77 wind turbines, with a hub height of 65 meters and a rotor-swept diameter of 82.5 meters, located in the southwestern foothills of the Tehachapi Mountains of southern California in northwestern Antelope Valley, which constitutes the westernmost extension of the Mojave Desert (Figure 1). The landscape is a gradually sloping alluvial fan incised by dry desert washes. The northwestern sector of the facility features more complex foothill topography adjacent to a primary riparian drainage, and the topography grades downslope to the southeast into a more-uniform plain. The desert scrub and woodland vegetation is typical of the upper Mojave Desert region. Seven DTBird systems were strategically installed here to support this research (Figure 1; H. T. Harvey & Associates 2018).

#### 4.3.1.2 Goodnoe Hills Wind Farm, Washington

The Goodnoe Hills Wind Farm has been in operation since 2008 and currently comprises 47 2.2 MW Vestas V110 Mark C and B wind turbines, with a hub height of 87 meters and a rotor-swept diameter of 110 meters located in south-central Washington atop an east-west ridgeline

flanking the Columbia River approximately 3–6 km away (Figure 2). The topography descends steeply south of the ridgeline approximately 610 meters to the Columbia River and more

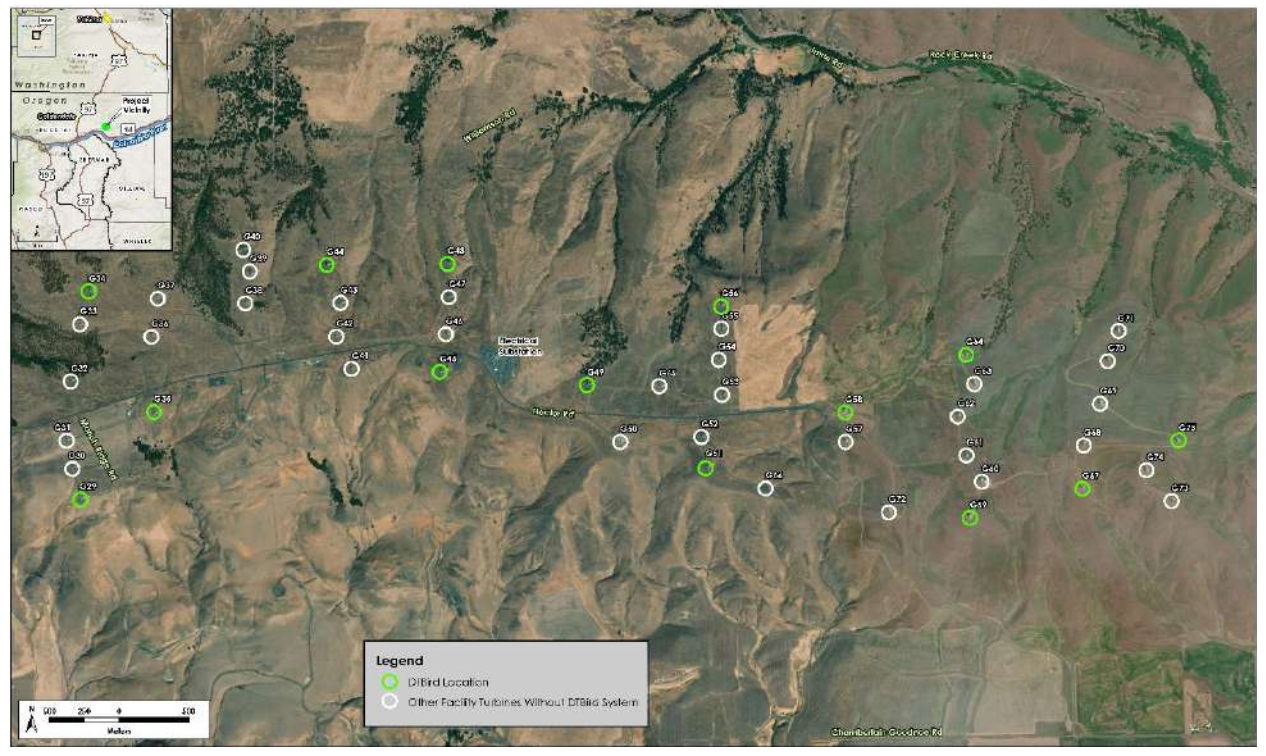


Figure 2. Layout of the Goodnoe Hills Wind Farm in south-central Washington showing locations of installed DTBird systems.

gradually to the north approximately 500 meters down into Rock Creek Canyon and associated riparian corridors. The project area is dominated by a mosaic of grazed grassland and shrubsteppe, with inclusions of ponderosa pine (Pinus ponderosa) and Oregon white oak (*Quercus garryana*) woodlands on the ridge's north-facing slopes. Fourteen DTBird systems were installed around the perimeter of this facility to support this research; however, the extent of effective operation varied among the installed systems during the 2-year study at this site (Attachment 3).

## 4.3.2 DTBird System Operation

DTBird is an automated detection and audio deterrent system created by the Spanish company Liquen, designed to discourage birds from entering the RSZ of spinning wind turbines. The system uses cameras to automatically detect airborne targets of interest, records each such event in an online database, and triggers a warning signal (loud sound) if the tracked object has moved close to the turbine. If the object moves even closer to the RSZ, a more aggressive dissuasion signal is broadcast.

The DTBird systems were set up with four 6-megapixel HD cameras arrayed in approximate cardinal directions on the turbine towers at a height of 4 m agl, and four speakers arrayed in similar fashion around the tower at a height close to the lower RSZ. The Goodnoe Hills

installations included a second ring of four broadcast speakers installed on the turbine towers just below hub height (Figure 3). This modification was implemented to account for taller turbines at the Goodnoe Hills and thereby help to ensure effective deterrent broadcasting throughout a larger overall detection envelope and collision risk zone. Field measurements correlated with known assigned camera numbers confirmed that the orientation of cameras of a given number was variable but nonetheless coarsely consistent across the seven installations. Camera 1 always faced to the west, Camera 2 to the south, Camera 3 to the east, and Camera 4 to the north. The systems included a light monitor that restricted their operation to periods when the lighting exceeded 50 lux, which translates to operation from civil dawn to civil twilight. In addition, during normal operations, the collision-avoidance module (deterrent signals) operated only when the turbine blades were spinning at a rate of ≥3 rpm. At the minimum cut-in wind speed for turbines at the study site (3.5 m/second [sec]), the blade rotors spun at a rate of approximately 12–14 rpm.

The broadcast volume of the deterrent signals can be adjusted depending on site-specific needs pertaining to the targeted bird species, local noise-management ordinances, and the specific facility layout. The factory setting broadcasts sounds at approximately 121 decibels (dB) at 1 m from the turbine. Sound-attenuation models and testing by Liquen during installation of the systems confirmed that broadcasting at the factory setting would not exceed the Kern County noise-ordinance restriction of  $\leq$ 65 dB at the exterior of the residence closest to a DTBird installation (approximately 0.5 km). On days when UAV flight trials occurred, deterrent signals were muted at the focal turbine during all daylight hours. This arrangement was necessary to allow the operations team to maintain clear verbal communication at all times, and because the

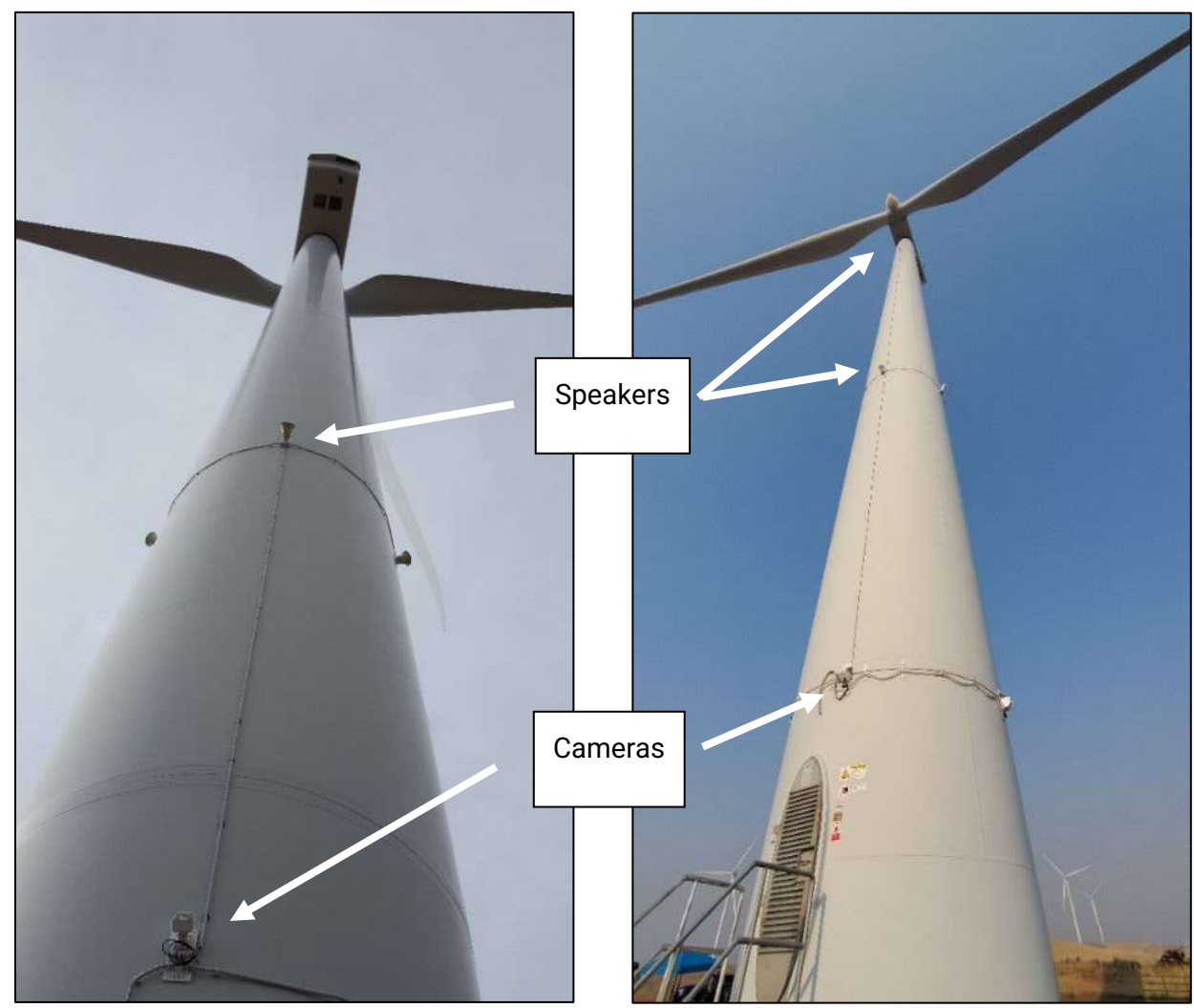


Figure 3. Depiction of DTBird video camera and broadcast speaker locations on turbines at the Manzana Wind Power Project (left panel, single ring of speakers) and Goodnoe Hills Wind Farm (right panel, two rings of speakers).

local time difference between the study site in the United States and the DTBird control operation in Spain precluded timelier coordination during the actual trials.

Each individual DTBird automated video system surveilled the sky around an individual turbine for moving objects that filled enough image pixels to qualify as a target of interest based on calibrations for the focal species of interest, in this case golden eagle. DTBird does not classify or enumerate targets, may target multiple objects simultaneously, and does not actually track individual objects—it simply repeatedly registers individual objects as targeted as long as they meet the calibrated targeting criteria. Analysts must subsequently review event records and video clips stored in the DAP to classify and enumerate the detected targets, which may be birds or false positive detections caused by airplanes, insects, debris, raindrops, snowflakes, or other inanimate objects moving through the detection envelope, as well as from by sky artifacts

(e.g., high-contrast, shifting elements caused by clouds and bright skies that are mistaken for flying objects).

DTBird systems are calibrated to target objects of a specified size range and, if a system registers that the turbine rotor is actively spinning at ≥2 rotations per minute (rpm) to trigger subsequent deterrent signals when the system estimates that a targeted object as within a specified distance from the turbine. Detection and trigger distances are determined based on pre-programmed criteria projecting how many image pixels a bird of the specified size is expected to fill at specified distances. The Manzana and Goodnoe Hills systems were calibrated to target golden eagles (wing span of 2.1–2.3 m), which translated to targeting objects that met specified criteria at an expected maximum line-of-sight distance from the turbine of approximately 240 m. Once an object is targeted and a new detection record initiated at a spinning turbine, the system triggers an initial audible warning signal if it perceives that a targeted object moves within 170–240 m of the turbine, and triggers a more aggressive dissuasion signal at distances of 100–170 m, depending on the flight altitude (Figure 4; and see H. T. Harvey & Associates 2018 for additional graphical illustrations and detailed information about the expected deterrent-triggering zones within the projected overall detection envelope).

When a DTBird system first detects a targeted object, it creates a new event record in the online digital analysis platform (DAP) database Liquen maintains to store detection records and extracted video clips for all DTBird installations. The DAP records a timestamp for each initial detection event along with other limited data. Other data automatically recorded in the DAP for each detection event include: (a) the average wind speed, rotor azimuth, and rotor rpm during the event record derived from the turbine SCADA system; (b) a binary indicator of whether or not the focal rotor was spinning sufficiently for DTBird deterrence module to be operating; (c) an estimate of the current amount of ambient illumination; and (d) length of the video tracking record. If a targeted object subsequently or simultaneously triggers one or both of two deterrent signals (early warning or a more raucous dissuasion signal if a target approaches closer to the turbine) information is added to the same DAP event record to document the unique timestamps and signal durations for each deterrent-triggering event. Each event record has video clips attached to it representing the four cameras, which the system extracts to begin 10 seconds before targeting began and continue for 30 seconds after the last targeted object exits the detection envelope. There must be no objects targeted for at least 26 seconds before a given DTBird system can initiate a new detection event record. If a system targets multiple objects concurrently during the same event period, timestamps are recorded only for the first detection, warning-trigger, and dissuasion-trigger events, and those respective events may not be triggered by the same object. In these cases, sometimes it can be difficult to determine exactly which bird or object was responsible for the timestamped events. Technicians must screen all relevant DAP records and videos to classify and enumerate the detected objects, which can include birds of all types and sizes as well as myriad other animate and inanimate flying objects, and to identify other sources of false positive detections caused by the detection system perceiving dynamic, high-contrast elements in the viewshed associated with moving turbine blades, clouds, and other turbine equipment as moving objects of interest.

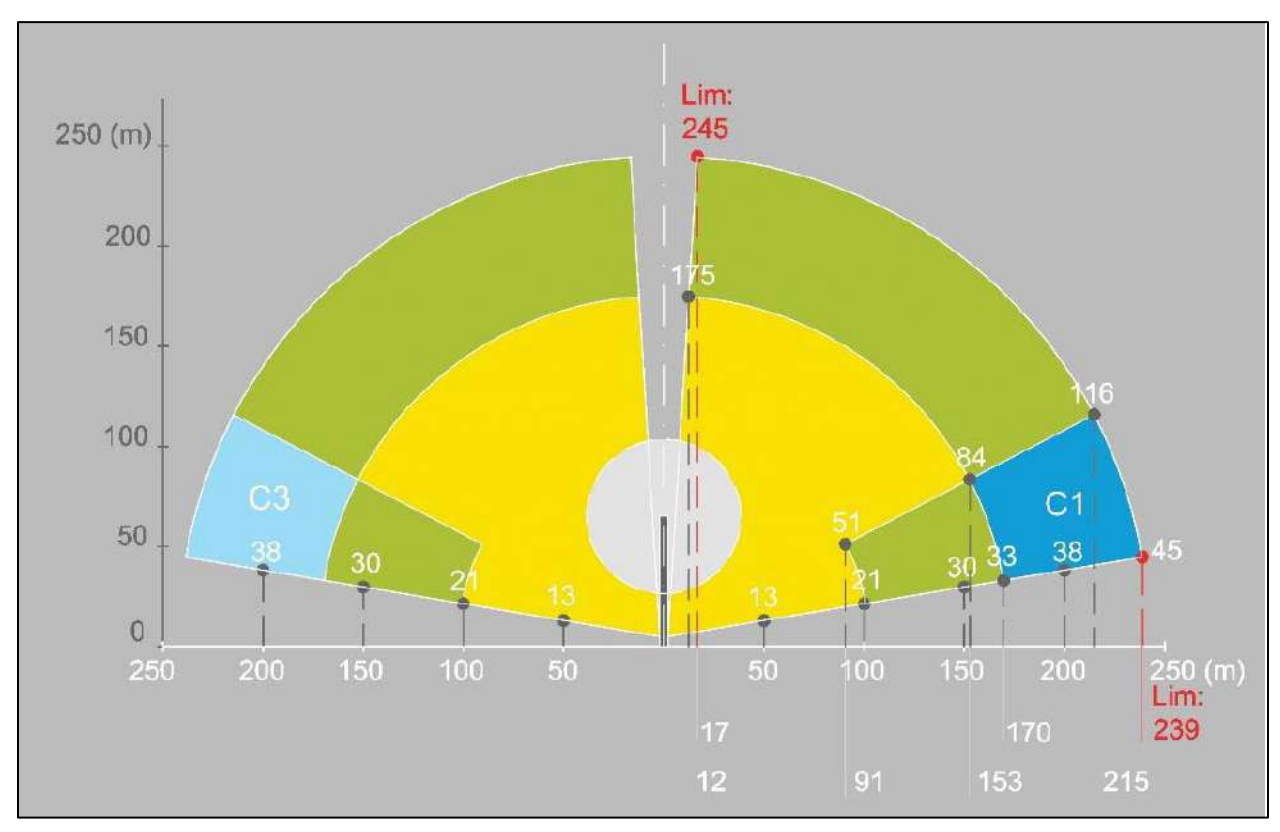


Figure 4. Vertical cross-section illustrating theoretical DTBird detection envelope calibrated for golden eagles, with light gray indicating rotor swept zone, blue indicating detection-only zones, green indicating variable warning-signal trigger zones, and yellow indicating variable dissuasion-signal trigger zones.

Under the DTBird targeting scenario and given calibration for golden eagles, much smaller objects (e.g., small birds and even insects) may trigger detections and deterrents if they are close enough to fill the same number of pixels as a golden eagle would at a much greater distance. Conversely, much larger objects (e.g., airplanes) may trigger detections when they are farther away but fill the requisite number of pixels to be perceived as a possible golden eagle at a relevant distance. Because of these system limitations, false-positive detections and deterrent triggering commonly occur, often at a much greater frequency than events related to target birds (May et al. 2012; Attachment 6).

The DTBird detection and targeting systems incorporate algorithms that reduce false positives caused by factors such as commercial aircraft, insects, and the focal turbine's spinning blades. The constant-pace, arrow-straight flights of high-altitude commercial aircraft are relatively easy to filter out and ignore. Many insects can be filtered out based on their rapid wing beats and erratic flights. Once a specific DTBird installation has been operational for period, a filtering "mask" can be developed that defines the rotor swept area each camera sees and thereby helps the system to filter out false triggers caused by the spinning blades.

Before beginning the Manzana pilot study (H. T. Harvey & Associates 2018), we did not understand that Liquen typically continues adjusting the True False Positive (TFP) filtering algorithms of the DTBird systems they install for as much as an additional 6–8 weeks after they deem the systems fully operational and "commissioned." Although standard practice, once we learned of this additional post-commissioning adjustment practice, we asked Liquen to cease making any further adjustments to create a stable platform for assessing system performance for the remainder of our research at the Manzana site. That point in time was mid-February 2017, approximately 2 months after the Manzana systems were commissioned, which means Liquen had already completed most of the typical post-commissioning adjustments by that time. The false positive performance standard established to guide expansion of this research to the Goodnoe Hills was set based on results derived under this Manzana setup history.

When the Goodnoe Hills systems were setup, we initially requested, once Liquen deemed a given system "fully commissioned", that they make no further algorithm adjustments to establish a consistent and stable platform for our subsequent evaluations. However, a preliminary analysis of the observed false positive rate recorded under this scenario during the first 6.5 months of DTBird operation at the Goodnoe Hills revealed an excessively high rate that greatly exceeded the relevant performance standard for the project. As a result, a proposal was made to the DOE to alter the setup during Year 2 of the overall Goodnoe Hills field study by allowing Liquen to make whatever further adjustments they could to minimize the overall false positive rate. It was agreed that doing so would provide a better basis for comparing DTBird's false positive performance at the two study sites using data collected subsequently at the Goodnoe Hills. Those further adjustments were completed in January 2023.

## 4.3.3 Sampling Protocol

We present Manzana results based on data collected from January through October 2017 (excludes initial partial month of data from December 2016). We present Goodnoe Hills results based on data collected from September 2021 through July 2023. For each DTBird installation, we randomly selected 10 days per sequential 28-day operational period as our sampling framework. We limited the selections to days when a given turbine and the associated DTBird system were operating at least mostly as expected, with the blades spinning and deterrents triggering when targets were registered to have crossed calibrated distance ranges. For both sites, we excluded from the sample selections all turbine-specific days where and when we conducted UAV flight trials (Attachment 5). On those days, our flight-trial activities undoubtedly influenced the otherwise typical patterns of bird activity around the focal turbines, biasing any other activity observations from those specific days.

#### 4.3.3.1 Classifying Avian Responses to Deterrents

The dataset we developed for this analysis was based on DTBird records that we randomly selected for evaluation to compose a larger experimental analysis (H. T. Harvey & Associates 2018). In 2017, the DAP recorded 19,562 detection events across the seven DTBird installations on days when no UAV flight trials were conducted as part of the pilot study; 8,953 (46%) of these events triggered a deterrent signal. To support investigating the behavioral responses of in situ eagles and other raptors exposed to the deterrent signals, we applied a sampling strategy

to select records to review and classify. Our sampling objective was to amass a temporally and taxonomically representative dataset sufficient to support robust assessments of the probability of deterrence for golden eagles, buteos (mostly red-tailed hawks [Buteo jamaicensis] year-round, as well as rough-legged hawks [B. lagopus] and ferruginous hawks [B. regalis] in Washington and California, respectively, during winter), and all raptors combined.

For each of the functioning DTBird installations, we selected 10 days per 28-day period (the cycling schedule for the larger experiment) across a full year and classifying all detected targets on those days. For evaluating the responses of *in situ* raptors to the deterrent signals, we applied a standardized approach to classifying the responses of all confirmed, suspected, and possible eagles, as well as samples of confirmed turkey vultures (*Cathartes aura*) and buteos for comparison. As described in the previous section, multiple birds occurring simultaneously in the viewsheds of a system's cameras typically confounded rendering precise temporal correlations between detectable changes in the flight behavior of individual birds and the broadcasting of specific warning and dissuasion signals (as reflected in specific triggering timestamps recorded in the DAP). For this reason, we generally excluded event records with multiple birds in view from our deterrence-response classification efforts, as did May et al. (2012). In a few such cases, however, the deterrent signaling could be unambiguously associated with an individual bird of interest, which generally meant the bird was traveling more or less alone and was clearly the only individual that was in a position to trigger the relevant deterrent signal.

To classify deterrence responses, we used the DAP and an on-screen protractor (Straffi 2016) to determine through 2D on-screen measurements whether a bird's flight path appeared to diverge appreciably and away from the RSZ within 5 sec of a warning or dissuasion signal being emitted. For comparative purposes, similar to the approach Liquen personnel typically use to classify deterrence responses, we considered a sustained flight path divergence of >15° away from the deterrent signal that precluded further passage toward the spherical RSZ of the turbine as indicative of a meaningful avoidance response. We also examined the video footage for evidence of correlations between detectable changes in flapping pattern or flight style and emittance of warning and dissuasion signals.

H. T. Harvey & Associates (2018) contains a step-by-step account of the classification process we used to categorize the responses of relevant raptors to the deterrent signals. The process incorporated several subjective and objective criteria for classifying the behavioral response of a given raptor upon exposure to a warning signal and/or dissuasion signal, culminating in a final classification of the response as one of the following:

- Y: Yes reacted in a way that, based on the change in flight pattern and direction, reduced the risk of collision with the turbine blades.
- *P: Potential* appeared to react to signal, but response was not definitive enough to be confident that the bird was at less risk after signal emission.
- N: No reacted to signal (e.g., temporarily altered its flapping rate) but did not alter its flight path away from RSZ.
- Z: Not relevant did not visibly react to signal.

 U: Unknown/undetermined – bird was already moving away from the turbine when the signal was emitted; the video quality or bird image quality was not favorable for determining the 3D reaction of the bird on the 2D video screen; or it simply was not possible to determine with any sense of confidence whether a reaction occurred or not due to other factors.

We excluded from further consideration all cases where we classified the response as "unknown/undetermined."

Along with evaluating behaviors and flight trajectories to classify a bird's response pattern when it triggered a deterrent signal, we classified the potential collision risk the bird was facing prior to triggering a deterrent as follows:

- High moving toward turbine on a trajectory and at an altitude that could take it near the current RSZ (defined for this purpose as the current, approximate 2D plane of rotation).
- Medium moving toward turbine on a trajectory and at an altitude that may take it near the turbine, but likely either below or above the RSZ.
- Low moving perpendicular to or away from the turbine distant from the RSZ, or at high altitude well above the RSZ.

### 4.3.3.2 Classifying Detected Targets for False Positives Assessment

Once the arrays of turbine-specific sampling days were selected, technicians reviewed the DAP records and videos from those days to classify the targets associated with all detection events recorded while the turbine blades were spinning. Then we focused this multi-site analysis on all such detection events for which the classified target was either a True Fals Positive (TFP) or Nontarget Avian False Positive (NTAFP) that triggered a deterrent signal. False positive detections that do not trigger an audio deterrent may result in excessively cluttered detection databases, which can hamper efficient evaluations of system operation, but they do not run the risk of excessively disturbing nontarget wildlife, wind technicians, and proximate human neighbors or contributing to negative habituation among target species of interest (H. T. Harvey & Associates 2018). Accordingly, for this multi-site assessment we focused exclusively on false positives that triggered deterrent signals.

The technicians classified the targets associated with selected detection events into a broad range of bird species, species groups, and general size categories (species-level identifications were difficult due to low-resolution video records), as well as a range of TFP subcategories. Classification subcategories we lumped together to assess overall TFP detection rates and proportions included several varieties of aircraft (i.e., airplane, helicopter, UAV [excluding our research UAVs], paraglider, and parachute), turbine blades (focal or neighboring turbine), insects, snow, rain, sky artifacts, equipment (i.e., sky artifacts triggered at edges of non-blade turbine features), debris (i.e., floating balloons, paper, plastic bags, etc.), and software/video failures (i.e., poor quality videos preclude target identification). We defined NTAFPs as birds other than large soaring raptors, including abundant common ravens, occasional distinctive falcons (*Falco* spp.) and accipiters (*Accipiter* spp.), and other species ranging from small

passerines to large geese, cranes, and pelicans (plus a few crepuscular bats). Typical large soaring raptors at both study sites were golden eagles, turkey vultures (*Cathartes aura*), redtailed hawks (*Buteo jamaicensis*), and northern harriers (*Circus hudsonicus*). Less common species at both sites were osprey (*Pandion haliaetus*), Swainson's hawk (*B. swainsoni*; migration and summer only), and ferruginous hawk (*B. regalis*; migration and winter only). Other relevant species unique to each site were abundant rough-legged hawks (*B. lagopus*) and less common bald eagles (*Haliaetus leucocephalus*) during migration/winter at Goodnoe Hills, and rare sitings of California condors (*Gymnogyps californicus*) at Manzana.

The generally poor resolution of the extracted video clips stored in the DAP precluded confidently identifying large proportions of the detected avian targets beyond coarse-scale size/group categories (H. T. Harvey & Associates 2018). Despite intensive QA/QC by the Project Manager/senior avian-raptor expert, nearly 800 Goodnoe Hills records and more than 1200 Manzana records relevant to evaluations of false positives remained classified only as unidentified "big size bird", "unknown medium/large raptor", or "unknown bird", with each classification potentially including some unconfirmed large soaring raptors. To bolster the overall comparative estimates of TFP and NTAFP rates and proportions, we manually classified all unidentified big size birds and unknown birds as either large raptors, medium/large raptors, or NTAFPs based on (a) carefully evaluating representations of other confirmed raptor, raven, and general NTAFP identifications at a given focal turbine on relevant days, (b) considering the general relative abundance of large raptors and ravens at the focal turbine, and (c) making logical assignments based on those considerations. Similarly, we reclassified some records the technicians originally classified as unknown medium/large raptors as large raptors or NTAFPs based on other proximate records identified to species or those two groups.

Partial and complete operational malfunctions of the DTBird systems—caused by several factors—were common at both sites, which led to a variety of sampling imbalances through time and among the different DTBird installations. Operational issues were particularly prevalent at one of the seven Manzana installations (Turbine V17, Figure 1; and see H. T. Harvey & Associates 2018). At the Goodnoe Hills, operational constraints and issues were comparatively rife throughout the study period there. The following constraints were most notable during the 23-month period of record considered in this report:

- System challenges resulted in no useful data being collected at 3 of 14 installations (G29, G51, and G56; see Figure 2) during Year 1 (Attachments 3, 4, and 5).
- The installation at turbine G56 was not fully commissioned until the second 28d Cycle of Year 2.
- The installation at turbine G48 failed and remained inoperable from mid-November 2022 through early March 2023.
- No useful data were collected at turbine G59 from December 2022 through early April 2023 and at turbine G64 during the month of December 2022.
- The Bonneville Power Administration shut off power to the entire facility from May 1–24, and most of the DTBird systems were not successfully rendered fully operational again until June 6, 2023.
- The installation at turbine G51 was nonfunctional after early July 2023.

- The installation at turbine G67 was largely nonfunctional from early June through early July 2023.
- Most of the installations were largely nonfunctional during the latter half of July 2023.

Given the scale of operational challenges at the Goodnoe Hills, in particular, and the fact that we were not specifically interested in evaluating variation among individual turbines for the assessments herein, we included in our analyses all available and useful data from selected sampling days that met the necessary turbine-DTBird operational criteria for inclusion, as described above. Then we standardized the dependent variables for analysis as the daily counts of TFPs and NTAFPs at each turbine on selected sampling days with relevant records (see Attachment 6: Appendixes A and B for summaries of the records used for analysis), and we included *Turbine ID* as a random effect in the statistical models we developed for analyzing variability among the sites and through time. This approach and the robustness of modern analytical models to sampling imbalances and modest violations of distributional assumptions (Schielzeth et al. 2020) helped to reduce potential biases caused by unequal sampling among the sites and DTBird installations.

## 4.3.4 Controlled Experimental Design at Goodnoe Hills

Data collection began on 1 September 2021 and was expected to continue for two annual rounds of 13 28-day sampling cycles. In the end, sampling was continued for one additional 28-cycle to account for the Bonneville Power Administration having unexpectedly shut down all power to the wind facility from 1–24 May 2023.

The experimental design involved, on a given day, having roughly half of the operational DTBird systems operating in control mode with the deterrent signals not actually broadcasting, and half operating in treatment mode with the deterrent signals broadcasting normally. Here it is important to note that the DTBird systems can be set to trigger and record the timing of deterrent signaling events virtually without the audio deterrents actually broadcasting. Assignments to the control and treatment groups were re-randomized on a daily basis, stratified to ensure (a) daily representation in both the eastern and western halves of the facility, and (b) that each system was operated in treatment mode for at least 10 days per 28-day cycle. Based on preselected rotation schedules (see Attachment 3: Appendix A), Liquen staff implemented and managed automated programming from Spain to control the daily deterrent settings, with necessary daily switching able to occur conveniently during daytime in Spain but nighttime in Washington (DTBird operates only during daylight hours). By randomly assigning treatments on a daily basis and using daily event metrics as the analytical data, we sought to: (1) minimize the potential for turbine-specific habituation; (2) ensure reasonable precision in matching environmental covariate values to response records on a daily basis, rather than seeking to apply covariate values that are averaged or classified across extended periods; and (3) enable effective subsampling of the DTBird event response data.

To select days from which we derived samples used in the analyses, for each operational DTBird turbine we randomly selected 10 days per 28-day cycle for screening, always seeking to the degree possible that each turbine-specific 28-day sample included data for 5 days when the deterrent signals were operating in treatment mode and 5 days when they were operating in

control mode. However, frequent operational failures greatly hindered achieving this intended sampling design. To reduce the effects of frequent system failures in producing unbalanced sampling relative to control-treatment modes, we often adjusted the selected sampling days compared to the initial random selections in an effort to maintain both the 10 days per 28-day cycle sampling objective and 50:50 ratios of control-treatment samples per turbine. Despite these efforts and due to issues beyond our control, the resulting sampling was far from ideal. Nevertheless, especially in this case with Turbine ID treated as a random variable, GLMMs tend to be fairly robust to sampling imbalances as long as the overall representation of data within predictors and covariate classes of interest is relatively robust.



Figure 5. Images portraying the five UAVs deployed during flight trials conducted during this study in California (images A and B) and in Washington (images C-E).

## 4.3.5 UAV Flight Trials to Assess False Negative Detection Rates

We conducted UAV flight trials at the Manzana site at all seven DTBird installations, with sessions spanning January through August in 2017, but most concentrated in August. We flew flight trials at three Goodnoe Hills DTBird turbines in August 2021 and at four turbines in July 2022. We flew two UAVs during the Manzana flight trials and three different UAVs during the Goodnoe Hills flight trials (see Figure 5). All five UAVs were similar in being fixed-wing plastic/foam-bodied models, with a wingspan, body length, and mass similar to a golden eagle, and painted brown to mimic golden eagle coloration. However, they differed somewhat in overall size, body morphology, and shade of coloration. The Manzana study results suggested that the distance at which the DTBird systems detected the two UAVs flown during those sessions differed significantly, which we interpreted as potentially mimicking differences that could pertain to detecting larger, darker female eagles versus smaller, lighter-colored male eagles (H. T. Harvey & Associates 2018). Accordingly, we purposefully sought to also fly more than one model during the Goodnoe Hills flight trials to support further investigation of this detectability factor. That said, some of the variability in models used stemmed from crashes destroying one of the two aircraft used during the Manzana study and two of the three aircraft used during the Goodnoe Hills study. Further contributing to the variability in UAV models used at each site, the second UAV used during the Manzana study was not available for use during the Goodnoe Hills study.

During both the Manzana and Goodnoe Hills flight-trial efforts, complicated flight conditions for flying light-bodied fixed-wing UAVs and unexpected calamities impinged on our ability to conduct robust suites of UAV flight trials repeated across different seasons with variable sky cover and flight conditions. In the end, both efforts commonly involved concentrated sampling during mid-summer, but differed in that other sampling occurred at the Manzana site at scattered times from mid-January to early March. The extent of sampling across daylight hours also varied at the two project sites. Most flight trial sessions occurred during morning hours when the wind conditions tended to be most compatible for flying fixed-wing UAVs; however, minimal winds allowed for extending the final 2022 sessions at the Goodnoe Hills later into early afternoon (at which point excessive heat precluded further flying for the day).

The key commonality at the two study sites was that we flew primarily pre-delineated linear transects orchestrated as automated flight missions at strategically selected DTBird-equipped turbines, with the goal of achieving representative sampling of the hemispheric, 240-m radius expected maximum-detection-distance envelopes around the sampled DTBird installations. The commonly applied randomized transect selection algorithm delineated flight transects based on multi-layer stratification by compass direction of the flight, flight trajectory (between a maximum 15° ascent and maximum 15° descent), lateral distance from the turbine, and altitude relative to the expected DTBird camera locations. We then packaged collections of 10–20 predelineated, turbine-specific transects to orchestrate efficient, single, battery-powered, mostly automated UAV flight sessions using professional pilots, Mission Planner software (ArduPilot Dev Team 2021) on a laptop, and automated radio communication to direct the UAV. Operating several such missions over a multi-hour period composed an individual flight-trial session at a specific turbine, and at both sites we sought to conduct at least half-day flight trial sessions at

several representative DTBird-equipped turbines with compatible landscape settings (i.e., relatively safe places from which to launch and land the UAV, limited topographic complexity, and minimal complications caused by elevated obstacles other than the focal turbine and usually one other adjacent turbine).

Each pre-delineated transect began and ended 100-m line-of-sight distance beyond the projected 240-m detection envelope to support the possibility of detections beyond the expected maximum range. Once the DTBird system targets an object and creates a new detection record in the DAP, no new detection record is created until no additional targeting has occurred for at least 26 seconds. Accordingly, to generate independent transect samples for evaluating the probability of detection and the DTBird system's response characteristics, the automated flight sessions included 30-second loiter periods between each delineated transect at 5–6 preselected, safe destinations located 500 m from the relevant study turbine (previously illustrated in H. T. Harvey & Associates 2018).

Each UAV was equipped with avionics that recorded myriad GPS position, ground and air speed, flight trajectory, and other flight metrics many times per second with high spatiotemporal accuracy. These data were automatically transmitted during the flights to a laptop used to control the automated missions, and could also be extracted directly from the avionics units post-flight. The resulting output from each individual flight was a continuous stream of non-parsed data that had to be translated to a useable format. To extract these data and prepare them for analysis, we followed the detailed procedures and protocols described in H. T. Harvey & Associates (2018). Concisely summarized, this process involved the following primary steps:

- 1) Translate UAV telemetry log files to spreadsheet format using a publicly available custom program (Fernie 2012).
- 2) Filter and translate variables recorded by the UAV avionics into useful formats and units of measure, with meaningful variable names.
- 3) Filter tracking records to:
  - a. Exclude data from periods when the UAV was not actually flying (pre-launch and post-landing) or was flying below or loitering outside of detection range.
  - b. Include only one record per second to match the resolution of the DAP records.
- 4) Use ArcGIS 3D Analyst (ESRI, Redlands, CA) to:
  - a. Exclude as outliers all loiter-point locations and any other locations recorded at a line-of-sight distance exceeding 340 m; i.e., more than 100 m beyond the expected DTBird maximum detection distance for golden eagles of 240 m.
  - b. Code all tracking locations with individual transect numbers based on relevant temporal breaks in the streams of tracking data.
  - c. Add additional GIS-derived position metrics and environmental covariates used in analyses.
- 5) Use the DAP to identify relevant UAV detection and deterrent-triggering event records, and to classify the sky backdrop behind the UAV at the time of each event.
- 6) Match DTBird detection and deterrent-triggering event records recorded in the DAP to the UAV tracking records based on matching 1-second-resolution timestamps.

7) Finalize datasets for analysis by eliminating all tracking records that are not matched with a DAP event record.

### 4.4 Analytical Methods

## 4.4.1 Factors Influencing DTBird Detection Capabilities (Objective 1)

#### 4.4.1.1 Factors Influencing Probability of Detection

To generate estimates of the probability of detecting an eagle-like UAV, we matched DAP detection event records in space and time (resolved to 1-second resolution) with the UAV tracking records to classify each independent UAV flight transect as Detected or Not Detected by the relevant DTBird system. We then calculated the proportions of flight transects detected and not detected at each turbine where we conducted flight trials. The grand-average of the proportions detected then represented the overall estimate of the probability of detecting an eagle-like UAV that passed within the expected 240-meter maximum detection range of the calibrated DTBird systems at each study site, and the converse represented the false negative rate (i.e., the percentage of flights that passed within detection range but were not detected by the DTBird systems).

To generate insight about patterns of variability in the probability of detection, we used ArcGIS tools to calculate the horizontal direction, vertical viewing angle, and line-of-sight (LoS) distance from the detection camera to each individual GPS point along a given UAV flight path, and we used circular statistics to calculate the average *Exposure Direction* (horizontal direction) for each flight transect (Zar 1998). Then we conducted a logistic regression analysis (Systat 13.2.01; Systat Software, Inc., San Jose, CA) with Detected or Not Detected as the binary response variable and several potential predictors considered in the models for evaluation. The relevant predictors were:

- Site (Manzana or Goodnoe Hills).
- Hour of the Day (e.g., 0900 or 1500 H Pacific Standard Time, using the majority value if the flight segment overlapped two hourly periods).
- Detection Angle (°; average vertical angle from camera to UAV).
- LoS Distance (minimum line-of-sight distance from camera to UAV).
- Exposure Direction (average horizontal angle from turbine to position of UAV, transformed to two orthogonal vectors: sine(Exposure Direction) representing a west [negatives values] to east [positive values] vector and cosine(Exposure Direction) representing a south [negatives values] to north [positive values] vector).

Given expectations of non-linear relationships from prior site-specific analyses, we considered second-order polynomial terms in the models for *Hour of the Day* and *Detection Angle*, and third-order polynomial terms for *LoS Distance*. We used Akaike's Information Criterion (AIC) scores, individual parameter tests, log-likelihood ratio chi-square tests, and Nagelkerke pseudo-R<sup>2</sup> values to identify the top predictive model given the predictors considered and evaluate the relative influences of various predictors on the probabilities of detection. The logistic GLMMs resulted in predictions of the ln(odds of a response). We used a standard formula

(100\*exp[ln[odds]]/[1+exp[ln[odds]]]) to transform the log-odds estimates to probabilities of response (0 to 1 translated to percentages) for the purpose of describing and graphically displaying relationships (Hosmer and Lemeshow 1989).

We also note here that Nagelkerke pseudo- $R^2$  values do not correlate with typical coefficients of determination  $R^2$  values for non-GLMM models reflecting the proportion of explained variance. Instead, although not well documented in published literature, a typical rule of thumb for interpreting Nagelkerke pseudo- $R^2$  values is that values  $\le 2$  indicate a weak relationship, values between 0.2 and 0.4 indicate a moderate relationship, and values  $\ge 4$  indicate a strong relationship (Shah 2023).

#### 4.4.1.2 Factors Influencing DTBird Detection and Deterrent-Triggering Response Distances

Development of candidate model sets should be guided as much as possible by a thorough understanding of the system being studied (Burnham and Anderson 2010). The multi-site analysis presented here benefited from insights gained from prior site-specific analyses conducted using data collected at the two study facilities (H. T. Harvey & Associates 2018).

The response variable for the analysis was the line-of-sight distance (LoS Response Distance) between the UAV and closest DTBird camera at the time a detection or deterrence event occurred. The operative assumption was that greater response distances can be interpreted as reflecting an improved detection or triggering response, in that earlier (more distant) detection and targeting is expected to provide more time for the deterrents to alter a target bird's behavior well before the risk of collision is acute. We calculated the distances based on the UAV GPS coordinates at the time of the event, using measuring tools in ArcGIS 3D Analyst. Flight samples included in these analyses were necessarily limited to those that triggered a relevant DTBird response. To fit the response-distance data, we built GLMMs and evaluated the influence of various potential random- and fixed-effect predictors. We implemented the models using the 'Ime4' package in R (R Core Team 2023; function *Imer*, Bates et al. 2015), with a Gaussian distribution and an identity link function. The initial full model for this analysis had the following structure (see Attachment 5: Appendix A for descriptions of each variable):

LoS Response Distance  $\sim (1 \mid Site : Turbine \mid ID) + (1 \mid Site : UAV Model) + Site + Event Type + Sky Backdrop + <math>\sin(Direction from Turbine \mid DFT \mid) + \cos(DFT) + \sin(Course Over Ground \mid COG \mid) + \cos(COG) + Ground Speed + Climb Rate + Roll Angle + Pitch Angle + Wind Speed + Solar Irradiation + Solar Irradiation<sup>2</sup> + Sun Azimuth + Sun Elevation + Roll Angle * Pitch Angle + <math>\sin(DFT)$  \* Sun Azimuth +  $\sin(DFT)$  \* Sun Azimuth +  $\sin(COG)$  \* Sun Azimuth +  $\sin(COG)$  \* Sun Azimuth +  $\sin(COG)$  \* Sun Azimuth

Because the predictor variables were on different scales, we centered and scaled all continuous predictors after applying the following transformations. We transformed *Roll Angles* and *Pitch Angles* to absolute values, expecting that rolling left versus right and pitching up versus down would modify exposure of the UAV profile to the camera similarly. We transformed the *DFT* and *COG* metrics to orthogonal east-west (cos[x]) and north-south (sin[x]) vectors to support linear analyses of these circular variables (Fisher 1995, Cremers and Klugkist 2018). In contrast, we did not similarly transform *Sun Azimuth*, because the range of that variable was only slight

greater than 180° (east in the morning, south at midday, and west in the evening) and therefore did not represent a potential for convergence errors caused by 0° and 360° being equivalent values.

We evaluated *Turbine ID* nested within *Site* (*Site*: *Turbine ID*) and *UAV Model* nested within *Site* (*Site*: *UAV Model*) as random effects, because we expected that DTBird's responses could vary depending on the unique setting at each turbine and variation among the UAVs used, yet neither component was similarly represented at the two sites. In addition, modeling these two factors as random rather than fixed effects acknowledged that the study involved repeated measures (flight sessions) at individual turbines and using different UAVs, such that there was a high likelihood of non-independence among the response distances measured within groupings of these factors. We also modeled *Site* as a fixed effect to determine if DTBird's overall response-distance performance appeared to vary significantly between the two study areas.

We evaluated two- and three-way interactions among the *DFT* and *COG* orthogonal vectors and *Sun Azimuth*, expecting that the influence on response distances of UAV travel direction and directional position from the turbine could markedly depend on the relative position of the sun due to illumination and glare. We also evaluated the two-way interaction between the two UAV "stability" metrics (*Pitch Angle* and *Roll Angle*), anticipating that modeling the interaction of these variables could more accurately reflect the collective influences on exposure of the UAV profile to the cameras than modeling any one metric alone, in part because preventing aircraft stalling effectively precludes maximizing more than one of these variables at the same time. We did not consider any other interactions due to inapplicability and limitations of the available dataset.

To investigate the validity of applying this full model to the multi-site dataset, after we fit the model we used diagnostic tests to evaluate whether the model violated any GLMM assumptions (Zuur et al. 2009, Wood 2017). Specific diagnostics included plotting model residuals to assess independence, equal variances, normal distributions, over- or under-dispersion, and outliers with high leverage. We conducted residual diagnostics using package 'DHARMa' (functions simulateResiduals, plotResiduals, testUniformity, testDispersion, testOutliers; Hartig 2021). Along with the residual diagnostics, we evaluated potential combinations of predictors for indications of collinearity, and specifically avoided variable combinations that produced variance inflation factors (VIFs) greater than 5 (Hair et al. 1998, Zuur et al. 2010).

To determine the best model for the analysis, we identified the subset of predictors that best explained variation in the observed response distances via stepwise model selection using the step function in R's base 'stats' package (R Core Team 2023) and following the GLMM model selection guidance of Zuur et al. (2009). This stepwise-selection was done in combination with the following criteria to select the best model: ANOVA-based comparisons of nested candidate models, R² values, and residual plots. To select final models using Akaike's Information Criterion (AIC), we evaluated only models that met the assumptions of GLMMs. Given the considerable number of predictors and unbalanced categorical factors with some groups having relatively small sample sizes, we used AIC corrected for small sample sizes (AICc) to

compare candidate models to avoid overfitting. We generated graphics resulting from the best model using 'siPlot' Lüdecke 2023) and 'emmeans' (Length 2023), both of which rely on 'ggplot2' (Wickham 2016).

In discussing the significance of statistical results, we label results with  $P \le 0.001$  as highly significant,  $P \le 0.05$  as significant, and  $P \le 0.10$  as marginally significant.

## 4.4.2 *In Situ* Behavioral Responses of Eagles and Raptors (Objective 2)

Implementing an analogous control-treatment design for evaluating responses to the deterrents was not feasible during the Manzana pilot study. Accordingly, to prepare this multi-site assessment we sought to achieve the following objectives:

- A. Use chi-square contingency table analyses with *Site* and categorical *Response* classifications as factors to determine if the apparent responses of eagles and other large raptors to DTBird deterrent signals broadcasted in association with spinning turbine blades differed at the two wind facilities.
- B. If the probability of effective deterrence in response to the combination of spinning turbine blades and broadcasted deterrents differs significantly at the two facilities:
  - a. Conduct additional logistic generalized linear model (LGLM) analyses to evaluate how various potential predictors influence the probability of effective deterrence at the two sites, limited to the "treatment" data collected at both facilities (i.e., responses to spinning turbines with the deterrents broadcasting).
  - b. Conduct no statistical analyses including the "control" data from the Goodnoe Hills site (i.e., responses to spinning turbines with the deterrents muted).
- C. If the probability of effective deterrence in response to the combination of spinning turbine blades and broadcasted deterrents does not differ significantly at the two facilities, expand the chi-square and LGLM analyses to include the full combination of treatment data from both sites and control data from the Goodnoe Hills, ignoring Site but including Treatment Group as a predictor. The objective here would be to enhance the single-site control-treatment analysis presented in Attachment 3 by substantially bolstering the available sample size of cases in the treatment group.
- D. Develop estimates of the probability of effective deterrence at the two sites that include consideration of the added benefit the DTBird audio deterrents appear to provide above and beyond the effect of spinning turbines alone. The derivation of such estimates will vary depending on whether option (2) or (3) above proves appropriate to pursue.

#### 4.5.2.1 Evaluating Differences in Behavioral Responses Between Sites

To evaluate differences in the categorical responses of raptors to broadcasted deterrent signals at the two study sites, we used 2-way Pearson chi-square analyses performed using the base R package version 4.3.1 (R Core Team 2023). For these analyses, classifications by Site (two groups) and Response (three groups) categories composed the 2 x 3 contingency tables of interest. If given at least a marginally significant ( $P \le 0.10$ ) overall chi-square test, we proceeded

to conduct post-hoc comparisons to further characterize the specific *Response* categories within which notable *Site*-specific differences were apparent. For these tests, we used the second post-hoc comparison approach outlined in McDonald (2014). To evaluate the individual significance of the three contrasts of interest, we compared the resulting P values to Bonferroniadjusted values of 0.017 for significance at the overall level of  $P \le 0.05$  and 0.033 for marginal significance at the overall level of  $P \le 0.10$ .

We prepared these chi-square analyses for all analyzed cases, all confirmed/probable golden eagles, all confirmed/probable turkey vultures, and all confirmed/probable buteos. Further, the datasets included three possible response variables, one pertaining to responses to warning signals alone, one pertaining to responses to dissuasion signals alone, and one including responses to single deterrents or to the combination of both deterrents signaling in sequence, where applicable. For this multi-site analysis we focused only on the combined response data to maximize sample sizes and emphasize the overall effects of the deterrent system. In a few cases, the resulting cell sample sizes were small, but Pearson chi-square tests are known to be robust as long as expected cell frequencies exceed 1.0 (Jeffreys 1939), and our preliminary investigations showed no notable differences in outcome using the alternative Fisher's Exact Test. We did not strive to develop more complicated 3-way chi-square statistical models that included consideration of relative collision risk prior to deterrent triggering as a third predictor (H. T. Harvey & Associates 2018). However, we ultimately addressed this important potential influence again using a LGLM approach.

#### 4.5.2.2 Evaluating Factors Influencing Behavioral Responses to Deterrents

As described further below, the initial chi-square analyses indicated that the probability of effective responses to broadcasted deterrents was often lower at the Goodnoe Hills facility than at the Manzana facility. Therefore, pursuing the second phase of Objective B rather than Objective C, as outlined above, was warranted. Accordingly, we did not seek to integrate the treatment data from both sites to compare against the control data generated only at the Goodnoe Hills. Instead, we sought to develop further insight about possible drivers of the difference in the probability of effective responses to broadcasted deterrents at the two sites by composing LGLM analyses to evaluate the influences of several potential predictors. These analyses were necessarily limited to cases involving responses to broadcasted deterrents. Further, we collapsed the Response variable from four to two categories to compose a binary response variable for the LGLM analysis: 1 = probable effective response (CE + PE classifications as described above) and 0 = no effective response (I = N + Z classifications). We prepared two analyses—one based on the multi-species dataset and one limited to probable golden eagles—and focused only on the combined deterrence response classifications. For the multi-species analysis, we included a Species Group variable in the model to highlight potential differences among the three primary species groups: eagles, vultures, and buteos. To facilitate evaluation of Species Group as a predictor, we reduced the dataset to only those cases that we could confidently identify as belonging to one of these three groups. The initial full model for the multi-species analysis was as follows:

 $In(Odds of effective deterrence) \sim Site (Manzana CA or Goodnoe WA) + Species Group (Eagle, Vulture, or Buteo) + Preexposure Risk (risk of exposure to turbine before$ 

deterrence: low, medium, or high) + Wind Speed (meters/second; measured by turbine anemometer) + all possible 2-way interactions

The initial full model for golden eagles was the same except for excluding the *Species Group* variable. We implemented the LGLM analyses using the 'glm' function in R (R Core Team 2023). To settle on final models, we used likelihood ratio tests for individual parameters and compared Akaike Information Criterion (AIC) scores for all possible candidate models reflected in the full model statements to identify the most parsimonious combinations of predictors (Burnham and Anderson 2010). In considering the merits of different candidate models, we also used diagnostic residual plots to evaluate conformity to the assumptions of LGLMs, plots of model residuals versus leverage and Cook's distance to identify potential outliers, and McFadden's pseudo- $R^2$  to assess the explanatory power of models (McFadden 1974, Friendly and Meyer 2016).

The LGLM resulted in predictions of the ln(odds of effective deterrence). We used a standard formula (100\*exp[ln[odds]]/[1+exp[ln[odds]]]) to transform the log-odds estimates to probabilities of response (0 to 1 translated to percentages) for the purpose of describing and graphically displaying relationships (Hosmer and Lemeshow 1989).

## 4.4.3 Factors Influencing False Positive Detection Rates (Objective 3)

We used R 4.3.2 (R Core Development Team, Vienna, Austria) to develop generalized linear mixed models (GLMMs) illustrating variation in TFP and NTAFP rates at the two study sites. We developed independent analyses for TFPs and NTAFPs, focusing on four model constructs for TFPs and two model constructs for NTAFPs. Given the additional false-positive filtering adjustments made during Year 2 of the Goodnoe Hills study, our first analytical objective was to compare TFP and NTAFP rates at the Goodnoe Hills across comparable periods of Year 1 and Year 2. Then we analyzed differences between the two study sites by comparing results from the Manzana site against results from only a comparable period of Year 2 at the Goodnoe Hills. For both sets of comparisons, we analyzed two models with the following variable structures:

#### Goodnoe Hills Year 1 versus Year 2

TFPs/Turbine/Day  $\sim$  (1|Turbine ID) + (1|28d Cycle:Date) + Year + 28d Cycle + Year\*28d Cycle NTAFPs/Turbine/Day  $\sim$  (1|Turbine ID) + (1|Month:Date) + Year + Month + Year \*Month

#### Manzana versus Goodnoe Hills Year 2

TFPs/Turbine/Day  $\sim$  (1|Turbine ID) + (1|28d Cycle:Date) + Site + 28d Cycle + Site\*28d Cycle NTAFPs/Turbine/Day  $\sim$  (1|Turbine ID) + (1|Month:Date) + Site + Month + Site\*Month

We included *Turbine ID* as a random effect in all models to account for uncontrolled variation resulting from the unique spatial and temporal influences of individual turbine locations and to avoid pseudo replication, and we treated *Date* as a random categorical factor nested within *28d Cycle* or *Month* to account for the influence of variable sampling days and avoid pseudo replication. We examined the models with *28d Cycle* and *Month* as alternative temporal

predictors to address different interests in examining patterns of variation though time. Specifically, we used 28d Cycle to evaluate the influences of operational duration on TFP rates, and we used Month to evaluate the seasonal influences of specific times of year on the prevalence of NTAFPs (including natural factors that vary seasonal, such as precipitation and insects).

We analyzed these data using negative binomial GLMMs, which account for typical overdispersion of count-based data. We used the 'glmmTMB' package in R (Brooks et al. 2017a, b; Magnussen et al. 2022) to generate the models with a log-link. The negative binomial response distribution ('binom2', with variance =  $\mu[1+\mu/k]$ , where  $\mu$  is the mean and k is the overdispersion parameter) accounted for overdispersion in the data.

We tested for differences in daily counts among 28d Cycles or Months using chi-squared maximum likelihood-ratio tests to evaluate the significance of the fixed factors in the models. To obtain estimated means for daily turbine-specific TFP and NTAFP counts based on the selected final models, we used the 'ggpredict' function ('ggeffects' package; Lüdecke et al. 2022). We identified differences among means using planned post-hoc comparisons following Tukey's Honestly Significant Differences test (Tukey 1949) to maintain a family-wise alpha of 0.05. The planned comparisons were limited to pairwise comparisons among 28d Cycles or Months within Years or Sites.

## 4.4.4 In Situ Experimental Evaluation of Raptor Responses (Objective 4)

The research hypotheses we formulated for the experiment were as follows:

<u>Hypothesis A:</u> The probability of an eagle triggering a dissuasion signal will be lower for DTBird turbines operating in treatment mode (deterrent signals broadcasting) compared to those operating in control mode, because broadcasted warning signals deter target raptors from approaching closer and triggering a dissuasion signal.

<u>Hypothesis B:</u> The average dwell time of eagles in the vicinity of DTBird-equipped turbines—as reflected in the length of relevant targeting videos recorded by the DTBird detection system—will be reduced around systems operating in treatment mode compared those operating in control mode, because broadcasted deterrent signals discourage birds from lingering near focal turbines.

**Hypothesis C:** The probability of an eagle crossing the active rotor swept area (RSA) of DTBird-equipped turbines will be lower for systems operating in treatment mode compared to those operating in control mode, because operation of the deterrent signals reduces the likelihood of target raptors entering the RSZ of turbines.

To analyze the full two-year experiment dataset, we used generalized linear mixed models (GLMMs) to evaluate the three research hypotheses using different response variables: 1) binary logistic response = whether or not a detected large raptor triggered a dissuasion signal, 2) continuous response (seconds) = tracking video length per large raptor targeting event, and 3) binary logistic response = whether or not a detected large raptor appeared to cross through or close to the RSA. Challenges producing a consistent, accurate, and robust dataset on

possible RSA crossings based on interpreting 3D responses from 2D video images limited our ability to evaluate research Hypothesis C.

Our GLMM designs considered DTBird turbines to be sampling units and included *Turbine ID* as a random effect in the models to account for inherent, localized, spatial variation in the landscape settings and eagle/raptor activity patterns at different turbines. All models also included sampling date nested within *Turbine ID* to account for highly variable temporal sampling at each turbine and inherent, localized, temporal variation in the environmental conditions, human activity patterns, and other factors that likely influenced the activity patterns and responses of target raptors around individual turbine locations. For this purpose, we transformed sampling dates to *Elapsed Days* since projection inception.

Given frequent uncertainties in species-specific identifications and attendant sample-size limitations for focal golden eagles, we developed independent models for three hierarchical taxonomic groups to provide effective insight: 1) confirmed and probable golden eagles, 2) confirmed and probable golden and bald eagles, with *Species* considered as a potential predictor; and 3) all confirmed and probable eagles, including unidentified eagles, without considering species as a potential predictor.

Predictors and covariates considered in the GLMMs were as follows:

- Random effects:
  - Turbine ID.
  - Days Elapsed nested within Turbine ID.
- Fixed effects:
  - o Treatment Group (binary): treatment or control.
  - Species (categorical): included in models focused on confirmed golden and bald eagles combined, but excluded from models focused on golden eagles alone and all possible eagles, including those not confirmed to species.
  - 28-day Cycle (discrete continuous): sequential series from 1 to 27 over 25-month period, with period 23 mostly not represented due to an unanticipated 1-month facility shut down.
  - Time of Day (continuous, Pacific Standard Time, translated to minutes of the day): second order term included to account for expected curvilinear relationship.
  - Cloud Cover (categorical): reflecting predominant daily condition gleaned from review of DTBird video records and coarsely classified by technicians as fair (mostly cloud free), partly cloudy (<50% cloud cover), cloudy (≥50% cloud cover with distinctly variable cloud definitions and brightness), or overcast (complete and largely uniform gray or darker cloud cover).
  - Wind Speed (continuous, meters/second): derived from turbine system metrics and averaged across duration of tracking event.
  - FPs per Day (discrete continuous): number of daily deterrent-trigger events resulting from false positives, including both true false positives (non-bird, including inanimate moving/flying objects, insects, precipitation, and sky artifacts) and non-target avian false positives (non-focal birds).

The selected covariates represented factors that: 1) were discernable using the DTBird DAP or were attainable from the wind facility; 2) we expected to have the potential to influence the ability of focal raptors to visualize the turbines and hear and respond to the deterrents; and 3) could influence the responses of focal raptors by increasing the frequency of deterrents being broadcasted. Given focal interest in evaluating *Treatment Group* as a predictor, we also evaluated all possible two-way interactions between *Treatment Group* and the other potential predictors/covariates. For all continuous independent variables, we centered and scaled the values as (value - mean)/SD prior to analysis.

For each species group, we developed GLMMs to test for the effects of *Treatment Group* and the five potential covariates on the three dependent variables. We used the R function 'glmer' in the lme4 package (Bolker 2023) to compile and evaluate GLMMs based on a binomial error distribution with a logit link (i.e., mixed-effects logistic regression), and maximum likelihood estimation with the *bobyqa* optimizer and the maximum number of function evaluations set to  $10^5$ , to model the probability of detection events triggering a dissuasion signal and whether or not an RSA cross occurred. We used the R Package 'glmmTMB' (Brooks et al. 2023) to compile and evaluate GLMMs based on a gamma error distribution with a log link and maximum likelihood estimation to analyze dwell time (recorded video length) as a dependent variable. We compared Akaike's Information Criterion (AIC) scores for candidate models to balance considerations of model fit and parsimony (considering a  $\Delta$ AICc of  $\leq$ 2 points indicative of similarly competitive models) and used Wald *z*-tests and Drop1 likelihood-ratio chi-square tests to further assess the relative importance of different predictor variables and ultimately identify a top model for each independent analysis (Burnham and Anderson 2002, Bolker et al. 2009, Symonds and Moussalli 2011).

To ensure a good model fit, normally distributed residuals, and homogeneous variances, we inspected residual plots for the selected models and individual grouping factors by plotting results using the 'simulateResiduals' function (package 'DHARMa'; Hartig 2019) applied to the selected model. We also conducted goodness-of-fit tests on these residuals using the 'testUniformity' function from the same package, which performs a Kolmogorov-Smirnov test for specified factors and combinations of factors (including the overall model) to evaluate conformity to a normal distribution. We used the functions 'testOutliers', 'testOverdispersion', and 'testZeroInflation' to confirm that the residuals did not include outliers nor exhibit overdispersion or zero-inflation (Hartig 2019).

To evaluate Wald z tests and Drop1 likelihood ratio chi-square parameter tests for individual predictors considered during GLMM development, we adopted  $P \le 0.10$  as our threshold for retaining predictors in the selected models. We chose this relatively liberal threshold to ensure representation of potentially noteworthy relationships that might have emerged more strongly had our sampling not suffered from frequent spatial and temporal imbalances in the operation of the study installations and resultant sampling, and uncertainties pertaining to species identifications. We refer to tests and contributions as marginally significant if  $0.05 < P \le 0.10$ , significant if  $0.01 < P \le 0.05$ , and highly significant if  $P \le 0.01$ .

For the logistic GLMMs, which resulted in predictions of the ln(odds of a response), we used a standard formula (100\*exp[ln[odds]]/[1+exp[ln[odds]]]) to transform the log-odds estimates to probabilities of response (0 to 1 translated to percentages) for the purpose of describing and graphically displaying relationships (Hosmer and Lemeshow 1989).

### 4.4.5 Multi-site Analysis of Collision Risk Reduction (Objective 5)

We used data generated by the two-site DTBird evaluations and the controlled experiment at Goodnoe Hills to quantify DTBird's effect on golden eagle collision risk, as described above. We initially intended to translate our results to applying the Bayesian collision risk model (CRM) recommended by the U.S. Fish and Wildlife Service (2013; and see New et al. 2015), using eagle flight times recorded by DTBird at control and treatment turbines as a proxy for eagle activity. However, we found comparisons of proportional responses to be most germane, because any estimates we could generate portraying absolute reductions in the number of eagles killed per year would be site specific, whereas proportional estimates have the potential to be applied across sites based on site-specific fatality projections.

### 4.4.6 Performance Reliability and Cost Analysis (Objective 6)

A more detailed breakdown of costs to purchase, acquire, install, and maintain DTBird is detailed in Attachment 9.

#### 4.5 Results

## 4.5.1 Factors Influencing Probability of Detection (Objective 1)

The sample sizes of independent site- and turbine-specific UAV flight transects that formed the basis for quantifying and investigating variation in the probability of detection ranged from 144–221 samples per turbine at the Manzana site and 54–131 samples per turbine at the Goodnoe Hills site (Table 1). At the Manzana site, DTBird detected 798 of 1,279 (62%) UAV flight transects, with the detected proportions ranging from 47–75% across seven sampled turbines. At Goodnoe Hills, DTBird detected 310 of 481 (64%) UAV flight transects, with the detected proportions ranging from 56–80% across five sampled turbines (Table 1).

Table 11. Numbers of UAV flight transects by sampled turbine analyzed to quantify and investigate variation in the probability of DTBird detecting an eagle-like UAV at the Manzana Wind Power Project in California and Goodnoe Hills Wind Farm in Washington.

Site	Turbine	Detected	Not Detected	Total	% Detected
Manzana	D01	80	64	144	56
	D04	129	62	191	68
	D08	106	65	171	62
	E11	143	54	197	73
	T13	116	38	154	75
	U7	130	91	221	59
	V17	94	107	201	47
Subtotal		798	481	1,279	62
Goodnoe Hills	G34	65	16	81	80

	G44	81	50	131	62	
	G58	69	36	105	66	
	G64	33	21	54	61	
	G75	62	48	110	56	
Subtotal		310	171	481	64	
Total		1,108	652	1,760	63	

The final model derived to illustrate the influence of spatial and temporal predictors on the probability of detection based on UAV flight trials had the following form:

 $In(Odds of Detection) \sim Site + Hour of the Day + LoS Distance + LoS Distance^2 + LoS Distance^3 + Detection Angle + Detection Angle^2$ 

The log-likelihood ratio goodness-of-fit test comparing the selected model and null model indicated a highly significant fit ( $\chi^2$  =476.7, df = 7, P < 0.001) and the Nagelkerke Psuedo-R² for the model was 0.324, indicating a moderate relationship. Comparisons with other candidate models are illustrated in Attachment 6: Appendix C, and coefficients, parameter tests, and diagnostics for the selected model are presented in Attachment 6: Appendix D.

The selected model indicated that the probability of detection:

- Averaged higher at Goodnoe Hills than at Manzana (discussed further below).
- Increased as the day progressed, from an average of approximately 57% during the 06:00 H to 75% during the 20:00 H (Figure 6).
- Was highest (estimated average ~75%) when the LoS Distance to a flight track was 50–75 meters from the cameras; decreased slightly at closer distances; and decreased at greater distances down to an estimated average of approximately 50% at the 240 meter

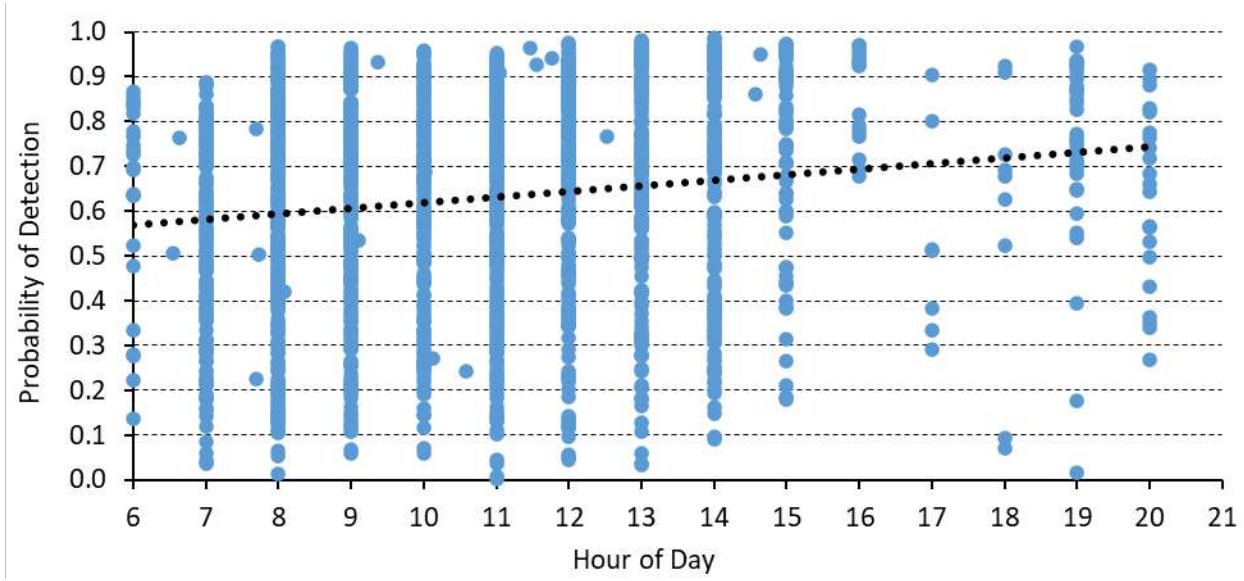


Figure 6. Modeled Linear Relationship Between Predicted DTBird Detection Probabilities for Individual UAV Flight Transects and Hour of the Day.

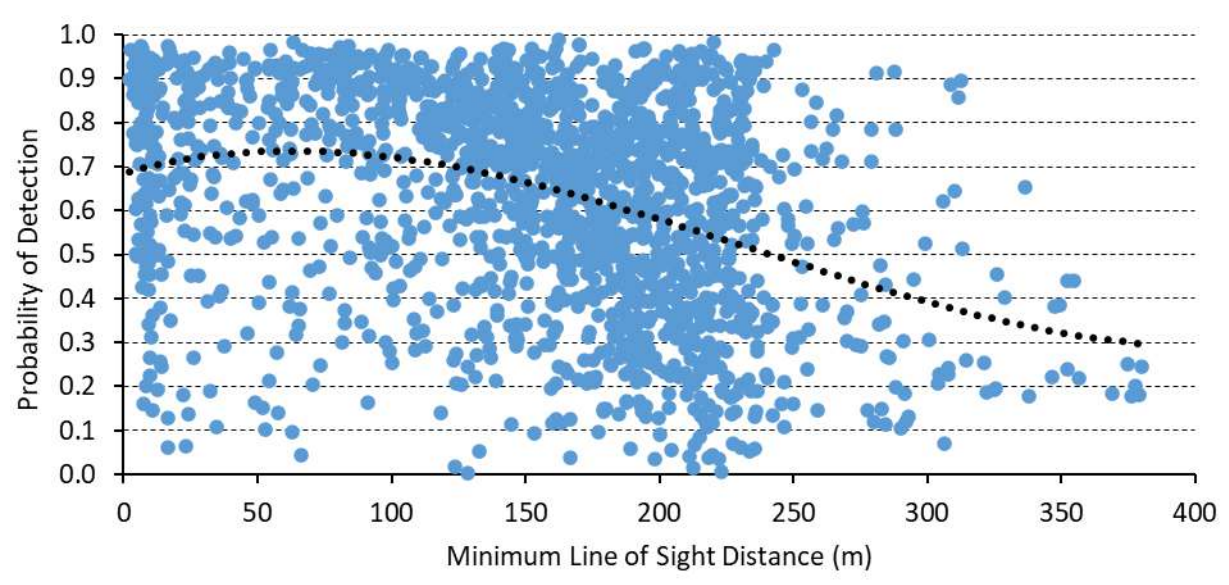


Figure 7. Modeled Third-Order Relationship Between Predicted DTBird Detection Probabilities for Individual UAV Flight Transects and the Minimum Line-of-Sight Distance to the DTBird Camera.

expected (calibrated) maximum detection distance for targets the size of golden eagles, but remained at an estimated 30% as far out as 380 meters from the cameras (Figure 7).

 Was highest (estimated mean ~65%) when the Average Detection Angle from the camera to a flight track was moderate (approximately 20-30° above horizontal from the camera) and decreased on average by 25-35% at minimum lower and maximum higher observed angles (Figure 8).

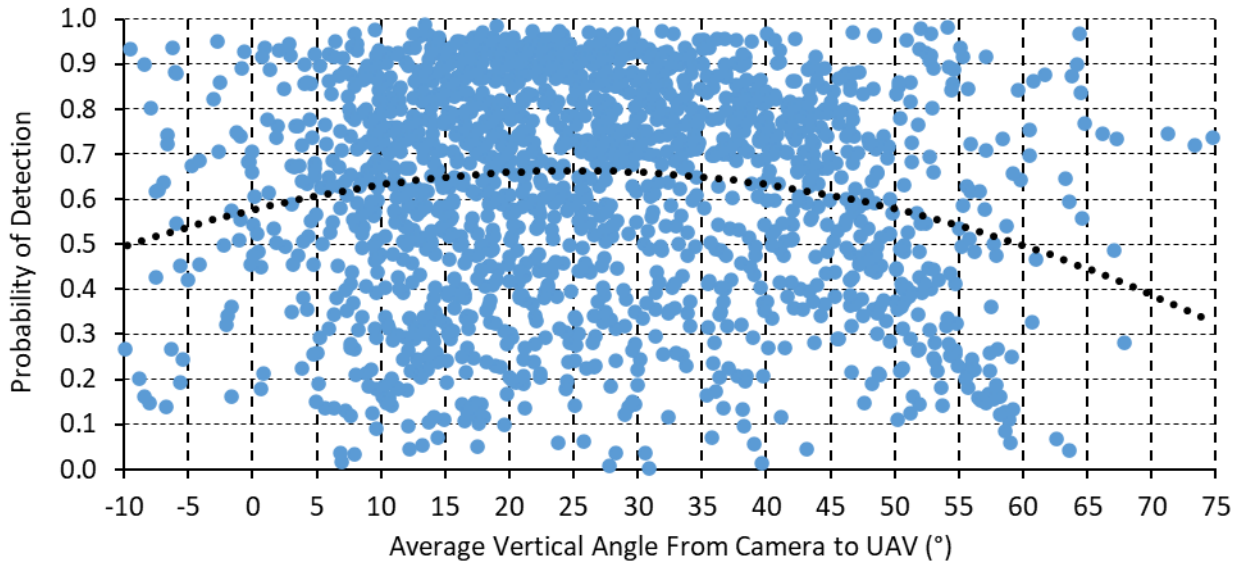


Figure 8. Modeled Second-Order Relationship Between Predicted DTBird Detection Probabilities for Individual UAV Flight Transects and the Average Vertical Angle from the DTBird Camera.

Based on the model output and the range of flights considered in formulating that model, the overall average probability of detecting an eagle-like UAV at the two study sites was  $63 \pm 1.1\%$  (95% CI). However, as the basis for the predictive model, we included a broad range of flights with LoS Distances extending out as far as 380 meters, including DTBird detection distances of up to 375 meters. The intent was to maximize good model fit by including useful data that extended spatially beyond the focal, calibrated maximum detection distance of 240 meters. For the purpose of comparing the estimated overall probability of detection (or conversely false negatives) against the performance standard established for this project (63%), a fairer metric is the probability of detecting an eagle-like UAV that flies within 240 meters or less of the cameras. Based on model output and this restriction, the relevant detection probabilities were  $66 \pm 1.3\%$  (95% CI) at Manzana,  $64 \pm 1.9\%$  at Goodnoe Hills, and  $65 \pm 1.1\%$  overall. Note that these indicators suggest that the probability of detection was slightly higher at the Manzana site, whereas the modeled full dataset suggested the opposite (Table 1), emphasizing that any difference between the two sites was at best marginal.

Flipped about to focus on false negatives, these results suggest that the probability of DTBird missing a detectable flight was overall <20% when the LoS Distance to the flight was between approximately 30–120 meters, <30% at distances of <20 meters and between 120–160 meters from the cameras, and exceeded 50% only beyond 200 meters. Otherwise, flights were missed more often at the Goodnoe Hills, during morning light, and at both low and high detection angles.

#### 4.4.1.2 Factors Influencing DTBird Detection and Deterrent-Triggering Response Distances

The flight trials conducted at the Manzana study site in 2017 occurred at all seven DTBird installations between 06:45 and 16:45 H Pacific Standard Time (PST) on 2 days in mid-January, 3 days in late February and early March, and 5 days in August (Table 2). The January and February/March flights involved an initial, custom-built aircraft (AES Custom; Figure 5A) flown by our first pilot, but unfortunately that aircraft crashed and was damaged beyond repair during the March flights. The August flights then involved a different pilot and custom-built aircraft (AUV Custom; Figure 5B). The Manzana missions resulted in a total of 1,279 usable, distinct flight segments (Table 2).

Table 22. Summary of UAV Flight Trials Conducted at the Manzana Wind Project Site in California that Contributed Data for Analysis.

Date	Sample Period (PST)	Turbine	Aircraft <sup>1</sup>	Missions Flown	Yield of Transect Samples
17-Jan-2017	08:15-11:40	V17	AES Custom	3	55
	13:05-16:45	E11	<b>AES Custom</b>	4	73
18-Jan-2017	08:45-12:05	D4	AES Custom	4	69
	13:15-14:25 <sup>2</sup>	D8	<b>AES Custom</b>	2	32
21-Feb-2017	07:55-12:05	U7	AES Custom	6	94
	13:15-13:50 <sup>2</sup>	D1	AES Custom	1	18
28-Feb-2017	10:45-15:45	T13	<b>AES Custom</b>	6	105
01-Mar-2017	08:35-10:10 <sup>3</sup>	E11	AES Custom	2	31
07-Aug-2017	07:35-13:55	V17	AUV Custom	8	146

08-Aug-2017	07:05-13:05	D8	AUV Custom	7	139
	13:55-15:50	U7	AUV Custom	2	37
09-Aug-2017	07:05-11:30	D4	AUV Custom	6	122
	12:35-13:15 <sup>3</sup>	U7	AUV Custom	1	16
10-Aug-2017	06:45-12:10	D1	AUV Custom	8	126
	13:00-15:00	T13	AUV Custom	3	49
11-Aug-2017	06:35-08:40	U7	AUV Custom	3	74
	09:25-12:25	E11	AUV Custom	5	93
			Totals	71	1,279

See Figure 5 for pictures of the aircraft.

At the Goodnoe Hills study site, the flight trials conducted in 2021 occurred at three turbines on two consecutive days in early August, involved a new pilot and mixed use of two UAVs (Clouds [Figure 5C] and Believer [Figure 5D]), and resulted in 210 flight samples suited to analysis (Table 3). Unfortunately, this flight trial session was terminated prematurely when both aircraft suffered fatal crashes. We also attempted an initial round of flight trials at this site in May 2021, but we were generally unable to proceed due to wind speeds that were incompatible with conducting flight trials with light-bodied UAVs. The flight trials conducted in 2022 then occurred at four turbines on four days in late July. They involved another piloting team and limited use of another Clouds aircraft, but primarily a new Ranger aircraft (Figure 5E), and resulted in 272 flight samples suited to analysis. We also conducted another apparently successful series of eight flights at turbine G51 during the trial session in July 2022, only to find out later that a DTBird hardware mismatch issue resulted in no recordings of those flights. Thus, our sampling at this site fell short of expectations, which we could not overcome due to budget limitations.

Table 33. Summary of UAV flight trials conducted at the Goodnoe Hills Wind Farm study site in Washington that contributed data for analysis.

Date	Sample Period (PST)	Turbine	Aircraft <sup>1</sup>	Missions Flown	Yield of Transect Samples
02-Aug-2021	07:42-08:46	G58	Believer	2	38
	11:05-13:04	G58	Clouds	2	67
	17:43-20:33	G34	Clouds	3	71
03-Aug-2021	08:34-09:292	G44	Believer	2	34
25-Jul-2022	11:57-12:10 <sup>2</sup>	G34	Clouds	1	10
26-Jul-2022	09:59-15:55	G64	Ranger	4	54
27-Jul-2022	08:15-15:41	G75	Ranger	7	111
29-Jul-2022	07:49-13:40	G44	Ranger	8	97
			Totals	29	482

See Figure 5 for pictures of the aircraft.

<sup>&</sup>lt;sup>2</sup> Aborted prematurely because of excessive wind or inclement weather.

<sup>&</sup>lt;sup>3</sup> Aborted prematurely because of UAV operational failure.

<sup>&</sup>lt;sup>2</sup> Aborted prematurely because of UAV operational failure.

The evaluation results for the initial full model and other models considered as part of the backward selection process used to identify the best model are portrayed in Attachment 5: Appendix B. The final, selected model had the following form:

LoS Response Distance ~ (1 | Site : Turbine ID) + (1 | Site : UAV Model) + Site + Event Type + Sky Backdrop + Ground Speed + Wind Speed + Roll Angle + Pitch Angle + Roll Angle \* Pitch Angle

A model with only the random effects included (AICc = 20010.06) reduced the AICc score by a substantial 223.48 points compared to the null model (AICc = 20233.54), and the selected model (AICc = 19918.34) reduced the AICc score by another substantial 91.2 points (315.2 total points compared to the null model). These results confirm noteworthy improvements in balancing parsimony and explanatory power (Burnham and Anderson 2010). The selected model also reduced the AICc score by 70.9 points compared to the full model (AICc = 19989.19), further reflecting a markedly improved model. However, the Nakagawa marginal pseudo-R² for the model (0.092) was low (Nakagawa and Shielzeth 2013), indicating that the included fixed effects provided only marginal explanatory power and a lot of variability in the dataset remained unexplained.

Diagnostics indicated that the final model satisfied the important assumptions of independence, normally distributed residuals, and the absence of significant collinearity among the predictors. However, Levene Tests for homogeneity of variances across groups within categorical variables (Zuur et al. 2009, Hartig 2021) confirmed modest deviations from ideal for *Site* and *Event Type*, but not for *Sky Backdrop*. These results suggest that the assumption of homogenous variances within groups was not completely met. Nevertheless, by incorporating random effects in the model, GLMMs estimate the variance components for the random effects, capturing the variability between groups and within groups. This flexibility in modeling allows for the accommodation of heteroscedasticity and helps to mitigate the impact of violations of the assumption of homogeneity of residual variances. Additionally, GLMMs can provide accurate parameter estimates and valid statistical inference even in the presence of heteroscedasticity; the mixed-effects structure helps to account for the correlation structure within the data, which reduces bias and provides robust standard errors for hypothesis testing (Zuur et al. 2009).

Output for the selected model indicated that including *Site*: *Turbine ID* as a random effect accounted for modest variation among turbines in modeled response distances (Figure 9). Specifically, the modeling results suggested that response distances were more variable among the seven Manzana turbines than among the five Goodnoe Hills turbines. Among the seven Manzana turbines, response distances were approximately 8.9 m shorter than the estimated global average at one turbine (V17), 7.7 m longer than average at one turbine (T13), and values for the other five turbines ranged from -0.9 m shorter to 1.7 m longer than the grand average. In comparison, the range of variation among the five Goodnoe Hills turbines was from 4.5 m shorter to 3.9 m longer than average, and values for the other three turbines ranged from -1.1 m shorter to 2.4 m longer than average. Although noteworthy but not particularly substantial

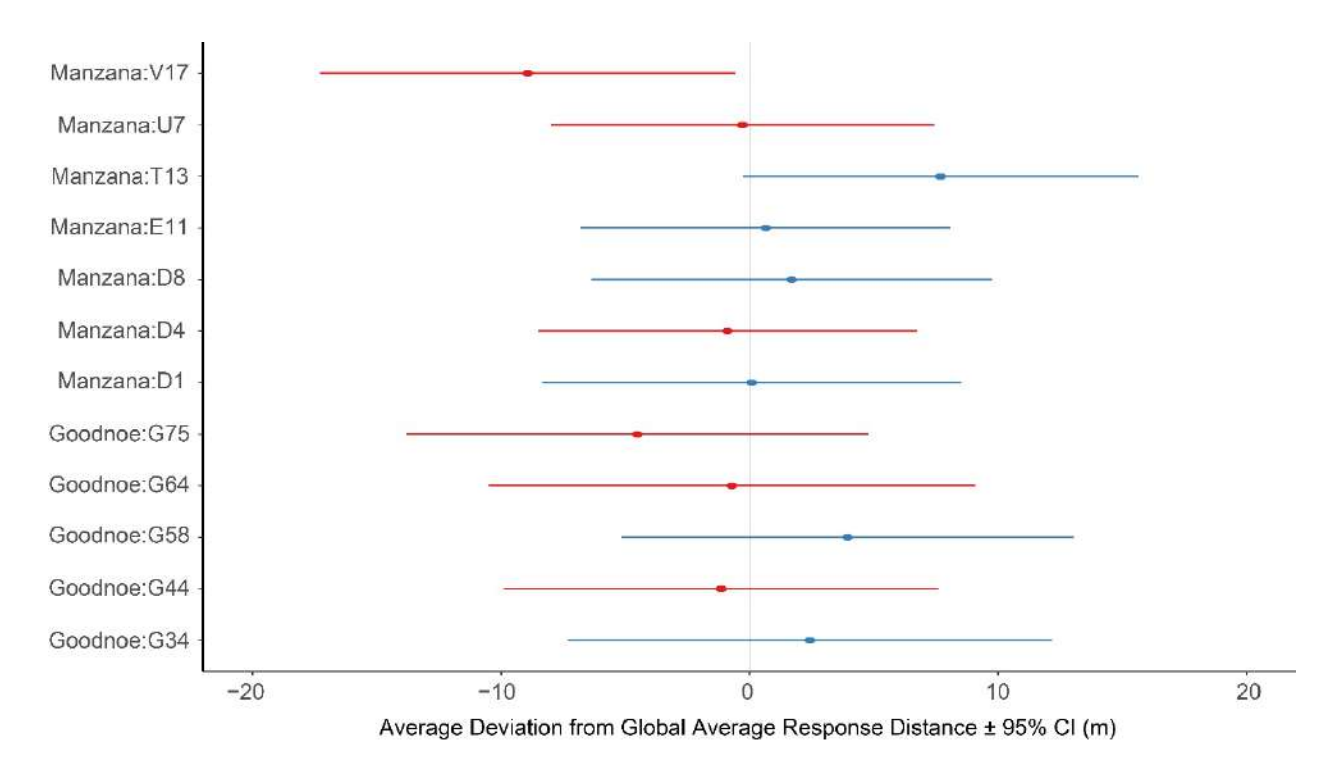


Figure 9. Deviations from the estimated global average DTBird response distance associated with different site-specific turbine installations, estimated as a nested random effect in the multi-site GLMM developed for the study.

differences, these apparent turbine-level variations likely reflect situation-specific landscape variation leading to modest variability in DTBird's ability to detect and target objects of interest.

Output for the selected model indicated that including *Site*: *UAV Model* as a random effect also captured noteworthy variation in the global average response levels attributable to the different UAV models used (Figure 10). The two UAV models used at the Manzana site showed the greatest variance in response distances: approximately 15.0 m shorter than the estimated global average across UAV types for the AUV Custom aircraft (with a skinny tubular hind body and more variable coloration; Figure 5A) and 15.0 m longer than average for the AES Custom aircraft (overall a more eagle-like torso and darker coloration; Figure 5B). At the Goodnoe Hills, variation among the three UAV models was less pronounced, ranging from an estimated 5.1 m shorter than average for the Believer aircraft (a relatively heavy, dark, and fast-flying aircraft; no picture available), 4.2 m longer than average for the Clouds aircraft (a relatively large and robust body and intermediate coloration; Figure 5D), and a nominal 0.9 m longer than average for the Ranger aircraft (longest wing span, but relatively narrow features and intermediate coloration; Figure 5C).

The coefficients and associated parameter tests for the fixed effects retained in the selected model are provided in Table 4. The selected model suggested that the retained fixed-effect predictors influenced the DTBird LoS Response Distances as summarized below.

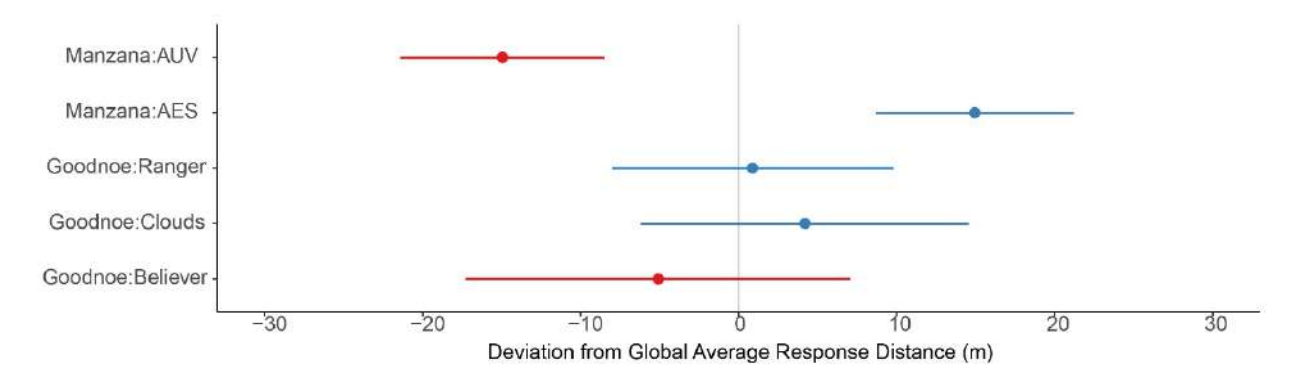


Figure 10. Deviation from the estimated global average DTBird response distance associated with site-specific use of different UAV models, estimated as a nested random effect in the multi-site GLMM developed for the study.

Table 44. Coefficients and parameter t-test results for fixed effects represented in the selected multi-site GLMM with DTBird response distance as the dependent variable.

Predictor	Coefficient	SE	df	t	P
(Intercept)	197.677	9.312	5.0	21.2	<0.0001
Site : Manzana <sup>1</sup>	-32.701	13.621	3.7	-2.4	0.0794
Event Type : Warning <sup>2</sup>	0.755	4.314	1798.7	0.2	0.8612
Event Type : Dissuasion <sup>2</sup>	-14.149	3.412	1793.9	-4.1	< 0.0001
Sky Backdrop : PartlyCloudy <sup>3</sup>	3.900	5.751	48.9	0.7	0.5008
Sky Backdrop : MostlyCloudy <sup>3</sup>	10.864	5.980	104.6	1.8	0.0721
Sky Backdrop : Overcast <sup>3</sup>	19.361	5.433	105.1	3.6	0.0006
Ground Speed	3.282	1.595	1744.8	2.1	0.0397
Wind Speed	3.229	1.657	1623.0	1.9	0.0515
Roll Angle	2.459	1.418	1798.4	1.7	0.0830
Pitch Angle	-0.719	1.429	1800.1	-0.5	0.6148
Roll Angle * Pitch Angle	-5.607	1.315	1796.0	-4.3	<0.0001

<sup>&</sup>lt;sup>1</sup> Reference category: Goodnoe Hills.

**Site:** The coefficient and parameter test for this fixed effect suggested that response distances averaged marginally shorter overall at the Manzana site than at the Goodnoe Hills site, and the post-hoc comparison of estimated means and variances illustrated that difference, but confirmed that it was not significant at  $P \le 0.05$  (Figure 11).

<sup>&</sup>lt;sup>2</sup> Reference category: Detection event.

<sup>&</sup>lt;sup>3</sup> Reference category: Fair skies.

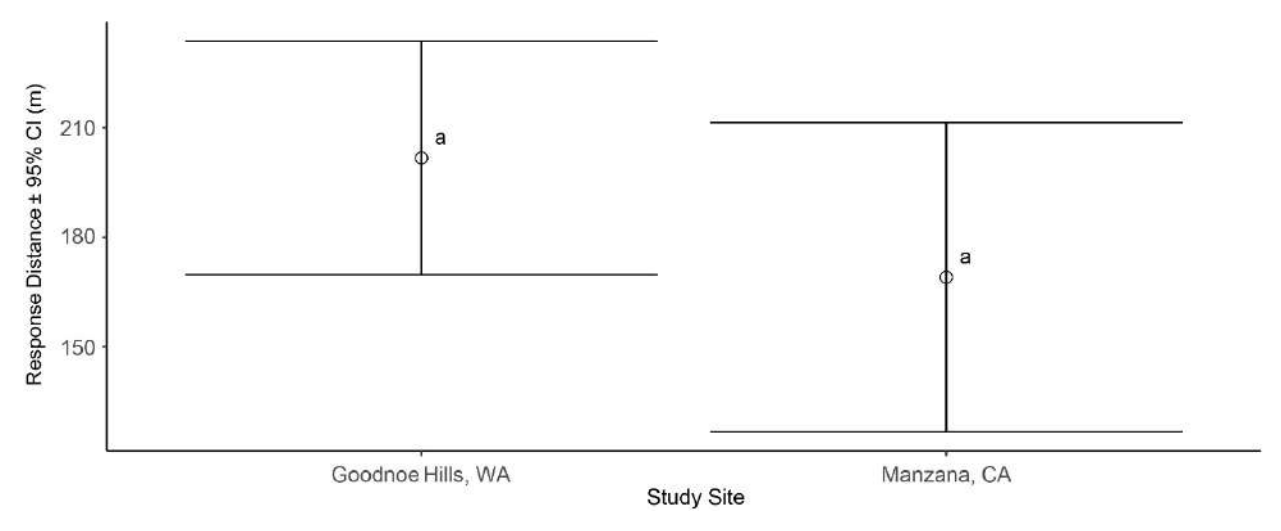


Figure 11. Modeled relationship between DTBird response distances and study site, with shared letters indicating pairwise differences that are not significant at  $P \le 0.05$ .

Event Type: Including Event Type as a fixed effect accounted for the significant "structural" (i.e., a system calibration/programming feature) difference in expected trigger distances for dissuasion signals compared to initial detections and warning signals (Figure 12). Calibrated for this study, initial detections were expected to occur at 240 m from the cameras throughout the projected detection envelope, while warning signals were also to be triggered at 240 m throughout the core envelope and at 170 m across lower, outer reaches of the detection envelope (see Figure 4 and H. T. Harvey & Associates 2018 for graphical illustrations). In contrast, dissuasion signals were expected to trigger at 170 m from the cameras throughout most of the expected detection envelope, and at 100 m across lower, outer reaches of the detection envelope. In contrast, the marginal means produced from the model for this parameter reflected the difference in average response distances for dissuasion signals (175.7) ± 7.34 m [SE]) and the comparatively minimal difference between the average response distances for initial detections (189.9 ± 7.00 m) and warning signals (190.61 ± 7.72 m). Also note, however, that the range of observed values for all three Event Types was wide (Figure 12). In addition, although the dissuasion-trigger response distances averaged close to the calibrated core-envelope trigger distance of 170 m, the averages for detections and warning signal triggers were notably shorter than the expected 240 m core-envelope trigger distances for those events.

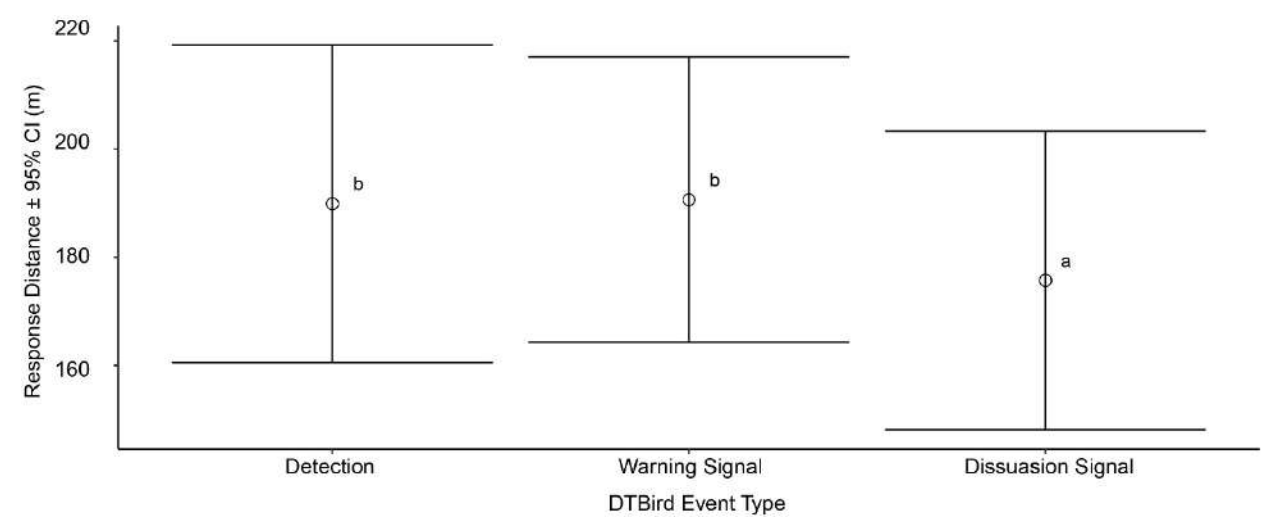


Figure 13. Modeled relationship between DTBird response distances and detection and deterrent-triggering event types, with shared letters indicating pairwise differences that are not significant at  $P \le 0.05$ .

Sky Backdrop: Response distances and cloud cover were positively correlated, with the average response distance increasing with the progression from fair to overcast skies (Figure 13). Parameter tests and post-hoc comparisons of estimated marginal means confirmed that response distances averaged a significant 19.4 m shorter under fair skies (defined as few if any small clouds in the sky) than under overcast skies (defined as complete or near-complete, dense cloud cover with little to no penetration of blue sky or large sunspots), with the average responses under partly cloudy (defined as more than a few small clouds but <50% cloud cover) and mostly cloudy skies (≥50% up to near-complete cloud cover but with distinct patches of

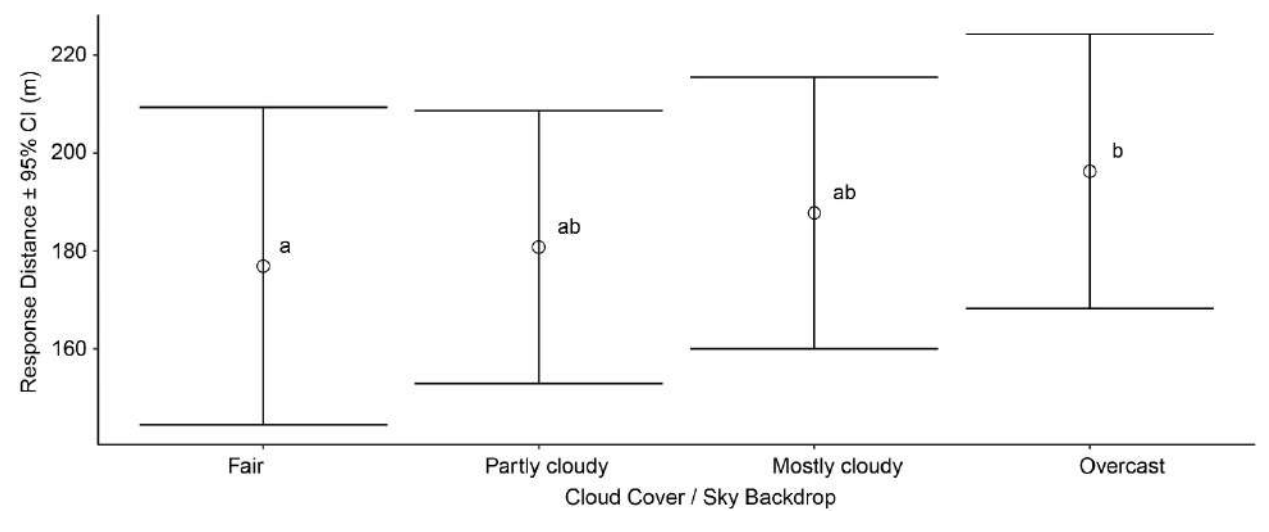


Figure 12. Modeled relationship between DTBird detection and deterrent-triggering response distances and sky backdrop / cloud cover categories, with shared letters indicating pairwise differences that are not significant at  $P \le 0.05$ .

blue and/or brighter clouds) intermediate in the progression and not significantly different from other categories.

**Ground Speed:** Response distances tended to increase as the rate of UAV travel relative to fixed points on the ground increased (Figure 14).

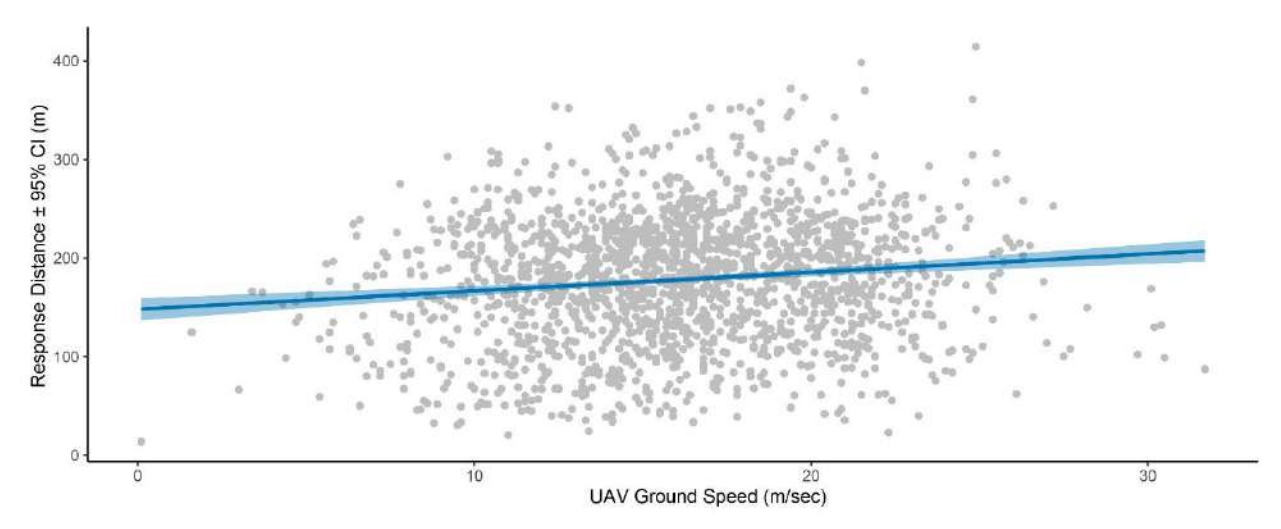


Figure 14. Modeled relationship (±95% confidence interval) between DTBird detection and deterrent-triggering response distances and UAV ground speed, or rate of travel relative to a fixed point on the ground, as measured by UAV avionics during sampling flights.

**Wind Speed:** Response distances tended to increase as the wind speed—measured in flight by the UAV avionics—increased (Figure 15).

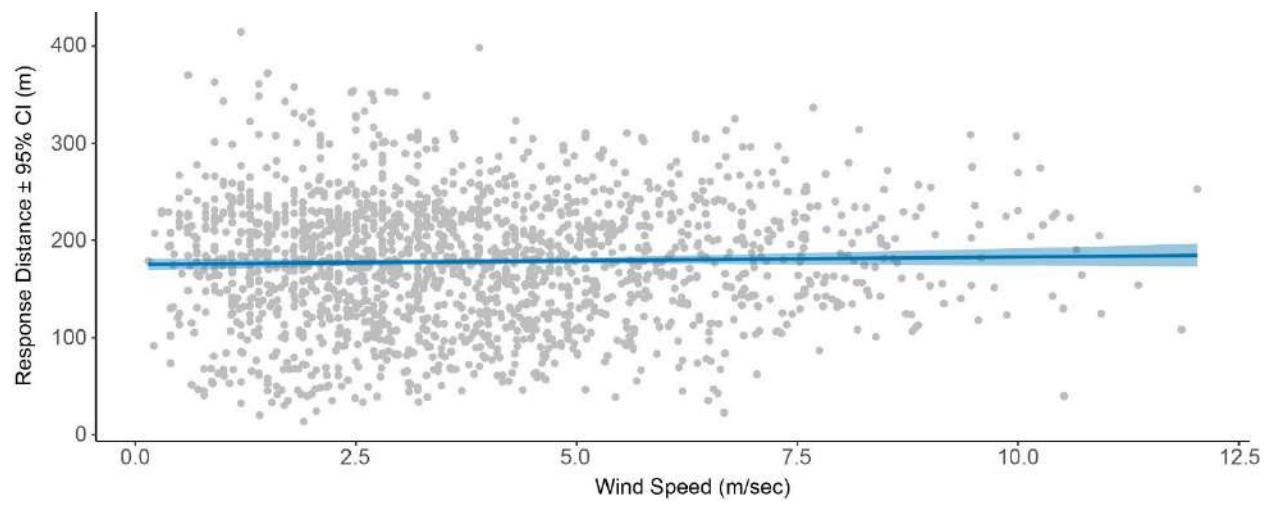


Figure 15. Modeled relationship between DTBird detection and deterrent-triggering response distances and wind speed as measured by UAV avionics during sampling flights.

Roll Angle: Pitch Angle Interaction: The degree to which a UAV rolled to one side or the other or pitched up or down while in flight influenced DTBird response distances in an interactive manner (Figure 16). Roll Angle was shown to be the strongest predictor of the two variables (Table 4), with observed values ranging from approximately -59° (left roll) to +41° (right roll). The interactive influence of Pitch Angle (observed values from -20° pitched down to +36° pitched up) reflected that pitching and rolling often acted in concert to increase exposure of the UAV profile to the cameras, but concurrent maximization of both metrics was effectively impractical.

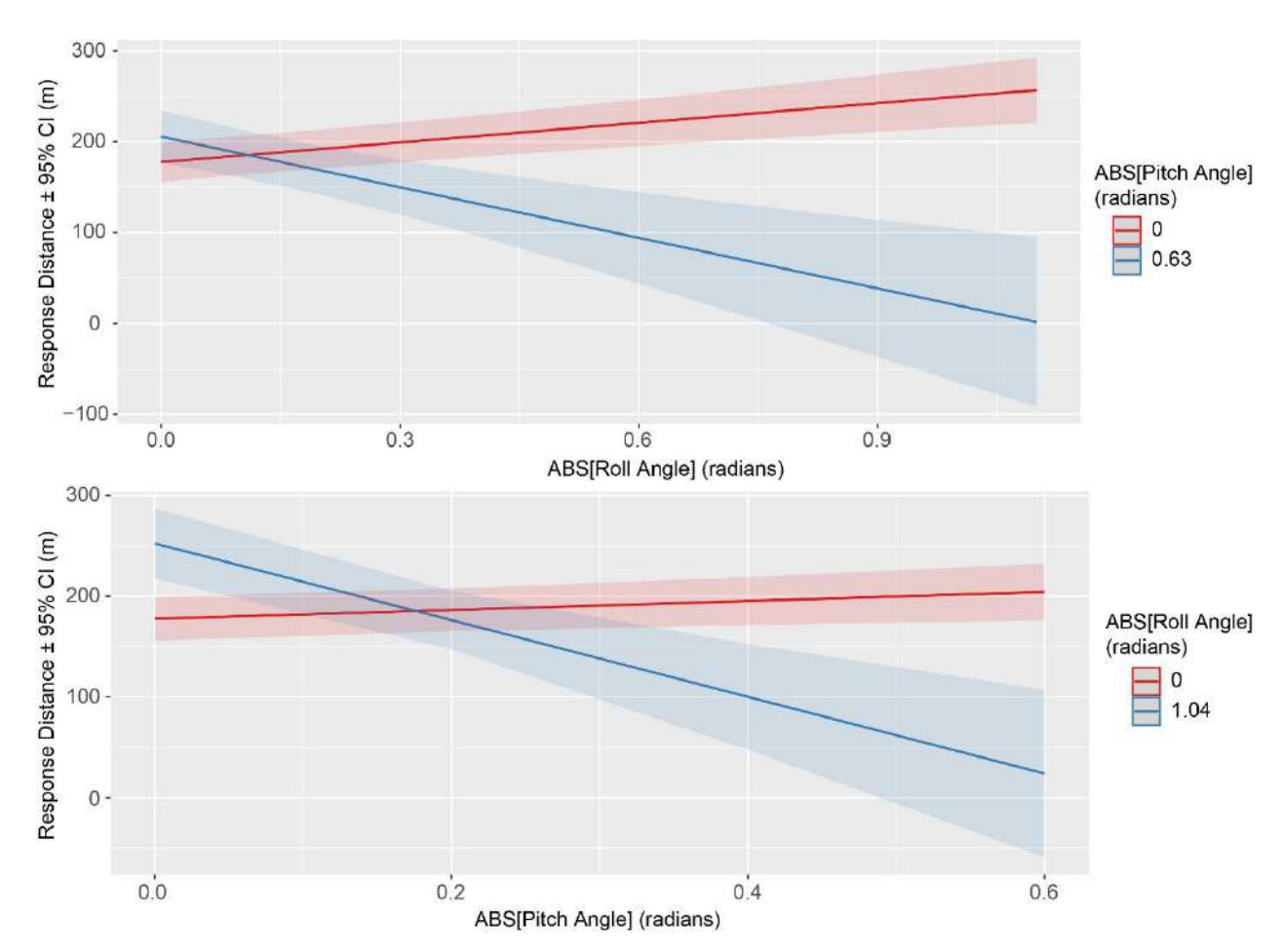


Figure 16. Modeled relationships between DTBird detection and deterrent-triggering response distances and the interactive influence of UAV pitch and roll angles.

More specifically, graphical illustrations of this interactive relationship indicated the following:

- With a low *Pitch Angle* (i.e., aircraft flying near nose-to-tail level), the more the UAV rolled from side to side (e.g., bouncing around in the wind or banking in a turn), the more the response distance increased.
- With a low *Roll Angle* (i.e., aircraft flying with wings near level), greater *Pitch Angles* also tended to increase response distances to a lesser degree.

Combinations of moderate pitch and roll angles were associated with moderate to
moderately high response distances, but concurrent maximization of both stability
metrics was effectively impractical, because it would translate to the aircraft stalling and
falling out of the sky. Hence, the indications in Figure 16 that as one stability metric
increased, the other generally declined, and vice versa, which was largely a result of the
automated avionics programming explicitly striving to avoid stalling the aircraft.

## 4.5.2 In Situ Behavioral Responses of Eagles and Raptors (Objective 2)

Table 5 summarizes the classified large-raptor deterrence events from the two study sites that we analyzed for this assessment.

Table 55. DTBird events recorded from January through August 2017 at the Manzana Wind Power Project in California and from September 2021 through August 2022 at the Goodnoe Hills Wind Farm in Washington, which formed the basis for assessing the behavioral responses of eagles and other large raptors to DTBird audio deterrents.

	Manzana	Goodnoe	e Hills	
Species <sup>1</sup>	Deterrents Broadcasting	Deterrents Broadcasting	Deterrents Muted	Total
Golden Eagle	80	33	45	158
Bald Eagle	1	14	25	40
Unknown Eagle	0	11	9	20
Turkey Vulture	21	52	54	127
Buteo <sup>2</sup>	122	52	55	229
Golden Eagle or Vulture	39	7	3	49
Golden Eagle or Buteo	7	3	6	16
Unknown Eagle/Vulture	11	34	49	94
Unknown Eagle/Buteo	0	16	22	38
Total	281	222	268	771

Classifications represent all cases where we either confirmed or strongly suspected ("probable") involvement of the relevant species or species group.

#### 4.5.2.1 Evaluating Differences in Behavioral Responses Between Sites

Given many cases where we could not confidently classify the species of raptor detected and tracked by the DTBird systems, we began our assessment by examining the deterrent response patterns reflected in all 503 of the selected cases involving large raptors exposed to broadcasted deterrents at the two study sites (Table 5). Overall, we classified 73% of the Manzana cases and 63% of the Goodnoe Hills cases as either confirmed or potentially effective responses (Table 6). The chi-square analysis of this dataset indicated a marginally significant difference (0.05 <  $P \le 0.10$ ) in the response patterns at the two sites ( $\chi^2 = 5.59$ , df = 2, P = 0.061). Post-hoc comparisons further indicated that the higher proportion of *Confirmed effective* responses approached significance only at the Manzana site (P = 0.076), the proportion of *Potentially effective* responses did not differ at the two sites (P = 0.683), and the proportion of *Ineffective* (P = 0.023 falls

<sup>&</sup>lt;sup>2</sup> Primarily red-tailed hawks year-round at both sites and rough-legged hawks during winter at the Goodnoe Hills.

below the Bonferroni-corrected significance threshold for maintaining an overall Type II error rate of  $\leq 0.10$ ).

Table 66. Classification of the effectiveness of behavioral responses (combined responses to warning and dissuasion signals acting alone or in tandem) in reducing collision risk for all large raptors combined (eagles, vultures, and buteos) at the Manzana Wind Power Project in California and the Goodnoe Hills Wind Farm in Washington.

Classified	Manzar	ıa	Goodnoe Hills		
Response	Number of Cases	%	Number of Cases	%	
Confirmed Effective (CE)	118	42.0	76	34.2	
Potentially Effective (PE)	87	31.0	69	29.3	
Not Effective (N)	13	4.6	17	7.2	
No Response $(Z)$	63	22.4	60	29.3	
Total	281	_	222	-	

Note: test of independence with N + Z lumped:  $\chi$ 2 = 5.59, df = 2, P = 0.061—indicating the overall pattern of responses was marginally different at the two sites. Bonferroni-corrected post-hoc comparisons confirmed a marginally higher proportion of Potentially effective responses and a marginally lower proportion of Ineffective (N+Z) responses at the Manzana site.

Focused on confirmed/probable golden eagles, the proportion of confirmed/potentially effective responses was again higher at the Manzana site (79%) compared to the Goodnoe Hills (60%) (Table 7), and the overall chi-square analysis again indicated that the pattern of variation among the *Response* classifications was at least marginally different at the two sites ( $\chi^2$  = 5.84, df = 2, P = 0.054). Post-hoc comparisons further indicated that the proportion of *Confirmed* effective responses was marginally higher at the Manzana site (P = 0.027), the proportion of *Potentially effective* responses did not differ at the two sites (P = 0.629), and the higher proportion of *Ineffective* responses at the Goodnoe Hills approached significance (P = 0.047).

Table 77. Classification of the effectiveness of behavioral responses (combined responses to warning and dissuasion signals acting alone or in tandem) in reducing collision risk for confirmed and probable golden eagles at the Manzana Wind Power Project in California and the Goodnoe Hills Wind Farm in Washington.

	<b>9</b>				
Classified	Manzar	na	Goodnoe Hills		
Response	Number of Cases	%	Number of Cases	%	
Confirmed Effective (CE)	40	50.0	9	27.3	
Potentially Effective (PE)	23	28.8	11	33.3	
Not Effective (N)	3	3.7	5	15.2	
No Response $(Z)$	14	17.5	8	24.2	
Total	80	_	33	_	

Note: chi-square test of independence with N+Z lumped:  $\chi^2 = 5.84$ , df = 2, P=0.054—indicating the overall pattern of responses was marginally different at the two sites. Bonferroni-corrected post-hoc comparisons confirmed a marginally higher proportion of Confirmed effective responses and a marginally lower proportion of Ineffective (N+Z) responses at the Manzana site.

For confirmed/probable turkey vultures, the proportion of confirmed/potentially effective responses was again higher at the Manzana site (81%) compared to the Goodnoe Hills site (61%) (Table 8), and the overall chi-square analysis indicated that the pattern of variation among the *Response* classifications differed at the two sites ( $\chi^2$  = 6.20, df = 2, P = 0.045). Post-hoc comparisons further indicated that the proportion of *Confirmed effective* responses was higher at the Manzana site (P = 0.015), the proportion of *Potentially effective* responses did not differ at the two sites (P = 0.424), and the higher proportion of P responses at the Goodnoe Hills approached significance (P = 0.069).

Table 88. Classification of the effectiveness of behavioral responses (combined responses to warning and dissuasion signals acting alone or in tandem) in reducing collision risk for confirmed and probable turkey vultures at the Manzana Wind Power Project in California and the Goodnoe Hills Wind Farm in Washington.

Classified	Manzar	na	Goodnoe Hills		
Response	Number of Cases	%	Number of Cases	%	
Confirmed Effective (CE)	11	52.4	12	23.1	
Potentially Effective (PE)	6	28.6	20	38.4	
Not Effective (N)	0	0	4	7.7	
No Response $(Z)$	4	19.0	16	30.8	
Total	21	_	52	_	

Note: Chi-square test of independence with N + Z lumped:  $\chi 2 = 6.20$ , df = 2, P = 0.045—indicating that the overall pattern of responses differed at the two sites. Bonferroni-corrected post-hoc comparisons confirmed a higher proportion of Confirmed effective responses at the Manzana site.

For confirmed/probable buteos, the difference between the overall proportions of confirmed/potentially effective responses was again notably higher at the Manzana site (72%) than at the Goodnoe Hills (56%). The chi-square analysis confirmed a significant difference in pattern at the two sites ( $\chi^2$  = 6.31, df = 2, P = 0.043; Table 9). Post-hoc comparisons further indicated that the proportion of *Confirmed effective* responses did not differ at the two sites (P = 0.095), but the proportion of *Potentially effective* responses was marginally higher (P = 0.028) and the proportion of P responses was marginally lower (P = 0.035) at the Manzana site.

Table 99. Classification of the effectiveness of behavioral responses (combined responses to warning and dissuasion signals acting alone or in tandem) in reducing collision risk for confirmed and probable buteos at the Manzana Wind Power Project in California and the Goodnoe Hills Wind Farm in Washington.

Classified Response	Manzar	ıa	Goodnoe Hills		
	Number of Cases	%	Number of Cases	%	
Confirmed Effective (CE)	44	36.1	19	36.6	
Potentially Effective (PE)	44	36.0	10	19.2	
Not Effective (N)	8	6.6	5	9.6	
No Response (Z)	26	21.3	18	34.6	
Total	122	_	52	-	

Note: Chi-square test of proportions:  $\chi 2 = 6.31$ , df = 2, P = 0.042—indicating the overall pattern of responses differed at the two sites. Bonferroni-corrected post-hoc comparisons confirmed a marginally higher proportion of Potentially effective responses and a marginally lower proportion of Ineffective (N + Z) responses at the Manzana site.

In relation to collision *Risk*, the raw percentage results for the multi-species Manzana dataset suggested that the proportion of *Confirmed effective* responses to broadcasted deterrents increased from 36% to 49% as the classified level of pre-exposure risk increased from low to high, whereas the proportions of *Potentially effective* and *I* responses each decreased by seven percentage points with increasing exposure risk (Table 10). In contrast, the multi-species Goodnoe Hills dataset suggested that the proportions of both *Confirmed effective* and *Potentially effective* responses were highest and the proportion of *I* responses lowest for birds at moderate pre-exposure risk.

Table 1010. Classification of the effectiveness of behavioral responses to broadcasted DTBird audio deterrents (combined responses to warning and dissuasion signals acting alone or in tandem) in reducing collision risk for all large raptors combined by site and classified risk level before deterrent exposure at the Manzana Wind Power Project in California and the Goodnoe Hills Wind Farm in Washington.

-				Site / Ri	sk Level			
	Manzana				Goodnoe Hills			
Response	Low	Med	High	Total	Low	Med	High	Total
Confirmed Effective (CE)	42	58	18	118	28	39	9	76
Potentially Effective (PE)	40	37	10	87	27	31	7	65
Ineffective $(I = N + Z)$ )	36	31	9	76	40	29	12	81
Total Cases	118	126	37	281	95	99	28	222
% Confirmed Effective	36	46	49	42	29	39	32	34
% Potentially Effective	34	29	27	31	28	31	25	29
% Ineffective	31	25	24	27	42	29	43	36

The Response–Risk data for confirmed/probable golden eagles were sparse across many cells of the relevant 3 x 3 contingency tables for both sites, especially the Goodnoe Hills, which may limit the value of generated insight (Table 11). The Manzana data suggested that the proportions of Confirmed effective responses were higher for birds at high (50%) and especially moderate (58%) risk of exposure than for birds at low risk of exposure (40%), and the proportions of *I* responses were concomitantly lower for birds at moderate to high risk. In contrast, the Goodnoe Hills data showed a modest increasing trend in the proportions of Confirmed effective responses as risk increased (22–33%); however, among birds at moderate risk of exposure, the highest proportion (44%) exhibited relatively subtle Potentially effective responses, and the highest proportions of birds at both low (56%) and high (50%) risk of exposure exhibited no effective responses.

Table 1111. Classification of the effectiveness of behavioral responses to broadcasted DTBird audio deterrents (combined responses to warning and dissuasion signals acting alone or in tandem) in reducing collision risk for confirmed and probable golden eagles by site and classified risk level before deterrent exposure at the Manzana Wind Power Project in California and the Goodnoe Hills Wind Farm in Washington.

				Site / Ri	sk Level			
	Manzana				Goodnoe Hills			
Response	Low	Med	High	Total	Low	Med	High	Total
Confirmed Effective (CE)	12	21	7	40	2	5	2	9
Potentially Effective (PE)	8	11	4	23	2	8	1	11
Ineffective $(I = N + Z)$	10	4	3	17	5	5	3	13
Total Cases	30	36	14	80	9	18	6	33
% Confirmed Effective	40	58	50	50	22	28	33	27
% Potentially Effective	27	31	29	29	22	44	17	33
% Ineffective	33	11	21	21	56	28	50	39

The Manzana sample sizes for confirmed/probable turkey vultures were sparse when broken out into a 3 x 3 Response–Risk table; however, the pattern of sparseness suggested that vultures at moderate to high risk of exposure exhibited a pronounced tendency to respond effectively, whereas birds at low risk of exposure were close to equally likely to exhibit any one

of the three responses (Table 12). In contrast, the Goodnoe Hills data suggested that *Confirmed effective* responses were least likely regardless of the pre-exposure risk level and were proportionately least common among birds at high risk, but no other consistent patterns were evident.

Table 1212. Classification of the effectiveness of behavioral responses to broadcasted DTBird audio deterrents (combined responses to warning and dissuasion signals acting alone or in tandem) in reducing collision risk for confirmed and probable turkey vultures by site and classified risk level before deterrent exposure at the Manzana Wind Power Project in California and the Goodnoe Hills Wind Farm in Washington.

				Site / Ri	sk Level			
	Manzana				Goodnoe Hills			
Response	Low	Med	High	Total	Low	Med	High	Total
Confirmed Effective (CE)	4	6	1	11	5	5	2	12
Potentially Effective (PE)	5	0	1	6	9	6	5	20
Ineffective $(I = N + Z)$	4	0	0	4	7	9	4	20
Total Cases	13	6	2	21	21	20	11	52
% Confirmed Effective	31	100	50	52	24	25	18	23
% Potentially Effective	38	0	50	29	43	30	45	38
% Ineffective	31	0	0	19	33	45	36	38

For confirmed/probable buteos, neither of the site-specific datasets exhibited distinctive trends in the response patterns in relation to pre-exposure risk levels (Table 13). At the Manzana site, overall variation across cells of the 3 x 3 Response–Risk table was not pronounced. The highest proportion of birds at high risk (44%) exhibited Confirmed effective responses, whereas marginally highest proportions of the birds at low (40%) and moderate (36%) risk exhibited Potentially effective responses. At the Goodnoe Hills, the proportions of I responses were notably highest for birds at both low and high risk, whereas the proportion of Confirmed effective responses was notably highest for birds at moderate risk.

Table 1313. Classification of the effectiveness of behavioral responses to broadcasted DTBird audio deterrents (combined responses to warning and dissuasion signals acting alone or in tandem) in reducing collision risk for confirmed and probable buteos by site and classified risk level before deterrent exposure at the Manzana Wind Power Project in California and the Goodnoe Hills Wind Farm in Washington.

				Site / Ri	sk Level			
	Manzana				Goodnoe Hills			
Response	Low	Med	High	Total	Low	Med	High	Total
Confirmed Effective (CE)	15	21	8	44	8	9	2	19
Potentially Effective (PE)	17	22	5	44	2	7	1	10
Ineffective $(I = N + Z)$ )	11	18	5	34	16	4	3	23
Total Cases	43	61	18	122	26	20	6	52
% Confirmed Effective	35	34	44	36	31	45	33	37
% Potentially Effective	40	36	28	36	8	35	17	19
% Ineffective	26	30	28	28	62	20	50	44

The performance standard of ≥50% successful or effective deterrence for golden eagles established based on the initial Manzana pilot study (H. T. Harvey & Associates 2018) was

further corroborated for that site by the initial 53% estimate derived from the subsequent expansion of that site-specific assessment to include a full year of data. Further minor adjustments to the relevant dataset in preparation for the multi-site evaluation presented herein modified that estimate to 50% *Confirmed effective* responses, with another 29% *Potentially effective* responses, yielding a total estimated probable effectiveness of 79% for golden eagles (Table 14). In comparison, the Goodnoe Hills results indicated a lower 27% confirmed effective responses, falling well below the established performance standard; however, the combined estimate of 60% confirmed/probable effective responses, though still notably lower than at the Manzana site, did exceed the 50% performance threshold. Similar patterns were shown for vultures and the multi-species group, except that the proportion of effective responses for the multi-species group fell below the 50% threshold. In contrast, for buteos the proportions of effective responses did not differ at the two sites and were well below the 50% threshold (27–29%); however, the combined proportion of confirmed/probable effective responses was again notably higher at the Manzana site (72%) than at the Goodnoe Hills site (56%) (Table 14).

Table 1414. Percentages of behavioral responses to broadcasted DTBird deterrents (combined responses to warning and dissuasion signals acting alone or in tandem) classified as effective or potentially effective in reducing collision risk for different species groups at the Manzana Wind Power Project in California and the Goodnoe Hills Wind Farm in Washington.

Species Group	Manzana	Goodnoe Hills
Golden Eagles	50 / 79 <sup>1</sup>	27 / 60
Vultures	52 / 81	23 / 61
Buteos	36 / 72	37 / 56
All Groups Combined	42 / 73	34 / 63

First number = % of responses confirmed effective; second number = overall % of confirmed + potentially effective responses.

#### 4.5.2.2 Evaluating Factors Influencing Behavioral Responses to Deterrents

Given that the initial chi-square analyses pointed to at least marginally significant differences in the deterrence response patterns of golden eagles and other large raptors at the two study sites, we did not consider pursuing Objective C as outlined in the Introduction. Instead, we pursued the second element of Objective B, which entailed preparing LGLM analyses to provide further insight about potential drivers of the evident site-specific differences in the apparent sensitivity of raptors to the broadcasted deterrents.

<u>Multi-species Model:</u> The LGLM analysis based on the multi-species dataset resulted in the final model listed below (and see Table 15) and the interpretations that follow:

Log(Odds of effective deterrence) ~ Site + Species Group + Preexposure Risk + Wind Speed + Species Group \* Wind Speed

Diagnostics for this final model revealed no outliers and residuals consistent with adequate model fit.

Table 1515. Comparison of AIC scoring results for top candidates and selected other multispecies logistic GLMs portraying potential relationships between the probability of effective deterrence and various predictors.

Candidate Model <sup>1</sup>	AIC <sup>2</sup>	ΔΑΙC	McFadden's R <sup>2</sup>
Site + Species Group + Preexposure Risk + Wind Speed + Species Group : Wind Speed	465.52	0.00	0.055
Site + Species Group + Preexposure Risk + Wind Speed + Species Group : Wind Speed + Site : Wind Speed	466.44	0.92	0.057
Site + Species Group + Wind Speed + Species Group : Wind Speed	466.87	1.35	0.044
Site	469.29	3.77	0.018
Site + Species Group	470.37	4.85	0.024
Site + Species Group + Preexposure Risk + Wind Speed + Species Group : Preexposure Risk + Species Group : Wind Speed + Site : Wind Speed	470.53	5.01	0.066
Site + Wind Speed	471.16	5.64	0.018
Site + Species Group + Wind Speed	471.92	6.40	0.025
Species Group*Wind Speed	474.30	8.78	0.024
Null model	475.60	10.08	_
Site + Species Group + Preexposure Risk + Wind Speed +Species Group : Site + Species Group : Preexposure Risk + Species Group : Wind Speed +Site : Preexposure Risk + Site : Wind Speed	477.23	11.71	0.068
Site + Species Group + Preexposure Risk + Wind Speed +Species Group : Site + Species Group : Preexposure Risk + Species Group : Wind Speed + Site : Wind Speed	477.33	11.81	0.068
Site + Species Group + Preexposure Risk + Wind Speed +Species Group : Site + Species Group : Preexposure Risk + Species Group : Wind Speed + Site : Preexposure Risk + Site : Wind Speed + Preexposure Risk : Wind Speed	481.22	15.70	0.068

Site = Manzana or Goodnoe Hills wind facility. Species Group = eagle, vulture or buteo. Preexposure Risk (of approaching rotor swept area of spinning turbine prior to deterrent triggering) = low, moderate or high. Wind Speed measured at turbine in meters / second.

<sup>&</sup>lt;sup>2</sup> Akaike Information Criterion score.

Table 1616. Parameters of final multi-species logistic GLM selected to represent relationship between the ln(odds of effective deterrence) and various predictors at the Manzana and Goodnoe Hills wind-energy facilities.

Parameter <sup>1</sup>	Estimate	SE	Z	P
Intercept	0.6394	0.5112	1.251	0.211
Site-Manzana	0.7416	0.2439	3.041	0.002
Species Group-Eagle	-0.8740	0.5548	-1.575	0.115
Species Group-Vulture	-0.6512	0.6965	-0.935	0.350
Preexposure Risk-Low	-0.2023	0.3355	-0.603	0.547
Preexposure Risk-Moderate	0.3748	0.3395	1.104	0.270
Wind Speed	-0.0725	0.0508	-1.427	0.153
Species Group-Eagle : Wind Speed	0.2220	0.0858	2.587	0.010
Species Group-Vulture : Wind Speed	0.1562	0.0993	1.574	0.116

<sup>1</sup> Site reference category = Goodnoe Hills. Species Group reference category = buteo. Preexposure Risk reference category = high.

Site effect (P = 0.002; Table 16) reflected a higher average probability of effective deterrence at the Manzana site (Figure 17).

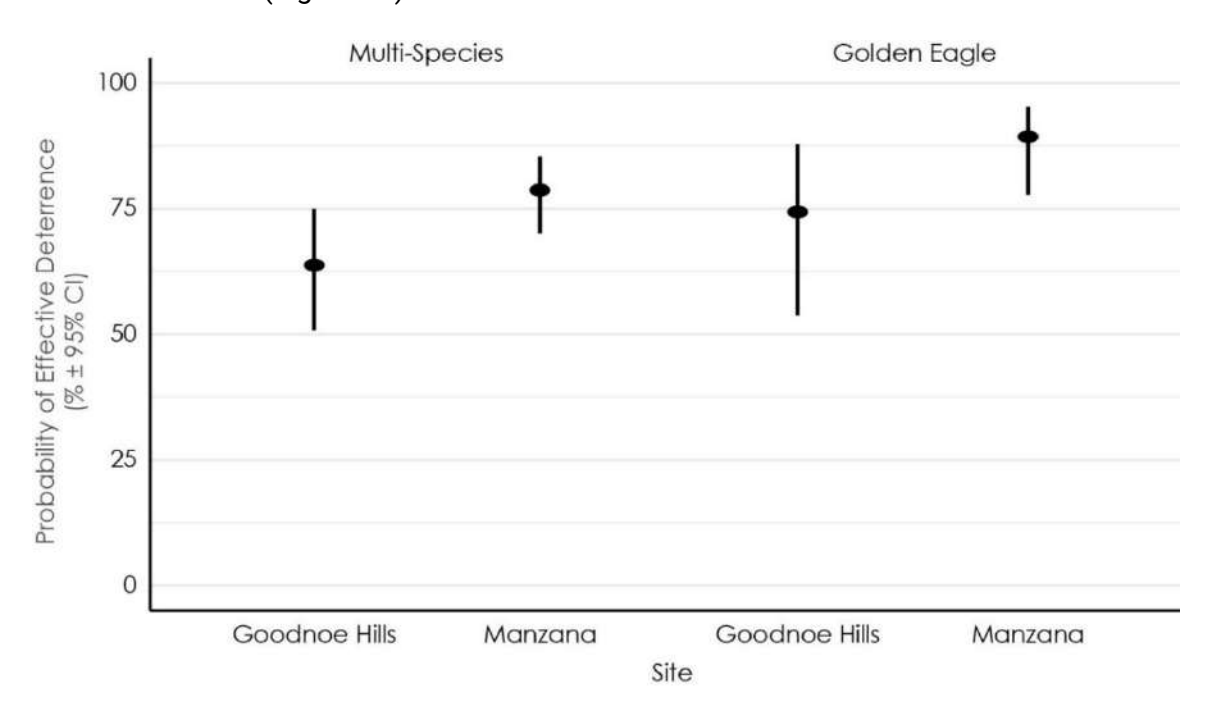


Figure 17. Modeled probability of effective DTBird deterrence for all large raptors combined and golden eagles alone at the two wind facilities evaluated in this study.

Preexposure Risk was only marginally significant (P = 0.069), but its inclusion reduced the AIC score by 1.35 points (Table 15). Birds facing moderate risk were the most likely to show effective deterrence responses, while birds facing low risk were the least likely to show effective responses; however, none of the pairwise differences were significant on their own, suggesting a gradient of variation rather than a discrete segregation of probability groups (Table 16, Table 20).

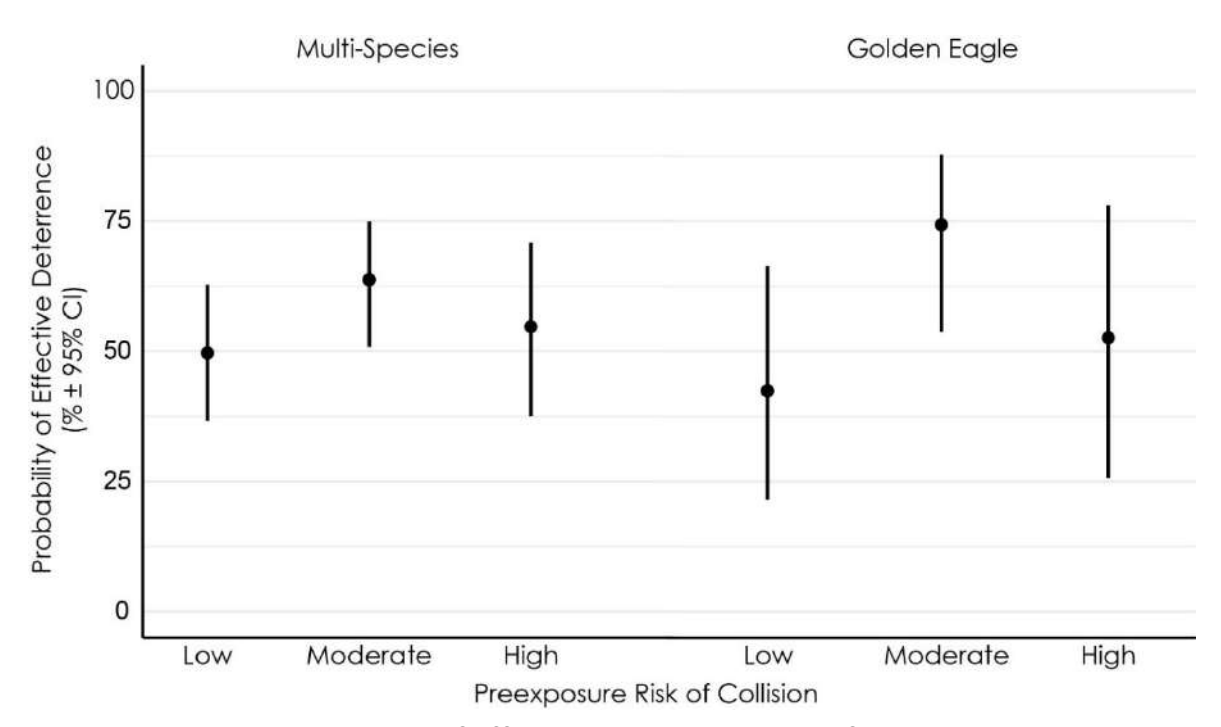


Figure 19. Modeled probability of effective DTBird deterrence for all large raptors combined and golden eagles alone in relation to classified risk of exposure to turbine collisions at the two wind facilities evaluated in this study.

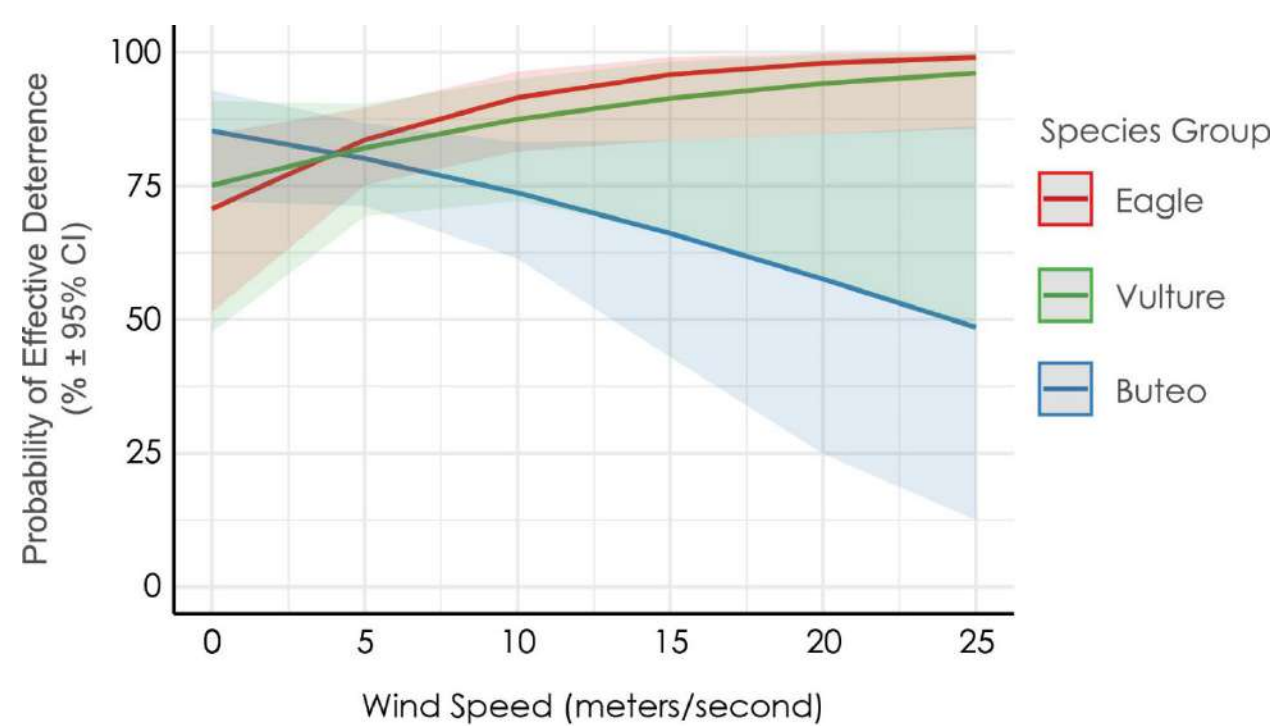


Figure 18. Modeled probability of effective DTBird deterrence for large raptors by species group and in relation to wind speed measured by turbine anemometer at time of events at the two wind facilities evaluated in this study.

Species Group and Wind Speed did not contribute significant main effects, but their 2-way

interaction was significant (P = 0.019). The Species Group \* Wind Speed interaction reflected the following (Table 16, Figure 19):

- At low wind speeds below approximately 4 meters/second (m/s) (just above the turbine cut-in speed of 3 m/s), the probability of effective deterrence was lowest for eagles, slightly higher for vultures, and slightly higher still for buteos, whereas wind speeds above 4 m/s resulted in the opposite pattern.
- At wind speeds above approximately 4 m/s, the probability of effective deterrence was:
  - o highest for eagles and increased strongly as wind speeds increased.
  - o second highest for vultures and increased moderately as wind speeds increased.
  - lowest for the smaller buteos and decreased moderately as wind speeds increased.

<u>Golden Eagle Model:</u> The LGLM analysis for golden eagles resulted in the final model listed below (and see Table 17) and the interpretations that follow:

Log(Odds of effective deterrence) ~ Site + Preexposure Risk + Wind Speed

Diagnostics for this final model revealed no influential outliers and residuals consistent with adequate model fit.

Site effect (P = 0.029; Table 18) reflected a higher average probability of effective deterrence at the Manzana site (Figure 17).

Preexposure Risk effect (P = 0.041) reflected that the probability of effective deterrence was highest for birds at moderate risk, moderate for birds at high risk, and significantly lowest for birds at low risk (Table 18, Figure 18).

Wind Speed was only marginally significant (P = 0.087; Table 18), but its inclusion reduced the AIC score by 1.2 pts (Table 17) and reflected a positive relationship with the probability of deterrence (Table 18, Figure 19).

Another model including the Site \* Wind Speed interaction scored lowest on the AIC scale, but improved the AIC score by only a nominal 0.45 points compared to the second-best model chosen as the final. Further, the parameter-test P value for the interaction (0.118) exceeded even the  $P \le 0.10$  threshold for marginal significance. Nevertheless, the suggested interactive relationship indicated a potentially interesting pattern, whereby (a) the probability of deterrence rose more quickly as wind speed increased at the Goodnoe Hills than at the Manzana site, and (b) as a consequence, was higher at the Manzana site at winds speeds below about 7 m/s, but was higher at the Goodnoe Hills at wind speeds greater than that (Figure 20).

Table 1717. Comparison of AIC scoring results for top candidates and selected other logistic GLMs portraying potential relationships for golden eagles between the ln(odds of effective deterrence) and various predictors.

Candidate Model <sup>1</sup>	AIC <sup>2</sup>	ΔΑΙC	McFadden's R <sup>2</sup>
Site + Preexposure Risk + Wind Speed + Site : Wind Speed	126.23	0.00	0.127
Site + Preexposure Risk + Wind Speed	126.68	0.45	0.108

Site + Preexposure Risk	127.90	1.67	0.083
Site + Wind Speed + Site : Wind Speed	128.64	2.41	0.078
Preexposure Risk + Wind Speed	129.47	3.24	0.071
Site + Preexposure Risk + Wind Speed + Site : Preexposure Risk + Site : Wind Speed	130.12	3.89	0.127
Site	131.01	4.78	0.029
Preexposure Risk	131.06	4.83	0.044
Wind Speed	131.92	5.69	0.022
Preexposure Risk + Wind Speed + Preexposure Risk : Wind Speed	132.51	6.28	0.079
Null model	132.51	6.28	-
Site + Preexposure Risk + Wind Speed + Site : Preexposure Risk + Site : Wind Speed + Preexposure Risk : Wind Speed	132.79	6.56	0.128

Site = Manzana or Goodnoe Hills wind facility. Species Group = eagle, vulture or buteo. Preexposure Risk (of approaching rotor swept area of spinning turbine prior to deterrent triggering) = low, moderate or high. Wind Speed measured at turbine in meters / second.

Table 1818. Parameters of final logistic GLM selected to represent relationship between the In (odds of effective deterrence) for golden eagles and various predictors at the Manzana and Goodnoe Hills wind-energy facilities.

Parameter <sup>1</sup>	Estimate	SE	Z	P
Intercept	-0.6933	0.7694	-0.901	0.3675
Site-Manzana	1.0615	0.4867	2.181	0.0292
Preexposure Risk-Low	-0.4103	0.6253	-0.656	0.5118
Preexposure Risk-Moderate	0.9581	0.6470	1.481	0.1386
Wind Speed	0.1612	0.0942	1.711	0.0870

<sup>&</sup>lt;sup>2</sup> Akaike Information Criterion score.

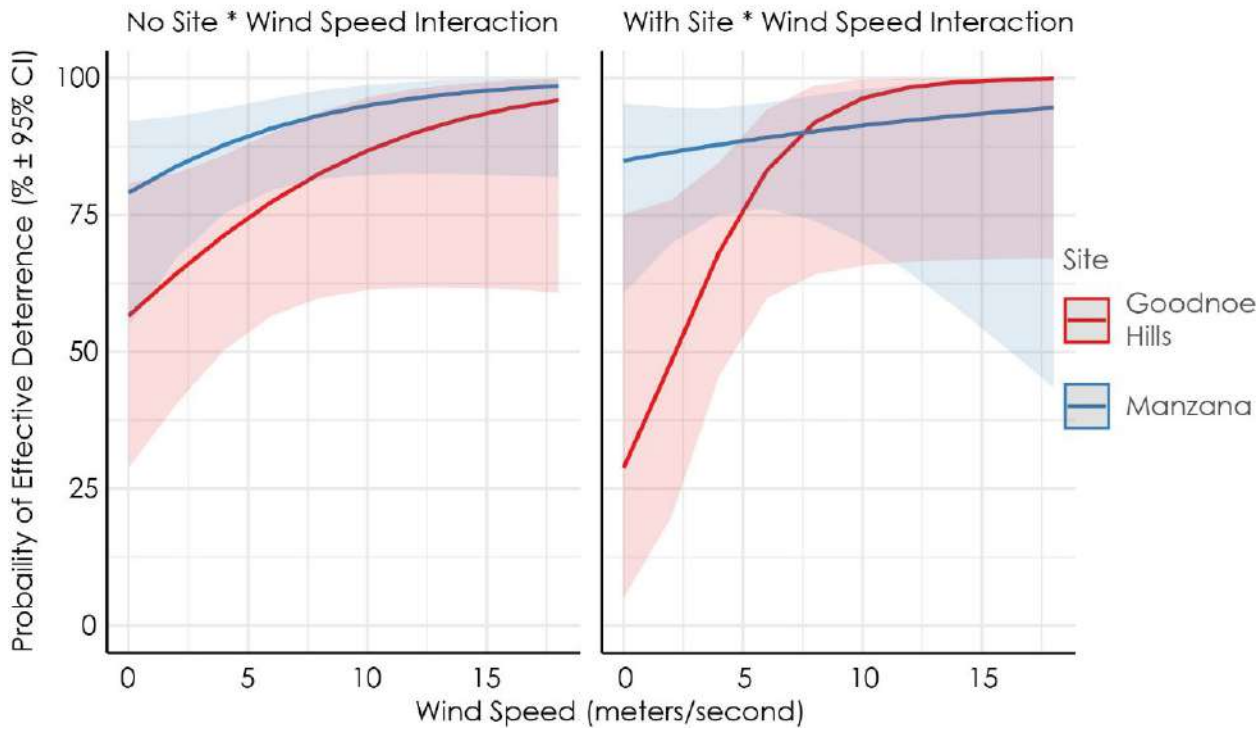


Figure 20. Modeled probability of effective DTBird deterrence for golden eagles in relation to wind speed measured by turbine anemometer at time of events at the two wind facilities evaluated in this study, showing results with and without Site \* Wind Speed interaction (improves AIC score but nonsignificant P = 0.118 parameter test).

The final model and the model including the *Site* \* *Wind Speed* interaction had a McFadden's pseudo- $R^2$  values of 0.108 and 0.127, respectively, and were the two models with the highest such values (Table 17). The closeness of the pseudo- $R^2$  values of these two models indicates that they have essentially equal ability to explain variation in deterrence probabilities. Both values are between 0.1 and 0.2, indicating "good" predictive value (values of 0.1–0.2 are considered a "good" result, while values of 0.2–0.4 are considered an "excellent" result; McFadden 1974, 1979).

## 4.5.3 Factors Influencing False Positive Detection Rates (Objective 3)

#### 4.5.3.1 DTBird Event Classifications

The 10-month, seven-turbine dataset analyzed from the Manzana site to derive results for this multi-site assessment involved 3,051 detections that triggered one or both deterrents (i.e., warning and/or dissuasion signals). With unknown big birds, unknown medium/large raptors, and unknown birds proportionately allocated where appropriate to the large raptors and NTAFP groups, the Manzana records included 789 detections classified as large soaring raptors, 917 detections classified as TFPs, and 1,212 detections classified as NTAFPs (Table 19). The analyzed 11-turbine dataset from Year 1 at the Goodnoe Hills involved 11,265 detections that triggered deterrents, including 1,529 classified as relevant raptors, 5,744 as TFPs, and 3,955 as NTAFPs. The analyzed intermittently 14-turbine dataset from Year 2 at the Goodnoe Hills

involved 8,075 detections that triggered deterrents, including 1,673 classified as relevant raptors, 3,441 as TFPs, and 2,958 as NTAFPs.

At Manzana, NTAFPs caused an estimated 40% of all deterrent triggers, TFPs caused 30%, large raptors caused 26%, and birds that remained classified as unknown medium/large raptors caused 4%. Particularly high raven activity at one DTBird turbine contributed to complaints from a residence approximately 500 meters away from that turbine. At Goodnoe Hills, adjusted NTAFPs caused a similar 36% of all deterrent triggers, whereas TFPs caused a higher 48% and large raptors caused a lower 17% of the total. Confirmed common ravens caused 24% of all false-positive deterrent triggers at Goodnoe Hills and 15% at Manzana.

Table 1919. DTBird Detection Events that Triggered Deterrents Classified as Large Raptors, True False Positives (TFPs), and Nontarget Avian False Positives (NTAFPs) at the Manzana Wind Power Project in California and Goodnoe Hills Wind Farm in Washington

	•				Large Raptors <sup>2</sup>		TFPs <sup>3</sup>		NTAFPs <sup>4</sup>	
Site	Number of Operational DTBird Systesms	Period of Record	Total Detection Events <sup>1</sup>	Number of Detection Events	Average Events/ Turbine/ Day	Number of Detection Events	Average Events/ Turbine/ Day	Number of Detection Events	Average Events/ Turbine/ Day	
Manzana	7	Jan-Oct 2017	3,051	789	1.1	917	1.3	1,212	1.7	
Goodnoe Hills Year 1	11	Sep 2021- Aug 2022	11,260	1,529	1.3	5,744	4.9	3,955	3.3	
Goodnoe Hills Year 2	14	Sep 2022- Jul 2023	8,075	1,673	1.5	3,441	3.0	2,958	2.6	
Total	Max 21	_	22,386	3,991	1.3	10,102	3.3	8,125	2.7	

<sup>3</sup> Includes unidentified medium/large raptors that we did not reclassify as Large Raptors or NTAFPs and were excluded from analyses.

#### 6.5.3.2 True False Positives

At Goodnoe Hills, the additional false-positive filtering adjustments made in January 2023 reduced the overall rate of TFP deterrent triggers from approximately 529 to 71 per month across all sampled turbines (87% reduction). Substantial proportional reductions in the monthly TFP deterrent triggering rates included those caused by insects (97%), sky artifacts (94%), floating debris (93%), other turbine equipment features (91%), spinning turbine blades (88%), precipitation (67%), and software/video issues (39%). Note, however, that unequal seasonal sampling and variation also could have affected the outcomes for insects, sky artifacts, floating debris, and precipitation. In addition, modifications of the absolute numbers substantially altered the proportional contributions of different types of TFPs observed at Goodnoe Hills in only a few cases. The proportion of blade-related TFPs declined only slightly from 32% of all TFP deterrent triggers in Year 1 to 28% post-adjustments in Year 2. The proportion of insect-related TFPs declined more substantially from 28% in Year 1 to 9% post-adjustments in Year 2, and the proportion of sky artifact TFPs declined from 23% in Year 1 to 9% post-adjustments in

<sup>4</sup> Restricted to large soaring species; i.e., eagles, vultures, buteos, harriers, and ospreys.

<sup>5</sup> Includes events triggered by inanimate objects, insects, and software/video interpretation errors and failures.

<sup>6</sup> Includes events triggered by birds other than large soaring raptors and unknown medium/large raptors.

Year 2. Concomitantly, the proportion of TFPs caused by aircraft increased from 11% in Year 1 to 30% post-adjustments in Year 2, and the proportion of TFPs caused by software failures increased from 4% in Year 1 to 18% post-adjustments in Year 2.

The range of TFP source types was similar but the percentage contributions of different sources varied at the two study sites (Attachment 6: Table 2). Before the false-positive filtering was adjusted at the Goodnoe Hills study, turbine blades (30-32% of TFPs) and insects (28-48%) variably ranked as the most and second-most common sources of TFPs, with TFPs caused by aircraft (6-11%) and sky artifacts (9-23%) variably ranked as the third and fourth most common sources. At Manzana by contrast, aircraft caused a majority of the TFPs (60%), sky artifacts caused the second highest proportion (25%), and insects caused a notably lower, third highest proportion (5%). The only other instance where another source caused more than 5% of the TFPs recorded during one of the four site-sampling periods involved software failures during the Goodnoe Hills Year 2 post-adjustments period (18% of TFPs) in that period).

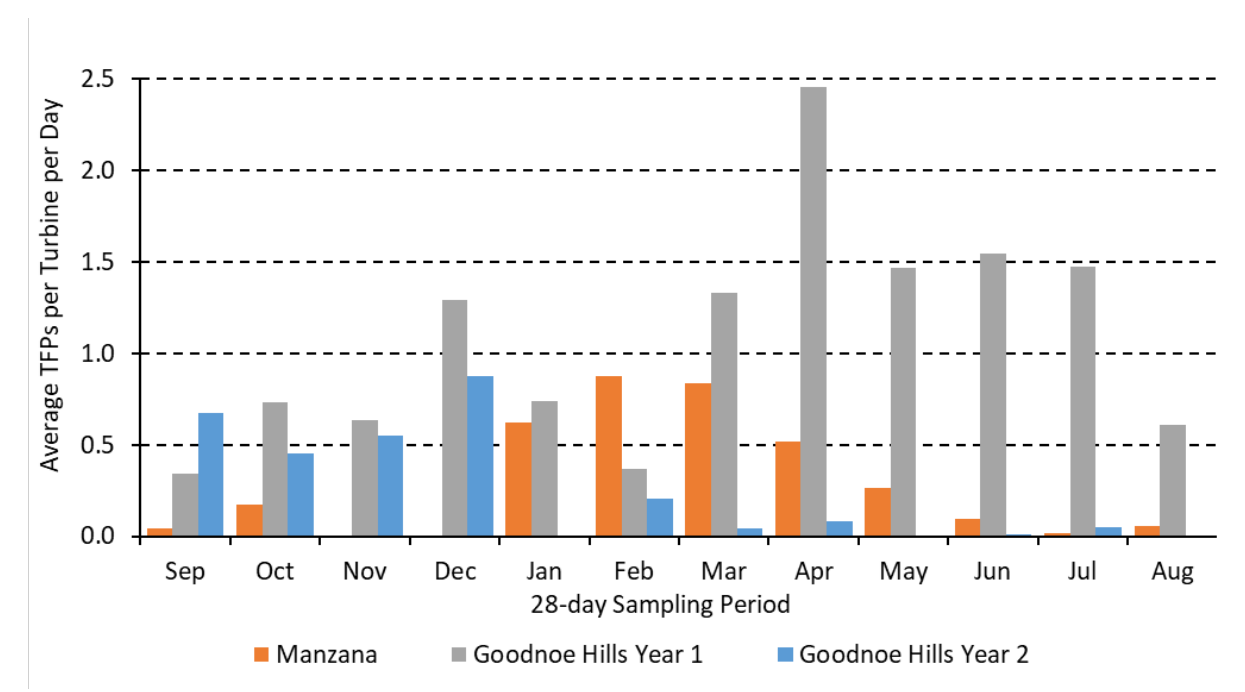


Figure 21. Rates of True False Positives Caused by Insects that Triggered DTBird Deterrents by Month at the Manzana Wind Power Project in California (January – October 2017) at the Goodnoe Hills Wind Farm in Washington (September-August 2021–2022 and 2022–2023).

The proportion of TFPs caused by insects showed distinctly different patterns both between years at Goodnoe Hills and between the two sites (Figure 21). At Manzana, insect TFPs were generally much less prevalent than at Goodnoe Hills and occurred mostly in early to midsummer. During Goodnoe Hills Year 1, insect TFPs started out high in the fall, were largely absent during winter, began to ramp up in spring, and peaked in summer. In contrast, during Goodnoe Hills Year 2, insect TFPs were very high initially during fall (expanding the summer peak from Year 1), dropped off and again were rare through winter, but unlike during Year 1, remained low and comparable to the Manzana rates after that.

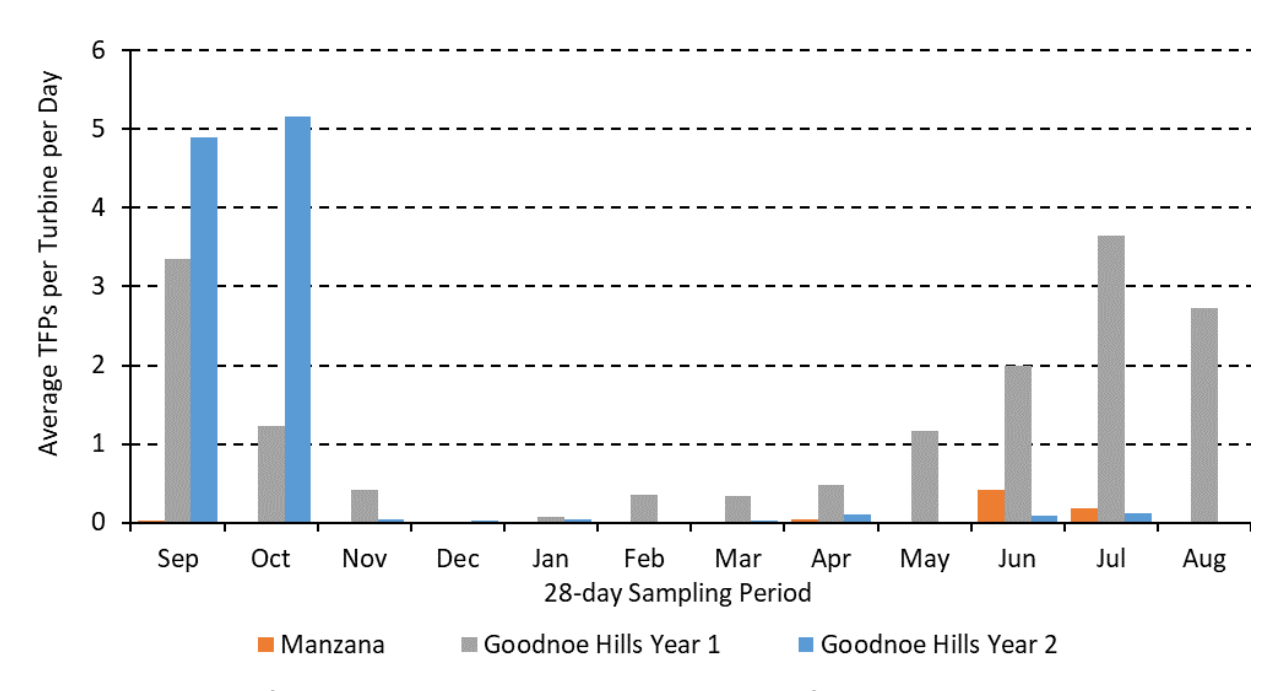


Figure 22. Rates of True False Positives Caused by Sky Artifacts that Triggered DTBird Deterrents by Month at the Manzana Wind Power Project in California (January–October 2017) and at the Goodnoe Hills Wind Farm in Washington (September–August 2021–2022 and 2022–2023).

The prevalence of TFPs caused by sky artifacts showed very different patterns across 28d Cycles in Years 1 and 2 at Goodnoe Hills, whereas the patterns were much more similar for Manzana and Goodnoe Hills Year 2 (Figure 22). After the fifth cycles, sky artifact TFPs dropped off markedly and remained low at both the Manzana site and at Goodnoe Hills during Year 2. Note that, while this drop-off marked the time when further changes were made in the false positive filtering algorithms at Goodnoe Hills, it did not correspond to any such change at Manzana. After this point, though showing comparable rates and variation through the first 4-5 cycles, the rate of sky artifact TFPs increased markedly during Goodnoe Hills Year 1 and remained high through the 12th cycle, before dropping back down again to a moderate level during the 13<sup>th</sup> cycle (Figure 22, noting that for Goodnoe Hills the indicated patterns across months are essentially the same as for 28d Cycles, whereas 28d Cycle 1 was in January at Manzana). Considering the patterns in relation to calendar months further suggested that seasonal variation in the relative prevalence of sky artifact TFPs also might have contributed to the observed patterns. Though temporal mismatches in the site-specific datasets confound seasonal comparisons, it appeared that sky artifact TFPs were most common at Manzana in late winter early spring and dropped off during summer, whereas the Goodnoe Hills Year 1 data suggested comparatively high rates across the year and an extended period of peak activity from spring through summer (Figure 22).

#### 6.5.3.3 Nontarget Avian False Positives

The range of general categories of NTAFP sources was similar at the two study sites. The only material difference in the proportional representations was that the percentage of confirmed

common ravens was lower at Manzana (28% of classified NTAFPs) than during either sampling year at the Goodnoe Hills (39–42%), whereas the proportion of unidentified big birds that we ultimately classified as NTAFPs was higher at Manzana (57%) than it was during both years at Goodnoe Hills (40–45%) (Attachment 6: Table 3).

#### 4.5.3.4 False Positive Deterrent Triggering Rates and Durations

The overall average large-raptor deterrent triggering rates were relatively consistent across the three primary site-sampling periods, ranging from 1.3–1.5 detections with deterrent triggers/turbine/day (Table 19). The overall average TFP deterrent triggering rates were more variable, ranging from a low of 1.3 detections with deterrent triggers/turbine/day at Manzana to a high of 4.9 detections with deterrent triggers/turbine/day during Year 1 at the Goodnoe Hills; the Year 2 TFP deterrent triggering rate at the Goodnoe Hills was midday between the other two estimates. The same general pattern of differences was evident among the NTAFP deterrent triggering rates (Table 20).

Table 2020. Overall Durations and Average Per Turbine Duration Rates for DTBird Deterrent Signals Triggered by True False Positives (TFPs) and Nontarget Avian False Positives (NTAFP) at the Manzana Wind Power Project in California and Goodnoe Hills Wind Farm in Washington.

			Warning Sig	nals	Dissuasion Signals			
Site	Sampling Period	Number of Triggers	Total Duration (minutes)	Average Duration/ Turbine/Day (seconds)	Number of Triggers	Total Duration (minutes)	Average Duration/ Turbine/Day (seconds)	
TFPs								
Manzana	10 months	487	294	17.3	662	370	33.5	
Goodnoe Hills	Year 1	654	217	27.0	4820	2465	30.7	
	Year 2 – 4.5 months pre- adjustments	493	78	26.5	2551	1361	32.0	
	Year 2 – 6.5 months post- adjustments	199	589	23.4	685	383	33.6	
NTAFPs								
Manzana	10 months	979	364	22.3	458	223	29.1	
Goodnoe Hills	Year 1	2510	1097	26.2	173.5	960	33.2	
	Year 2 – pre	1138	484	25.5	797	438	33.0	
	Year 2 – post	1083	458	25.4	602	321	32.0	

Standardized for variable sampling intensity, the overall average TFP-caused warning signal durations on turbine-days when deterrents were triggered averaged 17.3 seconds/turbine/day at the Manzana site and a significantly higher 26.2 seconds/turbine/day at the Goodnoe Hills site (Table 20). The average warning signal duration rate at the Goodnoe Hills declined from 27.0 seconds/turbine/day during Year 1 down to 23.4 seconds/turbine/day during the Year 2

post-adjustments period, but still remained notably longer than at Manzana. In contrast, the average duration rates for dissuasion signals rose slightly at Goodnoe Hills between Year 1 (30.7 seconds/turbine/day) and the Year 2 post-adjustments period (33.6 seconds/turbine/day), but in this case the higher Year 2 post-adjustments rate more closely matched the Manzana rate (33.5 seconds/turbine/day).

Similar patterns of variation were evident in the overall average NTAFP-caused deterrent signal duration rates (Table 20), except differences among the Goodnoe Hills sampling periods and between the two study sites were less pronounced, and the duration rates declined slightly for both warning and dissuasion signals between Year 1 and the post-adjustments Year 2 period at the Goodnoe Hills.

With the analysis limited to comparing results across 12 common 28d Cycles, the numbers of days from which samples were drawn to compose the GLMM relating daily turbine-specific counts of TFPs that triggered deterrents to Year and 28d Cycle at the Goodnoe Hills varied from 10-119 per turbine across 11 sampled turbines in Year 1, and from 57-97 per turbine across 14 sampled turbines in Year 2 (Table 21). For the analysis comparing Goodnoe Hills results by Year and Month, we excluded May from the comparison due to an absence of data from that month in Year 2. For this reason, the sample sizes used to compare Year 1 and Year 2 by Month at the Goodnoe Hills were slightly lower for Year 1 than in the 28d-Cycle analysis (Table 21). The GLMM relating daily turbine-specific TFP counts to Year and 28d Cycle revealed a highly significant main effect for Year (Wald x2, P < 0.0001), a non-significant main effect for 28d Cycle (P = 0.98), and a highly significant interaction term (P < 0.0001). Nakagawa's marginal pseudo-R2 for the model was 0.288, indicating that the fixed effects in the model provided moderate explanatory power (Nakagawa and Schielzeth 2013). Given the significant interaction, we conducted planned post-hoc comparisons to identify significant pairwise differences between Years within 28d Cycles and among 28d Cycles within Years. These comparisons confirmed the substantial shift in TFP prevalence after the additional filtering adjustments were made during the fifth 28d Cycle of Year 2 (Figure 23). Before that, the TFP rates did not differ markedly during corresponding 28d Cycles of the two sampling years. After that, the TFP rates remained significantly lower in Year 2 than in Year 1 during all subsequent 28d Cycles. Further, the postadjustments Year 2 rates remained consistently low post-adjustments, whereas the corresponding Year 1 rates rose steadily after the sixth cycle to the highest rate for the year during the twelfth cycle.

Table 2121. Numbers of turbine-specific days from which samples were drawn for investigating temporal differences in DTBird false-positive detection rates between sampling years at the Goodnoe Hills Wind Farm in Washington.

		y 28d Cycles: Cycles 1-12		Analysis by Month: All Months Except May			
Turbine	Year 1	Year 2	Total	Year 1	Year 2	Total	
G29	_	95	95	-	95	95	
G34	98	91	189	104	91	195	
G35	89	87	176	88	87	175	
G44	107	79	186	103	79	182	

G45	108	87	195	103	87	190	
G48	112	57	169	110	57	167	
G49	105	90	195	101	90	191	
G51	_	80	80	-	80	80	
G56	_	70	70	-	70	70	
G58	117	97	214	115	97	212	
G59	104	57	161	106	57	163	
G64	119	91	210	118	91	209	
G67	112	86	198	111	86	197	
G75	10	75	85	10	75	85	
Total	1,081	1,142	2,223	1,069	1,142	2,211	

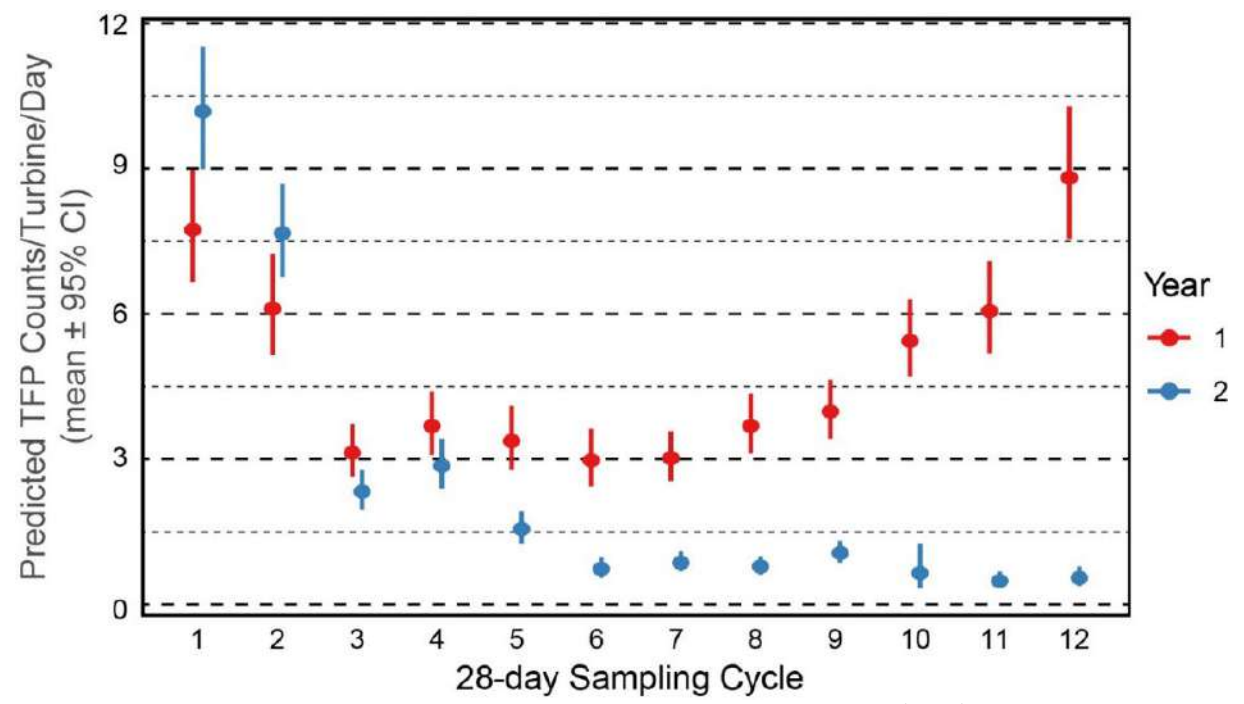


Figure 23. Predicted Average Daily Per Turbine True False Positive (TFP) DTBird Deterrent-Triggering Rates Across 28-day Sampling Periods During Study Years 1 and 2 at the Goodnoe Hills Wind Farm in Washington. Nonoverlapping Confidence Intervals Indicate Significant Pairwise Comparisons.

The GLMM relating daily turbine-specific counts of TFPs that triggered deterrents to *Site* and 28d *Cycles* at the Manzanas and during Goodnoe Hills Year 2 revealed a highly significant main effect for *Site* (Wald  $\chi^2$ , P < 0.0001), a non-significant main effect for 28d *Cycle* (P = 0.92), and a highly significant interaction term (P < 0.0001). Nakagawa's marginal pseudo- $R^2$  for the model was 0.219, indicating the fixed effects provided moderate explanatory power. Planned post-hoc pairwise comparisons confirmed that (a) both sites had relatively elevated TFP rates during the first two 28d *Cycles* of the respective sampling periods, (b) the early rates during Goodnoe Hills Year 2 were much higher than during the two corresponding cycles at the Manzanas, and (c) after adjustments were completed during the fifth cycle of Year 2 at the Goodnoe Hills, the TFP

deterrent-triggering rates followed similar patterns at the two sites, remained low and did not vary significantly across subsequent sampling cycles, and often were lower at the Goodnoe Hills post-adjustments than at the Manzanas (Figure 24).

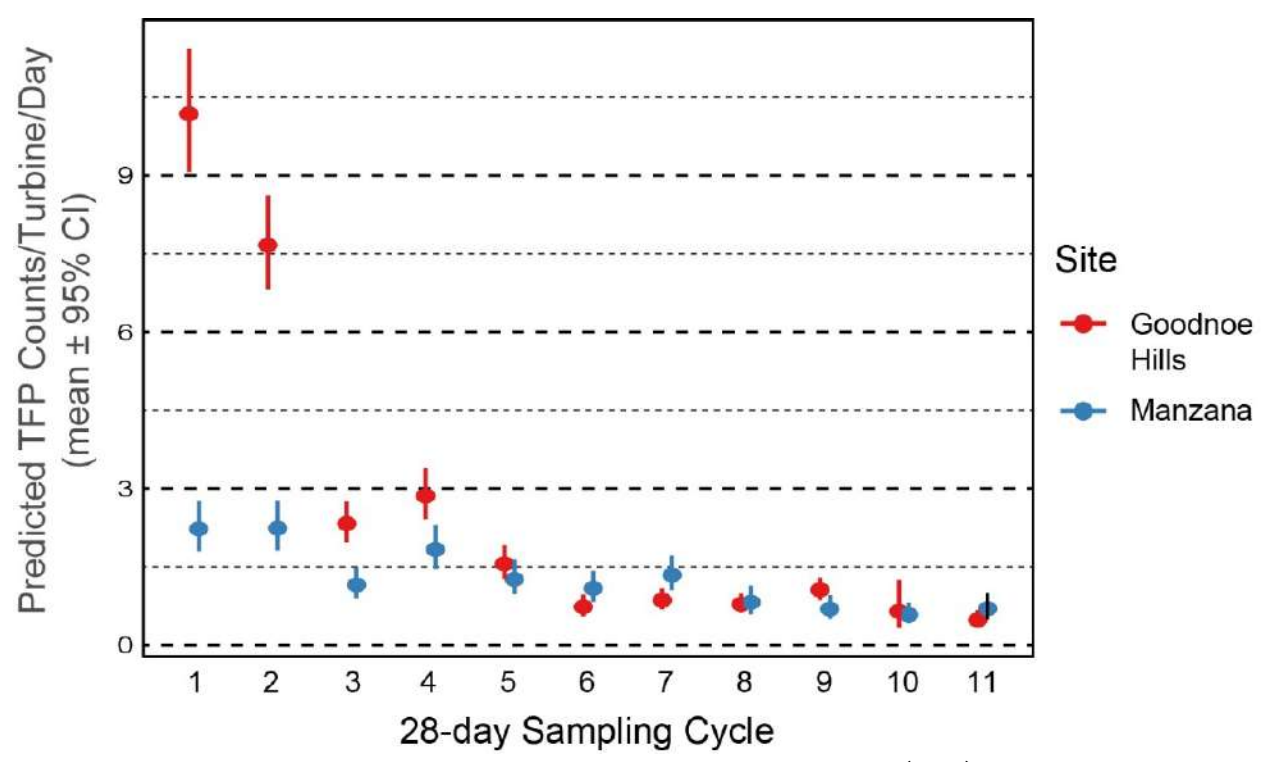


Figure 24. Predicted Average Daily Per Turbine True False Positive (TFP) DTBird Deterrent-Triggering Rates Across 12 28-day Sampling Periods (Variable Calendar Periods) at the Manzana Wind Power Project in California and During Study Year 2 at the Goodnoe Hills Wind Farm in Washington. Nonoverlapping Confidence Intervals Indicate Significant Pairwise Comparisons.

The GLMM relating daily turbine-specific counts of NTAFPs that triggered deterrents to *Year* and *Month* at the Goodnoe Hills revealed a highly significant main effect for *Year* (Wald  $\chi^2$ , *P* <0.0001), a non-significant main effect for *28d Cycle* (*P* = 0.99), and a highly significant interaction term (*P* <0.0001). Nakagawa's marginal pseudo- $R^2$  for the model was 0.085, indicating the fixed effects provided marginal explanatory power. Unlike the TFP results, no dramatic shift in NTAFP prevalence occurred post-adjustments at the Goodnoe Hills; however, the post-adjustment rates in Year 2 (after January) did generally remain significantly lower than during all corresponding months in Year 1 (Figure 25).

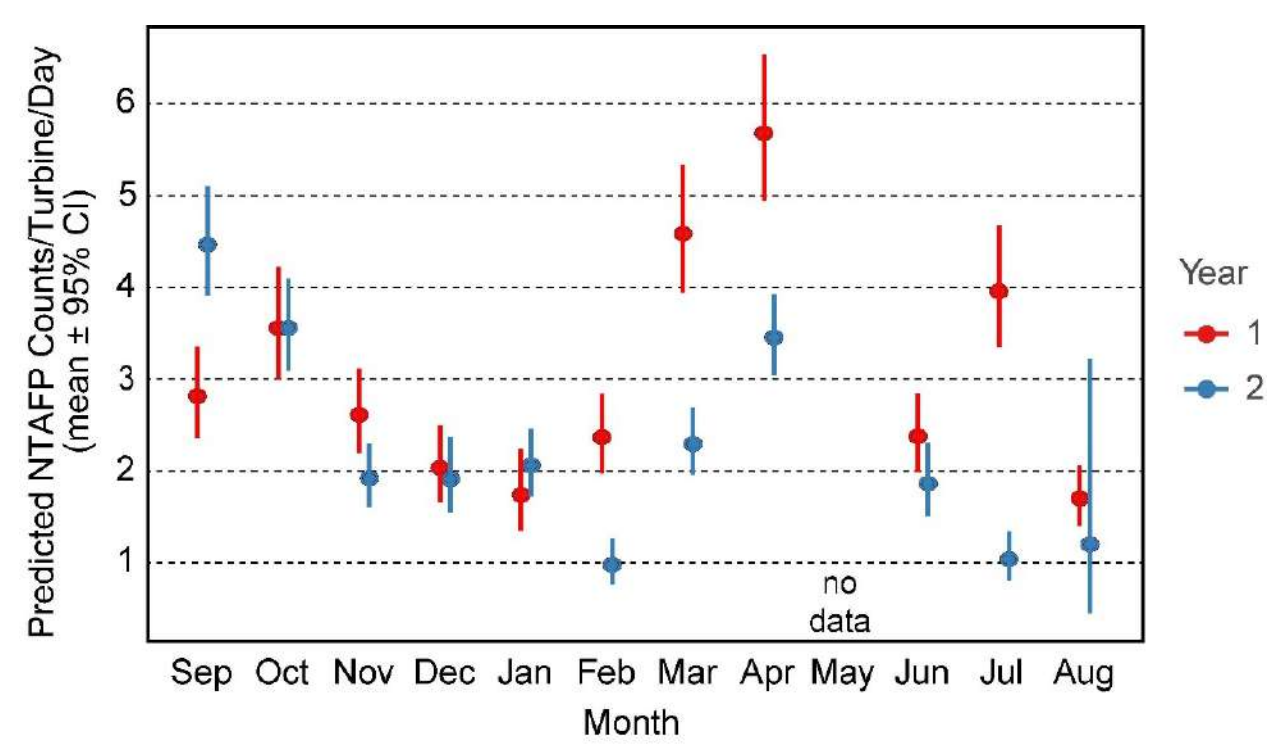


Figure 25. Predicted Average Daily Nontarget Avian False Positive (NTAFP) DTBird Deterrent-Triggering Rates Across 11 Months During Study Years 1 and 2 at the Goodnoe Hills Wind Farm in Washington. Nonoverlapping Confidence Intervals Indicate Significant Pairwise Comparisons.

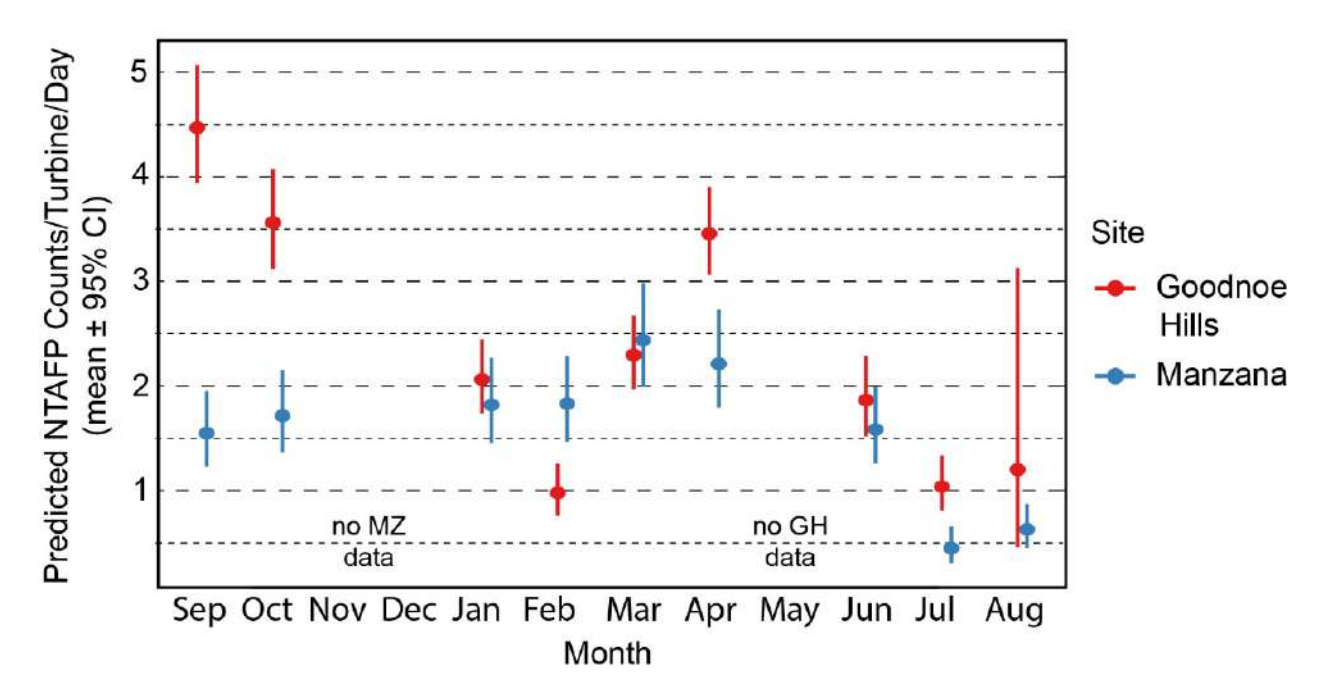


Figure 26. Predicted Average Daily Nontarget Avian False Positive (NTAFP) DTBird Deterrent-Triggering Rates Across Nine Common Sampling Months at the Manzana Wind Power Project in California and During Study Year 2 at the Goodnoe Hills Wind Farm in Washington. Nonoverlapping Confidence Intervals Indicate Significant Pairwise Comparisons.

The GLMM relating daily turbine-specific counts of NTAFPs that triggered deterrents to Site and Month at Manzana and at the Goodnoe Hills during sampling Year 2 revealed a non-significant main effect for Site (Wald  $\chi^2$ , P = 0.23), a non-significant main effect for 28d Cycle (P = 0.98), and a highly significant interaction term (P <0.0001). Nakagawa's marginal pseudo- $R^2$  for the model was 0.129, indicating the fixed effects provided marginal explanatory power. Across the nine relevant calendar months, the two sites showed similarities towards higher NTAFP prevalence in spring, declining into mid-summer, then increasing some again in fall (Figure 26). The only substantive difference in pattern was that NTAFP prevalence was notably elevated at Goodnoe Hills during September and October compared to Manzana, suggesting higher fall migratory activity of nontarget birds at Goodnoe Hills.

## 4.5.4 In Situ Experimental Evaluation of Raptor Responses (Objective 4)

Table 22 summarizes the samples of confirmed and probable eagles we derived from screening DTBird event records on selected sample days, including the numbers of records for each species/group that did and did not trigger a deterrent signal under conditions when deterrent triggering was expected to occur if a bird passed within triggering range. These samples formed the basis for our analyses.

Table 2222. Summary of DTBird Detection Samples Used to Evaluate Results of Two-year Experiment Comparing Responses of Large Raptors to Muted (Control) Versus Broadcasted (Treatment) Audio Deterrents

-	Days	No			Average	
Experiment Group – Species/Group <sup>1</sup>	With Samples	Deterrence Records <sup>2</sup>	Deterrence Records <sup>3</sup>	Total Records	Records Per Day	SD
Golden Eagles	71	6	99	105	0.8	1.04
Bald Eagles	64	6	70	76	0.8	0.75
All Eagles	135	15	199	209	0.9	1.18
Treatment						
Golden Eagles	70	11	91	102	0.8	1.11
Bald Eagles	40	2	51	53	0.5	0.72
All Eagles	123	13	168	181	0.8	1.05

<sup>&</sup>lt;sup>1</sup> In all cases, classifications include confirmed and probable identifications belonging to the specific species or species group.

# 4.5.4.1 Testing Hypothesis A Regarding Probability of Eagles Triggering a DTBird Dissuasion Signal

For confirmed and probable golden eagles alone, limited sample sizes constrained our ability to evaluate a full model including the complete suite of potential predictors and 2-way interactions of interest. Instead, we proceeded systematically to evaluate (1) the influences of *Treatment Group* combined with each of the other predictors alone and then with associated two-way interactions, and (2) more complex multi-variable models based on indications of potential significance during the preceding step (see Attachment 3: Appendix C for comparisons of selected candidate models). Throughout the process of considering candidate models and selecting a final logistic GLMM to represent the probability of golden eagles triggering a dissuasion signal, the prediction coefficients for *Treatment Group* were always negative, suggesting the expected effect of a lower probability of dissuasion triggers at turbines operating in treatment mode. *Treatment Group* never emerged as even a marginally significant predictor, however. In contrast, *Year, Time of Day*, and *Wind Speed* were at least marginally significant predictors and were retained in the final model. Accordingly, the dissuasion-trigger model selected to represent golden eagles alone, based on AIC scores, parameter tests, and positive model diagnostics, was as follows:

In(Odds of dissuasion trigger)  $\sim$  [1|Turbine ID] + [1|Turbine ID : Elapsed Days] + Treatment Group + Year + Time of Day + Wind Speed

The relationships indicated by the resulting model coefficients and individual parameter tests (Table 23) are described below.

- Non-significant 29% reduction (95% CI: 63% reduction 36% increase) in the probability
  of dissuasion triggers at installations operating in treatment mode.
- Marginally significant 46% reduction (95% CI: 73% reduction 9% increase) in the probability of dissuasion triggers in Year 2.

<sup>&</sup>lt;sup>2</sup> Cases where a target bird was detected but did not trigger a deterrent signal.

<sup>&</sup>lt;sup>3</sup> Cases where a target bird was detected and triggered one or both deterrent signals, either virtually (control mode) or with the deterrents actually broadcasting (treatment mode).

- Marginally significant positive relationship between the probability of dissuasion triggers and *Time of Day* (Figure 27).
- Significant negative relationship between the probability of dissuasion triggers and *Wind Speed* (Figure 28).

Table 2323. Model Coefficients and Fixed Effect Parameter Test Results for the Logistic GLMM Selected to Represent the Probability of Confirmed and Probable Golden Eagles Triggering a Dissuasion Signal at DTBird Installations Operating in Treatment (Deterrents Broadcasting) and Control (Deterrents Muted) Mode During Two-year Experiment

SD

Turbine	0.357 0.116 <b>Estimate</b>	0.5977 0.3409 <b>SE</b>				
Turbine: Elapsed Days <sup>1</sup> Fixed Effect			<b>z</b> <sup>2</sup>	P (> z ) <sup>2</sup>	LRT χ <sup>2</sup> <sup>3</sup>	P (>χ <sup>2</sup> ) <sup>3</sup>
Treatment Group: On4	-0.339	0.3304	-1.026	0.305	1.07	0.302
Year: 2 <sup>5</sup>	-0.614	0.3569	-1.721	0.085	3.06	0.080
Time of Day <sup>6</sup>	0.295	0.154	1.917	0.055	3.83	0.050
Wind Speed <sup>7</sup>	-0.385	0.1780	-2.161	0.031	5.10	0.024

Elapsed Days = days since data-collection began; a simpler equivalent of date.

Variance

**Random Effect** 

<sup>&</sup>lt;sup>2</sup> Wald test.

<sup>&</sup>lt;sup>3</sup> Drop1 likelihood ratio test.

<sup>&</sup>lt;sup>4</sup> Reference category – Off = control mode. On = treatment mode.

<sup>5</sup> Reference category – Year 1: 1 September 2021 – 31 August 2022. Year 2: 1 September 2022 – 30 September 2023 (extended due to facility shut down from 1–24 May 2023.

<sup>&</sup>lt;sup>6</sup> Translated to minutes of the day; centered and scaled ([value - mean]/SD).

<sup>&</sup>lt;sup>7</sup> Recorded in meters/second; centered and scaled ([value – mean]/SD).

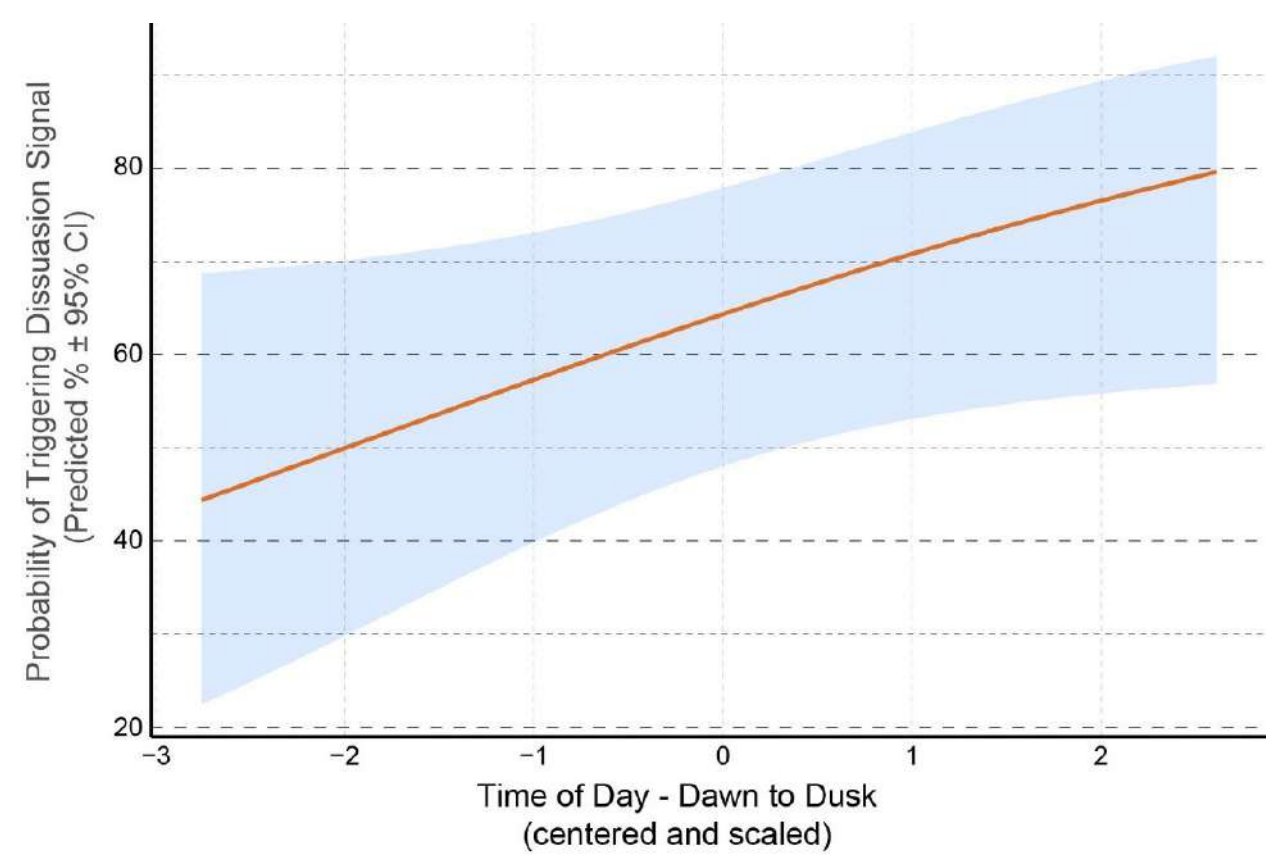


Figure 27. Illustration of predicted relationship between the probability of a golden eagle triggering a DTBird dissuasion signal and *Time of Day*.

Based on the dataset limited to eagles positively identified as either a golden eagle or a bald eagle, again no significant *Treatment Group* effects were evident but other indicators similar to

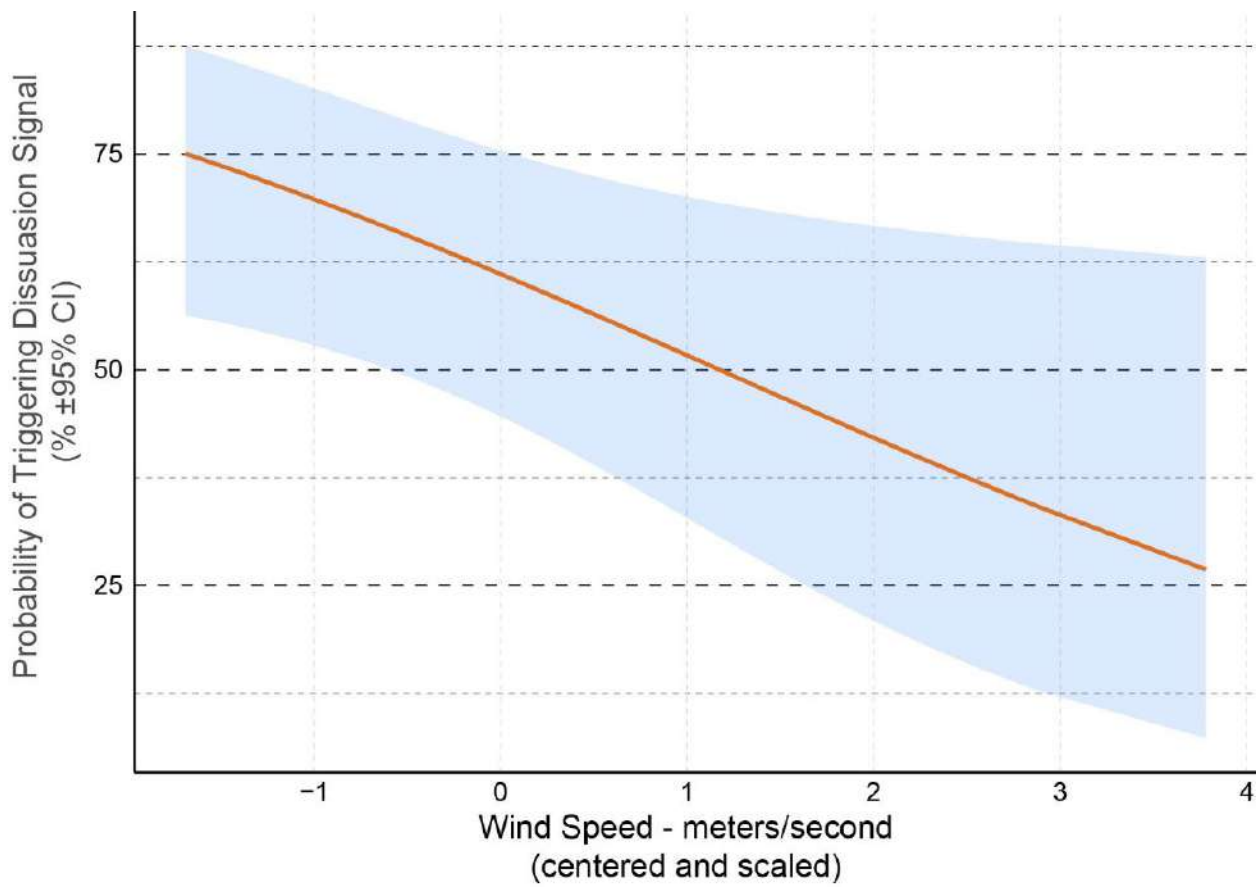


Figure 28. Illustration of predicted relationship between the probability of a golden eagle triggering a DTBird dissuasion signal and *Wind Speed*.

the results for golden eagles alone were evident. More importantly, although preliminary indications emerged suggesting potential marginal differences in the probability of dissuasion triggering for the two eagle species, those indications faded away once other covariates were included in the models. Therefore, we abandoned further consideration of models limited to identified golden and bald eagles with *Species* as a predictor in favor of evaluating models based on the larger all-eagles dataset (see Table 22) without considering *Species* as a potential predictor. Based on this dataset, we were able take both full backwards and forwards stepwise model building approaches to identify a top model (see Attachment 3: Appendix D for comparisons of models evaluated as part of a backwards elimination process to select the final model). The outcome of this approach again did not reveal a strong *Treatment Group* effect; however, the selected model included two at least marginally significant interactions between *Treatment Group* and other predictors, which provided important insight. The structure of the dissuasion-trigger logistic GLMM selected to represent all eagles combined was as follows:

In(Odds of dissuasion trigger)  $\sim$  [1|Turbine ID] + [1|Turbine ID : Elapsed Days] + Treatment Group + Time of Day + Time of Day<sup>2</sup> +Cloud Cover + FPs per Day + Treatment Group \* Cloud Cover + Treatment Group \* FPs per Day

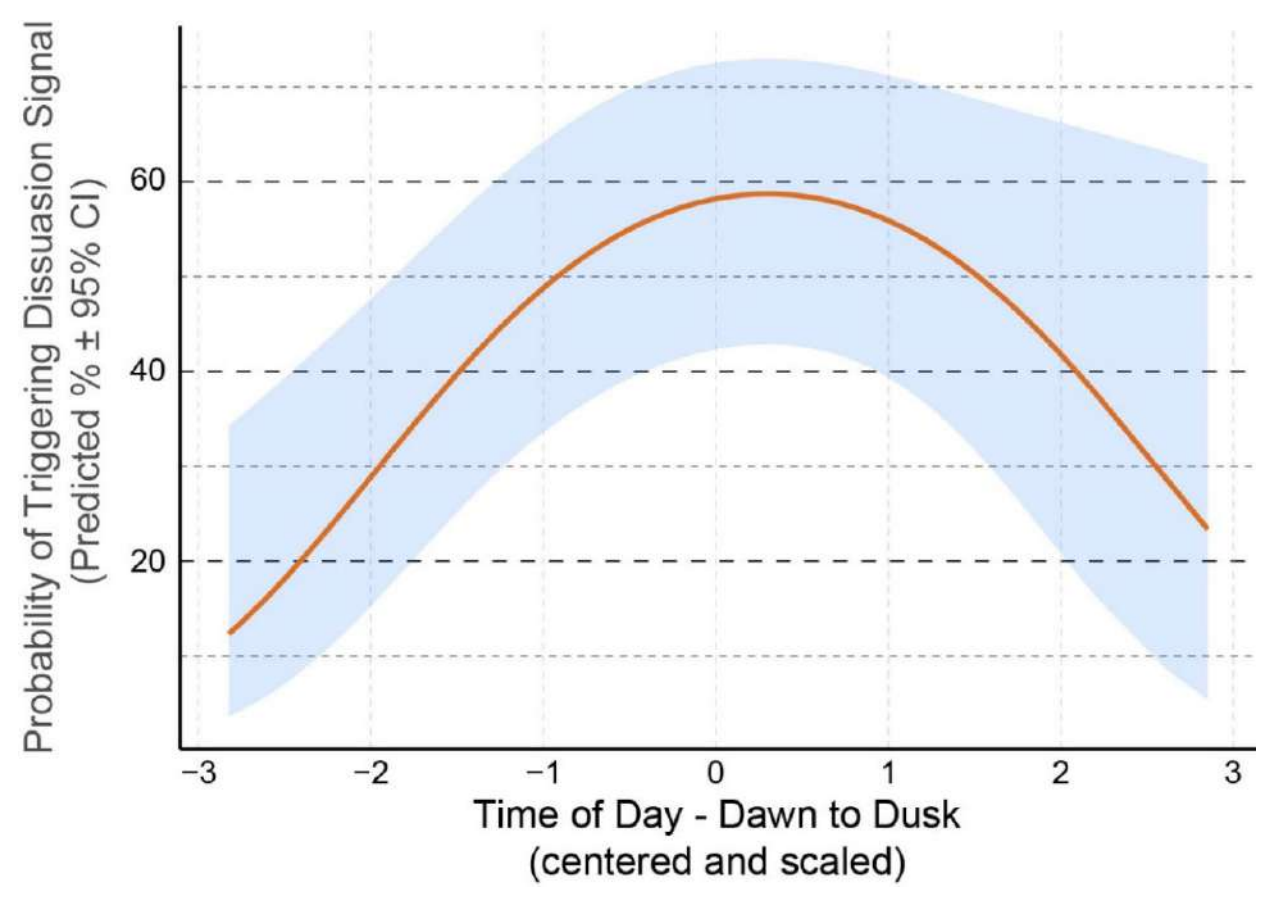


Figure 29. Illustration of predicted second-order relationship between the probability of an eagle triggering a DTBird dissuasion signal and time of day.

The relationships indicated by the resulting model coefficients and individual parameter tests (Table 24) are described below.

- Significant second-order relationship between the probability of dissuasion triggers and *Time of Day*, reflecting a higher probability of dissuasion triggering during midday compared to earlier and later in the day (Figure 29).
- When partly cloudy, cloudy, or overcast skies prevailed, the probability of dissuasion triggers was at least slightly lower at turbines operating in treatment mode compared to those operating in control mode, whereas when fair skies prevailed, the probability of dissuasion triggers was substantially lower at turbines operating in control mode (Figure 30).
- At turbines with DTBird systems operating in control mode, the probability of dissuasion triggers increased as the number of *FPs per Day* increased, whereas the opposite pattern applied at turbines operating in treatment mode (Figure 31).

Table 2424. Model Coefficients and Fixed Effect Parameter Test Results for the Logistic GLMM Selected to Represent the Probability of Confirmed and Probable Eagles (Golden and Bald Eagles Combined) Triggering a Dissuasion Signal at DTBird Installations Operating in Treatment (Deterrents Broadcasting) and Control (Deterrents Muted) Mode During Two-year Experiment

Random Effect	Variance	SD	<u> </u>			
Turbine ID	0.285	0.5338				
Turbine ID: Elapsed Days <sup>1</sup>	0.389	0.624				
Fixed Effect	Estimate	SE	<b>z</b> <sup>2</sup>	$P(> z )^{2}$	LRT χ <sup>2</sup> <sup>3</sup>	$P (> \chi^2)^3$
Intercept	0.374	0.3292	1.136	0.256	-	-
Treatment Group: On <sup>4</sup>	-0.263	0.3911	-0.672	0.501	-	-
Cloud Cover: Fair <sup>5</sup>	-1.278	0.5399	-2.367	0.018	-	-
Cloud Cover: Overcast <sup>5</sup>	0.377	0.5757	0.655	0.512	-	-
Cloud Cover: Partly Cloudy <sup>5</sup>	1.133	0.4120	2.751	0.006	-	-
Time of Day <sup>6</sup>	0.143	0.1226	1.165	0.244	1.359	0.244
Time of Day <sup>6</sup>	-0.237	0.0888	-2.668	0.008	7.939	0.004
FPs per Day <sup>7</sup>	0.395	0.1802	2.192	0.028	-	-
Treatment Group * Cloud Cover: Fair	2.040	0.7363	2.771	0.006	16.254	0.001
Treatment Group * Cloud Cover: Overcast	-0.297	0.8010	-0.371	0.710	-	-
Treatment Group * Cloud Cover: Partly Cloudy	-0.909	0.6004	-1.514	0.130	-	-
Treatment Group * FPs per Day	-0.492	0.2811	-1.750	0.080	2.965	0.085

<sup>&</sup>lt;sup>1</sup> Elapsed Days = days since data-collection began; a simpler equivalent of date.

<sup>&</sup>lt;sup>2</sup> Wald test.

<sup>&</sup>lt;sup>3</sup> Drop1 likelihood ratio test.

<sup>&</sup>lt;sup>4</sup> Reference category – Off = control mode. On = treatment mode.

<sup>5</sup> Reference category – Cloudy. Fair = mostly cloud free; Partly cloudy = <50% cloud cover; Cloudy = ≥50% cloud cover with distinctly variable cloud definitions and brightness; Overcast = complete and largely uniform gray or darker cloud cover.</p>

<sup>&</sup>lt;sup>6</sup> Translated to minutes of the day; centered and scaled ([value – mean]/SD).

FPs = false positives. Number of detection events triggered by true FPs and non-target avian FPs (see Section 2.4); centered and scaled ([value - mean]/SD).

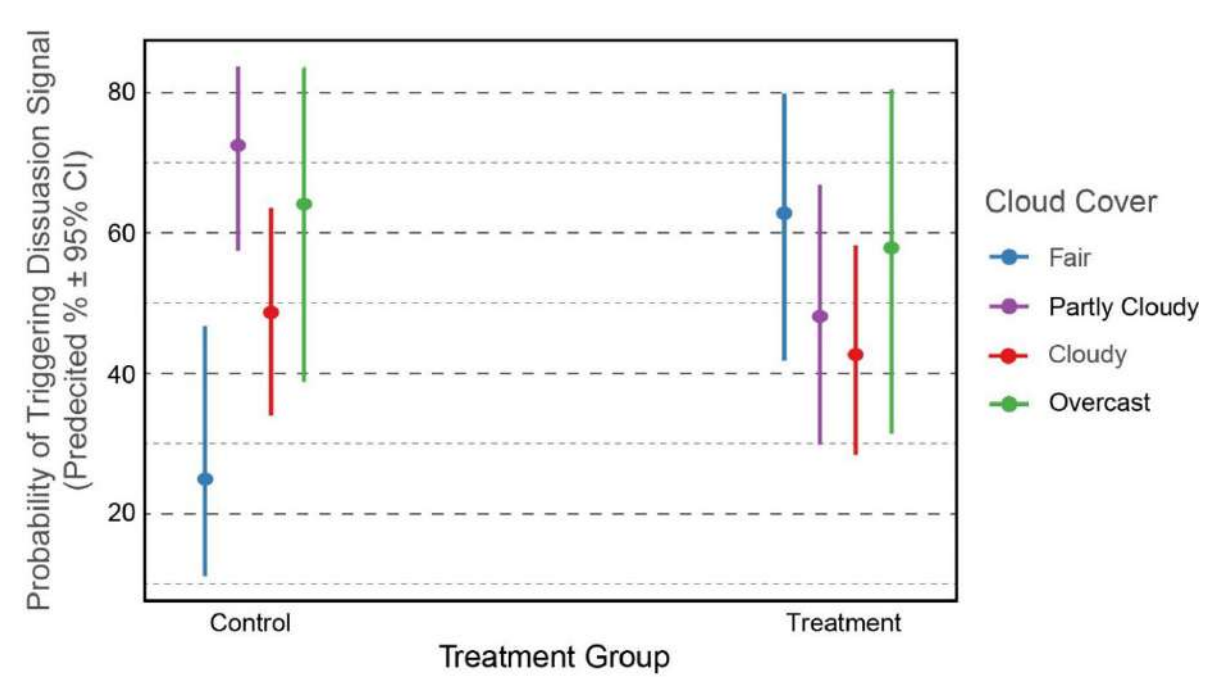


Figure 30. Illustration of predicted interactive relationship between treatment group and cloud cover in determining the probability of an eagle triggering a DTBird dissuasion signal.

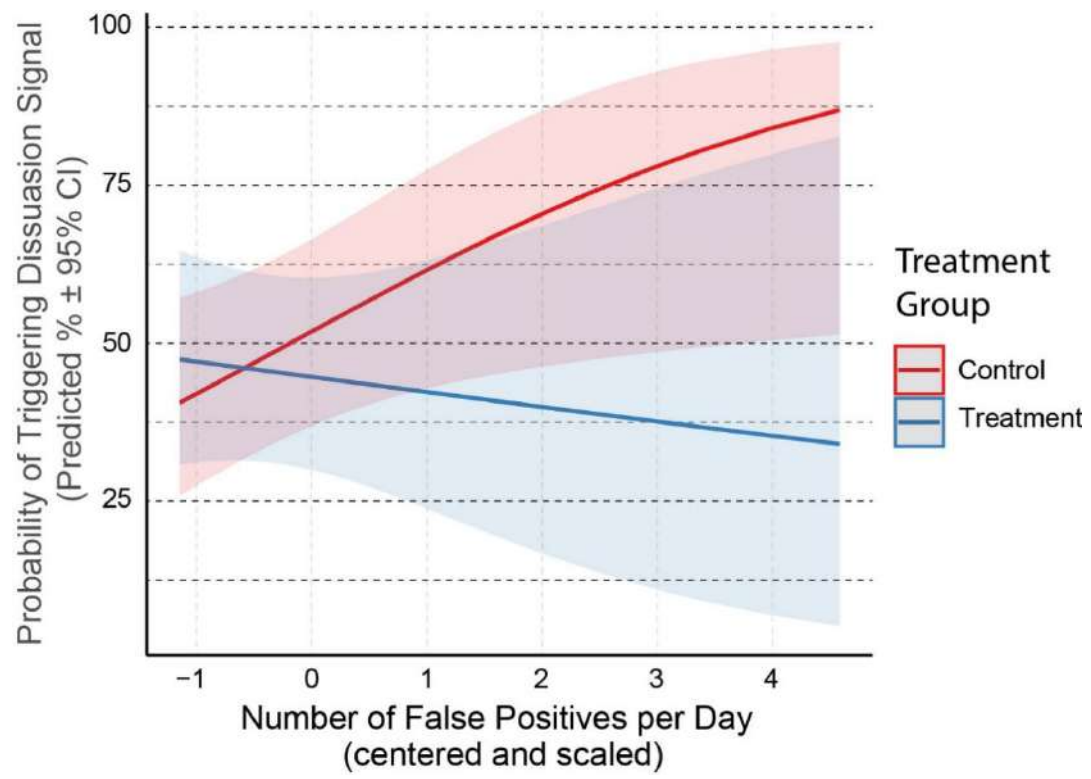


Figure 31. Illustration of predicted interactive relationship between treatment group and the daily numbers of false positives that triggered deterrent signals in determining the probability of an eagle (golden and bald eagles combined) triggering a DTBird dissuasion signal.

Augmenting the selected model above by including *Wind Speed* resulted in the lowest AIC score among the evaluated models (Attachment 3: Appendix D); however, the  $\Delta$ AIC was only 0.4 points and the *P* value for the likelihood ratio test evaluating the contribution of *Wind Speed* to the model (0.118) did not meet our criterion for retention in the model. Nevertheless, the negative parameter coefficient indicated a similar pattern as the significant relationship indicated for golden eagles alone, suggesting that wind speeds might have differentially influenced the responses of golden and bald eagles around the Goodnoe Hills turbines.

#### 4.5.4.2 Testing Hypothesis B Regarding Dwell Time of Eagles Around DTBird Deterrent Systems

To develop the GLMM for evaluating the influence of *Treatment Group* and other potential predictors on the dwell time of golden eagles around the study turbines, we were able take both full backwards and forwards stepwise model building approaches to identify a top model. The resulting selected model (see Attachment 3: Appendix E for comparisons of models evaluated as part of a backwards elimination process to select the final model) had the following form:

Dwell Time  $\sim$  [1|Turbine ID] + [1|Turbine ID : Elapsed Days] + Treatment Group + 28d Cycle + Time of Day + Time of Day 2 + FPs per Day + Treatment Group \* FPs per Day

The relationships indicated by the resulting model coefficients and individual parameter tests (Table 25) are described below.

- Significant 27% reduction (95% CI: 5–42%) in the average dwell time of golden eagles at installations operating in treatment mode, with the average dwell time reduced from approximately 26 to 17 seconds per event.
- Marginally significant overall declining trend in the dwell time of golden eagles in relation to the progression of 28d Cycles over the course of the two-year study (Figure 32).
- Significant main effect / marginally significant second-order relationship between dwell time and *Time of Day*, reflecting short dwell times in the morning, increasing through mid-afternoon, then tapering off again in the evening (Figure 33).
- Marginally significant interaction between Treatment Group and FPs per Day illustrating a
  positive relationship between dwell times and FP numbers around control turbines, but a
  negative relationship around treatment turbines (Figure 34). Put another way, the more
  that FPs contributed to actual deterrent broadcasting at treatment turbines, the less
  likely were eagles to dwell in the vicinity of those turbines.

Table 2525. Model Coefficients and Fixed Effect Parameter Test Results for the GLMM Selected to Represent the Relationship Between the Dwell Time of Confirmed and Probable Golden Eagles at DTBird Installations Operating in Treatment (Deterrents Broadcasting) and Control (Deterrents Muted) Mode During Two-year Experiment.

Random Effect	Variance	SD
Turbine	0.014	0.1166
Turbine: Elapsed Days <sup>1</sup>	2.15E-07	0.0005

Fixed Effect	Estimate	SE	<b>z</b> <sup>2</sup>	P (> z ) 2	LRT χ <sup>2</sup> <sup>3</sup>	P (>χ <sup>2</sup> ) <sup>3</sup>
Intercept	3.304	0.1082	30.54	<0.001	-	-
Treatment Group: On <sup>4</sup>	-0.319	0.1258	-2.54	0.011	-	-
28d Cycle <sup>5</sup>	-0.135	0.0661	-2.04	0.041	4.08	0.044
Time of Day <sup>6</sup>	0.166	0.0666	2.50	0.013	6.42	0.011
Time of Day <sup>2</sup>	-0.089	0.0451	-1.98	0.047	3.66	0.056
FPs per Day <sup>7</sup>	0.086	0.0754	1.14	0.255	-	-
Treatment Group: On * FPs per Day	-0.258	0.1361	-1.90	0.058	3.22	0.073

Elapsed Days = days since data-collection began; a simpler equivalent of date.

FPs = false positives. Number of detection events triggered by true FPs and non-target avian FPs (see Section 2.4); centered and scaled ([value – mean]/SD).

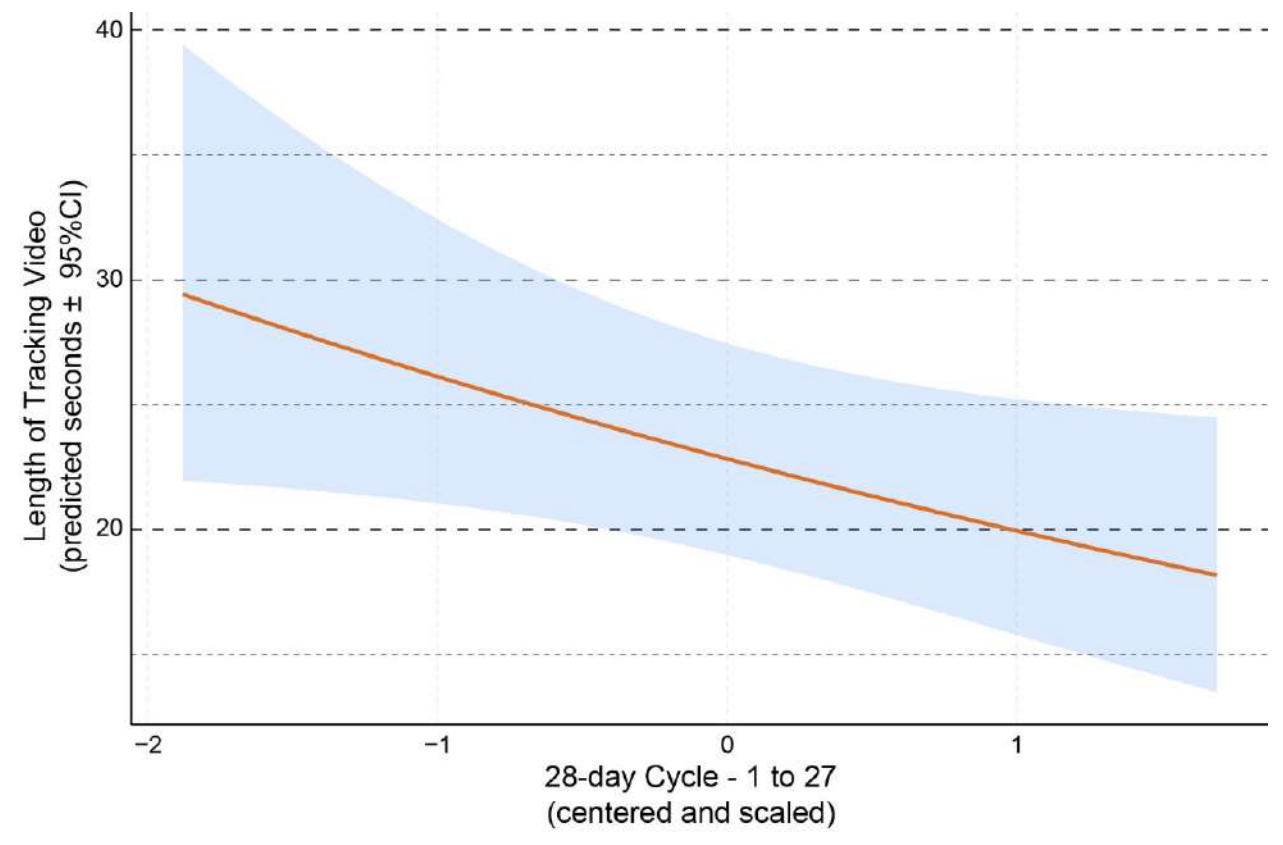


Figure 32. Illustration of predicted decline in the dwell time of golden eagles at DTBird turbines across the 27 28-day sampling cycles that composed this two-year experimental analysis.

<sup>&</sup>lt;sup>2</sup> Wald test.

<sup>&</sup>lt;sup>3</sup> Drop1 likelihood ratio test.

<sup>&</sup>lt;sup>4</sup> Reference category – Off = control mode. On = treatment mode.

<sup>&</sup>lt;sup>5</sup> Discrete continuous predictor representing 27 consecutive 28-day sampling periods from 1 September 2021 through 30 September 2023.

<sup>&</sup>lt;sup>6</sup> Translated to minutes of the day; centered and scaled ([value - mean]/SD).

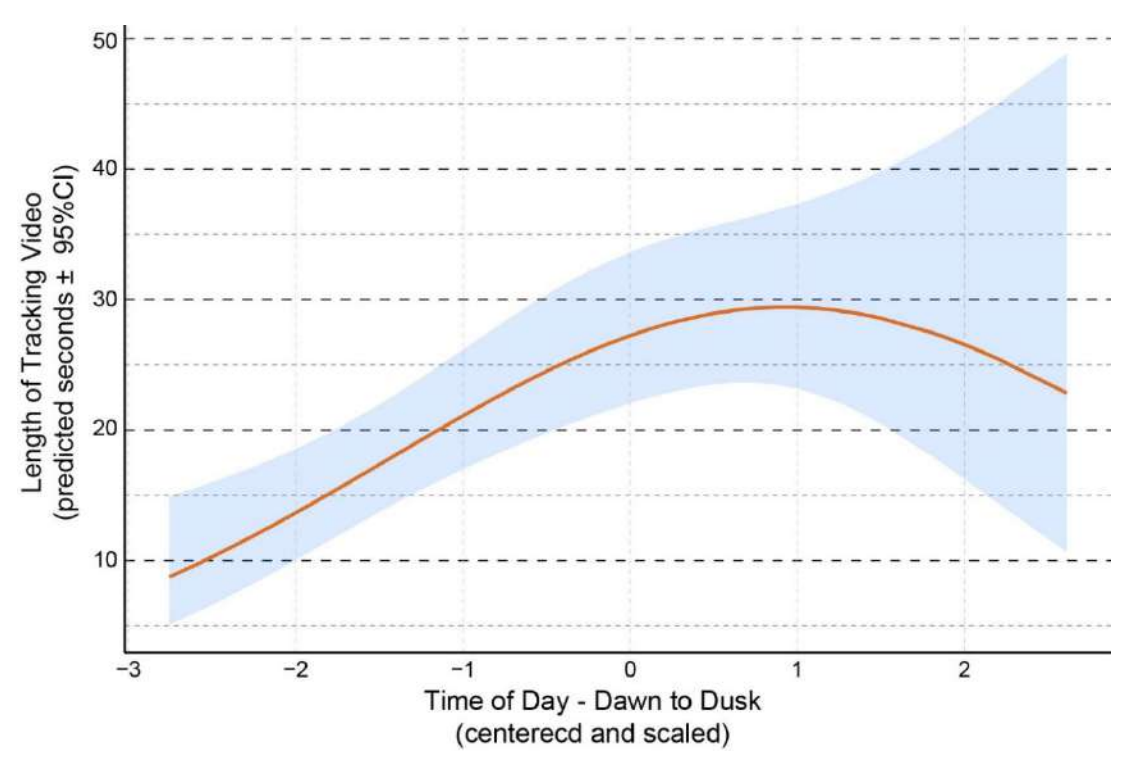


Figure 34. Illustration of predicted second-order relationship between the dwell time of golden eagles at DTBird turbines and time of day.

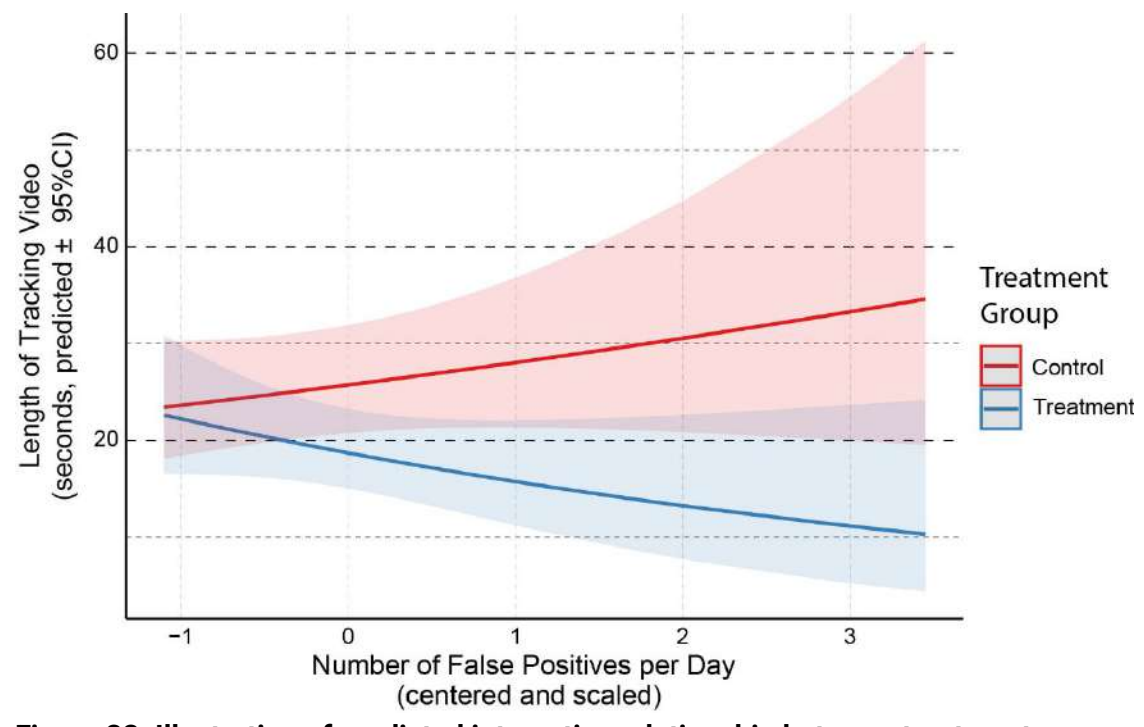


Figure 33. Illustration of predicted interactive relationship between treatment group and the daily numbers of false positives (FPs) that triggered deterrent signals in determining the dwell time of golden eagles around DTBird turbines.

Considering the dataset limited to eagles positively identified as either a golden eagle or a bald eagle yielded no evidence of Species as an influential predictor of dwell time. Hence, again we focused our further attention on evaluating models based on the larger all-eagles dataset without considering Species as a potential predictor. Running full models based on this dataset and dependent variable proved untenable due to dataset limitations; hence, we proceeded to identify a top model based on a similar iterative approach as described for golden eagles alone. The outcomes of this modeling effort yielded similar insights as for predicting the dwell time of golden eagles alone, with the same final model selected to represent all eagles combined (see Attachment 3: Appendix F for comparisons of selected candidate models) and the model coefficients confirming similar relationships as described above (Table 25, Figures 32-34). Most germane was a significant estimated 24% reduction (95% CI: 7-35%) in the dwell time of eagles at treatment turbines, with the average dwell time reduced from approximately 25 to 19 seconds per event. Note that, in deciding upon a final dwell-time model for all eagles combined, we retained FPs per Day and the Treatment Group \* FPs per Day interaction (see Figure 34) despite the P value for the interaction (0.129) being slightly greater than our  $P \le 0.10$  threshold for inclusion. We did this to retain a relationship that improved the AIC score of the final model and was common to two of the other three primary models we evaluated—albeit only marginally significant in each case (see Tables 25 and 26).

Table 2626. Model Coefficients and Fixed Effect Parameter Test Results for the GLMM Selected to Represent the Relationship Between the Dwell Time of All Confirmed and Probable Eagles at DTBird Installations Operating in Treatment (Deterrents Broadcasting) and Control (Deterrents Muted) Mode During Two-year Experiment.

Random Effect	Variance	SD				
Turbine	0.0016	0.03406				
Turbine: Elapsed Days <sup>1</sup>	1.82E-08	0.00014				
Fixed Effect	Estimate	SE	<b>z</b> <sup>2</sup>	P (> z ) 2	LRT χ <sup>2</sup> <sup>3</sup>	$P (> \chi^2)^3$
Intercept	3.305	0.0729	45.33	<0.001	-	-
Treatment Group: On <sup>4</sup>	-0.269	0.0934	-2.88	0.004	-	-
28d Cycle <sup>5</sup>	-0.114	0.0479	-2.37	0.018	5.64	0.018
Time of Day <sup>6</sup>	0.093	0.0453	2.09	0.037	4.49	0.034
Time of Day <sup>2</sup>	-0.093	0.0316	-2.93	0.003	7.92	0.005
FPs per Day <sup>7</sup>	0.124	0.0557	2.23	0.026	-	-
Treatment Group: On * FPs per Day	-0.149	0.0964	-1.55	0.121	2.31	0.129

Elapsed Days = days since data-collection began; a simpler equivalent of date.

<sup>2</sup> Wald test.

<sup>&</sup>lt;sup>3</sup> Drop1 likelihood ratio test.

<sup>&</sup>lt;sup>4</sup> Reference category – Off = control mode. On = treatment mode.

<sup>&</sup>lt;sup>5</sup> Discrete continuous predictor representing 27 consecutive 28-day sampling periods from 1 September 2021 through 30 September 2023.

<sup>&</sup>lt;sup>6</sup> Translated to minutes of the day; centered and scaled ([value – mean]/SD).

FPs = false positives. Number of detection events triggered by true FPs and non-target avian FPs (see Section 2.4); centered and scaled ([value – mean]/SD).

## 4.5.4.3 Testing Hypothesis C Regarding the Probability of Eagles Crossing the Rotor Swept Area of DTBird Equipped Turbines

Modeling the probability of an RSA crossing for golden eagles alone and for all eagles combined yielded no *Treatment Group* effects and no models that improved upon the null model. This outcome was not surprising given a paucity of consistent and reliable data to evaluate this dependent variable. Observations recorded by our data-entry technicians suggested that 9% of 105 golden eagle observations at turbines with DTBird systems operating in control mode a potential RSA cross, whereas a nominally lower 7% of 102 observations at turbines operating in treatment mode included a potential RSA cross. For all eagles combined, the comparisons were 13% of 209 observations included a potential RSA cross at control turbines, and 12% of 181 observations included a potential RSA cross at treatment turbines.

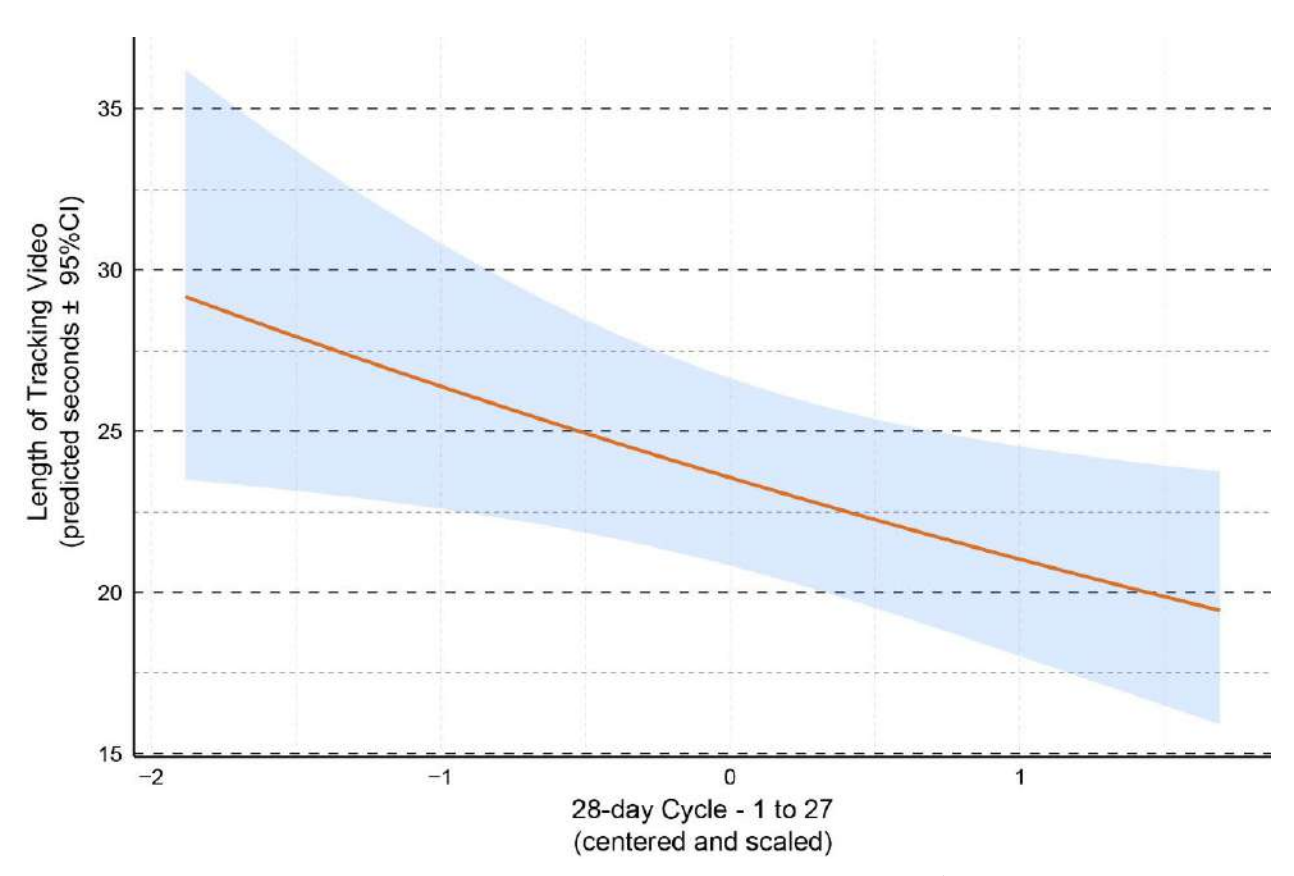


Figure 35. Illustration of predicted decline in the dwell time of eagles (golden and bald eagles combined) at DTBird turbines across the 27 28-day sampling cycles that composed this two-year experimental analysis.

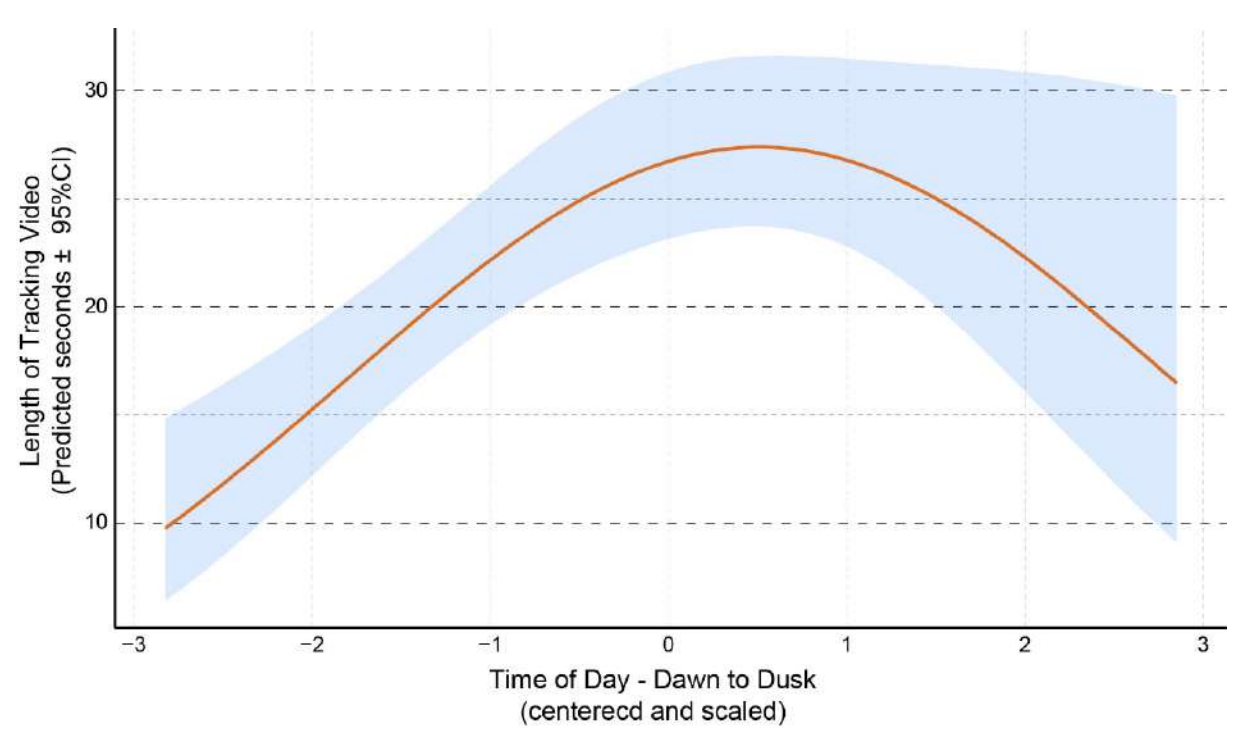


Figure 37. Illustration of predicted second-order relationship between the dwell time of eagles (golden and bald eagles combined) at DTBird turbines and time of day.

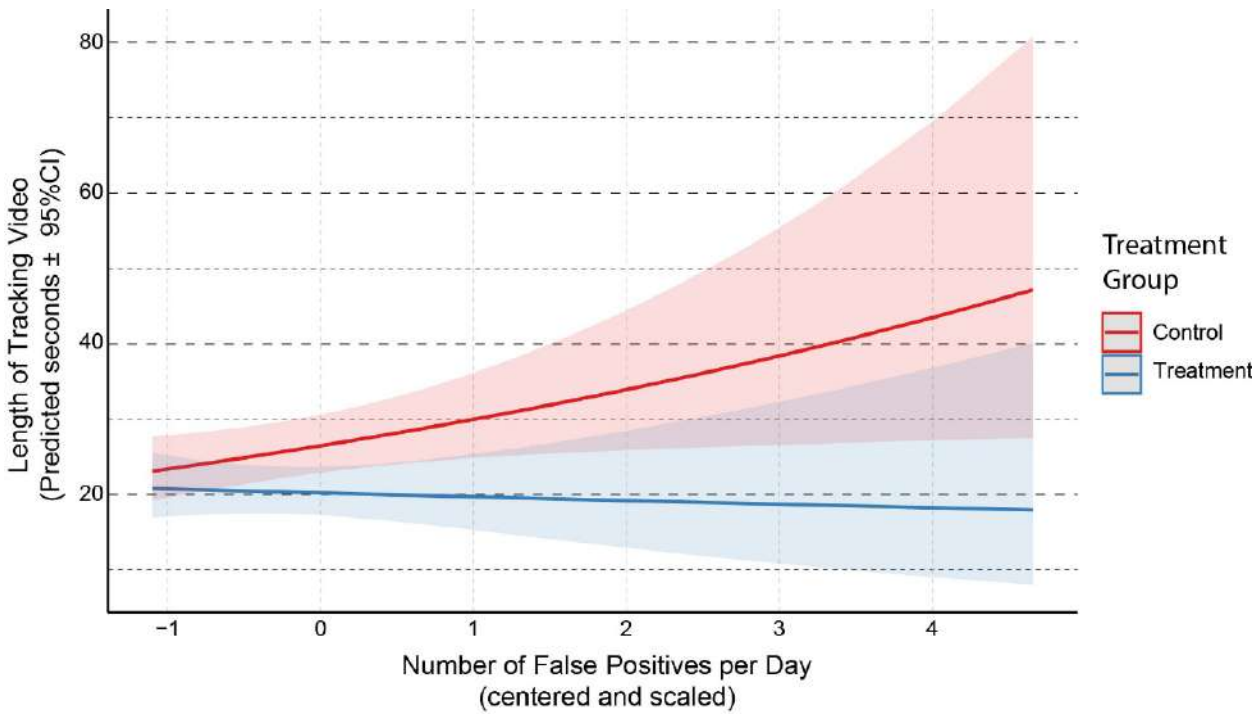


Figure 36. Illustration of predicted interactive relationship between treatment group and the daily numbers of false positives (FPs) that triggered deterrent signals in determining the dwell time of eagles (golden and bald eagles combined) around DTBird turbines.

#### 4.5.5 Multi-site Analysis of Collision Risk Reduction (Objective 5)

Our first approach to estimating the overall effectiveness of DTBird in reducing the risk of eagles entering the RSZ of spinning turbines involves the product of the estimated overall probability of detection from the UAV flight trials and the estimated probability of presumed effective deterrence from the behavioral analysis. For golden eagles alone, the results suggested variable performance at the two study sites as follows:

Manzana: 66% probability of detection x 79% probability of effective deterrence = 52% probability of reducing risk of entering RSZ of spinning turbines

Goodnoe Hills: 64% probability of detection x 60% probability of effective deterrence = 38% probability of reducing risk of entering RSZ of spinning turbines

Data for all eagles combined from the Goodnoe Hills (bald eagles rarely occur at the Manzana site) indicated similar results as for golden eagles alone, except that limited data suggested the probability of effective deterrence was higher for bald eagles than for golden eagles.

The Goodnoe Hills control-treatment experimental setup allowed for confirming that the addition of DTBird audio deterrents significantly increased the probability of effective deterrence compared to spinning turbines alone (deterrent signals muted). The difference amounted to a 1.8–2.3-fold (depending on signal type) increase in effective deterrence beyond the influence of spinning turbines for golden eagles alone, and a 2.1–2.9-fold increase for all golden and bald eagles combined, with bald eagles appearing more sensitive to the audio deterrents than golden eagles. We have no basis for comparison at the Manzana facility, but we suspect similar proportional effects would be evident there, perhaps heightened somewhat by evidence of greater overall deterrence effectiveness at that site.

Recalculating the estimates of DTBird's overall detection and deterrence effectiveness for golden eagles alone based on the added benefits estimate from the Goodnoe Hills results in the following modifications:

Manzana: 66% probability of detection x 40% probability of added effective deterrence = 24% probability of reducing risk of entering RSZ of spinning turbines

Goodnoe Hills: 64% probability of detection x 30% probability of effective deterrence = 19% probability of reducing risk of entering RSZ of spinning turbines

If we further narrow the focus to evaluating DTBird's effectiveness in detecting eagles (or UAV surrogates) and deterring eagles that were flying in core exposure locations (i.e., primary dissuasion-trigger risk zone within approximately 170 meters or less of the relevant turbines) and that we classified for behavioral analysis as at moderate to high risk of exposure to the RSZ of spinning turbines, the estimates of effectiveness across the two study sites increase markedly as follows:

Effectiveness of Spinning Turbines + Deterrents: 68% probability of detection x 80% probability of effective deterrence = 54% probability of reducing risk of entering RSZ of spinning turbines

Added Effectiveness of Deterrents: 68% probability of detection x 44% probability of effective deterrence = 30% probability of reducing risk of entering RSZ of spinning turbines

By eliminating from the equation eagles that were at low risk of approaching the RSZ of turbines and whose behavior was less likely to be influenced by either the spinning turbines or triggered audio deterrents, these heightened estimates of effectiveness are more likely to represent the true proportional benefits of the DTBird systems in reducing the risk of golden eagles entering the RSZ of focal turbines at the two study sites.

Our second approach to quantifying DTBird's overall effectiveness stems from the 2-year controlled experiment comparing eagle activity rates at DTBird installations operating in control mode with deterrents muted and in treatment mode with deterrents broadcasting normally. For golden eagles alone, the dissuasion-trigger and dwell-time models indicated similar reductions (27–29%) in indicative activity rates at turbines with the audio deterrents broadcasting compared to turbines with the audio deterrents muted. Assuming activity rates are positively correlated with the potential for collision risk, these percentage estimates of reduced activity levels in the vicinity of treatment turbines should represent roughly comparable estimates of DTBird's deterrence and collision-risk reduction benefits as those derived from our first estimation approach. Assuming this is true, the proportional estimates of collision-risk reduction from DTBird for golden eagles derived from the various estimation approaches were notably similar (19%, 27%, and 29%). Together these results suggest that, for golden eagles that fly anywhere within the calibrated maximum detection range for the species, operation of the DTBird automated detection and audio deterrence system can be expected to reduce the probability of approaching the RSZ of spinning turbines by 20–30%. Again we note, however, that further narrowing the focus to eagles (or surrogates) whose flight patterns exposed them to relatively high risk of entering the RSZ of turbines elevated the estimate of core effectiveness by at least 11%.

Properly scaled and tailored to the unique "survey" effort represented by the automated DTBird monitoring (not an easy task in this case due to highly variable turbine-specific sampling over 25 months), the dwell time data potentially could be translated to a surrogate for the preconstruction "eagle activity minutes" metrics used to project fatality rates at wind-energy facilities using the Bayesian collision risk model developed by the U.S. Fish & Wildlife Service (2013) and partners (New et al. 2015). If so, one could then theoretically compare independently projected post-construction fatality estimates tailored to the Goodnoe Hills based on dwell-time activity levels at control turbines versus treatment turbines to derive a quantitative estimate of projected fatality reduction from operation of DTBird at that facility. However, the magnitude of such a comparison (i.e., a reduced number of fatalities/year) could not be directly extrapolated to other facilities with different collision-risk infrastructure and eagle activity rates and behaviors. Instead, our perspective is that proportional/percentage estimates of effectiveness can be more easily tailored to projecting the magnitude of DTBird's beneficial effects in reducing collision risk at different facilities once initial pre-construction fatality projections tailored to the specific site are developed using the USFWS Bayesian risk model.

We designed this study to yield overarching insight about DTBird's effectiveness by sampling across an array of turbine-specific installations at two study sites, but with no expectation of producing facility-level estimates of effectiveness based on evaluating the influences of specific spatial arrays and densities of DTBird installations. As a result, the estimates of effects summarized herein should be thought of only as indicators of how individual DTBird systems can be expected to influence activity around the specific turbine on which a given system is installed. The estimated proportional effects can certainly be extrapolated across multiple turbines within a facility to develop a sense of the potential aggregate effects of installing multiple DTBird systems, but cannot be used to infer potential interactive benefits that could accrue from having multiple installations arrayed in particular configurations. Further, the comparative result we derived from the two study sites—one in a desert foothills landscape and one in temperate grassland ridgeline landscape—clearly indicated that DTBird's overall effectiveness may vary in different landscape/climatic settings with different resident and transient eagle populations and variable false-positive deterrent-triggering rates that may influence the eagle responses.

#### 4.5.6 Performance Reliability and Cost Analysis (Objective 6)

Sixteen DTBirdV4D8 units were manufactured in 2019 and delivered to Goodnoe Hills wind farm by the end of the year. 14 units operated under the evaluation and experimental design from August 2021 to September 2023. When including the overall cost of LIQUEN's Internal Services and R&D Department, the standard DTBirdV4D8 model sale cost (cameras model Falco and Larus software) is around \$18K - \$22K, and the yearly service sale cost around \$2K - \$3K. There are other project specific indirect costs for installation (around 4K\$-6K\$ per unit) and onsite maintenance (around 0.6 K\$-2K \$ per unit and year) (Table 27).

Table 2727. Actual Cost(s) to Install, Operate, and Maintain the DTBird system (2016-2024).

Project Cost(s)	Amount (USD)	Unitary cost for the 14 units (USD)
Actual purchase cost for 14 DTBirdV4D8 Units	\$208.619,64	\$14.901,40
Shipping and customs for DTBird Units to Goodnoe Hills*	\$17.114,49	\$1.069,66
Installation costs (travel and salary)	\$10.659,23	\$761,37
Year 1 service costs: 12 months of service, including travel costs to repair multiple maintenance issues August 2021 – July 2022	\$42.997,43	\$3.071,25
Year 2 service costs: 12 months of service, August 2022 – September 2023	\$35.199,41	\$2.514,24
Total	\$327.278,51	\$23.377,04

<sup>\*16</sup> units were delivered to the site

Ongoing technical complications reduced the team's ability to collect the intended level of data across the originally anticipated sample of turbines. PacifiCorp and Liquen experienced many technical troubles during repeated attempts to integrate installed DTBird units into the Goodnoe Hills Washington wind facility's SCADA and network.

Four units experienced repeated camera failures.

- Persistent malfunctions on GH40 and GH41 early in the commissioning process could
  not be resolved and the units were permanently removed from the experiment in favor of
  recovering other turbines further ahead in the commissioning process and maximizing
  the number of turbines commissioned in time for UAV flight trials. Parts from these units
  were used to resolve issues in other units.
- The malfunction on GH56 could not be resolved in time for the UAV flight trials or for the unit to participate in the Year 1 experiment, but PacifiCorp and Liquen continued to troubleshoot and with an onsite visit in C22-Q3 they have resolved the issues with this unit making it available for year 2 of the experiment.
- The onsite visit also revealed that during installation, equipment for G51 was mistakenly installed in G56 and equipment for G56 was installed in G51; data collected at G51 was mistakenly assigned to G56 and vice versa. Because of this confusion, data from G51 were not available for the analysis of the Year 1 experiment or from the UAV flight trial in July 2022. We are working to determine if data collected at G56 can be retrieved and included in further analysis of the experiment data
- Additionally, a month-long power outage at the Goodnoe Hills project site resulted in communication loss between DTBird and the SCADA system. The DTBird system was not responsible for this power loss and did not necessarily affect the system's ability to function as intended in detecting target species and triggering audio deterrents, it hindered our ability to evaluate the system in real time and the cause has not yet been resolved.

While some of the challenges resulted from less-than reliable maintenance at the study site, our experience suggests that reliable use of the DTBird system requires regular service at the systems. In addition to troubleshooting malfunctions, this includes:

- Two months of refining Liquen's detection algorithm in the field before installed DTBird systems can be considered fully commissioned
- Replacing all camera lenses at DTBird systems every six months, along with quality assurance to make sure camera positions have not changed during regular maintenance.

#### 4.6 Discussion

#### 4.6.1 DTBird Detection Performance

The specifications promulgated by Liquen (2017) specified that DTBird systems comparable to those installed at Manzana and Goodnoe Hills should be expected to result in a yearly average TFP deterrent trigger rate of 0.2–4.0 events/turbine/day, amounting to a total duration of 0.1–2.5 minutes/turbine/day. With seven turbines evaluated across 10 months, estimates from the Manzana study fell within these ranges: averages of 1.2–1.8 TFP deterrent triggers/turbine/day among the seven turbines and an overall average rate derived from the integrated analysis presented herein of 1.3 TFP detections with deterrent triggers/turbine/day. Similarly, the TFP

deterrent emittance rate (warning and dissuasion signals combined) was estimated to average 0.6–0.9 minutes/turbine/day among the seven installations, and the overall average rate derived from the integrated analysis presented herein was 0.8 minutes/turbine/day. Results from the Manzana study and other prior studies of DTBird technology (May et al. 2012, Aschwanden et al. 2015) formed the basis for the performance targets specified for the Goodnoe Hills study: maximum of 1.6–2.8 TFP deterrent triggers/turbine/day, and no more than 36% of all relevant detection events resulting from TFPs.

The overall-average TFP deterrent-triggering event rate at Goodnoe Hills across 23 months of sampling was 3.9 TFP deterrent triggers/turbine/day, which substantially exceeded the established performance target. However, after Liquen made additional adjustments to reduce the false positive rate in January 2023, the rate for the subsequent 7 months dropped to an average of 0.8 TFP deterrent triggers/turbine/day, well below the performance target. Similarly, although TFPs resulted in more than 50% of all detections that triggered deterrents before the adjustments were made, the proportion dropped to 25% post-adjustments, again falling below the established performance target. Moreover, in both cases the post-adjustment rates at Goodnoe Hills were lower than at Manzana, suggesting improvement in the filtering algorithms.

Across the periods of record, the overall TFP-caused deterrent signal durations (warning and dissuasion signals combined) on turbine-days when deterrents were triggered averaged 0.84 minutes/turbine/day at Manzana and 0.96 minutes/turbine/day at Goodnoe Hills. Post-adjustments, the combined deterrent signal duration rate at Goodnoe Hills fell only slightly to 0.95 minutes/turbine/day, despite the significant reduction in numbers of TFPs. This suggests that fewer signals averaged longer in duration per trigger after the adjustments, which may indicate that birds exposed to fewer TFP-triggered deterrents may have subsequently lingered more around the turbines with DTBird installations (a possible manifestation of negative habituation to prior excessive TFP signaling). Regardless, all documented signal duration rates fell below Liquen's desired standard of <2.5 minutes/turbine/day.

The results focused on variation in the prevalence of TFPs caused by insects during Goodnoe Hills Year 1 suggested the potential for substantial seasonal variation at this site, with a lesser magnitude of seasonal variation also evident at Manzana. However, the comparative results for Goodnoe Hills Year 2 suggested that the additional adjustments Liquen made in 2023 substantially mitigated/dampened what would otherwise have continued to be a significant source of excessive deterrent signaling during summer/fall at Goodnoe Hills (and perhaps at Manzana had earlier adjustments not been made there).

The notable contrasts in temporal patterns of sky artifact TFPs among years at Goodnoe Hills and between Manzana and Goodnoe Hills likely reflects a combination of factors. First, the documented difference in prevalence in Goodnoe Hills Years 1 and 2, showing a similar pattern as for insect TFPs, suggested that the further adjustments to the false positive filtering algorithms Liquen made in early 2023 probably also reduced the probability of sky artifact TFPs and contributed to the much lower post-adjustments sky artifact TFP rate in Year 2 compared to the corresponding cycles in Year 1. However, examining the patterns in relation to calendar months also suggested the possibility of weather-related differences in the source of TFPs at

the two sites. Specifically, sky artifact TFPs were generally common throughout the year at Goodnoe Hills and appeared to be particularly prevalent from spring through mid-summer (in Year 1 when not limited by additional filtering), whereas sky artifact TFPs appeared to be more restricted to late winter/early spring at Manzana. This suggests that the variable climatic regimes of the two study regions also contributed to the differences in the TFP rate between the two sites. Specifically, highly dynamic, partly cloudy skies tend to be more restricted to late winter/spring in the relatively xeric environment of the Mojave Desert where the Manzana site lies, whereas variable storminess and cloudy weather are often consistently more prevalent both during snowy winters and extending later in spring and into early summer in the Columbia Gorge region of Washington where the Goodnoe Hills site lies. Sky-artifact TFPs appear to arise more frequently when cloud cover is more prevalent and variable, dynamically producing more high-contrast elements that the DTBird system erroneously interprets as target movement.

Data from the Manzana and Goodnoe Hills study sites were also similar in showing some common species and seasonal patterns in the prevalence of detections reflecting the activities of NTAFPs. Common ravens were the most common source of NTAFPs at both sites, with generally higher activity during spring and fall migration, lowest activity during mid-summer in California, and moderate activity during winter in both areas.

Excessive false-positive detections hinder effective use of the DAP system for tracking activity and identifying exposure risk for focal species. This required investigators to sift through thousands of false positive records that did not trigger deterrents when the study motivation calls for screening such records (H. T. Harvey & Associates 2018). While burdensome for the purposes of this study, we did not find that excessive FPs led to negative habituation during the study period. Instead, we found evidence that excessive FPs may have led to positive habituation and potentially decreased risk to eagles. However, this does not address other potential burdens associated with FP detections excessively triggering deterrents, including potentially negative consequences of sound pollution to non-target wildlife and personnel. More generally, the results of this study clearly illustrate that limited AI discernment capabilities combined with audio deterrents may result in variable system effectiveness.

The probability of detection/false negatives models, resulting from the UAV flight trials, indicated similar patterns at the two study sites, with a nominally higher detection probability at Manzana (66%) than at Goodnoe Hills (64%). These estimates exceed the performance standard of 63% established as a basis for evaluating DTBird performance at Goodnoe Hills, though clearly nothing done to potentially improve the detection systems between the Manzana pilot study and the subsequent Goodnoe Hills study led to better performance at Goodnoe Hills. Instead, this outcome suggests consistent performance of the primary detection functions of the DTBird systems at both sites.

The probability of detection modeling analysis also provided useful perspective concerning factors that influence the overall probability of DTBird detecting an eagle-like UAV if it flies anywhere through the detection envelope projected based on calibration for golden eagles. The limitation of this analysis is that for flights that are not detected (false negatives) there are no reference points to use for precisely characterizing the flight, location, and environmental

characteristics at the time of a specific DTBird event to use as covariates. Consequently, we focused attention on discerning the influences of only a select few metrics derived by using GIS tools to calculate selected minimum and averaging position metrics across all points along a given sample flight. Nevertheless, this relatively simple approach illustrated variability in the probability of detection through the day, likely related to the relative influence of solar position and intensity.

More importantly, the results emphasized that the probability of detection was highest when the target flew at moderate distances from the turbine (generally high with average flight distances of 80–160 m) through the midsection of the camera viewshed (generally high with viewing angles from camera up to UAV of 25–40°). Conversely, the probability of detection averaged lower when the target flew either closer to or farther away from the camera or primarily within the lower or upper margins of the camera viewshed. These results are perhaps not surprising in suggesting that detection tends to be lower around the margins of the camera viewsheds and higher when a bird is flying at moderate distances from and in the center of a camera viewshed. The latter conditions are exactly when birds approaching a spinning turbine tend to be at greatest risk of entering the RSZ of spinning turbines. However, especially hunting or displaying raptors such as golden eagles often make very dynamic movements that can either rapidly drop them down from up high or pop them up from down low and quickly bring them into the RSZ danger zone at relatively close range. For this reason, poorer detection low and close or high and close to the turbine can result in problematic interactions with little time for the deterrents to trigger and discourage continued closer passage before entering the collision risk zone.

Characterizing the response-distance data for the three event types (detection, warning signal, and dissuasion signal) revealed some unexpected results. The average response distance for detection events (190 m) was longer than for dissuasion signals (176 m), as expected, but was considerably shorter than the 240-m theoretical maximum, calibrated detection distance. This result primarily reflected that initial detections often occurred when the UAV flew in low and first entered the detection envelope from the underside of the overall, inverted-cone-shaped envelope at relatively close distances to the turbine. Conversely, longer-than-expected response distances were comparatively uncommon.

A similar factor also contributed to the outcome for warning signals, where some initial triggers were expected to occur at distances of 100–170 (Figure 4); however, with the realm over which such warning signals could occur limited to less than one third of the perimeter area over which shorter detection distances could arise (Figure 4), the matching average detection and warning signal response distances were not expected. Reasons for this result are uncertain, but the outcome may reflect that, despite mostly common triggering calibration, longer than expected warning-signal response distances were proportionately less common than longer-than-expected detection response distances. This could be considered a desirable outcome, in that it means relevant targets were sometimes detected at greater than expected distances—increasing time for effective deterrent response if needed—but unnecessary warning signals targeting extra-distant birds were constrained.

The average response distance for triggering a dissuasion signal (176 m) nearly matched the calibrated core-envelope trigger distance for that event type (170 m), whereas the expectation was for a lower average reflecting a mix of expected response distances of approximately 170 m across the core-envelope surveillance area and 100-m in the outer, lower band of surveillance areas (see Figure 4). Instead, the observed outcome suggested that dissuasion signals were triggered more often than expected at distances exceeding the calibrated trigger distances. This result could be considered a beneficially conservative outcome in providing more time for an approaching bird to respond to a dissuasion signal, as long as it does not result in unnecessarily excessive triggering of the signals, with possible adverse consequences for non-target wildlife, facility staff, or facility neighbors (H. T. Harvey & Associates 2018).

The multi-site results illustrated notable random variation among turbines at the two study sites, and indicated that, given modeling of other random and fixed effects, the overall DTBird response distances tended to average marginally shorter at the Manzana study site compared to the Goodnoe Hills site. Reasons for this difference are uncertain, but it suggests that the overall targeting accuracy of the DTBird systems can vary slightly across different landscape settings, perhaps reflecting inherent differences in the overall visual clarity and complexity of different regional skies and landscape backdrops. DTBird does not reliably detect objects against a landscape, as opposed to sky, backdrop, and topographic complexity sometimes intrudes within the camera viewsheds to limit detectability. In this case, the proximate and elevated backdrop of the Tehachapi Mountains may have complicated detectability at the Manzana site more than the comparatively wide-open skies at the Goodnoe Hills site.

The multi-site results continued to support the notion that modeled variation in average response distances among the five UAV models we deployed in this study likely mimicked the kind of random variation that could be expected given eagles of different sizes and coloration patterns, such as those pertaining to differences among the sexes and age classes of golden eagles. As the initial Manzana site-specific analysis suggested (H. T. Harvey & Associates 2018), the demonstration that response distances tended to be relatively short for the AUV Custom aircraft is logical given its skinny tubular hind body and overall modest stature, with the relatively long-winged but slender Ranger aircraft also showing some of that tendency. In contrast, a tendency toward longer response distances was associated with the overall more eagle-like and robust-bodied AES Custom and Clouds models.

The multi-site results pertaining to the influence of cloud cover / sky backdrop on DTBird response distances suggested some similar patterns as the preceding site-specific analyses, but also some refinements. Specifically, all else equal, the updated analysis indicated that response distances generally increased as cloud cover increased and averaged significantly longer once the cloud cover extended throughout the viewshed under relatively uniform overcast skies. This outcome is logical in suggesting that the DTBird systems more readily detected the relatively dark eagle-like UAVs against relatively uniform high-contrast white or gray backgrounds than against less contrasting blue skies and or highly dynamic partly cloudy skies. These tendencies also mimic the challenges faced by observers scanning the skies for migrating raptors, where the presence of uniform cloud cover greatly increases the detectability of migrants passing overhead underneath the clouds (Bildstein et al. 2007).

The multi-site model uniquely indicated a significant positive association between response distances and UAV ground speed, which suggested that targeting performance improved significantly when a UAV was traveling relatively quickly from the perspective of the camera. This result may reflect that the DTBird detection algorithm focuses on targeting objects that both fill enough image pixels to warrant targeting from an estimated distance perspective, and that it perceives as moving in a manner that could be a flying bird. Our modeling results suggest that, across the UAV flight speeds documented in this study, slow-moving targets were generally harder for the DTBird system to detect than rapidly moving targets.

We included in our modeling effort consideration of a suite of variables as potential indicators of variation in the exposure of UAV profiles to the cameras, where greater profile exposure is expected to increase the accuracy of DTBird targeting based on calibrated settings. Our hypothesis was that the more a UAV climbs or descends, pitches up or down in the wind, rolls from side to side in the wind or while banking, or is generally bounced around by and quarters into the wind, the more the UAV profile should be exposed to the cameras and lead to more accurate targeting. Similar to the preceding site-specific modeling results, the final multi-site model continued to emphasize the importance of such variables in predicting DTBird response distances—specifically indicating a positive association with wind speed and the interactive influence of roll and pitch angels. The previous site-specific models also suggested that UAV Climb Rate was a relevant predictor, but that variable did not pan out as a significant predictor in the multi-site model, perhaps due to the combined data reflecting a stronger association with pitch and roll angles, with the former variable theoretically capturing a similar effect as variable climb rates (both descending and descending trajectories). The final model indicated relationships for wind speed and roll and pitch angles that were similar to the patterns reflected in the previous site-specific models, suggesting that response distances increased at higher wind speeds (UAV bouncing around more) and/or when the UAV was rolling side to side more, but only if the aircraft was not simultaneously pitching up or down to a substantial degree, because that combination would have caused the aircraft to stall and fall from the sky.

The initial Manzana site-specific model reflected a significant second-order relationship between response distances and the intensity of solar irradiation impinging on the UAV in the direction of the cameras. However, that relationship did not pan out again in the Goodnoe Hills site-specific model once we applied a more robust approach to developing that model. Similarly, none of the solar variables we considered were incorporated in the final multi-site model. There is no question that flying objects seen in the DTBird videos and targeted by the system routinely disappear from view when passing through major sunspots, and that high intensity solar insolation often increases the glare factor around such sunspots. In this case, however, we suspect that the combined-site dataset more effectively captured this effect in the refined relationship with sky backdrop/cloud cover. Specifically, situations where substantial sunspots obscured detectability were particularly prevalent under fair and partly cloudy skies, and greatly diminished when cloud cover was more complete, especially once overcast skies prevailed. Hence, the relative prevalence of sunspots may have been a primary driver behind the apparent positive relationship between response distances and cloud cover illustrated in the

multi-site model, to the exclusion of solar intensity or positioning proving to be of additional predictive value.

This investigation highlighted several flight metrics and environmental covariates that significantly influenced DTBird's detection and deterrent-triggering performance at the two wind-facility study sites. Here it is important to acknowledge that using eagle-like UAVs as surrogates for real eagles constrained the insights generated from the study. We think the fixedwing UAVs we used in the study did a good job of mimicking the non-flapping soaring and other flights of eagles, but were limited by not having wings that flap and tuck in the manner used by eagles to accomplish various maneuvers. The UAVs were also not capable of undertaking steep dive-and-roll or "roller-coaster" type display maneuvers that Golden Eagles sometimes make in pursuing prey or as part of their territorial behavior (Katzner et al. 2020). The degree to which more-dynamic wing action and flight maneuvers could alter the apparent targeting performance of the DTBird systems is uncertain. Wing flapping undoubtedly exposes more of a bird's profile to the cameras, at least intermittently; however, wing tucking does the opposite. In other words, these two components of real-bird flight dynamics may be offsetting factors that translate to average response distances similar to those reflected in the strictly fixed-wing UAV data we collected. If efforts to use UAVs as bird mimics are considered for similar future studies, some of the new robotic birds available today that actually fly with flapping wings should be considered, as long as the flapping rate of the robotic bird effectively mimics that of target birds of interest. In particular, a robotic bird with quick wingbeats and that flaps all the time to stay aloft would not be a good mimic for eagles, because eagles often spend most of their time in non-flapping soaring and sailing flight, rather than using powered flight (e.g., see Katzner et al. 2020).

Throughout these UAV flight trials, our effort was unexpectedly constrained to a high degree by incompatible weather and wind conditions. High winds and excess moisture in the air not only limited when we could fly, but also ultimately led to fatal crashes that took out four of the five aircraft we used, because we were compelled to fly in conditions that pushed the limits of tolerance for the light-weight, foam-bodied aircraft. On the positive front, having to replace several aircraft resulted in our flying a greater diversity of models than initially anticipated, which effectively mimicked some of the variability in DTBird performance that would likely occur given eagles of various sizes and color patterns. On the negative front, these unexpected complications significantly reduced the diversity of flight conditions during which we were able to conduct sampling flights, and substantially constrained the overall dataset compared to our original study-design projections. Nevertheless, we think the dataset we did amass provided valuable insight into how salient flight characteristics and environmental covariates influenced DTBird's performance in detecting eagles (or surrogates) and triggering deterrence signals compared to calibrated system settings.

Lastly, we acknowledge that the differences rated as statistically significant effects given our data sometimes amounted to effects magnitudes that may not have especially noteworthy biological or operational significance (e.g., 10–20 m differences in detection range for birds that may easily move farther than that in less than a second). However, our study was not designed to specifically quantify the relative effectiveness of different calibrated detection and deterrent

triggering distance thresholds nor the spatiotemporal aspects of what an eagle requires as deterrent warning to avoid calamity under different flight conditions. Therefore, we have no firm basis for presuming what may be biologically/operationally significant in this context.

#### 4.6.2 Behavioral Differences at Treatment vs Control Turbines

The *in situ* two-year experiment at Goodnoe Hills, Washington failed to reveal a significant overall treatment effect on the probability of a target bird triggering a dissuasion signal (Hypothesis A), but did reveal an effect of treatment on dwell time (Hypothesis B).

One possible reason the former relationship was not apparent concerns the efficacy of warning signals as a potential means to reduce the probability of an eagle triggering a subsequent dissuasion signal. Although eagles triggered warning and dissuasion signals with similar frequencies overall, a large majority of the triggered dissuasion signals were not preceded by a prior warning signal. In other words, the idea that broadcasted warning signals could be expected to reduce the probability of triggering a subsequent dissuasion signal actually did not apply very often. Two potential explanations for this pattern are: 1) within the primary detection envelope where sequential warning and dissuasion signaling is expected when relevant, the DTBird detection systems frequently did not detect eagles until they had already reached the closer dissuasion-triggering envelope; and 2) eagles often flew in relatively low and entered the detection envelope relatively close to the turbine where dissuasion signals were immediately triggered without a prior warning signal.

The significant effects of Treatment Group in the dwell-time models translated to predictions of golden eagles and all eagles combined averaging 24-27% less time dwelling in the vicinity of DTBird systems operating with their deterrents broadcasting normally compared to systems with muted deterrents. The golden eagle dissuasion-trigger model indicated a similar-albeit statistically nonsignificant-29% decrease in the probability of dissuasion triggers at treatment turbines. Quantifying estimated reductions in the probability of dissuasion triggers at treatment turbines based on the all-eagles model was complicated by the presence of interactions with both categorical (Cloud Cover) and continuous (FPs per Day) covariates. Under most sky conditions from partly cloudy to overcast, eagles tended to trigger approximately 9-30% fewer dissuasion signals at turbines with DTBird deterrents broadcasting normally (i.e., consistent with research Hypothesis A), whereas a much stronger, opposite pattern was shown when fair skies prevailed. Reasons for this unexpected anomaly are uncertain, but one possibility is that visibility typically tends to be clearer overall during fair weather. Better visibility might have allowed the eagles to more easily perceive the spinning turbines, take heed of the broadcasting deterrents, but also remain more comfortable flying and foraging closer to the turbines with less concern for the potential collision risk. In contrast, the indicated interactive relationship between Treatment Group and FPs per Day indicated further clear support for Hypothesis A in demonstrating that the positive effect of broadcasted deterrents at treatment turbines deterring eagles from triggering dissuasion signals was accentuated by higher FP deterrent-triggering activity, whereas no such effect was evident at control turbines. The difference in the probability of dissuasion triggers at control versus treatment turbines was nominal when the FP deterrent

triggering rate was low, but was approximately a 60% lower at treatment turbines when the FP deterrent triggering rate was elevated.

The model focused on presumed golden eagles triggering dissuasion signals indicated a novel relationship with monitoring *Year* as a predictor, suggesting that the probability of golden eagles triggering dissuasion signals declined overall by approximately 46% across the facility during Year 2 of the study. Neither *Year* nor *28d Cycle* emerged as a significant predictor in the alleagles dissuasion-trigger model; however, *28d Cycle* emerged as an important predictor in the dwell-time models for both golden eagles alone and all eagles combined. Similar to the result for golden eagles and dissuasion triggers, the indicated relationship for *28d Cycle* was an overall declining trend across the 2-year study in the dwell time of golden eagles alone and all eagles combined. Given that these trends did not emerge differentially around DTBird equipped turbines operating in treatment versus control mode, the overall pattern may provide evidence of positive habituation through time among resident and seasonally resident eagles. As such eagles became increasingly exposed to deterrents being broadcasted regularly around the perimeter of the facility, they might have grown increasingly wary of dwelling for extended periods in the vicinity.

Here it is important to note that this potential habituation pattern could have been accentuated by two factors: 1) an unusually high overall FP triggering rate through the first 19 months of the study, until Liquen was authorized to undertake further fine-tuning of the filtering algorithms to reduce the FP rate; and 2) due to an extended failure of communications between the DTBird and turbine SCADA systems following a forced 24-day site-wide power outage, all DTBird systems operated in default mode after May 2023, whereby the deterrents were being triggered whether or not the focal turbine was spinning. The first factor substantially reduced the overall FP deterrent triggering rate after January 2023; however, the second factor may have largely offset that effect by increasing the overall prevalence of superfluous deterrent triggering in after May 2023. This combination likely maintained an elevated rate of deterrent triggering throughout most of the 2-year study, which could have accelerated the pace of any positive habituation effects. What is equally important to note here, though, is that the results do not point to possible negative habituation, which would involve eagles learning to ignore the deterrents and remain at risk.

All of the models we developed reflected a pronounced diel pattern of variation in the documented eagle responses that operated independently of the applied deterrent treatment regime. Most of the modeled results captured the relationship as increasing strongly—whether the probability of dissuasion triggers or average dwell time—from dawn until reaching a midafternoon peak, followed by a lesser, gradual decline until dusk. We think this predominant pattern probably reflects the common general activity levels of eagles and other raptors during a typical day, with the flight activity of especially large soaring raptors typically dependent on thermal and wind activity increasing as the day warms up to provide energy-saving lift for active foraging, patrolling, and other flight-dependent activities.

Finally, Wind Speed emerged as significant covariate influencing the probability of golden eagles triggering dissuasion signals, independently of the implemented control-treatment design. The

indicated effect of higher wind speeds generally reducing the probability of dissuasion triggers suggests that the faster the turbines are spinning the more they themselves act as a deterrent to visually acute eagles, who then remain farther away from the perceived danger independent of the influence of DTBird deterrent signaling.

#### 4.6.3 Behavior Responses Across Both Sites

The results of the multi-site, integrative analysis of large-raptor behavioral responses to broadcasted DTBird audio deterrents illustrated noteworthy differences in the apparent responsiveness of golden eagles, turkey vultures, and buteos at the two wind facilities located in different landscape settings. When exposed to broadcasted deterrents, on average, the birds at the Manzana facility in a California foothills/desert landscape appeared to respond more effectively than their counterparts at the Goodnoe Hills facility occupying a ridgetop/grassland landscape bordering the Columbia River in Washington. Reasons for this difference are uncertain but could reflect the influence of differences in the relative proportions of different species and residents versus transients frequenting the two sites, with variable sensitivities and habituation tendencies. Alternatively, variable wind and climate regimes may have differentially influenced the response behaviors of birds at the two sites by influencing birds' abilities to hear and respond to the deterrents. Wind speeds recorded as part of the records analyzed for this analysis averaged and gusted slightly higher at the Goodnoe Hills (average 6.3 ± SD of 3.41 m/s, maximum 21.1 m/s) than at the Manzana site (average 5.7 ± 2.79 m/s, maximum 17.0 m/s); however, the modeling results suggested that higher wind speeds tended to increase rather than decrease the probability of effective deterrence. Note, however, that eagles tended to be increasingly more responsive to the deterrents than vultures and buteos as wind speeds increased, and there was some suggestion that, for golden eagles, the probability of effective deterrence tended to be higher at the Goodnoe Hills than at the Manzana site at moderate and higher wind speeds. These tendencies may have helped to ameliorate the evident site-specific difference in deterrence effectiveness during periods of high wind speeds and power production at the Goodnoe Hills. Regardless, the documented site differences clearly suggest that effectiveness of the DTBird deterrence system may vary significantly depending on the local landscape characteristics and species assemblages.

Both the multi-species and golden eagle models also reflected at least marginally significant relationships between the probability of deterrence and wind speed. Increasing wind speeds generally resulted in a higher probability of effective deterrence for larger eagles and vultures, but not for smaller buteos. We included wind speed as a potential predictor in the LGLMs thinking that higher wind speeds could reduce the probability of effective deterrence by either limiting a bird's ability to hear the deterrents and/or hindering its ability to maneuver effectively in response to the deterrents. The modeling results suggested our hypothesis was incorrect, however, at least for the larger eagles and vultures. One possibility is that faster-spinning turbine blades themselves act as a greater deterrent to approaching larger birds and more effectively amplify the effect of the audio deterrents. It is also possible that higher wind speeds actually facilitate greater maneuverability and responsiveness in many cases for large soaring raptors, which often strongly rely on the energy savings provided by wind-driven (or thermal) lift. In contrast, smaller buteos are generally more maneuverable and more easily constrained by

strong winds, such that increasing wind speeds may be a detriment rather than a benefit for them in influencing their ability to respond effectively to the deterrents.

Evidence that the probability of effective deterrence tended to be highest for birds we classified as at moderate risk of exposure to turbine collisions, rather than for those we classified as high risk of exposure, also may relate to birds having enough time and room to maneuver effectively in response to the deterrents. We expected responsiveness to be lower for birds at low risk of exposure, because such birds have little need to divert their flights to avoid risk. In contrast, birds at high risk of exposure may appear less responsive simply because they have less time and room to respond effectively if not deterred before entering a high-risk zone.

Accurately characterizing the behavioral responses of raptors to the DTBird audio deterrents was greatly confounded by two primary factors: 1) low-resolution video recordings frequently obscured the details of bird behaviors, such as changes in flapping rates, distinct "flinches" and head movements, and subtle flight path alterations; and 2) seeking insight about the degree of response based on evaluating two-dimensional renderings of three-dimensional movement scenarios, especially pertaining to measuring flight diversion angles as a relevant criteria. With this perspective in mind, if eagles and other raptors tended to respond to the deterrents less dramatically, but nonetheless effectively, at the Goodnoe Hills, then the limitations outlined above could have more easily reduced our ability to effectively discern subtler effective responses at the Goodnoe Hills. For this reason, comparing the proportions of only confirmed effective responses at the two sites may be misleading, as opposed to focusing on the combination of effective and potentially effective responses as a better comparative indicator of relative success.

The Goodnoe Hills results clearly did not meet the performance metric established based only on confirmed effective responses from the Manzana study. Further, combining CE and PE responses reduces but does not eliminate the indication of greater deterrence effectiveness at the Manzana facility, but it does result in effectiveness metrics for both sites and all species groups that exceed the ≥50% effectiveness threshold established as performance metric for this DOE-sponsored research project (Table 14). Taking this approach may overestimate DTBird's effectiveness to some degree. We expect, however, that there is a higher likelihood of underestimating the system's effectiveness by limiting the results to confirmed effective responses, because of our limited ability to confidently discern and classify relatively subtle but nonetheless effective behavioral responses.

The control-treatment setup for the Goodnoe Hills study provided further insight about the degree to which responses to spinning turbines and broadcasting audio deterrents contributed to the effectiveness statistics presented herein. Based on the comparative control-treatment results and for all analyzed groups and species, broadcasted deterrents consistently resulted in at least a doubling of the proportion of cases where an effective or potentially effective response was evident. Further, results for all four analyzed species groups consistently indicated that confirmed effective responses were more common when the deterrent signals were broadcasting, and that birds exhibiting no apparent response at the time a deterrent was triggered were always significantly more common when the deterrents were triggered only

virtually. However, we had no ability to conduct a similar control-treatment evaluation at the Manzana site to provide comparatively robust insight to determine if a similar proportional effect of spinning turbines and broadcasted deterrents would apply at the two sites.

In summary, the results of this investigation pointed to noteworthy differences in the apparent effectiveness of the DTBird deterrence system in different landscape settings, for undetermined reasons but with species and wind-regime differences potentially important. The results from the Goodnoe Hills site in Washington suggested a lower level of deterrence than the results from the Manzana site in California, which fell well below the ≥50% effective deterrence performance standard, when including confirmed effective responses alone. However, when considering both confirmed and potentially effective behavioral responses, the probability of effective deterrence given broadcasted deterrents exceeded the established performance standard for golden eagles at both the Manzana (79%) and Goodnoe Hills (61%) sites, with similar results obtained for the multi-species group and vultures and buteos as independent comparative groups.

#### 4.6.4 Eagle Collision Risk Reduction

The overarching goal of this research has been to evaluate the effectiveness of DTBird in detecting and discouraging especially golden eagles (*Aquila chrysaetos*), but also bald eagles (*Haliaeetus leucocephalus*) and other large soaring raptors from approaching the rotor swept zone (RSZ) of operating wind turbines. We initially intended to translate our results to applying the Bayesian collision risk model (CRM) recommended by the U.S. Fish and Wildlife Service (2013; and see New et al. 2015), using eagle flight times recorded by DTBird at control and treatment turbines as a proxy for eagle activity. However, we found comparisons of proportional responses to be most germane, because any estimates we could generate portraying absolute reductions in the number of eagles killed per year would be site specific, whereas proportional estimates have the potential to be applied across sites based on site-specific fatality projections. Therefore, we sought to estimate DTBird's overall effectiveness in reducing the risk of eagles entering the RSZ of spinning turbines, based on multiple complementary approaches.

The first approach involved combining probability of detection estimates derived from the UAV flight trials with probability of effective deterrence estimates derived from the behavioral analyses. The multiplicative combination of these estimates yielded an estimated 52% reduction in the probability of confirmed golden eagles entering the RSZ of spinning turbines with broadcasted deterrents at the Manzana facility, and a 38% reduction at the Goodnoe Hills facility. Data for all eagles combined from Goodnoe Hills (rare occurrences of bald eagles at Manzana) revealed similar results for golden eagles alone, except limited data suggested effective deterrence was higher for bald eagles than for golden eagles.

The Goodnoe Hills control-treatment experimental setup confirmed the addition of DTBird audio deterrents increased the likelihood of effective deterrence compared to just spinning turbines alone with deterrent signals muted. Recalculating the estimates of detection and deterrence effectiveness for golden eagles alone based on the Goodnoe Hills control-treatment results yielded a 24% probability of DTBird audio deterrents reducing risk of entering the RSZ of spinning turbines at Manzana and 19% for Goodnoe Hills. Narrowing the focus further to

estimating DTBird's effectiveness when an eagle-surrogate UAV was flying in core exposure locations and *in situ* eagles were classified for behavioral analysis as at moderate to high Preexposure Risk revealed that spinning turbines plus deterrents resulted in a 68% probability of reduced risk, with the added effectiveness of deterrents alone reducing estimated risk by 37%.

The second approach used to estimate risk reduction from DTBird was based on the Goodnoe Hills 2-year control-treatment experiment involving randomized daily rotations of muted and broadcasted deterrents. For golden eagles alone, the dissuasion-trigger (dependent variable = probability of triggering a dissuasion signal) and dwell-time (dependent variable = eagle dwell time as reflected in extent of video recording) models yielded similar estimated reductions (27–29%) in the two dependent variables at DTBird-equipped turbines when the audio deterrents were broadcasted compared to when the deterrents were muted. Combining insight from both approaches suggested that, for golden eagles that fly within the calibrated maximum detection range for the species, operation of DTBird can be expected to reduce the overall likelihood of approaching the RSZ by 20–30%, with that estimate potentially further elevated to near 40% for birds at moderate to high Preexposure Risk of entering the RSZ.

The dwell time data could potentially be used as a surrogate for the pre-construction "eagle activity minutes" metric used to project fatality rates at wind-energy facilities using the Bayesian collision risk model developed by the U.S Fish and Wildlife Service. We could have independently compared projected post-construction fatality estimates tailored to the Goodnoe Hills based on dwell time at control turbines versus treatment turbines to create an estimate of fatality reduction. However, a comparison (# of fatalities/per year) of that scale could not be extrapolated to other facilities with different collision risk infrastructure and eagle activity rates and behaviors. Therefore, we determined a better approach was to present percentage estimates of DTBird's beneficial effects in reducing post-construction collision risk, which could potentially be tailored to match initial pre-construction facility projections tailored to specific sites using the USFWS Bayesian risk model. The results from the two study sites—one in a desert foothills landscape and one in temperate grassland ridgeline landscape—clearly indicated that DTBird's overall effectiveness may vary in different landscape/climatic settings with different resident and transient eagle populations, and variable false-positive deterrent-triggering rates that may influence the eagle responses.

#### 4.7 Conclusion

Despite falling well short of our intended 2-year sampling design due to factors beyond our control, the results of our careful analyses yielded noteworthy insight about the factors affecting the ability of the DTBird deterrent system to reduce the activity of eagles around turbines where the deterrents were broadcasting normally. Particularly notable were indications of possible long-term positive habituation reducing the dwell time of eagles around the DTBird turbines independent of the control-treatment experimental design, likely reflecting the overarching influence of an atypically elevated overall deterrent triggering rate across the installed DTBird systems. We suspect that, had frequent operational failures not caused major unexpected imbalances in our intended sampling design and had the overall deterrent triggering

not been artificially elevated by various factors, our ability to demonstrate conclusive patterns of interest concerning the proximate effectiveness of DTBird would have been even greater.

Efficiently focusing a deterrent system such as DTBird on specific species of conservation interest is often the primary objective for facility managers. In this context, avoiding unnecessary detections and deterrent signaling caused by non-focal bird species will often be important to minimize the potential risk of negative habituation.

Natural seasonal cycles in the distribution and abundance of insects contributing to TFPs and birds contributing to NTAFPs are expected, but may also occur relative to sky artifacts as solar and cloud cover variations greatly influence that source of TFPs. If predictable enough through time, it may be possible to improve the DTBird false-positive filtering algorithms to be more sensitive to these factors and thereby efficiently reduce the overall false positive rate.

Collectively, our results suggest the following should be considered in future DTBird applications:

- DTBird systems should not be considered fully commissioned and maximally effective until at least 2 months after Liquen declares the systems "commissioned" and they complete fine-tuning to minimize false positives caused by spinning blades and other factors.
- Liquen should prioritize additional improvements of the DTBird filtering algorithms to further reduce the potential for especially blade-related, insect, and sky-artifact TFPs, which result in substantial clutter within the DAP and unnecessarily trigger an abundance of potentially deleterious deterrent signals.
- Liquen should develop and implement AI systems better able to distinguish target species. NTAFPs represent a complicated management issue, in that protecting all native bird species from unnecessary human-caused mortality is a worthy objective, but excessive deterrent triggering by nontarget birds could also have negative consequences.
- Regular replacement of camera lens cover to avoid solar degradation that can radically effect the clarity of the recorded videos
- Potentially use a higher resolution camera system and sophisticated AI/ML algorithms
  to obviate the need to manually screen the recorded videos to identify and enumerate
  detected targets and evaluated their behavior. This is especially necessary when
  evaluating the technology, but could have additional benefits as well.

#### 4.8 Literature Cited

ArduPilot Dev Team. 2021. Mission Planner. Version 1.3.77. <a href="https://firmware.ardupilot.org/Tools/MissionPlanner">https://firmware.ardupilot.org/Tools/MissionPlanner</a>. Accessed July 2022.

Bates, D., M. Maechler, B. Bolker, and S. Walker. 2015. Fitting Linear Mixed-Effects Models Using Ime4. Journal of Statistical Software 67:1-48. DOI 10.18637/jss.v067.i01.

Bildstein, K. L., J. P. Smith, and R. Yosef. 2007. Migration counts and monitoring. Pages 101–116 *in* D. M. Bird and K. L. Bildstein (Editors), Raptor Research and Management Techniques. Hancock House Publishers, Blaine, WA, USA, and Surrey, British Columbia, Canada.

Bolker, B. M. 2023. Package Ime4: linear mixed-effects models using 'eigen' and S4. Version 1.1-35.1 <a href="https://www.rdocumentation.org/packages/lme4">https://www.rdocumentation.org/packages/lme4</a>. Accessed December 2023.

Bolker, B. M., M. E. Brooks, C. J. Clark, S. W. Geange, J. R. Poulsen, M. H. H. Stevens, and J-S. S. White. 2009. Generalized linear mixed models: a practical guide for ecology and evolution. Trends in Ecology and Evolution 24:127–135.

Brooks, M., B. Bolker, K. Kristensen, M. Maechler, A. Magnusson, H. Skaug, A. Nielsen, C. Berg, and K. van Bentham. 2023. Package'glmmTMB'. Version 1.1.8. https://https://www.rdocumentation.org/packages/.

Brooks, M. E., K. Kristensen, K. J. van Benthem, A. Magnusson, C. W. Berg, A. Nielsen, H. J. Skaug, M. Mächler, and B. M. Bolker. 2017a. glmmTMB balances speed and flexibility among packages for zero-inflated generalized linear mixed modeling. The R Journal 9:378–400.

Brooks, M. E., K. Kristensen, K. J. van Benthem, A. Magnusson, C. W. Berg, A. Nielsen, H. J. Skaug, M. Mächler, and B. M. Bolker. 2017b. Modeling zero-inflated count data with glmmTMB. BioRxiv:132753. <a href="https://www.biorxiv.org/content/biorxiv/early/2017/05/01/132753.full.pdf">https://www.biorxiv.org/content/biorxiv/early/2017/05/01/132753.full.pdf</a>. glmmTMB/versions/1.1.8. Accessed December 2023.

Burnham, K. P., and D. R. Anderson. 2002. Model Selection and Multimodel Inference: A Practical Information-Theoretic Approach. Second edition. Springer, New York, NY.

Burnham, K. P., and D. R. Anderson. 2010. Model Selection and Multimodel Inference: A Practical Information-Theoretic Approach. Second Edition. Springer, New York, NY, USA.

De Lucas, M., G. F. Janss, D. P. Whitfield, and M. Ferrer. 2008. Collision fatality of Raptors in wind farms does not depend on Raptor abundance. *Journal of Applied Ecology*, 45(6), 1695–1703. https://doi.org/10.1111/j.1365-2664.2008.01549.x.

Erickson, W. P., G. D. Johnson, D. P. Young, Jr.. 2005. A summary and comparison of bird mortality from anthropogenic causes with an emphasis on collisions. Pages 1029-1042 *in C. J.* Ralph, C. and T. D. Rich (Editors). Bird Conservation Implementation and Integration in the Americas: Proceedings of the Third International Partners in Flight Conference. 2002 March 20-24; Asilomar, California, Volume 2 Gen. Tech. Rep. PSW-GTR-191. Albany, CA: U.S. Dept. of Agriculture, Forest Service, Pacific Southwest Research Station.

Fernie, A. 2012. TLogDataExtractor. Version 1.1. <a href="https://onedrive.live.com/?cid=2B4DC8F6BD223F57&id=2B4DC8F6BD223F57%212440">https://onedrive.live.com/?cid=2B4DC8F6BD223F57&id=2B4DC8F6BD223F57%212440</a>. Accessed August 2022.

Fisher, N. I. 1995. Statistical Analysis of Circular Data. Cambridge University Press, Cambridge, UK.

Friendly, M., and D. Meyer. 2016. Discrete Data Analysis with R: Visualization and Modeling Techniques for Categorical and Count Data. CRC Press, New York, New York, USA.

Hair, J.F., R. L. Tatham, and R. E. Anderson. 1998. Multivariate Data Analysis. Fifth edition. Prentice Hall, Englewood Cliffs, NJ, USA.

Hartig, F. 2019. Package DHARMa: residual diagnostics for hierarchical (multi-level/mixed) regression models. Version 0.2.6. <a href="https://cran.r-project.org/web/packages/DHARMa/index.html">https://cran.r-project.org/web/packages/DHARMa/index.html</a>. Accessed August 2022.

Hartig, F. 2021. DHARMa: Residual Diagnostics for Hierarchical (Multi-Level / Mixed) Regression Models. R package version 0.4.4. https://CRAN.R-project.org/package=DHARMa.

Hanagasioglu, M., J. Aschwanden, R. Bontadina, and M. de la Puente Nilsson. 2015. Investigation of the Effectiveness of Bat and Bird Detection of the DTBat and DTBird Systems at Calandawind Turbine. Final Report. Prepared for the Swiss Federal Office of Energy Research Program, Wind Energy and Federal Office for the Environment Species, Ecosystems, Landscapes Division. Bern, Switzerland.

Hosmer, D. W., and S. Lemeshow. 1989. Applied Logistic Regression. John Wiley & Sons, New York, NY, USA.

H. T. Harvey & Associates. 2018. Evaluating a Commercial-Ready Technology for Raptor Detection and Deterrence at a Wind Energy Facility in California. Research report. Los Gatos, California. Prepared for the American Wind Wildlife Institute, Washington, D.C.

Hunt, G. 2002. Golden Eagles in a Perilous Landscape: Predicting the Effects of Mitigation for Wind Turbine Blade-Strike Mortality. University of California-Santa Cruz. Prepared for the California Energy Commission, Public Interest Energy Research, Sacramento, CA, USA.

Jeffreys, H., 1939. Theory of Probability. Oxford University Press, Oxford, UK.

Katzner, T. E., M. N. Kochert, K. Steenhof, C. L. McIntyre, E. H. Craig, and T. A. Miller. 2020. Golden Eagle (*Aquila chrysaetos*), version 2.0. *In* P. G. Rodewald and B. K. Keeney (Editors), Birds of the World. Cornell Lab of Ornithology, Ithaca, NY, USA. <a href="https://doi.org/10.2173/bow.goleag.02">https://doi.org/10.2173/bow.goleag.02</a>.

Length, R. 2023. emmeans: Estimated Marginal Means, aka Least-Squares Means. R package version 1.8.6. <a href="https://CRAN.R-project.org/package=emmeans">https://CRAN.R-project.org/package=emmeans</a>.

Lüdecke, 2022. Package ggeffects: create tidy data frames of marginal effects for 'ggplot' from model outputs. Version 1.1.3. <a href="https://cran.r-project.org/web/packages/ggeffects/index.html">https://cran.r-project.org/web/packages/ggeffects/index.html</a>.

Lüdecke, D. 2023. sjPlot: Data Visualization for Statistics in Social Science. R package version 2.8.14. <a href="https://CRAN.R-project.org/package=sjPlot">https://CRAN.R-project.org/package=sjPlot</a>.

Magnussen, A., H. J. Skaug, A. Nielsen, C. W. Berg, K. Kristensen, M. Maechler, K. J. van Bentham, N. Sadat, B. M. Bolker, and M. E. Brooks. 2022. Package glmmTMB: generalized linear mixed models using template model builder. <a href="https://CRAN.R-project.org/package=glmmTMB">https://CRAN.R-project.org/package=glmmTMB</a>.

McFadden, D. 1974. Conditional logit analysis of qualitative choice behavior. Pages 105–142 *in* P. Zarembka, editor, Frontiers in Econometrics. Academic Press, New York, USA and London, UK.

May, R., Ø. Hamre, R. Vang, and T. Nygård. 2012. Evaluation of the DTBird Video-System at the Smøla Wind-Power Plant: Detection Capabilities for Capturing Near-Turbine Avian Behaviour. NINA Report 910. Norwegian Institute for Nature Rese arch, Trondheim, Norway.

Nakagawa, S., and H. Schielzeth. 2013. A general and simple method for obtaining R<sup>2</sup> from generalized linear mixed-effects models. Methods in Ecology and Evolution 4:133–142. https://doi.org/10.1111/j.2041-210x.2012.00261.x.

New, L., E. Bjerre, B. Millsap, M. C. Otto, and M. C. Runge. 2015. A collision risk model to predict avian fatalities at wind facilities: An example using golden eagles, Aquila Chrysaetos. PLOS ONE, 10(7). https://doi.org/10.1371/journal.pone.0130978.

R Core Team. 2023. R: A language and environment for statistical computing. R Foundation for Statistical Computing, Vienna, Austria. <a href="https://www.R-project.org/">https://www.R-project.org/</a>.

Smallwood, K. S. 2013. Comparing bird and bat fatality-rate estimates among North American wind-energy projects. *Wildlife Society Bulletin*, *37*(1), 19–33. <a href="https://doi.org/10.1002/wsb.260">https://doi.org/10.1002/wsb.260</a>.

Shah, M. 2023. Reply to inquiry: Could someone explain me about Nagelkerke R Square in logit regression analysis? Pakistan Institute of Development Economics. ResearchGate post, February 20, 2023.

https://www.researchgate.net/post/Could\_someone\_explain\_me\_about\_Nagelkerke\_R\_Square\_in\_Logit\_Regression\_analysis.

Schielzeth, H., N. J. Dingemanse, S. Nakagawa, D. F. Westneat, H. Allegue, C. Teplitsky, D. Réale, N. A. Dochtermann, L. Z. Garamszegi, and Y. G. Araya-Ajoy. 2020. Robustness of linear mixed-effects models to violations of distributional assumptions. Methods in Ecology and Evolution 11:1141–1152. https://doi.org/10.1111/2041-210X.13434.

Straffi, P. 2016. On Screen Protractor. v0.5. <a href="https://sourceforge.net/projects/osprotractor">https://sourceforge.net/projects/osprotractor</a>. Accessed June 2023.

Symonds, M. R., and A. Moussalli. 2011. A brief guide to model selection, multimodel inference and model averaging in behavioural ecology using Akaike's information criterion. Behavioral Ecology and Sociobiology 65:13–21.

Tukey, J. 1949. Comparing individual means in the analysis of variance. Biometrics 5:99–114.

U.S. Fish and Wildlife Service. 2013. Eagle Conservation Plan Guidance Module 1 – Land-based Wind Energy, Technical Appendix D. Version 2. Division of Migratory Bird Management, Washington, D.C., USA.

https://www.fws.gov/guidance/sites/guidance/files/documents/eagleconservationplanguidance.pdf.

Wickham, H. 2016. ggplot2: Elegant Graphics for Data Analysis. Springer-Verlag New York, NY, USA.

Wood, S. N. 2017. Generalized Additive Models: An Introduction with R. Second edition. CRC Press, Taylor & Francis Group, New York, NY, USA.

Zar, J. H. 1998. Biostatistical Analysis. Pearson.

Zuur, A. F., E. N. Ieno, and C. S. Elphick. 2010. A protocol for data exploration to avoid common statistical problems. Methods in Ecology and Evolution 1:3–14.

Zuur, A. F., E. N. Ieno, N. J. Walker, A. A. Saveliev, and G. M. Smith. 2009. Mixed Effects Models and Extensions in Ecology with R. Springer, New York, NY, USA.

### Section 5. Technical Scope and Objectives

## 5.1 Budget Period 1: Develop a detailed, peer-reviewed study design for expanded study, and evaluate results of California pilot study (Tasks 1-4)

<u>Timeline:</u> 1 June 2017 – 30 November 2018 (Q1:M1 – Q6:M18)

**Status:** Completed

#### **Objectives:**

- 1. Develop a peer-reviewed study plan for 1) testing of the DTBird System at the Washington host facility, and 2) conducting integrative analyses of information gathered at multiple study sites.
- 2. Evaluate results of independently funded California pilot study to inform refinements of the DTBird system and form the basis for developing the Washington-based study plan.
- 3. Complete an expanded evaluation of false positives at the California wind facility.

#### **Outcome Summary:**

The project team completed a final peer-reviewed Study Design, including a set of proposed Quantitative Performance Targets (QPTs) DOE approved in October 2018. In August 2018, H. T. Harvey & Associates completed an expanded 10.5-month assessment of false-positive detections from the California pilot study at the Manzana Wind Power Project. They revealed that, of the video clips identified and categorized, 63% involved false positive detections and 61% of those events triggered a deterrent signal. Eagles represented 2% of these detections, but identifying targets to species was difficult based on low-resolution DTBird videos (DTBird does not automatically identify nor enumerate targets; technicians must do that by reviewing extracted video clips). In evaluations of the pilot study, recommendations suggested that Liquen focus on (1) adjusting the duration of the deterrent signal and signal criteria, (2) applying

Al to reduce false positives, (3) increasing the accuracy and precision of the spatial targeting to increase consistency of deterrents triggered by at-risk targets, (4) refining algorithms to enable target detections against landscape backdrops. The QPTs were established based on the pilot study, assuming the DTBird systems would meet or exceed the proposed performance targets at the Washington facility. In coordination with DOE and reviewers, the research team established a QPT range of 53–73% for the probability of detection. Greater than 50% was established as the QPT for successful deterrence of eagles. The false positive QPT established that <36% of all screened event records should involve targets determined to be false positives, including inanimate objects and non-target birds.

#### Budget Period 1 (Go/No-go) Outcomes(s) (Q6: M17-18):

During Budget Period 1, REWI completed all SOPO tasks and milestones. The final study design was submitted to DOE in July 2018, and the final response to remaining peer review comments was submitted to DOE in August 2018. Documentation of the recommended upgrades, the false positive report, and the QTPs were submitted to DOE in August 2018. REWI requested a sixmonth extension to Budget Period 1 due to delays in the Award Negotiation process, a U.S. Fish and Wildlife Service roadblock in the NEPA analysis for the initial study site resulting in a need to identify a new site for the 2-year experiment, and the process of peer reviewing the study design. An award modification was provided in August 2018 and included the following:

- DOE approved a six-month extension.
- Relocation of the 2-year experiment from original host site in Wyoming to facility in Washington State
- DOE granted the project additional funds for unanticipated work associated with the delays.
- An additional \$200,000 in cost share for additional DTBird units used to increase the sample size of recordings of in situ raptor behavior responses and a more robust dataset.
- A revision of the study design to include a halfway checkpoint through the first year of the 2-year experiment whereby the project team analyzes the data accumulated and assesses whether there will be enough data in the first year to add a preliminary assessment of habituation to the study in the second year.

## 5.2 Budget Period 2: Expand evaluation of DTBird Detection and Deterrence Systems (Tasks 4-8)

<u>Timeline:</u> 1 December 2018 – 31 October 2022 (Q7-Q22:M19-M65)

**Status:** Completed

#### **Objectives:**

 Install DTBird and complete the first year of a controlled experiment at the Washington facility designed to evaluate DTBird's effectiveness as an impact minimization technology.

- Expand to a full year evaluation of DTBird deterrence capabilities at the California wind facility, focused on evaluating behavioral responses of in situ eagles based on DTBird video footage.
- 3. Conduct UAV flight trials at Washington wind facility.
- 4. Conduct a mid-year assessment to ascertain whether sufficient data were collected through Year 1 of a two-year controlled experiment to determine "proximate" effectiveness of DTBird with reasonable statistical power.

#### **Outcome Summary:**

Due to delays and equipment failures, of the 18 units originally proposed, only 14 DTBird units were installed in Washington, and usable data were provided by only 11 of these units during Year 1 of the Goodnoe Hills study, with no other departures from the approved study design. An estimated 53 ± 16.7% of confirmed eagles were considered to have been effectively deterred in an evaluation of the expanded dataset from the Manzana facility. The proportion of false negatives as determined from UAV flight trials at the Goodnoe Hills was 37 ± 10.7%, essentially identical to the estimate from the Manzana pilot study. In contrast, the rate at which false positives triggered deterrent signals substantially exceeded the relevant QPT at Goodnoe Hills. True false positives (TFPs; i.e., detections triggered by inanimate objects, insects, and software limitations/glitches) triggered an average of 3.6 ± 0.79 deterrent signals/turbine/day and resulted in an average of 1.9 ± 0.42 minutes of deterrent signaling/turbine/day at Goodnoe Hills. Non-target avian false positives (NTAFPs; i.e., birds other than focal large soaring raptors) triggered an average of 2.2 ± 0.86 deterrent signals/turbine/day and resulted in an average of 1.2 ± 0.48 minutes of deterrent signaling/turbine/ day at Goodnoe Hills. When averaged across turbines, the probability of detection was 63 ± 11% at Goodnoe Hills, which was similar to the estimate derived from the previous Manzana study (63 ± 10%) and fell in the middle of the established QPT range (53–73%). The overall probability of detection estimate derived from combining data across all turbines and trial sessions at Goodnoe Hills (67%) also fell within the QPT range.

#### Budget Period 2 Go/No-go Outcomes (Q20 - Q22: M60-64):

During Budget Period 2, REWI completed all SOPO tasks and milestones. The project team requested a 12+ month extension of BP2, which the DOE granted in September 2020 to complete the commissioning of all DTBird units and the UAV flight trials. The project team came together in Spring 2021 to reschedule and rescope BP2 tasks, given the anticipated extension request. The project team completed two successful rounds of UAV flight trials to evaluate the detection and deterrent-triggering functions of DTBird at Goodnoe Hills in August 2021 and July 2022. The expanded full-year evaluation of *in situ* raptor behavioral responses to DTBird deterrents at the Manzana facility was reported on in August 2019. The project team completed the first year of the controlled experiment at the Goodnoe Hills facility in August 2022. This experiment evaluated the ability of DTBird to deter eagles and surrogate raptors from entering the RSZ of DTBird-equipped turbines. Based on the mid-year statistical-power assessment of data collected through Year 1, the project team recommended continuing a second year of the controlled experiment focused on evaluating DTBird's proximate

effectiveness, instead of pivoting to the alternative objective to evaluate potential habituation behavior. An updated budget justification was provided for BP1 and BP2 to include the following changes:

- An additional \$200,000 in cost share for the overall project
- An additional 5 DTBird units (total 18) for the Washington experiment
- Addition of allowable indirect costs not included in the original budget justification.
- Increase in the budget for DTBird installation at the Washington site to reflect increased units.
- Redistribution of funds intended for trained raptor flight trials (originally task 6) to now cover additional screening and analysis of DTBird data (UAV flight trials and in situ raptor videos)
- Redistribution of funds allocated to REWI, Liquen, and H. T. Harvey & Associates to better reflect accurate predictions of project needs based on the completed pilot study and BP1.

# 5.3 Budget Period 3: Complete primary or alternative controlled experiment & video evaluation at Washington Facility; Conduct multi-site analyses (Task 8-12)

<u>Timeline:</u> 1 September 2022 – 31 May 2024 (Q22-Q28:M65-M84)

Status: Completed

#### **Objectives:**

- 1. Based on results of mid-year statistical power assessment, either extend to two years the controlled experiment focused on evaluating proximate effectiveness or pivot to Alternative Objective at Washington wind facility.
  - **1.a. Alternative Objective:** Complete one (1) year of a controlled experiment at the Washington facility designed to assess the potential for habituation behavior.
- 2. Conduct multi-site analyses of field data.

#### **Outcome Summary:**

The project team completed the classification of in-situ raptor responses to deterrents. The resulting estimate of the proportion of successful deterrence responses with turbines spinning and deterrents broadcasting (53−100%) exceeded the established QPT of ≥50% successful deterrence for eagles. Additionally, the two-year experiment results indicated that broadcasted DTBird deterrents significantly reduced the dwell time of eagles around relevant turbines, especially when combined with elevated rates of deterrent triggering caused by false positives. However, broadcasted warning signals did not significantly influence the rate at which eagles triggered dissuasion signals, partly because eagles often entered the dissuasion signal zone without first being detected by DTBird within a warning signal zone. In the multi-site analysis, false positives were distinguished as TFPs and NTAFPs. Liquen adjusted the algorithms in January 2023, lowering TFPs from 3.9 to 0.8 triggers/turbine/day at spinning turbines. Post-

adjustments, the TFP triggering rate fell within or under the established QPT (1.6–2.8 triggers/turbine/day). Overall, turbine-specific counts of TFPs varied by site and 28-day sampling cycles.

Proportions of false negatives were determined by evaluating the number of UAV flight transects that should have triggered a DTBird detection but did not. The multi-site analysis revealed similar probabilities of detection at both sites (66% at Manzana and 64% at Goodnoe Hills) which exceeded the QPT established from the pilot study ( $\geq$ 63% detection probability or  $\leq$ 37% false negative proportion).

The multi-site analysis of detection and deterrence triggering performance based on UAV flight and landscape characteristics revealed situation-specific landscape variations between Manzana and Goodnoe Hills that led to variability in DTBird's ability to detect and target objects of interest. Cloudy skies, wind speed, different UAV models (potentially reflecting differences in sexes and age classes), UAV speed, and pitch and roll angles all influenced the DTBird response distances.

The multi-species and golden eagle analyses confirmed significant differences in the probability of successful behavioral responses to broadcasted DTBird deterrents at the two study sites and indicated an effect of pre-exposure risk as well as an interacting effect of wind speed and raptor species. The probability of effective deterrence generally was highest for eagle/large raptors classified as at moderate risk of exposure to collision, likely because such birds had more time to respond effectively before entering the high-risk RSZ compared to birds that were initially at high risk of exposure.

Overall, for golden eagles flying within DTBird's calibrated maximum detection range for the species, the operation of DTBird appeared to reduce the likelihood of approaching the RSZ of spinning turbines by 20–30%. The study results also emphasized that DTBird's overall effectiveness may vary in different landscape/climatic settings and depending on the focal raptor species.

# Section 6. Award and Modifications to Prime Award and the Statement of Project Objectives (SOPO)

Overall, the project award received fourteen modifications associated with delays and extensions, personnel changes, cost-share assistance, COVID-19, and technical DTBird system-related issues:

<u>Modification 1</u> was created to allow for the deletion and replacement of Special Terms and Conditions to incorporate the following revisions: (a) delete and replace Term 13 Publications changing 'Wind Program' to 'Wind Energy Technologies Office' and (b) delete and replace Term 26 Cost Sharing to authorize providing the cost share on a Budget Period basis.

<u>Modification 2</u> was created to delete and replace the SOPO and Federal Assistance Reporting Checklist and extend the period of performance from to 6/1/2017 – 8/21/2021 and adjust the special terms and conditions to delete and replace Term 8, NEPA requirements.

Modification 3 was created to delete and replace the Federal Assistance Reporting Checklist.

<u>Modification 4</u> was created to obligate an additional \$16,558 in Federal funding for the award, to delete and replace the SOPO, Federal Assistance Reporting Checklist, and Budget information, in addition to deleting and replace Term 26 Cost Sharing and Term 29 Indirect Costs.

**Modification 5** was created to update the DOE Award Administrator.

Modification 6 was created to approve the continuation application and allow the recipient to move from Budget Period 1 to Budget Period 2. It also extended the period of performance for the award to 6/1/2017 – 5/31/2022, adding a 12+ month extension in Budget Period 2 and continuing to increase the cost share on the awardee's end.

<u>Modification 7</u> was created to extend the period of performance to 6/1/2017 – 5/31/2023, revise the Government share, cost share, and total, provide additional funding, delete and replace the SOPO and Budget information, and delete and replace the Special Terms and Conditions to add Term 41, Foreign National Access Under DOE order 142.3A "Unclassified Foreign Visits and Assignments Program", Term 14 Publications, Term 26 Cost Sharing, and Term 32 Payment Procedures were also deleted and replaced.

**Modification 8** was created to update the DOE Project Officer.

Modification 9 was created to extend the period of performance by 13+ months to 6/1/2017 – 5/31/2024 with Budget Period 2 specifically extended from 12/01/2018 – 09/30/2021 to 10/31/2022, and deleted and replace the following terms in the Special Terms and Conditions, Terms 41 Foreign National Access and add Term 42 Environmental, Safety and Heath Performance of Work at DOE Facilities, Term 43 Export Control, and Term 44 Prohibition on Certain Telecommunications and Video Surveillance Services or Equipment.

<u>Modification 10</u> was created to delete and replace the SOPO, Budget Information, Term 26 Cost Sharing in the Special Terms and Conditions and reconfirm the project period. This modification confirmed the start and end date for the rest of the project timelines, per MOD 9.

**Modification 11** was created to correct the period of performance start date.

<u>Modification 12</u> was created to approve the continuation application, allowing the recipient to move from Budget Period 2 to Budget Period 3; approve the extension of the period of performance end date; update the recipient cost share and total project costs; and delete and replace Term 26 Cost Sharing and Term 29 Indirect Costs.

**Modification 13** was created to update the DOE Award Administrator.

**Modification 14** was created to update the Recipient Principal Investigator.

### Section 7. Issues and Changes in Approach

During BP2 and towards BP3, due to delays in equipment shipping, personnel changes, and equipment challenges all exacerbated by COVID (Liquen staff could not travel to the U.S. to expedite addressing equipment issues), REWI requested and received multiple project extensions resulting in the project continuing three plus years after the originally proposed end date. Additionally, the project team contributed substantial added cost share to cover unanticipated costs related to the project challenges, as well as additional support provided by DOE related to COVID-19.

**Equipment:** 16 units were ordered, built, shipped, installed, and attempted to be commissioned. However, due to COVID restricting in-person servicing by Liquen, only 14 units were determined to be commissionable within a feasible timeline. Therefore, 16 units remain as Equipment costs, with Liquen covering the costs of the two unusable units as cost share.

#### Cost share changes:

- H. T. Harvey & Associates: additional cost share provided for UAV preparations.
- Liquen: additional cost share for two unusable units, as noted above.
- PacifiCorp: shifting BP allocation of cost share, as noted above. Additional costs to capture additional labor by PacifiCorp contractors in lieu of on-site support by Liquen (Liquen could not travel due to COVID).
- Portland General Electric: shifting cash cost share from external funders into BP2 to reflect anticipated timing of applying these funds.
- Puget Sound Energy: shifting cash cost share from external funders into BP2 to reflect anticipated timing of applying these funds.
- REWI: additional cost share in BP3 to ensure total project cost share percentage remains the same (57.76%).

During BP3, consistent issues occurred for DTBird systems at various turbines at the Goodnoe Hills sight, which required a considerable amount of additional project team time and PacifiCorp staff time to mitigate issues. Most notable were issues related to a delay in camera lens cover replacements, which were to be completed every six months and were not replaced until over a year after their initial replacement. Additional issues arose due to camera outages, analysis unit replacements, Vesta's server disconnections, and the unexpected Bonneville Power Administration (BPA) outage that lasted for approximately 26 days in May 2023. PacifiCorp was able to provide data that helped overcome a complete DTBird system communication failure after the BPA power outage that extended for the remainder of the study, but this resulted in Liquen and H. T. Harvey & Associates spending time beyond their scopes to format and align the PacifiCorp data and records stored in the DTBird on-line Data Analysis Platform (DAP).

### Section 8. Task Accomplishments & Milestones

## 8.1 Task 1.0: Project Launch and Development of Peer-reviewed Study Design

## 8.1.1 Milestone 1.1.1: Completed peer-reviewed study design and quantitative performance targets (Q5:M15)

The final, peer-reviewed study design and a companion document, Response to Peer Reviewer Comments, were **submitted to DOE** in **July 2018 (Q5:M14)**. Following coordination with DOE, The National Renewable Energy Laboratory (NREL), and peer reviewers, the updated study design was **submitted to DOE** in **August 2018 (Q5:M15)** and **approved by DOE** in **October 2018 (Q6:M17)**. In the original SOPO, the study design was intended to be completed in the third month of the project, but multiple delays pushed back the process, so the final draft was submitted to the DOE in the 14th month of the project. The study design was updated with respect to resident raptor observations at the Washington site to include a "partial year assessment" of data collected in the first half of Year 1 of the 2-year experiment to determine whether enough data were likely to be available to effectively analyze the "proximate" effectiveness of DTBird's audible deterrents for deterring eagles and other raptors. The additional assessment was designed to determine if the DTBird units would be assigned a continued daily control-treatment rotation schedule in Year 2, designed to minimize the potential for turbine-specific habituation, or a permanent control or treatment mode during Year 2 to enable evaluating the potential for habituation.

## 8.2 Task 2.0: Evaluate false positives using data collected during the pilot study at California wind facility

# 8.2.1 Milestone 2.1 False positive rates quantified at California wind facility (Q5:Q15)

A final report on false positive detections at the Manzana Wind Power Project in southern California was **submitted to DOE in August 2018 (Q5:M15)**. H. T. Harvey & Associates analyzed footage collected by DTBird from December 2016 through October 2017. The team sampled 5,212 detection events and were able to classify the detected targets in 5,208 of those records. The classifications included estimates of 33% (1,712) TFPs 30% (1,567) NTAFPs. There was an average of 2.2 TFP detections/turbine/day, and 1.9 NTAFP detections/turbine/day. Of the TFP detections, 61% triggered a deterrent signal, resulting in an average of 1.7 extraneous deterrent signals/turbine/day. Of the NTAFP detections, 58% triggered a deterrent signal, resulting in an average of 1.2 deterrent signals/turbine/day. False positive rates varied among turbines and months. For example, there was an increase in TFPs caused by insects in June reflecting a seasonal increase in insect abundance, rather than variation in DTBird performance. Of the TFPs, 45% were associated with various aircraft, 23% turbine blades, 21% various sky artifacts, 8% insects, 1% precipitation, and <1% other objects such as balloons or floating leaves. Eagles

represented approximately 2% of all detections, however, DTBird does not identify or filter targets by species. Per their preceding standard practice, Liquen implemented some adjustments to the filtering algorithms that significantly reduced the instances of TFPs triggered by turbine blades after February 2017, more than 2 months after the systems were declared "fully commissioned."

### 8.3 Task 3.0: Evaluation of pilot study

## 8.3.1 Milestone 3.1 Recommended updates to DTBird system delivered to technology vendor (Q6:M16)

With insights from the DTBird 2016–2017 pilot study at the Manzana Wind Project, H. T. Harvey & Associates, Liquen, and REWI created a set of feasible recommendations for future updates and upgrades to the DTBird system. **These recommendations were submitted to DOE in August 2018 (Q5:M15)** and **received review from DOE in September 2018 (Q6:M16)**. All comments and revisions to the recommended system updates **were submitted to DOE in December 2019 (Q7:M19)**. REWI and Liquen recommended updates focused on the following four topics:

- 1. Reducing the duration of deterrent signals and signal criteria to ignore fast moving targets that cannot be birds.
- 2. Artificial intelligence/machine learning capabilities to reduce false positives.
- 3. Increasing accuracy and precision of spatial targeting to increase the consistency of deterrents signaled in response to at-risk targets.
- 4. Refine algorithms to enable target detections against landscape backdrops.

# 8.3.2 Milestone 3.2 QTPs established based on analysis of pilot study (Q6:M18)

A set of QPTs were *proposed to DOE in the study design submitted August 2018 (Q5:M15)*. Performance targets were established based on the results of the Manzana pilot study and with the expectation that DTBird would meet or exceed the performance targets.

As part of Milestone 3.2, the following QPTs were established for future Milestones 6.1-7.1, to be completed in BP2:

<u>Milestone 6.1:</u> 53-73% overall UAV detection rate; false negative rate (inverse of detection rate) 27-47%. This detection rate was selected based on data from the pilot study, in which 63%  $\pm$  10% SD of the UAV flights were detected in the flight trials. The false negative rate (inverse of the detection rate - UAV flights that occurred but were not recorded by DTBird), was 37%  $\pm$  10% SD.

<u>Milestone 6.2:</u> ≥ 50% successful deterrence rate for eagles. At least 50% of bald and golden eagles should exhibit avoidance behavior to a DTBird system within 5 seconds of the deterrent signal when sound is "on". This deterrence rate was selected based on data from the pilot study, in which 36% of raptors (overall) responded effectively to the deterrent signals. We selected this target because our expectation is that DTBird's performance in the two-year study

will meet or exceed the performance observed in the pilot study. The project team anticipated having access to higher resolution video footage for the DOE study, and the ability to better identify birds in the DTBird video clips.

<u>Milestone 6.3</u>: Not to exceed 1.6 -2.8 TFPs triggers/turbine/day or ≤36% of total video records collected by DTBird units. This false positive rate is based on data from the False Positives Analysis of data collected during the pilot study, in which DTBird systems detected 2.2 ± 0.64 TFPs/turbine/day, and 36% of video records from DTBird contained targets determined to be non-avian objects (e.g., turbine blades, aircraft, insects, raindrops).

<u>Milestone 7.1:</u> Complete a summary of the mid-year assessment and provide a recommendation of which objective to pursue in Year 2 of the experiment (proximate effectiveness or habituation focused).

The team provided responses to comments regarding the proposed target detection rates of 53% for eagle-surrogate UAVs *in September 2018 (Q6:M16)*. As part of this response, the team clarified that a lower confidence interval would be incorporated for drones (63% ±10% detection rate) and accommodating unidentified large birds for the eagle detection rate (36% detection rate) due to the likelihood that an unknown percentage of unidentified large birds were eagles. Since the DTBird system does not distinguish between eagles and other bird species that trigger detections and deterrents and in the United States, where the primary species of concern are bald and/or golden eagles, triggering for non-target species could be deemed excessive. Therefore, the project team sought to quantify the percentage of each event type triggered by eagles (i.e., detections, warning signals, and dissuasion signals) compared to non-eagles and false positives as well as the rate of deterrent signal triggers per turbines per day.

## 8.4 Task 4.0: Update DTBird system and revise study design for BP2 and BP3 as appropriate

### 8.4.1 Milestone 4.1 Study design revised (Q7:M19)

A revision to the study design was **submitted to DOE in August 2018 (Q5:Q15)**, response to comments from expert review were **submitted to DOE in January 2019 (Q7:M20)**. The following was clarified/updated:

- The presumption of an effective DTBird deterrent signal relative to North American eagle species, as Liquen's rational noted that the deterrent signal was developed for a range of species both European and North American (including golden eagles). The presumed similar reaction to the technology is expected by bald eagles and European white-tailed eagles, both in *Haliaeetus*.
- The rational for using the Akaike Information Criterion (AIC) in the proposed statistical approach. H. T. Harvey & Associates noted that the AIC had several potential predictor variables under consideration. AIC scores would be used to support deriving an optimized model best predicting future observed outcomes while minimizing predictor variables. Additionally, use of AIC was with respect to the detection efficacy related to drones, not eagle activity or deterrence.

- An evaluation of the pilot study was completed with the adjusted false positive and deterrent response analyses of the California dataset; the results of the two analyses informed the decision to not revise the study design.
- In addition, the numbers of units scheduled for deployment at the Goodnoe Hills site was adjusted from 18 to 16; concerns were raised about whether this change would compromise the study design or project objectives, but ultimately determined it would not affect the statistical power of the study.

#### 8.4.2 Milestone 4.2 Updates to DTBird system completed (Q8:M22)

The recommended DTBird system updates were **submitted to DOE in August 2018 (Q5:M15)** and were **provided to Liquen in November 2018 (Q6:M18)**. Liquen confirmed the incorporation of the following updates in advance of the next phase of fieldwork at the Goodnoe Hills site.

- An increase in the size of the red box in the DTBird video footage showing the location of targets.
- An increase in the size of the time stamps on video footage.
- DAP ID number included in file name by default.
- Use of higher megapixel resolution to facilitate improved target identification.
- A second ring of speakers to broadcast deterrent signals.
- Increased frequency of replacement of lens covers to reduce impacts of sun glare, specifically polarized lenses, if feasible.

All updates were incorporated with one exception regarding a change to polarized lens covers which needed further assessment, therefore the project team decided to modify preventative maintenance of camera lens cover changes from annual to biannual.

Longer term recommendations for updates that were to continue to be researched and developed include:

- A new statistical analysis will be done by DTBird, and results incorporated in the second year of fieldwork to optimize the sounding of the deterrence trigger and refine the triggering criteria and duration of signal.
- Liquen's evaluation of whether a sample turbine at Goodnoe Hills can incorporate a set of polarized lenses during Year 1 data collection compared to standard lens but has not determined whether this would complicate the experimental design.
- An updated version of the DTBird software set to be implemented at Goodnoe Hills, which will allow the operation of AI software over the detections of the videos, data collection and preliminary testing set to be completed following the first year of service.
- Improvements to the precision of detection, warning-trigger, and dissuasion-trigger
  targeting to ensure effective deterrence responses and reducing unnecessary signaling
  are expected to be longer-term, but increased image quality, new software algorithms,
  and sound triggering criteria, as noted above, should reduce unnecessary deterrence
  signaling.

 Incorporation of an algorithm that summarizes all instances of video failure at individual cameras to allow more comprehensive evaluations of system performance, is set for Year 2 of field testing at Goodnoe Hills.

All 16 DTBird units arrived at Goodnoe Hills, all but four were partially installed due to special equipment required to install a second ring of speakers. Liquen reverted to the previous software platform due to technical difficulties, but the previously noted recommendations were included prior to UAV flight trials and Year 1 data collection **completing this milestone in May 2021 (Q16:M48)**.

#### 8.5 Task 5.0: Install DTBird systems at Washington wind facility

# 8.5.1 Milestone 5.1 DTBird systems installed and commissioned at Washington wind facility (Q13:M37)

Liquen and PacifiCorp experienced several unanticipated delays in acquiring parts for units, sending personnel for installation, and integrating the DTBird units to the SCADA and network amid the COVID-19 pandemic. All 16 DTBird units arrived at Goodnoe Hills in October 2019 (Q11:M29) where all but four, due to weather concerns, were assembled and fully installed. PacifiCorp contracted a Vestas crew on site to conduct their part of the cost-share to conduct assembly and installation. Liquen and Pacificorp began integration of the units into the Washington wind facility's online network. In the Spring of 2020 (Q12) Liquen and PacifiCorp continued integrating the 12 fully installed units into the online network and enabled remote control access. A 13+ month extension was awarded in September 2020 (Q14:M40) starting with BP2 to allow for the complete commissioning of DTBird units and to allow for UAV flight trials. Thirteen of 14 DTBird units were fully commissioned for the Year 1 experiment, however only 11 were operating sufficiently and consistently enough to yield usable data. Following a myriad of system maintenance issues involving camera outages, communication failures, and analysis units without remote access, all 14 DTBird units were fully commissioned and effectively functional in early September 2022 (Q22:M64), though additional significant (> 30 days) gaps in functionality continued for several units.

# 8.6 Task 6.0: Expand evaluation of *in situ* bird video footage at California and Washington wind facilities, conduct UAV flight trials at Washington wind facility, and analyze site-specific results

# 8.6.1 Milestone 6.1: UAV flight trials completed at Washington wind facility (Q18:M53)

H. T. Harvey & Associates and Remote Intelligence attempted to conduct an initial round of UAV flight trials at the Washington facility during May 2021 (Q16:M48); however, excessive wind and a DTBird system failure resulted in no usable data from that attempt. **The first round of successful flight trials at this facility occurred in early August 2021 (Q17:M51).** This trial session involved two UAV models and provided approximately 8 hours of usable data collected

at three DTBird turbines, but ended prematurely when both UAVs were destroyed in crashes. In September 2021, H. T. Harvey & Associates coordinated with Remote Intelligence to prepare two new UAV aircraft—for use during a third round of flight trials. The third round was then conducted during the last week of July 2022 and provided additional data collected at four DTBird turbines, but with one of the new aircraft also destroyed in a crash caused by an equipment failure. UAV flight trials at Goodnoe Hills were **completed at the end of July 2022** (Q21:M62), with useable data collected during 29 individual, automated flight missions conducted at five DTBird-equipped turbines, which yielded 482 distinct flight-transect samples suitable for analysis. Results of this site-specific investigation were provided as part of the **project's Continuation Application in September 2022 (Q22:M64)**.

# 8.6.2 Milestone 6.2 DTBird video data collection and enhanced site-specific evaluation of *in situ* eagle responses to deterrents completed for California facility, with evaluation restricted to first year of data collection (Q10:M28)

The objective was to expand a preliminary pilot-study evaluation based on one full year of data collected at the Manzana wind facility to support quantification of the effectiveness of DTBird audible deterrents to deter golden eagles from approaching equipped turbines. The analysis evaluated the behavioral responses of *in-situ* eagles to deterrence signals using DTBird data collected from January through December 2017 at the seven turbines outfitted with DTBird systems. Event data recorded in the DAP were processed and analyzed to estimate the probability of effective deterrence for golden eagles and other large soaring raptors.

For this analysis, H. T. Harvey & Associates randomly selected 10 days/month during the sampling period and collected behavioral data for all large raptors detected by the DTBird system and exposed to deterrent signals. The following behaviors were recorded for each relevant deterrence event: approximate direction of travel relative to turbine before and after signal emittance, risk of approaching RSZ before signal emittance (i.e., *Preexposure Risk*), whether the raptor appeared to respond to the deterrent signal, and whether the raptor's response to the signal reduced its risk of approaching the RSZ (i.e., *Reduced Risk*). H. T. Harvey & Associates used this final behavioral classification, *Reduced Risk*, as the response variable in a series of general linear models (GLMs) to evaluate the influence of month, initial risk level (*Risk*), and raptor group (i.e., eagles, vultures, and buteos) on the probability of deterrence.

The assessment indicated that, across all evaluated events, the DTBird collision avoidance module effectively deterred at least 53% confirmed golden eagles, 57% of turkey vultures, 38% of buteos, 64% of falcons, and 43% of all raptors combined. Adding in cases where deterrent responses were classified as potentially effective elevated the estimated probability of deterrence for golden eagles to 74%, for turkey vultures to 81%, for buteos to 69%, for falcons to 100%, and for all raptors combined to 72%.

The GLM results suggested that birds at moderate to high risk of approaching the RSZ were more likely to respond effectively and tended to divert away from the risk zone more strongly when exposed to the deterrent signals compared to birds that were at low risk of exposure. The GLMs also suggested that eagles were slightly more likely than buteos to respond to deterrence

signals and responded with greater diversion angles. The interpretability of these results had limited rigor due to modest sample sizes and the lack of control (i.e., to support evaluating the differential effect of spinning turbines alone versus spinning turbines plus broadcasted DTBird deterrents). H. T. Harvey & Associates **produced a final summary report in August 2019** (Q9:M27) documenting the enhanced analysis.

# 8.6.3 Milestone 6.3 Preliminary site-specific estimates of rates of false positives and false negatives produced for Washington wind facility (Q20:M60)

The probability of false negatives as determined from UAV flight trials conducted at Goodnoe Hills was  $37 \pm 10.7\%$ , identical to the false negative probability estimated for the Manzana site based on the pilot study ( $37 \pm 10\%$ ). This outcome suggests consistent performance of the primary detection functions of the DTBird system.

A probability of detection (converse of probability of false negatives) logistic GLM (LGLM) analysis provided additional perspective concerning factors that influence the overall probability of DTBird detecting an eagle-like UAV if it flies anywhere through the 240-meter-radius detection envelope projected based on calibration for golden eagles. The limitation of this analysis was that for flights that were not detected (false negatives) there were no reference points to use for precisely characterizing the flight, location, and environmental characteristics at the time of a specific event to use as covariates. Consequently, we focused attention on discerning the influences of only a select few metrics derived by averaging across all points along a given sample flight. Nevertheless, this approach illustrated some variability in the probability of detection through the day, perhaps related to influence of the sun's position and intensity, but more importantly emphasized that the probability of detection was highest when the target flew at moderate distances from the turbine (generally high with average flight distances of 80-160 m) through the mid-section of the camera viewshed (generally high with viewing angles from camera up to UAV of 25-40°). The probability of detection averaged lower when the target flew closer to or farther away from the camera or within the lower or upper margins of the camera viewshed.

The rate at which false positives triggered deterrent signals exceeded the QPT during Year 1 of the Washington study. TFPs triggered an average  $3.6 \pm 0.79$  deterrent signals/turbine/day and resulted in an average of  $1.9 \pm 0.42$  minutes of deterrent signaling/turbine/day. NTAFPs, defined as birds other than focal large raptors (eagles, vultures, buteos, and ospreys), averaged  $2.2 \pm 0.86$  deterrent signals/turbine/day, and  $1.2 \pm 0.48$  minutes of deterrent signaling/turbine/day. Calculation of False Positive rates was based on 12,962 detections (defined as triggering a video recording). An estimated 66% of those detections resulted from TFPs, 25% from NTAFPs, and 9% from presumed eagles and other large raptors. Approximately 33% of the TFPs and 52% of the NTAFPs triggered a deterrent signal. TFPs averaged  $11.2 \pm 3.46$  (SD) detections/turbine/day, and NTAFPs averaged  $4.2 \pm 1.49$  detections/turbine/day. A report was produced to accompany this milestone in the **Continuation Application submitted in September 2022 (Q22:M64)**.

# 8.6.4 Milestone 6.4 Initial site-specific models developed to quantify the spatial accuracy of the DTBird detection and deterrent-triggering system at Washington wind facility (Q20:M60)

UAV flight-trial data were analyzed, and site-specific statistical models were developed to evaluate the influence of flight and environmental covariates on DTBird detection and deterrent-triggering response distances at the Goodnoe Hills facility. This site-specific analysis used the final Manzana site-specific model as a template but did not consider the same full suite of variables initially considered to develop the Manzana model. We made this choice primarily because unanticipated and unavoidable lengthy delays in our ability to conduct a successful series of UAV flight trials at the Goodnoe Hills severely compressed the time available for analysis ahead of the deadline for submitting a BP2 Continuation Application to the DOE to support moving into BP3. Nevertheless, this initial modeling effort was informative in suggesting similar relationships at the two sites for several key covariates of interest. We then developed further insight during BP3 in conducting an integrated assessment based on combining data from the two sites (see Task 10.1).

The initial Goodnoe Hills response-distance modeling effort revealed both similarities and some notable differences compared to the previous Manzana modeling effort. The similarities included (a) different UAV models influenced the response distances similar to what one might expect to occur in relation to eagles of different sizes and colorations, (b) eagle-like UAVs flying at relatively high altitudes were detected at greater distances than those flying at lower altitudes relative to the turbine base, c) greater degrees of ascent and rolling from side to side generally increased the response distances as a result of increasing the degree the UAV profile was exposed to the DTBird cameras, and (d) response distances were generally higher under uniformly bright mostly cloudy skies and lower under uniformly dark overcast skies, with clear blue and partly cloudy skies showing variably intermediate responses. Notable contrasts in the two sets of site-specific results included significant contributions of Turbine ID, solar intensity, wind speed, and UAV elevation angle in the Manzana model but not in the Goodnoe Hills model.

A report was produced to accompany this milestone in the Continuation Application submitted in September 2022 (Q22:M64).

# 8.7 Task 7.0: Conduct first year of controlled experiment at Washington Wind Facility

# 8.7.1 Milestone 7.1 First year data collection completed for controlled experiment (Q21:M63)

Thirteen of 14 DTBird units installed on turbines were fully commissioned, and H. T. Harvey & Associates and Liquen implemented the full 14-turbine 28-day muting rotation schedule for all available DTBird units. The project team ended Year 1 experimental data collection in August 2022 (Q21:M63).

8.7.2 Milestone 7.2 A summary of progress and findings up to 10 months of data will be included in the Go/No Go report for BP2. This summary will include a power analysis performed on at least 6 months of data, as well as a recommendation of which objective (proximate effectiveness or habituation) to pursue in Year 2 of the experiment (Q21:M63)

The estimated effect size based on the existing dataset of seven 28-day cycles was a 66% reduction in the number of dissuasion signals at treatment turbines compared to control turbines. This difference was not significant (p = 0.192); our statistical power to detect an effect of that amount with  $\alpha$  = 0.05 was estimated to be approximately 23%. The simulation portraying what we could expect based on an expanded 13-cycle dataset with comparable per-cycle sample sizes boosted the estimate of power to detect a 66% effect to approximately 42%, but still falling well short of an optimal power target of 80%. The 13-cycle projections suggested that we would have 80% power to detect only a >85% effect size, assuming the sampling results remained comparable to the initial 7 cycles across the extended 13-cycle period.

Based on these results, it was recommended to continue with the experiment as designed for testing DTBird's proximate effectiveness. **REWI submitted this mid-year assessment and recommendation along with its Continuation Application at the beginning of September 2022 (Q22:M64)**.

### 8.8 Task 8.0: Complete controlled experiment and analyze results

## 8.8.1 Milestone 8.1 First two months of controlled experiment's Year 2 DTBird data collected at Washington site (Q21:M65)

REWI, H. T. Harvey & Associates, PacifiCorp, and Liquen continued with the second year of the experimental design to ensure sufficient data to evaluate the proximate effectiveness of DTBird, starting in September 2022 (Q22:M64). Liquen implemented updates to the algorithm from November 2022 – March 2023, effectively allowing for full commissioning of the DTBird units for use in Year 2 of the experiment.

# 8.8.2 Milestone 8.2 Controlled experiment completed, and results analyzed; an estimate of eagle collision risk reduction from DTBird calculated (Q26:M78)

The 14 turbines included in the experiment were randomly assigned to control and treatment groups daily. Those assigned to the treatment group broadcasted warning and dissuasion deterrents when triggered. Those assigned to the control group triggered deterrents virtually but did not result in audible deterrents. Results indicated that the presence of broadcasted warning signals did not significantly influence the rate at which eagles triggered dissuasion signals, likely because eagles often entered the dissuasion signal zone without ever being detected by DTBird within the warning signal zone. However, results also indicated that broadcasted deterrent signals significantly reduced the time eagles spent near DTBird-equipped turbines

(aka dwell time). There was also a strong interactive effect of treatment group and false positive rates, meaning that if warning/dissuasion signals were triggered and broadcasted more frequently at treatment turbines by false positives, this led eagles to spend less time around those turbines. These results suggest that, despite our concerns that high false positive rates might cause eagles to become less responsive to deterrent signals, negative habituation did not occur over the 2-year course of this experiment. Instead, positive habituation appeared to occur over the 2-year course of this study, likely because the deterrent triggering rate caused by false positives was atypically high through the first 18 months of the study and the overall deterrent triggering rate was excessive during the last 5 months of the study due to a DTBird operations issue stemming from a facility-wide power outage. A report for this milestone was submitted to DOE in December 2023. (Attachment 3).

## 8.9 Task 9.0: Evaluate behavioral responses of raptors exposed to deterrent signals at Washington wind facility

8.9.1 Milestone 9.1 All DTBird video evaluation and classification of in-situ raptor responses to deterrent signals completed. Target performance is ≥50% successful deterrence for eagles (Q27:M79)

H. T. Harvey & Associates reviewed detection videos from the 14 DTBird turbines, sampling 10 randomly selected days within each 28-day period for the first year of the experiment. For all screened records in which a deterrent signal was triggered by a confirmed or probable eagle, vulture, or buteo, investigators evaluated the bird's flight behavior, including path divergence and changes in flapping style to classify each event into one of four response categories: Yes (Confirmed Effective), Potential (Potentially Effective), No Response, Not Relevant (response did not reduce risk). Records were also categorized by collision risk prior to deterrent exposure. H. T. Harvey & Associates then evaluated the differences in the categorical response proportions among the control (deterrents muted) and treatment (deterrents broadcasting) groups using a 2-way Pearson chi-square analysis and estimated the probable successful deterrence rate as the combination of responses classified as confirmed and potentially effective.

Of the 19 instances in which a golden eagle triggered a warning signal, 13 resulted in a successful or potentially successful deterrence response (68%). Similarly, 10 out of 19 of the instances in which a golden eagle triggered a dissuasion signal resulted in a successful or potentially successful deterrence response (53%). Small sample sizes did not allow for a comparative analysis between control and treatment groups for each species of eagle; however, based on the comparative control-treatment results and for all analyzed groups and species, broadcasted deterrents consistently resulted in at least a doubling of the proportion of cases where a successful or potentially successful response was evident. In addition, although the percentage of golden eagle responses classified as confirmed effective (32%) fell below the QPT established based on the Manzana pilot study, the combination of confirmed effective and potentially effective responses exceeded 50% for all analyzed species groups and for both warning and dissuasion signals (overall range 53–100%). A report for this milestone was submitted to DOE in June 2023 (Q25:M73) (Attachment 4).

### 8.10 Task 10.0: Complete combined multi-site analyses

8.10.1 Milestone 10.1 Multi-site analyses of detection and deterrence triggering capabilities as a function of flight and landscape characteristics completed (Q24: M72)

H. T. Harvey & Associates modeled DTBird response distances as a function of several environmental and UAV variables. The general linear mixed model (GLMM) that best explained variation in DTBird response distances suggested that response distances were more variable among the seven Manzana DTBird turbines than among the five Goodnoe Hills DTBird turbines where UAV flight trials were conducted, likely reflecting situation-specific landscape variation leading to modest variability in DTBird's ability to detect and target objects of interest. The average response distance at the Manzana facility was marginally lower than that at the Goodnoe Hills facility. Overcast skies significantly increased detection and deterrence-triggering distances compared to fair skies, suggesting greater detectability given a contrasting sky backdrop. Response distances tended to increase as the wind speed increased, but this relationship was only moderately significant. Increased wind speeds increased the degree to which the UAVs bounced around in the air, increasing profile exposure to the DTBird cameras and thereby increasing detectability as suggested by increasing response distances. Detection and deterrent-triggering response distances also tended to increase with UAV ground speed, suggesting that DTBird could more easily detect faster moving targets. DTBird response distances were also dependent on the interactive influences of UAV pitch and roll angles, whereby pitching and rolling acted in concert to increase exposure of the UAV profile to the cameras.

Output for the best performing GLMM also indicated that the different UAV models used accounted for a noteworthy difference in detection and deterrent-triggering distances. The two UAV models used at the Manzana site showed the greatest variance in response distances, whereas variation among the three distinct UAV models used at Goodnoe Hills was less pronounced. As the initial pilot study at Manzana suggested, response distances tended to be shorter for the skinnier-bodied UAV models when compared with the more eagle-like, robust-bodied models. Some of the variation observed potentially mimicked the kind of variation that could be expected with physical differences associated with eagles of different sexes and age classes.

We also note here that the differences rated as statistically significant effects given our data sometimes amounted to magnitudes that may not have especially noteworthy biological or operational significance (e.g., 10–20 m differences in detection range for birds that may easily move farther than that in less than a second). However, our study was not designed to specifically quantify the relative effectiveness of different calibrated detection and deterrent triggering distance thresholds nor the spatiotemporal aspects of what an eagle requires as deterrent warning to avoid calamity under different flight conditions. Therefore, we have no basis for presuming what may be biologically/operationally significant in this context.

The best performing GLMM did not include the UAV's climb rate, location of the UAV in relation to focal turbine (i.e., direction from turbine), the UAV direction of travel (i.e., course over ground), sun azimuth, solar irradiation, or sun elevation angle. A report for this milestone was submitted to DOE on May 2023 (Q24:M72) (Attachment 5).

## 8.10.2 Milestone 10.2 Complete multi-site analyses of false positives and false negatives (Q25:M73)

We used flight trials involving UAVs designed to coarsely mimic the general size, weight, and coloration of golden eagles to quantify the probability of false negatives (or conversely the probability of detection) at the two study sites. To investigate false positives, we used DTBird event data recorded for *in situ* eagles and other large raptors. A high false-positive rate during Year 1 of the Goodnoe Hills study proved concerning and required, upon DOE approval, that Liquen update the DTBird filtering algorithms to reduce the potential for blade-related, insect, and sky-artifact sources of false positives.

Based on the Manzana pilot study, a QPT for the probability of detection of 63% (or 37% false negatives) was established to evaluate the comparative performance of DTBird systems installed at the Goodnoe Hills. A multi-site GLMM revealed an overall 65% probability of detecting an eagle-like UAV within 240 meters or less of the cameras, with a nominally higher detection probability at the Manzana site (66%) than at the Goodnoe Hills site (64%). This outcome suggested consistent performance of the primary DTBird detection function at both sites. The results also indicated a higher chance of detection when the target flew within 80–160 meters of the turbine, versus closer or farther away, and at elevation angles that placed it within the middle of the camera viewsheds, versus high or lower.

The false positive analyses distinguished between TFPs (representing non-avian factors such as aircraft, insects, spinning turbine blades, and high-contrast sky conditions that sometimes trigger false detections, called sky artifacts) and NTAFPs (representing detections of birds other than focal large raptors, defined in this study as eagles, vultures, buteos, and ospreys). The established QPTs stipulated that (a) the overall TFP deterrent-trigger rate should not exceed 1.6–2.8 triggers/turbine/day; and (b) no more than 36% of all relevant and classified detections recorded by the DTBird systems should result from TFPs.

The TFP deterrent-triggering event rate exhibited interactive effects of site and time (28-day cycle). The overall average TFP rate at the Goodnoe Hills across the full 23 months of sampling was 3.9 TFP detections with deterrent triggers/turbine/day, which exceeded the established QPT. However, after Liquen made additional adjustments to reduce the false positive rate in January 2023, the TFP deterrent-trigger rate for the subsequent 7 months dropped to an average of 0.8 triggers/turbine/day, well below the performance target and comparable to contemporaneous rates at Manzana. Similarly, although TFPs resulted in more than 50% of all detections that triggered deterrents before the adjustments were made, the proportion dropped to 25% post-adjustments, again falling below the established performance target. Moreover, in both cases the post-adjustment rates at Goodnoe Hills were lower than at Manzana, suggesting

improvement in the filtering algorithms. A report for this milestone was submitted to DOE in November 2023 (Q26:M78) (Attachment 6).

# 8.10.3 Milestone 10.3 Complete multi-site analyses of behavioral responses of in-situ raptors to deterrence signals (Q26:M76)

To accomplish this task, H. T. Harvey & Associates observed video data of eagles and other large raptors approaching DTBird-equipped turbines and classified the eagles' behavior during/after deterrent signals were broadcasted. They included data from both the observational study at the Manzana Wind Power Project and Year 1 of the experimental study at the Goodnoe Hills Wind Farm. The analyses focused on evaluating individual eagle/large raptor behavior at both study sites in response to spinning blades with broadcast deterrents, but also qualified those multi-site results based on the site-specific control-treatment results from the Goodnoe Hills that allowed for quantifying the differential deterrence effects of spinning turbines alone versus spinning turbines plus broadcasted DTBird audio deterrents.

H. T. Harvey & Associates reviewed detection records and videos collected for one full year at both study sites, including at all seven DTBird-equipped turbines at the Manzana facility and 11 acceptably functional DTBird turbines at the Goodnoe Hills facility. Sampling at both sites included screening all records that triggered a deterrent signal on 10 randomly selected days/28-day period during the first year of data collection at each site. For all records where the target was classified as a confirmed or probable eagle, vulture, or buteo, investigators evaluated the bird's flight behavior, including path divergence and changes in flapping style, and classified its response to the triggered deterrent into one of four categories: Yes (Confirmed Effective), Potential (Potentially Effective), No Response, Not Relevant (evident response but did not reduce risk). H. T. Harvey & Associates then evaluated differences in the proportions of categorical responses by site using 2-way Pearson chi-square analyses for each raptor group (eagles, vultures, and buteos). Records were also classified and evaluated by Preexposure Risk, but limited sample sizes precluded preparing 3-way chi-square analyses including Site and Preexposure Risk as predictors.

H. T. Harvey & Associates used a LGLM to evaluate how the probability of effective deterrence (reduced to binary dependent variable) was influenced by Site, Species Group, Preexposure Risk, and Wind Speed. The multi-species and golden eagle specific LGLM analyses confirmed effects of Site and Preexposure Risk, and an interactive effect of Wind Speed and Species Group. The probability of effective deterrence was overall slightly higher at the Manzana site, for unknown reasons, but possibly reflecting factors such as region-specific species sensitivities, habituation patterns of resident vs non-resident birds, and variation in landscape or climatic features. The probability of effective deterrence was highest for birds classified as at moderate Preexposure Risk, likely reflecting such birds having more time than birds at higher risk to effectively respond before closely approaching the RSZ. Higher wind speeds resulted in a higher probability of effective deterrence for eagles and vultures, but not buteos, potentially because larger raptors are more reliant on, and capable of using, wind for in-flight maneuvering.

Because of the poor quality of videos that DTBird uses, we took a conservative approach to classifying behavioral responses, meaning that we categorized responses based on the degree to which we could discern a behavior as effectively reducing risk for the eagle. Partially in order to maintain a sufficient sample size for analysis, we chose to consider effectiveness estimates that included both confirmed effective and potentially effective deterrence responses to evaluate the potential for DTBird deterrents to reduce the risk of eagles and other large raptors entering the RSZ of spinning turbines at the two study sites. This may overestimate DTBird's effectiveness to some degree. However, it is just as likely, if not more likely, limiting the results to confirmed effective responses would have underestimated the rate at which DTBird effectively reduced risk for eagles, because of our limited ability to confidently discern and classify relatively subtle but nonetheless effective behavioral responses. All further results summarized below are based on statistics representing the combination of confirmed and potentially effective responses as the basis for estimating the probability of effective deterrence. A report for this milestone was submitted to DOE in September 2023 (Q26:M76) (Attachment 7).

# 8.10.4 Milestone 10.4 Produce a multi-site estimate of collision risk reduction, estimate of eagle fatality reduction (# eagles/year) attributable to DTBird completed (Q27:M79)

The objective was to estimate DTBird's overall effectiveness in reducing the risk of eagles entering the RSZ of spinning turbines, based on multiple complementary approaches. The first approach involved combining probability of detection estimates derived from the UAV flight trials with probability of effective deterrence estimates derived from the behavioral analyses. The multiplicative combination of these estimates yielded an estimated 52% reduction in the probability of confirmed golden eagles entering the RSZ of spinning turbines with broadcasted deterrents at the Manzana facility, and a 38% reduction at the Goodnoe Hills facility. Data for all eagles combined from Goodnoe Hills (rare occurrences of bald eagles at Manzana) revealed similar results for golden eagles alone, except limited data suggested effective deterrence was higher for bald eagles than for golden eagles.

The Goodnoe Hills control-treatment experimental setup confirmed the addition of DTBird audio deterrents increased the likelihood of effective deterrence compared to just spinning turbines alone with deterrent signals muted. Recalculating the estimates of detection and deterrence effectiveness for golden eagles alone based on the Goodnoe Hills control-treatment results yielded a 24% probability of DTBird audio deterrents reducing risk of entering the RSZ of spinning turbines at Manzana and 19% for Goodnoe Hills. Narrowing the focus further to estimating DTBird's effectiveness when an eagle-surrogate UAV was flying in core exposure locations and *in situ* eagles were classified for behavioral analysis as at moderate to high Preexposure Risk revealed that spinning turbines plus deterrents resulted in a 68% probability of reduced risk, with the added effectiveness of deterrents alone reducing estimated risk by 37%.

The second approach used to estimate risk reduction from DTBird was based on the Goodnoe Hills 2-year control-treatment experiment involving randomized daily rotations of muted and broadcasted deterrents. For golden eagles alone, the dissuasion-trigger (dependent variable =

probability of triggering a dissuasion signal) and dwell-time (dependent variable = eagle dwell time as reflected in extent of video recording) models yielded similar estimated reductions (27–29%) in the two dependent variables at DTBird-equipped turbines when the audio deterrents were broadcasted compared to when the deterrents were muted. Combining insight from both approaches suggested that, for golden eagles that fly within the calibrated maximum detection range for the species, operation of DTBird can be expected to reduce the overall likelihood of approaching the RSZ by 20–30%, with that estimate potentially further elevated to near 40% for birds at moderate to high Preexposure Risk of entering the RSZ.

The dwell time data could potentially be used as a surrogate for the pre-construction "eagle activity minutes" metric used to project fatality rates at wind-energy facilities using the Bayesian collision risk model developed by the U.S Fish and Wildlife Service. We could have independently compared projected post-construction fatality estimates tailored to the Goodnoe Hills based on dwell time at control turbines versus treatment turbines to create an estimate of fatality reduction. However, a comparison (# of fatalities/per year) of that scale could not be extrapolated to other facilities with different collision risk infrastructure and eagle activity rates and behaviors. Therefore, we determined a better approach was to present percentage estimates of DTBird's beneficial effects in reducing post-construction collision risk, which could potentially be tailored to match initial pre-construction facility projections tailored to specific sites using the USFWS Bayesian risk model. The results from the two study sites—one in a desert foothills landscape and one in temperate grassland ridgeline landscape-clearly indicated that DTBird's overall effectiveness may vary in different landscape/climatic settings with different resident and transient eagle populations, and variable false-positive deterrenttriggering rates that may influence the eagle responses. A report for this milestone was submitted to DOE in January 2024 (Q27:M80) (Attachment 8).

### 8.11 Task 11.0: Prepare systems cost analysis

### 8.11.1 Milestone 11.1 System cost analysis completed (Q28:M84)

When including the overall cost of Liquen's Internal Services and R&D Department, the standard DTBirdV4D8 model sale cost (cameras model Falco and Larus software) is around \$18K - \$22K, and the yearly service sale cost around \$2K - \$3K. There are other project specific indirect costs for installation (around \$4–6K/unit) and onsite maintenance (around \$0.6–2K/unit/year). For the project, 16 DTBirdV4D8 units were manufactured in 2019 and delivered to Goodnoe Hills wind farm by the end of the year. Fourteen units operated under the evaluation and experiment from August 2021 to September 2023. **A report for this milestone is attached (Attachment 9)** 

Table 2828. Actual Cost(s) to Install, Operate, and Maintain the DTBird system, Liquen ONLY (2016-2024).

Project Cost(s)	Amount (USD)	Unitary cost for the 14 units (USD)
ACTUAL DTBIRD PURCHASE COST FOR 14 UNITS	\$208.619,64	\$14.901,40

SHIPPING DTBIRDV4D8 UNITS TO GOODNOE HILLS SITE AND US CUSTOMS *	\$17.114,49	\$1.069,66
INSTALLATION COSTS (TRAVEL & SALARIES COSTS) – OCT $26^{\text{TH}}$ TO NOV $3^{\text{RD}}$ 2019	\$10.659,23	\$761,37
YEAR 1: TOTAL YEARLY SERVICE 13 DTBirdV4D8 (12 months) including technician travelling costs to repair multiple maintenance issues - August 2021 till July 2022	\$42.997,43	\$3.071,25
YEAR 2: TOTAL YEARLY SERVICE 14 DTBirdV4D8 (12 months) – August 2022 till September 2023	\$35.199,41	\$2.514,24
TOTAL 14 SYSTEMS + 24 MONTHS OF SERVICE	\$327.278,51	\$23.377,04

<sup>\*16</sup> units were delivered to the site

### Section 9. Project Output/STI

#### 9.1 Publications

No publications resulting from work performed under this Cooperative Agreement. Three draft manuscripts have been prepared to date, but they have not yet been submitted for publication.

#### 9.2 Technologies/Techniques

No technologies or techniques were developed related to any aspect of the project with our knowledge under this Cooperative Agreement.

### 9.3 Status Reports

As part of the monthly check-in calls which REWI established with the DOE Contracting Team, unofficial status reports on this project were generated in advance of each monthly call. These status reports served as an agenda and guided the discussions during the calls and are preserved as attachments via email record between REWI and DOE.

### 9.4 Media Reports

In November 2022, REWI mentioned "support from the U.S. Department of Energy, evaluation minimization technologies, including IdentiFlight and DTBird" in a REWI Special Update on the Eagle Rule. **See** <u>https://rewi.org/2022/11/09/eagle-rule/</u>.

#### 9.5 Invention Disclosures

No invention disclosures about any aspect of the project were made with our knowledge under this Cooperative Agreement.

### 9.6 Patent Applications

No patent applications related to any aspect of the project were submitted with our knowledge under this Cooperative Agreement.

#### 9.7 Licensed Technologies

No subject inventions were licensed to third parties under this Cooperative Agreement.

#### 9.8 Networks/Collaborations Fostered

No partnerships, networks or other means of collaboration were formed or concluded under this Cooperative Agreement.

#### 9.9 Websites Featuring Project Work or Results

In September 2018, REWI (then AWWI) released "DTBird Technology Evaluation" and an accompanying technical report by H. T. Harvey & Associates detailing the results of an initial independent, site-specific pilot study of the DTBird detection/deterrence system at a wind facility in California. This initial study used UAVs and in-situ raptors to evaluate DTBird's ability to detect and deter large raptors, particularly golden eagles and reduce the risk of collisions with wind turbines. **See** <a href="https://rewi.org/resources/dtbird-technical-report">https://rewi.org/resources/dtbird-technical-report</a>.

#### 9.10 Other Products

No additional project output was generated under this Cooperative Agreement.

### 9.11 Awards, Prizes, and Recognition

No awards or other forms of recognition were received by any party under this Cooperative Agreement.

### Section 10. Project Summary Table

		Task Completion Date					
Ta	Sk Title / Task Description	Original Plan	Revised Plan (Mod 10)	Current Plan	Status	Percent Complete	Progress Notes

1.0	Project Launch and Development of Peer- Reviewed Study Design	Q1M3	Q5M15	Q5M15	Complet e	100%	Task Completed
2.0	Expand Analysis of False Positives Using Data Collected During Pilot Study at California Wind Facility	Q4M9	Q5M15	Q5M15	Complet e	100%	Task Completed
3.0	Evaluation of Pilot Study	Q4M10	Q6M18	Q6M18	Complet e	100%	Task Completed
4.0	Update DTBird System and Revise Study Design for BP2 and BP3 As Appropriate	Q5M13	Q8M22	Q8M22	Complet e	100%	Task Completed
5.0	Install DTBird at Goodnoe Hills, WA	Q5M15	Q18M53	Q18M53	Complet e	100%	Task Completed
6.0	In situ CA, WA; UAV Trials WA	Q9M25	Q20M60	Q20M60	Complet e	100%	Task Completed
7.0	Experiment Year 1	Q9M27	Q22M65	Q22M65	Complet e	100%	Task Completed
8.0	Complete Controlled Experiment and Analyze Results	Q15M4 5	Q26M78	Q27: M79	Complet e	100%	Task Completed
9.0	Evaluate Behavioral Responses of Raptors at Goodnoe Hills	Q15M4 5	Q27M79	Q25:M7 3	Complet e	100%	Task Completed
10.0	Complete Combined Multi- Site Analyses	Q15M4 5	Q27M79	Q27:M8 0	Complet e	100%	Task Completed
11.0	Systems Cost Analysis	Q15M4 5	Q28:M8 4	Q28:M8 4	Complet e	100%	Task Completed
12.0	Final Report	Q15M4 5	Q28:M8 4	Q28:M8 4	Complet e	100%	Task Completed



DE-EE0007883.0010
Attachment 1

#### Statement of Project Objectives (SOPO)

#### **American Wind Wildlife Institute**

#### Evaluating the Effectiveness of a Detection and Deterrent System in Reducing Golden Eagle Fatalities at Operational Wind Facilities

#### A. Project Goal and Objectives

The goal of this study is to evaluate the effectiveness of the current DTBird system in minimizing the risk of golden eagles (*Aquila chrysaetos*) colliding with wind turbines. AWWI will quantify the expected reduction in collision risk for golden eagles from operation of the detection and deterrence modules in a manner that supports the approach used by the U.S. Fish & Wildlife Service (USFWS) to assess and credit facility operators for their efforts to minimize predicted collision fatalities. AWWI will also provide information to help improve the technology to maximize its effectiveness. Golden eagles will be the focus of this study, but because eagle fatalities and interactions with wind turbines are infrequent, AWWI also may use suitable surrogate species, such as red-tailed hawks (*Buteo jamaicensis*), to accomplish statistically robust analyses.

At the end of the project AWWI will provide an analysis of DTBird's technical performance, its impact on eagle fatality reduction, and a detailed system cost analysis to provide the broadest inferences possible regarding the performance of DTBird in minimizing impacts to eagles from wind energy development in the U.S.

#### **Budget Period 1:**

- **Objective:** Develop a peer-reviewed study plan for 1) testing of the DTBird System at the Washington host facility, 2) potential to focus second year of evaluation to preliminarily assess for habituation, and 3) conducting integrative analyses of information gathered at multiple study sites.
- **Objective:** Evaluate results of a concurrent and independently funded California pilot study to inform refinements of the DTBird system and potential revisions to the study plan.
- **Objective**: Complete a preliminary evaluation of false positives at the California wind facility.
- Outcome: An initial assessment of DTBird effectiveness in detecting and deterring eagles and suitable surrogates based on an independent pilot study, recommendations to the technology provider for improving the DTBird system, development of a peer- reviewed study plan, and completed preparations for the second study site.

#### **Budget Period 2:**

- Objective: Install DTBird and conduct unmanned aerial vehicle (UAV) flight trials at the Washington wind facility.
- Objective: Conduct a second year of evaluation of DTBird detection and deterrence capabilities at the California wind facility, focusing on in situ bird

- video footage.
- Objective: Complete the first year of a controlled experiment at the Washington facility designed to evaluate DTBird's effectiveness as an impact minimization technology.
- Objective: Conduct a mid-year assessment to ascertain whether sufficient data were collected through year one to determine effectiveness of the deterrent with reasonable statistical power.
- **Outcome**: Field data collection completed at California wind facility, UAV flight trials and first year of controlled experiment completed at Washington wind facility.

### **Budget Period 3:**

- **Objective:** Based on results of mid-year dataset assessment, either complete the controlled experiment or pivot to Alternative Objective at Washington wind facility.
- Alternative Objective: Complete one (1) year of a controlled experiment at the Washington facility designed to evaluate for eagle and raptor habituation behavior.
- Objective: Conduct multi-site analyses of field data.
- Outcome: A rigorous evaluation of DTBird's ability to reduce eagle fatalities and calculation of the fatality reduction credit applicable to the development of Eagle Conservation Plans.

#### **B.** Technical Scope Summary

AWWI will conduct independent tests of DTBird detection and deterrence functions using:

- 1. UAVs equipped with high-resolution GPS tracking devices; and
- 2. DTBird video data of in situ golden eagles and suitable surrogate raptors.

AWWI will use these results to model expected reductions in fatality risk. Conducted in two distinctly different landscapes in California and Washington, these tests will support rigorous evaluation of the accuracy, primary dependent factors, and limitations of the DTBird system in detecting and deterring eagles and suitable surrogate raptors at the two study sites.

AWWI will rigorously support these analyses by conducting a two-year controlled experiment at the Washington wind facility to evaluate whether operation of DTBird reduces the probability of raptors entering the collision risk zone of equipped turbines. If the first year of data collection elicits sound results for the effectiveness objective, an alternative objective of a preliminary evaluation of habituation will be conducted in year 2. Regardless the overall approach taken, these efforts intend to enable a robust evaluation of DTBird's ability to successfully deter eagles entering the Rotor Swept Zone (RSZ) of turbines in landscapes similar to the study areas.

AWWI proposes a three-phase study over 84 months (7 years) beginning June 01, 2017 and ending May 31, 2024.

#### **Budget Period 1 – AWWI will:**

- Develop a detailed study design for Budget Period (BP) 2 and BP3 and revise the design in response to comments from peer reviewers.
- Incorporate the results of a separately funded pilot study initiated in November 2016 at the California host wind facility based on a previously approved peerreviewed study plan. The pilot study will provide an initial assessment of the DTBird detection and deterrence-triggering functions and the behavioral responses of *in situ* raptors exposed to deterrence signals.
- Results from the pilot study will support initial refinements of the DTBird system and updates to our study design prior to expanding the study during Budget Periods 2 and 3 at the California wind facility and to the south-central Washington wind facility.



#### **Budget Period 2 - AWWI will:**

- Expand the evaluation of the first, initial year of in situ raptors' behavioral responses to DTBird at the California wind facility;
- Conduct a second year of video evaluation of in situ raptors' behavioral responses to DTBird at the California wind facility;
- Incorporate lessons learned from the California pilot study, expand evaluation of DTBird to a second geographically distinct wind facility in the Columbia Plateau Steppe and Grassland of Washington;
- Conduct UAV flight trials to evaluate the detection and deterrence-triggering functions of DTBird at the Washington wind facility.
- Complete the first year of the controlled experiment at the Washington wind facility. This experiment will evaluate the ability of DTBird to deter eagles and surrogate raptors from entering the rotor-swept zone (RSZ) of DTBirdequipped turbines; and
- Evaluate whether first year dataset is sufficient to address primary objective. If so, pivot to Alternative Objective described under Task 8 to preliminarily assess for habituation.

#### **Budget Period 3 – AWWI will:**

- Complete the second year of the controlled experiment at the Washington wind facility, either the primary or alternative objective, effectiveness or habituation, respectively.
- Complete multi-site analyses of flight trial and in situ video footage to provide the broadest possible inferences of the effectiveness of the DTBird detection anddeterrent system.
- Prepare a final technical report and one or more manuscripts for publication in peer- reviewed journals.

#### C. Tasks To Be Performed

BUDGET PERIOD 1: DEVELOP A DETAILED, PEER-REVIEWED STUDY DESIGN FOR EXPANDED STUDY, AND EVALUATE RESULTS OF CALIFORNIA PILOT STUDY (Q1-Q6: M1-M18)

Task 1.0: Project Launch and Development of Peer-Reviewed Study Design (Q2-5: M4- M15)

**Task Summary:** Develop a detailed study design, coordinate and complete internal, logistical aspects of the project in preparation for the project launch.

**Subtask 1.1:** Develop a detailed study design (Q2-5: M4-M15) AWWI will develop a peer-reviewed study plan. The study design will include field testing of the DTBird System at the Washington wind facility using drones and, if deemed feasible, trained raptors and integrative analyses of information gathered at multiple study sites.

Milestone 1.1.1: Completed peer-reviewed study design (Q5: M15)

Task 2.0: Evaluate False Positives Using Data Collected During Pilot Study at California Wind Facility (Q2-Q5: M4-M15)

**Task Summary:** Quantify and evaluate false-positive detections at the California wind facility based on DTBird video data collected during pilot study.

**Expected End Result:** Initial site-specific evaluation of the probability of false positives.

**Milestone 2.1:** False positive rates quantified at California wind facility (Q5: M15)

#### Task 3.0: Evaluation of Pilot Study (Q3-6: M8-M18)

**Task Summary:** Produce comprehensive evaluation of pilot study that (a) summarizes results and presents an initial objective assessment of DTBird effectiveness in detecting and deterring eagles and suitable surrogates and (b) provide recommended updates to technology partner and facilitate relevant refinements of DTBird hardware and/or software system.

**Expected End Result:** Comprehensive technical evaluation to facilitate updates to DTBird technology, as appropriate.

**Milestone 3.1:** Recommended updates to DTBird system delivered to technology vendor (Q6: M16)

**Milestone 3.2**: Quantitative performance targets established based on analysis of pilot study (Q6: M18)

**Task 4.0 (Bridge Task):** Update DTBird System and Revise Study Design for BP2 and BP3 as appropriate (Q6-8: M17-22)

Task Summary: Based on the comprehensive evaluation of the pilot study,

update the study design for use in further DTBird evaluations, and update the DTBird system.

**Expected End Result:** Study design for BP2 and BP3 revised, as appropriate, based on evaluation of pilot study results.

#### **Budget Period 1 Go/No-go Decision Point (Q6: M17-18)**

AWWI will submit a continuation application at least 60 days before end of BP1, including a progress report summarizing results to date.

Continuation into the subsequent budget period will be based on project performance, adherence to project schedule, meeting milestone objectives, and overall contribution to the program goals and objectives. The Go/No-Go decision to proceed with BP2 activities is based on the following criteria:

- Successful development and peer review of study plan for BP2 and BP3 activities.
- Determination of whether anticipated DTBird refinements can be made prior to initiating expanded study.
- 3. Initial quantification of false positives and false negatives and estimate of collision risk reduction from use of DTBird completed.
- 4. Adherence to schedule, budget, and submission of deliverables in BP1, and quality of plans for BP2 work.
- 5. Evaluation of technical performance goals established in BP1.

AWWI will provide a presentation summarizing the results of the work performed during and planned for the remainder of BP1. During the Go/No-Go review, the project's technical merits, schedule, budget, and deliverables from Tasks 1-3 and plans for the next budget period will be evaluated based on the criteria as specified above.

As a result of the Go/No-Go decision point, DOE may, at its discretion, authorize the following actions by the Recipient:

- 1. Continue to fund the project, depending on appropriations;
- 2. Recommend redirection of the work under the project;
- 3. Place a hold on the project, pending further supporting data or funding; or
- 4. Cancel the project because of insufficient progress, change in strategic direction, or lack of funding.

### BUDGET PERIOD 2: EXPAND EVALUATION OF DTBIRD DETECTION AND DETERRENCE SYSTEMS (Q7-Q22: M19-M65)

Task 4.0 (Bridge Task): Update DTBird System and Revise Study Design for BP2 and BP3 as Appropriate (Q6-8: M17-22)

**Task Summary:** Based on the comprehensive evaluation of the pilot study, update the study design for use in further DTBird evaluations and update the DTBird system.

**Expected End Result:** Study design for BP2 and BP3 revised, as appropriate, based on evaluation of pilot study results.

Milestone 4.1: Study design revised (Q7: M19)

Milestone 4.2: Updates to DTBird system completed (Q8: M22)

#### Task 5.0: Install DTBird Systems at Washington Wind Facility (Q10-18: M28-M53)

**Task Summary:** Install and commission updated DTBird systems on multiple turbines at Washington wind facility; selected turbines will be located in areas with higher golden eagle and surrogate raptor activity and distributed to ensure independence among installations and to support the controlled experiment and installation requirements of the facility.

**Expected End Result:** Completed installation and commissioning of DTBird systems at Washington wind facility.

**Milestone 5.1:** DTBird systems installed and commissioned at Washington wind facility (Q18: M53)

# Task 6.0: Expand Evaluation of *In Situ* Bird Video Footage at California and Washington Wind Facilities, Conduct UAV Flight Trials at Washington Wind Facility, and Analyze Site-Specific Results (Q10-Q20: M28-M60)

**Task Summary:** HTH will expand the evaluation to encompass the first, initial year of behavioral response data of *in situ* raptors to deterrence signals at the California wind facility. Based on the approved study design, HTH will conduct UAV flight trials at the Washington wind facility and will analyze results to improve understanding of how landscape setting and behavioral covariates influence DTBird's performance of both detection and deterrence-triggering functions. HTH will evaluate DTBird video footage and UAV flight trial results to quantify false positives and false negatives at Washington wind facility.

**Expected End Results:** Enhanced site-specific evaluations of detection and deterrence-triggering system at the California wind facility. Site-specific evaluations of detection and deterrence-triggering systems at the Washington wind facility.

Subtask 6.1: Conduct UAV Flight Trials at Washington Wind Facility (Q10-

Q18: M28- M53)

Conduct UAV flight trials at the Washington facility to evaluate detection and deterrence-triggering functions.

**Milestone 6.1.1:** UAV flight trials completed at Washington Wind Facility (Q18: M53)

**Subtask 6.2:** Expand evaluation of Behavioral Responses of *In Situ* Eagles to Deterrence Signals at California Wind Facility using DTBird data collected between September 2017 – December 2018 (Q10–Q13: M28–M39)

**Milestone 6.2.1:** DTBird video data collection and enhanced site-specific evaluation of *in situ* eagle responses to deterrents completed for California facility. Evaluation is restricted to first, initial year of data collection at California facility. (Q10: M28)

#### **Quantitative Performance Target:**

 Deterrence Rate for Eagles: ≥50% estimated deterrence rate for eagles.

From those data collected during first, initial year at California facility, at least 50% of bald and golden eagles should exhibit avoidance behavior to a DTBird system within 5 seconds of deterrent signal when sound is "on".

This deterrence rate was selected based on data from the pilot study, in which 36% of raptors (overall) responded effectively to the deterrent signals. We selected this target because our expectation is that DTBird's performance, as measured at the Washington facility, will meet or exceed the performance observed in the pilot study. The project team anticipates having access to higher resolution video footage from the Washington facility and therefore improved bird identification capabilities from the DTBird video clips.

**Subtask 6.3:** Conduct Preliminary Analysis of False Positives and False Negatives at Washington Wind Facility (Q18–Q20: M54–M60)

Analyze DTBird video footage and data to quantify rates of false positives and false negatives at Washington wind facility.

**Milestone 6.3.1:** Preliminary site-specific estimates of rates of false positives and false negatives produced for Washington wind facility (Q20: M60)

#### **Quantitative Performance Targets:**

1) False Negative Rate: 27 – 47%; this is the complement of the detection rate of UAV flights by DTBird system.

The false negative rate (complement of the detection rate;

- UAV flights that occurred but were not recorded by DTBird) was  $37\% \pm 10\%$  SD in the pilot study.
- False Positive Rate: Not to exceed 1.6 2.8 False Positive triggers/turbine/day, or 36% of total video records collected by DTBird units.

This false positive rate is based on data from the False Positives Analysis of data collected during the pilot study, in which DTBird systems detected  $2.2 \pm 0.64$  TFPs/turbine/day, and 36% of video records from DTBird contained targets determined to be non-avian objects such as turbine blades, aircraft, insects, raindrops, etc.

#### Additional Metrics for Context and Applicability

The DTBird technology in its current form does not distinguish between eagles and other bird species that trigger detection and deterrent responses, though the system can be calibrated and optimized for targets of a specified wingspan. In the United States, where the primary species of concern are bald and/or golden eagles, deterrent signals triggered by non-target species may be considered either excessive or a nuisance to nearby humans and wildlife. For this study, we will quantify the percent of each event type (detection, warning signal, dissuasion signal) triggered by eagles compared to other species of birds and false positives, as well as the rate of deterrent signal triggers per turbine per day when the system is calibrated for eagle-size birds.

**Subtask 6.4:** Analyze Detection and Deterrence-Triggering Responses as a Function of Flight and Landscape Characteristics at Washington Wind Facility (Q14-Q20: M40- M60)

Analyze UAV flight data and develop site-specific statistical models to evaluate the influence of flight and environmental covariates on DTBird detection and deterrence- triggering responses.

**Milestone 6.4.1:** Initial site-specific models developed to quantify the spatial accuracy of the DTBird detection and deterrence-triggering system at Washington wind facility (Q20: M60)

#### **Quantitative Performance Target:**

1) UAV Detection Rate: 53 - 73% overall UAV detection rate.

This detection rate was selected based on data from the pilot study, in which  $63\% \pm 10\%$  standard deviation (SD) of the UAV flights were detected in the flight trials.

Task 7.0: Conduct First Year of Controlled Experiment at Washington Wind Facility (Q18-Q22: M52-M65)

**Task Summary:** Conduct the first year of the controlled experiment to evaluate the collision risk reduction capability of DTBird and conduct partial-year assessment to assess whether sufficient data will be collected in year one of the controlled experiment to determine effectiveness of the deterrent with reasonable statistical power.

**Expected End Result:** Completion of first year of the controlled experiment. If we are unable to sufficiently determine whether the DTBird deterrent is effective in year one, then we will continue to evaluate effectiveness in year two. If effectiveness is detected statistically, then we will obtain a preliminary assessment of habituation by eagles to the deterrent.

**Subtask 7.1:** Collect first year of data at the Washington wind facility for the controlled experiment to evaluate the collision risk reduction capacity of DTBird. (Q18-Q21: M52-M63)

**Milestone 7.1.1:** First year data collection completed for controlled experiment (Q21: M63)

**Subtask 7.2:** Use at least first six months of data from controlled experiment to conduct partial-year assessment of whether data collected in year one of the controlled experiment will be sufficient to evaluate effectiveness of the technology with reasonable statistical power. If appropriate, the Project Team will update the assessment with some or all data collected during months 7-10 of the controlled experiment. The assessment will be used to determine whether our objective in year two will be to evaluate short-term habituation of eagles to the deterrent. (Q20-21: M58-M63)

Milestone 7.2.1: A summary of progress and findings up to 10 months' worth of data will be included in the Go/No Go report for Budget Period 2. This summary will include a power analysis performed on at least 6 months' worth of data as well as a recommendation of which objective (effectiveness or habituation) to pursue in year two of the experiment. (Q21: M63)

### Task 8.0 (Bridge Task): Complete Controlled Experiment and Analyze Results (Q22: M64-M65)

**Task Summary:** Implement the second year of the controlled experiment following the primary objective or undertake the alternative objective that assesses for evidence of habituation.

**Expected End Result:** Completed controlled experiment and analysis of experiment results to evaluate potential for DTBird to reduce raptor activity in collision risk zone.

**Milestone 8.1:** First two months of controlled experiment's Year 2 DTBird data collected at Washington site (Q21: M65)

### **Budget Period 2 Go/No-Go Decision Point (Q20-Q22: M60-M64)**

AWWI will submit a continuation application at least 60 days before the end of BP2, which includes a progress report summarizing the results of the work performed to date.

Continuation into the subsequent budget period will be based on project performance, adherence to project schedule, meeting milestone objectives and overall contribution to the program goals and objectives. The Go/No-Go decision to proceed with BP3 activities is based on the following criteria:

- Successful performance of detection, identification, and deterrence functions, including successful performance relative to updated Quantitative Performance Targets:
  - 1) ≥50% successful deterrence rate for eagles (Subtask 6.2)
  - 2) False Negative Rate: 27 47%; this is the complement of the detection rate of UAV flights by DTBird system (Subtask 6.3);
  - False Positive Rate: Not to exceed 1.6 2.8 False Positive triggers/turbine/day, or 36% of total video records collected by DTBird units (Subtask 6.3); and
  - 4) 53-73% Detection rate of UAVs (Subtask 6.4)
- 2. Adherence to schedule, budget, and submission of deliverables in BP2 and quality of plans for BP3 work.
- 3. Determine if year one eagle activity is sufficient enough to complete the controlled experiment; if not continue year one controlled experiment in year two (Milestone 7.1). The final decision will be made in conjunction with the DOE and peer review team during the Go/No-Go decision.
- 4. Any marked departure from the study design determined to be of importance will be evaluated in a revised, peer-reviewed study design.

AWWI will provide a presentation summarizing the results of the work performed during and planned for the remainder of BP2. During the Go/No-Go review, the project's technical merits, schedule, budget, and deliverables from Tasks 4–8 and plans for the next budget period will be evaluated based on the criteria as specified above.

As a result of the Go/No-Go decision point, DOE may, at its discretion authorize the following actions by the Recipient:

- 1) Continue to fund the project, depending on appropriations;
- 2) Recommend redirection of the work under the project;
- 3) Place a hold on the project, pending further supporting data or funding; or
- 4) Cancel the project because of insufficient progress, change in strategic

direction, or lack of funding.

# BUDGET PERIOD 3: COMPLETE PRIMARY OR ALTERNATIVE CONTROLLED EXPERIMENT & VIDEO EVALUATION AT WASHINGTON FACILITY; CONDUCT MULTI-SITE ANALYSES (Q22-Q28: M65-M84)

Task8.0: Complete Controlled Experiment and Analyze Results (Q22-Q26: M64-M78)

**Task Summary:** Implement the second year of the controlled experiment following the primary objective or undertake the alternative objective that assesses for evidence of habituation.

**Expected End Result:** Completed controlled experiment and analysis of experiment results to evaluate potential for DTBird to reduce raptor activity in collision risk zone.

**Milestone 8.2:** Controlled experiment completed and results analyzed; an estimate of eagle collision risk reduction from DTBird is calculated. (Q26: M78)

Task 9.0: Evaluate Behavioral Responses of Raptors Exposed to Deterrence Signals at Washington Wind Facility (Q22-Q27: M65-M79)

**Task Summary:** Review year one of DTBird video footage from Washington wind facility to classify behavioral responses of *in situ* raptors exposed to deterrence signals at treatment turbines using DTBird Digital Analysis Platform (see Subtask 2.2).

**Expected End Result:** DTBird effectiveness in causing successful behavioral responses among *in situ* raptors, based on a measured divergence in flight path, and other changes in flight as described in the study design (section 2.4.2. Classifying Deterrent Responses) evaluated with sufficient statistical power.

Milestone 9.1: All DTBird video evaluation and classification of *in situ* raptor responses to deterrence signals completed. Target performance is ≥50% successful deterrence rate for eagles (Q27: M79)

Task 10.0: Complete Combined Multi-Site Analyses (Q22-Q27: M65-M79)

**Task Summary:** Conduct analyses that integrate data from studies at the California and Washington wind facilities and, if relevant, the test facility.

**Expected End Result:** Broader-based inferences about the performance characteristics and effectiveness of the DTBird system in different landscape settings.

**Subtask 10.1:** Complete Multi-Site Analyses of Detection and Deterrence-Triggering Capabilities as a Function of Flight and Landscape Characteristics (Q22–Q24: M65– M70)

Milestone 10.1.1: Multi-site analyses completed (Q24: M70)

**Subtask 10.2:** Complete Multi-Site Analyses of False Positives and False Negatives (Q24-Q25: M71-M73)

Milestone 10.2.1: Multi-site analyses completed (Q25: M73)

**Subtask 10.3:** Complete Multi-Site Analyses of Behavioral Responses of *In Situ* Raptors to Deterrence Signals (Q25-Q26: M74–M76)

The basic approach to accomplishing Subtasks 10.1–10.3 integrated analyses is adding site as a blocking factor in relevant GLMMs and GLMs (see Subtasks 2.2–2.4); some analyses may require covariate modifications to represent variation in landscape settings.

Milestone 10.3.1: Multi-site analyses completed (Q26: M76)

**Subtask 10.4:** Produce Multi-site Estimate of Collision Risk Reduction (Q26-Q27: M77 – M79)

Use data generated by the two-site DTBird evaluations, the controlled experiment, and the Bayesian risk analysis recommended by the USFWS, to quantify DTBird's effect on golden eagle collision risk.

**Milestone 10.4.1:** Estimate of eagle fatality reduction (# eagles/year) attributable to DTBird completed (Q27: M79).

#### Task 11.0: Prepare systems cost analysis (Q27-28: M79-84)

**Task Summary:** An analysis of DTBird system cost including cost of instrumentation, data management, data analysis, and deployment or retrieval, operation, and maintenance will be completed for comparison with the cost-effectiveness of other minimization technologies.

**Milestone 11.1:** System cost analysis completed (Q28: M84)

**Deliverable 11.1:** Final report with detailed technical summary, results of performance testing, and system cost analysis of instrumentation, data management and analysis, and the deployment or retrieval, operation, and maintenance of the technology (Q28: M84).

**Expected End Result:** Systems cost analysis

### Task 12.0: Prepare and Submit Manuscripts on Project Methodology and Results for Publication in Peer-Reviewed Journals (Q27-28: M79-84)

**Task Summary:** As appropriate, one or more manuscripts will be prepared for publication in peer-reviewed journals. Review and revision of manuscript(s) may extend beyond the timeframe of the DOE study.

**Deliverable 12.1:** Submission of one or more manuscripts for publication in peer-reviewed journals (Q28: M84).

**Expected End Result:** One or more peer-reviewed publications in respected scientific journals.

**End of Project Goal:** AWWI will have developed a model that evaluates DTBird's technical performance under a range of environmental conditions, AWWI will have

quantified DTBird's ability to reduce eagle fatalities at wind facilities. AWWI will have estimated the cost of the minimization achieved.

#### D. Project Management and Reporting

AWWI will coordinate all meetings and project team activities. At a minimum, this will include monthly calls on the progress of field evaluations and quarterly briefing calls with all members of project team. AWWI will also work with DOE's designated coordinating entity on peer review of the study design and project results, and any meta-analyses across multiple projects.

Prior to each Budget Period and Task, the project team will meet to discuss the potential risks and management strategies to minimize the negative impacts of those risks. AWWI will clearly articulate the objectives of each Task throughout the study and assign specific responsibilities and deliverables to team members. In consultation with DOE, a change control process will be designed and implemented. If a minor change occurs, project team members are responsible for notifying other members of the project team within three business days. If a major change is identified, AWWI will convene the team within 48 hours and consult with DOE to discuss the most viable option to continue with the study. AWWI will facilitate handoff points to team members and manage all logistics and finances for this study. AWWI will be responsible for all reporting to the DOE/EERE.

Deliverables will be provided in accordance with the Federal Assistance Reporting Checklist:

- 1. Quarterly reports outlining progress made on all awarded tasks
- 2. Annual technical reports for each year of the study
- 3. Written summaries and/or presentations for DOE Program Office Peer Reviews
- 4. Final report with detailed technical summary, results of performance testing, and system cost analysis of instrumentation, data management and analysis, and the deployment or retrieval, operation, and maintenance of the technology
- 5. Submission of one or more manuscripts for publication in peer-reviewed journals

E. Milestone Summary Table: American Wind Wildlife Institute. Project Title: Evaluating the Effectiveness of a Detection and Deterrent System in Reducing Golden Eagle Fatalities at Operational Wind Facilities

Task #	Task/Subtask Title	Milestone		Milestone Description	Verification	Expected	Expected
		Туре	#	1	Process	Month	Quarter
1.1	Develop a Detailed Study Design	Milestone	1.1.1	Completed and peer-reviewed study design	Report to EERE	15	5
2.0	Augment Pilot Study with Analysis of False Positives at California Wind Facility	Milestone	2.1	False positives rates quantified at California wind facility	Report to EERE	15	5
		Milestone	3.1	Recommended updates to DTBird system delivered to technology vendor	Report to EERE	16	6
3.0	Evaluation of Pilot Study	Milestone	3.2	Quantitative performance targets established based on analysis of pilot study	Report to EERE	18	6
4.1	Study design revised	Milestone	4.1	Study design revised	Report to EERE	19	7
4.2	Updates to DTBird system completed	Milestone	4.2	Updates to DTBird system completed	Report to EERE	22	8
		Go/No-Go	BP1 Go/ No-Go	Successful development and peer review of study plan for BP2 and BP3 activities.  Determination of whether anticipated DTBird refinements can be made prior to initiating expanded study.  -Successful performance of detection, identification and deterrence functions. Initial quantification of false positives and false negatives and estimate of collision risk reduction from use of DTBird.  -Adherence to schedule, budget, and submission of deliverables in BP1, and quality of plans for BP2 work.	Report to EERE	18	6
5.0	Install DTBird Systems at Washington Facility	Milestone	5.1	DTBird systems installed at Washington wind facility	Report to EERE	49	17

Task #	Task/Subtask Title	Milestone		Milestone Description	Verification	Expected	Expected
		Туре	#		Process	Month	Quarter
6.1	Conduct UAV Flight Trials at Washington Facility	Milestone	6.1.1	UAV flight trials completed at Washington wind facility	Report to EERE	53	18
6.2	Expand Analysis of Behavioral Responses of In Situ Eagles to Deterrence Signals at California Facility	Milestone	6.2.1	DTBird video data collection and enhanced site- specific evaluation of in situ eagle responses to deterrents completed for California wind facility. Evaluation is restricted to first, initial year of data collection at California facility.	Report to EERE	28	10
6.3	Analyze False Positives and False Negatives at Washington Facility	Milestone	6.3.1	Site-specific estimates of rates of false positives and false negatives produced for Washington wind facility	Report to EERE	60	20
6.4	Analyze Detection and Deterrence Triggering Responses as a Function of Flight and Landscape Characteristics at Washington Facility	Milestone	6.4.1	Initial site-specific models developed to quantify the spatial accuracy of the DTBird detection and deterrence-triggering system at Washington wind facility	Report to EERE	60	20
7.1	Conduct First Year of Controlled Experiment at Washington Facility	Milestone	7.1.1	First-year baseline data collection completed for controlled experiment	Report to EERE	63	21
7.2	Partial-year assessment	Milestone	7.2.1	Conduct a partial-year assessment to assess whether sufficient data were collected in year one of the controlled experiment to determine effectiveness of the deterrent with reasonable statistical power.  Summary of progress and findings of controlled experiment to date submitted with Go/No Go report	Report to EERE	64	22
		Go/No-Go	BP2 Go/ No-Go	Successful performance of detection, identification, and deterrence functions. Adherence to schedule, budget, and submission of deliverables in BP2 and quality of plans for BP3 work. Determine if eagle activity is high enough to complete the controlled experiment; if not stop experiment and consider whether and how to proceed.	Provide analysis to EERE	64	21

8.0	Complete Controlled Experiment and Analyze Results (Bridge Task)	Milestone		First two months of controlled experiment's Year 2 DTBird data collected at Washington site.	Report to EERE	65	21	
-----	--	-----------	--	---	-------------------	----	----	--

Task #	Task/Subtask Title	Milestone		Milestone Description	Verification	Expected	Expected	
		Туре	#		Process	Month	Quarter	
8.0	Complete Controlled Experiment and Analyze Results	Milestone	8.2	, , ,	Report to EERE	78	26	
9.0	Evaluate Behavioral Responses of Raptors Exposed to Deterrence Signals at Washington Facility	Milestone	9.1		Report to EERE	79	24	
10.1	Complete Multi-Site Analyses of Detection and Deterrence- Triggering Capabilities as a Function of Flight and Landscape Characteristics	Milestone	10.1.1	Multi-site analyses completed	Report to EERE	70	24	
10.2	Complete Multi-site Analysis of False Positives and False Negatives	Milestone	10.2.1	Multi-site analyses completed	Report to EERE	73	25	
10.3	Complete Multi-site Analysis of Behavioral Responses of In Situ Raptors to Deterrence Signals	Milestone	10.3.1	Multi-site analyses completed	Report to EERE	76	26	
10.4	Produce Multi-Site Estimate of Collision Risk Reduction	Milestone	10.4.1	Estimate of eagle fatality reduction (# eagles/year) attributable to DTBird completed	Report to EERE	79	27	
11.0	Prepare systems cost analysis	Milestone	11.1	Systems cost analysis completed	Report to EERE	84	28	
12.0	Prepare and Submit Manuscripts on Project Methodology and Results for Publication in Peer-Reviewed Journals	End of Projec t Goal	12.1	A model that evaluates DTBird's technical performance under a range of environmental conditions, and quantification of its ability to reduce eagle fatalities at wind facilities.	Report to EERE	84	28	

DBA Renewable Energy Wildlife Applicant Name: Institute

Award Number:

## DE-EE0007883.0012 **Budget Information - Non Construction Programs**

OMB Approval No. 0348-0044

Section A - Budget Summary  Grant Program Function or	Catalog of Federal	Estimated Unol	oligated Funds			
Activity Domestic Assistance		Federal	Non-Federal	Federal	New or Revised Budget  Non-Federal	Total
(a)	Number (b)	(c)	(d)	(e)	(f)	(g)
Budget Period 1	81.087			\$116,480	\$147,021	\$263,50
2. Budget Period 2	81.087			\$341,423	\$888,856	\$1,230,27
3. Budget Period 3	81.087			\$258,616	\$5,270	\$263,886
4.						
5. Totals				\$716,519	\$1,041,146	\$1,757,665
Section B - Budget Categories						
6. Object Class Catagories				Total (5)		
6. Object Class Categories		Budget Period 1	Budget Period 2	Budget Period 3		Total (5)
a. Personnel		\$45,667	\$77,477	\$13,446		\$136,59 <sup>2</sup>
b. Fringe Benefits		\$8,964	\$15,209	\$2,640		\$26,813
c. Travel		\$1,357	\$1,090	\$0		\$2,447
d. Equipment		\$0	\$265,249	\$0		\$265,249
e. Supplies		\$0	\$0	\$0		\$(
f. Contractual		\$183,462	\$794,685	\$207,301		\$1,185,448
g. Construction		\$0	\$0	\$0		\$(
h. Other		\$0	\$42,997	\$36,788		\$79,785
i. Total Direct Charges (sum of 6a-6h)		\$239,451	\$1,196,707	\$260,175		\$1,696,333
j. Indirect Charges		\$24,050	\$33,571	\$3,711		\$61,332
k. Totals (sum of 6i-6j)		\$263,501	\$1,230,278	\$263,886		\$1,757,665
7. Program Income		\$0	\$0	\$0		\$0













50 years of field notes, exploration, and excellence

## **Research Report**

Results of Controlled Two-Year Experiment to Evaluate
Effectiveness of the DTBird® Automated Detection and
Deterrence System in Reducing Collision Risk for Eagles and
Other Large Raptors at the Goodnoe Hills Wind Farm,
Washington

Project #4080-01

Prepared for:

Renewable Energy Wildlife Institute

1990 K Street NW, Suite 620 Washington, D.C. 20006-1189

Prime Contractor: DOE Cooperative Agreement DE-EE0007883

Prepared by:

H. T. Harvey & Associates

Final - May 17, 2024

## **Executive Summary**

DTBird® is an automated detection and audio deterrent system designed to discourage birds from entering the rotor swept zone of spinning wind turbines (see https://dtbird.com). This report focuses on a portion of research conducted in collaboration with the Renewable Energy Wildlife Institute (REWI), funded by the Department of Energy (DOE), involving 14 DTBird systems installed at the Goodnoe Hills Wind Farm in south-central Washington. The overarching goal of this research has been to evaluate the effectiveness of DTBird in detecting and discouraging golden eagles (*Aquila chrysaetos*) and other large soaring raptors from approaching the rotor swept zone (RSZ) of operating wind turbines.

The DTBird video surveillance system detects and tracks objects based on calibrated metrics reflecting how many image pixels a bird of a targeted size range is expected to fill at specific distances from the turbine. The system automatically records an initial detection/tracking-initiation event in an online database once it registers a target of interest, and then triggers a warning signal and/or a more aggressive dissuasion signal (both of which comprise deterrent signals) if it registers that the tracked object has moved closer and crossed a specific distance threshold. The Goodnoe Hills study included a 2-year control-treatment experiment involving randomized daily operation of DTBird systems with and without the audio deterrents actually broadcasting. The objective was to evaluate the effectiveness of DTBird in reducing collision risk for eagles and surrogate raptors as indicated by a reduction in detectable eagle/raptor activity near the RSZ of turbines with active deterrent signals. For the purposes of this in situ experiment, DTBird units at all 14 turbines continued to produce and record warning- and dissuasion-trigger events, but the audio signals for these events were not broadcast at control turbines.

In this report, we present an analysis of data collected during 27 consecutive 28-day sampling cycles (hereafter 28d Cycles) from September 2021 through September 2023 to evaluate DTBird's "proximate" effectiveness in deterring eagles from approaching the RSZ of spinning turbines. The research hypotheses we formulated for the experiment were as follows:

**Hypothesis A:** The probability of an eagle triggering a dissuasion signal will be lower for DTBird turbines operating in treatment mode (deterrent signals broadcasting) compared to those operating in control mode, because broadcasted warning signals deter target raptors from approaching closer and triggering a dissuasion signal.

**Hypothesis B:** The average dwell time of eagles in the vicinity of DTBird-equipped turbines—as reflected in the length of relevant targeting videos recorded by the DTBird detection system—will be reduced around systems operating in treatment mode compared those operating in control mode, because broadcasted deterrent signals discourage birds from lingering near focal turbines.

**Hypothesis C:** The probability of an eagle crossing the active rotor swept area (RSA) of DTBird-equipped turbines will be lower for systems operating in treatment mode compared to those operating in control mode, because operation of the deterrent signals reduces the likelihood of target raptors entering the RSZ of turbines.

Because DTBird does not identify or enumerate detected targets (technicians must do that manually by reviewing recorded videos) and due to a preponderance of false-positive detections and other abundant raptors besides eagles, amassing the datasets considered here required screening more than 27,000 detection records to generate a dataset of 390 useable records representing confirmed and probable eagles. In addition, substantial issues beyond our control with maintaining effective operations of the 14 DTBird systems greatly hindered achieving our intended, rigorously balanced sampling design for the 2-year experiment. Despite these challenges, we developed independent generalized linear mixed models (GLMMs) that allowed us to effectively address Hypotheses A and B. In contrast, challenges producing a consistent, accurate, and robust dataset on possible RSA crossings based on interpreting 3D responses from 2D video images precluded effective evaluation of Hypothesis C.

We developed independent GLMMs for all confirmed and probable golden eagles, and for all confirmed and probable eagles (including all golden eagles, bald eagles [Haliaetus leucocephalus], and unidentified eagles). For each group and dependent variable, we tested for effects of Treatment Group and five potential covariates: sampling Year (1 or 2) or 28d Cycle (temporal variables considered only in separate models), Time of Day (evaluated including a second-order term), Cloud Cover (fair, partly cloudy, or overcast), Wind Speed, and the number of false positives that triggered deterrent signals each day (FPs per Day). We also considered all possible 2-way interactions between Treatment Group and the other independent variables, and all models included Turbine ID and Elapsed Days since project inception nested within Turbine ID as random effects.

For the logistic GLMMs, which resulted in predictions of the ln(odds of a response), we used a standard formula (100\*exp[ln[odds]]/[1+exp[ln[odds]]]) to transform the log-odds estimates to probabilities of response (0 to 1 translated to percentages) for the purpose of describing and graphically displaying relationships.

#### Results

The final dissuasion-trigger GLMM selected to represent golden eagles alone was as follows:

```
ln(Odds \ of \ dissuasion \ trigger) \sim [1 \ | \ Turbine \ ID] + [1 \ | \ Turbine \ ID : Elapsed \ Days] + Treatment \ Group + Year + Time \ of \ Day + Wind \ Speed
```

The model coefficients indicated the following relationships:

- Nonsignificant (P > 0.10) 29% reduction in the probability of dissuasion triggers at installations operating in treatment mode.
- Marginally significant (0.05 <  $P \le 0.10$ ) 46% reduction in the probability of dissuasion triggers in Year 2.
- Marginally significant positive relationship between the probability of dissuasion triggers and Time of Day.
- Significant (P ≤ 0.05) negative relationship between the probability of dissuasion triggers and Wind Speed.

Based on the large all-eagles dataset, the top GLMM was similar to the above, but also included two at least marginally significant interactions between *Treatment Group* and other predictors, which provided important insight:

```
ln(Odds \ of \ dissuasion \ trigger) \sim [1 \ | \ Turbine \ ID] + [1 \ | \ Turbine \ ID : Elapsed \ Days] + Treatment \ Group + Time \ of \ Day^2 + Cloud \ Cover + FPs \ per \ Day + Treatment \ Group * Cloud \ Cover + Treatment \ Group * FPs \ per \ Day
```

The model coefficients of this model indicated the following relationships:

- No significant overall effect of *Treatment Group*.
- Significant second-order relationship with *Time of Day*, reflecting a higher probability of dissuasion triggering during midday compared to earlier and later in the day.
- When partly cloudy, or overcast skies prevailed, the probability of dissuasion triggers was estimated to be 9–33% lower at turbines operating in treatment mode compared to those operating in control mode, whereas when fair skies prevailed, the probability of dissuasion triggers was substantially lower at turbines operating in control mode.
- The probability of dissuasion triggers did not differ between turbines operating in control or treatment mode when the number of FPs per Day was low, but was approximately 60% lower at turbines operating in treatment when the number of FPs per Day that triggered deterrents was high.

Using dwell-time as a dependent variable revealed much clearer expected effects of *Treatment Group* consistent with research Hypothesis B. For both golden eagles alone and all eagles combined, the selected models had the same structure:

```
Dwell Time \sim [1 \mid Turbine] + [1 \mid Turbine : Elapsed Days] + Treatment Group + 28d Cycle + Time of Day + Time of Day^2 + FPs per Day + Treatment Group * FPs per Day
```

The model coefficients of these models indicated the following relationships:

- Significant 24–27% reductions in the dwell time of golden eagles at installations operating in treatment mode.
- Marginally significant overall declining trend in the dwell time of golden eagles in relation to the progression of 28d Cycles over the course of the two-year study.
- Marginally significant second-order relationship between dwell time and *Time of Day*, reflecting short
  dwell times in the morning, increasing through mid-afternoon, then tapering off again in the evening.
- Marginally significant interaction between *Treatment Group* and *FPs per Day* illustrating that, the more that FPs contributed to actual deterrent broadcasting at treatment turbines, the less likely were eagles to dwell in the vicinity of those turbines.

#### **Discussion**

The modeling results failed to reveal a significant overall treatment effect based on the probability of triggering a dissuasion signal as the binary dependent variable, but those models did reveal some potentially insightful interactive relationships between *Treatment Group* and other predictors. Although *Treatment Group* did not emerge as a significant predictor of the probability of dissuasion triggers, the indicated association for golden eagles alone and all eagles combined was as predicted in Hypothesis A—at least a slightly lower probability of dissuasion triggers at turbines when the DTBird deterrents were broadcasting. Much stronger overall *Treatment Group* effects emerged when we modeled dwell time as the dependent variable, and the indicators were again consistent with the prediction of Hypothesis B. The more-robust dwell-time models also emphasized both some common and novel influences of the evaluated covariates compared to the dissuasion-trigger models.

One possible reason why greater support for Hypothesis A was not apparent concerns the efficacy of warning signals as a potential means to reduce the probability of an eagle triggering a subsequent dissuasion signal. The idea that broadcasted warning signals could be expected to reduce the probability of triggering a subsequent dissuasion signal actually did not apply very often.

The significant effects of *Treatment Group* in the dwell-time models translated to predictions of golden eagles and all eagles combined averaging 24–27% less time dwelling in the vicinity of DTBird systems operating with their deterrents broadcasting normally compared to systems with muted deterrents. Quantifying estimated reductions in the probability of dissuasion triggers at treatment turbines based on the all-eagles model was complicated by the presence of interactions with both categorical (*Cloud Cover*) and continuous (*FPs per Day*) covariates. Under most sky conditions from partly cloudy to overcast, eagles tended to trigger approximately 9–30% fewer dissuasion signals at turbines with DTBird deterrents broadcasting normally (i.e., consistent with research Hypothesis A); however, the opposite pattern was apparent when fair skies prevailed. Reasons for this unexpected anomaly are uncertain, possibly related better visibility under fair skies allowing the eagles to more effectively perceive and avoid conflict with spinning turbines at closer distances independent of the audio deterrents. In contrast, the indicated interactive relationship between *Treatment Group* and *FPs per Day* provided further clear support for Hypothesis A in demonstrating that the positive effect of broadcasted deterrents at treatment turbines deterring eagles from triggering dissuasion signals was accentuated by higher FP deterrent-triggering activity.

The model focused on presumed golden eagles triggering dissuasion signals indicated a novel relationship with monitoring *Year* as a predictor, suggesting that the probability of golden eagles triggering dissuasion signals declined overall by approximately 46% across the facility during Year 2 of the study, independent of the control-treatment deterrent broadcasting scenario. In contrast, the dwell-time models consistently revealed *28d Cycle* as an important predictor, illustrating an overall declining trend across the 2-year study in the average dwell time of golden eagles alone and all eagles combined around DTBird equipped turbines, again independent of the control-treatment experimental scenario. These apparent relationships appeared to provide evidence of positive habituation to the overall presence of DTBird deterrent broadcasting at the facility, which may have been accentuated by two factors: 1) an unusually high overall FP triggering rate through the first 19 months of the study, until Liquen was authorized to undertake further fine-tuning of the filtering algorithms to reduce the FP rate; and 2) due to an extended failure of communications between the

DTBird and turbine SCADA systems following a forced 24-day site-wide power outage, all DTBird systems operated in default mode after May 2023, whereby the deterrents were being triggered whether or not the focal turbine was spinning. What is equally important to note here, though, is that the results did not point to possible negative habituation, which would involve eagles learning to ignore the deterrents and remain at risk.

All of the models we developed reflected a pronounced diel pattern of variation in the documented eagle responses that operated independently of the applied deterrent treatment regime, with peak responses during mid-afternoon and lesser responses earlier and later in the day. We think this predominant pattern probably reflects the common general activity levels of eagles and other raptors during a typical day. In addition, *Wind Speed* emerged as a significant covariate influencing the probability of golden eagles triggering dissuasion signals, independently of the implemented control-treatment design. The indicated effect suggested that the faster the turbines were spinning, the more they themselves acted as a deterrent to visually acute golden eagles, who then remain farther away from the perceived danger independent of the influence of DTBird deterrent signaling.

In conclusion, despite falling well short of our intended 2-year sampling design due to factors beyond our control, the results of our careful analyses yielded noteworthy insight about the positive benefits of the DTBird deterrent system in reducing the activity of eagles around turbines where the deterrents were broadcasting normally, and both the related and independent influences of various environmental factors on the eagle responses around the facility to the presence of operating DTBird systems. We suspect that, had frequent operational failures not caused major unexpected imbalances in our intended sampling design and had the overall deterrent triggering not been artificially elevated by various factors, our ability to demonstrate conclusive patterns of interest concerning the proximate effectiveness of DTBird would have been even greater.

## **Table of Contents**

Section 1.0	O Introduction	1
Section 2.0	) Methods	3
2.1	Study Site and DTBird Setup	3
2.2	Control-Treatment Sampling Design	4
2.3	Data Processing	5
2.4	Analytical Models	6
Section 3.0	) Results	9
3.1	Sampling Results	9
3.2	Model Selection	9
3.	2.1 Testing Hypothesis A Regarding Probability of Eagles Triggering a DTBird  Dissuasion Signal	9
3.	2.2 Testing Hypothesis B Regarding Dwell Time of Eagles Around DTBird Deterrent Systems	
3.	2.3 Testing Hypothesis C Regarding the Probability of Eagles Crossing the Rotor Swept  Area of DTBird Equipped Turbines	19
Section 4.0	Discussion	22
Section 5.0	O References	25
Figures	S	
Figure 1.	Layout of the Goodnoe Hills Wind Farm in south-central Washington showing locations of installed DTBird systems.	4
Figure 2.	Illustration of predicted relationship between the probability of a golden eagle triggering a DTBird dissuasion signal and <i>Time of Day</i>	11
Figure 3.	Illustration of predicted relationship between the probability of a golden eagle triggering a DTBird dissuasion signal and <i>Wind Speed</i> .	12
Figure 4.	Illustration of predicted second-order relationship between the probability of an eagle triggering a DTBird dissuasion signal and time of day.	14
Figure 5.	Illustration of predicted interactive relationship between treatment group and cloud cover in determining the probability of an eagle triggering a DTBird dissuasion signal	14
Figure 6.	Illustration of predicted interactive relationship between treatment group and the daily numbers of false positives (FPs) that triggered deterrent signals in determining the	

	probability of an eagle (golden and bald eagles combined) triggering a DTBird dissuasion signal.	15
Figure 7.	Illustration of predicted decline in the dwell time of golden eagles at DTBird turbines across the 27 28-day sampling cycles that composed this two-year experimental analysis	17
Figure 8.	Illustration of predicted second-order relationship between the dwell time of golden eagles at DTBird turbines and time of day.	17
Figure 9.	Illustration of predicted interactive relationship between treatment group and the daily numbers of false positives (FPs) that triggered deterrent signals in determining the dwell time of golden eagles around DTBird turbines.	18
Figure 10.	Illustration of predicted decline in the dwell time of eagles (golden and bald eagles combined) at DTBird turbines across the 27 28-day sampling cycles that composed this two-year experimental analysis	20
Figure 11.	Illustration of predicted second-order relationship between the dwell time of eagles (golden and bald eagles combined) at DTBird turbines and time of day	20
Figure 12.	Illustration of predicted interactive relationship between treatment group and the daily numbers of false positives (FPs) that triggered deterrent signals in determining the dwell time of eagles (golden and bald eagles combined) around DTBird turbines	21
Tables		
Table 1.	Summary of DTBird Detection Samples Used to Evaluate Results of Two-year Experiment Comparing Responses of Large Raptors to Muted (Control) Versus Broadcasted (Treatment) Audio Deterrents	9
Table 2.	Model Coefficients and Fixed Effect Parameter Test Results for the Logistic GLMM Selected to Represent the Probability of Confirmed and Probable Golden Eagles Triggering a Dissuasion Signal at DTBird Installations Operating in Treatment (Deterrents Broadcasting) and Control (Deterrents Muted) Mode During Two-year Experiment	11
Table 3.	Model Coefficients and Fixed Effect Parameter Test Results for the Logistic GLMM Selected to Represent the Probability of Confirmed and Probable Eagles (Golden and Bald Eagles Combined) Triggering a Dissuasion Signal at DTBird Installations Operating in Treatment (Deterrents Broadcasting) and Control (Deterrents Muted) Mode During Two-year Experiment	13
Table 4.	Model Coefficients and Fixed Effect Parameter Test Results for the GLMM Selected to Represent the Relationship Between the Dwell Time of Confirmed and Probable Golden Eagles at DTBird Installations Operating in Treatment (Deterrents Broadcasting) and Control (Deterrents Muted) Mode During Two-year Experiment	16

Table 5.	Model Coefficients and Fixed Effect Parameter Test Results for the GLMM Selected to	
	Represent the Relationship Between the Dwell Time of All Confirmed and Probable	
	Eagles at DTBird Installations Operating in Treatment (Deterrents Broadcasting) and	
	Control (Deterrents Muted) Mode During Two-year Experiment	19
Apper	ndixes	
Appendix	A. Randomized Deterrent-Broadcasting Control-Treatment Rotation Schedules for Two-Year Experiment	A-1
Appendix	B. Selected Days within 28-day Sampling Cycles at DTBird-Equipped Turbines When	
	Records Were Screened to Compose Dataset for Two-Year Experiment	B-1
Appendix	C. Evaluation of GLMM Candidates Considered to Identify the Best Model Used to Represent Relationships Between the Probability of Confirmed and Probable Golden Eagles Triggering a DTBird Dissuasion Signal and Various Predictors	
Appendix		
Appendix	E. Results of Backwards Selection Approach Used to Identify Selected GLMM Representing Relationships Between the Dwell Time of Confirmed and Probable Golden Eagles Around DTBird Installations and Various Predictors	E-1
Appendix	F. Evaluation of GLMM Candidates Considered to Identify the Best Model Used to Represent Relationships Between the Dwell Time of Confirmed and Probable Eagles Around DTBird Installations and Various Predictors	F-1
List of	Preparers and Contributors	
Jeff P. Sm	ith, Ph.D., Associate Wildlife Ecologist—Project Manager	
Scott B. T	errill, Ph.D., Principal, Wildlife Ecology—Principal-in-Charge	
John Rom	nansic, Ph.D., Wildlife/Quantitative Ecologist	
Sophie Be	ernstein. M.S., Wildlife/Quantitative Ecologist	
Stephanie	Schneider, M.S., Wildlife/Quantitative Ecologist	
Alex Henr	ry, B.S., Field Biologist	
Cooper Sr	mith, B.S., Field Biologist	
Zach Han	npson, B.S., Field Biologist	
Cassandra	Butler, B.S., Field Biologist	

#### **Section 1.0 Introduction**

DTBird® (Liquen Consultoría Ambiental, S.L., Madrid, Spain; hereafter Liquen) is an automated detection and audio deterrent system designed to discourage birds from entering the rotor swept zone (RSZ) of spinning wind turbines (see https://dtbird.com). The research results presented herein represent the culminating component of a multi-faceted, multi-year evaluation of the DTBird system conducted in collaboration with the Renewable Wildlife Energy Institute (REWI) at two commercial wind-energy facilities in California and Washington (H. T. Harvey & Associates 2018, 2019a). The overarching goal of this research is to evaluate the effectiveness of DTBird in detecting and discouraging golden eagles (*Aquila chrysaetos*) and other large raptors from approaching the rotor swept zone of operating wind turbines.

The results presented herein derive from a two-year control-treatment experiment conducted at the Goodnoe Hills Wind Farm in south-central Washington. The experiment involved 14 DTBird systems installed on turbines strategically selected to effectively represent the 48-turbine facility. The control-treatment design involved the randomized operation of those systems with (treatment) and without (control) the audio deterrents actually broadcasting (but always triggering virtually in control mode). The goal of this experiment was to evaluate the effectiveness of DTBird in reducing collision risk for eagles and surrogate raptors as indicated by a reduction in detectable eagle/raptor activity in the vicinity of the RSZ of turbines with active deterrent signals. For this purpose, we employed an experimental design that explicitly minimized the potential for target raptors to become habituated to deterrent signals being broadcasted consistently at any one turbine. The potential for turbine-specific habituation was minimized by randomizing treatment assignments among turbines on a daily basis to capitalize on the presence of initially naïve birds and limit the potential for learning from stable operational configurations. By quantifying the "proximate" effectiveness of the DTBird deterrence system under this scenario, we sought to assess the system's ability to reduce collision risk for eagles and other raptors under naïve exposure conditions. Nevertheless, one might suppose that yearround resident raptors could nevertheless become habituated to deterrents being regularly broadcasted across the facility in general; hence, we considered temporal variables in our analytical models to help determine whether any such patterns were evident across the extended study.

The DTBird detection system comprises four 6-megapixel video cameras installed on a given turbine tower at 4–5 meters (m) above ground level, oriented approximately in cardinal directions, and angled upwards approximately 12° to focus the overlapping surveillance viewsheds on the expected RSZ. The DTBird deterrence system comprises two types of deterrent signals: initial *warning* signals meant to alert target birds to the presence of the spinning turbine, and more aggressive *dissuasion* signals meant to actively discourage birds from approaching the RSZ. The signals are triggered at various estimated distances from the focal turbine whenever the DTBird system registers—through communication with the turbine SCADA system—that the turbine rotor is spinning at ≥2 revolutions per minute (rpm). The DTBird detection system coarsely estimates the position of detected targets based on calibration for targeted birds of a specified size. In this case, the systems were calibrated for detecting and deterring moving targets that filled the number of image pixels an average golden eagle with a wingspan of approximately 2.1–2.3 meters would be expected to fill when

1

exposed perpendicular to a given camera with its wings fully spread. Based on this calibration, the estimated maximum detection distance for an average golden eagle was expected to be 240 m; the expected trigger distance for *warning* signals was expected to be in the range of 170–240 m from the turbine (depending on the target's distance and altitude above ground level); and the expected trigger distance for *dissuasion* signals was expected to be 100–170 m. H. T. Harvey & Associates (2018) contains a detailed summary of the typical system configuration and operation, including graphical portrayals of the expected deterrent-triggering zones within the projected overall detection envelope, and H. T. Harvey & Associates (2019a, 2022a) contains additional information about the specific Goodnoe Hills DTBird setups.

The research hypotheses we formulated for the experiment (H. T. Harvey & Associates 2019a) were as follows:

**Hypothesis A:** The probability of an eagle triggering a dissuasion signal will be lower for DTBird turbines operating in treatment mode (deterrent signals broadcasting) compared to those operating in control mode, because broadcasted warning signals deter target raptors from approaching closer and triggering a dissuasion signal.

**Hypothesis B:** The average dwell time of eagles in the vicinity of DTBird-equipped turbines—as reflected in the length of relevant targeting videos recorded by the DTBird detection system—will be reduced around systems operating in treatment mode compared those operating in control mode, because broadcasted deterrent signals discourage birds from lingering near focal turbines. (Note that we reframed this hypothesis compared to our original study plan to focus on a related but more informative dependent variable).

**Hypothesis C:** The probability of an eagle crossing the active rotor swept area (RSA) of DTBird-equipped turbines will be lower for systems operating in treatment mode compared to those operating in control mode, because operation of the deterrent signals reduces the likelihood of target raptors entering the RSZ of turbines.

#### Section 2.0 Methods

### 2.1 Study Site and DTBird Setup

The Goodnoe Hills Wind Farm comprises 48 2.2-MW Vestas V110 Mark C and B wind turbines situated atop an east-west ridgeline flanking the Columbia River to the south (Figure 1). Fourteen DTBird systems spread around the perimeter of the overall facility were installed at the facility beginning in 2019 to support this research,; however, three of these systems were not rendered effectively operational until during the second year of the experiment (located at turbines G29, G51, and G56; Figure 1). Four video cameras were installed on each DTBird turbine tower approximately 5 m off the ground, and the systems installed at the Goodnoe Hills included two rings of four broadcast speakers each situated on the turbine tower at just below rotor-swept height and just below hub height to help ensure effective deterrent broadcasting throughout a relatively large overall detection envelope and collision risk zone (H. T. Harvey & Associates 2019a). The automated detection systems surveilled the skies throughout daylight hours, and created new event records in the DTBird Data Analysis Platform (DAP) on-line database whenever a moving object was perceived to fill enough image pixels to qualify as a target of interest. DTBird does not identify or enumerate targets; analysts must do that manually by reviewing event records and video clips stored in the DAP. The system is calibrated to begin tracking objects of a specified size range and trigger subsequent deterrent signals (only if the system registers that the turbine rotor as actively spinning) when it perceives that the object has reached specified distances from the turbine, which it determines based on pre-programmed criteria projecting how many image pixels a target of the specified size is expected to fill at specified distances (as described in the Introduction).

When the system begins tracking an object, it creates a new event record in the DAP and records a timestamp for the initial detection event. If that tracked object subsequently or simultaneously triggers one or both deterrent signals, information is added to the same DAP event record to document the unique timestamps and signal durations for each deterrent-triggering event. Other data automatically recorded in the DAP for each detection event include: (a) the average wind speed, rotor azimuth, and rotor rpm during the event record derived from the turbine SCADA system; (b) a binary indicator of whether or not the focal rotor was spinning sufficiently for DTBird deterrence module to be operating; (c) an estimate of the current amount of ambient illumination; and (d) length of the video tracking record. Each event record also ultimately has attached to it video clips representing each of the four cameras, which the system extracts from bulk footage to begin 10 seconds before the detection event was initiated and continue for 30 seconds after the last tracked object exits the detection envelope. There must have been no objects tracked by a given system for at least 26 seconds before a new independent event record can be recorded. If a system tracks multiple objects concurrently during the same event period, timestamps are recorded only for the first detection, warningtrigger, and/or dissuasion-trigger events, and those respective events may not be triggered by the same individual bird or object. In these cases, it is sometimes difficult to determine exactly which bird or object was responsible for the timestamped events.

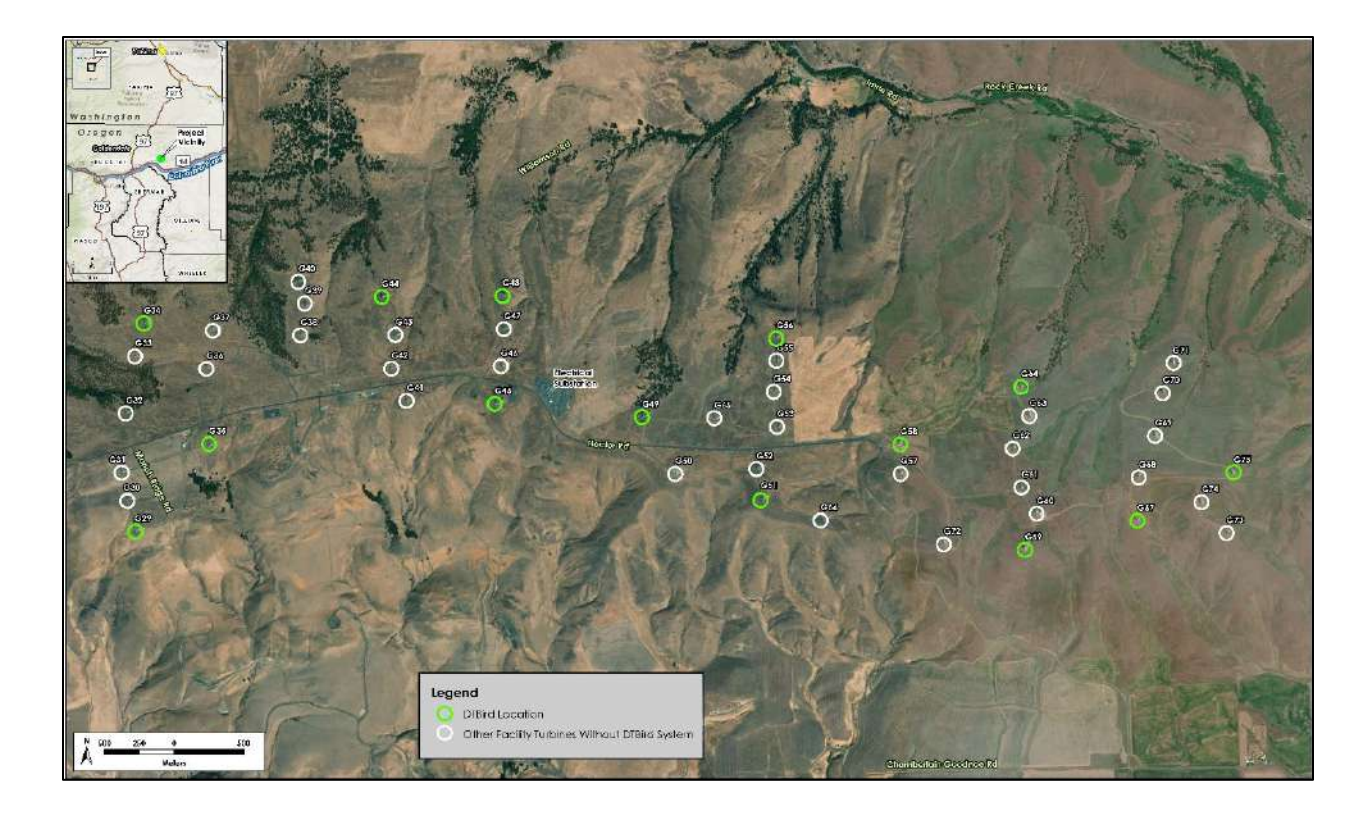


Figure 1. Layout of the Goodnoe Hills Wind Farm in south-central Washington showing locations of installed DTBird systems.

Under the DTBird targeting scenario and given calibration for golden eagles, much smaller objects (e.g., small birds and even insects) may trigger detections and deterrents if they are sufficiently close to a camera to fill the same number of pixels as a golden eagle would at a much greater distance. Conversely, much larger objects (e.g., airplanes) may trigger detections and deterrents when they are farther away but fill the requisite number of image pixels to register as a possible golden eagle at a relevant distance. Because of these system limitations, false-positive detections and deterrent triggering commonly occur, often at a much greater frequency than events related to target birds (May et al. 2012; H. T. Harvey & Associates 2019b, 2022b, 2023a).

## 2.2 Control-Treatment Sampling Design

Data collection began on 1 September 2021 and was expected to continue for two annual rounds of 13 28-day sampling cycles. In the end, sampling was continued for one additional 28-cycle to account for the Bonneville Power Administration having unexpectedly shut down all power to the wind facility from 1–24 May 2023.

The experimental design involved, on a given day, having roughly half of the operational DTBird systems operating in control mode with the deterrent signals not actually broadcasting, and half operating in treatment mode with the deterrent signals broadcasting normally. Here it is important to note that the DTBird systems can be set to trigger and record the timing of deterrent signaling events virtually without the audio deterrents

actually broadcasting. Assignments to the control and treatment groups were re-randomized on a daily basis, stratified to ensure (a) daily representation in both the eastern and western halves of the facility, and (b) that each system was operated in treatment mode for at least 10 days per 28-day cycle. Based on preselected rotation schedules (see Appendix A), Liquen staff implemented and managed automated programming from Spain to control the daily deterrent settings, with necessary daily switching able to occur conveniently during daytime in Spain but nighttime in Washington (DTBird operates only during daylight hours). By randomly assigning treatments on a daily basis and using daily event metrics as the analytical data, we sought to: (1) minimize the potential for turbine-specific habituation; (2) ensure reasonable precision in matching environmental covariate values to response records on a daily basis, rather than seeking to apply covariate values that are averaged or classified across extended periods; and (3) enable effective subsampling of the DTBird event response data.

To select days from which we derived samples used in the analyses, for each operational DTBird turbine we randomly selected 10 days per 28-day cycle for screening, always seeking to the degree possible that each turbine-specific 28-day sample included data for 5 days when the deterrent signals were operating in treatment mode and 5 days when they were operating in control mode. However, as reflected in Appendix B, frequent operational failures greatly hindered achieving this intended sampling design. To reduce the effects of frequent system failures in producing unbalanced sampling relative to control-treatment modes, we often adjusted the selected sampling days compared to the initial random selections in an effort to maintain both the 10 days per 28-day cycle sampling objective and 50:50 ratios of control-treatment samples per turbine. Despite these efforts and due to issues beyond our control, the resulting sampling was far from ideal. Nevertheless, especially in this case with *Turbine ID* treated as a random variable, GLMMs tend to be fairly robust to sampling imbalances as long as the overall representation of data within predictors and covariate classes of interest is relatively robust.

## 2.3 Data Processing

To compose the dataset considered here, technicians initially screened all relevant DAP event records and videos recorded on selected sampling days when the focal turbine rotor was spinning at rate sufficient to trigger operation of the DTBird deterrence function when relevant. The technicians identified the apparent targets involved in each event to the degree possible, and recorded data to classify the sky backdrop (i.e., fair skies, partly cloudy, cloudy, or overcast) at the time of each detection/deterrent event. Due to a preponderance of false-positive detections (see H. T. Harvey & Associates 2019b, 2022b, 2023a) and other abundant raptors besides eagles, this involved screening more than 27,000 records to generate a dataset of 390 useable records representing confirmed and probable eagles (golden eagles and bald eagles [Haliaeetus leucocephalus]). Even after intensive QA/QC by the project manager/raptor specialist, high proportions of the event records involving large raptors could be confidently identified only as eagle, buteo, eagle/buteo, eagle/vulture, or simply unknown large raptor. More generally, positively identifying species based on reviewing poor-resolution DTBird video records was very difficult and substantially limited our ability to generate species-specific insights (H. T. Harvey & Associates 2023a, 2023b).

### 2.4 Analytical Models

To analyze the experiment dataset, we used generalized linear mixed models (GLMMs) to evaluate the three research hypotheses using different response variables: 1) binary logistic response = whether or not a detected large raptor triggered a dissuasion signal, 2) continuous response (seconds) = tracking video length per large raptor targeting event, and 3) binary logistic response = whether or not a detected large raptor appeared to cross through or close to the RSA. Challenges producing a consistent, accurate, and robust dataset on possible RSA crossings based on interpreting 3D responses from 2D video images limited our ability to evaluate research Hypothesis C.

Our GLMM designs considered DTBird turbines to be sampling units and included *Turbine ID* as a random effect in the models to account for inherent, localized, spatial variation in the landscape settings and eagle/raptor activity patterns at different turbines. All models also included sampling date nested within *Turbine ID* to account for highly variable temporal sampling at each turbine and inherent, localized, temporal variation in the environmental conditions, human activity patterns, and other factors that likely influenced the activity patterns and responses of target raptors around individual turbine locations. For this purpose, we transformed sampling dates to *Elapsed Days* since projection inception.

Given frequent uncertainties in species-specific identifications and attendant sample-size limitations for focal golden eagles, we developed independent models for three hierarchical taxonomic groups to provide effective insight: 1) confirmed and probable golden eagles, 2) confirmed and probable golden and bald eagles, with *Species* considered as a potential predictor; and 3) all confirmed and probable eagles, including unidentified eagles, without considering species as a potential predictor.

Predictors and covariates considered in the GLMMs were as follows:

#### Random effects:

- Turbine ID
- Days Elapsed nested within Turbine ID

#### Fixed effects:

- Treatment Group (binary): treatment or control
- Species (categorical): included in models focused on confirmed golden and bald eagles combined, but excluded from models focused on golden eagles alone and all possible eagles, including those not confirmed to species
- 28-day Cycle (discrete continuous): sequential series from 1 to 27 over 25-month period, with period 23 mostly not represented due to an unanticipated 1-month facility shut down
- *Time of Day* (continuous, Pacific Standard Time, translated to minutes of the day): second order term included to account for expected curvilinear relationship

- Cloud Cover (categorical): reflecting predominant daily condition gleaned from review of DTBird video records and coarsely classified by technicians as fair (mostly cloud free), partly cloudy (<50% cloud cover), cloudy (≥50% cloud cover with distinctly variable cloud definitions and brightness), or overcast (complete and largely uniform gray or darker cloud cover)
- Wind Speed (continuous, meters/second): derived from turbine system metrics and averaged across duration of tracking event
- FPs per Day (discrete continuous): number of daily deterrent-trigger events resulting from false positives, including both true false positives (non-bird, including inanimate moving/flying objects, insects, precipitation, and sky artifacts) and non-target avian false positives (non-focal birds) (see H. T. Harvey & Associates 2023a)

The selected covariates represented factors that: 1) were discernable using the DTBird DAP or were attainable from the wind facility; 2) we expected to have the potential to influence the ability of focal raptors to visualize the turbines and hear and respond to the deterrents; and 3) could influence the responses of focal raptors by increasing the frequency of deterrents being broadcasted. Given focal interest in evaluating *Treatment Group* as a predictor, we also evaluated all possible two-way interactions between *Treatment Group* and the other potential predictors/covariates. For all continuous independent variables, we centered and scaled the values as (value - mean)/SD prior to analysis.

For each species group, we developed GLMMs to test for the effects of *Treatment Group* and the five potential covariates on the three dependent variables. We used the R function 'glmer' in the lme4 package (Bolker 2023) to compile and evaluate GLMMs based on a binomial error distribution with a logit link (i.e., mixed-effects logistic regression), and maximum likelihood estimation with the *bobyqa* optimizer and the maximum number of function evaluations set to  $10^5$ , to model the probability of detection events triggering a dissuasion signal and whether or not an RSA cross occurred. We used the R Package 'glmmTMB' (Brooks et al. 2023) to compile and evaluate GLMMs based on a gamma error distribution with a log link and maximum likelihood estimation to analyze dwell time (recorded video length) as a dependent variable. We compared Akaike's Information Criterion (AIC) scores for candidate models to balance considerations of model fit and parsimony (considering a  $\Delta$ AICc of  $\leq$ 2 points indicative of similarly competitive models) and used Wald  $\approx$ 2 tests and Drop1 likelihood-ratio chi-square tests to further assess the relative importance of different predictor variables and ultimately identify a top model for each independent analysis (Burnham and Anderson 2002, Bolker et al. 2009, Symonds and Moussalli 2011).

To ensure a good model fit, normally distributed residuals, and homogeneous variances, we inspected residual plots for the selected models and individual grouping factors by plotting results using the 'simulateResiduals' function (package 'DHARMa'; Hartig 2019) applied to the selected model. We also conducted goodness-of-fit tests on these residuals using the 'testUniformity' function from the same package, which performs a Kolmogorov-Smirnov test for specified factors and combinations of factors (including the overall model) to evaluate conformity to a normal distribution. We used the functions 'testOutliers', 'testOverdispersion', and 'testZeroInflation' to confirm that the residuals did not include outliers nor exhibit overdispersion or zero-inflation (Hartig 2019).

To evaluate Wald z tests and Drop1 likelihood ratio chi-square parameter tests for individual predictors considered during GLMM development, we adopted  $P \le 0.10$  as our threshold for retaining predictors in the selected models. We chose this relatively liberal threshold to ensure representation of potentially noteworthy relationships that might have emerged more strongly had our sampling not suffered from frequent spatial and temporal imbalances in the operation of the study installations and resultant sampling, and uncertainties pertaining to species identifications. We refer to tests and contributions as marginally significant if  $0.05 < P \le 0.10$ , significant if  $0.01 < P \le 0.05$ , and highly significant if  $P \le 0.01$ .

For the logistic GLMMs, which resulted in predictions of the ln(odds of a response), we used a standard formula (100\*exp[ln[odds]]/[1+exp[ln[odds]]]) to transform the log-odds estimates to probabilities of response (0 to 1 translated to percentages) for the purpose of describing and graphically displaying relationships (Hosmer and Lemeshow 1989).

#### Section 3.0 Results

#### 3.1 Sampling Results

Table 1 summarizes the samples of confirmed and probable eagles we derived from screening DTBird event records on selected sample days, including the numbers of records for each species/group that did and did not trigger a deterrent signal under conditions when deterrent triggering was expected to occur if a bird passed within triggering range. These samples formed the basis for our analyses.

Table 1. Summary of DTBird Detection Samples Used to Evaluate Results of Two-year Experiment Comparing Responses of Large Raptors to Muted (Control) Versus Broadcasted (Treatment) Audio Deterrents

Experiment Group – Species/Group <sup>1</sup>	Days With Samples	No Deterrence Records <sup>2</sup>	Deterrence Records <sup>3</sup>	Total Records	Average Records Per Day	SD
Control						
Golden Eagles	71	6	99	105	0.8	1.04
Bald Eagles	64	6	70	76	0.8	0.75
All Eagles	135	15	199	209	0.9	1.18
Treatment						
Golden Eagles	70	11	91	102	0.8	1.11
Bald Eagles	40	2	51	53	0.5	0.72
All Eagles	123	13	168	181	0.8	1.05

<sup>&</sup>lt;sup>1</sup> In all cases, classifications include confirmed and probable identifications belonging to the specific species or species group.

#### 3.2 Model Selection

# 3.2.1 Testing Hypothesis A Regarding Probability of Eagles Triggering a DTBird Dissuasion Signal

For confirmed and probable golden eagles alone, limited sample sizes constrained our ability to evaluate a full model including the complete suite of potential predictors and 2-way interactions of interest. Instead, we proceeded systematically to evaluate (1) the influences of *Treatment Group* combined with each of the other predictors alone and then with associated two-way interactions, and (2) more complex multi-variable models based on indications of potential significance during the preceding step (see Appendix C for comparisons of selected candidate models). Throughout the process of considering candidate models and selecting a final logistic GLMM to represent the probability of golden eagles triggering a dissuasion signal, the prediction

<sup>&</sup>lt;sup>2</sup> Cases where a target bird was detected but did not trigger a deterrent signal.

<sup>3</sup> Cases where a target bird was detected and triggered one or both deterrent signals, either virtually (control mode) or with the deterrents actually broadcasting (treatment mode).

coefficients for *Treatment Group* were always negative, suggesting the expected effect of a lower probability of dissuasion triggers at turbines operating in treatment mode. *Treatment Group* never emerged as even a marginally significant predictor, however. In contrast, *Year*, *Time of Day*, and *Wind Speed* were at least marginally significant predictors and were retained in the final model. Accordingly, the dissuasion-trigger model selected to represent golden eagles alone, based on AIC scores, parameter tests, and positive model diagnostics, was as follows:

```
ln(Odds \ of \ dissuasion \ trigger) \sim [1 \ | \ Turbine \ ID] + [1 \ | \ Turbine \ ID : Elapsed \ Days] + Treatment \ Group + Year + Time \ of \ Day + Wind \ Speed
```

The relationships indicated by the resulting model coefficients and individual parameter tests (Table 2) are described below.

- Non-significant 29% reduction (95% CI: 63% reduction 36% increase) in the probability of dissuasion triggers at installations operating in treatment mode.
- Marginally significant 46% reduction (95% CI: 73% reduction 9% increase) in the probability of dissuasion triggers in *Year 2*.
- Marginally significant positive relationship between the probability of dissuasion triggers and *Time of Day* (Figure 2).
- Significant negative relationship between the probability of dissuasion triggers and Wind Speed (Figure 3).

Based on the dataset limited to eagles positively identified as either a golden eagle or a bald eagle, again no significant *Treatment Group* effects were evident but other indicators similar to the results for golden eagles alone were evident. More importantly, although preliminary indications emerged suggesting potential marginal differences in the probability of dissuasion triggering for the two eagle species, those indications faded away once other covariates were included in the models. Therefore, we abandoned further consideration of models limited to identified golden and bald eagles with *Species* as a predictor in favor of evaluating models based on the larger all-eagles dataset (see Table 1) without considering *Species* as a potential predictor. Based on this dataset, we were able take both full backwards and forwards stepwise model building approaches to identify a top model (see Appendix D for comparisons of models evaluated as part of a backwards elimination process to select the final model). The outcome of this approach again did not reveal a strong *Treatment Group* effect; however, the selected model included two at least marginally significant interactions between *Treatment Group* and other predictors, which provided important insight. The structure of the dissuasion-trigger logistic GLMM selected to represent all eagles combined was as follows:

```
ln(Odds \ of \ dissuasion \ trigger \sim [1 \ | \ Turbine \ ID] + [1 \ | \ Turbine \ ID : Elapsed \ Days] + Treatment \ Group + Time \ of \ Day^2 + Cloud \ Cover + FPs \ per \ Day + Treatment \ Group * FPs \ per \ Day
```

Table 2. Model Coefficients and Fixed Effect Parameter Test Results for the Logistic GLMM
Selected to Represent the Probability of Confirmed and Probable Golden Eagles
Triggering a Dissuasion Signal at DTBird Installations Operating in Treatment
(Deterrents Broadcasting) and Control (Deterrents Muted) Mode During Two-year
Experiment

Random Effect	Variance	SD
Turbine	0.357	0.5977
Turbine: Elapsed Days <sup>1</sup>	0.116	0.3409

Fixed Effect	Estimate	SE	<b>z</b> <sup>2</sup>	P(> z ) <sup>2</sup>	LRT $\chi^{23}$	P (>χ <sup>2</sup> ) <sup>3</sup>
Intercept	0.546	0.3421	1.597	0.110	-	_
Treatment Group: On4	-0.339	0.3304	-1.026	0.305	1.07	0.302
Year: 2 <sup>5</sup>	-0.614	0.3569	-1.721	0.085	3.06	0.080
Time of Day <sup>6</sup>	0.295	0.154	1.917	0.055	3.83	0.050
Wind Speed <sup>7</sup>	-0.385	0.1780	-2.161	0.031	5.10	0.024

Elapsed Days = days since data-collection began; a simpler equivalent of date.

Recorded in meters/second; centered and scaled ([value – mean]/SD).

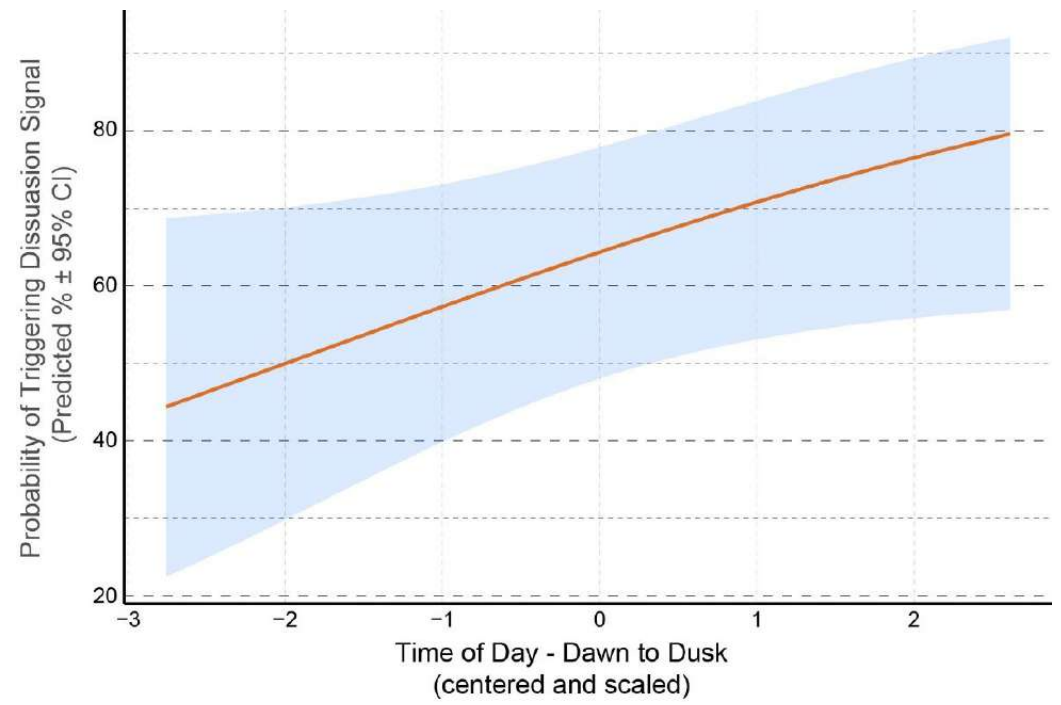


Figure 2. Illustration of predicted relationship between the probability of a golden eagle triggering a DTBird dissuasion signal and *Time of Day*.

<sup>&</sup>lt;sup>2</sup> Wald test.

<sup>&</sup>lt;sup>3</sup> Drop1 likelihood ratio test.

<sup>&</sup>lt;sup>4</sup> Reference category – Off = control mode. On = treatment mode.

<sup>&</sup>lt;sup>5</sup> Reference category – Year 1: 1 September 2021 – 31 August 2022. Year 2: 1 September 2022 – 30 September 2023 (extended due to facility shut down from 1–24 May 2023.

<sup>&</sup>lt;sup>6</sup> Translated to minutes of the day; centered and scaled ([value – mean]/SD).

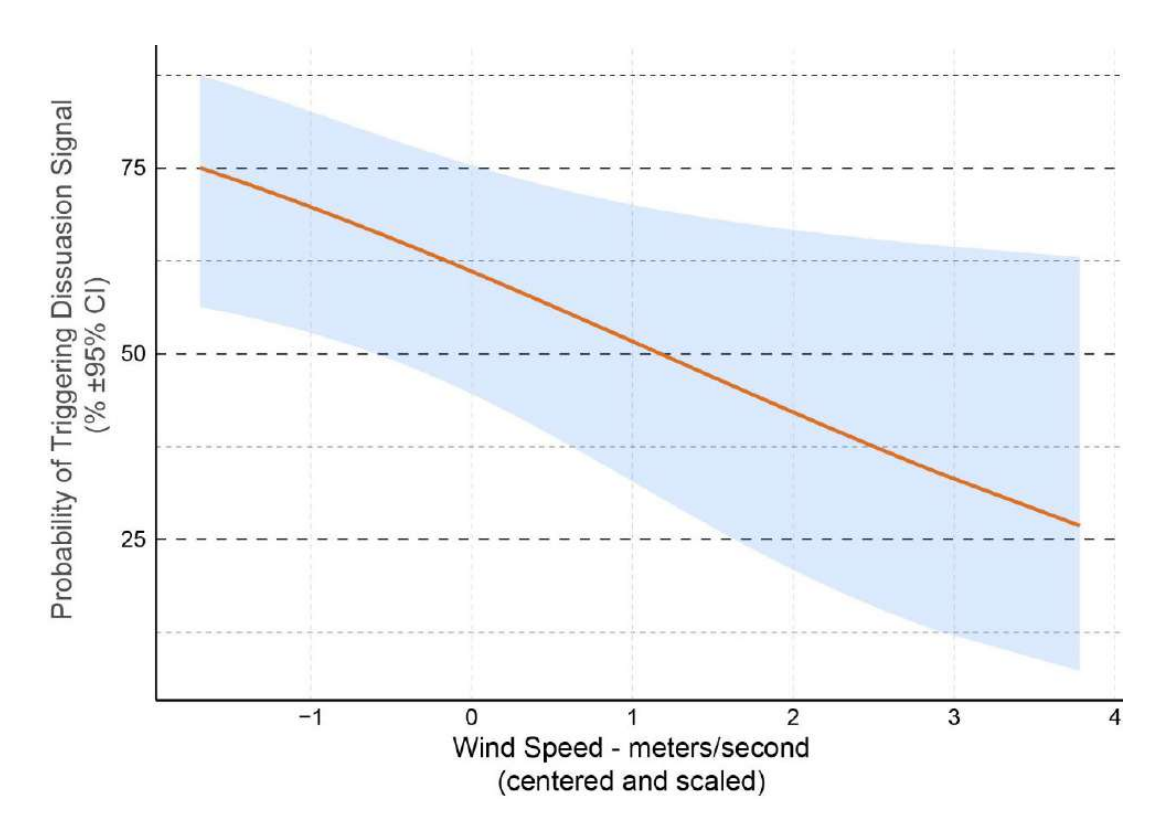


Figure 3. Illustration of predicted relationship between the probability of a golden eagle triggering a DTBird dissuasion signal and *Wind Speed*.

The relationships indicated by the resulting model coefficients and individual parameter tests (Table 3) are described below.

- Significant second-order relationship between the probability of dissuasion triggers and *Time of Day*, reflecting a higher probability of dissuasion triggering during midday compared to earlier and later in the day (Figure 4).
- When partly cloudy, cloudy, or overcast skies prevailed, the probability of dissuasion triggers was at least slightly lower at turbines operating in treatment mode compared to those operating in control mode, whereas when fair skies prevailed, the probability of dissuasion triggers was substantially lower at turbines operating in control mode (Figure 5).
- At turbines with DTBird systems operating in control mode, the probability of dissuasion triggers increased as the number of *FPs per Day* increased, whereas the opposite pattern applied at turbines operating in treatment mode (Figure 6).

Table 3. Model Coefficients and Fixed Effect Parameter Test Results for the Logistic GLMM
Selected to Represent the Probability of Confirmed and Probable Eagles (Golden and
Bald Eagles Combined) Triggering a Dissuasion Signal at DTBird Installations
Operating in Treatment (Deterrents Broadcasting) and Control (Deterrents Muted) Mode
During Two-year Experiment

Random Effect	Variance	SD
Turbine ID	0.285	0.5338
Turbine ID: Elapsed Days <sup>1</sup>	0.389	0.624

Fixed Effect	Estimate	SE	<b>z</b> <sup>2</sup>	P(> z ) <sup>2</sup>	LRT $\chi^2$ 3	P (>x <sup>2</sup> ) <sup>3</sup>
Intercept	0.374	0.3292	1.136	0.256	_	_
Treatment Group: On4	-0.263	0.3911	-0.672	0.501	_	_
Cloud Cover: Fair⁵	-1.278	0.5399	-2.367	0.018	_	-
Cloud Cover: Overcast <sup>5</sup>	0.377	0.5757	0.655	0.512	_	_
Cloud Cover: Partly Cloudy <sup>5</sup>	1.133	0.4120	2.751	0.006	_	_
Time of Day <sup>6</sup>	0.143	0.1226	1.165	0.244	1.359	0.244
Time of Day <sup>6</sup>	-0.237	0.0888	-2.668	0.008	7.939	0.004
FPs per Day <sup>7</sup>	0.395	0.1802	2.192	0.028	_	_
Treatment Group * Cloud Cover: Fair	2.040	0.7363	2.771	0.006	16.254	0.001
Treatment Group * Cloud Cover: Overcast	-0.297	0.8010	-0.371	0.710	_	_
Treatment Group * Cloud Cover: Partly Cloudy	-0.909	0.6004	-1.514	0.130	-	_
Treatment Group * FPs per Day	-0.492	0.2811	-1.750	0.080	2.965	0.085

Elapsed Days = days since data-collection began; a simpler equivalent of date.

<sup>&</sup>lt;sup>2</sup> Wald test.

<sup>&</sup>lt;sup>3</sup> Drop1 likelihood ratio test.

<sup>&</sup>lt;sup>4</sup> Reference category – Off = control mode. On = treatment mode.

<sup>5</sup> Reference category - Cloudy. Fair = mostly cloud free; Partly cloudy = <50% cloud cover; Cloudy = ≥50% cloud cover with distinctly variable cloud definitions and brightness; Overcast = complete and largely uniform gray or darker cloud cover.</p>

<sup>&</sup>lt;sup>6</sup> Translated to minutes of the day; centered and scaled ([value - mean]/SD).

<sup>&</sup>lt;sup>7</sup> FPs = false positives. Number of detection events triggered by true FPs and non-target avian FPs (see Section 2.4); centered and scaled ([value – mean]/SD).

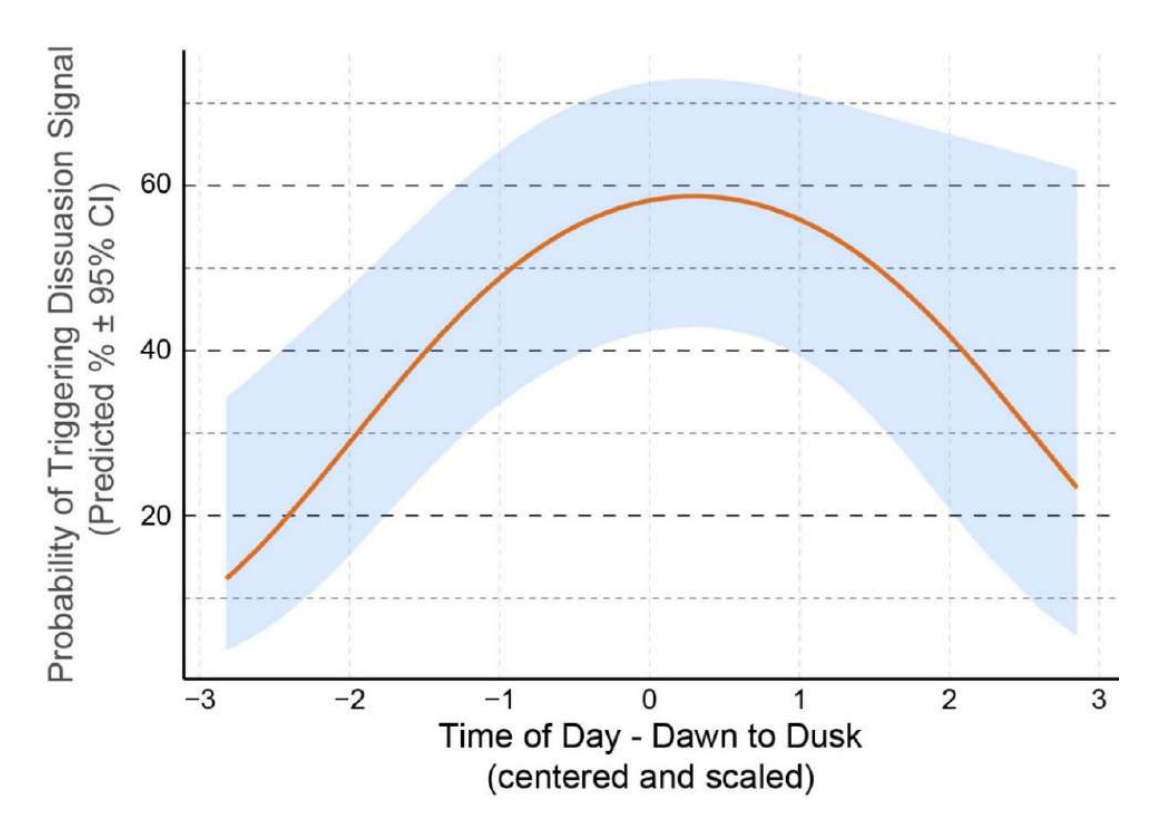


Figure 4. Illustration of predicted second-order relationship between the probability of an eagle triggering a DTBird dissuasion signal and time of day.

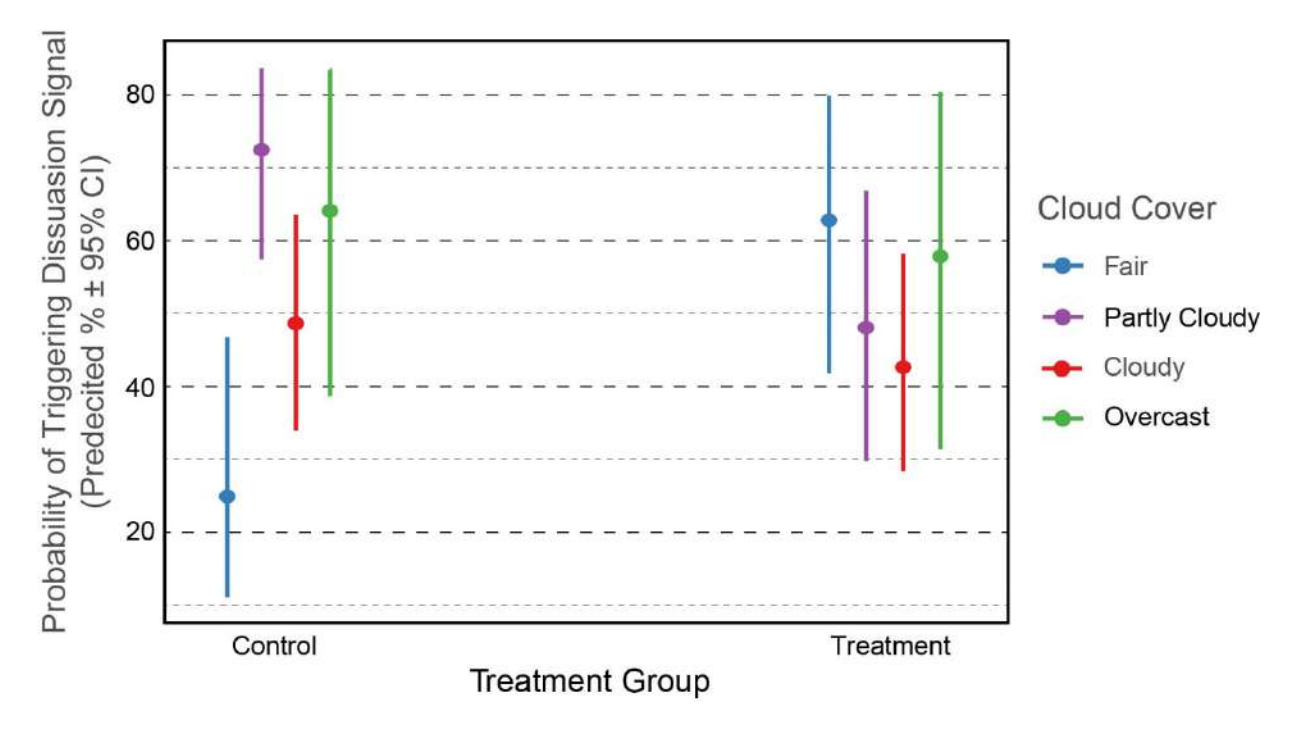


Figure 5. Illustration of predicted interactive relationship between treatment group and cloud cover in determining the probability of an eagle triggering a DTBird dissuasion signal.

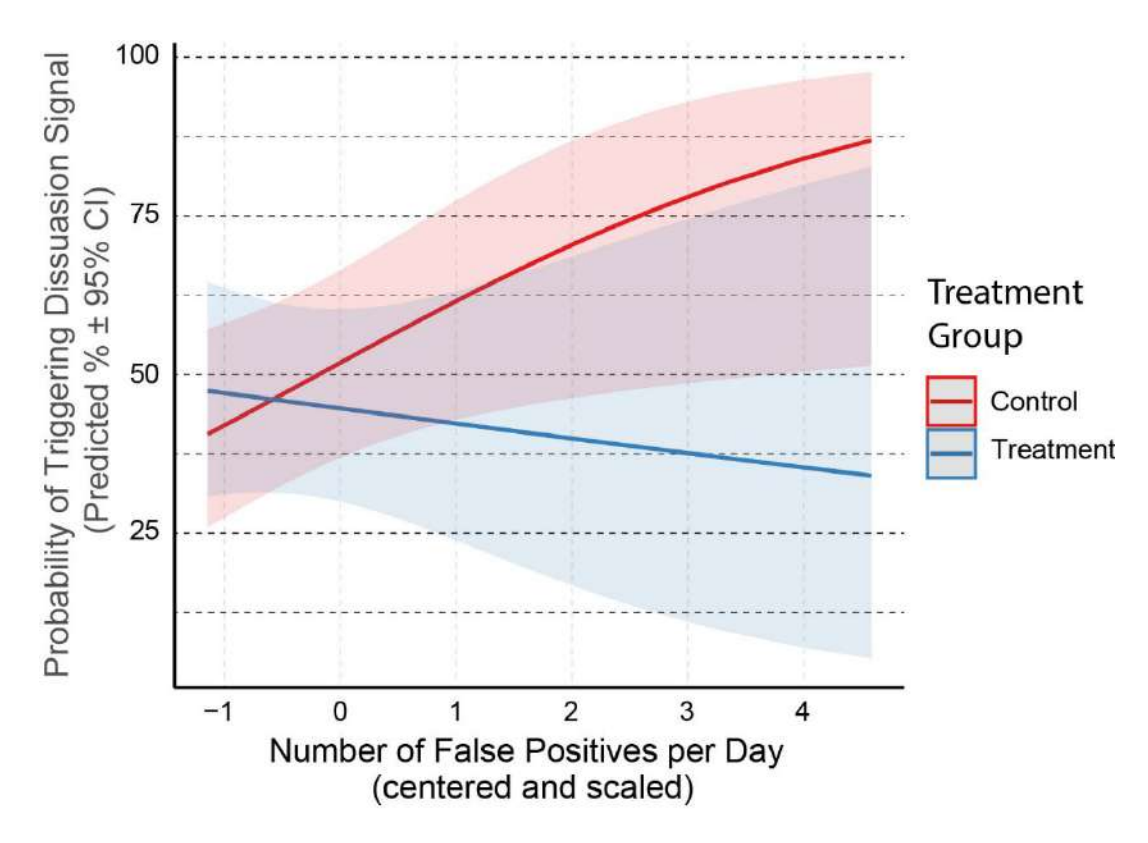


Figure 6. Illustration of predicted interactive relationship between treatment group and the daily numbers of false positives (FPs) that triggered deterrent signals in determining the probability of an eagle (golden and bald eagles combined) triggering a DTBird dissuasion signal.

Augmenting the selected model above by including  $Wind\ Speed$  resulted in the lowest AIC score among the evaluated models (Appendix D); however, the  $\Delta$ AIC was only 0.4 points and the P value for the likelihood ratio test evaluating the contribution of  $Wind\ Speed$  to the model (0.118) did not meet our criterion for retention in the model. Nevertheless, the negative parameter coefficient indicated a similar pattern as the significant relationship indicated for golden eagles alone, suggesting that wind speeds might have differentially influenced the responses of golden and bald eagles around the Goodnoe Hills turbines.

# 3.2.2 Testing Hypothesis B Regarding Dwell Time of Eagles Around DTBird Deterrent Systems

To develop the GLMM for evaluating the influence of *Treatment Group* and other potential predictors on the dwell time of golden eagles around the study turbines, we were able take both full backwards and forwards stepwise model building approaches to identify a top model. The resulting selected model (see Appendix E for comparisons of models evaluated as part of a backwards elimination process to select the final model) had the following form:

Dwell Time  $\sim [1 \mid Turbine ID] + [1 \mid Turbine ID : Elapsed Days] + Treatment Group + 28d Cycle + Time of Day + Time of Day<sup>2</sup> + FPs per Day + Treatment Group * FPs per Day$ 

The relationships indicated by the resulting model coefficients and individual parameter tests (Table 4) are described below.

- Significant 27% reduction (95% CI: 5–42%) in the average dwell time of golden eagles at installations operating in treatment mode, with the average dwell time reduced from approximately 26 to 17 seconds per event.
- Marginally significant overall declining trend in the dwell time of golden eagles in relation to the progression of *28d Cycles* over the course of the two-year study (Figure 7).
- Significant main effect / marginally significant second-order relationship between dwell time and *Time of Day*, reflecting short dwell times in the morning, increasing through mid-afternoon, then tapering off again in the evening (Figure 8).
- Marginally significant interaction between Treatment Group and FPs per Day illustrating a positive
  relationship between dwell times and FP numbers around control turbines, but a negative
  relationship around treatment turbines (Figure 9). Put another way, the more that FPs contributed to
  actual deterrent broadcasting at treatment turbines, the less likely were eagles to dwell in the vicinity
  of those turbines.

Table 4. Model Coefficients and Fixed Effect Parameter Test Results for the GLMM Selected to Represent the Relationship Between the Dwell Time of Confirmed and Probable Golden Eagles at DTBird Installations Operating in Treatment (Deterrents Broadcasting) and Control (Deterrents Muted) Mode During Two-year Experiment

Random Effect	Variance	SD		
Turbine	0.014	0.1166		
Turbine: Elapsed Days <sup>1</sup>	2.15E-07	0.0005		
Fixed Effect	Estimate	SE	<b>z</b> <sup>2</sup>	P
Intercent	2 204	0.1000	20 54	

Fixed Effect	Estimate	SE	<b>z</b> <sup>2</sup>	P(> z ) <sup>2</sup>	LRT $\chi^2$ 3	P (>χ <sup>2</sup> ) <sup>3</sup>
Intercept	3.304	0.1082	30.54	<0.001	-	_
Treatment Group: On4	-0.319	0.1258	-2.54	0.011	-	-
28d Cycle <sup>5</sup>	-0.135	0.0661	-2.04	0.041	4.08	0.044
Time of Day <sup>6</sup>	0.166	0.0666	2.50	0.013	6.42	0.011
Time of Day <sup>2</sup>	-0.089	0.0451	-1.98	0.047	3.66	0.056
FPs per Day <sup>7</sup>	0.086	0.0754	1.14	0.255	-	-
Treatment Group: On * FPs per Day	-0.258	0.1361	-1.90	0.058	3.22	0.073

Elapsed Days = days since data-collection began; a simpler equivalent of date.

<sup>&</sup>lt;sup>2</sup> Wald test.

<sup>&</sup>lt;sup>3</sup> Drop1 likelihood ratio test.

<sup>&</sup>lt;sup>4</sup> Reference category – Off = control mode. On = treatment mode.

<sup>&</sup>lt;sup>5</sup> Discrete continuous predictor representing 27 consecutive 28-day sampling periods from 1 September 2021 through 30 September 2023.

<sup>&</sup>lt;sup>6</sup> Translated to minutes of the day; centered and scaled ([value – mean]/SD).

<sup>&</sup>lt;sup>7</sup> FPs = false positives. Number of detection events triggered by true FPs and non-target avian FPs (see Section 2.4); centered and scaled ([value – mean]/SD).

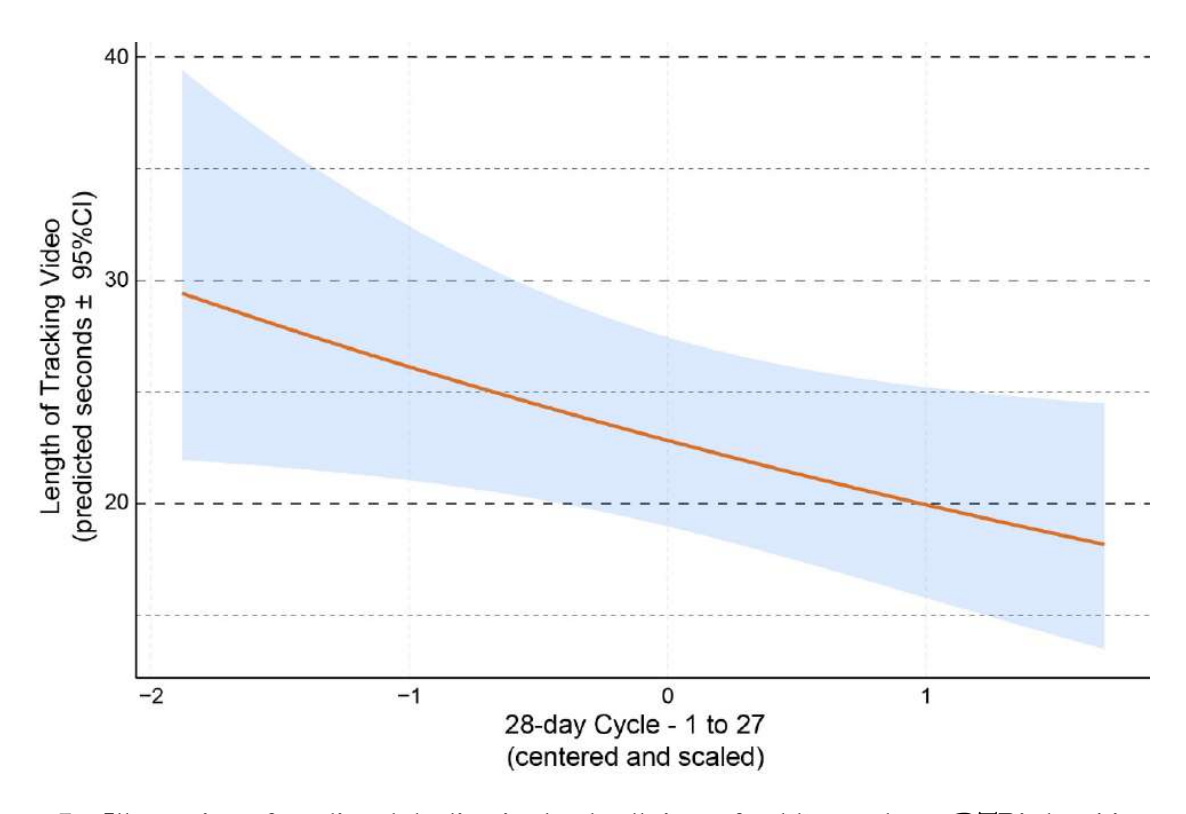


Figure 7. Illustration of predicted decline in the dwell time of golden eagles at DTBird turbines across the 27 28-day sampling cycles that composed this two-year experimental analysis.

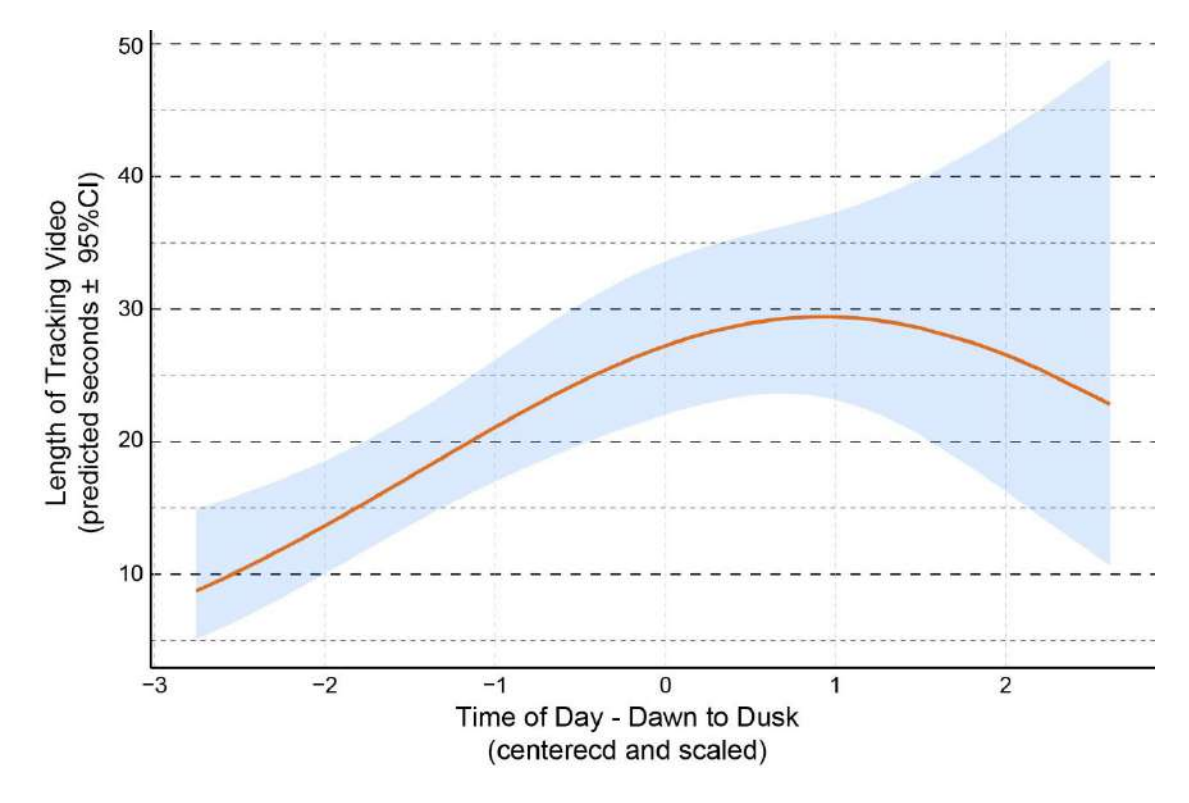


Figure 8. Illustration of predicted second-order relationship between the dwell time of golden eagles at DTBird turbines and time of day.

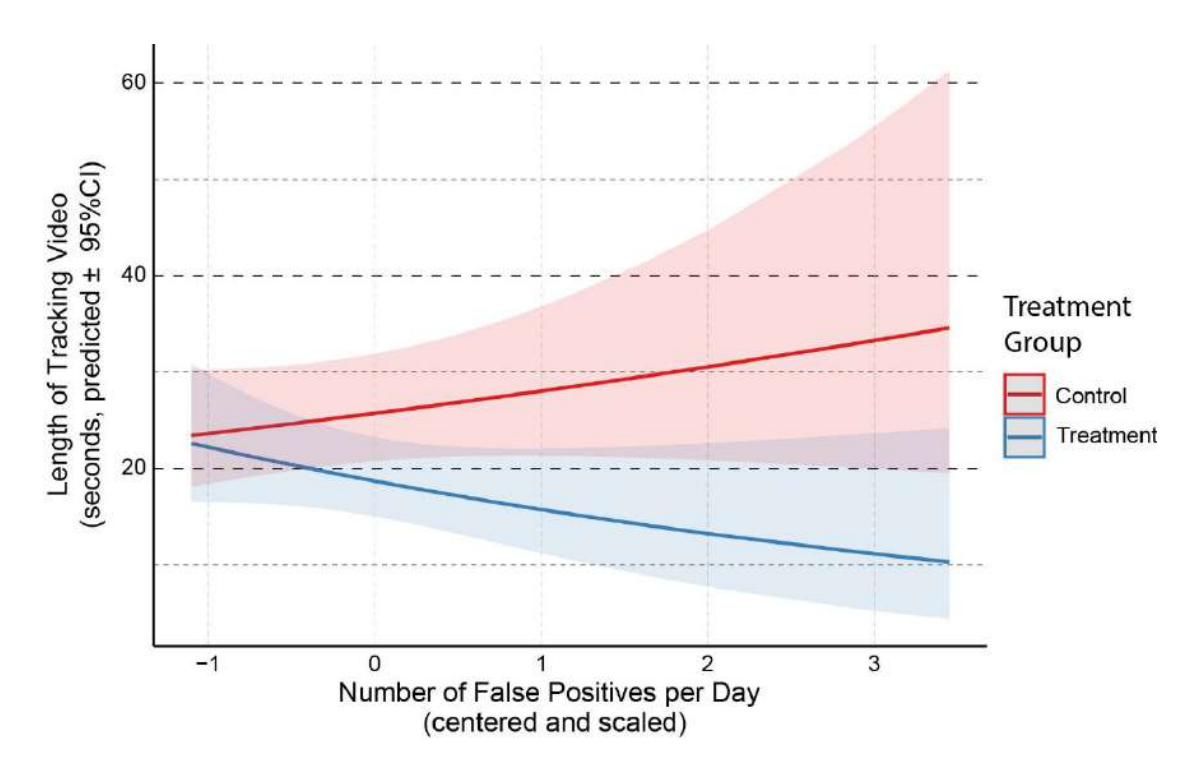


Figure 9. Illustration of predicted interactive relationship between treatment group and the daily numbers of false positives (FPs) that triggered deterrent signals in determining the dwell time of golden eagles around DTBird turbines.

Considering the dataset limited to eagles positively identified as either a golden eagle or a bald eagle yielded no evidence of Species as an influential predictor of dwell time. Hence, again we focused our further attention on evaluating models based on the larger all-eagles dataset without considering *Species* as a potential predictor. Running full models based on this dataset and dependent variable proved untenable due to dataset limitations; hence, we proceeded to identify a top model based on a similar iterative approach as described for golden eagles alone in Section 3.2.1. The outcomes of this modeling effort yielded similar insights as for predicting the dwell time of golden eagles alone, with the same final model selected to represent all eagles combined (see Appendix F for comparisons of selected candidate models) and the model coefficients confirming similar relationships as described above (Table 5, Figures 10–12). Most germane was a significant estimated 24% reduction (95% CI: 7-35%) in the dwell time of eagles at treatment turbines, with the average dwell time reduced from approximately 25 to 19 seconds per event. Note that, in deciding upon a final dwelltime model for all eagles combined, we retained FPs per Day and the Treatment Group \* FPs per Day interaction (see Figure 12) despite the P value for the interaction (0.129) being slightly greater than our  $P \le 0.10$  threshold for inclusion. We did this to retain a relationship that improved the AIC score of the final model and was common to two of the other three primary models we evaluated—albeit only marginally significant in each case (see Tables 3 and 4).

Table 5. Model Coefficients and Fixed Effect Parameter Test Results for the GLMM Selected to Represent the Relationship Between the Dwell Time of All Confirmed and Probable Eagles at DTBird Installations Operating in Treatment (Deterrents Broadcasting) and Control (Deterrents Muted) Mode During Two-year Experiment

Random Effect	Variance	SD				
Turbine	0.0016	0.03406				
Turbine: Elapsed Days <sup>1</sup>	1.82E-08	0.00014				
Fixed Effect	Estimate	SE	<b>Z</b> <sup>2</sup>	P(> z ) <sup>2</sup>	LRT $\chi^2$ 3	P (>χ <sup>2</sup> ) <sup>3</sup>
Intercept	3.305	0.0729	45.33	<0.001	_	-
Treatment Group: On4	-0.269	0.0934	-2.88	0.004	_	_
28d Cycle <sup>5</sup>	-0.114	0.0479	-2.37	0.018	5.64	0.018
Time of Day <sup>6</sup>	0.093	0.0453	2.09	0.037	4.49	0.034
Time of Day <sup>2</sup>	-0.093	0.0316	-2.93	0.003	7.92	0.005
FPs per Day <sup>7</sup>	0.124	0.0557	2.23	0.026	_	_

Elapsed Days = days since data-collection began; a simpler equivalent of date.

-0.149

Treatment Group: On \* FPs per Day

0.0964

-1.55

0.121

2.31

0.129

# 3.2.3 Testing Hypothesis C Regarding the Probability of Eagles Crossing the Rotor Swept Area of DTBird Equipped Turbines

Modeling the probability of an RSA crossing for golden eagles alone and for all eagles combined yielded no *Treatment Group* effects and no models that improved upon the null model. This outcome was not surprising given a paucity of consistent and reliable data to evaluate this dependent variable. Observations recorded by our data-entry technicians suggested that 9% of 105 golden eagle observations at turbines with DTBird systems operating in control mode a potential RSA cross, whereas a nominally lower 7% of 102 observations at turbines operating in treatment mode included a potential RSA cross. For all eagles combined, the comparisons were 13% of 209 observations included a potential RSA cross at control turbines, and 12% of 181 observations included a potential RSA cross at treatment turbines.

<sup>&</sup>lt;sup>2</sup> Wald test.

<sup>&</sup>lt;sup>3</sup> Drop1 likelihood ratio test.

<sup>&</sup>lt;sup>4</sup> Reference category – Off = control mode. On = treatment mode.

<sup>5</sup> Discrete continuous predictor representing 27 consecutive 28-day sampling periods from 1 September 2021 through 30 September 2023.

<sup>&</sup>lt;sup>6</sup> Translated to minutes of the day; centered and scaled ([value - mean]/SD).

FPs = false positives. Number of detection events triggered by true FPs and non-target avian FPs (see Section 2.4); centered and scaled ([value - mean]/SD).

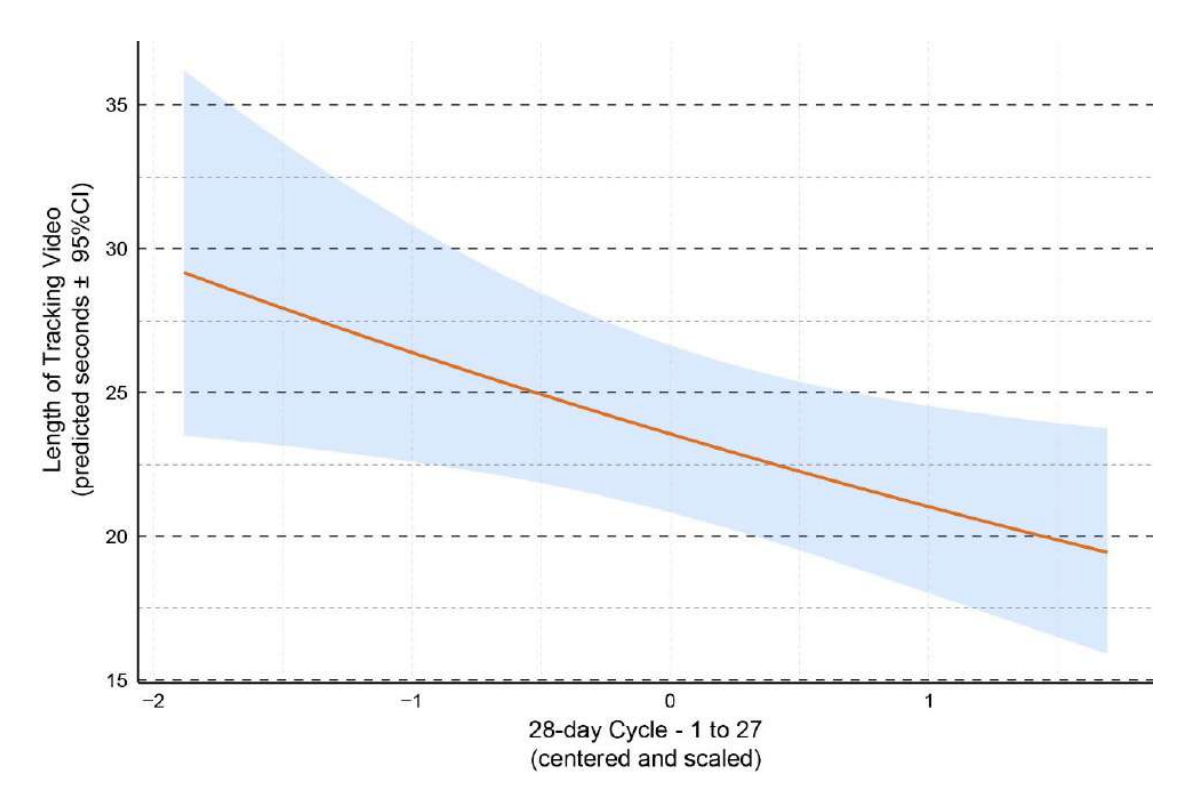


Figure 10. Illustration of predicted decline in the dwell time of eagles (golden and bald eagles combined) at DTBird turbines across the 27 28-day sampling cycles that composed this two-year experimental analysis.

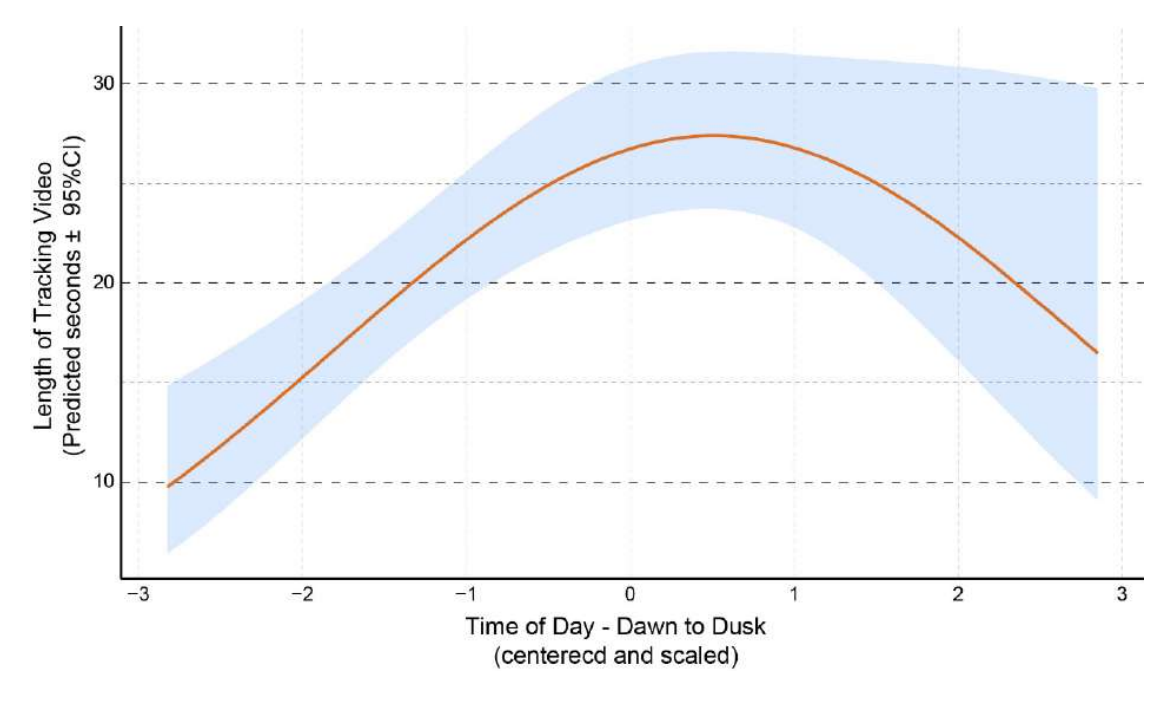


Figure 11. Illustration of predicted second-order relationship between the dwell time of eagles (golden and bald eagles combined) at DTBird turbines and time of day.

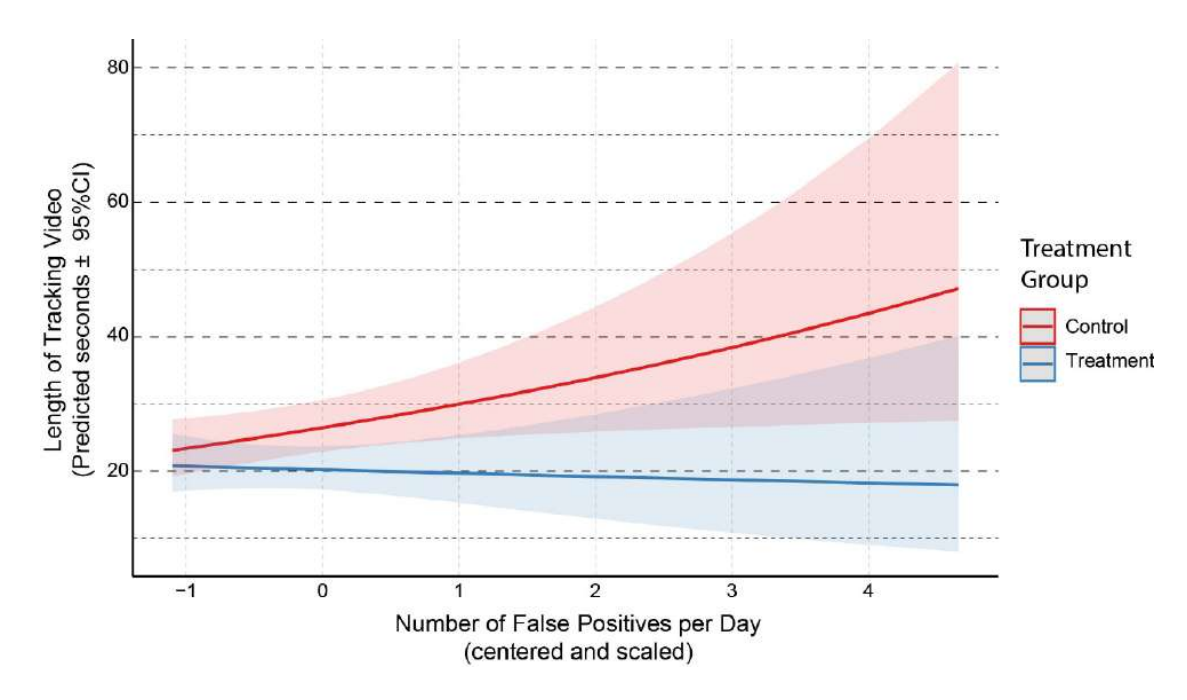


Figure 12. Illustration of predicted interactive relationship between treatment group and the daily numbers of false positives (FPs) that triggered deterrent signals in determining the dwell time of eagles (golden and bald eagles combined) around DTBird turbines.

#### **Section 4.0 Discussion**

The modeling results failed to reveal a significant overall treatment effect based on the probability of triggering a dissuasion signal as the binary dependent variable, but those models did reveal some potentially insightful interactive relationships between *Treatment Group* and other predictors. Although *Treatment Group* did not emerge as a significant predictor of the probability of dissuasion triggers, the indicated association for golden eagles alone and all eagles combined was as predicted in Hypothesis A—at least a slightly lower probability of dissuasion triggers at turbines when the DTBird deterrents were broadcasting. Much stronger overall *Treatment Group* effects emerged when we modeled dwell time as the dependent variable, and the indicators were again consistent with the prediction of Hypothesis B. The more-robust dwell-time models also emphasized both some common and novel influences of the evaluated covariates compared to the dissuasion-trigger models. Unfortunately, evaluating Hypothesis C simply did not pan out due to poor data quality, as predicted.

One possible reason why greater support for Hypothesis A was not apparent concerns the efficacy of warning signals as a potential means to reduce the probability of an eagle triggering a subsequent dissuasion signal. Although eagles triggered warning and dissuasion signals with similar frequencies overall, a large majority of the triggered dissuasion signals were not preceded by a prior warning signal. In other words, the idea that broadcasted warning signals could be expected to reduce the probability of triggering a subsequent dissuasion signal actually did not apply very often. Two potential explanations for this pattern are: 1) within the primary detection envelope where sequential warning and dissuasion signaling is expected when relevant, the DTBird detection systems frequently did not detect eagles until they had already reached the closer dissuasion-triggering envelope; and 2) eagles often flew in relatively low and entered the detection envelope relatively close to the turbine where dissuasion signals were immediately triggered without a prior warning signal.

The significant effects of *Treatment Group* in the dwell-time models translated to predictions of golden eagles and all eagles combined averaging 24–27% less time dwelling in the vicinity of DTBird systems operating with their deterrents broadcasting normally compared to systems with muted deterrents. The golden eagle dissuasion-trigger model indicated a similar—albeit statistically nonsignificant—29% decrease in the probability of dissuasion triggers at treatment turbines. Quantifying estimated reductions in the probability of dissuasion triggers at treatment turbines based on the all-eagles model was complicated by the presence of interactions with both categorical (*Cloud Cover*) and continuous (*FPs per Day*) covariates. Under most sky conditions from partly cloudy to overcast, eagles tended to trigger approximately 9–30% fewer dissuasion signals at turbines with DTBird deterrents broadcasting normally (i.e., consistent with research Hypothesis A), whereas a much stronger, opposite pattern was shown when fair skies prevailed. Reasons for this unexpected anomaly are uncertain, but one possibility is that visibility typically tends to be clearer overall during fair weather. Better visibility might have allowed the eagles to more easily perceive the spinning turbines, take heed of the broadcasting deterrents, but also remain more comfortable flying and foraging closer to the turbines with less concern for the potential collision risk. In contrast, the indicated interactive

relationship between *Treatment Group* and *FPs per Day* indicated further clear support for Hypothesis A in demonstrating that the positive effect of broadcasted deterrents at treatment turbines deterring eagles from triggering dissuasion signals was accentuated by higher FP deterrent-triggering activity, whereas no such effect was evident at control turbines. The difference in the probability of dissuasion triggers at control versus treatment turbines was nominal when the FP deterrent triggering rate was low, but was approximately a 60% lower at treatment turbines when the FP deterrent triggering rate was elevated.

The model focused on presumed golden eagles triggering dissuasion signals indicated a novel relationship with monitoring Year as a predictor, suggesting that the probability of golden eagles triggering dissuasion signals declined overall by approximately 46% across the facility during Year 2 of the study. Neither Year nor 28d Cycle emerged as a significant predictor in the all-eagles dissuasion-trigger model; however, 28d Cycle emerged as an important predictor in the dwell-time models for both golden eagles alone and all eagles combined. Similar to the result for golden eagles and dissuasion triggers, the indicated relationship for 28d Cycle was an overall declining trend across the 2-year study in the dwell time of golden eagles alone and all eagles combined. Given that these trends did not emerge differentially around DTBird equipped turbines operating in treatment versus control mode, the overall pattern may provide evidence of positive habituation through time among resident and seasonally resident eagles. As such eagles became increasingly exposed to deterrents being broadcasted regularly around the perimeter of the facility, they might have grown increasingly wary of dwelling for extended periods in the vicinity. Here it is important to note that this potential habituation pattern could have been accentuated by two factors: 1) an unusually high overall FP triggering rate through the first 19 months of the study, until Liquen was authorized to undertake further fine-tuning of the filtering algorithms to reduce the FP rate; and 2) due to an extended failure of communications between the DTBird and turbine SCADA systems following a forced 24-day site-wide power outage, all DTBird systems operated in default mode after May 2023, whereby the deterrents were being triggered whether or not the focal turbine was spinning. The first factor substantially reduced the overall FP deterrent triggering rate after January 2023 (H. T. Harvey & Associates 2023a); however, the second factor may have largely offset that effect by increasing the overall prevalence of superfluous deterrent triggering in after May 2023. This combination likely maintained an elevated rate of deterrent triggering throughout most of the 2-year study, which could have accelerated the pace of any positive habituation effects. What is equally important to note here, though, is that the results do not point to possible negative habituation, which would involve eagles learning to ignore the deterrents and remain at risk.

All of the models we developed reflected a pronounced diel pattern of variation in the documented eagle responses that operated independently of the applied deterrent treatment regime. Most of the modeled results captured the relationship as increasing strongly—whether the probability of dissuasion triggers or average dwell time—from dawn until reaching a mid-afternoon peak, followed by a lesser, gradual decline until dusk. We think this predominant pattern probably reflects the common general activity levels of eagles and other raptors during a typical day, with the flight activity of especially large soaring raptors typically dependent on thermal and wind activity increasing as the day warms up to provide energy-saving lift for active foraging, patrolling, and other flight-dependent activities.

Finally, *Wind Speed* emerged as significant covariate influencing the probability of golden eagles triggering dissuasion signals, independently of the implemented control-treatment design. The indicated effect of higher wind speeds generally reducing the probability of dissuasion triggers suggests that the faster the turbines are spinning the more they themselves act as a deterrent to visually acute eagles, who then remain farther away from the perceived danger independent of the influence of DTBird deterrent signaling.

In conclusion, despite falling well short of our intended 2-year sampling design due to factors beyond our control, the results of our careful analyses yielded noteworthy insight about the positive benefits of the DTBird deterrent system in reducing the activity of eagles around turbines where the deterrents were broadcasting normally, and both the related and independent influences of various environmental factors on the eagle responses around the facility to the presence of operating DTBird systems. Particularly notable among the latter were indications of possible long-term positive habituation reducing the dwell time of eagles around the DTBird turbines independent of the control-treatment experimental design, likely reflecting the overarching influence of an atypically elevated overall deterrent triggering rate across the installed DTBird systems. We suspect that, had frequent operational failures not caused major unexpected imbalances in our intended sampling design and had the overall deterrent triggering not been artificially elevated by various factors, our ability to demonstrate conclusive patterns of interest concerning the proximate effectiveness of DTBird would have been even greater.

#### **Section 5.0 References**

- Bolker, B. M. 2023. Package lme4: linear mixed-effects models using 'eigen' and S4. Version 1.1-35.1 <a href="https://www.rdocumentation.org/packages/lme4">https://www.rdocumentation.org/packages/lme4</a>. Accessed December 2023.
- Bolker, B. M., M. E. Brooks, C. J. Clark, S. W. Geange, J. R. Poulsen, M. H. H. Stevens, and J-S. S. White. 2009. Generalized linear mixed models: a practical guide for ecology and evolution. Trends in Ecology and Evolution 24:127–135.
- Brooks, M., B. Bolker, K. Kristensen, M. Maechler, A. Magnusson, H. Skaug, A. Nielsen, C. Berg, and K. van Bentham. 2023. Package'glmmTMB'. Version 1.1.8.

  <a href="https://www.rdocumentation.org/packages/glmmTMB/versions/1.1.8">https://www.rdocumentation.org/packages/glmmTMB/versions/1.1.8</a>. Accessed December 2023.
- Burnham, K. P., and D. R. Anderson. 2002. Model Selection and Multimodel Inference: A Practical Information-Theoretic Approach. Second edition. Springer, New York, NY.
- Hartig, F. 2019. Package DHARMa: residual diagnostics for hierarchical (multi-level/mixed) regression models. Version 0.2.6. <a href="https://cran.r-project.org/web/packages/DHARMa/index.html">https://cran.r-project.org/web/packages/DHARMa/index.html</a>. Accessed August 2022.
- Hosmer, D. W., and S. Lemeshow. 1989. Applied Logistic Regression. John Wiley & Sons, New York, NY, USA.
- H. T. Harvey & Associates. 2018. Evaluating a Commercial-Ready Technology for Raptor Detection and Deterrence at a Wind Energy Facility in California. Research report. Los Gatos, California. Prepared for the American Wind Wildlife Institute, Washington, D.C.
- H. T. Harvey & Associates. 2019a. Evaluating the Effectiveness of a Detection and Deterrent System in Reducing Eagle Fatalities at Operational Wind Facilities: Detailed Study Plan. Los Gatos, California. Prepared for the American Wind Wildlife Institute, Washington, D.C., in conjunction with U.S. Department of Energy Cooperative Agreement DE-EE0007883.
- H. T. Harvey & Associates. 2019b. Analysis of DTBird False Positive Detections at the Manzana Wind Power Project Through October 2017. Research Report. Los Gatos, California. Prepared for the American Wind Wildlife Institute, Washington, D.C., in conjunction with U.S. Department of Energy Cooperative Agreement DE-EE0007883.
- H. T. Harvey & Associates. 2022a. Initial Analyses of DTBird Detection and Deterrent-Triggering Response Distances and Probability of Detection at the Goodnoe Hills Wind Farm, Washington. Research Report. Research Report. Los Gatos, CA, USA. Prepared for the Renewable Energy Wildlife Institute, Washington, D.C., USA, in conjunction with U.S. Department of Energy Cooperative Agreement DE-EE0007883.

- H. T. Harvey & Associates. 2022b. Initial Analysis of DTBird False Positive Detections at the Goodnoe Hills Wind Farm, Washington: September 1, 2021 – March 15, 2022. Research Report. Draft – August 25, 2022. Los Gatos, California. Prepared for the Renewable Energy Wildlife Institute, Washington, D.C., in conjunction with U.S. Department of Energy Cooperative Agreement DE-EE0007883.
- H. T. Harvey & Associates. 2023a. Analysis of DTBird False Negatives and False Positives at Commercial Wind-Energy Facilities in California and Washington. Research Report. DOE Review Draft November 29, 2023. Los Gatos, California. Prepared for the Renewable Energy Wildlife Institute, Washington, D.C., in conjunction with U.S. Department of Energy Cooperative Agreement DE-EE0007883.
- H. T. Harvey & Associates. 2023b. Analysis of Behavioral Responses of Eagles and Other Large Raptors to DTBird Audio Deterrents at Commercial Wind-Energy Facilities in California and Washington. Los Gatos, CA, USA. Prepared for the Renewable Energy Wildlife Institute, Washington, D.C., USA, in conjunction with U.S. Department of Energy Cooperative Agreement DE-EE0007883.
- May, R., Ø. Hamre, R. Vang, and T. Nygård. 2012. Evaluation of the DTBird Video-System at the Smøla Wind-Power Plant: Detection Capabilities for Capturing Near-Turbine Avian Behaviour. NINA Report 910. Norwegian Institute for Nature Rese arch, Trondheim, Norway.
- Symonds, M. R., and A. Moussalli. 2011. A brief guide to model selection, multimodel inference and model averaging in behavioural ecology using Akaike's information criterion. Behavioral Ecology and Sociobiology 65:13–21.

### Appendix A. Randomized Deterrent-Broadcasting Control-Treatment Rotation Schedules for Two-Year Experiment

	28-day							Turbine	<b></b>						
Date	Cycle	G29	G34	G35	G44	G45	G48	G49	G51	G56	G58	G59	G64	G67	G75
01-Sep-21	1	na¹	Off1	Off	On¹	Off	On	Off	na	na	On	On	Off	Off	On
02-Sep-21	1	na	Off	On	Off	On	Off	Off	na	na	Off	On	On	On	Off
03-Sep-21	1	na	Off	Off	On	Off	On	Off	na	na	On	Off	On	On	Off
04-Sep-21	1	na	Off	Off	On	On	Off	On	na	na	On	Off	On	Off	Off
05-Sep-21	1	na	On	Off	On	On	Off	On	na	na	On	Off	Off	Off	On
06-Sep-21	1	na	Off	On	Off	On	On	Off	na	na	Off	On	Off	On	On
07-Sep-21	1	na	Off	On	Off	Off	On	Off	na	na	On	Off	On	On	Off
08-Sep-21	1	na	On	On	Off	Off	Off	On	na	na	Off	On	Off	Off	On
09-Sep-21	1	na	Off	On	On	Off	Off	On	na	na	On	Off	On	Off	Off
10-Sep-21	1	na	On	Off	On	Off	Off	On	na	na	Off	Off	On	Off	On
11-Sep-21	1	na	On	Off	Off	On	On	Off	na	na	On	Off	Off	On	On
12-Sep-21	1	na	On	Off	On	On	Off	On	na	na	On	Off	On	Off	Off
13-Sep-21	1	na	Off	Off	On	On	On	Off	na	na	On	Off	On	Off	On
14-Sep-21	1	na	On	Off	On	Off	Off	Off	na	na	On	Off	On	Off	On
15-Sep-21	1	na	On	Off	On	Off	Off	On	na	na	Off	On	On	Off	Off
16-Sep-21	1	na	Off	On	Off	Off	On	On	na	na	Off	On	Off	Off	On
17-Sep-21	1	na	Off	On	On	On	Off	On	na	na	Off	Off	On	Off	On
18-Sep-21	1	na	Off	Off	On	On	On	Off	na	na	Off	On	On	On	Off
19-Sep-21	1	na	On	Off	On	Off	On	Off	na	na	On	On	On	Off	Off
20-Sep-21	1	na	On	Off	Off	On	On	On	na	na	Off	Off	On	Off	On
21-Sep-21	1	na	Off	Off	Off	On	On	On	na	na	Off	On	On	Off	Off
22-Sep-21	1	na	Off	Off	On	On	On	Off	na	na	Off	On	On	Off	On
23-Sep-21	1	na	On	Off	Off	Off	On	Off	na	na	On	On	Off	Off	On
24-Sep-21	1	na	Off	On	Off	Off	On	On	na	na	On	On	Off	Off	Off
25-Sep-21	1	na	On	On	On	Off	Off	On	na	na	Off	On	On	Off	Off
26-Sep-21	1	na	On	Off	Off	On	On	On	na	na	On	Off	Off	On	Off
27-Sep-21	1	na	On	On	Off	Off	On	Off	na	na	On	Off	Off	On	On
28-Sep-21	1	na	On	Off	On	Off	On	On	na	na	Off	On	On	Off	Off
29-Sep-21	2	na	On	On	Off	Off	On	Off	na	na	Off	Off	On	On	On
30-Sep-21	2	na	On	On	Off	On	Off	Off	na	na	On	Off	Off	On	On
01-Oct-21	2	na	Off	On	On	On	Off	On	na	na	Off	On	On	Off	Off
02-Oct-21	2	na	On	Off	On	On	Off	On	na	na	Off	On	On	Off	Off
03-Oct-21	2	na	Off	Off	Off	On	On	On	na	na	Off	Off	On	On	Off
04-Oct-21	2	na	On	Off	Off	On	On	On	na	na	Off	Off	On	Off	On
05-Oct-21	2	na	On	Off	On	On	Off	On	na	na	Off	Off	On	On	Off
06-Oct-21	2	na	On	Off	On	Off	On	Off	na	na	Off	On	On	On	Off
07-Oct-21	2	na	On	On	Off	Off	On	On	na	na	On	Off	On	Off	Off
08-Oct-21	2	na	On	Off	Off	Off	On	Off	na	na	Off	On	On	On	Off
09-Oct-21	2	na	On	On	On	Off	Off	On	na	na	On	Off	On	Off	Off
10-Oct-21	2	na	On	Off	On	Off	On	On	na	na	On	Off	Off	Off	On
11-Oct-21	2	na	Off	On	On	Off	On	On	na	na	Off	Off	On Off	On	Off
12-Oct-21	2	na	Off	On	On	Off	On Off	On	na	na	Off	On Off	Off	On	Off
13-Oct-21	2	na	Off	Off	On	On	Off	On	na	na	Off	Off	On	On Off	Off
14-Oct-21	2	na	Off	Off	On On	On Off	On On	On Off	na	na	On	Off	On Off	Off	Off
15-Oct-21	2	na	Off	Off	On	Off	On Off	Off	na	na	On	On	Off	On	Off
16-Oct-21	2	na	Off	On	On	Off	Off	Off	na	na	On	On	Off	On	Off

	28-day							Turbine	9						
Date	28-aay Cycle	G29	G34	G35	G44	G45	G48	G49	G51	G56	G58	G59	G64	G67	G75
17-Oct-21	2	na	On	On	Off	Off	On	On	na	na	Off	On	Off	Off	On
18-Oct-21	2	na	Off	On	Off	On	On	Off	na	na	Off	On	On	Off	On
19-Oct-21	2	na	Off	On	Off	On	On	Off	na	na	Off	On	On	Off	On
20-Oct-21	2	na	On	On	On	Off	Off	On	na	na	Off	Off	On	On	Off
21-Oct-21	2	na	On	On	Off	Off	On	Off	na	na	On	On	On	Off	Off
22-Oct-21	2	na	On	On	Off	On	Off	Off	na	na	On	Off	Off	On	On
23-Oct-21	2	na	Off	Off	On	On	On	Off	na	na	Off	On	On	On	Off
24-Oct-21	2	na	On	Off	On	On	Off	On	na	na	On	Off	Off	Off	On
25-Oct-21	2	na	Off	On	On	Off	Off	Off	na	na	Off	On	On	On	Off
26-Oct-21	2	na	Off	On	Off	Off	On	On	na	na	On	Off	Off	On	Off
27-Oct-21	3	na	Off	Off	On	On	Off	Off	na	na	On	On	On	Off	Off
28-Oct-21	3	na	Off	On	Off	Off	On	Off	na	na	Off	On	On	On	Off
29-Oct-21	3	na	Off	Off	On	On	On	On	na	na	Off	On	Off	Off	On
30-Oct-21	3	na	On	On	On	Off	Off	Off	na	na	Off	Off	On	On	On
31-Oct-21	3	na	On	On	On	Off	Off	Off	na	na	On	Off	Off	On	On
01-Nov-21	3	na	Off	On	On	Off	On	On	na	na	On	On	Off	Off	Off
02-Nov-21	3	na	Off	On	Off	Off	On	Off	na	na	On	On	Off	Off	On
03-Nov-21	3	na	On	Off	Off	On	On	Off	na	na	On	Off	On	On	Off
04-Nov-21	3	na	Off	Off	On	On	Off	Off	na	na	On	On	Off	Off	On
05-Nov-21	3		Off	Off	On	On	On	On			On	On	Off	Off	Off
		na							na	na					
06-Nov-21	3	na	On	Off	Off	On	On	Off	na	na	Off	On	On	Off	On
07-Nov-21	3	na	Off	On	On	Off	On	Off	na	na	Off	On	On	Off	On
08-Nov-21	3	na	Off	On	Off	On	Off	On	na	na	On	Off	Off	On	Off
09-Nov-21	3	na	On	Off	On	Off	Off	On	na	na	Off	On	On	Off	Off
10-Nov-21	3	na	On	On	Off	On	Off	Off	na	na	On	Off	On	On	Off
11-Nov-21	3	na	On	On	On	Off	Off	Off	na	na	Off	Off	On	On	On
12-Nov-21	3	na	On	On	On	Off	Off	Off	na	na	On	On	Off	Off	On
13-Nov-21	3	na	On	Off	On	Off	Off	Off	na	na	On	Off	On	On	Off
14-Nov-21	3	na	Off	On	Off	On	On	On	na	na	On	Off	Off	Off	On
15-Nov-21	3	na	Off	Off	On	On	Off	On	na	na	Off	On	Off	On	Off
16-Nov-21	3	na	On	Off	On	On	Off	On	na	na	Off	On	On	Off	Off
17-Nov-21	3	na	Off	On	Off	On	On	Off	na	na	Off	On	On	On	Off
18-Nov-21	3	na	On	Off	On	Off	Off	Off	na	na	On	On	Off	Off	On
19-Nov-21	3	na	On	Off	On	Off	Off	Off	na	na	Off	On	Off	On	On
20-Nov-21	3	na	On	Off	On	Off	Off	On	na	na	On	Off	On	Off	Off
21-Nov-21	3	na	Off	On	Off	On	Off	On	na	na	On	Off	Off	On	Off
22-Nov-21	3	na	Off	Off	Off	On	On	On	na	na	Off	Off	Off	On	On
23-Nov-21	3	na	Off	On	On	On	Off	On	na	na	On	Off	Off	On	Off
24-Nov-21	4	na	Off	Off	On	On	On	Off	na	na	On	Off	On	Off	On
25-Nov-21	4	na	On	Off	Off	Off	On	Off	na	na	Off	Off	On	On	On
26-Nov-21	4	na	On	Off	On	Off	Off	On	na	na	Off	On	Off	Off	On
27-Nov-21	4	na	On	Off	Off	On	On	On	na	na	On	Off	Off	Off	On
28-Nov-21	4	na	On	Off	Off	On	On	Off	na	na	Off	Off	On	On	On
29-Nov-21	4	na	Off	On	On	Off	Off	On	na	na	On	Off	On	Off	Off
30-Nov-21	4	na	Off	On	On	On	Off	Off	na	na	Off	Off	On	On	On
01-Dec-21	4	na	Off	On	Off	Off	On	On	na	na	Off	On	On	Off	Off
02-Dec-21	4	na	On	Off	On	Off	Off	On	na	na	Off	On	Off	On	Off
03-Dec-21	4	na	Off	Off	Off	On	On	On	na	na	On	Off	Off	Off	On
04-Dec-21	4	na	Off	On	Off	On	On	On	na	na	Off	Off	On	Off	On
05-Dec-21	4	na	On	Off	Off	On	On	On	na	na	Off	On	Off	Off	On
06-Dec-21	4	na	Off	On	On	On	Off	On	na	na	On	Off	Off	Off	On
07-Dec-21	4	na	Off	On	Off	On	On	On			On	On	Off	Off	Off
07-DGC-21	4	nu	Oil	OH	OII	OH	OH	OH	na	na	OH	OH	OII	OII	OII

	28-day							Turbine	<del></del>						
Date	Cycle	G29	G34	G35	G44	G45	G48	G49	G51	G56	G58	G59	G64	G67	G75
08-Dec-21	4	na	On	Off	Off	Off	On	On	na	na	Off	On	Off	Off	On
09-Dec-21	4	na	Off	On	On	On	Off	On	na	na	On	On	Off	Off	Off
10-Dec-21	4	na	Off	On	On	Off	Off	On	na	na	Off	Off	On	On	Off
11-Dec-21	4	na	Off	On	Off	On	On	Off	na	na	Off	On	On	On	Off
12-Dec-21	4	na	Off	On	On	Off	On	On	na	na	On	Off	Off	On	Off
13-Dec-21	4	na	Off	On	Off	Off	On	Off	na	na	Off	On	On	Off	On
14-Dec-21	4	na	On	Off	On	On	Off	Off	na	na	On	On	Off	On	Off
15-Dec-21	4	na	Off	On	On	Off	Off	Off	na	na	On	Off	Off	On	On
16-Dec-21	4	na	On	Off	On	Off	Off	On	na	na	On	Off	Off	On	Off
17-Dec-21	4	na	Off	On	On	Off	Off	On	na	na	On	Off	On	Off	Off
18-Dec-21	4	na	On	Off	On	Off	On	Off	na	na	On	On	On	Off	Off
19-Dec-21	4	na	Off	On	Off	On	On	Off	na	na	Off	On	On	On	Off
20-Dec-21	4	na	Off	Off	On	Off	On	Off	na	na	On	Off	On	Off	On
21-Dec-21	4	na	On	Off	Off	On	Off	On	na	na	Off	Off	On	On	Off
22-Dec-21	5	na	Off	On	Off	Off	On	On	na	na	Off	On	On	Off	Off
23-Dec-21	5	na	Off	Off	On	On	Off	On	na	na	Off	Off	On	Off	On
24-Dec-21	5	na	On	On	On	Off	Off	On	na	na	On	Off	On	Off	Off
25-Dec-21	5	na	On	On	Off	On	Off	On	na	na	On	Off	Off	Off	On
26-Dec-21	5	na	Off	On	Off	On	On	On	na	na	Off	Off	On	On	Off
27-Dec-21	5	na	On	Off	On	On	Off	Off	na	na	On	Off	On	On	Off
28-Dec-21	5	na	Off	On	On	On	Off	Off	na	na	On	On	Off	Off	On
29-Dec-21	5	na	Off	On	On	Off	Off	On	na	na	Off	On	Off	On	Off
30-Dec-21	5	na	Off	Off	Off	On	On	On	na	na	Off	On	Off	Off	On
31-Dec-21	5	na	On	On	Off	On	Off	Off	na	na	On	On	Off	Off	On
01-Jan-22	5	na	Off	Off	On	On	Off	Off	na	na	Off	Off	On	On	On
02-Jan-22	5	na	On	Off	On	Off	On	On	na	na	Off	On	On	Off	Off
03-Jan-22	5	na	Off	Off	Off	On	On	On	na	na	Off	Off	On	On	Off
04-Jan-22	5	na	Off	Off	On	Off	On	Off	na	na	Off	On	On	On	Off
05-Jan-22	5	na	Off	Off	On	On	On	On	na	na	Off	Off	On	Off	On
06-Jan-22	5	na	On	Off	On	Off	On	Off	na	na	Off	On	On	Off	On
07-Jan-22	5	na	On	Off	Off	On	On	Off	na	na	Off	Off	On	On	On
08-Jan-22	5	na	Off	Off	On	On	Off	On	na	na	On	Off	Off	Off	On
09-Jan-22	5	na	Off	Off	On	On	On	On	na	na	On	Off	Off	Off	On
10-Jan-22	5	na	On	Off	Off	On	On	On	na	na	On	Off	On	Off	Off
11-Jan-22	5	na	On	On	Off	On	Off	On	na	na	Off	Off	Off	On	On
12-Jan-22	5	na	Off	Off	On	On	Off	On	na	na	Off	Off	On	Off	On
13-Jan-22	5	na	Off	On	On	Off	On	Off	na	na	On	Off	On	Off	On
14-Jan-22	5	na	On	On	Off	Off	Off	Off	na	na	Off	On	On	On	Off
15-Jan-22	5	na	Off	On	On	Off	On	On	na	na	Off	On	On	Off	Off
16-Jan-22	5	na	Off	Off	On	Off	On	On	na	na	Off	On	Off	On	Off
17-Jan-22	5	na	Off	Off	On	Off	On	Off	na	na	Off	On	On	On	Off
18-Jan-22	5	na	On	On	Off	On	Off	Off	na	na	Off	On	On	Off	On
19-Jan-22	6	na	Off	Off	On	Off	On	Off	na	na	On	Off	On	On	Off
20-Jan-22	6	na	Off	On	Off	On	Off	Off	na	na	On	Off	On	Off	On
21-Jan-22	6		Off	On	On	Off	Off	On			On	On	Off	Off	Off
	6	na			Off		Off	Off	na	na				Off	Off
22-Jan-22		na	On Off	On Off	On	On Off		On	na	na	On On	On Off	On Off	Off	
23-Jan-22	6	na					On Off		na	na	On				On
24-Jan-22	6	na	Off	Off	On Off	On On	Off	Off	na	na	On Off	On	Off	Off	On Off
25-Jan-22	6	na	Off	On	Off	On	On Off	Off	na	na	Off	On	On	On Off	Off
26-Jan-22	6	na	Off	Off	On	On	Off	Off	na	na	Off	On	On	Off	On
27-Jan-22	6	na	Off	Off	On	On	On	On	na	na	On	On	Off	Off	Off
28-Jan-22	6	na	On	Off	Off	Off	On	On	na	na	Off	On	Off	Off	On

-	28-day							Turbine	9						
Date	28-aay Cycle	G29	G34	G35	G44	G45	G48	G49	G51	G56	G58	G59	G64	G67	G75
29-Jan-22	6	na	On	On	Off	Off	On	On	na	na	Off	Off	On	On	Off
30-Jan-22	6	na	Off	Off	On	On	On	Off	na	na	On	Off	Off	On	On
31-Jan-22	6	na	Off	On	On	Off	Off	Off	na	na	On	Off	Off	On	On
01-Feb-22	6	na	Off	On	Off	On	On	Off	na	na	On	Off	Off	On	On
02-Feb-22	6	na	On	Off	Off	On	Off	On	na	na	Off	On	On	Off	Off
03-Feb-22	6	na	On	On	Off	Off	On	On	na	na	Off	On	Off	Off	On
04-Feb-22	6	na	On	Off	On	Off	Off	On	na	na	On	On	Off	Off	Off
05-Feb-22	6	na	On	On	On	Off	Off	Off	na	na	On	Off	Off	On	On
06-Feb-22	6	na	On	On	Off	Off	Off	On	na	na	On	Off	On	Off	Off
07-Feb-22	6	na	Off	On	On	On	Off	On	na	na	On	Off	On	Off	Off
08-Feb-22	6	na	On	Off	On	On	Off	On	na	na	Off	Off	Off	On	On
09-Feb-22	6	na	Off	On	On	Off	On	Off	na	na	On	Off	Off	On	On
10-Feb-22	6	na	Off	On	On	On	Off	Off	na	na	Off	On	On	On	Off
11-Feb-22	6	na	On	On	Off	On	Off	Off	na	na	On	On	On	Off	Off
12-Feb-22	6	na	On	Off	On	Off	Off	Off	na	na	Off	On	On	Off	On
13-Feb-22	6	na	On	Off	Off	On	Off	On	na	na	On	Off	Off	On	Off
14-Feb-22	6		Off	Off	Off	On	On	Off			On	Off	Off	On	On
14-Feb-22 15-Feb-22	6	na	Off	On	Off	On		Off	na	na	On	Off	On	Off	On
	7	na		Off		Off	On Off		na	na	Off		Off		Off
16-Feb-22		na	On Off		On			On	na	na		On		On	
17-Feb-22	7	na	Off	On	Off	Off	On	On	na	na	Off	On	Off	On	Off
18-Feb-22	7	na	On	Off	On	Off	Off	On	na	na	On	On	On	On	Off
19-Feb-22	7	na	On	On	Off	On	Off	Off	na	na	On	Off	Off	Off	Off
20-Feb-22	7	na	Off	Off	On	Off	On	Off	na	na	Off	On	On	On	On
21-Feb-22	7	na	Off	Off	On	On	Off	On	na	na	Off	On	Off	Off	On
22-Feb-22	7	na	Off	Off	On	On	Off	On	na	na	On	Off	On	Off	Off
23-Feb-22	7	na	On	On	Off	On	On	Off	na	na	Off	On	On	Off	On
24-Feb-22	7	na	On	Off	Off	On	Off	Off	na	na	On	Off	Off	Off	On
25-Feb-22	7	na	Off	On	On	Off	Off	On	na	na	Off	Off	On	Off	On
26-Feb-22	7	na	Off	Off	Off	On	Off	On	na	na	Off	Off	On	On	On
27-Feb-22	7	na	On	On	Off	On	Off	On	na	na	Off	On	Off	On	On
28-Feb-22	7	na	On	On	Off	Off	Off	On	na	na	On	On	Off	Off	On
01-Mar-22	7	na	On	On	Off	Off	On	On	na	na	Off	Off	Off	Off	On
02-Mar-22	7	na	Off	Off	Off	Off	On	On	na	na	On	On	On	Off	On
03-Mar-22	7	na	On	On	Off	Off	On	On	na	na	Off	On	On	Off	On
04-Mar-22	7	na	On	Off	On	Off	On	Off	na	na	On	On	On	On	Off
05-Mar-22	7	na	On	Off	On	On	Off	Off	na	na	Off	Off	On	Off	On
06-Mar-22	7	na	Off	On	On	Off	On	Off	na	na	Off	On	Off	Off	On
07-Mar-22	7	na	On	On	On	On	Off	Off	na	na	Off	Off	On	Off	On
08-Mar-22	7	na	On	On	Off	Off	Off	On	na	na	On	Off	Off	On	On
09-Mar-22	7	na	On	Off	On	Off	On	Off	na	na	Off	Off	Off	On	On
10-Mar-22	7	na	Off	On	Off	On	On	Off	na	na	On	Off	Off	On	On
11-Mar-22	7	na	Off	Off	Off	On	On	On	na	na	Off	Off	Off	On	Off
12-Mar-22	7	na	Off	On	On	Off	Off	On	na	na	On	Off	On	Off	Off
13-Mar-22	7	na	Off	On	Off	On	Off	On	na	na	Off	On	On	On	Off
14-Mar-22	, 7	na	Off	Off	Off	On	On	Off	na	na	On	On	Off	On	Off
15-Mar-22	7	na	Off	On	On	On	On	Off	na	na	Off	Off	Off	On	On
16-Mar-22	8	na	Off	Off	On	Off	Off	On	na	na	On	On	On	Off	Off
17-Mar-22	8	na	On	Off	On	Off	On	Off	na	na	On	Off	Off	On	On
17-Mar-22	8	na	On	On	Off	On	Off	Off	na	na	Off	On	On	Off	On
19-Mar-22	8		Off	Off	On	Off	On	On			Off	On	Off	On	Off
20-Mar-22	8	na	Off	Off	On		Off	On	na	na				Off	
		na				On Off			na	na	Off	On	On		On
21-Mar-22	8	na	On	Off	Off	Off	On	On	na	na	Off	On	Off	Off	On

-	28-day							Turbine	9						
Date	Cycle	G29	G34	G35	G44	G45	G48	G49	G51	G56	G58	G59	G64	G67	G75
22-Mar-22	8	na	Off	On	On	Off	On	Off	na	na	Off	On	On	Off	On
23-Mar-22	8	na	On	On	Off	Off	On	On	na	na	Off	Off	Off	On	On
24-Mar-22	8	na	On	Off	Off	On	Off	Off	na	na	On	Off	On	Off	On
25-Mar-22	8	na	On	Off	On	On	Off	On	na	na	Off	Off	On	On	On
26-Mar-22	8	na	Off	On	Off	Off	On	On	na	na	Off	Off	On	Off	On
27-Mar-22	8	na	Off	Off	On	On	On	Off	na	na	Off	On	Off	Off	Off
28-Mar-22	8	na	Off	Off	Off	On	On	Off	na	na	Off	On	Off	On	On
29-Mar-22	8	na	Off	On	Off	On	On	Off	na	na	On	Off	On	Off	Off
30-Mar-22	8	na	On	Off	On	On	Off	Off	na	na	On	Off	On	On	Off
31-Mar-22	8	na	On	On	Off	On	Off	Off	na	na	On	On	On	Off	Off
01-Apr-22	8	na	On	Off	Off	Off	On	On	na	na	Off	On	On	Off	On
02-Apr-22	8	na	Off	Off	On	On	On	On	na	na	On	Off	Off	On	On
03-Apr-22	8	na	Off	On	Off	Off	Off	On	na	na	On	On	On	On	Off
04-Apr-22	8	na	Off	On	Off	On	Off	On	na	na	On	On	Off	Off	Off
05-Apr-22	8	na	On	Off	On	Off	On	Off	na	na	On	Off	On	Off	Off
06-Apr-22	8	na	Off	Off	Off	On	On	On	na	na	Off	Off	Off	On	On
07-Apr-22	8		On	Off	Off	Off	On	Off	na		Off	On	Off	On	On
07-Apr-22 08-Apr-22	8	na	On	Off	Off	On	On	On	na	na	Off	On	Off	On	On
		na	Off		Off			Off		na	Off		Off		
09-Apr-22	8	na		Off		On	On		na	na		On Off		On	On Off
10-Apr-22	8	na	Off	Off	Off	On	On	On	na	na	On	Off	Off	Off	Off
11-Apr-22	8	na	Off	Off	On	Off	Off	On	na	na	On	Off	On	Off	On
12-Apr-22	8	na	On	Off	On	Off	On	On	na	na	Off	On	Off	On	Off
13-Apr-22	9	na	Off	On	On	Off	On	Off	na	na	On	On	Off	Off	On
14-Apr-22	9	na	On	On	Off	Off	On	On	na	na	Off	Off	On	On	On
15-Apr-22	9	na	Off	On	Off	On	Off	Off	na	na	Off	On	On	On	Off
16-Apr-22	9	na	Off	On	Off	On	On	Off	na	na	On	Off	On	On	Off
17-Apr-22	9	na	On	Off	On	On	Off	Off	na	na	On	Off	On	On	Off
18-Apr-22	9	na	Off	Off	On	Off	On	On	na	na	On	Off	Off	Off	On
19-Apr-22	9	na	On	On	On	Off	Off	Off	na	na	On	Off	On	Off	On
20-Apr-22	9	na	On	On	Off	Off	On	On	na	na	Off	Off	On	Off	On
21-Apr-22	9	na	Off	Off	Off	Off	On	On	na	na	Off	Off	On	On	On
22-Apr-22	9	na	On	Off	On	Off	On	On	na	na	Off	On	Off	Off	On
23-Apr-22	9	na	Off	On	Off	Off	On	On	na	na	On	On	Off	On	Off
24-Apr-22	9	na	Off	Off	Off	On	On	On	na	na	Off	Off	Off	On	Off
25-Apr-22	9	na	On	On	Off	Off	Off	Off	na	na	On	Off	Off	On	Off
26-Apr-22	9	na	Off	On	Off	On	On	Off	na	na	On	Off	On	On	Off
27-Apr-22	9	na	On	On	Off	Off	On	Off	na	na	On	Off	Off	On	On
28-Apr-22	9	na	Off	Off	On	On	On	Off	na	na	On	On	Off	Off	On
29-Apr-22	9	na	On	Off	On	Off	On	Off	na	na	Off	Off	On	Off	On
30-Apr-22	9	na	Off	Off	On	On	Off	On	na	na	Off	On	On	Off	Off
01-May-22	9	na	Off	Off	Off	On	Off	On	na	na	On	Off	Off	On	On
02-May-22	9	na	On	On	On	Off	On	Off	na	na	On	Off	Off	Off	Off
03-May-22	9	na	On	Off	On	Off	Off	Off	na	na	On	On	Off	On	On
04-May-22	9	na	Off	On	On	Off	Off	On	na	na	On	Off	Off	Off	On
05-May-22	9	na	On	Off	Off	On	Off	On	na	na	On	On	On	Off	Off
06-May-22	9	na	On	Off	On	Off	On	Off	na	na	On	On	Off	Off	Off
07-May-22	9	na	On	Off	Off	On	Off	On	na	na	On	On	Off	On	On
08-May-22	9	na	Off	On	Off	On	Off	On	na	na	On	Off	Off	Off	Off
09-May-22	9	na	Off	On	Off	Off	On	On	na	na	Off	Off	On	On	On
10-May-22	9	na	On	On	On	Off	On	Off	na	na	Off	On	Off	Off	Off
10-May-22 11-May-22	10		Off	Off	Off	On	On	Off	na		On	Off	On	Off	On
		na								na					
12-May-22	10	na	Off	On	On	Off	Off	On	na	na	On	Off	On	Off	Off

								Turbine							
Date	28-day Cycle	G29	G34	G35	G44	G45	G48	G49	G51	G56	G58	G59	G64	G67	G75
13-May-22	10	na	Off	Off	On	Off	On	Off	na	na	Off	On	Off	On	On
14-May-22	10	na	Off	Off	On	On	On	On	na	na	On	On	On	Off	Off
15-May-22	10	na	On	On	On	Off	Off	Off	na	na	On	Off	On	On	On
16-May-22	10	na	On	Off	On	On	Off	On	na	na	On	On	Off	Off	Off
17-May-22	10	na	Off	Off	Off	On	On	On	na	na	On	Off	Off	On	Off
18-May-22	10	na	Off	On	Off	Off	On	On	na	na	Off	On	Off	On	Off
19-May-22	10	na	Off	Off	On	On	On	Off	na	na	Off	On	On	Off	On
20-May-22	10	na	On	On	On	Off	On	Off	na	na	Off	On	Off	Off	Off
21-May-22	10	na	On	On	Off	Off	Off	Off	na	na	Off	Off	Off	On	On
22-May-22	10	na	On	Off	On	Off	On	On	na	na	On	On	On	Off	Off
23-May-22	10	na	On	Off	Off	Off	Off	On	na	na	On	On	On	On	Off
24-May-22	10	na	Off	Off	On	On	On	Off	na	na	Off	Off	Off	On	Off
25-May-22	10	na	Off	On	Off	Off	On	Off	na	na	On	Off	Off	Off	On
26-May-22	10	na	Off	On	On	Off	On	Off	na	na	On	Off	Off	Off	On
27-May-22	10	na	On	Off	Off	Off	On	On	na	na	Off	Off	On	Off	On
28-May-22	10	na	On	Off	Off	On	Off	On	na	na	On	On	Off	Off	Off
29-May-22	10	na	Off	Off	Off	On	On	On	na	na	On	On	On	Off	Off
30-May-22	10	na	On	On	Off	On	Off	On	na	na	On	Off	Off	On	Off
31-May-22	10	na	On	Off	Off	On	On	Off	na	na	On	Off	On	Off	On
01-Jun-22	10	na	Off	On	On	Off	Off	On	na	na	On	On	On	Off	Off
02-Jun-22	10	na	On	Off	On	Off	On	Off	na	na	Off	On	On	Off	On
03-Jun-22	10	na	On	Off	On	Off	Off	On	na	na	Off	Off	Off	Off	On
04-Jun-22	10	na	On	Off	On	Off	Off	On	na	na	On	Off	Off	On	On
05-Jun-22	10	na	On	On	On	Off	Off	Off	na	na	Off	Off	Off	On	On
06-Jun-22	10	na	On	Off	Off	On	On	Off	na	na	Off	Off	On	Off	On
07-Jun-22	10	na	Off	On	On	On	Off	Off	na	na	On	Off	Off	Off	On
08-Jun-22	11	na	Off	On	On	Off	Off	Off	na	na	On	On	On	Off	Off
09-Jun-22	11	na	Off	On	Off	On	On	Off	na	na	Off	Off	On	On	Off
10-Jun-22	11	na	Off	On	Off	Off	Off	On	na	na	Off	On	Off	On	On
11-Jun-22	11	na	Off	On	On	On	Off	Off	na	na	On	On	On	Off	Off
12-Jun-22	11	na	Off	Off	Off	On	On	On	na	na	On	On	Off	Off	On
13-Jun-22	11	na	Off	On	On	On	Off	On	na	na	Off	Off	On	Off	On
14-Jun-22	11	na	On	On	Off	Off	Off	On	na	na	Off	Off	Off	On	On
14-Jun-22	11	na	Off	Off	On	On	Off	On	na	na	On	On	Off	Off	Off
16-Jun-22	11	na	On	On	Off	Off	Off	Off	na	na	On	Off	Off	On	On
17-Jun-22	11	na	On	On	Off	On	Off	On	na	na	On	On	Off	On	Off
17-Jun-22	11	na	Off	Off	On	Off	Off	On	na	na	On	Off	On	On	Off
19-Jun-22	11	na	Off	Off	On	On	On	Off	na	na	On	Off	On	Off	Off
20-Jun-22	11	na	Off	Off	On	On	Off	On	na	na	On	Off	Off	On	Off
21-Jun-22	11	na	On	Off	On	On	Off	Off	na	na	On	On	Off	On	Off
22-Jun-22	11		Off	On	Off	Off	On	Off			On	On	Off	On	Off
		na							na	na					
23-Jun-22	11	na	On	Off	Off	On Off	Off	On	na	na	On Off	Off	On	Off	On
24-Jun-22	11	na	Off	Off	On	Off	Off	On	na	na	Off	Off	On Off	On O#	Off
25-Jun-22	11	na	On	Off	On	Off	Off	On Off	na	na	Off	Off	Off	Off	On
26-Jun-22	11	na	Off	On	On	On	Off	Off	na	na	On Off	Off	Off	On O#	Off
27-Jun-22	11	na	Off	On	On	Off	On	On	na	na	Off	On	Off	Off	On
28-Jun-22	11	na	Off	Off	Off	On	On	Off	na	na	Off	On	On	On	Off
29-Jun-22	11	na	On	On	On	Off	Off	On	na	na	Off	Off	Off	On	On
30-Jun-22	11	na	On	Off	Off	On	On	Off	na	na	On	On	Off	Off	On
01-Jul-22	11	na	On	Off	Off	Off	On	On	na	na	Off	Off	On	Off	On
02-Jul-22	11	na	On	Off	Off	On	Off	Off	na	na	Off	On	On	On	Off
03-Jul-22	11	na	On	On	On	On	Off	Off	na	na	Off	Off	On	On	Off

	28-day							Turbine	<del></del>						
Date	28-aay Cycle	G29	G34	G35	G44	G45	G48	G49	G51	G56	G58	G59	G64	G67	G75
04-Jul-22	11	na	Off	Off	On	On	Off	On	na	na	Off	Off	On	Off	On
05-Jul-22	11	na	On	On	Off	Off	On	Off	na	na	On	Off	On	On	Off
06-Jul-22	12	na	On	Off	On	On	Off	Off	na	na	On	Off	On	Off	Off
07-Jul-22	12	na	On	On	On	Off	On	Off	na	na	Off	Off	Off	On	Off
08-Jul-22	12	na	Off	On	Off	On	Off	Off	na	na	On	On	Off	Off	Off
09-Jul-22	12	na	On	On	Off	Off	On	On	na	na	Off	On	Off	Off	On
10-Jul-22	12	na	Off	Off	Off	Off	On	On	na	na	On	On	On	Off	Off
11-Jul-22	12	na	On	On	On	Off	On	Off	na	na	Off	On	Off	Off	Off
12-Jul-22	12	na	Off	On	Off	Off	On	Off	na	na	On	On	Off	On	Off
13-Jul-22	12	na	On	Off	On	On	Off	On	na	na	On	Off	Off	Off	On
14-Jul-22	12	na	Off	On	On	Off	Off	On	na	na	On	Off	On	On	Off
15-Jul-22	12	na	On	Off	On	On	Off	Off	na	na	Off	Off	On	Off	On
16-Jul-22	12	na	Off	Off	On	On	On	Off	na	na	On	On	Off	On	Off
17-Jul-22	12	na	Off	Off	On	Off	On	On	na	na	On	On	Off	Off	On
18-Jul-22	12	na	Off	Off	On	Off	On	On	na	na	Off	On	Off	Off	On
19-Jul-22	12	na	On	Off	Off	On	Off	On	na	na	On	On	Off	On	Off
20-Jul-22	12	na	On	Off	On	Off	On	Off	na	na	On	On	Off	Off	On
21-Jul-22	12	na	On	On	On	Off	Off	Off	na	na	Off	On	Off	Off	On
22-Jul-22	12	na	Off	Off	Off	On	On	Off	na	na	Off	On	Off	Off	On
23-Jul-22	12	na	Off	On	Off	On	On	On	na	na	Off	Off	Off	On	On
24-Jul-22	12	na	Off	Off	On	Off	On	Off	na	na	Off	On	On	On	On
25-Jul-22	12	na	On	Off	Off	On	On	Off	na	na	On	On	Off	Off	Off
26-Jul-22	12	na	On	Off	Off	Off	On	On	na	na	On	Off	On	Off	On
27-Jul-22	12	na	Off	On	On	On	Off	Off	na	na	Off	On	Off	On	On
28-Jul-22	12	na	On	Off	On	On	Off	Off	na	na	Off	On	Off	On	Off
29-Jul-22	12	na	On	Off	On	On	On	Off	na	na	On	Off	Off	Off	On
30-Jul-22	12	na	On	Off	Off	Off	On	Off	na	na	Off	Off	Off	On	On
31-Jul-22	12	na	Off	Off	On	On	On	Off	na	na	Off	On	Off	On	Off
01-Aug-22	12	na	Off	Off	Off	On	On	On	na	na	Off	On	On	On	Off
02-Aug-22	12	na	On	On	On	Off	On	Off	na	na	Off	On	On	On	Off
03-Aug-22	13	na	On	Off	On	On	Off	Off	na	na	On	On	Off	Off	Off
04-Aug-22	13	na	Off	Off	On	On	Off	On	na	na	Off	Off	Off	On	Off
05-Aug-22	13	na	Off	Off	Off	On	On	Off	na	na	On	Off	On	On	Off
06-Aug-22	13	na	Off	Off	On	On	On	On	na	na	Off	Off	On	On	Off
07-Aug-22	13	na	Off	Off	On	On	On	Off	na	na	On	On	Off	Off	Off
08-Aug-22	13	na	On	On	Off	On	Off	On	na	na	On	Off	Off	On	On
09-Aug-22	13	na	Off	On	Off	Off	On	Off	na	na	Off	On	On	On	Off
10-Aug-22	13	na	Off	On	Off	On	On	Off	na	na	Off	Off	Off	On	On
11-Aug-22	13	na	Off	On	On	Off	Off	Off	na	na	Off	On	Off	Off	On
12-Aug-22	13	na	On	On	Off	Off	On	Off	na	na	On	On	On	Off	Off
12-Aug-22 13-Aug-22	13	na	Off	Off	On	On	On	Off	na		On	Off	Off	On	Off
										na					
14-Aug-22	13	na	On	On Off	On	Off	Off	Off	na	na	Off	On	On	Off	On
15-Aug-22	13	na	Off	Off	On	Off	On	Off	na	na	On	On	On	Off	On
16-Aug-22	13	na	Off	On Off	Off	On	On	Off	na	na	Off	On	Off	On	On
17-Aug-22	13	na	Off	Off	Off	On	Off	On	na	na	On	Off	Off	On	On
18-Aug-22	13	na	On	Off	On	Off	On	Off	na	na	Off	On Off	Off	On	On
19-Aug-22	13	na	On	Off	On	Off	On	Off	na	na	Off	Off	On	On	Off
20-Aug-22	13	na	Off	On	Off	On	On	Off	na	na	On	On	Off	Off	On
21-Aug-22	13	na	Off	Off	Off	Off	On	On	na	na	On	On	On	On	Off
22-Aug-22	13	na	Off	Off	Off	On	On	On	na	na	On	On	Off	On	Off
23-Aug-22	13	na	On	On	Off	Off	Off	Off	na	na	On	On	Off	On	Off
24-Aug-22	13	na	Off	Off	On	On	On	On	na	na	Off	On	Off	Off	On

-	28-day							Turbine	<del>)</del>						
Date	28-aay Cycle	G29	G34	G35	G44	G45	G48	G49	G51	G56	G58	G59	G64	G67	G75
25-Aug-22	13	na	On	Off	Off	Off	Off	On	na	na	On	Off	On	On	Off
26-Aug-22	13	na	Off	Off	On	On	Off	On	na	na	Off	On	On	Off	Off
27-Aug-22	13	na	Off	On	Off	Off	On	On	na	na	Off	Off	On	On	On
28-Aug-22	13	na	On	On	Off	On	Off	On	na	na	On	Off	On	Off	On
29-Aug-22	13	na	On	Off	On	Off	Off	Off	na	na	On	Off	Off	On	On
30-Aug-22	13	na	Off	On	On	On	On	Off	na	na	On	On	On	Off	Off
31-Aug-22	13	na	Off	On	On	Off	On	Off	na	na	On	Off	Off	Off	On
01-Sep-22	14	On	Off	On	Off	Off	On	Off	On	na	Off	On	Off	Off	On
02-Sep-22	14	Off	On	Off	On	Off	On	On	Off	na	On	Off	On	Off	Off
03-Sep-22	14	On	Off	Off	Off	On	On	Off	On	na	On	Off	On	Off	Off
04-Sep-22	14	Off	Off	Off	On	On	On	On	Off	na	On	Off	On	On	Off
05-Sep-22	14	Off	On	Off	Off	Off	On	On	Off	na	Off	On	Off	On	On
06-Sep-22	14	On	On	On	On	Off	Off	Off	On	na	Off	Off	Off	On	Off
07-Sep-22	14	Off	Off	On	Off	Off	On	On	On	na	Off	On	On	Off	Off
08-Sep-22	14	Off	On	On	Off	On	On	Off	On	na	Off	On	On	Off	Off
09-Sep-22	14	On	Off	Off	On	On	Off	Off	Off	na	Off	Off	On	On	On
10-Sep-22	14	On	On	Off	On	Off	Off	On	Off	na	Off	On	Off	On	On
11-Sep-22	14	On	Off	Off	Off	Off	On	On	On	na	Off	On	Off	On	Off
12-Sep-22	14	Off	Off	On	Off	On	On	On	Off	na	On	Off	Off	On	Off
12-3ep-22 13-Sep-22	14	Off	On	Off	On	On	Off	Off	Off		Off	On	On	Off	On
-	14		Off			Off			On	na			Off		Off
14-Sep-22		On		Off	On		On	On		na	On	Off		On	
15-Sep-22	14	Off	Off	Off	On	On	Off	On	On	na	On	Off	On	Off	On
16-Sep-22	14	Off	Off	On	Off	On	On	On	Off	na	Off	On	Off	On	On
17-Sep-22	14	Off	Off	Off	On	On	Off	On	On	na	Off	On	Off	Off	On
18-Sep-22	14	Off	Off	On	Off	On	On	On	On	na	Off	Off	On	Off	Off
19-Sep-22	14	Off	On	On	Off	On	Off	Off	On	na	On	Off	Off	On	On
20-Sep-22	14	On	Off	On	Off	On	On	Off	On	na	Off	Off	Off	On	On
21-Sep-22	14	Off	On	On	On	Off	Off	Off	On	na	Off	On	On	On	Off
22-Sep-22	14	Off	Off	On	Off	On	On	On	Off	na	On	Off	Off	On	Off
23-Sep-22	14	Off	Off	On	Off	Off	On	On	Off	na	On	Off	On	On	Off
24-Sep-22	14	Off	On	Off	On	On	On	Off	Off	na	Off	On	On	Off	Off
25-Sep-22	14	On	Off	Off	On	Off	Off	On	On	na	On	Off	Off	On	Off
26-Sep-22	14	On	Off	On	Off	On	Off	On	Off	na	On	Off	On	Off	Off
27-Sep-22	14	On	On	Off	Off	Off	On	Off	Off	On	On	Off	On	On	Off
28-Sep-22	14	On	On	On	Off	On	Off	Off	Off	On	Off	Off	On	Off	On
29-Sep-22	15	Off	Off	On	Off	Off	On	On	On	Off	Off	On	On	On	Off
30-Sep-22	15	On	On	Off	On	Off	On	Off	On	On	Off	On	Off	Off	Off
01-Oct-22	15	Off	On	Off	Off	Off	On	On	Off	On	Off	On	Off	On	On
02-Oct-22	15	Off	On	On	Off	On	Off	On	Off	On	Off	Off	Off	On	On
03-Oct-22	15	Off	On	Off	Off	On	Off	On	On	Off	Off	On	On	Off	On
04-Oct-22	15	Off	Off	On	On	On	Off	On	Off	On	Off	Off	Off	On	On
05-Oct-22	15	Off	On	On	Off	Off	Off	On	On	Off	On	Off	On	Off	On
06-Oct-22	15	Off	On	Off	On	On	Off	On	Off	On	Off	Off	Off	On	On
07-Oct-22	15	On	Off	Off	On	Off	On	Off	On	On	On	Off	On	Off	Off
08-Oct-22	15	On	Off	Off	On	On	Off	On	On	Off	On	On	Off	Off	Off
09-Oct-22	15	On	Off	On	On	Off	Off	Off	On	Off	On	Off	On	Off	On
10-Oct-22	15	Off	Off	On	Off	On	On	On	Off	On	Off	On	Off	On	Off
11-Oct-22	15	On	Off	Off	Off	On	On	Off	On	Off	On	Off	On	Off	On
12-Oct-22	15	On	Off	Off	On	On	Off	On	Off	Off	Off	On	Off	On	On
13-Oct-22	15	Off	Off	Off	On	On	On	Off	On	On	Off	On	Off	Off	On
14-Oct-22	15	On	Off	Off	Off	On	On	On	Off	On	Off	Off	On	On	Off
15-Oct-22	15	On	Off	Off	Off	On	Off	On	On	On	Off	Off	On	Off	On
10 001 22	10		011	<b>J</b> 11	011	011		<b>0</b> 11	011	<b>O</b> 11	011	011	011	011	011

-	28-day							Turbine	9						
Date	28-day Cycle	G29	G34	G35	G44	G45	G48	G49	G51	G56	G58	G59	G64	G67	G75
16-Oct-22	15	On	On	On	Off	On	Off	Off	On	Off	Off	On	On	Off	Off
17-Oct-22	15	Off	On	Off	On	Off	On	Off	On	Off	On	On	Off	Off	On
18-Oct-22	15	On	On	Off	Off	On	Off	On	Off	On	Off	On	Off	On	Off
19-Oct-22	15	Off	On	Off	On	Off	Off	On	On	On	Off	On	Off	Off	On
20-Oct-22	15	On	On	Off	On	Off	Off	On	Off	Off	Off	On	Off	On	On
21-Oct-22	15	On	Off	Off	Off	Off	On	On	On	On	On	Off	Off	On	Off
22-Oct-22	15	On	On	Off	Off	On	Off	On	On	Off	Off	On	Off	On	Off
23-Oct-22	15	On	Off	Off	Off	On	On	Off	On	Off	Off	Off	On	On	On
24-Oct-22	15	On	On	On	Off	On	Off	Off	Off	Off	On	Off	Off	On	On
25-Oct-22	15	On	Off	Off	On	Off	On	Off	Off	On	Off	On	On	Off	On
26-Oct-22	15	Off	On	Off	Off	On	On	On	Off	On	Off	Off	Off	On	On
27-Oct-22	16	Off	Off	On	On	On	Off	Off	Off	On	Off	On	On	On	Off
28-Oct-22	16	On	Off	On	Off	On	Off	On	On	On	Off	Off	Off	On	Off
29-Oct-22	16	On	Off	Off	Off	Off	On	On	On	Off	On	On	Off	On	Off
30-Oct-22	16	On	On	Off	Off	On	Off	On	Off	On	On	Off	Off	Off	On
31-Oct-22	16	On	On	On	Off	Off	Off	Off	Off	On	Off	On	On	Off	On
		Off				Off		Off	Off			Off	Off		
01-Nov-22	16 16		On Off	On Off	On Off		On Off			Off	On Off			On Off	On Off
02-Nov-22		On				On		On Off	On	On Off		On	On		
03-Nov-22	16	On	Off	Off	On	On	On	Off	Off	Off	Off	On	On	On	Off
04-Nov-22	16	Off	On	On	Off	On	Off	Off	On	On	Off	On	Off	On	Off
05-Nov-22	16	On	Off	On	Off	Off	On	On	Off	On	Off	Off	On	On	Off
06-Nov-22	16	On	On	Off	Off	Off	Off	On	Off	Off	On	On	On	Off	On
07-Nov-22	16	Off	Off	On	On	On	Off	On	Off	On	On	Off	Off	On	Off
08-Nov-22	16	On	Off	Off	On	Off	Off	On	On	On	Off	Off	On	Off	On
09-Nov-22	16	On	Off	On	On	Off	On	Off	Off	On	On	Off	Off	Off	On
10-Nov-22	16	On	Off	On	Off	Off	Off	On	On	On	Off	On	Off	Off	On
11-Nov-22	16	On	On	On	On	Off	Off	Off	On	Off	Off	On	Off	On	Off
12-Nov-22	16	Off	Off	Off	Off	On	On	On	On	Off	Off	On	Off	On	On
13-Nov-22	16	Off	On	On	On	Off	Off	On	On	Off	Off	On	Off	On	Off
14-Nov-22	16	Off	On	On	Off	Off	Off	On	Off	Off	On	On	Off	On	On
15-Nov-22	16	Off	On	Off	Off	On	On	On	Off	On	On	Off	On	Off	Off
16-Nov-22	16	Off	On	Off	Off	On	Off	On	On	Off	On	Off	Off	On	On
17-Nov-22	16	Off	On	On	Off	Off	On	On	On	On	Off	On	Off	Off	Off
18-Nov-22	16	Off	On	On	Off	Off	Off	On	Off	Off	On	On	Off	On	On
19-Nov-22	16	On	Off	On	On	Off	Off	On	On	Off	Off	On	Off	Off	On
20-Nov-22	16	On	Off	On	Off	On	Off	Off	On	Off	On	Off	On	Off	On
21-Nov-22	16	On	On	Off	On	Off	Off	On	Off	On	On	Off	On	Off	Off
22-Nov-22	16	Off	On	Off	On	Off	Off	On	Off	Off	On	On	On	On	Off
23-Nov-22	16	Off	On	On	Off	On	Off	On	Off	Off	On	Off	On	On	Off
24-Nov-22	17	Off	On	Off	Off	Off	On	On	Off	On	Off	On	On	On	Off
25-Nov-22	17	On	On	On	Off	On	Off	Off	Off	On	Off	Off	Off	On	On
26-Nov-22	17	Off	On	On	Off	On	Off	Off	Off	On	On	Off	Off	On	On
27-Nov-22	17	On	On	Off	On	Off	Off	On	On	On	Off	On	Off	Off	Off
28-Nov-22	17	On	Off	Off	On	On	Off	Off	Off	Off	On	On	On	Off	On
29-Nov-22	17	Off	Off	On	On	Off	On	On	On	Off	Off	On	On	Off	Off
30-Nov-22	17	On	Off	Off	On	Off	Off	On	Off	On	Off	Off	On	On	On
01-Dec-22	17	Off	Off	On	On	On	On	Off	Off	On	On	On	Off	Off	Off
01-Dec-22 02-Dec-22	17	On	On	Off	Off	Off	On	Off	Off	Off	On	On	On	On	Off
03-Dec-22	17	On	On	Off	Off	On	Off	On	Off	Off	Off	On	Off	On	On
04-Dec-22	17	Off	Off	On On	Off	On Off	On	Off	Off	On Off	Off	On Off	On	On	Off
05-Dec-22	17	On	Off	On	Off	Off	On	On	Off	Off	Off	Off	On	On Off	On
06-Dec-22	17	Off	Off	Off	Off	On	On	On	On	On	Off	On	On	Off	Off

	28-day							Turbine	<b></b>						
Date	Cycle	G29	G34	G35	G44	G45	G48	G49	G51	G56	G58	G59	G64	G67	G75
07-Dec-22	17	On	Off	Off	Off	On	On	On	On	Off	Off	Off	Off	On	On
08-Dec-22	17	Off	Off	On	Off	On	Off	On	On	Off	Off	Off	On	On	On
09-Dec-22	17	Off	On	On	Off	On	Off	On	On	On	Off	Off	On	Off	Off
10-Dec-22	17	Off	Off	On	On	Off	Off	On	Off	On	Off	Off	On	On	On
11-Dec-22	17	Off	On	Off	On	On	On	Off	Off	On	On	On	Off	Off	Off
12-Dec-22	17	On	On	Off	Off	Off	Off	On	On	Off	On	Off	Off	On	On
13-Dec-22	17	Off	On	On	On	Off	Off	On	Off	Off	On	Off	On	On	Off
14-Dec-22	17	Off	Off	On	Off	On	Off	On	On	Off	On	Off	On	Off	On
15-Dec-22	17	Off	On	Off	On	Off	On	On	Off	On	On	On	Off	Off	Off
16-Dec-22	17	On	Off	Off	Off	On	Off	On	On	Off	Off	Off	On	On	On
17-Dec-22	17	Off	Off	On	On	On	On	Off	Off	On	Off	Off	Off	On	On
18-Dec-22	17	On	On	On	Off	Off	Off	Off	On	Off	On	On	On	Off	Off
19-Dec-22	17	Off	On	Off	On	On	Off	On	On	On	Off	On	Off	Off	Off
20-Dec-22	17	On	Off	On	Off	Off	On	Off	Off	Off	Off	On	On	On	On
21-Dec-22	17	On	Off	On	On	On	Off	Off	On	On	On	Off	Off	Off	Off
22-Dec-22	18	On	Off	Off	Off	On	On	Off	On	Off	Off	On	Off	On	On
23-Dec-22	18	On	Off	On	On	Off	Off	On	Off	Off	Off	On	On	On	Off
24-Dec-22	18	On	Off	On	Off	On	Off	Off	Off	Off	On	On	On	Off	On
25-Dec-22	18	On	On	On	Off	Off	On	Off	Off	On	On	Off	Off	Off	On
26-Dec-22	18	On	Off	Off	On	Off	Off	On	On	On	Off	Off	Off	On	On
27-Dec-22	18	Off	On	Off	Off	On	On	On	Off	On	On	Off	Off	On	Off
28-Dec-22	18	On	Off	On	Off	Off	Off	On	On	On	Off	Off	Off	On	On
29-Dec-22	18	On	On		On	Off	Off	Off	On	On	Off	Off	Off	On	Off
30-Dec-22	18	Off	Off	On Off			Off	On	Off	Off	Off	On	On	On	On
	18			Off	On Off	On			Off		Off				Off
31-Dec-22	18	On Off	Off			On	On Off	On Off	Off	On Off	Off	On	On	Off	
01-Jan-23	18		Off	On	On	On	Off	Off		Off	Off	On Off	On Off	On	On
02-Jan-23		On	On	Off	On	Off	On		Off	On				On	On
03-Jan-23	18	On	On	On	Off	Off	Off	Off	On	On	Off	On	Off	On	Off
04-Jan-23	18	Off	On	Off	On	Off	On	On Off	Off	Off	Off	Off	On	On	On
05-Jan-23	18	On	Off	Off	Off	On	On	Off	On	Off	On	Off	Off	On	On
06-Jan-23	18	On	Off	On	On	Off	Off	On	On	Off	Off	Off	On	Off	On
07-Jan-23	18	On	Off	Off	Off	On	Off	On	Off	Off	On	On	On	Off	On
08-Jan-23	18	On	Off	On	Off	On	Off	On	Off	Off	On	On	On	Off	Off
09-Jan-23	18	Off	Off	Off	On	On	On	Off	On	Off	On	Off	On	Off	On
10-Jan-23	18	On	On	Off	On	Off	Off	On	On	Off	On	Off	Off	Off	On
11-Jan-23	18	Off	On	Off	Off	Off	On	On	Off	On	On	On	Off	On	Off
12-Jan-23	18	Off	On	Off	On	Off	On	On	Off	Off	On	On	Off	Off	On
13-Jan-23	18	On	Off	Off	Off	Off	On	On	On	Off	Off	Off	On	On	On
14-Jan-23	18	On	On	Off	Off	On	On	Off	On	Off	Off	On	Off	On	Off
15-Jan-23	18	On	Off	Off	On	On	Off	Off	Off	On	On	Off	On	Off	On
16-Jan-23	18	Off	Off	Off	On	On	On	On	Off	Off	Off	On	On	Off	On
17-Jan-23	18	Off	Off	On	On	Off	On	Off	On	Off	Off	On	On	Off	On
18-Jan-23	18	On	Off	On	Off	Off	On	On	On	On	Off	Off	On	Off	Off
19-Jan-23	19	On	Off	Off	On	Off	On	Off	Off	On	Off	On	Off	On	On
20-Jan-23	19	Off	Off	On	On	On	On	Off	Off	On	Off	On	On	Off	Off
21-Jan-23	19	On	On	On	Off	Off	Off	Off	On	Off	On	Off	Off	On	On
22-Jan-23	19	On	Off	On	On	On	Off	Off	On	Off	On	On	Off	Off	Off
23-Jan-23	19	On	On	Off	On	Off	Off	Off	Off	Off	On	On	On	Off	On
24-Jan-23	19	On	On	Off	Off	On	On	Off	On	Off	Off	Off	On	Off	On
25-Jan-23	19	Off	On	Off	Off	On	Off	On	Off	On	On	Off	On	On	Off
26-Jan-23	19	On	Off	On	On	On	Off	Off	Off	Off	Off	On	Off	On	On
27-Jan-23	19	Off	Off	Off	Off	On	On	On	Off	Off	Off	On	On	On	On
20			٠		J	<b>-</b>		J	٠	J	٠	٠	~	٠	٠

	20 4							Turbine	•						
Date	28-day Cycle	G29	G34	G35	G44	G45	G48	G49	G51	G56	G58	G59	G64	G67	G75
28-Jan-23	19	Off	On	On	On	On	Off	Off	Off	Off	On	Off	On	Off	On
29-Jan-23	19	On	On	Off	Off	Off	On	Off	Off	On	On	On	Off	On	Off
30-Jan-23	19	Off	On	On	On	Off	Off	On	Off	On	On	On	Off	Off	Off
31-Jan-23	19	On	Off	On	Off	Off	Off	On	On	Off	On	On	Off	Off	On
01-Feb-23	19	Off	Off	Off	On	On	On	On	Off	Off	Off	Off	On	On	On
02-Feb-23	19	Off	Off	On	On	On	Off	Off	On	On	Off	Off	Off	On	On
03-Feb-23	19	Off	Off	On	On	Off	On	On	Off	On	Off	Off	Off	On	On
04-Feb-23	19	Off	Off	On	On	Off	Off	On	Off	On	On	Off	Off	On	On
05-Feb-23	19	On	On	Off	Off	On	Off	On	Off	On	Off	Off	On	Off	On
06-Feb-23	19	Off	Off	On	Off	On	Off	On	Off	On	On	On	Off	Off	On
07-Feb-23	19	Off	On	Off	Off	On	On	On	Off	On	On	Off	Off	On	Off
08-Feb-23	19	Off	On	On	Off	Off	Off	On	Off	Off	On	On	On	On	Off
09-Feb-23	19	Off	On	Off	On	On	Off	On	On	Off	On	Off	Off	Off	On
10-Feb-23	19	On	On	On	Off	Off	Off	Off	On	Off	On	On	Off	Off	On
11-Feb-23	19	Off	On	On	Off	On	Off	On	On	Off	Off	Off	On	Off	On
12-Feb-23	19	On	On	Off	Off	Off	Off	On	On	Off	On	On	On	Off	Off
13-Feb-23	19	On	Off	On	Off	Off	On	On	On	On	Off	Off	On	Off	Off
14-Feb-23	19	Off	On	Off	Off	Off	On	On	On	On	Off	On	Off	Off	On
15-Feb-23	19	Off	On	On	Off	On	On	Off	On	Off	Off	Off	On	On	Off
16-Feb-23	20	Off	On	On	Off	On	Off	Off	Off	Off	On	On	Off	On	On
17-Feb-23	20	On	On Off	Off	On	On	Off	Off	Off	Off	Off	On	On	On	Off
18-Feb-23	20	On	Off	On	Off	On	Off	Off	On	On	Off	On	Off	On	Off
19-Feb-23	20	On	Off	On	Off	On	On	Off	Off	On	Off	On	Off	On	Off
20-Feb-23	20	Off	Off	On	Off	On	Off	On	Off	Off	On	On	On	Off	On
21-Feb-23	20	Off	Off	On	On	Off	On	On	Off	On	On	Off	On	Off	Off
22-Feb-23	20	On	Off	On	Off	Off	Off	On	Off	On	Off	On	On	Off	On
23-Feb-23	20	Off	Off	Off	On	On	On	On	Off	On	Off	On	Off	On	Off
24-Feb-23	20	On	Off	Off	On	Off	Off	On	On	Off	On	Off	On	On	Off
25-Feb-23	20	Off	Off	On	On	On	Off	On	Off	Off	Off	On	Off	On	On
26-Feb-23	20	Off	Off	On	On	On	Off	Off	On	Off	Off	On	On	Off	On
27-Feb-23	20	On	On	On	Off	Off	Off	On	On	Off	Off	On	Off	On	Off
28-Feb-23	20	Off	On	Off	Off	Off	On	On	On	On	Off	Off	On	Off	On
01-Mar-23	20	On	Off	Off	On	On	Off	On	On	Off	On	On	Off	Off	Off
02-Mar-23	20	Off	On	On	Off	On	Off	Off	On	Off	Off	On	On	On	Off
03-Mar-23	20	Off	On	On	On	Off	On	Off	Off	Off	On	On	Off	On	Off
04-Mar-23	20	On	Off	On	Off	Off	On	Off	On	Off	On	Off	On	Off	On
05-Mar-23	20	On	Off	On	Off	Off	On	On	On	Off	Off	Off	Off	On	On
06-Mar-23	20	Off	Off	On	Off	On	Off	On	On	On	Off	On	Off	On	Off
07-Mar-23	20	On	On	Off	Off	Off	On	On	Off	Off	Off	On	On	Off	On
08-Mar-23	20	Off	On	Off	Off	On	On	Off	Off	On	On	On	On	Off	Off
09-Mar-23	20	On	On	On	Off	Off	On	Off	Off	Off	On	On	Off	Off	On
10-Mar-23	20	Off	Off	On	On	On	Off	Off	On	Off	On	Off	On	On	Off
11-Mar-23	20	On	Off	Off	On	On	On	Off	Off	Off	On	Off	Off	On	On
12-Mar-23	20	Off	Off	Off	On	On	On	Off	On	On	Off	On	Off	On	Off
13-Mar-23	20	On	Off	On	Off	On	On	Off	On	On	Off	Off	Off	Off	On
14-Mar-23	20	On	On	Off	Off	Off	On	Off	Off	Off	On	On	On	Off	On
15-Mar-23	20	Off	Off	On	On	On	Off	On	Off	On	Off	On	On	Off	Off
16-Mar-23	21	On	Off	Off	Off	On	Off	On	On	Off	Off	Off	On	On	On
17-Mar-23	21	Off	On	On	On	Off	On	Off	Off	Off	Off	Off	On	On	On
18-Mar-23	21	Off	Off	On	Off	Off	On	On	On	Off	Off	Off	On	On	On
19-Mar-23	21	On	On	Off	On	Off	Off	On	On	Off	On	Off	Off	Off	On
20-Mar-23	21	On	Off	On	Off	Off	On	Off	On	Off	On	On	On	Off	Off

	28-day							Turbine	9						
Date	Cycle	G29	G34	G35	G44	G45	G48	G49	G51	G56	G58	G59	G64	G67	G75
21-Mar-23	21	Off	On	Off	Off	On	On	On	Off	On	Off	Off	On	Off	On
22-Mar-23	21	On	Off	Off	Off	On	On	Off	On	On	Off	Off	Off	On	On
23-Mar-23	21	On	On	On	Off	Off	Off	On	Off	Off	Off	On	Off	On	On
24-Mar-23	21	Off	On	On	On	Off	Off	Off	On	On	Off	On	On	Off	Off
25-Mar-23	21	On	Off	On	On	Off	Off	On	Off	Off	Off	Off	On	On	On
26-Mar-23	21	On	On	Off	Off	Off	Off	On	On	On	Off	On	Off	On	Off
27-Mar-23	21	Off	Off	On	Off	On	On	On	On	Off	Off	On	Off	Off	On
28-Mar-23	21	Off	On	Off	Off	Off	On	On	Off	On	On	On	Off	Off	On
29-Mar-23	21	On	On	On	Off	Off	On	Off	On	Off	Off	Off	On	Off	On
30-Mar-23	21	Off	Off	On	Off	On	On	Off	On	Off	Off	Off	On	On	On
31-Mar-23	21	On	On	Off	Off	On	On	Off	Off	On	On	Off	Off	On	Off
01-Apr-23	21	On	Off	Off	On	Off	Off	On	On	Off	On	Off	On	Off	On
02-Apr-23	21	On	Off	On	On	Off	Off	On	On	Off	On	Off	On	Off	Off
03-Apr-23	21	Off	On	Off	On	Off	Off	On	Off	Off	On	On	On	Off	On
04-Apr-23	21	On	Off	Off	On	On	On	Off	Off	Off	On	Off	On	Off	On
05-Apr-23	21	Off	Off	On	Off	Off	On	On	Off	Off	On	On	On	Off	On
06-Apr-23	21	On	On	Off	On	Off	Off	On	On	On	Off	Off	Off	On	Off
07-Apr-23	21	On	On	Off	Off	Off	On	Off	On	Off	Off	On	On	Off	On
08-Apr-23	21	On	Off	On	On	On	Off	Off	On	Off	Off	Off	Off	On	On
09-Apr-23	21	On	Off	Off	On	Off	On	Off	On	Off	On	On	Off	On	Off
10-Apr-23	21	On	Off	On	Off	On	Off	On	Off	Off	Off	On	On	Off	On
11-Apr-23	21	On	Off	On	Off	Off	Off	On	On	On	Off	On	Off	Off	On
12-Apr-23	21	Off	On	On	Off	On	On	Off	Off	Off	Off	On	On	Off	On
•	22	Off	On	Off	Off	Off	On	On	Off	Off	On	On	Off	On	On
13-Apr-23	22			Off	Off			Off			Off	Off	Off		Off
14-Apr-23		On Off	On		Off	On	On	Off	On	On Off	Off			On Off	
15-Apr-23	22		On	Off		On	On Off	Off	On Off		Off	On	On Off	Off	On
16-Apr-23	22	On	On Off	Off	On	On				On Off		On			On
17-Apr-23	22	Off	Off	Off	On	On	On	Off	On	Off	Off	On	Off	On	On
18-Apr-23	22	On	On	Off	On	Off	Off	On	On	On	Off	Off	Off	On	Off
19-Apr-23	22	On	Off	Off	Off	On	Off	On	On	On	Off	Off	On	Off	On
20-Apr-23	22	Off	On	Off	Off	On	On	On	On	Off	On	Off	Off	Off	On
21-Apr-23	22	On	Off	On	Off	Off	Off	On	Off	Off	On	On	On	Off	On
22-Apr-23	22	On	Off	On	Off	On	On	Off	Off	Off	On	On	On	Off	Off
23-Apr-23	22	On	On	Off	Off	Off	Off	On	Off	On	Off	On	On	Off	On
24-Apr-23	22	On	On	Off	Off	On	Off	On	On	On	Off	Off	Off	Off	On
25-Apr-23	22	Off	On	Off	On	Off	On	Off	Off	Off	Off	On	On	On	On
26-Apr-23	22	On	On	Off	Off	Off	On	On	Off	On	Off	Off	On	On	Off
27-Apr-23	22	On	Off	On	Off	Off	On	Off	On	On	Off	On	On	Off	Off
28-Apr-23	22	On	On	Off	On	On	Off	Off	Off	Off	On	Off	On	Off	On
29-Apr-23	22	Off	On	Off	On	On	Off	Off	On	On	Off	On	On	Off	Off
30-Apr-23	22	Off	Off	Off	On	On	On	On	Off	Off	On	On	Off	Off	On
01-May-23	22	Off	Off	Off	On	Off	On	On	On	On	On	Off	Off	Off	On
02-May-23	22	On	On	Off	Off	On	Off	On	On	Off	On	On	Off	Off	Off
03-May-23	22	Off	Off	On	On	Off	On	Off	On	On	On	On	Off	Off	Off
04-May-23	22	Off	Off	On	On	On	Off	On	Off	Off	On	Off	On	Off	On
05-May-23	22	On	Off	On	Off	On	Off	Off	On	Off	On	Off	On	On	Off
06-May-23	22	Off	Off	On	On	On	On	Off	Off	Off	On	On	Off	Off	On
07-May-23	22	Off	On	On	Off	Off	On	Off	On	Off	On	On	Off	On	Off
08-May-23	22	On	On	Off	On	Off	Off	On	Off	Off	On	On	Off	On	Off
09-May-23	22	Off	Off	Off	On	On	On	Off	Off	Off	On	Off	On	On	On
10-May-23	22	On	On	On	On	Off	Off	Off	Off	On	On	Off	On	Off	Off
11-May-23	23	Off	On	Off	Off	On	Off	On	On	Off	On	Off	On	On	Off
,															

	28-day							Turbine	<del></del>						
Date	28-day Cycle	G29	G34	G35	G44	G45	G48	G49	G51	G56	G58	G59	G64	G67	G75
12-May-23	23	Off	On	On	Off	On	On	Off	On	On	Off	Off	Off	Off	On
13-May-23	23	Off	Off	Off	On	Off	On	On	On	On	Off	Off	Off	On	On
14-May-23	23	On	Off	On	Off	On	Off	On	On	Off	Off	Off	On	Off	On
15-May-23	23	On	Off	Off	On	On	Off	Off	On	On	Off	On	On	Off	Off
16-May-23	23	On	Off	On	Off	On	On	Off	Off	Off	On	Off	On	Off	On
17-May-23	23	On	On	On	Off	Off	Off	Off	On	On	Off	On	Off	On	Off
18-May-23	23	On	Off	On	On	Off	Off	On	On	On	Off	Off	On	Off	Off
19-May-23	23	On	Off	Off	On	Off	Off	On	Off	Off	Off	On	On	On	On
20-May-23	23	Off	On	On	On	Off	Off	On	Off	Off	Off	On	Off	On	On
21-May-23	23	Off	Off	On	Off	On	Off	On	On	On	Off	Off	On	Off	On
22-May-23	23	On	On	Off	Off	On	Off	On	On	Off	Off	On	Off	On	Off
23-May-23	23	Off	Off	On	Off	On	On	Off	Off	On	On	Off	On	On	Off
24-May-23	23	On	On	On	On	Off	Off	Off	Off	Off	Off	On	On	On	Off
25-May-23	23	Off	On	Off	On	Off	Off	On	On	Off	Off	On	On	On	Off
26-May-23	23	Off	Off	On	On	Off	On	On	Off	Off	On	Off	Off	On	On
27-May-23	23	Off	On	On	Off	Off	On	Off	On	On	On	Off	Off	On	Off
28-May-23	23	Off	On	On	On	Off	Off	On	Off	Off	On	Off	Off	On	On
29-May-23	23	Off	Off	Off	On	Off	On	On	Off	Off	On	On	On	On	Off
30-May-23	23	On	Off	Off	On	On	On	Off	On	Off	Off	Off	Off	On	On
31-May-23	23	Off	On	Off	Off	On	On	Off	On	On	Off	On	Off	On	Off
01-Jun-23	23	On	Off	On	Off	Off	On	On	On	Off	Off	Off	On	On	Off
02-Jun-23	23	Off	Off	On	On	Off	Off	On	On	Off	Off	Off	On	On	On
03-Jun-23	23	On	Off	On	Off	On	On	Off	Off	On	Off	Off	On	On	Off
04-Jun-23	23	On	On	Off	Off	On	Off	Off	On	On	On	Off	Off	On	Off
05-Jun-23	23	Off	Off	On	Off	On	On	On	Off	Off	On	On	On	Off	Off
06-Jun-23	23	Off	Off	On	On	Off	Off	On	On	On	On	Off	On	Off	Off
07-Jun-23	23	On	On	On	On	Off	Off	Off	Off	Off	Off	On	Off	On	On
08-Jun-23	24	On	Off	Off	On	On	Off	Off	On	On	Off	Off	On	On	Off
09-Jun-23	24	On	Off	On	On	Off	Off	On	Off	Off	Off	On	On	Off	On
10-Jun-23	24	On	On	Off	Off	On	Off	Off	On	Off	Off	On	On	Off	On
11-Jun-23	24	On	Off	On	Off	Off	On	On	Off	Off	On	On	Off	On	Off
12-Jun-23	24	Off	On	Off	On	On	Off	Off	Off	On	Off	On	On	On	Off
13-Jun-23	24	Off	On	On	On	On	Off	Off	Off	Off	Off	Off	On	On	On
14-Jun-23	24	On	Off	On	Off	Off	On	Off	Off	On	On	On	Off	On	Off
15-Jun-23	24	On	On	On	Off	Off	Off	On	On	On	On	Off	Off	Off	Off
16-Jun-23	24	On	On	Off	On	Off	Off	Off	Off	On	On	On	Off	On	Off
17-Jun-23	24	On	Off	On	Off	On	On	Off	Off	Off	Off	On	On	On	Off
18-Jun-23	24	On	On	Off	Off	On	Off	Off	Off	On	On	On	Off	Off	On
19-Jun-23	24	On	On	Off	Off	On	Off	On	On	Off	On	On	Off	Off	Off
20-Jun-23	24	Off	On	On	On	Off	Off	Off	On	Off	On	Off	On	Off	On
21-Jun-23	24	Off	On	On	Off	On	Off	On	Off	On	Off	On	Off	Off	On
21-Jun-23 22-Jun-23	24	On		Off	Off	Off		Off		Off	Off			Off	
23-Jun-23	24		On			Off	On	Off	On Off			On Off	On	Off	On Off
		On On	On	Off	On Off		On Off			On Off	On Off		On		Off
24-Jun-23	24	On On	On Off	On Off	Off	Off	Off	Off	Off	Off	Off	On On	On Off	On Off	On On
25-Jun-23	24	On On	Off	Off	Off	On	On Off	On	Off	On	Off	On	Off	Off	On
26-Jun-23	24	On	Off	Off	Off	On Off	Off	On	On	On Off	Off	On	Off	On Off	Off
27-Jun-23	24	Off	Off	On	On	Off	On	On	Off	Off	On	On Off	Off	Off	On
28-Jun-23	24	Off	On	Off	Off	Off	On	On	Off	On	On	Off	On	Off	On
29-Jun-23	24	On	On	Off	On	Off	Off	On	On	Off	On	Off	On	Off	Off
30-Jun-23	24	Off	On	On	Off	Off	Off	On	Off	On	On	Off	On	Off	On
01-Jul-23	24	On	Off	On	Off	Off	On	On	Off	Off	On	Off	On	Off	On
02-Jul-23	24	Off	On	Off	Off	Off	On	On	Off	Off	On	On	Off	On	On

	28-day							Turbine	<del></del>						
Date	28-day Cycle	G29	G34	G35	G44	G45	G48	G49	G51	G56	G58	G59	G64	G67	G75
03-Jul-23	24	Off	On	Off	On	On	On	Off	Off	Off	On	Off	On	Off	On
04-Jul-23	24	On	On	Off	Off	On	Off	Off	Off	Off	On	On	On	Off	On
05-Jul-23	24	Off	On	On	On	On	Off	Off	Off	Off	Off	On	On	Off	On
06-Jul-23	25	On	On	Off	Off	Off	Off	On	On	On	On	Off	On	Off	Off
07-Jul-23	25	On	Off	On	Off	On	Off	On	On	Off	Off	Off	Off	On	On
08-Jul-23	25	On	Off	On	Off	On	Off	Off	On	Off	On	On	On	Off	Off
09-Jul-23	25	On	Off	On	On	Off	On	Off	Off	On	On	Off	Off	On	Off
10-Jul-23	25	Off	Off	Off	On	On	Off	On	On	On	On	Off	On	Off	Off
11-Jul-23	25	On	Off	On	On	Off	Off	On	Off	Off	On	On	Off	Off	On
12-Jul-23	25	On	On	Off	Off	On	Off	Off	On	Off	On	On	On	Off	Off
13-Jul-23	25	On	On	On	Off	On	Off	Off	Off	Off	On	On	Off	On	Off
14-Jul-23	25	Off	Off	On	On	Off	On	Off	On	Off	On	Off	On	Off	On
15-Jul-23	25	On	On	Off	Off	On	On	Off	On	Off	On	Off	Off	Off	On
16-Jul-23	25	Off	On	On	Off	Off	Off	On	On	On	On	Off	On	Off	Off
17-Jul-23	25	On	On	On	Off	Off	On	Off	Off	Off	On	Off	Off	On	On
18-Jul-23	25	On	On	Off	Off	On	Off	Off	On	On	Off	On	On	Off	Off
19-Jul-23	25	Off	Off	On	On	On	Off	On	On	Off	On	Off	Off	Off	On
20-Jul-23	25	On	Off	On	Off	On	Off	Off	On	Off	On	Off	On	Off	On
21-Jul-23	25	On	On	Off	Off	Off	On	On	Off	Off	Off	On	Off	On	On
22-Jul-23	25	Off	Off	Off	On	Off	On	On	Off	On	On	Off	On	On	Off
23-Jul-23	25	On	On	Off	Off	On	On	Off	Off	Off	On	On	On	Off	Off
24-Jul-23	25	Off	On	On	Off	Off	Off	On	Off	On	Off	Off	On	On	On
25-Jul-23	25	On	Off	Off	On	Off	On	On	Off	Off	On	Off	Off	On	On
26-Jul-23	25	Off	Off	On	On	Off	Off	On	On	Off	Off	Off	On	On	On
27-Jul-23	25	Off	On	On	Off	Off	On	On	On	Off	Off	On	Off	On	Off
28-Jul-23	25	On	Off	On	Off	Off	Off	On	Off	On	Off	On	On	On	Off
29-Jul-23	25	Off	Off	On	On	On	On	Off	Off	On	Off	On	Off	On	Off
30-Jul-23	25	Off	Off	On	Off	On	Off	On	Off	On	Off	On	On	Off	On
31-Jul-23	25	On	On	Off	On	Off	On	Off	On	On	Off	Off	Off	Off	On
01-Aug-23	25	Off	Off	Off	On	On	Off	On	Off	On	On	On	Off	On	Off
02-Aug-23	25	On	On	Off	On	Off	On	Off	On	Off	On	Off	Off	Off	On
03-Aug-23	26	Off	On	Off	On	Off	Off	On	Off	On	Off	On	Off	On	On
04-Aug-23	26	On	On	Off	Off	On	Off	On	On	Off	On	Off	Off	Off	On
05-Aug-23	26	Off	On	Off	On	On	Off	Off	Off	On	On	On	On	Off	Off
06-Aug-23	26	Off	On	On	On	On	Off	Off	Off	On	Off	On	On	Off	Off
07-Aug-23	26	Off	On	Off	Off	Off	On	On	Off	On	On	Off	On	Off	On
08-Aug-23	26	On	On	Off	Off	On	Off	On	Off	Off	Off	On	Off	On	On
09-Aug-23	26	Off	On	Off	On	Off	On	Off	On	On	Off	Off	On	On	Off
10-Aug-23	26	Off	Off	On	On	Off	On	On	Off	On	Off	Off	Off	On	On
_															
11-Aug-23	26	On	Off	On	Off	On	Off	Off	On	On	On	Off	Off	On	Off
12-Aug-23	26	Off	On	Off	On	Off	On	On	Off	Off	On	On	Off	On	Off
13-Aug-23	26	On	On	Off	Off	Off	Off	On Off	On	On	Off	On	On	Off	Off
14-Aug-23	26	On	On	Off	On	Off	On	Off	On	Off	Off	On	On	Off	Off
15-Aug-23	26	Off	Off	On	Off	Off	On	On	Off	Off	On	On	On	On	Off
16-Aug-23	26	Off	On	On	Off	On	Off	On	Off	Off	On	Off	On	Off	On
17-Aug-23	26	Off	On	Off	On	Off	On	Off	Off	Off	On	On	On	Off	On
18-Aug-23	26	On	On	Off	Off	On	On	Off	On	Off	On	Off	Off	On	Off
19-Aug-23	26	Off	On	Off	On	Off	Off	On	On	On	Off	On	Off	Off	On
20-Aug-23	26	Off	On	Off	On	On	Off	On	Off	Off	Off	Off	On	On	On
21-Aug-23	26	Off	Off	Off	On	On	Off	On	On	On	Off	On	Off	Off	On
22-Aug-23	26	Off	On	On	On	On	Off	Off	Off	On	Off	Off	On	Off	On
23-Aug-23	26	On	Off	On	Off	On	Off	Off	On	On	Off	Off	On	Off	On

	28-day							Turbine	•						
Date	Cycle	G29	G34	G35	G44	G45	G48	G49	G51	G56	G58	G59	G64	G67	G75
24-Aug-23	26	On	Off	Off	On	On	On	Off	On	On	On	Off	Off	Off	Off
25-Aug-23	26	Off	Off	On	On	On	Off	Off	On	Off	Off	On	On	Off	On
26-Aug-23	26	On	Off	Off	On	On	On	Off	On	On	On	Off	Off	Off	Off
27-Aug-23	26	Off	On	Off	Off	On	Off	On	Off	Off	On	Off	On	On	On
28-Aug-23	26	Off	Off	On	On	On	On	Off	On	On	Off	On	Off	Off	Off
29-Aug-23	26	On	Off	On	Off	Off	On	Off	Off	On	On	Off	On	On	Off
30-Aug-23	26	Off	On	Off	On	Off	On	On	Off	On	Off	Off	On	Off	On
31-Aug-23	27	Off	Off	Off	On	Off	On	On	On	On	On	Off	Off	Off	On
01-Sep-23	27	On	On	Off	Off	On	Off	On	On	Off	On	On	Off	Off	Off
02-Sep-23	27	Off	Off	On	On	Off	On	Off	On	On	On	On	Off	Off	Off
03-Sep-23	27	Off	Off	On	On	On	Off	On	Off	Off	On	Off	On	Off	On
04-Sep-23	27	On	Off	On	Off	On	Off	Off	On	Off	On	Off	On	On	Off
05-Sep-23	27	Off	Off	On	On	On	On	Off	Off	Off	On	On	Off	Off	On
06-Sep-23	27	Off	On	On	Off	Off	On	Off	On	Off	On	On	Off	On	Off
07-Sep-23	27	On	On	Off	On	Off	Off	On	Off	Off	On	On	Off	On	Off
08-Sep-23	27	Off	Off	Off	On	On	On	Off	Off	Off	On	Off	On	On	On
09-Sep-23	27	On	On	On	On	Off	Off	Off	Off	On	On	Off	On	Off	Off
10-Sep-23	27	Off	On	Off	Off	On	Off	On	On	Off	On	Off	On	On	Off
11-Sep-23	27	Off	On	On	Off	On	On	Off	On	On	Off	Off	Off	Off	On
12-Sep-23	27	Off	Off	Off	On	Off	On	On	On	On	Off	Off	Off	On	On
13-Sep-23	27	On	Off	On	Off	On	Off	On	On	Off	Off	Off	On	Off	On
14-Sep-23	27	On	Off	Off	On	On	Off	Off	On	On	Off	On	On	Off	Off
15-Sep-23	27	On	Off	On	Off	On	On	Off	Off	Off	On	Off	On	Off	On
16-Sep-23	27	On	On	On	Off	Off	Off	Off	On	On	Off	On	Off	On	Off
17-Sep-23	27	On	Off	On	On	Off	Off	On	On	On	Off	Off	On	Off	Off
18-Sep-23	27	On	Off	Off	On	Off	Off	On	Off	Off	Off	On	On	On	On
19-Sep-23	27	Off	On	On	On	Off	Off	On	Off	Off	Off	On	Off	On	On
20-Sep-23	27	Off	Off	On	Off	On	Off	On	On	On	Off	Off	On	Off	On
21-Sep-23	27	On	On	Off	Off	On	Off	On	On	Off	Off	On	Off	On	Off
22-Sep-23	27	Off	Off	On	Off	On	On	Off	Off	On	On	Off	On	On	Off
23-Sep-23	27	On	On	On	On	Off	Off	Off	Off	Off	Off	On	On	On	Off
24-Sep-23	27	Off	On	Off	On	Off	Off	On	On	Off	Off	On	On	On	Off
25-Sep-23	27	Off	Off	On	On	Off	On	On	Off	Off	On	Off	Off	On	On
26-Sep-23	27	Off	On	On	Off	Off	On	Off	On	On	On	Off	Off	On	Off
27-Sep-23	27	Off	On	On	On	Off	Off	On	Off	Off	On	Off	Off	On	On

On = deterrents broadcasting; Off = deterrents muted but triggering virtually; na = not applicable because DTBird system was not effectively operational (also see Appendix B).

### Appendix B. Selected Days within 28-day Sampling Cycles at DTBird-Equipped Turbines When Records Were Screened to Compose Dataset for Two-Year Experiment

Cells highlighted in red represent periods when a given DTBird system was either not yet commissioned and operational or when a commissioned system was not effectively functional. Cells highlighted in orange represent selected sampling days on which no detection events were recorded when the focal turbine was spinning and the DTBird deterrents were set to trigger as expected.

Sampling days were initially selected randomly for each turbine within each 28-day Cycle sampling period, balanced to ensure that 5 days were selected when the deterrents were set to trigger virtually but not actually broadcast (control mode) and 5 days were selected when the deterrents were set to broadcast normally (treatment mode) (see Appendix A). However, intermittent operational failures frequently dictated the need to modify the initial random sampling in an effort to achieve 10 days of useful sampling per 28-day period and maintain a 50:50 ratio of sampled control-treatment days at each turbine. Notes at the bottom of some turbine-specific columns under certain 28-day Cycles highlight when operational failures constrained the distribution of days available for sampling.

					28	-day Cycle	1: 1–28 Se	ptember 20	21					
Sample Day	G29	G34	G35	G44	G45	G48	G49	G51	G56	G58	G59	G64	G67	G75
1		1-Sep	3-Sep	2-Sep	1-Sep	1-Sep	4-Sep			1-Sep	3-Sep	3-Sep	3-Sep	3-Sep
2		5-Sep	5-Sep	3-Sep	3-Sep	5-Sep	7-Sep			2-Sep	6-Sep	5-Sep	7-Sep	5-Sep
3		7-Sep	9-Sep	4-Sep	4-Sep	8-Sep	10-Sep			5-Sep	9-Sep	6-Sep	8-Sep	6-Sep
4		12-Sep	13-Sep	6-Sep	7-Sep	13-Sep	13-Sep			10-Sep	10-Sep	7-Sep	11-Sep	7-Sep
5		16-Sep	15-Sep	15-Sep	12-Sep	14-Sep	17-Sep			12-Sep	11-Sep	15-Sep	14-Sep	10-Sep
6		17-Sep	16-Sep	18-Sep	14-Sep	15-Sep	20-Sep			13-Sep	15-Sep	16-Sep	16-Sep	19-Sep
7		23-Sep	17-Sep	21-Sep	17-Sep	17-Sep	22-Sep			15-Sep	16-Sep	17-Sep	18-Sep	21-Sep
8		24-Sep	21-Sep	23-Sep	18-Sep	23-Sep	23-Sep			18-Sep	21-Sep	19-Sep	22-Sep	23-Sep
9		25-Sep	25-Sep	24-Sep	19-Sep	26-Sep	24-Sep			21-Sep	24-Sep	23-Sep	25-Sep	26-Sep
10		26-Sep	27-Sep	28-Sep	21-Sep	27-Sep	27-Sep			24-Sep	27-Sep	27-Sep	26-Sep	27-Sep
	faulty operation in Year 1		no useable records 1–2, 5–11 Sep					faulty operation in Year 1	faulty operation in Year 1					

					28-day	Cycle 2: 29	September	- 26 Octob	per 2021					
Sample Day	G29	G34	G35	G44	G45	G48	G49	G51	G56	G58	G59	G64	G67	G75
1		4-Oct	30-Sep	29-Sep	1-Oct	1-Oct	30-Sep			30-Sep	3-Oct	30-Sep	1-Oct	29-Sep
2		6-Oct	5-Oct	1-Oct	2-Oct	3-Oct	1-Oct			2-Oct	5-Oct	2-Oct	5-Oct	3-Oct
3		7-Oct	6-Oct	2-Oct	8-Oct	5-Oct	3-Oct			4-Oct	7-Oct	8-Oct	6-Oct	4-Oct
4		13-Oct	8-Oct	3-Oct	12-Oct	8-Oct	6-Oct			7-Oct	15-Oct	10-Oct	9-Oct	6-Oct
5		14-Oct	11-Oct	10-Oct	14-Oct	9-Oct	7-Oct			12-Oct	16-Oct	11-Oct	12-Oct	8-Oct
6		15-Oct	14-Oct	14-Oct	19-Oct	13-Oct	13-Oct			14-Oct	17-Oct	17-Oct	13-Oct	10-Oct
7		19-Oct	18-Oct	19-Oct	20-Oct	18-Oct	15-Oct			15-Oct	18-Oct	19-Oct	15-Oct	13-Oct
8		21-Oct	22-Oct	20-Oct	21-Oct	23-Oct	18-Oct			18-Oct	21-Oct	22-Oct	17-Oct	18-Oct
9		24-Oct	24-Oct	21-Oct	22-Oct	25-Oct	23-Oct			19-Oct	22-Oct	24-Oct	18-Oct	21-Oct
10		26-Oct	25-Oct	26-Oct	25-Oct	26-Oct	24-Oct			21-Oct	24-Oct	25-Oct	21-Oct	22-Oct
					28-day	Cycle 3: 27	October –	23 Novemb	er 2021					
Sample Day	G29	G34	G35	G44	G45	G48	G49	G51	G56	G58	G59	G64	G67	G75
1		27-Oct	27-Oct	31-Oct	1-Nov	27-Oct	27-Oct			27-Oct	27-Oct	29-Oct	28-Oct	29-Oct
2		30-Oct	29-Oct	1-Nov	4-Nov	29-Oct	29-Oct			30-Oct	29-Oct	30-Oct	1-Nov	31-Oct
3		1-Nov	31-Oct	2-Nov	6-Nov	1-Nov	30-Oct			31-Oct	30-Oct	4-Nov	5-Nov	5-Nov
4		3-Nov	6-Nov	3-Nov	7-Nov	3-Nov	1-Nov			5-Nov	31-Oct	7-Nov	7-Nov	6-Nov
5		9-Nov	9-Nov	4-Nov	8-Nov	5-Nov	6-Nov			7-Nov	2-Nov	8-Nov	13-Nov	8-Nov
6		10-Nov	12-Nov	16-Nov	11-Nov	11-Nov	13-Nov			11-Nov	4-Nov	9-Nov	15-Nov	10-Nov
7		13-Nov	14-Nov	17-Nov	13-Nov	13-Nov	16-Nov			12-Nov	9-Nov	10-Nov	17-Nov	11-Nov
8		16-Nov	16-Nov	20-Nov	15-Nov	14-Nov	18-Nov			20-Nov	13-Nov	16-Nov	20-Nov	15-Nov
9		21-Nov	19-Nov	21-Nov	22-Nov	15-Nov	22-Nov			21-Nov	20-Nov	17-Nov	21-Nov	18-Nov
10		23-Nov	23-Nov	22-Nov	23-Nov	19-Nov	23-Nov			22-Nov	23-Nov	19-Nov	22-Nov	21-Nov
					28-day C	Cycle 4: 24	November -	21 Decem	ber 2021					
Sample Day	G29	G34	G35	G44	G45	G48	G49	G51	G56	G58	G59	G64	G67	G75
1		26-Nov	24-Nov	24-Nov	25-Nov	25-Nov	30-Nov			1-Dec	24-Nov	27-Nov	24-Nov	26-Nov
2		27-Nov	28-Nov	25-Nov	27-Nov	26-Nov	2-Dec			3-Dec	26-Nov	30-Nov	25-Nov	28-Nov
3		28-Nov	29-Nov	27-Nov	28-Nov	29-Nov	6-Dec			4-Dec	29-Nov	1-Dec	27-Nov	1-Dec
4		3-Dec	30-Nov	30-Nov	29-Nov	2-Dec	7-Dec			5-Dec	6-Dec	2-Dec	29-Nov	4-Dec
5		9-Dec	3-Dec	3-Dec	30-Nov	3-Dec	9-Dec			6-Dec	8-Dec	3-Dec	4-Dec	5-Dec
6		11-Dec	7-Dec	4-Dec	1-Dec	10-Dec	11-Dec			8-Dec	13-Dec	15-Dec	5-Dec	15-Dec
7		13-Dec	8-Dec	10-Dec	2-Dec	11-Dec	15-Dec			9-Dec	14-Dec	16-Dec	8-Dec	16-Dec
8		15-Dec	12-Dec	16-Dec	3-Dec	12-Dec	18-Dec			11-Dec	16-Dec	19-Dec	11-Dec	17-Dec
9		16-Dec	14-Dec	18-Dec	14-Dec	17-Dec	19-Dec			14-Dec	20-Dec	20-Dec	12-Dec	19-Dec

10		18-Dec	19-Dec	19-Dec	15-Dec	19-Dec	21-Dec			20-Dec	21-Dec	21-Dec	14-Dec	21-Dec
							ecember 20	)21 – 18 Jar	nuary 2022					
Sample Day	G29	G34	G35	G44	G45	G48	G49	G51	G56	G58	G59	G64	G67	G75
1		25-Dec	23-Dec	27-Dec	7-Jan	22-Dec	24-Dec			23-Dec	22-Dec	25-Dec	22-Dec	23-Dec
2		27-Dec	24-Dec	31-Dec	10-Jan	23-Dec	25-Dec			24-Dec	24-Dec	26-Dec	26-Dec	25-Dec
3		29-Dec	27-Dec	2-Jan	11-Jan	31-Dec	27-Dec			25-Dec	25-Dec	30-Dec	27-Dec	26-Dec
4		30-Dec	29-Dec	3-Jan	12-Jan	1-Jan	28-Dec			26-Dec	27-Dec	31-Dec	1-Jan	30-Dec
5		2-Jan	2-Jan	4-Jan	13-Jan	4-Jan	2-Jan			27-Dec	28-Dec	2-Jan	4-Jan	31-Dec
6		4-Jan	9-Jan	10-Jan	14-Jan	6-Jan	4-Jan			2-Jan	29-Dec	3-Jan	5-Jan	5-Jan
7		5-Jan	11-Jan	12-Jan	15-Jan	8-Jan	12-Jan			3-Jan	1-Jan	4-Jan	6-Jan	8-Jan
8		6-Jan	13-Jan	14-Jan	16-Jan	10-Jan	13-Jan			13-Jan	10-Jan	5-Jan	9-Jan	10-Jan
9		14-Jan	15-Jan	16-Jan	17-Jan	13-Jan	14-Jan			16-Jan	14-Jan	8-Jan	16-Jan	14-Jan
10		17-Jan	18-Jan	18-Jan	18-Jan	17-Jan	15-Jan			17-Jan	17-Jan	9-Jan	18-Jan	17-Jan
					only partially operational 7 Jan		inoperable 7– 10 Jan					mostly inoperable 9 Jan–7 Feb		
					28-day	Cycle 6: 1	9 January –	15 Februai	ry 2022					
Sample Day	G29	G34	G35	G44	G45	G48	G49	G51	G56	G58	G59	G64	G67	G75
1		24-Jan	20-Jan	19-Jan	20-Jan	19-Jan	19-Jan			21-Jan	19-Jan	29-Jan	21-Jan	19-Jan
2		26-Jan	21-Jan	23-Jan	22-Jan	20-Jan	20-Jan			23-Jan	21-Jan	3-Feb	25-Jan	21-Jan
3		29-Jan	24-Jan	25-Jan	23-Jan	24-Jan	28-Jan			25-Jan	28-Jan	4-Feb	29-Jan	23-Jan
4		1-Feb	27-Jan	26-Jan	28-Jan	26-Jan	5-Feb			29-Jan	4-Feb	5-Feb	1-Feb	28-Jan
5		5-Feb	29-Jan	28-Jan	3-Feb	27-Jan	6-Feb			31-Jan	9-Feb	7-Feb	2-Feb	29-Jan
6		6-Feb	2-Feb	29-Jan	4-Feb	28-Jan	7-Feb			1-Feb	10-Feb	8-Feb	4-Feb	2-Feb
7		7-Feb	5-Feb	31-Jan	8-Feb	29-Jan	8-Feb			2-Feb	11-Feb	9-Feb	8-Feb	4-Feb
8		11-Feb	8-Feb	5-Feb	9-Feb	6-Feb	9-Feb			3-Feb	13-Feb	10-Feb	10-Feb	6-Feb
9		12-Feb	10-Feb	7-Feb	14-Feb	10-Feb	13-Feb			7-Feb	14-Feb	11-Feb	11-Feb	12-Feb
10		14-Feb	13-Feb	15-Feb	15-Feb	13-Feb	15-Feb			12-Feb	15-Feb	14-Feb	12-Feb	14-Feb
					inoperable 24, 26–27 Jan							mostly inoperable 9 Jan–7 Feb		
			,		28-da	y Cycle 7:	16 February	– 15 March	n 2022		,			
Sample Day	G29	G34	G35	G44	G45	G48	G49	G51	G56	G58	G59	G64	G67	G75
1		20-Feb	18-Feb	23-Feb	16-Feb	21-Feb	16-Feb			19-Feb	16-Feb	16-Feb	16-Feb	17-Feb
2		24-Feb	19-Feb	25-Feb	23-Feb	25-Feb	20-Feb			21-Feb	18-Feb	18-Feb	23-Feb	19-Feb
3		26-Feb	24-Feb	26-Feb	1-Mar	27-Feb	24-Feb			22-Feb	19-Feb	24-Feb	26-Feb	25-Feb
4		28-Feb	25-Feb	28-Feb	3-Mar	1-Mar	26-Feb			23-Feb	24-Feb	25-Feb	1-Mar	27-Feb

5		O Mar	27-Feb	1 1400	/ Mar	/ Mar	27-Feb			24-Feb	25-Feb	1 Mar	2 14 0 5	3-Mar
6		2-Mar	27-reb 2-Mar	1-Mar	6-Mar 7-Mar	6-Mar				24-reb 28-Feb	26-Feb	1-Mar	3-Mar	
7		5-Mar		4-Mar		7-Mar	2-Mar					7-Mar	5-Mar	4-Mar
		6-Mar	10-Mar	5-Mar	9-Mar	9-Mar	3-Mar			3-Mar	3-Mar	11-Mar	7-Mar	6-Mar
8		7-Mar	11-Mar	6-Mar	10-Mar	11-Mar	7-Mar			8-Mar	8-Mar	13-Mar	10-Mar	11-Mar 13-Mar
		9-Mar	14-Mar	12-Mar	13-Mar	13-Mar	10-Mar			9-Mar	12-Mar	14-Mar	13-Mar	
10		10-Mar	15-Mar	14-Mar	15-Mar	14-Mar	11-Mar <b>3: 16 March</b>	10 Amril 0	0000	12-Mar	14-Mar	15-Mar	14-Mar	15-Mar
Companie					20-0	ady Cycle (	o. 16 Maich	- 12 April 2	1022					
Sample Day	G29	G34	G35	G44	G45	G48	G49	G51	G56	G58	G59	G64	G67	G75
1		16-Mar	18-Mar	16-Mar	16-Mar	17-Mar	16-Mar			17-Mar	18-Mar	18-Mar	19-Mar	16-Mar
2		17-Mar	20-Mar	18-Mar	22-Mar	18-Mar	22-Mar			20-Mar	21-Mar	19-Mar	22-Mar	20-Mar
3		19-Mar	23-Mar	19-Mar	23-Mar	20-Mar	23-Mar			21-Mar	25-Mar	21-Mar	26-Mar	25-Mar
4		27-Mar	27-Mar	20-Mar	24-Mar	21-Mar	26-Mar			22-Mar	29-Mar	25-Mar	30-Mar	28-Mar
5		2-Apr	29-Mar	24-Mar	28-Mar	26-Mar	27-Mar			23-Mar	3-Apr	27-Mar	31-Mar	31-Mar
6		3-Apr	30-Mar	26-Mar	31-Mar	30-Mar	29-Mar			31-Mar	4-Apr	3-Apr	2-Apr	4-Apr
7		5-Apr	4-Apr	30-Mar	1-Apr	31-Mar	1-Apr			2-Apr	5-Apr	5-Apr	4-Apr	7-Apr
8		7-Apr	7-Apr	3-Apr	2-Apr	2-Apr	5-Apr			5-Apr	7-Apr	6-Apr	7-Apr	8-Apr
9		11-Apr	8-Apr	6-Apr	3-Apr	5-Apr	6-Apr			7-Apr	9-Apr	10-Apr	8-Apr	9-Apr
10		12-Apr	10-Apr	9-Apr	12-Apr	11-Apr	10-Apr			10-Apr	10-Apr	11-Apr	9-Apr	12-Apr
												inoperable 22–24 Mar	inoperable 23–24 Mar	
					28-	day Cycle	9: 13 April -	- 10 May 20	)22					
Sample Day	G29	G34	G35	G44	G45	G48	G49	G51	G56	G58	G59	G64	G67	G75
1		14-Apr	13-Apr	14-Apr	13-Apr	15-Apr	17-Apr			14-Apr	13-Apr	19-Apr	16-Apr	14-Apr
2		16-Apr	19-Apr	15-Apr	18-Apr	17-Apr	18-Apr			16-Apr	18-Apr	20-Apr	23-Apr	16-Apr
3		17-Apr	22-Apr	18-Apr	19-Apr	21-Apr	19-Apr			22-Apr	22-Apr	22-Apr	24-Apr	18-Apr
4		18-Apr	24-Apr	19-Apr	20-Apr	22-Apr	22-Apr			24-Apr	24-Apr	25-Apr	25-Apr	19-Apr
5		20-Apr	26-Apr	23-Apr	22-Apr	23-Apr	24-Apr			25-Apr	25-Apr	27-Apr	27-Apr	20-Apr
6		23-Apr	30-Apr	24-Apr	24-Apr	24-Apr	25-Apr			26-Apr	29-Apr	29-Apr	28-Apr	24-Apr
7		26-Apr	1-May	2-May	26-Apr	26-Apr	29-Apr			30-Apr	30-Apr	30-Apr	29-Apr	26-Apr
8		29-Apr	3-Мау	4-May	1-May	28-Apr	1-May			1-May	2-May	3-May	30-Apr	29-Apr
9		30-Apr	6-May	6-May	5-May	1-May	3-May			5-May	4-May	4-May	5-May	3-May
10		7-May	9-Мау	8-May	8-May	5-May	4-May			10-Мау	5-May	10-Мау	9-Мау	6-May
					inoperable14– 17 Apr							inoperable13– 17 Apr and 1– 2, 5–9 May		

					28-	day Cycle	10: 11 May	- 07 June 2	022					
Sample Day	G29	G34	G35	G44	G45	G48	G49	G51	G56	G58	G59	G64	G67	G75
1		11-May	16-May	11-May	12-May	12-May	12-May			13-May	11-May	11-May	11-May	14-May
2		13-May	18-May	14-May	13-May	16-May	13-May			15-May	12-May	17-May	16-May	16-May
3		14-May	23-May	16-May	18-May	23-May	18-May			20-May	13-May	19-May	18-May	18-May
4		18-May	25-May	17-May	19-May	24-May	20-May			21-May	14-May	23-May	20-May	20-May
5		22-May	26-May	18-May	23-May	25-May	21-May			22-May	16-May	28-May	23-May	25-May
6		30-May	27-May	19-May	24-May	26-May	22-May			24-May	20-May	29-May	24-May	26-May
7		1-Jun	28-May	23-May	29-May	28-May	23-May			26-May	29-May	31-May	29-May	28-May
8		2-Jun	1-Jun	31-May	31-May	29-May	25-May			29-May	30-May	2-Jun	30-Мау	1-Jun
9		6-Jun	3-Jun	1-Jun	3-Jun	2-Jun	30-May			3-Jun	2-Jun	3-Jun	1-Jun	2-Jun
10		7-Jun	5-Jun	7-Jun	6-Jun	3-Jun	6-Jun			4-Jun	3-Jun	7-Jun	4-Jun	7-Jun
					inoperable 4– 5 Jun							mostly inoperable 1 Jun		
		1		•	28-	day Cycle	11: 08 June	- 05 July 2	022	1	•	•	•	
Sample Day	G29	G34	G35	G44	G45	G48	G49	G51	G56	G58	G59	G64	G67	G75
1		9-Jun	10-Jun	11-Jun	10-Jun	8-Jun	9-Jun			8-Jun	9-Jun	9-Jun	10-Jun	9-Jun
2		10-Jun	11-Jun	13-Jun	11-Jun	12-Jun	13-Jun			12-Jun	14-Jun	12-Jun	12-Jun	12-Jun
3		11-Jun	13-Jun	17-Jun	12-Jun	17-Jun				17-Jun	17-Jun	14-Jun	13-Jun	14-Jun
4		14-Jun	15-Jun	21-Jun	14-Jun	19-Jun				21-Jun	18-Jun	22-Jun	16-Jun	16-Jun
5		16-Jun	18-Jun	24-Jun	17-Jun	21-Jun				23-Jun	22-Jun	23-Jun	19-Jun	19-Jun
6		20-Jun	19-Jun	27-Jun	18-Jun	22-Jun				25-Jun	23-Jun	29-Jun	23-Jun	20-Jun
7		23-Jun	22-Jun	29-Jun	30-Jun	23-Jun				27-Jun	24-Jun	30-Jun	24-Jun	23-Jun
8		24-Jun	25-Jun	1-Jul	2-Jul	24-Jun				28-Jun	28-Jun	2-Jul	25-Jun	30-Jun
9		29-Jun	26-Jun	2-Jul	4-J∪l	25-Jun				30-Jun	2-Jul	4-J∪l	26-Jun	3-Jul
10		1-Jul	30-Jun	5-Jul	5-Jul	30-Jun				3-Jul	3-Jul	5-Jul	3-Jul	5-Jul
		problematic operation 19 Jun–4 Aug											inoperable 11 Jun	
					28-0	lay Cycle 1	2: 06 July –	02 August	2022		·	·		
Sample Day	G29	G34	G35	G44	G45	G48	G49	G51	G56	G58	G59	G64	G67	G75
1		10-Jul	19-Jul	12-Jul	9-Jul	10-Jul	7-Jul			8-Jul	10-Jul	6-Jul	10-Jul	7-Jul
2		11-Jul	22-Jul	15-Jul	10-Jul	11-Jul	9-Jul			9-Jul	11-Jul	10-Jul	13-Jul	8-Jul
3		16-Jul	23-Jul	16-Jul	14-Jul	14-Jul	12-Jul			10-Jul	13-Jul	14-Jul	17-Jul	9-Jul
4		17-Jul	24-Jul	19-Jul	15-Jul	19-Jul	17-Jul			12-Jul	14-Jul	15-Jul	20-Jul	13-Jul
5		22-Jul	25-Jul	21-Jul	19-Jul	21-Jul	18-Jul			15-Jul	15-Jul	19-Jul	21-Jul	16-Jul

The complete	6		24-Jul	27-Jul	22-Jul	20-Jul	27-Jul	19-Jul			18-Jul	18-Jul	20-Jul	24-Jul	17-Jul
Somple   Part															
9   30-Jul   30-Jul   30-Jul   31-Jul   27-Jul   24-Jul   21-Jul   23-Jul   1-Aug   25-Jul   1-Aug   25-Jul   23-Jul   1-Aug   25-Jul   23-Jul   2-Aug   2-A															
10   2-Aug   31-Jul   31-Jul   2-Aug   1-Aug   31-Jul   25-Jul   30-Jul   24-Jul   2-Aug   3-Aug   3															
Sample   Debtarratic   Properties 28   Debtarratic   Debtarratic   Properties 28   Debtarratic   Debta															
Somple	10		<u> </u>		31-301	z-Aug	1-Aug	31-JUI			25-JUI	30-301	Z4-JUI	z-Aug	Z-Aug
Sample   Day   G29   G34   G35   G44   G45   G48   G49   G51   G56   G58   G59   G64   G67   G75				inoperable 28											
Sample													Jul-21 Aug		
Day   G29   G34   G35   G44   G45   G48   G49   G51   G56   G58   G59   G64   G67   G75		•				2	8-day Cycl	le 13: 03–30	August 202	22					
2		G29	G34	G35	G44	G45	G48	G49	G51	G56	G58	G59	G64	G67	G75
2	1		3-Aug		5-Aug	4-Aug	3-Aug	4-Aug			8-Aug	8-Aug		3-Aug	4-Aug
4	2		4-Aug	22-Aug	6-Aug	6-Aug	5-Aug	6-Aug				9-Aug	22-Aug	6-Aug	8-Aug
12-Aug   25-Aug   13-Aug   17-Aug   10-Aug   14-Aug   18-Aug   15-Aug   25-Aug   13-Aug   14-Aug   6   20-Aug   26-Aug   14-Aug   21-Aug   11-Aug   19-Aug   21-Aug   17-Aug   26-Aug   15-Aug   15-Aug   16-Aug   7   22-Aug   27-Aug   23-Aug   23-Aug   20-Aug   24-Aug   19-Aug   27-Aug   20-Aug   18-Aug   19-Aug   27-Aug   27-Aug   20-Aug   28-Aug   29-Aug   28-Aug   29-Aug   28-Aug   29-Aug   28-Aug   29-Aug   28-Aug   29-Aug   29-Aug   29-Aug   28-Aug   29-Aug   29	3		8-Aug	23-Aug	9-Aug	8-Aug	6-Aug	9-Aug			14-Aug	10-Aug	23-Aug	8-Aug	9-Aug
6 20-Aug 26-Aug 14-Aug 21-Aug 11-Aug 19-Aug 21-Aug 17-Aug 26-Aug 15-Aug 16-Au 7 22-Aug 27-Aug 15-Aug 23-Aug 23-Aug 20-Aug 24-Aug 19-Aug 27-Aug 27-Aug 20-Aug 19-Aug 27-Aug 27-Aug 28-Aug 17-Aug 24-Aug 26-Aug 25-Aug 25-Aug 26-Aug 26-Aug 27-Aug 27-Aug 27-Aug 27-Aug 27-Aug 27-Aug 26-Aug 26-Aug 26-Aug 26-Aug 26-Aug 26-Aug 26-Aug 26-Aug 26-Aug 29-Aug 27-Aug 27-Aug 27-Aug 27-Aug 28-Aug 28-Aug 29-Aug 30-Aug 30-Aug 30-Aug 30-Aug 29-Aug 28-Aug 29-Aug 30-Aug 29-Aug 30-Aug 29-Aug 30-Aug 29-Aug 30-Aug	4		10-Aug	24-Aug	10-Aug	12-Aug	9-Aug	12-Aug			16-Aug	12-Aug	24-Aug	11-Aug	10-Aug
7	5		12-Aug	25-Aug	13-Aug	17-Aug	10-Aug	14-Aug			18-Aug	15-Aug	25-Aug	13-Aug	14-Aug
8	6		20-Aug	26-Aug	14-Aug	21-Aug	11-Aug	19-Aug			21-Aug	17-Aug	26-Aug	15-Aug	16-Aug
9 26-Aug 29-Aug 27-Aug 27-Aug 27-Aug 26-Aug 26-Aug 26-Aug 29-Aug 26-Aug	7		22-Aug	27-Aug	15-Aug	23-Aug	23-Aug	20-Aug			24-Aug	19-Aug	27-Aug	20-Aug	19-Aug
10   28-Aug   30-Aug   30-Aug   30-Aug   29-Aug   28-Aug   29-Aug   30-Aug   29-Aug   30-Aug   30-Au	8		25-Aug	28-Aug	17-Aug	24-Aug	26-Aug	22-Aug			25-Aug	24-Aug	28-Aug	22-Aug	23-Aug
Problematic operation   Page	9		26-Aug	29-Aug	27-Aug	27-Aug	27-Aug	26-Aug			26-Aug	26-Aug	29-Aug	26-Aug	26-Aug
Sample Day   Aug -most of   22 Aug   24 Sep   2-Sep   2-Sep   13-Sep   11-Sep   11-Sep   11-Sep   12-Sep   13-Sep   11-Sep   13-Sep   14-Sep   14	10		28-Aug	30-Aug	30-Aug	30-Aug	29-Aug	28-Aug			28-Aug	29-Aug	30-Aug	29-Aug	30-Aug
Sample Day   G34   G35   G44   G45   G48   G49   G51   G56   G58   G59   G64   G67   G75			operation 19	Aug-most of											
Day         G2Y         G34         G35         G44         G45         G48         G47         G51         G56         G58         G57         G64         G67         G75           1         1-Sep         2-Sep         2-Sep         1-Sep         1-Sep         2-Sep         3-Sep         1-Sep						28-day Cy	cle 14 (Beg	gin Year 2):	1–28 Septe	mber 2022					
1         1-Sep         2-Sep         4-Sep         1-Sep         2-Sep         3-Sep         3-Sep         2-Sep         3-Sep         1-Sep         2-Sep         3-Sep         3-S	-	G29	G34	G35	G44	G45	G48	G49	G51	G56	G58	G59	G64	G67	G75
2         2-Sep         6-Sep         6-Sep         9-Sep         2-Sep         4-Sep         9-Sep         3-Sep         5-Sep         9-Sep         3-Sep         2-Sep         3-Sep         2-Sep         3-Sep         3-Sep         3-Sep         10-Sep         10-Sep         11-Sep         11-Se		1-Sep	2-Sep	2-Sep	4-Sep	1-Sep	2-Sep	3-Sep	3-Sep		2-Sep	3-Sep	1-Sep	2-Sep	1-Sep
4     8-Sep     8-Sep     8-Sep     14-Sep     11-Sep     10-Sep     13-Sep     13-Sep     14-Sep     13-Sep     14-Sep     14-Sep     10-Sep     13-Sep     14-Sep     11-Sep     <	2	2-Sep	<del> </del>		9-Sep	2-Sep	4-Sep	1	9-Sep			5-Sep	9-Sep		2-Sep
5         10-Sep         10-Sep         12-Sep         15-Sep         13-Sep         11-Sep         14-Sep         14-Sep         10-Sep         13-Sep         15-Sep         11-Sep         12-Sep         11-Sep         12-Sep         11-Sep         12-Sep         11-Sep         12-Sep         11-Sep         12-Sep         11-Sep	3	6-Sep	7-Sep	7-Sep	12-Sep	10-Sep	9-Sep	8-Sep	11-Sep		4-Sep	8-Sep	10-Sep	4-Sep	9-Sep
6     13-Sep     12-Sep     14-Sep     16-Sep     19-Sep     14-Sep     16-Sep     13-Sep     17-Sep     16-Sep     14-Sep     15-Sep       7     14-Sep     16-Sep     23-Sep     17-Sep     20-Sep     17-Sep     19-Sep     17-Sep     16-Sep     19-Sep     21-Sep     21-Sep     21-Sep     18-Sep     21-Sep     21-Sep     21-Sep     21-Sep     22-Sep     22-Sep     22-Sep     22-Sep     22-Sep     22-Sep     23-Sep     23-S	4	8-Sep	8-Sep	8-Sep	14-Sep	11-Sep	10-Sep	9-Sep	13-Sep		6-Sep	9-Sep	14-Sep	8-Sep	10-Sep
6     13-Sep     12-Sep     14-Sep     16-Sep     19-Sep     14-Sep     16-Sep     13-Sep     17-Sep     16-Sep     14-Sep     15-Sep       7     14-Sep     16-Sep     23-Sep     17-Sep     20-Sep     17-Sep     19-Sep     17-Sep     16-Sep     19-Sep     21-Sep     21-Sep     21-Sep     18-Sep     21-Sep     21-Sep     21-Sep     21-Sep     22-Sep     22-Sep     22-Sep     22-Sep     22-Sep     22-Sep     23-Sep     23-S	5	10-Sep	10-Sep	12-Sep	15-Sep	13-Sep		11-Sep				13-Sep	15-Sep	11-Sep	12-Sep
8     16-Sep     21-Sep     24-Sep     22-Sep     24-Sep     21-Sep     21-Sep     21-Sep     21-Sep     21-Sep     22-Sep     22-Sep     22-Sep     22-Sep     22-Sep     22-Sep     23-Sep     21-Sep     22-Sep     23-Sep     21-Sep     23-Sep     21-Sep     23-Sep	6	13-Sep	12-Sep	14-Sep	16-Sep	19-Sep	14-Sep	14-Sep	16-Sep		13-Sep	17-Sep	16-Sep	14-Sep	15-Sep
9         24-Sep         23-Sep         25-Sep         25-Sep         27-Sep         22-Sep         23-Sep         23-Sep         21-Sep         23-Sep         21-Sep         23-Sep         24-Sep         23-Sep         25-Sep	7	14-Sep	16-Sep	23-Sep	17-Sep	20-Sep	17-Sep	19-Sep	17-Sep		16-Sep	19-Sep	21-Sep	18-Sep	17-Sep
10 27-Sep 26-Sep 27-Sep 28-Sep 26-Sep 28-Sep 28-Sep 23-Sep 27-Sep 25-Sep 25-Sep 25-Sep 25-Sep 25-Sep	8	16-Sep	21-Sep	24-Sep	22-Sep	24-Sep	21-Sep	21-Sep	21-Sep		18-Sep	20-Sep	22-Sep	21-Sep	22-Sep
	9	24-Sep	23-Sep	25-Sep	23-Sep	25-Sep	27-Sep	22-Sep	23-Sep		23-Sep	21-Sep	23-Sep	24-Sep	23-Sep
no event no event no event no event no event not	10	27-Sep	26-Sep	27-Sep	28-Sep	26-Sep	28-Sep	23-Sep	27-Sep		25-Sep	23-Sep	27-Sep	25-Sep	25-Sep
records 5.7															
records 5-7 records 5-7 records 5-7 records 5-7 sep Sep Sep Sep until 27 Sep															

					28-day	Cycle 15: 29	Septembe	er – 26 Octo	ber 2022					
Sample Day	G29	G34	G35	G44	G45	G48	G49	G51	G56	G58	G59	G64	G67	G75
1	29-Sep	30-Sep	29-Sep	29-Sep	29-Sep	29-Sep	6-Oct	1-Oct	30-Sep	29-Sep	30-Sep	29-Sep	30-Sep	29-Sep
2	2-Oct	4-Oct	1-Oct	1-Oct	30-Sep	4-Oct	8-Oct	6-Oct	1-Oct	30-Sep	1-Oct	30-Sep	2-Oct	2-Oct
3	5-Oct	5-Oct	4-Oct	4-Oct	5-Oct	6-Oct	9-Oct	8-Oct	7-Oct	5-Oct	4-Oct	1-Oct	6-Oct	7-Oct
4	6-Oct	10-Oct	5-Oct	6-Oct	9-Oct	7-Oct	10-Oct	9-Oct	12-Oct	6-Oct	7-Oct	4-Oct	8-Oct	10-Oct
5	10-Oct	14-Oct	9-Oct	11-Oct	11-Oct	10-Oct	11-Oct	11-Oct	14-Oct	9-Oct	8-Oct	5-Oct	9-Oct	13-Oct
6	14-Oct	15-Oct	11-Oct	13-Oct	13-Oct	11-Oct	16-Oct	14-Oct	16-Oct	10-Oct	11-Oct	7-Oct	12-Oct	15-Oct
7	15-Oct	17-Oct	15-Oct	17-Oct	19-Oct	12-Oct	17-Oct	18-Oct	19-Oct	15-Oct	14-Oct	10-Oct	16-Oct	16-Oct
8	16-Oct	20-Oct	19-Oct	18-Oct	22-Oct	15-Oct	21-Oct	22-Oct	20-Oct	17-Oct	16-Oct	11-Oct	17-Oct	18-Oct
9	21-Oct	23-Oct	20-Oct	19-Oct	24-Oct	20-Oct	24-Oct	23-Oct	22-Oct	21-Oct	20-Oct	17-Oct	20-Oct	25-Oct
10	25-Oct	24-Oct	24-Oct	21-Oct	26-Oct	26-Oct	26-Oct	26-Oct	23-Oct	24-Oct	23-Oct	25-Oct	24-Oct	26-Oct
												effectively Inoperable 2– 3, 6, 8–9, 12, 14–16, 19, 22– 23, 26 Oct		
					28-day	Cycle 16: 27	7 October –	23 Novem	ber 2022					
Sample Day	G29	G34	G35	G44	G45	G48	G49	G51	G56	G58	G59	G64	G67	G75
1	31-Oct	29-Oct	28-Oct	28-Oct	2-Nov	1-Nov	29-Oct	29-Oct	27-Oct	30-Oct	28-Oct	27-Oct	29-Oct	27-Oct
2	8-Nov	1-Nov	2-Nov	5-Nov	4-Nov	2-Nov	31-Oct	30-Oct	30-Oct	1-Nov	29-Oct	29-Oct	31-Oct	29-Oct
3	10-Nov	5-Nov	6-Nov	6-Nov	5-Nov	3-Nov	2-Nov	2-Nov	31-Oct	2-Nov	1-Nov	3-Nov	2-Nov	30-Oct
4	12-Nov	8-Nov	8-Nov	7-Nov	6-Nov	6-Nov	4-Nov	6-Nov	3-Nov	7-Nov	4-Nov	4-Nov	7-Nov	6-Nov
5	14-Nov	9-Nov	10-Nov	9-Nov	7-Nov	8-Nov	6-Nov	10-Nov	7-Nov	10-Nov	5-Nov	7-Nov	9-Nov	11-Nov
6	15-Nov	14-Nov	14-Nov	11-Nov	8-Nov	9-Nov	9-Nov	11-Nov	8-Nov	11-Nov	8-Nov	10-Nov	12-Nov	14-Nov
7	17-Nov	15-Nov	16-Nov	12-Nov	11-Nov	12-Nov	11-Nov	13-Nov	11-Nov	12-Nov	10-Nov	15-Nov	14-Nov	18-Nov
8	18-Nov	16-Nov	17-Nov	18-Nov	12-Nov	13-Nov	16-Nov	18-Nov	13-Nov	14-Nov	13-Nov	16-Nov	19-Nov	20-Nov
9	20-Nov	19-Nov	20-Nov	21-Nov	14-Nov	14-Nov	20-Nov	21-Nov	16-Nov	16-Nov	18-Nov	22-Nov	21-Nov	22-Nov
10	21-Nov	21-Nov	21-Nov	22-Nov	23-Nov	15-Nov	23-Nov	22-Nov	18-Nov	19-Nov	23-Nov	23-Nov	23-Nov	23-Nov
					inoperable 17–20 Nov	inoperable 28- 29, 31 Oct, 16 Nov–8 Mar			inoperable 21, 23-29 Nov					
	1	1	1	1	28-day C	ycle 17: 24	November	– 21 Decei	mber 2022	1	1	T	1	1
Sample Day	G29	G34	G35	G44	G45	G48	G49	G51	G56	G58	G59	G64	G67	G75
1	25-Nov	29-Nov	24-Nov	24-Nov	24-Nov		25-Nov	27-Nov	30-Nov	24-Nov	24-Nov	24-Nov	25-Nov	25-Nov
2	26-Nov	1-Dec	25-Nov	26-Nov	29-Nov		26-Nov	30-Nov	5-Dec	25-Nov	25-Nov	25-Nov	28-Nov	26-Nov
3	29-Nov	2-Dec	27-Nov	28-Nov	1-Dec		29-Nov	4-Dec	6-Dec	2-Dec	26-Nov	28-Nov	1-Dec	29-Nov
4	3-Dec	3-Dec	30-Nov	2-Dec	3-Dec		4-Dec	7-Dec	7-Dec	6-Dec	27-Nov	29-Nov	6-Dec	1-Dec

5	4-Dec	5-Dec	1-Dec	4-Dec	7-Dec		5-Dec	8-Dec	8-Dec	7-Dec	28-Nov	30-Nov	8-Dec	4-Dec
6	7-Dec	9-Dec	2-Dec	8-Dec	8-Dec		9-Dec	10-Dec	9-Dec	10-Dec	29-Nov	1-Dec	9-Dec	9-Dec
7	9-Dec	10-Dec	4-Dec	10-Dec	13-Dec		11-Dec	12-Dec	10-Dec	14-Dec		2-Dec	10-Dec	11-Dec
8	12-Dec	12-Dec	8-Dec	13-Dec	15-Dec		15-Dec	15-Dec	11-Dec	15-Dec			12-Dec	14-Dec
9	15-Dec	14-Dec	10-Dec	17-Dec	18-Dec		17-Dec	17-Dec	12-Dec	18-Dec			16-Dec	17-Dec
10	18-Dec	18-Dec	16-Dec	21-Dec	21-Dec		19-Dec	18-Dec	13-Dec	21-Dec			21-Dec	20-Dec
				inoperable 25 Nov, 5 Dec	inoperable intermittently Nov-Dec				inoperable 23-29 Nov, 1– 4, 14–29 Dec		no useable event records 30 Nov–9 Apr	inoperable 26–27 Nov, 3 Dec–1 Jan		
					28-day Cy	cle 18: 22 D	ecember 2	2022 – 18 Jo	nuary 2023	•				
Sample Day	G29	G34	G35	G44	G45	G48	G49	G51	G56	G58	G59	G64	G67	G75
1	26-Dec	23-Dec	24-Dec	29-Dec	30-Dec		1-Jan	30-Dec	30-Dec	29-Dec		2-Jan	30-Dec	29-Dec
2	27-Dec	25-Dec	28-Dec	30-Dec	2-Jan		2-Jan	31-Dec	2-Jan	2-Jan		3-Jan	31-Dec	30-Dec
3	29-Dec	29-Dec	31-Dec	31-Dec	3-Jan		5-Jan	3-Jan	3-Jan	4-Jan		4-Jan	5-Jan	2-Jan
4	4-Jan	1-Jan	1-Jan	2-Jan	5-Jan		8-Jan	4-Jan	4-Jan	6-Jan		5-Jan	6-Jan	3-Jan
5	5-Jan	2-Jan	6-Jan	4-Jan	8-Jan		9-Jan	5-Jan	9-Jan	7-Jan		9-Jan	7-Jan	6-Jan
6	6-Jan	3-Jan	8-Jan	7-Jan	9-Jan		10-Jan	8-Jan	11-Jan	9-Jan		10-Jan	9-Jan	8-Jan
7	11-Jan	8-Jan	11-Jan	9-Jan	10-Jan		11-Jan	10-Jan	13-Jan	10-Jan		11-Jan	10-Jan	10-Jan
8	12-Jan	11-Jan	12-Jan	11-Jan	12-Jan		12-Jan	13-Jan	15-Jan	11-Jan		13-Jan	13-Jan	13-Jan
9	13-Jan	15-Jan	14-Jan	13-Jan	15-Jan		16-Jan	14-Jan	16-Jan	14-Jan		15-Jan	14-Jan	14-Jan
10	16-Jan	16-Jan	16-Jan	14-Jan	17-Jan		17-Jan	15-Jan	18-Jan	15-Jan		18-Jan	17-Jan	18-Jan
			inoperable 30 Dec	inoperable 18 Jan	inoperable 18 Jan				Inoperable 14–29 Dec, 1, 8 Jan			inoperable 3 Dec-1 Jan, 6- 8 Jan		
					28-day	Cycle 19:	19 January	– 15 Febru	ary 2023					•
Sample Day	G29	G34	G35	G44	G45	G48	G49	G51	G56	G58	G59	G64	G67	G75
1	21-Jan	20-Jan	19-Jan	20-Jan	20-Jan		19-Jan	21-Jan	19-Jan	20-Jan		19-Jan	20-Jan	21-Jan
2	24-Jan	22-Jan	24-Jan	25-Jan	23-Jan		24-Jan	23-Jan	20-Jan	23-Jan		29-Jan	23-Jan	22-Jan
3	29-Jan	26-Jan	27-Jan	28-Jan	25-Jan		28-Jan	25-Jan	24-Jan	25-Jan		1-Feb	25-Jan	25-Jan
4	30-Jan	27-Jan	30-Jan	30-Jan	26-Jan		29-Jan	29-Jan	29-Jan	27-Jan		2-Feb	26-Jan	26-Jan
5	31-Jan	28-Jan	1-Feb	1-Feb	27-Jan		31-Jan	31-Jan	1-Feb	30-Jan		3-Feb	30-Jan	31-Jan
6	3-Feb	29-Jan	3-Feb	7-Feb	30-Jan		4-Feb	2-Feb	5-Feb	2-Feb		7-Feb	1-Feb	2-Feb
7	4-Feb	5-Feb	6-Feb	8-Feb	3-Feb		5-Feb	6-Feb	7-Feb	4-Feb		8-Feb	5-Feb	7-Feb
8	6-Feb	8-Feb	9-Feb	9-Feb	4-Feb		7-Feb	7-Feb	8-Feb	8-Feb		11-Feb	6-Feb	9-Feb
9	12-Feb	9-Feb	10-Feb	12-Feb	6-Feb		11-Feb	11-Feb	9-Feb	13-Feb		13-Feb	8-Feb	13-Feb
10	14-Feb	13-Feb	11-Feb	15-Feb	10-Feb		15-Feb	14-Feb	12-Feb	15-Feb		15-Feb	15-Feb	15-Feb
		inoperable 10 Feb		inoperable 19, 21, 24 Jan	inoperable 19, 21, 24 Jan				inoperable 21–23 Jan			inoperable 20–28, 30–31		

												Jan, 4–6, 9–10, 12 Feb		1
	1				28-day	y Cycle 20:	16 February	y – 15 Marc	h 2023			12100		
Sample Day	G29	G34	G35	G44	G45	G48	G49	G51	G56	G58	G59	G64	G67	G75
1	16-Feb	17-Feb	17-Feb	17-Feb	16-Feb		19-Feb	16-Feb	16-Feb	17-Feb		16-Feb	17-Feb	16-Feb
2	17-Feb	18-Feb	20-Feb	18-Feb	17-Feb		20-Feb	18-Feb	17-Feb	18-Feb		18-Feb	18-Feb	17-Feb
3	18-Feb	19-Feb	4-Mar	21-Feb	20-Feb		3-Mar	20-Feb	18-Feb	19-Feb		19-Feb	21-Feb	18-Feb
4	19-Feb	20-Feb	6-Mar	2-Mar	21-Feb	9-Mar	5-Mar	21-Feb	19-Feb	3-Mar		20-Feb	2-Mar	20-Feb
5	3-Mar	21-Feb	7-Mar	3-Mar	3-Mar	10-Mar	6-Mar	2-Mar	20-Feb	4-Mar		2-Mar	3-Mar	3-Mar
6	5-Mar	2-Mar	8-Mar	6-Mar	4-Mar	11-Mar	7-Mar	4-Mar	21-Feb	5-Mar		5-Mar	6-Mar	5-Mar
7	9-Mar	3-Mar	12-Mar	7-Mar	7-Mar	12-Mar	8-Mar	6-Mar	8-Mar	7-Mar		7-Mar	8-Mar	6-Mar
8	10-Mar	9-Mar	13-Mar	10-Mar	9-Mar	13-Mar	10-Mar	11-Mar	9-Mar	8-Mar		8-Mar	9-Mar	7-Mar
9	12-Mar	12-Mar	14-Mar	14-Mar	11-Mar	14-Mar	12-Mar	12-Mar	13-Mar	10-Mar		11-Mar	13-Mar	9-Mar
10	15-Mar	14-Mar	15-Mar	15-Mar	13-Mar	15-Mar	15-Mar	14-Mar	14-Mar	14-Mar		15-Mar	14-Mar	15-Mar
	effectively inoperable 22 Feb-1 Mar	effectively inoperable 22 Feb–1 Mar	effectively inoperable 22 Feb–1 Mar	effectively inoperable 22 Feb–1 Mar	effectively inoperable 22 Feb–1 Mar		effectively inoperable 22 Feb–1 Mar	effectively inoperable 22 Feb-1 Mar	effectively inoperable 22 Feb–7 Mar	effectively inoperable 22 Feb–1 Mar		effectively inoperable 17 Feb, 19 Feb–4 Mar, 6, 9–10, 12–14 Mar	effectively inoperable 22 Feb–1 Mar, 7, 10 Mar	effectively inoperable 22 Feb–1 Mar, 13 Mar
					28-d	ay Cycle 2	1: 16 March	– 12 Aprril	2023					
Sample Day	G29	G34	G35	G44	G45	G48	G49	G51	G56	G58	G59	G64	G67	G75
1	17-Mar	17-Mar	18-Mar	16-Mar	16-Mar	16-Mar	19-Mar	17-Mar	16-Mar	18-Mar		16-Mar	17-Mar	20-Mar
2	24-Mar	19-Mar	21-Mar	24-Mar	18-Mar	18-Mar	22-Mar	18-Mar	17-Mar	20-Mar		23-Mar	23-Mar	21-Mar
3	26-Mar	22-Mar	23-Mar	25-Mar	22-Mar	23-Mar	24-Mar	19-Mar	19-Mar	22-Mar		25-Mar	25-Mar	24-Mar
4	27-Mar	27-Mar	28-Mar	26-Mar	28-Mar	30-Mar	26-Mar	24-Mar	22-Mar	28-Mar		28-Mar	26-Mar	26-Mar
5	29-Mar	29-Mar	30-Mar	1-Apr	31-Mar	31-Mar	29-Mar	26-Mar	24-Mar	30-Mar		30-Mar	3-Apr	27-Mar
6	31-Mar	2-Apr	4-Apr	2-Apr	1-Apr	3-Apr	2-Apr	29-Mar	25-Mar	3-Apr		31-Mar	7-Apr	30-Mar
7	2-Apr	4-Apr	7-Apr	6-Apr	3-Apr	5-Apr	3-Apr	3-Apr	31-Mar	4-Apr		3-Apr	8-Apr	2-Apr
8	3-Apr	6-Apr	9-Apr	10-Apr	4-Apr	7-Apr	5-Apr	4-Apr	6-Apr	7-Apr		4-Apr	10-Apr	4-Apr
9	8-Apr	7-Apr	10-Apr	11-Apr	8-Apr	10-Apr	8-Apr	5-Apr	10-Apr	9-Apr		6-Apr	11-Apr	6-Apr
10	12-Apr	11-Apr	12-Apr	12-Apr	11-Apr	11-Apr	12-Apr	10-Apr	11-Apr	12-Apr		8-Apr	12-Apr	10-Apr
										mostly inoperable 1– 2 Apr	effectively inoperable 10–13 Apr	inoperable 17–20, 22 Mar, 2, 7, 9 Apr	inoperable 20, 25, 30 Mar	inoperable 7, 9, 12, 19, 21 Apr
					28-	day Cycle	22: 13 April	– 10 May 2	023					
Sample Day	G29	G34	G35	G44	G45	G48	G49	G51	G56	G58	G59	G64	G67	G75
1	13-Apr	14-Apr	14-Apr	14-Apr	13-Apr	14-Apr	13-Apr	13-Apr	13-Apr	13-Apr	13-Apr	13-Apr	13-Apr	14-Apr
2	15-Apr	15-Apr	16-Apr	15-Apr	17-Apr	16-Apr	14-Apr	15-Apr	14-Apr	14-Apr	14-Apr	16-Apr	17-Apr	15-Apr
3	18-Apr	17-Apr	20-Apr	16-Apr	18-Apr	17-Apr	16-Apr	16-Apr	15-Apr	15-Apr	15-Apr	18-Apr	18-Apr	18-Apr

4	20-Apr	20-Apr	21-Apr	19-Apr	19-Apr	21-Apr	17-Apr	18-Apr	16-Apr	17-Apr	16-Apr	21-Apr	20-Apr	20-Apr
5	21-Apr	21-Apr	22-Apr	23-Apr	20-Apr	22-Apr	19-Apr	19-Apr	17-Apr	20-Apr	17-Apr	23-Apr	21-Apr	25-Apr
6	23-Apr	22-Apr	24-Apr	24-Apr	21-Apr	23-Apr	21-Apr	22-Apr	18-Apr	21-Apr	18-Apr	24-Apr	23-Apr	26-Apr
7	25-Apr	24-Apr	25-Apr	25-Apr	23-Apr	24-Apr	24-Apr	24-Apr	20-Apr	22-Apr	19-Apr	25-Apr	25-Apr	27-Apr
8	26-Apr	25-Apr	26-Apr	28-Apr	25-Apr	25-Apr	25-Apr	28-Apr	23-Apr	23-Apr	20-Apr	27-Apr	26-Apr	28-Apr
9	27-Apr	27-Apr	27-Apr	29-Apr	28-Apr	27-Apr	27-Apr	29-Apr	27-Apr	25-Apr	21-Apr	28-Apr	28-Apr	29-Apr
10	30-Apr	30-Apr	29-Apr	30-Apr	29-Apr	28-Apr	30-Apr	30-Apr	28-Apr	30-Apr	22-Apr	30-Apr	29-Apr	30-Apr
	Entire	facility shut do	wn 1–24 May a	nd then no fund	tional deterren	t triggering unti	l 6 Jun		inoperable 22, 25–26 Apr		inoperable 22 Apr			Inoperable 19, 21 Apr
	Tenth 28-day Cycle: 11 May – 07 Jun 2023													
Sample Day	G29	G34	G35	G44	G45	G48	G49	G51	G56	G58	G59	G64	G67	G75
1														
2														
3														
4														
5														
6														
7														
8														
9		6-Jun		6-Jun	6-Jun		6-Jun	6-Jun						6-Jun
10	7-Jun	7-Jun	6-Jun	7-Jun	7-Jun	6-Jun	7-Jun	7-Jun	7-Jun	6-Jun	7-Jun	7-Jun	6-Jun	7-Jun
				mostly inoperable 7 Jun									no spinning records 7 Jun- 6 Jul	
		•			28-	day Cycle	24: 08 June	e – 05 July 2	023	•	•			
Sample Day	G29	G34	G35	G44	G45	G48	G49	G51	G56	G58	G59	G64	G67	G75
1	12-Jun	9-Jun	10-Jun	9-Jun	8-Jun	8-Jun	8-Jun	8-Jun	8-Jun	10-Jun	8-Jun	10-Jun		8-Jun
2	14-Jun	10-Jun	12-Jun	11-Jun	9-Jun	10-Jun	10-Jun	9-Jun	11-Jun	11-Jun	11-Jun	12-Jun		9-Jun
3	15-Jun	11-Jun	16-Jun	15-Jun	15-Jun	15-Jun	13-Jun	10-Jun	13-Jun	12-Jun	13-Jun	16-Jun		10-Jun
4	19-Jun	13-Jun	18-Jun	19-Jun	18-Jun	18-Jun	15-Jun	14-Jun	17-Jun	14-Jun	18-Jun	18-Jun		11-Jun
5	20-Jun	14-Jun	21-Jun	23-Jun	20-Jun	22-Jun	18-Jun	15-Jun	20-Jun	17-Jun	19-Jun	19-Jun		12-Jun
6	24-Jun	17-Jun	24-Jun	25-Jun	24-Jun	25-Jun	23-Jun	19-Jun	21-Jun	20-Jun	24-Jun	21-Jun		18-Jun
7	1-Jul	21-Jun	26-Jun	29-Jun	26-Jun	27-Jun	26-Jun	20-Jun	24-Jun	24-Jun	28-Jun	24-Jun		19-Jun
8	2-Jul	23-Jun	30-Jun	2-Jul	30-Jun	28-Jun	28-Jun	25-Jun	25-Jun	28-Jun	29-Jun	27-Jun		20-Jun
9	3-Jul	24-Jun	1-Jul	3-Jul	3-Jul	1-Jul	30-Jun	3-Jul	28-Jun	30-Jun	3-Jul	1-Jul		23-Jun
10	5-Jul	25-Jun	5-Jul	5-Jul	5-Jul	5-Jul	2-Jul	4-Jul	30-Jun	5-Jul	5-Jul	4-Jul		27-Jun
	effectively inoperable 21, 27–29 Jun		inoperable 19–20, 22 Jun	inoperable 8– 10, 26–28 Jun, 1 Jul	inoperable 4, 19 Jun			inoperable 5 Jul-27 Sep	inoperable 22–23 Jun		inoperable 14, 20 Jun, 2 Jul	inoperable 13, 15, 17, 26 Jun, 2 Jul		few spinning records 24 Jun-31 Aug

					28-d	ay Cycle 2	.5: 06 July –	02 August	2023					
Sample Day	G29	G34	G35	G44	G45	G48	G49	G51	G56	G58	G59	G64	G67	G75
1	6-Jul	6-Jul	6-Jul	6-Jul	6-Jul	6-Jul	6-Jul		6-Jul	6-Jul	7-Jul	6-Jul	6-Jul	6-J∪l
2	7-Jul	7-Jul	7-Jul	7-Jul	7-Jul	7-Jul	7-Jul		7-Jul	7-Jul	8-Jul	7-Jul	7-Jul	7-Jul
3	8-Jul	8-Jul	8-Jul	8-Jul	8-Jul	8-Jul	8-Jul		8-Jul	9-Jul	9-Jul	8-Jul	8-Jul	8-Jul
4	9-Jul	9-Jul	9-Jul	9-Jul	9-Jul	9-Jul	9-Jul		9-Jul	13-Jul	11-Jul	9-Jul	9-Jul	9-Jul
5	10-Jul	10-Jul	10-Jul	11-Jul	10-Jul	10-Jul	10-Jul		10-Jul	14-J∪l	12-Jul	10-Jul	10-Jul	10-Jul
6	11-Jul	11-Jul	11-Jul		11-Jul	11-Jul	11-Jul			18-Jul	13-Jul	11-Jul		11-Jul
7	12-Jul	12-Jul	12-Jul		12-Jul	12-J∪l	12-Jul			21-Jul	14-J∪l	12-Jul	12-Jul	12-Jul
8	13-Jul	13-Jul	13-Jul		13-Jul	13-Jul	13-Jul			22-Jul	20-Jul	13-Jul	13-Jul	13-Jul
9	14-Jul	14-J∪l	14-Jul		14-Jul	14-Jul				26-Jul	21-Jul	14-J∪l	14-Jul	15-Jul
10		2-Aug	2-Aug	2-Aug	2-Aug	2-Aug	2-Aug		2-Aug	31-Jul	2-Aug	2-Aug	2-Aug	2-Aug
	effectively inoperable most of 15 Jul– 2 Aug	effectively inoperable most of 15 Jul- 2 Aug	effectively inoperable most of 15 Jul- 2 Aug	inoperable 10, - 12 Jul–1 Aug	inoperable 15 Jul-1 Aug	Jul-1 Aug	inoperable 14 Jul-1 Aug e 26: 03-30	August 202	inoperable 11 Jul-1 Aug	inoperable 24–25 Jul, 1–2 Aug	inoperable 16–19, 22 Jul–1 Aug	inoperable most of 16 Jul– 1 Aug	no spinning records 7 Jun- 6 Jul, mostly inoperable 10 Jul, inoperable 11, 15 Jul-1 Aug	mostly no spinning records 24 Jun-31 Aug
Sample	G29	G34	G35	G44	G45	G48	G49	G51	G56	G58	G59	G64	G67	G75
Day 1	3-Aug	3-Aug	6-Aug	3-Aug	4-Aug	3-Aug	3-Aug		4-Aug	4-Aug	4-Aug	3-Aug	3-Aug	
2	4-Aug	5-Aug	7-Aug	6-Aug	5-Aug	6-Aug	5-Aug		5-Aug	6-Aug	5-Aug	5-Aug	5-Aug	
3	5-Aug	10-Aug	8-Aug	10-Aug	6-Aug	8-Aug	8-Aug		8-Aug	7-Aug	8-Aug	7-Aug	6-Aug	
4	10-Aug	12-Aug	9-Aug	11-Aug	7-Aug	9-Aug	12-Aug		9-Aug	11-Aug	9-Aug	10-Aug	7-Aug	
5	11-Aug	16-Aug	10-Aug	13-Aug	13-Aug	10-Aug	14-Aug		12-Aug	13-Aug	11-Aug	11-Aug	8-Aug	
6	14-Aug	19-Aug	11-Aug	16-Aug	17-Aug	13-Aug	17-Aug		13-Aug	15-Aug	13-Aug	13-Aug	07.09	
7	15-Aug	24-Aug	15-Aug	17-Aug	19-Aug	16-Aug	19-Aug		16-Aug	19-Aug	15-Aug	15-Aug		
8	16-Aug	26-Aug	16-Aug	24-Aug	24-Aug	24-Aug	24-Aug		25-Aug	25-Aug	17-Aug	19-Aug		
9	24-Aug	28-Aug	18-Aug	26-Aug	26-Aug	26-Aug	27-Aug		29-Aug	28-Aug	24-Aug	28-Aug		
10	29-Aug	29-Aug	19-Aug	29-Aug	30-Aug	28-Aug	28-Aug		30-Aug	29-Aug	26-Aug	30-Aug		
	few spinning records after 17 Aug, inoperable 20–23 Aug	inoperable 20–23 Aug	inoperable 20–23 Aug	inoperable 20-23 Aug	inoperable 10, 20–23 Aug	inoperable 20-23 Aug	inoperable 20-23 Aug		inoperable 20-23 Aug	inoperable 20–23 Aug	inoperable 20-23 Aug	inoperable 20–23 Aug	no spinning records 9 Aug-1 Sep	
					28-day	Cycle 27: 3	1 August – 2	27 Septem	ber 2023					
Sample Day	G29	G34	G35	G44	G45	G48	G49	G51	G56	G58	G59	G64	G67	G75
1	1-Sep	1-Sep	31-Aug	1-Sep	1-Sep	1-Sep	2-Sep		31-Aug	5-Sep	31-Aug	31-Aug	2-Sep	1-Sep
2	8-Sep	2-Sep	1-Sep	3-Sep	8-Sep	2-Sep	3-Sep		2-Sep	6-Sep	1-Sep	3-Sep	5-Sep	2-Sep

3	11-Sep	4-Sep	3-Sep	4-Sep	9-Sep	9-Sep	4-Sep	6-Sep	10-Sep	5-Sep	4-Sep	9-Sep	3-Sep
4	12-Sep	12-Sep	4-Sep	8-Sep	10-Sep	10-Sep	9-Sep	12-Sep	11-Sep	7-Sep	5-Sep	10-Sep	8-Sep
5	13-Sep	16-Sep	7-Sep	9-Sep	11-Sep	12-Sep	15-Sep	16-Sep	16-Sep	10-Sep	6-Sep	15-Sep	11-Sep
6	17-Sep	18-Sep	9-Sep	11-Sep	15-Sep	20-Sep	16-Sep	18-Sep	17-Sep	15-Sep	7-Sep	16-Sep	16-Sep
7	21-Sep	19-Sep	14-Sep	16-Sep	17-Sep	22-Sep	17-Sep	22-Sep	18-Sep	20-Sep	17-Sep	17-Sep	19-Sep
8	22-Sep	21-Sep	16-Sep	17-Sep	18-Sep	23-Sep	19-Sep	23-Sep	23-Sep	23-Sep	18-Sep	22-Sep	21-Sep
9	23-Sep	25-Sep	18-Sep	20-Sep	23-Sep	25-Sep	21-Sep	24-Sep	25-Sep	24-Sep	22-Sep	26-Sep	25-Sep
10	24-Sep	27-Sep	22-Sep	25-Sep	24-Sep	26-Sep	25-Sep	27-Sep	27-Sep	26-Sep	27-Sep	27-Sep	26-Sep
				inoperable 5, 13–14 Sep	inoperable 13–14, 19 Sep	inoperable 13–14 Sep	inoperable 13–14 Sep	Inoperable 9/13-14>>>>	Inoperable 9/12-14>>>>		Inoperable 9/1-2, part 9/8-9/16, 19- 21, 23-25	no spinning turbine records 8/9- 9/1, inoperable 9/3	Inoperable 9/9, 13, 15, 23

# Appendix C. Evaluation of GLMM Candidates Considered to Identify the Best Model Used to Represent Relationships Between the Probability of Confirmed and Probable Golden Eagles Triggering a DTBird Dissuasion Signal and Various Predictors

Fixed Effects Candidate Model <sup>1</sup>	AICc	ΔAICc
PDS ~ Treatment Group + Year + Time of Day + Wind Speed	282.3	-
PDS ~ Treatment Group + Year + Time of Day + Time of Day $^2$ + Wind Speed	282.8	0.5
PDS ~ Treatment Group + 28d Cycle + Time of Day + Wind Speed	283.2	0.9
PDS ~ Treatment Group + Time of Day + Wind Speed	283.4	1.1
PDS ~ Treatment Group + Year + Wind Speed	284.2	1.9
PDS ~ Treatment Group + Year + Time of Day	285.4	3.1
PDS ~ Treatment Group + Wind Speed	285.9	3.6
PDS ~ Treatment Group + Time of Day + Time of Day $^2$	286.0	3.7
PDS ~ Treatment Group + Year + Time of Day + Wind Speed + Cloud Cover + Treatment Group * Cloud Cover	286.4	4.1
PDS ~ Treatment Group + 28d Cycle + Time of Day + Wind Speed + Cloud Cover + Treatment Group * Cloud Cover	286.6	4.3
PDS ~ Treatment Group + Time of Day	287.1	4.8
PDS ~ Treatment Group + Year	287.7	5.4
PDS ~ Treatment Group + Time of Day + Time of Day $^2$ + Treatment Group *	289.1	6.8
Time of Day + Treatment Group $^*$ Time of Day $^2$		
PDS ~ Treatment Group * Time of Day	288.6	5.8
PDS ~ Treatment Group + 28d Cycle	288.9	6.1
PDS ~ Treatment Group * Year	289.2	6.4
Null model – random effects only	289.7	7.4
PDS ~ Treatment Group	290.2	7.9
PDS ~ Treatment Group * Wind Speed	290.2	7.9
PDS ~ Treatment Group * 28d Cycle	290.3	8.0
PDS ~ Treatment Group + Cloud Cover	291.7	9.4
PDS ~ Treatment Group * Cloud Cover	291.4	9.7
PDS ~ Treatment Group + FPs per Day	292.1	10.4
PDS ~ Treatment Group * FPs per Day	292.1	10.4

<sup>&</sup>lt;sup>1</sup> PDS = Probability of Dissuasion Signal being triggered, initially represented as predicted In(odds of response) and transformed to percentage probabilities using a standard conversion formula. All models also include Turbine and Turbine: Elapsed Days as random effects. Selected model is highlighted in green; null model in gray.

### Appendix D. Results of Backwards Selection Approach Used to Identify Selected GLMM Representing Relationships Between the Probability of Confirmed and Probable Eagles Triggering a DTBird Dissuasion Signal and Various Predictors

Fixed Effects Candidate Model <sup>1</sup>	AICc	ΔΑΙСα
PDS ~ Treatment Group + Year + Time of Day + Time of Day <sup>2</sup> + Wind Speed + Cloud Cover + FPs per Day + Treatment Group * Year + Treatment Group * Time of Day+ Treatment Group * Wind Speed + Treatment Group * Cloud Cover + Treatment Group * FPs per Day <sup>2</sup>	521.0	3.6
Drop Treatment Group * Time of Day (Drop1 LRT $P = 0.295$ ) <sup>3</sup>	520.1	2.7
Drop Treatment Group * Wind Speed (Drop1 LRT $P = 0.308$ )	519.1	2.1
Drop Treatment Group * Year (Drop1 LRT P = 0.273)	518.3	1.3
Drop Year (Drop1 LRT $P = 0.418$ )	517.0	-
Drop Wind Speed (Drop1 LRT P = 0.118)	517.4	0.4
PDS ~ Treatment Group + Time of Day + Time of Day <sup>2</sup> + Cloud Cover + FPs per Day + Treatment Group * Cloud Cover + Treatment Group * FPs per Day	517.4	0.4
Null Model – random effects only	535.7	18.7

<sup>&</sup>lt;sup>1</sup> PDS = Probability of Dissuasion Signal being triggered, initially represented as predicted In(odds of response) and transformed to percentage probabilities using a standard conversion formula. All models also include *TurbinelD* and *TurbinelD*: *Elapsed Days* as random effects. See text for variable descriptions. Selected model is highlighted in green; null model in gray.

<sup>&</sup>lt;sup>2</sup> Starting the selection process with 28d Cycle in place of Year led to the same end result.

<sup>&</sup>lt;sup>3</sup> Drop1 likelihood ratio chi-square test evaluating fit of model with and without the focal variable; a nonsignificant result indicates no significant influence on the dependent variable.

## Appendix E. Results of Backwards Selection Approach Used to Identify Selected GLMM Representing Relationships Between the Dwell Time of Confirmed and Probable Golden Eagles Around DTBird Installations and Various Predictors

Fixed Effects Candidate Model <sup>1</sup>	AICc	ΔAICc
Dwell Time ~ Treatment Group + 28d Cycle + Time of Day + Time of Day <sup>2</sup> + Wind Speed + Cloud Cover + FPs per Day + Treatment Group * Year + Treatment Group * Time of Day+ Treatment Group * Wind Speed + Treatment Group * Cloud Cover + Treatment Group * FPs per Day <sup>2</sup>	1680.6	15.6
Drop Treatment Group * 28d Cycle (Drop1 LRT $P = 0.472$ ) <sup>3</sup>	1679.0	14.0
Drop Treatment Group * Time of Day (Drop1 LRT $P = 0.418$ )	1677.7	12.7
Drop Treatment Group * Time of Day <sup>2</sup> (Drop1 LRT $P = 0.537$ )	1676.1	11.1
Drop Treatment Group * Cloud Cover (Drop1 LRT P = 0.455)	1672.7	7.7
Drop Cloud Cover (Drop1 LRT P = 0.893)	1667.3	2.3
Drop Treatment Group * Wind Speed (Drop1 LRT $P = 0.221$ )	1666.8	1.8
Drop Wind Speed (Drop1 LRT P = 0.682)	1665.0	-
Dwell Time $\sim$ Treatment Group + 28d Cycle + Time of Day + Time of Day $^2$ + FPs per Day + Treatment Group * FPs per Day	1665.0	-
Null Model – random effects only	1687.3	22.3

All models also include *TurbineID* and *TurbineID*: *Elapsed Days* as random effects. Selected model is highlighted in green; null model in gray. See text for variable descriptions.

<sup>&</sup>lt;sup>2</sup> Starting the selection process with Year in place of 28d Cycle led to a similar end result but with a slightly higher AICc score/worse fit

<sup>&</sup>lt;sup>3</sup> Drop1 likelihood ratio chi-square test evaluating fit of model with and without the focal variable; a nonsignificant result indicates no significant influence on the dependent variable.

Appendix F. Evaluation of GLMM Candidates Considered to Identify the Best Model Used to Represent Relationships Between the Dwell Time of Confirmed and Probable Eagles Around DTBird Installations and Various Predictors

Fixed Effects Candidate Model <sup>1</sup>	AICc	ΔΑΙСα
Dwell Time $\sim$ Treatment Group + 28d Cycle + Time of Day + Time of Day + FPs per Day + Treatment Group * FPs per Day	3161.9	-
Dwell Time $\sim$ Treatment Group + 28d Cycle + Time of Day + Time of Day    Treatment Group * 28d Cycle	3162.1	0.2
Dwell Time $\sim$ Treatment Group + 28d Cycle + Time of Day + Time of Day $^2$ + FPs per Day	3162.2	0.3
Dwell Time $\sim$ Treatment Group + 28d Cycle + Time of Day + Time of Day $^2$	3162.5	0.6
Dwell Time $\sim$ Treatment Group + Year + Time of Day + Time of Day <sup>2</sup>	3166.0	4.1
Dwell Time $\sim$ Treatment Group + Time of Day + Time of Day <sup>2</sup>	3167.5	5.6
Dwell Time ~ Treatment Group + 28d Cycle + Time of Day	3167.7	5.8
Dwell Time ~ Treatment Group + Time of Day + Time of Day $^2$ + Treatment Group * Time of Day + Treatment Group * Time of Day $^2$	3171.1	9.2
Dwell Time ~ Treatment Group + Year + Time of Day	3172.5	10.6
Dwell Time ~ Treatment Group * 28d Cycle	3174.8	12.9
Dwell Time ~ Treatment Group + Time of Day	3175.0	13.1
Dwell Time ~ Treatment Group + 28d Cycle	3175.1	13.2
Dwell Time ~ Treatment Group * Time of Day	3176.6	14.7
Dwell Time ~ Treatment Group * Year	3180.1	18.2
Dwell Time ~ Treatment Group + Year	3180.7	18.8
Dwell Time ~ Treatment Group + FPs per Day	3182.1	20.2
Dwell Time ~ Treatment Group * FPs per Day	3182.8	20.9
Dwell Time ~ Treatment Group	3184.7	22.8
Dwell Time ~ Treatment Group + Wind Speed	3185.0	23.1
Dwell Time ~ Treatment Group * Wind Speed	3186.5	24.6
Dwell Time ~ Treatment Group + Cloud Cover	3190.1	28.2
Null model – random effects only	3190.2	28.3
Dwell Time ~ Treatment Group * Cloud Cover	3192.7	30.8

All models also include *TurbineID* and *TurbineID*: *Elapsed Days* as random effects. Selected model is highlighted in green; null model in gray. See text for variable descriptions.



50 years of field notes, exploration, and excellence

**Research Report** 

Analysis of the Behavioral Responses of Eagles to DTBird® Audio Deterrents at a Commercial Wind-Energy Facility in Washington

Project #4080-01

Prepared for:

Renewable Energy Wildlife Institute

1990 K Street NW, Suite 620 Washington, D.C. 20006-1189

Prime Contractor: DOE Cooperative Agreement DE-EE0007883

Prepared by:

H. T. Harvey & Associates











#### **Executive Summary**

DTBird® is an automated detection and audio deterrent system designed to discourage birds from entering the rotor swept zone (RSZ) of spinning wind turbines. As part of a multi-faceted research program conducted in collaboration with the Renewable Energy Wildlife Institute, we previously conducted site-specific analyses of of DTBird performance based on seven systems installed and operated for the first time at the Manzana Wind Power Project in southern California, USA. We then expanded the research with funding from the U. S. Department of Energy to include comparative assessments and expanded research involving 14 DTBird systems installed and operated for the first time at the Goodnoe Hills Wind Farm in south-central Washington, USA. The overarching goal of this research is to evaluate the effectiveness of DTBird in detecting and discouraging golden eagles (*Aquila chrysaetos*) and other large raptors from approaching the RSZ of operating wind turbines.

Herein we present a new initial site-specific analysis of the behavioral responses of eagles and other large raptors to the audio deterrents broadcasted by the DTBird systems operated at the Goodnoe Hills study site. Based on results from the Manzana pilot study, a performance metric was established to gauge the comparative effectiveness of the DTBird systems in deterring eagles and other large raptors from entering the RSZ of spinning turbines at the Goodnoe Hills site. The established performance metric stipulated that the Goodnoe Hills DTBird systems should result in at least a 53% rate of successful deterrence for golden eagles. Because it is often difficult to confidently identify the species and to precisely gauge the behavioral responses (e.g., flight diversion angles) of birds evident in DTBird videos, this metric was based on (a) combining data for confirmed and probable golden eagles, and (b) including both confirmed and potentially successful deterrence events in the "successful" category.

This new Goodnoe Hills assessment differed in one key way from the similar Manzana pilot-study analysis we conducted previously, in that the broader experimental research agenda for the expanded study presented the opportunity for conducting a control-treatment evaluation at the Goodnoe Hills site that supported distinguishing between the deterrence effects of spinning turbines alone versus spinning turbines plus audio deterrents.

In brief, the results of this new investigation confirmed matching or greater values (53–100%) for all analyzed species groups (i.e., all large raptors, all probable eagles, probable golden eagles, and probable bald eagles) and types of deterrent signals (warning signals and more raucous dissuasion signals triggered at close distance from the turbine) in comparison to the established performance metric. Broadcasted deterrents consistently resulted in at least a doubling of the proportion of cases where a successful or potentially successful response was evident compared to when no signals were actually broadcasting. The differential patterns of responses for the four analyzed groups were largely similar, but smaller sample sizes limited the demonstration of statistical significance for species-specific analyses. Nevertheless, eagles appeared to exhibit at least slightly greater sensitivity to the deterrents than the larger all large raptors group, which included representative samples of vultures and buteos. Further, though limited by modest samples sizes, the results also suggested that bald eagles were more sensitive to the deterrents than golden eagles.

i

### **Table of Contents**

Executive	Summary	i
Section 1.	Introduction	1
Section 2.	Methods	2
2.1 Stud	ly Site and DTBird Installations	2
	Bird System Operation	
2.3 Clas	sifying Responses to Deterrents	4
2.4 Ana	lyses	6
Section 3.	Results	7
3.1 Sam	pling Results	7
3.2 Res	ponse to Deterrents	7
Section 4.	Discussion	12
Section 5.	References	14
Figures		
Figure 1.	Layout of Goodnoe Hills Wind Farm in south-central Washington showing the locations of installed DTBird systems and where UAV flight trials were conducted	2
Figure 2.	Depiction of DTBird video camera and broadcast speaker locations on turbines at the Goodnoe Hills Wind Farm.	3
Tables		
Table 1.	DTBird events recorded from September 2012 though August 2022 at the Goodnoe Hills Wind Farm in Washington that formed the basis for assessing the behavioral responses of eagles and other large raptors to DTBird audio deterrents	7
Table 2.	Classification of deterrent responses by treatment group and risk level for all analyzed cases, including all confirmed, probable, and possible eagles, plus representative samples of vultures and buteos	8
Table 3.	Classification of deterrent responses by treatment group and risk level for all probable eagles.	9
Table 4.	Classification of responses to deterrent signals for confirmed and probable golden eagles in relation to treatment group.	
Table 5.	Classification of responses to deterrent signals for confirmed and probable golden eagles in relation to treatment group.	10
Table 6.	Percentages of responses to broadcasting deterrents classified as successful or potentially successful for different species groups at the Goodnoe Hills.	12

#### **List of Primary Preparers**

Jeff P. Smith, Ph.D., Associate Wildlife Ecologist—Project Manager Stephanie R. Schneider, M.S., Wildlife and Quantitative Ecologist

Scott B. Terrill, Ph.D., Principal in Wildlife Ecology and Senior Ornithologist—Principal-in-Charge

#### **Section 1. Introduction**

DTBird® (Liquen Consultoría Ambiental, S.L., Madrid, Spain; hereafter "Liquen") is an automated detection and audio deterrent system designed to discourage birds from entering the rotor swept zone of spinning wind turbines (see <a href="https://dtbird.com">https://dtbird.com</a>). DTBird can also include an automated turbine control-stop module that was not installed as part of the systems evaluated herein. Funded by the American Wind Wildlife Institute (now the Renewable Energy Wildlife Institute [REWI]), H. T. Harvey & Associates (2018) previously analyzed the performance of seven DTBird systems operated for the first time at the Manzana Wind Power Project in southern California. Following this pilot study, we continued the research in collaboration with REWI, funded by the U.S. Department of Energy, by augmenting some of the pilot-study analyses and expanding the investigations to a second facility: the Goodnoe Hills Wind Farm in south-central Washington (H. T. Harvey & Associates 2019a).

The ultimate goal of this research is to quantify the effectiveness of DTBird as a measure to reduce collision risk for golden eagles (*Aquila chrysaetos*) and other large raptors. If found to be effective and accepted by the U.S. Fish and Wildlife Service (USFWS), DTBird could be considered for use by commercial wind energy facilities in conservation plans, as a best management practice under the Bald and Golden Eagle Protection Act (Eagle Act) (16 U.S.C. §668–668c), as a minimization measure for take permits or habitat conservation plans, or as an adaptive management measure.

In this report, we present an analysis of the behavioral responses of golden eagles, bald eagles (*Haliaeetus leucocephalus*), and other large raptors to the audio deterrents broadcasted by the DTBird systems at the Goodnoe Hills Wind Farm, based on one year of data collection from September 2021 through August 2022. The response data were derived from reviewing detection and tracking videos recorded in the online digital analysis platform (DAP) database maintained by Liquen for this project. Our approved study plan for this overall project (H. T. Harvey & Associates 2019a) established a performance standard for this behavioral-response analysis of a 53% successful or potentially successful deterrence rate. Here it is important to recognize that this performance metric was based on the results of our pilot study at the Manzana Wind Power Project in California, which did not involve a control-treatment design to facilitate distinguishing between behavioral responses with and without the deterrents broadcasting. Therefore, evaluating the Goodnoe Hills data in relation to this performance metric must be constrained to comparing the deterrence rate for cases where the deterrents were broadcasting; however, the control-treatment design of the Goodnoe Hills investigation will shed new light on the degree to which the observed responses reflected reactions to the spinning turbines alone versus spinning turbines plus broadcasted audio deterrents.

1

#### Section 2. Methods

#### 2.1 Study Site and DTBird Installations

The Goodnoe Hills Wind Farm has been in operation since 2008 and currently comprises 47 2.2 MW Vestas V110 Mark C and B wind turbines, with a hub height of 87 m and a rotor-swept diameter of 110 m located in south-central Washington atop an east-west ridgeline flanking the Columbia River approximately 3–6 km away (Figure 1). The topography descends steeply south of the ridgeline approximately 610 meters (m) to the Columbia River and more gradually to the north approximately 500 m down into Rock Creek Canyon and associated riparian corridors. The project area is dominated by a mosaic of grazed grassland and shrubsteppe, with inclusions of ponderosa pine (*Pinus ponderosa*) and Oregon white oak (*Quercus garryana*) woodlands on the ridge's north-facing slopes.

Fourteen DTBird systems were installed at this facility to support this research (Figure 1). We spread the installations around the outer perimeter of the overall facility with sufficient spacing to minimize the potential for target raptors to be simultaneously exposed to multiple deterrent signals.

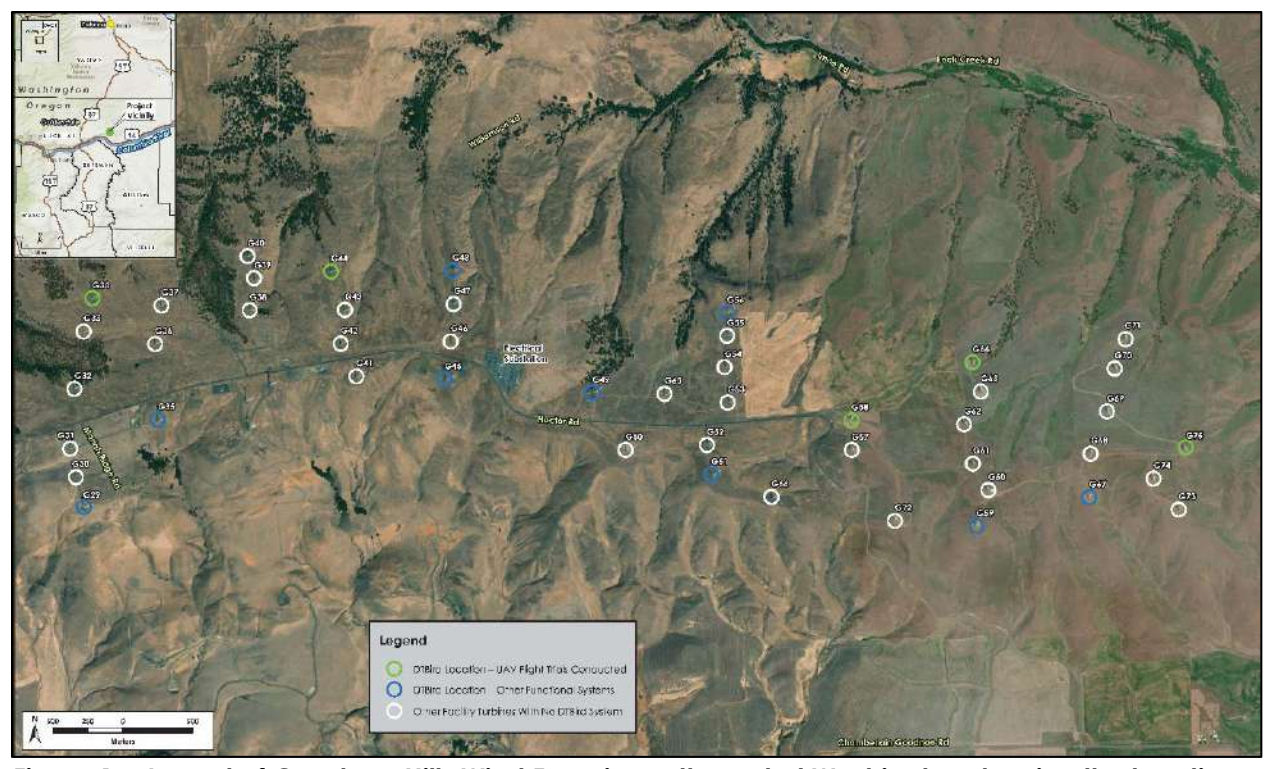


Figure 1. Layout of Goodnoe Hills Wind Farm in south-central Washington showing the locations of installed DTBird systems and where UAV flight trials were conducted.

#### 2.2 DTBird System Operation

A detailed description of the DTBird system set up and operation can be found in H. T. Harvey & Associates (2018). Each turbine-specific DTBird monitoring system comprised four video cameras (6-megapixel resolution) installed on the turbine tower approximately 5 m off the ground, which surveilled the skies throughout daylight hours, and two rings of four broadcast speakers installed on the tower just below the lower rotor swept zone and just below hub height (Figure 2).

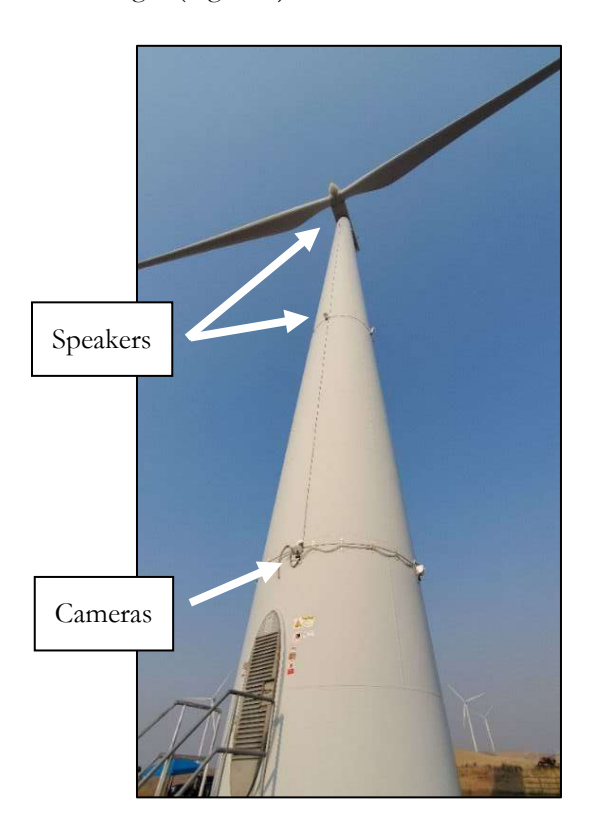


Figure 2. Depiction of DTBird video camera and broadcast speaker locations on turbines at the Goodnoe Hills Wind Farm.

When a DTBird system first detects a targeted object, it creates a new event record in the DAP and records a timestamp for the initial *detection* event along with other limited data. If a targeted object subsequently or simultaneously triggers one or both of the deterrent signals (early *warning* or a more raucous *dissuasion* signal if a target approaches closer to the turbine) information is added to the same DAP event record to document the unique timestamps and signal durations for each deterrent-triggering event. Each event record ultimately has attached to it video clips representing the four cameras, which the system extracts to begin 10 seconds before targeting began and continue for 30 seconds after the last targeted object exits the detection envelope. There must be no objects targeted for at least 26 seconds before a given DTBird system can initiate a new event record. If a system targets multiple objects concurrently during the same event period, timestamps are recorded only for the first detection, warning-trigger, and dissuasion-trigger events, and those respective events may not be triggered by the same object. In these cases, it can be difficult to determine exactly which bird or object was responsible for the timestamped events.

For the purpose of the overall Goodnoe Hills DTBird performance assessment (H. T. Harvey & Associates 2019a), the DTBird-equipped turbines were operated on a schedule whereby, on a given day, approximately half of the operating units were run with the deterrent signals triggered virtually but not actually broadcasting, while the other half were operating normally with the deterrents broadcasting. The suite of DTBird units operating in each mode varied on daily basis according to a stratified, randomized schedule that sought to equitably distribute broadcasting and non-broadcasting units across the facility each day. This experimental setup (design to support another overall project objective) provided an ideal circumstance for composing a control-treatment design for the behavioral analyses represented here. That is, our data-entry technicians reviewed all relevant videos without knowledge of whether or not a given DTBird unit was actually broadcasting the triggered deterrent signals. The motivation for this "deaf"-trial assessment acknowledged that approaching birds may divert their flight in response to the presence of spinning blades alone. The implemented control-treatment design provided a means of comparing the patterns of responses with and without the deterrents broadcasting, and thereby isolating responses to the broadcasted deterrents.

#### 2.3 Classifying Responses to Deterrents

The dataset we developed for this analysis was based on DTBird records that we randomly selected for evaluation to compose a larger experimental analysis (H. T. Harvey & Associates 2018), which entailed selecting 10 days per 28-day period (the cycling schedule for the larger experiment) across a full year and classifying all detected targets on those days. For evaluating the responses of *in situ* raptors to the deterrent signals, we applied a standardized approach to classifying the responses of all confirmed, suspected, and possible eagles, as well as samples of confirmed turkey vultures (*Cathartes aura*) and buteos for comparison. As described in the previous section, multiple birds occurring simultaneously in the viewsheds of a system's cameras typically confounded rendering precise temporal correlations between detectable changes in the flight behavior of individual birds and the broadcasting of specific warning and dissuasion signals (as reflected in specific triggering timestamps recorded in the DAP). For this reason, we generally excluded event records with multiple birds in view from our deterrence-response classification efforts, as did May et al. (2012). In a few such cases, however, the deterrent signaling could be unambiguously associated with an individual bird of interest, which generally meant the bird was traveling more or less alone and was clearly the only individual that was in a position to trigger the relevant deterrent signal.

Our sampling objective was to amass a temporally and taxonomically representative dataset sufficient to support a robust assessment of the probability of effective deterrence for *in situ* eagles and other large raptors as a group, reasonable independent assessments for all probable golden eagles, all probable bald eagles, and all probable eagles combined, and representative samples of probable turkey vultures and buteos (mostly red-tailed hawks [*Buteo jamaicensis*] year-round and rough-legged hawks [*B. lagopus*] during winter).

To classify deterrence responses, we used the DAP and an on-screen protractor (Straffi 2016) to determine through 2D on-screen measurements whether a bird's flight path appeared to diverge appreciably and away from the RSZ within 5 sec of a warning or dissuasion signal being emitted. For comparative purposes, similar to the approach Liquen personnel typically use to classify deterrence responses, we considered a sustained flight

path divergence of >15° away from the deterrent signal that precluded further passage toward the spherical RSZ of the turbine as indicative of a meaningful avoidance response. We also examined the video footage for evidence of correlations between detectable changes in flapping pattern or flight style and emittance of warning and dissuasion signals.

H. T. Harvey & Associates (2018: Appendix A) contains a step-by-step account of the classification process we used to categorize the responses of relevant raptors to the deterrent signals. The process incorporated several subjective and objective criteria for classifying the behavioral response of a given raptor upon exposure to a warning signal and/or dissuasion signal, culminating in a final classification of the response as one of the following:

- Y: Yes reacted in a way that, based on the change in flight pattern and direction, reduced the risk of collision with the turbine blades
- P: Potential appeared to react to signal, but response was not definitive enough to be confident that the bird was at less risk after signal emission
- N: No reacted to signal (e.g., temporarily altered its flapping rate) but did not alter its flight path away from RSZ
- Z: Not relevant did not visibly react to signal
- U: *Unknown/undetermined* bird was already moving away from the turbine when the signal was emitted; the video quality or bird image quality was not favorable for determining the 3D reaction of the bird on the 2D video screen; or it simply was not possible to determine with any sense of confidence whether a reaction occurred or not due to other factors.

We excluded from further consideration all cases where we classified the response as "unknown/undetermined."

Along with evaluating behaviors and flight trajectories to classify a bird's response pattern when it triggered a deterrent signal, we classified the potential collision risk the bird was facing prior to triggering a deterrent as follows:

- a. High moving toward turbine on a trajectory and at an altitude that could take it near the current RSZ (defined for this purpose as the current, approximate 2D plane of rotation).
- b. Medium moving toward turbine on a trajectory and at an altitude that may take it near the turbine, but likely either below or above the RSZ.
- c. Low moving perpendicular to or away from the turbine distant from the RSZ, or at high altitude well above the RSZ.

#### 2.4 Analyses

To evaluate differences in the categorical response rates among the control and treatment groups, we used 2-way Pearson chi-square analyses performed using the base R package (R Core Team 2023), with treatment group and the four deterrent response categories as the two classification variables. We prepared analyses for all analyzed cases, all probable eagles, all probable golden eagles, and all probable bald eagles. In some cases, cell sample sizes were small, but Pearson chi-square is known to be robust as long as expected cell frequencies exceed 1.0 (Jeffreys 1939) and our preliminary investigations showed no notable differences in outcome using the alternative Fisher's Exact Test. At this juncture, we did not strive to develop a more complicated 3-way statistical model that included consideration of relative collision risk prior to deterrent triggering as a third predictor (H. T. Harvey & Associates 2018). Increasingly sparse sample matrices will further complicate such analyses, but we do expect to explore additional possibilities here in preparing the final multi-site assessment that will form our Milestone 10.3 deliverable for this overall project due this fall. We do, however, provide raw outcome data tables herein that illustrate the relevant samples collected in relation to our classifications of relative risk and provide initial insight about relevant patterns of interest for all large raptors combined and all probable eagles combined (small sample sizes precluded meaningful assessments for either eagle species alone).

#### Section 3. Results

#### 3.1 Sampling Results

Table 1 summarizes the classified large-raptor deterrent events that we extracted from the DAP and analyzed for this assessment.

Table 1. DTBird events recorded from September 2012 through August 2022 at the Goodnoe Hills Wind Farm in Washington that formed the basis for assessing the behavioral responses of eagles and other large raptors to DTBird audio deterrents.

Species <sup>1</sup>	Deterrents Broadcasting	Deterrents Muted	Total
Golden Eagle	33	45	78
Bald Eagle	14	25	39
Unknown Eagle	11	9	20
Turkey Vulture	52	54	106
Buteo <sup>1</sup>	52	55	107
Unknown Eagle/Vulture	41	52	93
Unknown Eagle/Buteo	19	28	47
Total	222	268	490

<sup>1</sup> Classifications represent all cases where we either confirmed or strongly suspected involvement of the relevant species or species group.

#### 3.2 Response to Deterrents

Given large numbers of cases where we could not confidently classify the species of the raptors detected and tracked by the DTBird systems (e.g., see H. T. Harvey & Associates 2019b, 2022a, 2022b), we began our assessment by examining the deterrent response patterns reflected in all 490 cases involving large raptors that we analyzed (Table 2). These cases consistently indicated that confirmed successful responses were far more likely to occur when the deterrents were actually broadcasting (33–36% of relevant cases) than when they were muted (6–7%). Apparently successful responses also occurred when the deterrents were not broadcasting, however, suggesting that the spinning blades alone also sometimes elicited successful avoidance behavior. Overall, we classified 22–27% of the analyzed cases as potentially successful responses, and the percentages of cases classified as such were slightly higher for the treatment group (deterrents broadcasting; 26–29% of relevant cases) versus the control group (deterrents muted; 19–25%).

The percentages of cases where a bird appeared to respond when a deterrent was triggered by briefly flinching or changing its flight style, but ultimately did not alter is pathway toward the RSZ, also were marginally higher for the treatment group (7% of relevant cases) compared to the control group (4–6%). In contrast, the percentages of birds that showed no evidence of responding to the triggering of deterrent signals were much lower for the treatment group (30–34%) than for the control group (65–68%).

<sup>&</sup>lt;sup>2</sup> Primarily red-tailed hawks year-round and rough-legged hawks during winter.

Table 2. Classification of deterrent responses by treatment group and risk level for all analyzed cases, including all confirmed, probable, and possible eagles, plus representative samples of vultures and buteos.

	Treatment Group / Risk Level								
	Deterrent Broadcasting			Deterrent Muted <sup>1</sup>			– — Grand		
Warning Response	High	Medium	Low	Total	High	Medium	Low	Total	Total
Successful	3	12	18	33	0	5	3	8	41
Potentially Successful	1	14	17	32	0	10	23	33	65
Ineffective	0	2	6	8	0	1	4	5	13
No Response	0	9	28	37	4	19	64	87	124
Total Cases	4	37	69	110	4	35	94	133	243
Dissuasion Response									
Successful	7	30	13	50	4	5	3	12	62
Potentially Successful	7	18	11	36	8	11	15	34	70
Ineffective	5	3	2	10	5	4	1	10	20
No Response	7	21	14	42	16	46	59	121	163
Total Cases	26	72	40	138	33	66	78	177	315

<sup>1</sup> With the deterrent muted, any apparent responses are presumed to have been elicited by the spinning turbine alone.

The chi-square analyses for all large raptors combined indicated highly significant overall tests for both warning signals ( $\chi^2 = 34.24$ , df = 3, P < 0.0001) and dissuasion signals ( $\chi^2 = 57.69$ , df = 3, P < 0.0001). Bonferroniadjusted post-hoc comparisons further confirmed that, for both warning and dissuasion signals, "Successful" deterrent responses were far more likely to occur when the deterrents were broadcasting, whereas "No Response" was far more likely to occur when the deterrents were not broadcasting (P < 0.0001 in both cases). In contrast, the proportions of cases classified is "Potentially Successful" or "Ineffective" responses did not differ significantly between the control and treatment groups for either signal type (P > 0.40).

Broken down further in relation to classified collision risk, the raw percentage results for the all large raptors dataset suggested that the probability of a successful or potentially successful response to a broadcasted warning signal was highest for birds at high risk of entering the RSZ (100% of relevant cases, but a small sample size), lower for birds at medium risk (70%), and lower still for birds at low risk of entering the RSZ (51%) (Table 2). In contrast, with the deterrents muted, no birds at high risk exhibited a detectable response when a warning signal was triggered virtually, and notably lower percentages of the documented cases exhibited apparently or potentially successful responses when birds were at medium risk (43%) or low risk (27%). The results for broadcasted dissuasion signals differed from the indicated pattern for broadcasted warning signals in suggesting that a lower 54% of birds at high risk and a higher 61% of birds at low risk exhibited successful or potentially successful responses, whereas the proportion of birds at medium risk that exhibited such responses (67%) was similar to the proportion that responded favorably to warning signals.

Focusing in on cases involving all confirmed and probable eagles showed similar patterns as for all large raptors combined (Table 3). The probability of a successful or potentially successful response to a broadcasted warning signal was highest for birds at high risk (100%), lower for birds at medium risk (82%), and lower still for birds at low risk (58%) of entering the RSZ (Table 3). In contrast, with the deterrents muted, no birds at high risk exhibited a detectable response when a warning signal was triggered virtually, and notably lower percentages of the documented cases exhibited apparently or potentially successful responses when birds were at medium risk (39%) or low risk (34%). The results for broadcasted dissuasion signals suggested a similar pattern as for broadcasted warning signals, but the percentages of successful or potentially successful responses were unexpectedly lower for all risk categories (51% for high risk, 72% for medium risk, and 9% for low risk).

Table 3. Classification of deterrent responses by treatment group and risk level for all probable eagles.

	Treatment Group / Risk Level								
	D	Deterrent Broadcasting			Deterrent Muted <sup>1</sup>			_ _ Grand	
Warning Response	High	Medium	Low	Total	High	Medium	Low	Total	Total
Successful	2	7	3	12	0	3	1	4	16
Potentially Successful	0	7	4	11	0	4	6	10	21
Ineffective	0	0	2	2	0	0	0	0	2
No Response	0	3	3	6	1	11	15	27	33
Total Cases	2	17	12	31	1	18	22	41	72
Dissuasion Response									
Successful	3	8	0	11	0	1	0	1	12
Potentially Successful	1	5	3	9	0	8	2	10	19
Ineffective	3	1	1	5	1	0	1	2	7
No Response	1	4	3	8	5	16	19	40	48
Total Cases	8	18	7	33	6	25	22	53	86

<sup>1</sup> With the deterrent muted, any apparent responses are presumed to have been elicited by the spinning turbine alone.

The chi-square analyses of the all probable eagles dataset indicated highly significant overall tests for both warning signals ( $\chi^2 = 18.12$ , df = 3, P = 0.0004) and dissuasion signals ( $\chi^2 = 27.86$ , df = 3, P < 0.0001). Bonferroni-adjusted post-hoc comparisons confirmed that the proportion of successful responses to warning signals was not significantly higher for the control group but approached significance (P = 0.0455 compared to a Bonferroni-corrected target value of 0.0125) and confirmed a significantly higher proportion of successful responses for dissuasion signals when broadcasted versus muted (P = 0.0039). In addition, for both analyses, post-hoc comparisons confirmed that the proportions of no responses were much higher when the deterrents were not broadcasting ( $P \le 0.0002$ ). In contrast, similar to the results for all large raptors combined, the proportions of cases classified as potentially successful or ineffective responses did not differ significantly between the control and treatment groups (P > 0.157).

Smaller samples sizes confounded independently focusing on confirmed and probable golden eagles and bald eagles as distinct groups, but suggested that golden eagles exhibited a lower overall sensitivity to broadcasted signals (53–68% successful or potentially successful deterrence; Table 4) than did bald eagles (89–100%; Table 5). In addition, similar to the scenario portrayed for all large raptors combined, 23–38% of the relevant cases involving golden eagles and 18–42% of the relevant cases involving bald eagles showed apparently successful or potentially successful deterrence when the deterrents were not broadcasting.

Table 4. Classification of responses to deterrent signals for confirmed and probable golden eagles in relation to treatment group.

Classified Response	Warning	Signal	Dissuasion Signal		
	Broadcasting	Muted	Broadcasting	Muted	
Successful	6	2	6		
Potentially Successful	7	7	4	7	
Ineffective	0	0	5	2	
No Response	6	15	4	22	
Total Cases	19	24	19	31	

Table 5. Classification of responses to deterrent signals for confirmed and probable bald eagles in relation to treatment group.

Classified Response	Warning S	Signal <sup>1</sup>	Dissuasion Signal <sup>1</sup>		
	Broadcasting	Muted	Broadcasting	Muted	
Successful	3	2	4	1	
Potentially Successful	3	3	4	2	
Ineffective	0	0	0	0	
No Response	0	7	1	14	
Total Cases	6	12	9	17	

The suggested patterns of responses for all probable golden eagles were similar to the patterns indicated for all large raptors combined and all eagles combined. However, for warning signals the chi-square analysis for probable golden eagles indicated only a marginally significant overall test ( $\chi^2 = 5.35$ , df = 2, P = 0.069) and Bonferroni-adjusted post-hoc comparisons confirmed no significant contrasts for the control versus treatment groups within response categories. In contrast, the chi-square analysis for probable golden eagles responding to dissuasion signals indicated a highly significant overall test ( $\chi^2 = 18.77$ , df = 3, P = 0.0003), with post-hoc comparisons indicating that the higher percentage of successful and potentially successful responses for the control group versus the treatment group was only marginally significant (P = 0.0143 compared to a Bonferroni-corrected target value of 0.0125), whereas the much higher percentage of no responses for the treatment group was highly significant (P < 0.0004).

The chi-square analysis results for probable bald eagles were similar to the results for probable golden eagles. For warning signals, the overall test was only marginally significant ( $\chi^2 = 5.85$ , df = 2, P = 0.0537), but post-

hoc comparisons suggested that the higher percentage of no responses when the deterrents were muted exceeded the Bonferroni-corrected threshold for significance (P = 0.0082). For dissuasion signals, the overall test was significant ( $\chi^2 = 12.451$ , df = 2, P = 0.0020), and post-hoc comparisons suggested that the higher percentage of no responses when the deterrents were muted was highly significant (P = 0.0008).

For both probable golden eagles and probable bald eagles, smaller sample sizes likely precluded demonstrating higher degrees of significance for some of the comparisons described above, and precluded conducting meaningful statistical comparisons with the classifications further broken down according to classified risk levels.

#### Section 4. Discussion

The 53% estimate of "successful" deterrence from the pilot study, which formed the performance metric of interest here, was derived as the proportion of responses that were either confirmed or potentially successful with the deterrents broadcasting (H. T. Harvey & Associates 2018). The comparative estimates from this new Goodnoe Hills study for the analyzed subgroups are summarized in Table 6, all of which matched or exceeded the 53% performance metric.

Table 6. Percentages of responses to broadcasting deterrents classified as successful or potentially successful for different species groups at the Goodnoe Hills.

Species Group	Warning Signal	Dissuasion Signal
All Large Raptors	59	62
All Probable Eagles	74	61
Probable Golden Eagles	68	53
Probable Bald Eagles	100	89

The control-treatment setup for the Goodnoe Hills study provided further insight about the degree to which responses to spinning turbines and broadcasting audio deterrents contributed to these statistics. For all large raptors combined, the warning signal data indicated a 31% successful or potentially successful response proportion due to spinning turbines alone (control group) and a comparative 59% positive responses to the combination of a spinning turbine and broadcasting deterrent (treatment group). This suggests that broadcasted warning signals almost doubled the positive response rate. The comparison for dissuasion signals suggested a slightly greater benefit, with broadcasted signals resulting in 62% successful or potentially successful responses versus 26% with the deterrents muted.

The same general pattern was shown for all probable eagles combined, with the differences between the control and treatment groups slightly greater than for all large raptors combined: 36% presumed successful responses for the control group versus 74% for the treatment group for warning signals, and 21% control versus 61% treatment for dissuasion signals. This suggests that eagles tended to be more sensitive to the deterrents than vultures and buteos.

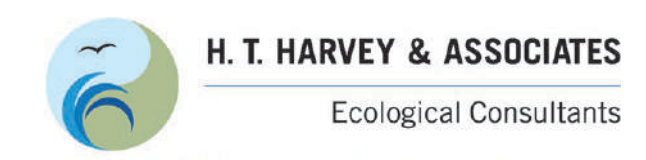
The same general patterns were evident based on the independent assessments for all probable golden eagles and all probable bald eagles, but suggested variable sensitivity for the two species. The magnitudes of the effects indicated for golden eagles (38% control vs. 68% treatment for warning signals; 23% vs. 53% for dissuasion signals) were substantially similar to the results for all large raptors combined and all probable eagles. In contrast, the results for bald eagles suggested greater sensitivity to broadcasted signals (42% control vs. 100% treatment for warning signals; 18% vs. 89% for dissuasion signals); however, smaller sample sizes for confirmed and probable bald eagles may limit the value of this comparison.

In summary, the results of this new Goodnoe Hills analysis yielded the following key results and insights:

- 1) Limited to the same manner of comparisons that formed the basis for the established performance metric, the proportions of analyzed cases that reflected a successful or potentially successful deterrence response when both the focal turbine was spinning and the deterrents were broadcasting consistently (53–100%) matched or exceeded the established 53% performance metric for all analyzed species groups and for both warning and dissuasion signals.
- 2) Based on the comparative control-treatment results and for all analyzed groups and species, broadcasted deterrents consistently resulted in at least a doubling of the proportion of cases where a successful or potentially successful response was evident.
- 3) The patterns of differential response classifications for the control and treatment groups were largely similar across the four analyzed groups and species; however, smaller sample sizes more often precluded confirming significant results for independent assessments of probable golden eagles and probable bald eagles.
- 4) Results for all four analyzed species groups consistently indicated that confirmed successful responses to the deterrents were more common (with variable levels of statistical significance) when the deterrent signals were actually broadcasting, and that birds exhibiting no apparent response at the time a deterrent was triggered were always significantly more common when the deterrents were triggered virtually but the signals were muted (i.e., not broadcasting at all).
- 5) At this juncture, sparsely distributed samples hindered expanding the statistical analysis to a 3-way classification analysis with level of risk prior to deterrence triggering as a third classification variable. Nevertheless, preliminary examinations of raw classification totals suggested that birds classified as at moderate risk of entering the RSZ generally were the most likely to exhibit discernable positive responses to broadcasted deterrents, while birds classified as at low risk were the least likely to do so. In comparison, the results for birds classified as at high risk were more equivocal, especially regarding responses to dissuasion signals (a much more raucous signal triggered at closer distances to the turbine compared to warning signals). Reasons for this pattern are uncertain but could suggest that birds are more likely to exhibit a discernable positive response to the deterrents when they are still far enough away to have plenty of time to react favorably.

#### Section 5. References

- H. T. Harvey & Associates. 2018. Evaluating a Commercial-Ready Technology for Raptor Detection and Deterrence at a Wind Energy Facility in California. Research Report. Los Gatos, CA, USA. Prepared for the American Wind Wildlife Institute, Washington, D.C., USA
- H. T. Harvey & Associates. 2019a. Evaluating the Effectiveness of a Detection and Deterrent System in Reducing Eagle Fatalities at Operational Wind Facilities: Detailed Study Plan. Los Gatos, CA, USA. Prepared for the American Wind Wildlife Institute, Washington, D.C., USA, in conjunction with U.S. Department of Energy Cooperative Agreement DE-EE0007883.
- H. T. Harvey & Associates. 2019b. Analysis of DTBird False Positive Detections at the Manzana Wind Power Project Through October 2017. Research Report. Los Gatos, CA, USA. Prepared for the American Wind Wildlife Institute, Washington, D.C., USA, in conjunction with U.S. Department of Energy Cooperative Agreement DE-EE0007883.
- H. T. Harvey & Associates. 2022a. Initial Analysis of DTBird False Positive Detections at the Goodnoe Hills Wind Farm, Washington: September 1, 2021 March 15, 2022. Research Report. Los Gatos, CA, USA. Prepared for the Renewable Energy Wildlife Institute, Washington, D.C., USA, in conjunction with U.S. Department of Energy Cooperative Agreement DE-EE0007883.
- H. T. Harvey & Associates. 2022b. Initial Analyses of DTBird Detection and Deterrent-Triggering Response Distances and Probability of Detection at the Goodnoe Hills Wind Farm, Washington. Research Report. Research Report. Los Gatos, CA, USA. Prepared for the Renewable Energy Wildlife Institute, Washington, D.C., USA, in conjunction with U.S. Department of Energy Cooperative Agreement DE-EE0007883.
- Jeffreys, H., 1939. Theory of Probability. Oxford University Press, Oxford, UK.
- May, R., Ø. Hamre, R. Vang, and T. Nygård. 2012. Evaluation of the DTBird Video-System at the Smøla Wind-Power Plant: Detection Capabilities for Capturing Near-Turbine Avian Behaviour. NINA Report 910. Norwegian Institute for Nature Research, Trondheim, Norway.
- R Core Team (2023). R: A language and environment for statistical computing. R Foundation for Statistical Computing, Vienna, Austria. <a href="https://www.R-project.org/">https://www.R-project.org/</a>.
- Straffi, P. 2016. On Screen Protractor. v0.5. <a href="https://sourceforge.net/projects/osprotractor">https://sourceforge.net/projects/osprotractor</a>>. Accessed June 2023.



50 years of field notes, exploration, and excellence

**Research Report** 

Analysis of DTBird® Detection and Deterrent-Triggering
Response Distances at Commercial Wind-Energy Facilities
in California and Washington

Project #4080-01

Prepared for:

Renewable Energy Wildlife Institute 1990 K Street NW, Suite 620 Washington, D.C. 20006-1189

Prime Contractor: DOE Cooperative Agreement DE-EE0007883

Prepared by:

H. T. Harvey & Associates











### **Executive Summary**

DTBird® is an automated detection and audio deterrent system designed to discourage birds from entering the rotor swept area of spinning wind turbines. As part of a multi-faceted research program conducted in collaboration with the Renewable Energy Wildlife Institute, we previously conducted site-specific analyses of the detection and deterrent-triggering performance of seven DTBird systems operated for the first time at the Manzana Wind Power Project in southern California, USA, and of 5 of 11 DTBird systems operated for the first time at the Goodnoe Hills Wind Farm in south-central Washington, USA. The overarching goal of this research is to evaluate the effectiveness of DTBird in detecting and discouraging golden eagles (Aquila chrysaetos) and other large raptors from approaching the rotor-swept area of operating wind turbines. Herein we present a new multi-site analysis of DTBird detection and deterrent-triggering performance based on integrating data collected at the two study sites.

We used unmanned aerial vehicles (UAVs, also commonly called drones) as surrogates for live eagles in experimental flight trials. The fixed-wing UAVs were similar in size and mass to, and were painted to resemble, a golden eagle, and they carried onboard avionics that provided high spatiotemporal resolution Geographic Information System (GPS) tracking and other flight metrics data, which enabled precise comparisons against temporally matched DTBird event records. We flew mostly pre-delineated flight transects, with the sampling arrays developed based on a stratified random selection algorithm and delineated to support evaluating DTBird responses within a 240-m radius of focal turbines—the maximum, calibrated distance that DTBird was expected to detect birds the size of golden eagles. We used detection and deterrent events recorded in the online DTBird digital analysis platform during the flight trials, matched with data derived from the UAV navigation systems, to evaluate system performance.

We built a generalized linear mixed-effects model (GLMM) to evaluate the influence on DTBird detection and deterrent-triggering response distances of random effects including *Turbine ID* and *UAV Model* (different models used at the two sites) nested within *Site* (i.e., wind facility); categorical fixed effects including *Site*, DTBird *Event Type* (detection, initial warning signal trigger, or raucous dissuasion signal trigger), and *Sky Backdrop* (fair, partly cloudy, mostly cloudy, or overcast) categories; a UAV *Direction from Turbine* positioning metric; flight characteristic covariates including UAV *Course Over Ground*, *Ground Speed*, *Climb Rate*, *Pitch Angle*, and *Roll Angle*; and environmental covariates including *Wind Speed*, *Solar Irradiation*, *Sun Azimuth*, and *Sun Elevation Angle*.

The final GLMM had the following form:

```
Line-of-Sight (LoS) Response Distance \sim (1 \mid Site : Turbine ID) + (1 \mid Site : UAV) + Site + Event Type + Sky Backdrop + Ground Speed + Wind Speed + Roll Angle + Pitch Angle + Roll Angle * Pitch Angle
```

Output for the selected model indicated the following relationships:

Site: Turbine ID: modest variation among turbines in modeled response distances.

*Site : UAV*: average response distances varied by as much as 30 m among the five UAV models used, indicating fairly substantial variation likely to also pertain to eagles of variable size and coloration.

*Site*: even after controlling for variability in site due to turbines and UAV types, response distances averaged 32 m shorter (indicating poorer detectability) at the Manzana site than at the Goodnoe Hills site, suggesting that the overall targeting accuracy of the DTBird systems can vary across different landscape settings.

**Event Type:** confirmed a significant "structural" difference in expected trigger distances for dissuasion signals compared to initial detections and warning signals.

Sky Backdrop: response distances increased (indicating improved detectability) with increasing cloud cover.

*Ground Speed:* response distances increased as the rate of UAV travel relative to fixed points on the ground increased.

Wind Speed: response distances generally increased as the wind speed increased.

Roll Angle: Pitch Angle Interaction: the degree to which a UAV rolled to one side or the other or pitched up or down while in flight influenced DTBird response distances in an interactive manner. Roll Angle was shown to be the strongest predictor of the two variables, and both metrics were positively correlated with response distances when the other variable was held constantly low; however, concurrent maximization of both stability metrics was effectively impractical, because that would translate to the aircraft stalling and falling out of the sky.

This investigation highlighted several flight metrics and environmental covariates that significantly influenced DTBird's detection and deterrent-triggering performance at the two wind-facility study sites. Here it is important to acknowledge that using eagle-like UAVs as surrogates for real eagles may have constrained the insights generated from the study. Nevertheless, the indicated relationships can help future system users understand the environmental conditions in which DTBird is likely to perform best and other factors that can substantially influence the targeting accuracy of the systems.

## **Table of Contents**

Section 1.	Introduction	1
Section 2.	Methods	3
2.1 Stu	dy Sites and DTBird Installations	3
2.	1.1 Manzana Site	3
2.	1.2 Goodnoe Hills Site	4
2.2 DT	Bird System Operation	4
2.3 UA	V Flight Trials	7
2.4 Pos	st-processing of UAV Tracking Data and Matching with DTBird Detection Records	9
2.5 Fac	ctors Influencing DTBird Detection and Deterrent-Triggering Response Distances	10
Section 3.	Results	13
3.1 Sar	npling Results	13
3.2 Mc	deling Response Distances	14
Section 4.	Discussion	22
4.1 Co	ncluding Statements	24
Section 5.		
	A. Variables Considered in DTBird Detection and Deterrent-Triggering Response	29
	B. Evaluation Results for the Initial Full and Other Candidate Models Considered as Part kward Selection Approach Used to Identify the Best Model	31
Figure	S	
Figure 1.	Layout of Manzana Wind Power Project in southern California showing the locations of installed DTBird systems and where UAV flight trials were conducted	3
Figure 2.	Layout of Goodnoe Hills Wind Farm in south-central Washington showing the locations of installed DTBird systems and where UAV flight trials were conducted	5
Figure 3.	Depiction of DTBird video camera and broadcast speaker locations on turbines at the Manzana Wind Power Project (left panel, single ring of speakers) and Goodnoe Hills Wind Farm (right panel, two rings of speakers)	5
Figure 4.	Vertical cross-section illustrating theoretical DTBird detection envelope calibrated for golden eagles, with light gray indicating rotor swept zone, blue indicating detection-only zones, green indicating variable warning-signal trigger zones, and yellow indicating variable dissuasion-signal trigger zones.	7
Figure 5.	Images portraying the five UAVs deployed during flight trials conducted during this study in California (images A and B) and in Washington (images C–E).	8
Figure 6.	Deviations from the estimated global average DTBird response distance associated with different site-specific turbine installations, estimated as a nested random effect in the multi-site GLMM developed for the study	16

Figure 7.	Deviation from the estimated global average DTBird response distance associated with site-specific use of different UAV models, estimated as a nested random effect in the multi-site GLMM developed for the study	16
Figure 8.	Modeled relationship between DTBird response distances and study site, with shared letters indicating pairwise differences that are not significant at $P \le 0.05$ .	17
Figure 9.	Modeled relationship between DTBird response distances and detection and deterrent-triggering event types, with shared letters indicating pairwise differences that are not significant at $P \le 0.05$	18
Figure 10.	Modeled relationship between DTBird detection and deterrent-triggering response distances and sky backdrop / cloud cover categories, with shared letters indicating pairwise differences that are not significant at $P \le 0.05$	19
Figure 11.	Modeled relationship (±95% confidence interval) between DTBird detection and deterrent-triggering response distances and UAV ground speed, or rate of travel relative to a fixed point on the ground, as measured by UAV avionics during sampling flights	19
Figure 12.	Modeled relationship between DTBird detection and deterrent-triggering response distances and wind speed as measured by UAV avionics during sampling flights	20
Figure 13.	Modeled relationships between DTBird detection and deterrent-triggering response distances and the interactive influence of UAV pitch and roll angles	21
Tables		
Table 1.	Summary of UAV Flight Trials Conducted at the Manzana Wind Project Site in California that Contributed Data for Analysis	13
Table 2.	Summary of UAV flight trials conducted at the Goodnoe Hills Wind Farm study site in Washington that contributed data for analysis	
Table 3.	Coefficients and parameter t-test results for fixed effects represented in the selected multi-site GLMM with DTBird response distance as the dependent variable.	17
Appen	adices	
Appendix	A. Variables Considered in DTBird Detection and Deterrent-Triggering Response  Distance Analysis	29
Appendix	B. Evaluation Results for the Initial Full and Other Candidate Models Considered as Part of the Backward Selection Approach Used to Identify the Best Model	31
List of F	Primary Preparers	
Jeff P. Smi	ith, Ph.D., Associate Wildlife Ecologist—Project Manager	
Stephanie	R. Schneider, M.S., Wildlife and Quantitative Ecologist	
Scott B. To	errill, Ph.D., Principal in Wildlife Ecology and Senior Ornithologist—Principal-in-Charge	
List of C	Contributors to Collective Research	
Judd How	ell, Ph.D., Senior Associate Wildlife Ecologist (Retired)	
Jeff Zirpol	li, M.S., Senior Wildlife Ecologist	
Ken Lindk	xe, M.S., Quantitative Ecologist	
Kristina W	Volf, Ph.D., Quantitative Ecologist	

Allison Gibson, M.A., GIS Specialist

Steve Watt, M.S., Senior GIS Specialist

Alex Henry, B.S., Field Biologist / Data Entry Technician

Cooper Smith, B.S., Field Biologist / Data Entry Technician

#### Research Conducted with Logistical/In-kind Support From:

Liquen Consultoría Ambiental, S.L., Madrid, Spain

Avangrid, Manzana Wind Power Project, Kern County, California, USA

PacifiCorp Wind Operations, Goodnoe Hills Wind Farm, Goldendale, Washington, USA

Vestas - American Wind Technology, Inc., Goodnoe Hills Wind Farm, Goldendale, Washington, USA

Remote Intelligence, LLC, Wellsboro, Pennsylvania, USA

TerraData Unmanned, LLC, Archer, Florida, USA

AUV Flight Services, Tucson, Arizona, USA

Alta Environmental Services, LLC, San Diego, California, USA

#### **Section 1. Introduction**

DTBird® (Liquen Consultoría Ambiental, S.L., Madrid, Spain) is an automated detection and audio deterrent system designed to discourage birds from entering the rotor swept zone of spinning wind turbines (see <a href="https://dtbird.com">https://dtbird.com</a>). DTBird can also include an automated turbine control-stop module that was not installed as part of the systems evaluated herein. Funded by the American Wind Wildlife Institute (now the Renewable Energy Wildlife Institute [REWI]), H. T. Harvey & Associates (2018) previously analyzed the performance of seven DTBird systems operated for the first time at the Manzana Wind Power Project in southern California. Following this pilot study, we continued the research in collaboration with REWI, funded by the U.S. Department of Energy, by augmenting some of the pilot-study analyses and expanding the investigations to a second facility: the Goodnoe Hills Wind Farm in south-central Washington (H. T. Harvey & Associates 2019a).

The ultimate goal of this research is to quantify the effectiveness of DTBird as a measure to reduce collision risk for golden eagles (*Aquila chrysaetos*) and other large raptors. If found to be effective and accepted by the U.S. Fish and Wildlife Service (USFWS), DTBird could be considered for use by commercial wind energy facilities in conservation plans, as a best management practice under the Bald and Golden Eagle Protection Act (Eagle Act) (16 U.S.C. §668–668c), as a minimization measure for take permits or habitat conservation plans, or as an adaptive management measure.

Another DTBird pilot study was previously conducted in Norway (May et al. 2012) and other more limited evaluations were conducted in Switzerland (Aschwanden et al. 2015, Hanagasioglu et al. 2015) and Sweden (Litsgård et al. 2016), but our study represents the first comprehensive effort to evaluate the DTBird system in North America. May et al. (2012) evaluated the ability of the DTBird system to detect and deter raptors flying near and in the risk zone of wind turbines in Norway, with the system calibrated to detect and deter large raptors such as white-tailed sea eagles (*Haliaeetus albicilla*) and golden eagles. They compared the detection rates of the DTBird camera and video surveillance system against detections documented by a radar system. Using this approach, they were able to quantify the probability of false positives (defined as video recordings without birds) and false negatives (defined as the detection system failing to trigger video surveillance of a targeted bird that the radar system indicated passed by in detectable range). This study, as well as other preliminary DTBird evaluations (Aschwanden et al. 2015, Litsgård et al. 2016), did not, however, explicitly address potential limitations in the spatial coverage provided by the surveillance system, nor did it evaluate detectability as a function of factors such as 1) distance from the turbine; 2) flight altitude, trajectory, and angle of approach relative to the camera(s); and 3) variation in visibility conditions caused by weather, ambient lighting, and different visual backdrops.

A primary component of our research implemented at both study sites involved using fixed-wing unmanned aerial vehicles (UAVs) designed to mimic golden eagles to evaluate how DTBird detection and deterrent-triggering response distances varied depending on a variety of flight characteristics and environmental covariates. These investigations involved using detection and deterrent event records automatically recorded in the DTBird on-line digital analysis platform (DAP) database during standardized UAV flight trials, matched with data derived from the UAV GPS-based navigation systems, to associate specific DTBird detection and

1

deterrent events with high spatiotemporal resolution UAV position, flight characteristics, and covariate data. We then used generalized linear mixed-effects models (GLMMs) to discern how the DTBird detection and deterrent triggering response distances varied depending on factors such as the facility location, UAV model, UAV ground speed, UAV flight stability and trajectory, and environmental covariates such as wind speed, cloud cover, and solar positioning and intensity relative to the UAV at the time a given detection or deterrent-triggering event occurred. The analysis incorporating data from two distinct study sites, one located in a Mojave desert environment and the other in a north-temperate grassland/scrub landscape above the Columbia River gorge, yielded important insight about the effectiveness and limitations of DTBird's overall detection and deterrent-triggering performance, which will ultimately compliment other testing and evaluation elements of this overall research program.

#### Section 2. Methods

#### 2.1 Study Sites and DTBird Installations

#### 2.1.1 Manzana Site

The Manzana Wind Project has been in operation since 2012 and comprises 126 1.5 MW GE 1.5-77 wind turbines, with a hub height of 65 m and a rotor-swept diameter of 82.5 m, located in the southwestern foothills of the Tehachapi Mountains of southern California in northwestern Antelope Valley, which constitutes the westernmost extension of the Mojave Desert (Figure 1). The landscape is a gradually sloping alluvial fan incised by dry desert washes. The northwestern sector of the facility features more complex foothill topography adjacent to a primary riparian drainage, and the topography grades downslope to the southeast into a more-uniform plain. The vegetation is typical of the upper Mojave Desert region, featuring cover types such as Mojave Desert scrub communities, southern willow (*Salix* spp.) scrub, native and nonnative grasslands, juniper (*Juniperus* spp.) and Joshua tree (*Yucca brevifolia*) woodlands, and, at the upper margins of the facility, pine-oak (*Pinus-Querus* spp.) woodlands characteristic of middle elevations in the Tehachapi Mountains (Sapphos Environmental 2006).

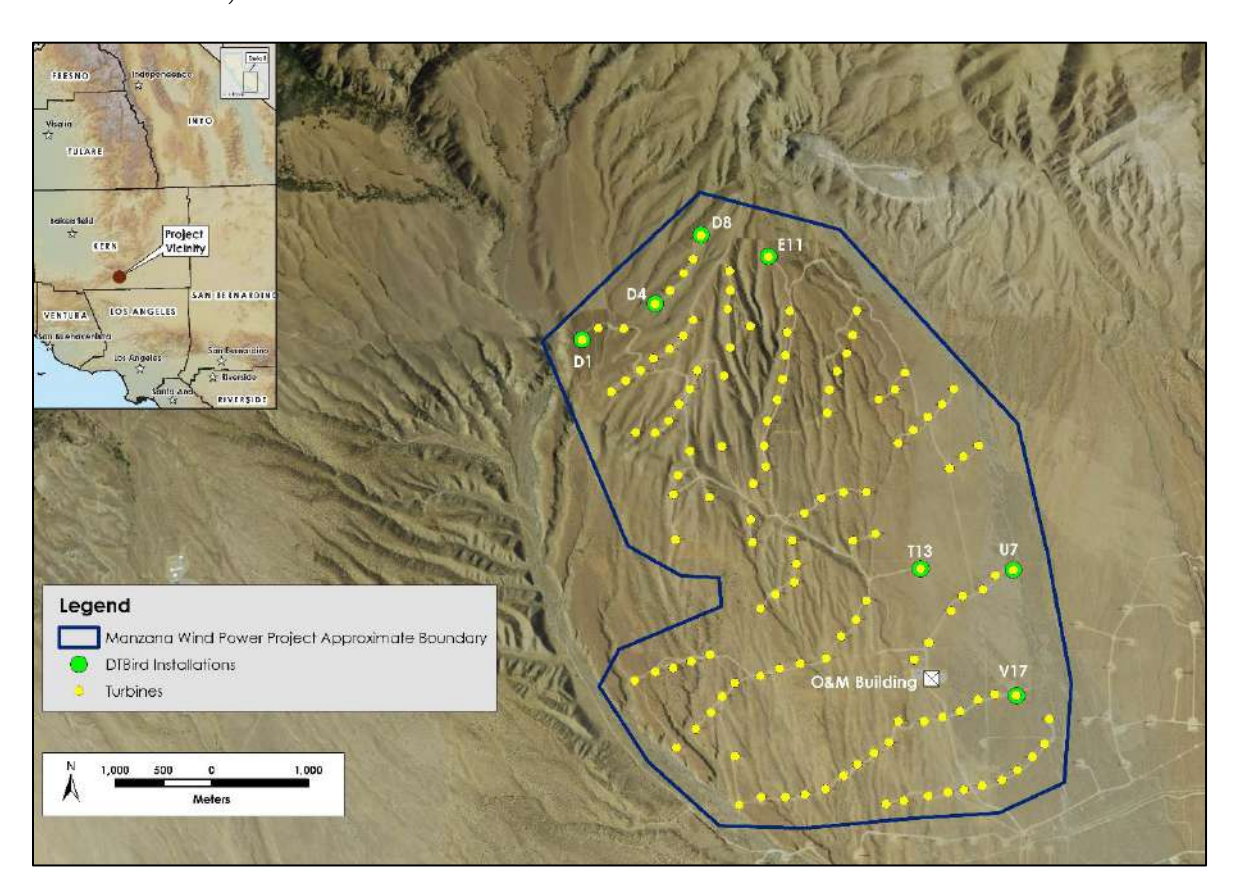


Figure 1. Layout of Manzana Wind Power Project in southern California showing the locations of installed DTBird systems and where UAV flight trials were conducted.

Seven DTBird systems were installed at this facility to support the pilot study (Figure 1). This number of DTBird systems was insufficient to characterize the behavior of the systems across the entire facility; hence, we did not randomize the selection of installation locations for sampling purposes. Instead, we focused our selection of study turbines on achieving practical cost and logistical efficiencies for the facility, to encompass important landscape features represented within the facility, to provide necessary spacing of the installations to ensure that the deterrent responses of raptors at one installation were not influenced by deterrent signals emitted at another installation, and to maximize the chances of recording the activities of *in situ* raptors of interest. We derived insight about the latter element from prior post-construction monitoring studies, including knowledge of a proximate golden eagle nesting territory (Bloom Biological 2015b, c; Bloom Biological and Cardno ENTRIX 2015; Kuehn 2016).

#### 2.1.2 Goodnoe Hills Site

The Goodnoe Hills Wind Farm has been in operation since 2008 and currently comprises 47 2.2 MW Vestas V110 Mark C and B wind turbines, with a hub height of 87 m and a rotor-swept diameter of 110 m located in south-central Washington atop an east-west ridgeline flanking the Columbia River approximately 3–6 km away (Figure 2). The topography descends steeply south of the ridgeline approximately 610 meters (m) to the Columbia River, and descends more gradually to the north approximately 500 m down into Rock Creek Canyon and associated riparian corridors. The project area is dominated by a mosaic of grazed grassland and shrubsteppe, with inclusions of ponderosa pine (*Pinus ponderosa*) and Oregon white oak (*Quercus garryana*) woodlands on the ridge's north-facing slopes.

Fourteen DTBird systems were installed at this facility to support this research (Figure 2). We spread the installations around the outer perimeter of the overall facility with sufficient spacing to minimize the potential for target raptors to be simultaneously exposed to multiple deterrent signals and thereby confound achieving independent assessments at individual installations.

### 2.2 DTBird System Operation

A detailed description of the DTBird system set up and operation can be found in H. T. Harvey & Associates (2018). Each turbine-specific DTBird monitoring system comprised four video cameras (6 megapixel resolution) installed on the turbine tower approximately 5 m off the ground, which surveilled the skies throughout daylight hours, and at least one ring of four broadcast speakers installed on the tower just below the lower rotor swept zone (Figure 3). The only noteworthy difference between the installations at the Manzana and Goodnoe Hills sites was that the latter systems included a second set of deterrent broadcast speakers located on the turbine tower just below hub height (Figure 3). This modification was necessary because the Goodnoe Hills turbines are taller than the Manzana turbines, and installing a second set of speakers higher up on the tower was expected to help ensure effective deterrent broadcasting throughout a larger overall detection envelope and collision risk zone.

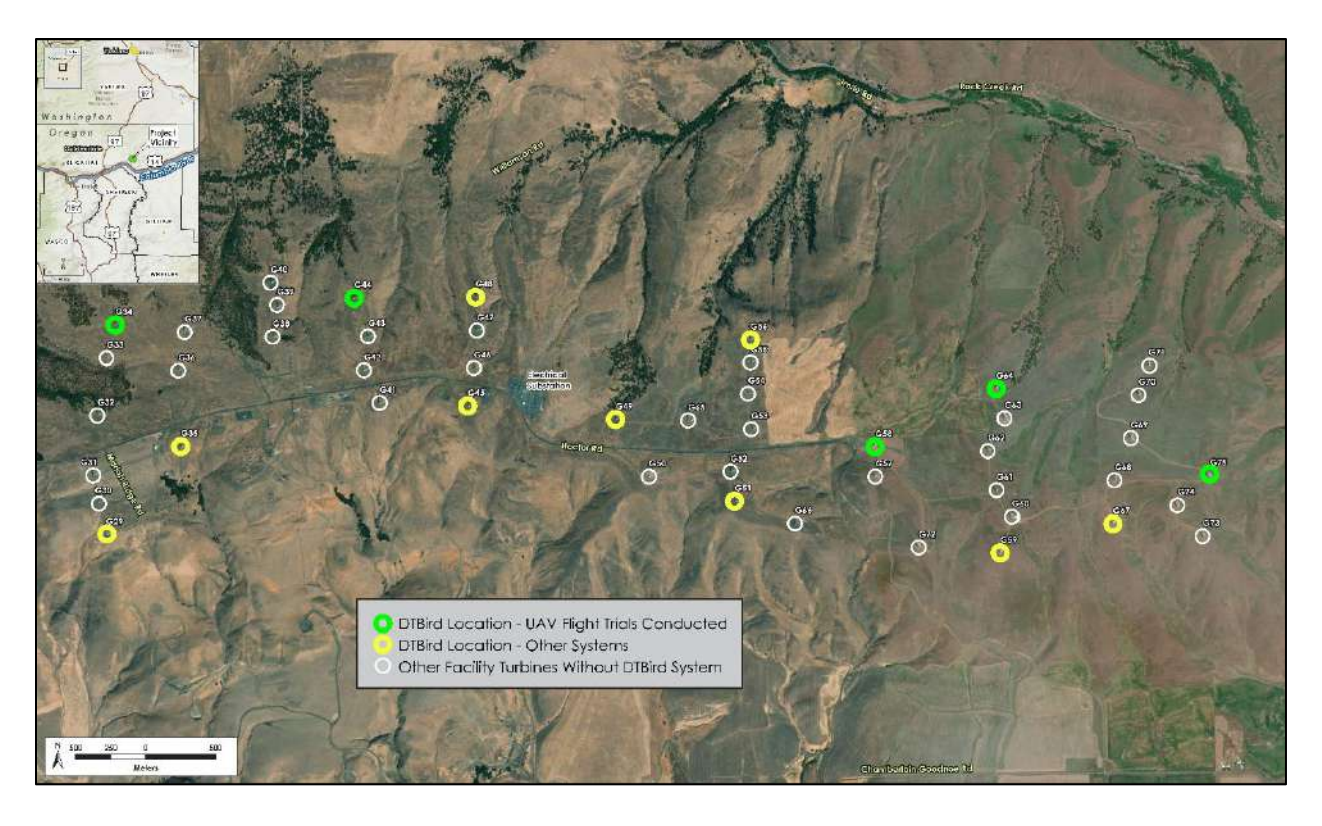


Figure 2. Layout of Goodnoe Hills Wind Farm in south-central Washington showing the locations of installed DTBird systems and where UAV flight trials were conducted.

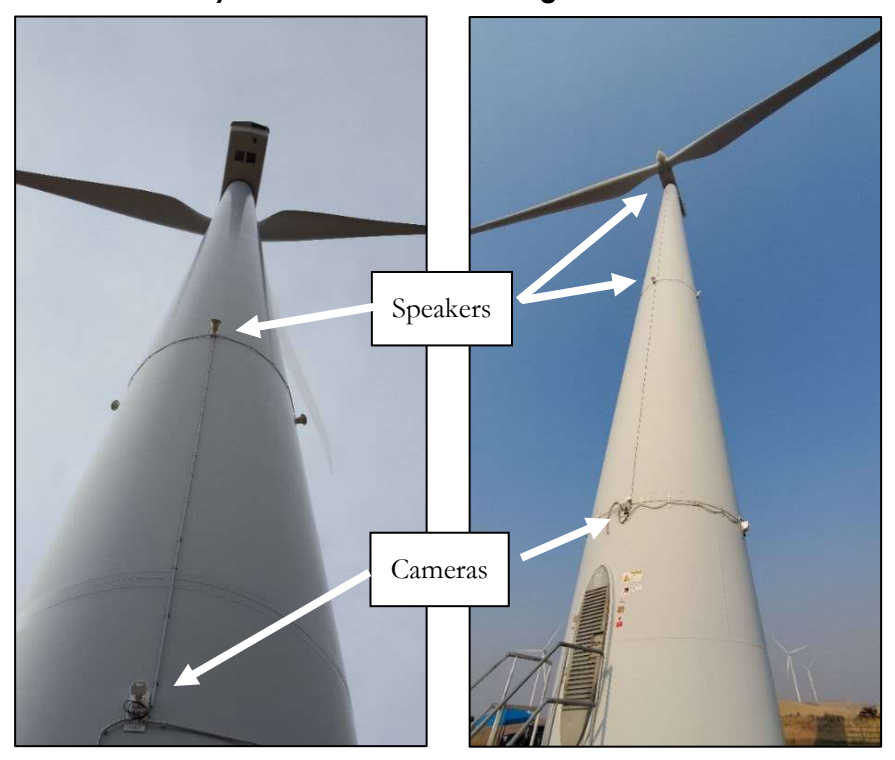


Figure 3. Depiction of DTBird video camera and broadcast speaker locations on turbines at the Manzana Wind Power Project (left panel, single ring of speakers) and Goodnoe Hills Wind Farm (right panel, two rings of speakers).

Each individual DTBird automated video system surveilled the sky around an individual turbine for moving objects that filled enough image pixels to qualify as a target of interest based on calibrations for the focal species of interest, in this case golden eagle. DTBird does not classify or enumerate targets, may target multiple objects simultaneously, and does not actually track individual objects—it simply repeatedly registers individual objects as targeted as long as they meet the calibrated targeting criteria. Analysts must subsequently review event records and video clips stored in the DAP to classify and enumerate the detected targets, which may be birds or *false positive* detections caused by airplanes, insects, debris, raindrops, snowflakes, or other inanimate objects moving through the detection envelope, as well as from by *sky artifacts* (e.g., high-contrast, shifting elements caused by clouds and bright skies that are mistaken for flying objects).

DTBird systems are calibrated to target objects of a specified size range and, if a system registers that the turbine rotor is actively spinning at ≥2 rotations per minute (rpm) to trigger subsequent deterrent signals when the system estimates that a targeted object as within a specified distance from the turbine. Detection and trigger distances are determined based on pre-programmed criteria projecting how many image pixels a bird of the specified size is expected to fill at specified distances. The Manzana and Goodnoe Hills systems were calibrated to target golden eagles (wing span of 2.1–2.3 m), which translated to targeting objects that met specified criteria at an expected maximum line-of-sight distance from the turbine of approximately 240 m. Once an object is targeted and a new detection record initiated at a spinning turbine, the system triggers an initial audible warning signal if it perceives that a targeted object moves within 170–240 m of the turbine, and triggers a more aggressive dissuasion signal at distances of 100–170 m, depending on the flight altitude (Figure 4; and see H. T. Harvey & Associates 2018 for additional graphical illustrations and detailed information about the expected deterrent-triggering zones within the projected overall detection envelope).

When a system first detects a targeted object, it creates a new event record in the DAP and records a timestamp for the initial *detection* event along with other limited data. If a targeted object subsequently or simultaneously triggers one or both of the deterrent signals, information is added to the same DAP event record to document the unique timestamps and signal durations for each deterrent-triggering event. Each event record ultimately has attached to it video clips representing the four cameras, which the system extracts to begin 10 seconds before targeting began and continue for 30 seconds after the last targeted object exits the detection envelope. There must be no objects targeted for at least 26 seconds before a given DTBird system can initiate a new event record. If a system targets multiple objects concurrently during the same event period, timestamps are recorded only for the first detection, warning-trigger, and dissuasion-trigger events, and those respective events may not be triggered by the same object. In these cases, it can be difficult to determine exactly which bird or object was responsible for the timestamped events.

Under the DTBird targeting scenario and given calibration for golden eagles, much smaller objects (e.g., small birds and even insects) may trigger detections and deterrents if they are close enough to fill the same number of pixels as a golden eagle would at a much greater distance. Conversely, much larger objects (e.g., airplanes) may trigger detections when they are farther away but fill the requisite number of pixels to be perceived as a possible golden eagle at a relevant distance. Because of these system limitations, false-positive detections and deterrent triggering commonly occur, often at a much greater frequency than events related to target birds (May et al. 2012; H. T. Harvey & Associates 2019b, 2022a).

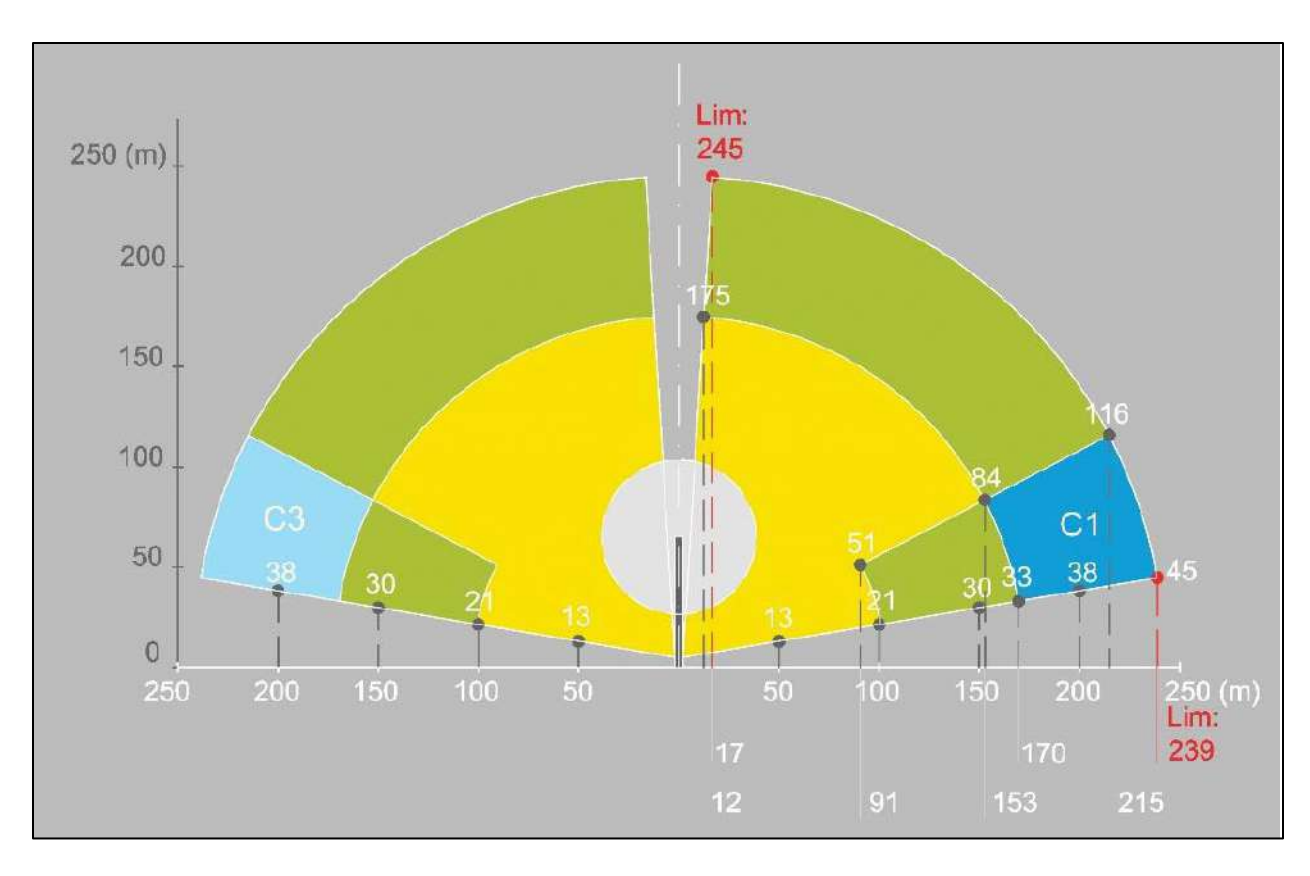


Figure 4. Vertical cross-section illustrating theoretical DTBird detection envelope calibrated for golden eagles, with light gray indicating rotor swept zone, blue indicating detection-only zones, green indicating variable warning-signal trigger zones, and yellow indicating variable dissuasion-signal trigger zones.

### 2.3 UAV Flight Trials

We conducted UAV flight trials at the Manzana site at all seven DTBird installations, with sessions spanning January through August in 2017, but most concentrated in August. We flew flight trials at three Goodnoe Hills DTBird turbines in August 2021 and at four turbines in July 2022. The ultimate timing of the successful flight trials, mostly concentrated in July and August at both sites, was not the intended sampling design; however, several unexpected UAV failures, extended replacement timeframes complicated by changes in piloting/aircraft service companies, and other unavoidable logistical, weather-related, and pandemic-related constraints ultimately limited our options.

We flew two UAVs during the Manzana flight trials and three different UAVs during the Goodnoe Hills flight trials (Figure 5). All five UAVs were similar in being fixed-wing plastic/foam-bodied models, with a wingspan (~1.9–2.2 m), body length (~0.8–1.1 m), and mass (~3–4 kg) similar to a golden eagle, and variably painted brown to mimic golden eagle coloration. However, they differed in overall size, body morphology, and shade of coloration. The Manzana study results suggested that the distance at which the DTBird systems detected the two UAVs flown during those sessions differed significantly, which we interpreted as potentially mimicking

differences that could pertain to detecting larger, darker female eagles versus smaller, lighter-colored male eagles (H. T. Harvey & Associates 2018).

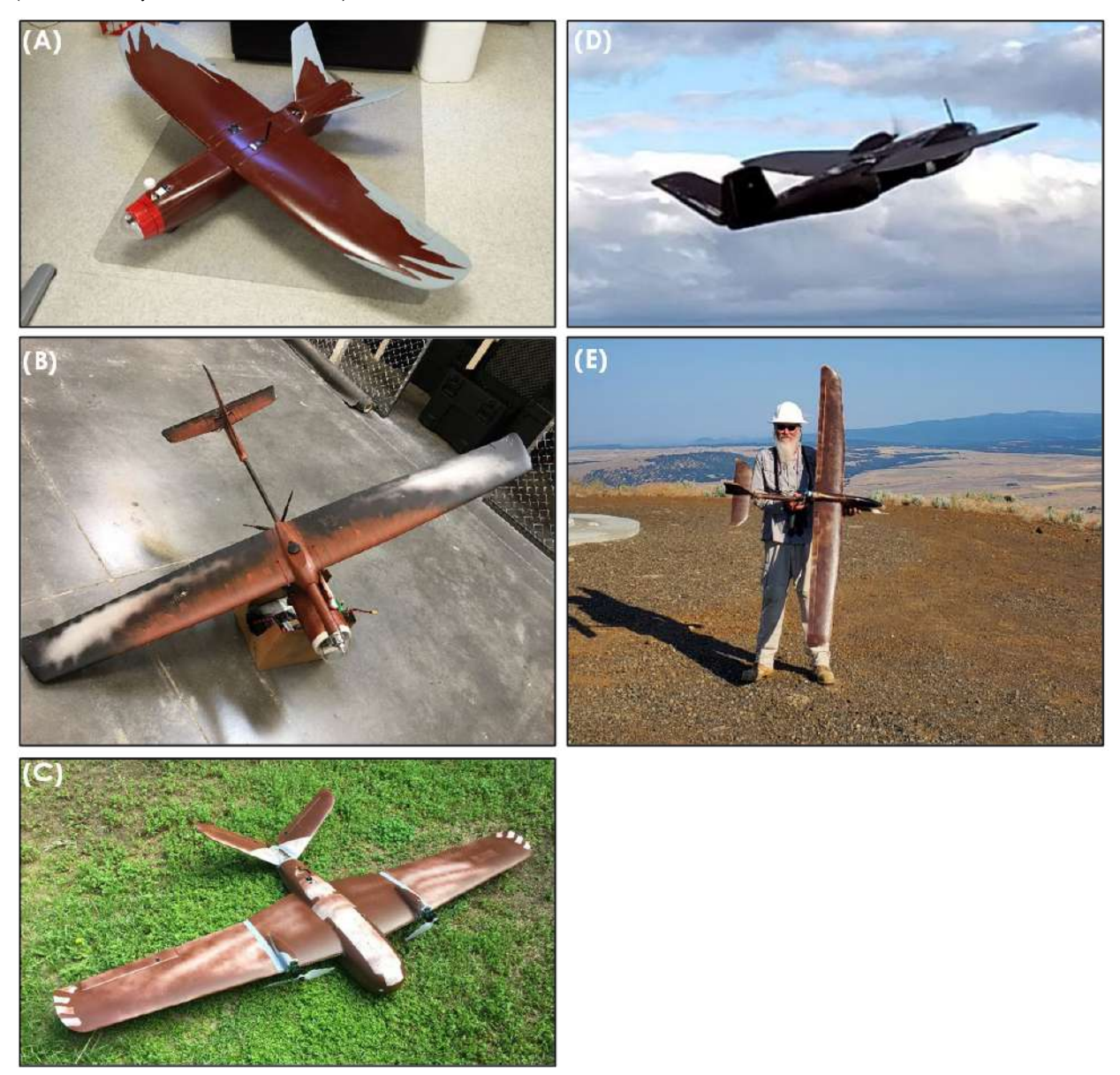


Figure 5. Images portraying the five UAVs deployed during flight trials conducted during this study in California (images A and B) and in Washington (images C–E).

Accordingly, we purposefully sought to also fly more than one model during the Goodnoe Hills flight trials to support further investigation of this detectability factor. That said, some of the variability in models used stemmed from crashes destroying one of the two aircraft used during the Manzana study and two of the three aircraft used during the Goodnoe Hills study. Further contributing to the variability in UAV models used at each site, the second UAV used during the Manzana study was not available for use during the Goodnoe Hills study.

During both the Manzana and Goodnoe Hills flight-trial efforts, complicated flight conditions for flying light-bodied fixed-wing UAVs and unexpected calamities impinged on our ability to conduct robust suites of UAV flight trials repeated across different seasons with variable sky cover and flight conditions. In the end, both efforts commonly involved concentrated sampling during mid-summer, but differed in that other sampling occurred at the Manzana site at scattered times from mid-January to early March. The extent of sampling across daylight hours also varied at the two project sites. Most flight trial sessions occurred during morning hours when the wind conditions tended to be most compatible for flying fixed-wing UAVs; however, minimal winds allowed for extending the final 2022 sessions at the Goodnoe Hills later into early afternoon (at which point excessive heat precluded further flying for the day).

The key commonality at the two study sites was that we flew primarily pre-delineated linear transects orchestrated as automated flight missions at strategically selected DTBird-equipped turbines, with the goal of achieving representative sampling of the hemispheric, 240-m radius expected maximum-detection-distance envelopes around the sampled DTBird installations. The commonly applied randomized transect selection algorithm delineated flight transects based on multi-layer stratification by compass direction of the flight, flight trajectory (between a maximum 15° ascent and maximum 15° descent), lateral distance from the turbine, and altitude relative to the expected DTBird camera locations. We then packaged collections of 10–20 pre-delineated, turbine-specific transects to orchestrate efficient, single, battery-powered, mostly automated UAV flight sessions using professional pilots, Mission Planner software (ArduPilot Dev Team 2021) on a laptop, and automated radio communication to direct the UAV. Operating several such missions over a multi-hour period composed an individual flight-trial session at a specific turbine, and at both sites we sought to conduct at least half-day flight trial sessions at several representative DTBird-equipped turbines with compatible landscape settings (i.e., relatively safe places from which to launch and land the UAV, limited topographic complexity, and minimal complications caused by elevated obstacles other than the focal turbine and usually one other adjacent turbine).

Each pre-delineated transect began and ended 100-m line-of-sight distance beyond the projected 240-m detection envelope to support the possibility of detections beyond the expected maximum range. Once the DTBird system targets an object and creates a new detection record in the DAP, no new detection record is created until no additional targeting has occurred for at least 26 seconds. Accordingly, to generate independent transect samples for evaluating the probability of detection and the DTBird system's response characteristics, the automated flight sessions included 30-second loiter periods between each delineated transect at 5–6 preselected, safe destinations located 500 m from the relevant study turbine (previously illustrated in H. T. Harvey & Associates 2018).

# 2.4 Post-processing of UAV Tracking Data and Matching with DTBird Detection Records

Each UAV was equipped with avionics that recorded during all flights myriad GPS position, ground and air speed, flight trajectory, and other flight metrics many times per second with high spatiotemporal accuracy. These data were automatically transmitted during the flights to a laptop used to control the automated missions,

and could also be extracted directly from the avionics units post-flight. The resulting output from each individual flight was a continuous stream of non-parsed data that had to be translated to a useable format. To extract these data and prepare them for analysis, we followed the detailed procedures and protocols described in H. T. Harvey & Associates (2018). Concisely summarized, this process involved the following primary steps:

- 1) Translate UAV telemetry log files to spreadsheet format using a publicly available custom program (Fernie 2012).
- 2) Filter and translate variables recorded by the UAV avionics into useful formats and units of measure, with meaningful variable names.
- 3) Filter UAV tracking records to:
  - a. Exclude data from periods when the UAV was not actually flying (pre-launch and post-landing) or was flying below or loitering outside of detection range.
  - b. Include only one record per second to match the resolution of the DAP records.
- 4) Use ArcGIS 3D Analyst (ESRI, Redlands, CA) to:
  - a. Exclude as outliers all UAV loiter-point locations and any other locations recorded at a line-of-sight distance exceeding 340 m; i.e., more than 100 m beyond the expected DTBird maximum detection distance for golden eagles of 240 m.
  - b. Code all UAV tracking locations with individual transect numbers based on relevant temporal breaks in the streams of tracking data.
  - c. Add additional GIS-derived position metrics and environmental covariates used in analyses.
- 5) Use the DAP to identify relevant UAV detection and deterrent-triggering event records, and to classify the sky backdrop behind the UAV at the time of each event.
- 6) Match DTBird detection and deterrent-triggering event records recorded in the DAP to the UAV tracking records based on matching 1-second-resolution timestamps.
- 7) Finalize datasets for analysis by eliminating all tracking records that are not matched with a DAP event record.

# 2.5 Factors Influencing DTBird Detection and Deterrent-Triggering Response Distances

Development of candidate model sets should be guided as much as possible by a thorough understanding of the system being studied (Burnham and Anderson 2010). The multi-site analysis presented here benefited from insights gained from prior site-specific analyses conducted using data collected at the two study facilities (H. T. Harvey & Associates 2018, 2022b).

The response variable for the analysis was the line-of-sight distance (LoS Response Distance) between the UAV and closest DTBird camera at the time a detection or deterrence event occurred. The operative assumption was

that greater response distances can be interpreted as reflecting an improved detection or triggering response, in that earlier (more distant) detection and targeting is expected to provide more time for the deterrents to alter a target bird's behavior well before the risk of collision is acute. We calculated the distances based on the UAV GPS coordinates at the time of the event, using measuring tools in ArcGIS 3D Analyst. Flight samples included in these analyses were necessarily limited to those that triggered a relevant DTBird response. To fit the response-distance data, we built GLMMs and evaluated the influence of various potential random- and fixed-effect predictors. We implemented the models using the 'lme4' package in R (R Core Team 2023; function *lmer*, Bates et al. 2015), with a Gaussian distribution and an identity link function. The initial full model for this analysis had the following structure (see Appendix A for descriptions of each variable):

LoS Response Distance  $\sim (1 \mid Site : Turbine ID) + (1 \mid Site : UAV Model) + Site + Event Type + Sky Backdrop + sin(Direction from Turbine [DFT]) + cos(DFT) + sin(Course Over Ground [COG]) + cos(COG) + Ground Speed + Climb Rate + Roll Angle + Pitch Angle + Wind Speed + Solar Irradiation + Solar Irradiation<sup>2</sup> + Sun Azimuth + Sun Elevation + Roll Angle * Pitch Angle + sin(DFT) * Sun Azimuth + cos(DFT) * Sun Azimuth + sin(COG) * Sun Azimuth + cos(COG) * Sun Azimuth + sin(COG) * Sun Azimuth.$ 

Because the predictor variables were on different scales, we centered and scaled all continuous predictors after applying the following transformations. We transformed *Roll Angles* and *Pitch Angles* to absolute values, expecting that rolling left versus right and pitching up versus down would modify exposure of the UAV profile to the camera similarly. We transformed the *DFT* and *COG* metrics to orthogonal east-west (cos[x]) and north-south (sin[x]) vectors to support linear analyses of these circular variables (Fisher 1995, Cremers and Klugkist 2018). In contrast, we did not similarly transform *Sun Azimuth*, because the range of that variable was only slight greater than 180° (east in the morning, south at midday, and west in the evening) and therefore did not represent a potential for convergence errors caused by 0° and 360° being equivalent values.

We evaluated *Turbine ID* nested within *Site* (*Site*: *Turbine ID*) and *UAV Model* nested within *Site* (*Site*: *UAV Model*) as random effects, because we expected that DTBird's responses could vary depending on the unique setting at each turbine and variation among the UAVs used, yet neither component was similarly represented at the two sites. In addition, modeling these two factors as random rather than fixed effects acknowledged that the study involved repeated measures (flight sessions) at individual turbines and using different UAVs, such that there was a high likelihood of non-independence among the response distances measured within groupings of these factors. We also modeled *Site* as a fixed effect to determine if DTBird's overall response-distance performance appeared to vary significantly between the two study areas.

We evaluated two- and three-way interactions among the *DFT* and *COG* orthogonal vectors and *Sun Azimuth*, expecting that the influence on response distances of UAV travel direction and directional position from the turbine could markedly depend on the relative position of the sun due to illumination and glare. We also evaluated the two-way interaction between the two UAV "stability" metrics (*Pitch Angle* and *Roll Angle*), anticipating that modeling the interaction of these variables could more accurately reflect the collective influences on exposure of the UAV profile to the cameras than modeling any one metric alone, in part because preventing aircraft stalling effectively precludes maximizing more than one of these variables at the same time. We did not consider any other interactions due to inapplicability and limitations of the available dataset.

To investigate the validity of applying this full model to the multi-site dataset, after we fit the model we used diagnostic tests to evaluate whether the model violated any GLMM assumptions (Zuur et al. 2009, Wood 2017). Specific diagnostics included plotting model residuals to assess independence, equal variances, normal distributions, over- or under-dispersion, and outliers with high leverage. We conducted residual diagnostics using package 'DHARMa' (functions *simulateResiduals*, *plotResiduals*, *testUniformity*, *testDispersion*, *testOutliers*; Hartig 2021). Along with the residual diagnostics, we evaluated potential combinations of predictors for indications of collinearity, and specifically avoided variable combinations that produced variance inflation factors (VIFs) greater than 5 (Hair et al. 1998, Zuur et al. 2010).

To determine the best model for the analysis, we identified the subset of predictors that best explained variation in the observed response distances via stepwise model selection using the step function in R's base 'stats' package (R Core Team 2023) and following the GLMM model selection guidance of Zuur et al. (2009). This stepwise-selection was done in combination with the following criteria to select the best model: ANOVA-based comparisons of nested candidate models, R<sup>2</sup> values, and residual plots. To select final models using Akaike's Information Criterion (AIC), we evaluated only models that met the assumptions of GLMMs. Given the considerable number of predictors and unbalanced categorical factors with some groups having relatively small sample sizes, we used AIC corrected for small sample sizes (AICc) to compare candidate models to avoid overfitting. We generated graphics resulting from the best model using 'siPlot' Lüdecke 2023) and 'emmeans' (Length 2023), both of which rely on 'ggplot2' (Wickham 2016).

In discussing the significance of statistical results, we label results with  $P \le 0.001$  as highly significant,  $P \le 0.05$  as significant, and  $P \le 0.10$  as marginally significant.

#### Section 3. Results

#### 3.1 Sampling Results

The flight trials conducted at the Manzana study site in 2017 occurred at all seven DTBird installations between 06:45 and 16:45 H Pacific Standard Time (PST) on 2 days in mid-January, 3 days in late February and early March, and 5 days in August (Table 1). The January and February/March flights involved an initial, custom-built aircraft (AES Custom; Figure 5A) flown by our first pilot, but unfortunately that aircraft crashed and was damaged beyond repair during the March flights. The August flights then involved a different pilot and custom-built aircraft (AUV Custom; Figure 5B). The Manzana missions resulted in a total of 1,279 usable, distinct flight segments (Table 1).

Table 1. Summary of UAV Flight Trials Conducted at the Manzana Wind Project Site in California that Contributed Data for Analysis

Date	Sample Period (PST)	Turbine	Aircraft <sup>1</sup>	Missions Flown	Yield of Transect Samples
17-Jan-2017	08:15–11:40	V17	AES Custom	3	55
	13:05–16:45	E11	<b>AES</b> Custom	4	73
18-Jan-2017	08:45–12:05	D4	AES Custom	4	69
	13:15–14:25 <sup>2</sup>	D8	<b>AES</b> Custom	2	32
21-Feb-2017	07:55–12:05	U7	AES Custom	6	94
	13:15–13:50 <sup>2</sup>	D1	<b>AES</b> Custom	1	18
28-Feb-2017	10:45–15:45	T13	AES Custom	6	105
01-Mar-2017	08:35-10:10 <sup>3</sup>	E11	AES Custom	2	31
07-Aug-2017	07:35–13:55	V17	AUV Custom	8	146
08-Aug-2017	07:05–13:05	D8	AUV Custom	7	139
	13:55–15:50	U7	AUV Custom	2	37
09-Aug-2017	07:05–11:30	D4	AUV Custom	6	122
	12:35–13:15 <sup>3</sup>	U7	<b>AUV</b> Custom	1	16
10-Aug-2017	06:45–12:10	D1	AUV Custom	8	126
	13:00-15:00	T13	AUV Custom	3	49
11-Aug-2017	06:35-08:40	U7	AUV Custom	3	74
	09:25-12:25	E11	AUV Custom	5	93
			Totals	71	1,279

See Figure 5 for pictures of the aircraft.

At the Goodnoe Hills study site, the flight trials conducted in 2021 occurred at three turbines on two consecutive days in early August, involved a new pilot and mixed use of two UAVs (Clouds [Figure 5C] and Believer [Figure 5D]), and resulted in 210 flight samples suited to analysis (Table 2). Unfortunately, this flight

<sup>&</sup>lt;sup>2</sup> Aborted prematurely because of excessive wind or inclement weather.

<sup>&</sup>lt;sup>3</sup> Aborted prematurely because of UAV operational failure.

trial session was terminated prematurely when both aircraft suffered fatal crashes. We also attempted an initial round of flight trials at this site in May 2021, but we were generally unable to proceed due to wind speeds that were incompatible with conducting flight trials with light-bodied UAVs. The flight trials conducted in 2022 then occurred at four turbines on four days in late July. They involved another piloting team and limited use of another Clouds aircraft, but primarily a new Ranger aircraft (Figure 5E), and resulted in 272 flight samples suited to analysis. We also conducted another apparently successful series of eight flights at turbine G51 during the trial session in July 2022, only to find out later that a DTBird hardware mismatch issue resulted in no recordings of those flights. Thus, our sampling at this site fell short of expectations, which we could not overcome due to budget limitations.

Table 2. Summary of UAV flight trials conducted at the Goodnoe Hills Wind Farm study site in Washington that contributed data for analysis.

Date	Sample Period (PST)	Turbine	Aircraft <sup>1</sup>	Missions Flown	Yield of Transect Samples
02-Aug-2021	07:42-08:46	G58	Believer	2	38
	11:05–13:04	G58	Clouds	2	67
	17:43–20:33	G34	Clouds	3	71
03-Aug-2021	08:34–09:292	G44	Believer	2	34
25-Jul-2022	11:57-12:102	G34	Clouds	1	10
26-Jul-2022	09:59–15:55	G64	Ranger	4	54
27-Jul-2022	08:15–15:41	G75	Ranger	7	111
29-Jul-2022	07:49-13:40	G44	Ranger	8	97
			Totals	29	482

See Figure 5 for pictures of the aircraft.

#### 3.2 Modeling Response Distances

The evaluation results for the initial full model and other models considered as part of the backward selection process used to identify the best model are portrayed in Appendix B. The final, selected model had the following form:

LoS Response Distance  $\sim (1 \mid Site : Turbine ID) + (1 \mid Site : UAV Model) + Site + Event Type + Sky Backdrop + Ground Speed + Wind Speed + Roll Angle + Pitch Angle + Roll Angle * Pitch Angle$ 

A model with only the random effects included (AICc = 20010.06) reduced the AICc score by a substantial 223.48 points compared to the null model (AICc = 20233.54), and the selected model (AICc = 19918.34) reduced the AICc score by another substantial 91.2 points (315.2 total points compared to the null model). These results confirm noteworthy improvements in balancing parsimony and explanatory power (Burnham and Anderson 2010). The selected model also reduced the AICc score by 70.9 points compared to the full model (AICc = 19989.19), further reflecting a markedly improved model. However, the Nakagawa marginal pseudo-

<sup>&</sup>lt;sup>2</sup> Aborted prematurely because of UAV operational failure.

R<sup>2</sup> for the model (0.092) was low (Nakagawa and Shielzeth 2013), indicating that the included fixed effects provided only marginal explanatory power and a lot of variability in the dataset remained unexplained.

Diagnostics indicated that the final model satisfied the important assumptions of independence, normally distributed residuals, and the absence of significant collinearity among the predictors. However, Levene Tests for homogeneity of variances across groups within categorical variables (Zuur et al. 2009, Hartig 2021) confirmed modest deviations from ideal for *Site* and *Event Type*, but not for *Sky Backdrop*. These results suggest that the assumption of homogenous variances within groups was not completely met. Nevertheless, by incorporating random effects in the model, GLMMs estimate the variance components for the random effects, capturing the variability between groups and within groups. This flexibility in modeling allows for the accommodation of heteroscedasticity and helps to mitigate the impact of violations of the assumption of homogeneity of residual variances. Additionally, GLMMs can provide accurate parameter estimates and valid statistical inference even in the presence of heteroscedasticity; the mixed-effects structure helps to account for the correlation structure within the data, which reduces bias and provides robust standard errors for hypothesis testing (Zuur et al. 2009).

Output for the selected model indicated that including *Site*: *Turbine ID* as a random effect accounted for modest variation among turbines in modeled response distances (Figure 6). Specifically, the modeling results suggested that response distances were more variable among the seven Manzana turbines than among the five Goodnoe Hills turbines. Among the seven Manzana turbines, response distances were approximately 8.9 m shorter than the estimated global average at one turbine (V17), 7.7 m longer than average at one turbine (T13), and values for the other five turbines ranged from -0.9 m shorter to 1.7 m longer than the grand average. In comparison, the range of variation among the five Goodnoe Hills turbines was from 4.5 m shorter to 3.9 m longer than average, and values for the other three turbines ranged from -1.1 m shorter to 2.4 m longer than average. Although noteworthy but not particularly substantial differences, these apparent turbine-level variations likely reflect situation-specific landscape variation leading to modest variability in DTBird's ability to detect and target objects of interest.

Output for the selected model indicated that including *Site*: *UAV Model* as a random effect also captured noteworthy variation in the global average response levels attributable to the different UAV models used (Figure 7). The two UAV models used at the Manzana site showed the greatest variance in response distances: approximately 15.0 m shorter than the estimated global average across UAV types for the AUV Custom aircraft (with a skinny tubular hind body and more variable coloration; Figure 5A) and 15.0 m longer than average for the AES Custom aircraft (overall a more eagle-like torso and darker coloration; Figure 5B). At the Goodnoe Hills, variation among the three UAV models was less pronounced, ranging from an estimated 5.1 m shorter than average for the Believer aircraft (a relatively heavy, dark, and fast-flying aircraft; no picture available), 4.2 m longer than average for the Clouds aircraft (a relatively large and robust body and intermediate coloration; Figure 5D), and a nominal 0.9 m longer than average for the Ranger aircraft (longest wing span, but relatively narrow features and intermediate coloration; Figure 5C).

The coefficients and associated parameter tests for the fixed effects retained in the selected model are provided in Table 3. The selected model suggested that the retained fixed-effect predictors influenced the DTBird LoS Response Distances as summarized below.

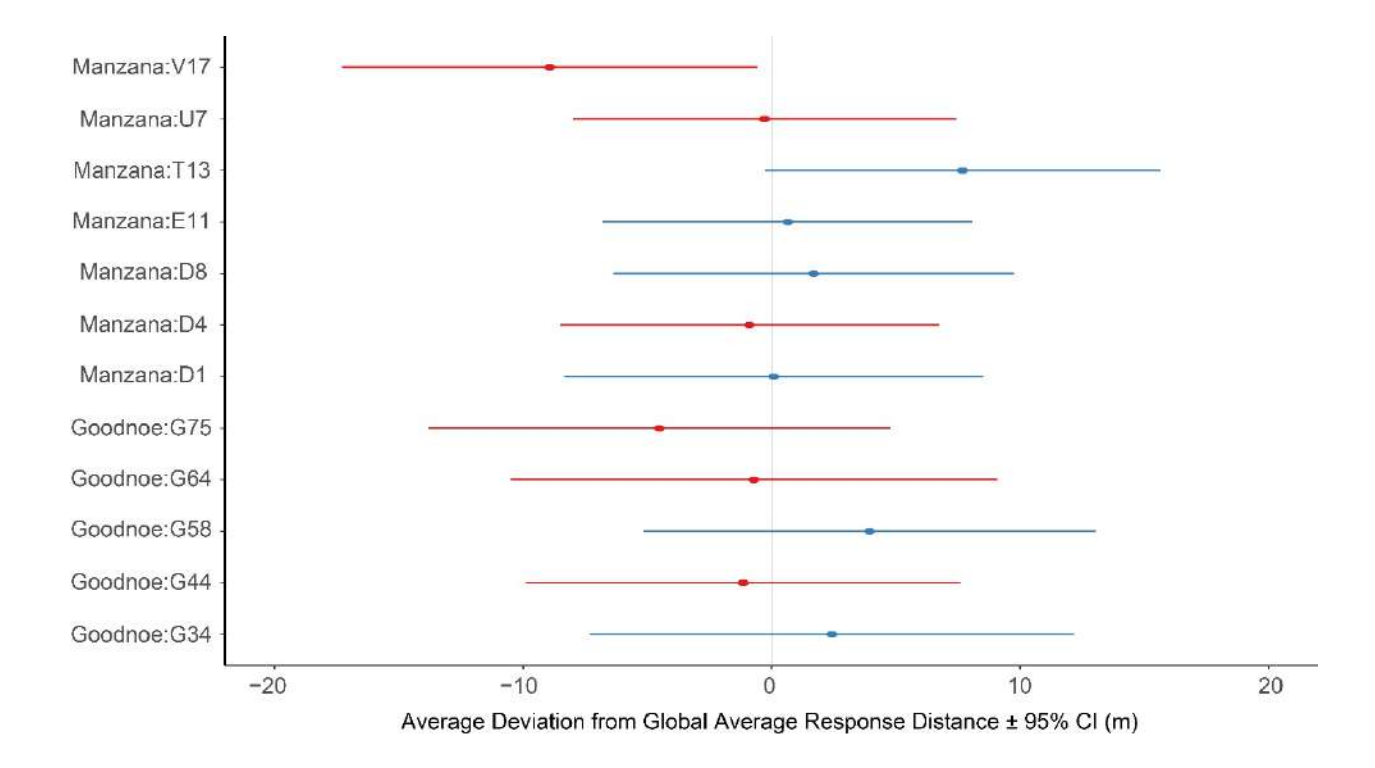


Figure 6. Deviations from the estimated global average DTBird response distance associated with different site-specific turbine installations, estimated as a nested random effect in the multi-site GLMM developed for the study.

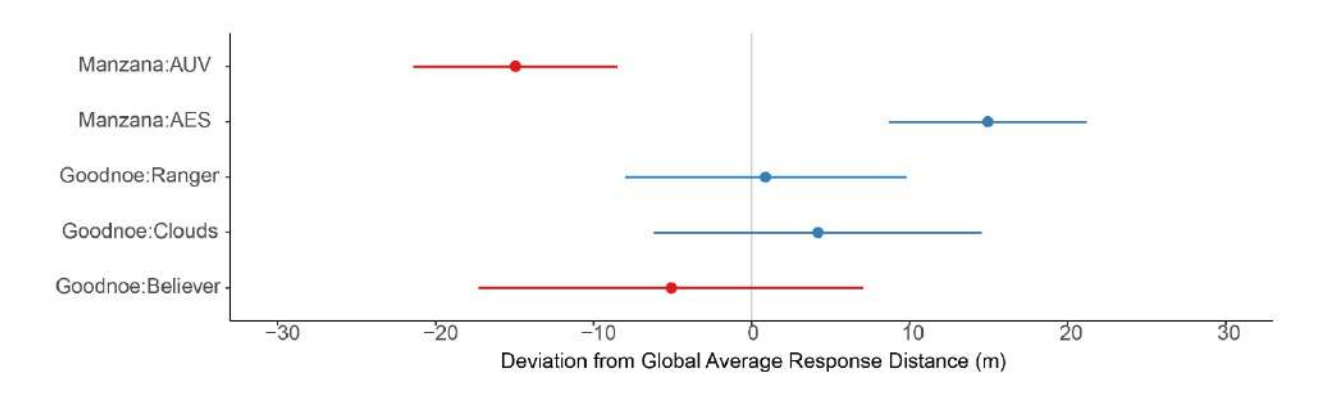


Figure 7. Deviation from the estimated global average DTBird response distance associated with site-specific use of different UAV models, estimated as a nested random effect in the multi-site GLMM developed for the study.

Table 3. Coefficients and parameter t-test results for fixed effects represented in the selected multi-site GLMM with DTBird response distance as the dependent variable.

Predictor	Coefficient	SE	df	t	Р
(Intercept)	197.677	9.312	5.0	21.2	<0.0001
Site : Manzana <sup>1</sup>	-32.701	13.621	3.7	-2.4	0.0794
Event Type : Warning <sup>2</sup>	0.755	4.314	1798.7	0.2	0.8612
Event Type : Dissuasion <sup>2</sup>	-14.149	3.412	1793.9	-4.1	< 0.0001
Sky Backdrop : PartlyCloudy <sup>3</sup>	3.900	5.751	48.9	0.7	0.5008
Sky Backdrop : MostlyCloudy <sup>3</sup>	10.864	5.980	104.6	1.8	0.0721
Sky Backdrop : Overcast <sup>3</sup>	19.361	5.433	105.1	3.6	0.0006
Ground Speed	3.282	1.595	1744.8	2.1	0.0397
Wind Speed	3.229	1.657	1623.0	1.9	0.0515
Roll Angle	2.459	1.418	1798.4	1.7	0.0830
Pitch Angle	-0.719	1.429	1800.1	-0.5	0.6148
Roll Angle * Pitch Angle	-5.607	1.315	1796.0	-4.3	<0.0001

<sup>&</sup>lt;sup>1</sup> Reference category: Goodnoe Hills.

Site: The coefficient and parameter test for this fixed effect suggested that response distances averaged marginally shorter overall at the Manzana site than at the Goodnoe Hills site, and the post-hoc comparison of estimated means and variances illustrated that difference, but confirmed that it was not significant at  $P \le 0.05$  (Figure 8).

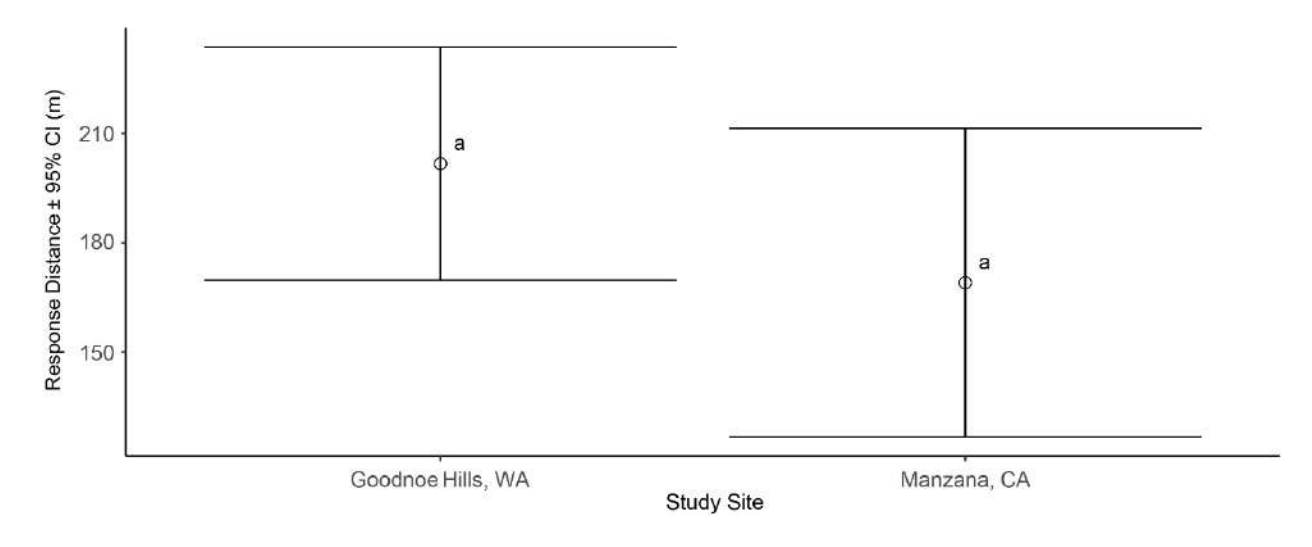


Figure 8. Modeled relationship between DTBird response distances and study site, with shared letters indicating pairwise differences that are not significant at  $P \le 0.05$ .

<sup>&</sup>lt;sup>2</sup> Reference category: Detection event.

<sup>3</sup> Reference category: Fair skies.

Event Type: Including Event Type as a fixed effect accounted for the significant "structural" (i.e., a system calibration/programming feature) difference in expected trigger distances for dissuasion signals compared to initial detections and warning signals (Figure 9). Calibrated for this study, initial detections were expected to occur at 240 m from the cameras throughout the projected detection envelope, while warning signals were also to be triggered at 240 m throughout the core envelope and at 170 m across lower, outer reaches of the detection envelope (see H. T. Harvey & Associates 2018 for graphical illustrations). In contrast, dissuasion signals were expected to trigger at 170 m from the cameras throughout most of the expected detection envelope, and at 100 m across lower, outer reaches of the detection envelope. In contrast, The marginal means produced from the model for this parameter reflected the difference in average response distances for dissuasion signals (175.7  $\pm$  7.34 m [SE]) and the comparatively minimal difference between the average response distances for initial detections (189.9  $\pm$  7.00 m) and warning signals (190.61  $\pm$  7.72 m). Also note, however, that the range of observed values for all three Event Types was wide (Figure 9). In addition, although the dissuasion-trigger response distances averaged close to the calibrated core-envelope trigger distance of 170 m, the averages for detections and warning signal triggers were notably shorter than the expected 240 m core-envelope trigger distances for those events.

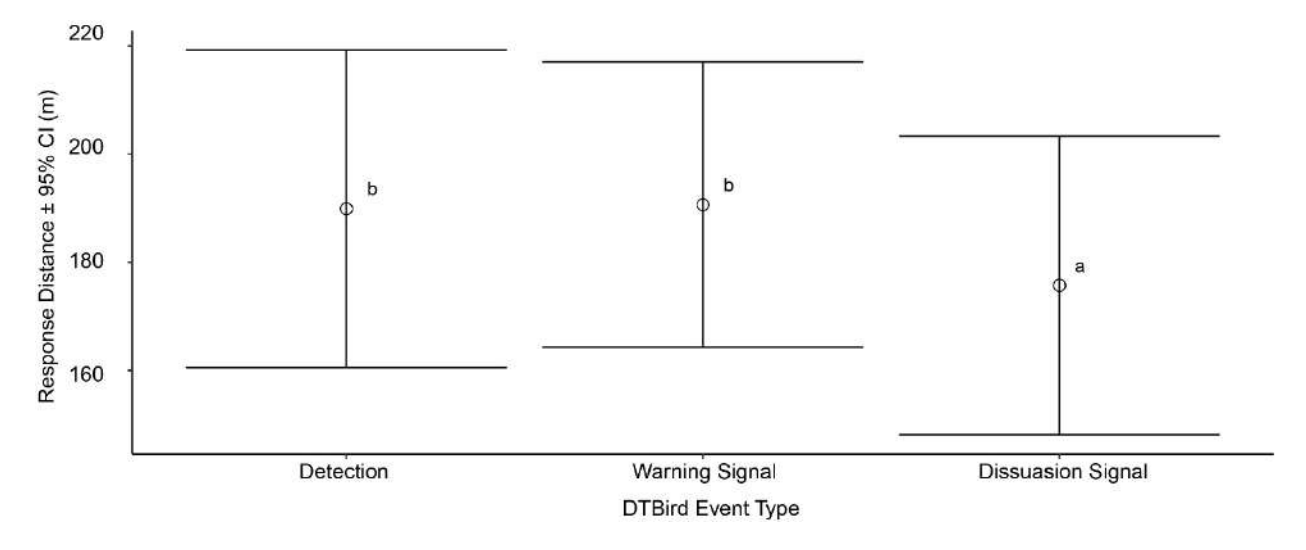


Figure 9. Modeled relationship between DTBird response distances and detection and deterrent-triggering event types, with shared letters indicating pairwise differences that are not significant at  $P \le 0.05$ .

Sky Backdrop: Response distances and cloud cover were positively correlated, with the average response distance increasing with the progression from fair to overcast skies (Figure 10). Parameter tests and post-hoc comparisons of estimated marginal means confirmed that response distances averaged a significant 19.4 m shorter under fair skies (defined as few if any small clouds in the sky) than under overcast skies (defined as complete or near-complete, dense cloud cover with little to no penetration of blue sky or large sunspots), with the average responses under partly cloudy (defined as more than a few small clouds but <50% cloud cover) and mostly cloudy skies (≥50% up to near-complete cloud cover but with distinct patches of blue and/or brighter clouds) intermediate in the progression and not significantly different from other categories.

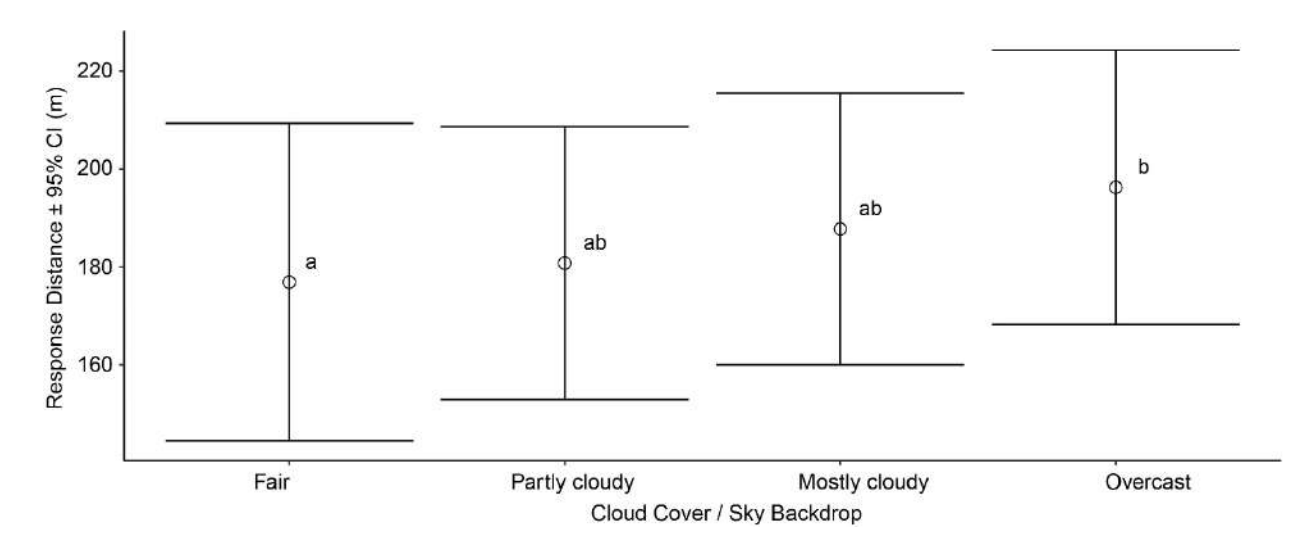


Figure 10. Modeled relationship between DTBird detection and deterrent-triggering response distances and sky backdrop / cloud cover categories, with shared letters indicating pairwise differences that are not significant at  $P \le 0.05$ .

*Ground Speed:* Response distances tended to increase as the rate of UAV travel relative to fixed points on the ground increased (Figure 11).

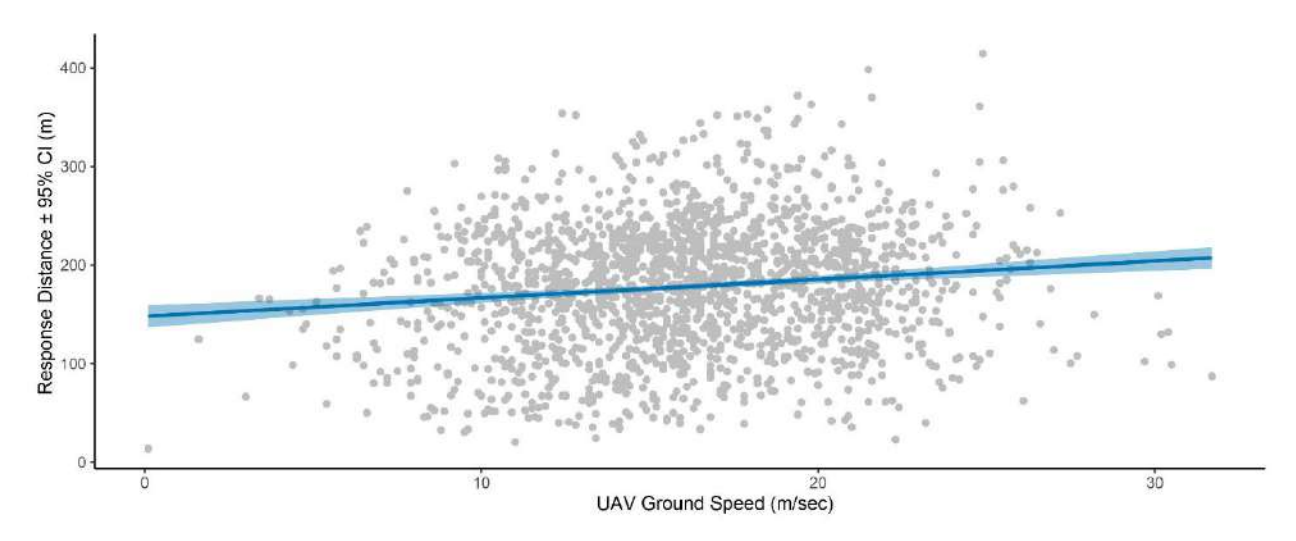


Figure 11. Modeled relationship (±95% confidence interval) between DTBird detection and deterrent-triggering response distances and UAV ground speed, or rate of travel relative to a fixed point on the ground, as measured by UAV avionics during sampling flights.

Wind Speed: Response distances tended to increase as the wind speed—measured in flight by the UAV avionics—increased (Figure 12).

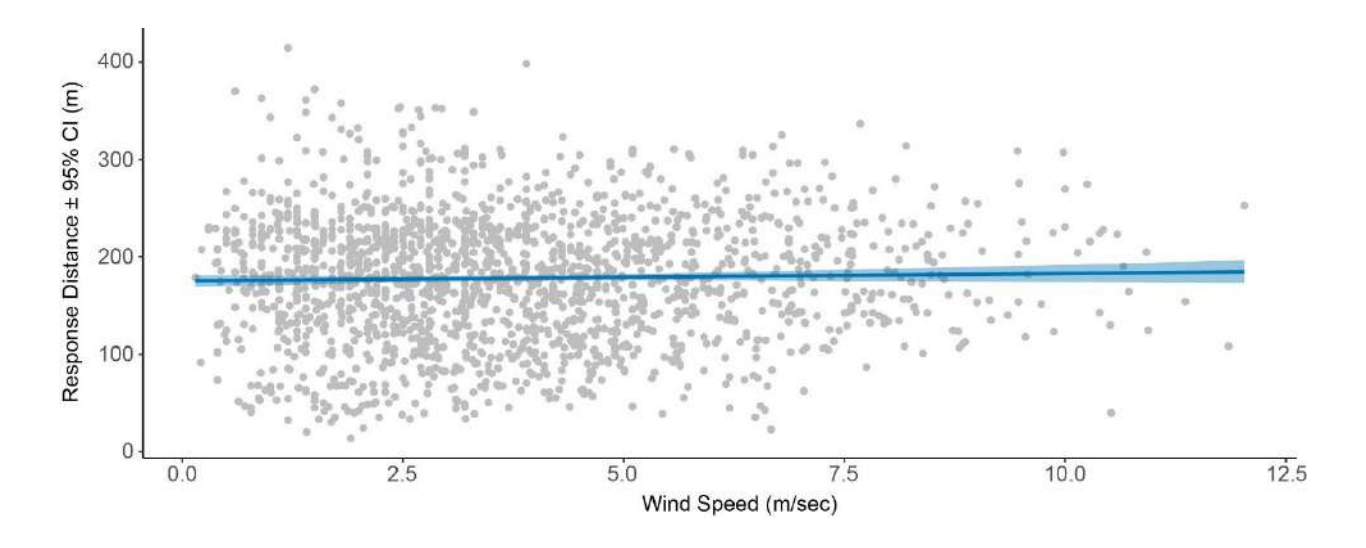


Figure 12. Modeled relationship between DTBird detection and deterrent-triggering response distances and wind speed as measured by UAV avionics during sampling flights.

Roll Angle: Pitch Angle Interaction: The degree to which a UAV rolled to one side or the other or pitched up or down while in flight influenced DTBird response distances in an interactive manner (Figure 13). Roll Angle was shown to be the strongest predictor of the two variables (Table 3), with observed values ranging from approximately -59° (left roll) to +41° (right roll). The interactive influence of Pitch Angle (observed values from -20° pitched down to +36° pitched up) reflected that pitching and rolling often acted in concert to increase exposure of the UAV profile to the cameras, but concurrent maximization of both metrics was effectively impractical.

More specifically, graphical illustrations of this interactive relationship indicated the following:

- With a low *Pitch Angle* (i.e., aircraft flying near nose-to-tail level), the more the UAV rolled from side to side (e.g., bouncing around in the wind or banking in a turn), the more the response distance increased.
- With a low Roll Angle (i.e., aircraft flying with wings near level), greater Pitch Angles also tended to increase response distances to a lesser degree.
- Combinations of moderate pitch and roll angles were associated with moderate to moderately high
  response distances, but concurrent maximization of both stability metrics was effectively impractical,
  because it would translate to the aircraft stalling and falling out of the sky. Hence, the indications in
  Figure 13 that as one stability metric increased, the other generally declined, and vice versa, which
  was largely a result of the automated avionics programming explicitly striving to avoid stalling the
  aircraft.

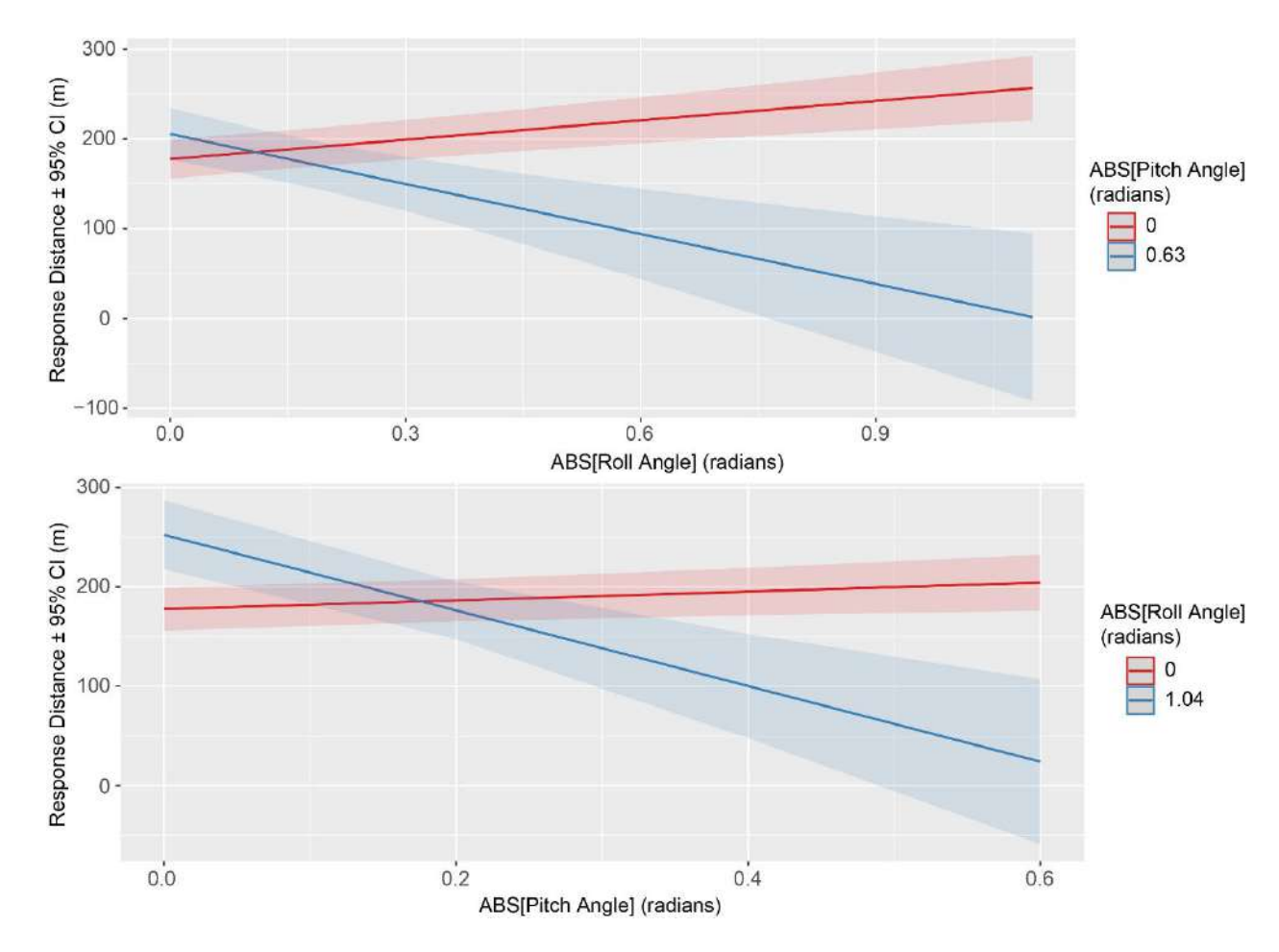


Figure 13. Modeled relationships between DTBird detection and deterrent-triggering response distances and the interactive influence of UAV pitch and roll angles.

#### Section 4. Discussion

The results of this multi-site modeling effort, based on data collected at the Manzana wind facility in California and Goodnoe Hills wind facility in Washington, benefited from previous site-specific analyses and, analyzed together, bolstered insight about factors that influence performance of the DTBird detection and deterrent-triggering systems. Innovations brought to bear in this new analysis included:

- 1) Understanding that modeling some of the position covariates we included before (e.g., lateral distance from turbine, relative altitude, and UAV elevation angle; see H. T. Harvey & Associates 2018) was inappropriate due to their being mathematically related by simple geometry and trigonometry to the response variable.
- 2) Including UAV model as a random effect nested within *Site*, rather than as a fixed effect, because no common UAV usage occurred at the two sites and the data involved repeated measures with each individual UAV model.
- 3) Given bolstered sample sizes, considering anew some variables (e.g., *DFT*, *COG*, *Sun Azimuth*, and *Sun Elevation Angle*) previously considered but that did not figure into the final site-specific models compared in H. T. Harvey & Associates (2022b).
- 4) Considering new transformations to effectively evaluate the influence of certain circular variables, including interactions with sun-positioning metrics.

Characterizing the response-distance data for the three event types revealed some unexpected results. The average response distance for detection events (190 m) was longer than for dissuasion signals (176 m), as expected, but was considerably shorter than the 240-m theoretical maximum, calibrated detection distance. This result primarily reflected that initial detections often occurred when the UAV flew in low and first entered the detection envelope from the underside of the overall, inverted-cone-shaped envelope at relatively close distances to the turbine. Conversely, longer-than-expected response distances were comparatively uncommon.

A similar factor also contributed to the outcome for warning signals, where some initial triggers were expected to occur at distances of 100–170 (Figure 4); however, with the realm over which such warning signals could occur limited to less than one third of the perimeter area over which shorter detection distances could arise (Figure 4), the matching average detection and warning signal response distances were not expected. Reasons for this result are uncertain, but the outcome may reflect that, despite mostly common triggering calibration, longer than expected warning-signal response distances were proportionately less common than longer-than-expected detection response distances. This could be considered a desirable outcome, in that it means relevant targets were sometimes detected at greater than expected distances—increasing time for effective deterrent response if needed—but unnecessary warning signals targeting extra-distant birds were constrained.

The average response distance for triggering a dissuasion signal (176 m) nearly matched the calibrated core-envelope trigger distance for that event type (170 m), whereas the expectation was for a lower average reflecting a mix of expected response distances of approximately 170 m across the core-envelope surveillance area and

100-m in the outer, lower band of surveillance areas (see Figure 4). Instead, the observed outcome suggested that dissuasion signals were triggered more often than expected at distances exceeding the calibrated trigger distances. This result could be considered a beneficially conservative outcome in providing more time for an approaching bird to respond to a dissuasion signal, as long as it does not result in unnecessarily excessive triggering of the signals, with possible adverse consequences for non-target wildlife, facility staff, or facility neighbors (H. T. Harvey & Associates 2018).

The multi-site results illustrated notable random variation among turbines at the two study sites, and indicated that, given modeling of other random and fixed effects, the overall DTBird response distances tended to average marginally shorter at the Manzana study site compared to the Goodnoe Hills site. Reasons for this difference are uncertain, but it suggests that the overall targeting accuracy of the DTBird systems can vary slightly across different landscape settings, perhaps reflecting inherent differences in the overall visual clarity and complexity of different regional skies and landscape backdrops. DTBird does not reliably detect objects against a landscape, as opposed to sky, backdrop, and topographic complexity sometimes intrudes within the camera viewsheds to limit detectability. In this case, the proximate and elevated backdrop of the Tehachapi Mountains may have complicated detectability at the Manzana site more than the comparatively wide-open skies at the Goodnoe Hills site.

The multi-site results continued to support the notion that modeled variation in average response distances among the five UAV models we deployed in this study likely mimicked the kind of random variation that could be expected given eagles of different sizes and coloration patterns, such as those pertaining to differences among the sexes and age classes of golden eagles. As the initial Manzana site-specific analysis suggested (H. T. Harvey & Associates 2018), the demonstration that response distances tended to be relatively short for the AUV Custom aircraft is logical given its skinny tubular hind body and overall modest stature, with the relatively long-winged but slender Ranger aircraft also showing some of that tendency. In contrast, a tendency toward longer response distances was associated with the overall more eagle-like and robust-bodied AES Custom and Clouds models.

The multi-site results pertaining to the influence of cloud cover / sky backdrop on DTBird response distances suggested some similar patterns as the preceding site-specific analyses, but also some refinements. Specifically, all else equal, the updated analysis indicated that response distances generally increased as cloud cover increased and averaged significantly longer once the cloud cover extended throughout the viewshed under relatively uniform overcast skies. This outcome is logical in suggesting that the DTBird systems more readily detected the relatively dark eagle-like UAVs against relatively uniform high-contrast white or gray backgrounds than against less contrasting blue skies and or highly dynamic partly cloudy skies. These tendencies also mimic the challenges faced by observers scanning the skies for migrating raptors, where the presence of uniform cloud cover greatly increases the detectability of migrants passing overhead underneath the clouds (Bildstein et al. 2007).

The multi-site model uniquely indicated a significant positive association between response distances and UAV ground speed, which suggested that targeting performance improved significantly when a UAV was traveling relatively quickly from the perspective of the camera. This result may reflect that the DTBird detection algorithm focuses on targeting objects that both fill enough image pixels to warrant targeting from an estimated

distance perspective, and that it perceives as moving in a manner that could be a flying bird. Our modeling results suggest that, across the UAV flight speeds documented in this study, slow-moving targets were generally harder for the DTBird system to detect than rapidly moving targets.

We included in our modeling effort consideration of a suite of variables as potential indicators of variation in the exposure of UAV profiles to the cameras, where greater profile exposure is expected to increase the accuracy of DTBird targeting based on calibrated settings. Our hypothesis was that the more a UAV climbs or descends, pitches up or down in the wind, rolls from side to side in the wind or while banking, or is generally bounced around by and quarters into the wind, the more the UAV profile should be exposed to the cameras and lead to more accurate targeting. Similar to the preceding site-specific modeling results, the final multi-site model continued to emphasize the importance of such variables in predicting DTBird response distances specifically indicating a positive association with wind speed and the interactive influence of roll and pitch angels. The previous site-specific models also suggested that UAV Climb Rate was a relevant predictor, but that variable did not pan out as a significant predictor in the multi-site model, perhaps due to the combined data reflecting a stronger association with pitch and roll angles, with the former variable theoretically capturing a similar effect as variable climb rates (both descending and descending trajectories). The final model indicated relationships for wind speed and roll and pitch angles that were similar to the patterns reflected in the previous site-specific models, suggesting that response distances increased at higher wind speeds (UAV bouncing around more) and/or when the UAV was rolling side to side more, but only if the aircraft was not simultaneously pitching up or down to a substantial degree, because that combination would have caused the aircraft to stall and fall from the sky.

The initial Manzana site-specific model reflected a significant second-order relationship between response distances and the intensity of solar irradiation impinging on the UAV in the direction of the cameras. However, that relationship did not pan out again in the Goodnoe Hills site-specific model once we applied a more robust approach to developing that model. Similarly, none of the solar variables we considered were incorporated in the final multi-site model. There is no question that flying objects seen in the DTBird videos and targeted by the system routinely disappear from view when passing through major sunspots, and that high intensity solar insolation often increases the glare factor around such sunspots. In this case, however, we suspect that the combined-site dataset more effectively captured this effect in the refined relationship with sky backdrop/cloud cover. Specifically, situations where substantial sunspots obscured detectability were particularly prevalent under fair and partly cloudy skies, and greatly diminished when cloud cover was more complete, especially once overcast skies prevailed. Hence, the relative prevalence of sunspots may have been a primary driver behind the apparent positive relationship between response distances and cloud cover illustrated in the multi-site model, to the exclusion of solar intensity or positioning proving to be of additional predictive value.

#### 4.1 Concluding Statements

This investigation highlighted several flight metrics and environmental covariates that significantly influenced DTBird's detection and deterrent-triggering performance at the two wind-facility study sites. Here it is important to acknowledge that using eagle-like UAVs as surrogates for real eagles constrained the insights

generated from the study. We think the fixed-wing UAVs we used in the study did a good job of mimicking the non-flapping soaring and other flights of eagles, but were limited by not having wings that flap and tuck in the manner used by eagles to accomplish various maneuvers. The UAVs were also not capable of undertaking steep dive-and-roll or "roller-coaster" type display maneuvers that Golden Eagles sometimes make in pursuing prey or as part of their territorial behavior (Katzner et al. 2020). The degree to which more-dynamic wing action and flight maneuvers could alter the apparent targeting performance of the DTBird systems is uncertain. Wing flapping undoubtedly exposes more of a bird's profile to the cameras, at least intermittently; however, wing tucking does the opposite. In other words, these two components of real-bird flight dynamics may be offsetting factors that translate to average response distances similar to those reflected in the strictly fixed-wing UAV data we collected. If efforts to use UAVs as bird mimics are considered for similar future studies, some of the new robotic birds available today that actually fly with flapping wings should be considered, as long as the flapping rate of the robotic bird effectively mimics that of target birds of interest. In particular, a robotic bird with quick wingbeats and that flaps all the time to stay aloft would not be a good mimic for eagles, because eagles often spend most of their time in non-flapping soaring and sailing flight, rather than using powered flight (e.g., see Katzner et al. 2020).

Throughout these UAV flight trials, our effort was unexpectedly constrained to a high degree by incompatible weather and wind conditions. High winds and excess moisture in the air not only limited when we could fly, but also ultimately led to fatal crashes that took out four of the five aircraft we used, because we were compelled to fly in conditions that pushed the limits of tolerance for the light-weight, foam-bodied aircraft. On the positive front, having to replace several aircraft resulted in our flying a greater diversity of models than initially anticipated, which effectively mimicked some of the variability in DTBird performance that would likely occur given eagles of various sizes and color patterns. On the negative front, these unexpected complications significantly reduced the diversity of flight conditions during which we were able to conduct sampling flights, and substantially constrained the overall dataset compared to our original study-design projections. Nevertheless, we think the dataset we did amass provided valuable insight into how salient flight characteristics and environmental covariates influenced DTBird's performance in detecting eagles (or surrogates) and triggering deterrence signals compared to calibrated system settings.

Lastly, we acknowledge that the differences rated as statistically significant effects given our data sometimes amounted to effects magnitudes that may not have especially noteworthy biological or operational significance (e.g., 10–20 m differences in detection range for birds that may easily move farther than that in less than a second). However, our study was not designed to specifically quantify the relative effectiveness of different calibrated detection and deterrent triggering distance thresholds nor the spatiotemporal aspects of what an eagle requires as deterrent warning to avoid calamity under different flight conditions. Therefore, we have no firm basis for presuming what may be biologically/operationally significant in this context.

#### Section 5. References

- ArduPilot Dev Team. 2021. Mission Planner. Version 1.3.77. <a href="https://firmware.ardupilot.org/">https://firmware.ardupilot.org/</a> Tools/MissionPlanner>. Accessed July 2022.
- Aschwanden, J., S. Wanner, and F. Liechti. 2015. Investigation on the Effectivity of Bat and Bird Detection at a Wind Turbine: Final Report Bird Detection. Prepared for Interwind AG, Swiss Federal Office of Energy, and Federal Office for the Environment. Schweizerische Vogelwarte, Sempach, Switzerland.
- Bates, D., M. Maechler, B. Bolker, and S. Walker. 2015. Fitting Linear Mixed-Effects Models Using Ime4. Journal of Statistical Software 67:1-48. DOI 10.18637/jss.v067.i01.
- Bildstein, K. L., J. P. Smith, and R. Yosef. 2007. Migration counts and monitoring. Pages 101–116 in D. M. Bird and K. L. Bildstein (Editors), Raptor Research and Management Techniques. Hancock House Publishers, Blaine, WA, USA, and Surrey, British Columbia, Canada.
- Burnham, K. P., and D. R. Anderson. 2010. Model Selection and Multimodel Inference: A Practical Information-Theoretic Approach. Second Edition. Springer, New York, NY, USA.
- Cremers, J., and I. Klugkist. One direction? A tutorial for circular data analysis using R with examples in cognitive psychology. Frontiers in Psychology 9:2040. 13 pp. doi:10.3389/fpsyg.2018.02040.
- Fernie, A. 2012. TLogDataExtractor. Version 1.1. <a href="https://onedrive.live.com/?cid=2B4DC8F6BD223F57">https://onedrive.live.com/?cid=2B4DC8F6BD223F57</a>% &id=2B4DC8F6BD223F57% 212440>. Accessed August 2022.
- Fisher, N. I. 1995. Statistical Analysis of Circular Data. Cambridge University Press, Cambridge, UK.
- Hair, J.F., R. L. Tatham, and R. E. Anderson. 1998. Multivariate Data Analysis. Fifth edition. Prentice Hall, Englewood Cliffs, NJ, USA.
- Hanagasioglu, M., J. Aschwanden, R. Bontadina, and M. de la Puente Nilsson. 2015. Investigation of the Effectiveness of Bat and Bird Detection of the DTBat and DTBird Systems at Calandawind Turbine. Final Report. Prepared for the Swiss Federal Office of Energy Research Program, Wind Energy and Federal Office for the Environment Species, Ecosystems, Landscapes Division. Bern, Switzerland.
- Hartig, F. 2021. DHARMa: Residual Diagnostics for Hierarchical (Multi-Level / Mixed) Regression Models. R package version 0.4.4. <a href="https://CRAN.R-project.org/package=DHARMa">https://CRAN.R-project.org/package=DHARMa</a>.
- H. T. Harvey & Associates. 2018. Evaluating a Commercial-Ready Technology for Raptor Detection and Deterrence at a Wind Energy Facility in California. Research Report. Los Gatos, CA, USA. Prepared for the American Wind Wildlife Institute, Washington, D.C., USA
- H. T. Harvey & Associates. 2019a. Evaluating the Effectiveness of a Detection and Deterrent System in Reducing Eagle Fatalities at Operational Wind Facilities: Detailed Study Plan. Los Gatos, CA, USA. Prepared for the American Wind Wildlife Institute, Washington, D.C., USA, in conjunction with U.S. Department of Energy Cooperative Agreement DE-EE0007883.

- H. T. Harvey & Associates. 2019b. Analysis of DTBird False Positive Detections at the Manzana Wind Power Project Through October 2017. Research Report. Los Gatos, CA, USA. Prepared for the American Wind Wildlife Institute, Washington, D.C., USA, in conjunction with U.S. Department of Energy Cooperative Agreement DE-EE0007883.
- H. T. Harvey & Associates. 2022a. Initial Analysis of DTBird False Positive Detections at the Goodnoe Hills Wind Farm, Washington: September 1, 2021 March 15, 2022. Research Report. Los Gatos, CA, USA. Prepared for the Renewable Energy Wildlife Institute, Washington, D.C., USA, in conjunction with U.S. Department of Energy Cooperative Agreement DE-EE0007883.
- H. T. Harvey & Associates. 2022b. Initial Analyses of DTBird Detection and Deterrent-Triggering Response Distances and Probability of Detection at the Goodnoe Hills Wind Farm, Washington. Research Report. Research Report. Los Gatos, CA, USA. Prepared for the Renewable Energy Wildlife Institute, Washington, D.C., USA, in conjunction with U.S. Department of Energy Cooperative Agreement DE-EE0007883.
- Katzner, T. E., M. N. Kochert, K. Steenhof, C. L. McIntyre, E. H. Craig, and T. A. Miller. 2020. Golden Eagle (*Aquila chrysaetos*), version 2.0. *In P. G. Rodewald and B. K. Keeney (Editors)*, Birds of the World. Cornell Lab of Ornithology, Ithaca, NY, USA. <a href="https://doi.org/10.2173/bow.goleag.02">https://doi.org/10.2173/bow.goleag.02</a>.
- Length, R. 2023. emmeans: Estimated Marginal Means, aka Least-Squares Means. R package version 1.8.6. <a href="https://CRAN.R-project.org/package=emmeans">https://CRAN.R-project.org/package=emmeans</a>.
- Litsgård, F., A. Eriksson, T. Wizelius, and T. Säfström. 2016. DTBird System Pilot Installation in Sweden. Possibilities for Bird Monitoring Systems Around Wind Farms. Experiences from Sweden's First DTBird Installation. Ecocom AB, Kalmar, Sweden. (English summary provided by DTBird Team).
- Lüdecke, D. 2023. sjPlot: Data Visualization for Statistics in Social Science. R package version 2.8.14. <a href="https://CRAN.R-project.org/package=sjPlot">https://CRAN.R-project.org/package=sjPlot</a>.
- May, R., Ø. Hamre, R. Vang, and T. Nygård. 2012. Evaluation of the DTBird Video-System at the Smøla Wind-Power Plant: Detection Capabilities for Capturing Near-Turbine Avian Behaviour. NINA Report 910. Norwegian Institute for Nature Rese arch, Trondheim, Norway.
- Nakagawa, S., and H. Schielzeth. 2013. A general and simple method for obtaining R<sup>2</sup> from generalized linear mixed-effects models. Methods in Ecology and Evolution 4:133–142. https://doi.org/10.1111/j.2041-210x.2012.00261.x.
- R Core Team (2023). R: A language and environment for statistical computing. R Foundation for Statistical Computing, Vienna, Austria. <a href="https://www.R-project.org/">https://www.R-project.org/</a>.
- Wickham, H. 2016. ggplot2: Elegant Graphics for Data Analysis. Springer-Verlag New York, NY, USA.
- Wood, S. N. 2017. Generalized Additive Models: An Introduction with R. Second edition. CRC Press, Taylor & Francis Group, New York, NY, USA.
- Zuur, A. F., E. N. Ieno, and C. S. Elphick. 2010. A protocol for data exploration to avoid common statistical problems. Methods in Ecology and Evolution 1:3–14.

Zuur, A. F., E. N. Ieno, N. J. Walker, A. A. Saveliev, and G. M. Smith. 2009. Mixed Effects Models and Extensions in Ecology with R. Springer, New York, NY, USA.

## Appendix A. Variables Considered in DTBird Detection and Deterrent-Triggering Response Distance Analysis

		_	Response Distance
Variable	Description	Source	Model Input
Line-of-Sight (LoS) Response Distance (m)	Line-of-sight distance from camera to UAV at time of event	UAV avionics and GIS measurement	Dependent variable
Site: Turbine ID	ID# of focal turbine during trial session	Analyst input	Random effect, categorical predictor nested within Site
Site : UAV Model	Five UAV models used, different ones at the two study sites	Analyst input	Random effect, categorical predictor nested within Site
Site	Wind facility study sites: Manzana, CA and Goodnoe Hills, WA	Analyst input	Fixed effect, categorical predictor
Event Type	DTBird detection, warning signal, or dissuasion signal	DTBird DAP	Fixed effect, categorical predictor
Sky Backdrop	Fair, partly cloudy, mostly cloudy, overcast	DTBird DAP	Fixed effect, categorical predictor
Climb Rate (m/sec)	UAV climb rate	UAV Avionics	Fixed effect, continuous covariate
Roll Angle (radians)	UAV lateral roll angle (-1.6 = 90° roll left; +1.6 = 90° roll right. Observed -1.04–0.71 or -60–41°)	UAV Avionics :	Fixed effect, continuous covariate
Pitch Angle (radians)	UAV nose-tail Pitch Angle (-1.6 = 90° pitch nose down; +1.6 = 90° pitch nose up. Observed: -0.34–0.63 or -20–36°)	UAV Avionics	Fixed effect, continuous covariate
Direction From Turbine (DFT) (°)	Direction from turbine to UAV (1–360° compass heading)	GIS measurement	Fixed effect, continuous covariate transformed to orthogonal east-west (cos[x]) and north-south (sin[x]) vectors
Course Over Ground (COG) (°)	UAV course over ground (1–360° compass heading)	UAV Avionics	Fixed effect, continuous covariate transformed to orthogonal east-west (cos[x]) and north-south (sin[x]) vectors
Solar Irradiation (watt-hours/m²)	Solar radiation impinging on UAV in line of sight with camera	GIS measurement using national solar database	Fixed effect, continuous covariate, and second-order term
Sun Elevation Angle (°)	Vertical angle from camera to sun (range ~ -2–71°)	GIS measurement using national solar database	Fixed effect, continuous covariate
Sun Azimuth (°)	Compass direction to position of sun from turbine (range ~82–297°)	GIS measurement using national solar database	Fixed effect, continuous covariate

Wind Speed (m/sec)	-	UAV avionics	Fixed effect, continuous covariate
Ground Speed (m/sec)	UAV travel speed relative to ground	UAV avionics	Fixed effect, continuous covariate

# Appendix B. Evaluation Results for the Initial Full and Other Candidate Models Considered as Part of the Backward Selection Approach Used to Identify the Best Model

All models reflected below included the random effects:  $(1 \mid Site : Turbine ID) + (1 \mid Site : UAV Model)$ . For additional reference the "full model" was as follows:

LoS Response Distance  $\sim (1 \mid Site : Turbine ID) + (1 \mid Site : UAV Model) + Site + Event Type + Sky Backdrop + sin(DFT) + cos(DFT) + sin(COG) + cos(COG) + Ground Speed + Climb Rate + Roll Angle + Pitch Angle + Wind Speed + Solar Irradiation + Solar Irradiation<sup>2</sup> + Sun Azimuth + Sun Elevation Angle + Roll Angle * Pitch Angle + sin(DFT) * Sun Azimuth + cos(DFT) * Sun Azimuth + sin(COG) * Sun Azimuth + cos(COG) * Sun Azimuth + sin(DFT) * Cos(DFT) * Sun Azimuth + sin(COG) * Sun Azimuth$ 

			Deviance	Nakagawa
Candidate Model	AICc	$\Delta$ AIC	Test ( <i>P</i> )	Marginal R <sup>2</sup>
Full Model	19989.14	21.26	na	0.106
Remove Solar Irradiation <sup>2</sup>	19987.08	19.10	0.9366	0.106
Remove Sun Azimuth*sin(COG)*cos(COG)	19985.05	17.07	0.8292	0.106
Remove Sun Azimuth*sin(DFT)* cos(DFT)	19983.11	15.13	0.7210	0.106
Remove Climb Rate	19981.31	13.33	0.6100	0.106
Remove Solar Irradiation	19979.57	11.59	0.5693	0.104
Remove Sun Azimuth*sin(COG)	19977.84	9.86	0.5628	0.104
Remove Sun Azimuth*sin(DFT)	19976.35	8.37	0.4516	0.104
Remove sin(DFT)*cos(DFT)	19974.91	6.93	0.4336	0.103
Remove sin(DFT)	19973.08	5.10	0.6370	0.103
Remove Sun Elevation Angle	19971.60	3.62	0.4485	0.101
Remove Sun Azimuth*cos(DFT)	19971.15	3.17	0.2065	0.100
Remove cos(DFT)	19969.10	1.12	0.9419	0.100
Remove sin(COG)*cos(COG)	19968.74	0.76	0.1943	0.099
Remove Sun Azimuth*cos(COG)	19968.55	0.57	0.1740	0.098
Remove cos(COG)	19967.98	0.00	0.2245	0.098
Remove sin(COG)	19968.14	0.16	0.1389	0.096
Remove Sun Azimuth = <b>Selected Model</b>	19968.05	0.07	0.1630	0.095
No Fixed Effects Null Model	20016.57	48.59	NA	0.000



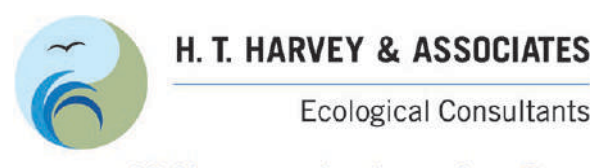












50 years of field notes, exploration, and excellence

#### Research Report

Analysis of DTBird False Negatives and False Positives at Commercial Wind-Energy Facilities in California and Washington

Project #4080-01

Prepared for:

Renewable Energy Wildlife Institute 1990 K Street NW, Suite 620 Washington, D.C. 20006-1189

Prime Contractor: DOE Cooperative Agreement DE-EE0007883

Prepared by:

H. T. Harvey & Associates

Final - May 17, 2024

#### **Executive Summary**

DTBird® (Liquen Consultoría Ambiental, S.L., Madrid, Spain) is an automated detection and audio deterrent system designed to discourage birds from entering the rotor swept zone of spinning wind turbines (see https://dtbird.com). In this report, we present integrated results from research conducted at two commercial wind energy facilities in California (Manzana Wind Power Project operated by Avangrid Renewables) and Washington (Goodnoe Hills Wind Farm operated by PacifiCorp) designed to evaluate the prevalence of false negatives and false positives at the two study sites. These assessments constitute two facets of a broader research agenda focused on evaluating the effectiveness of DTBird in detecting and discouraging golden eagles (Aquila chrysaetos) and other large soaring raptors (e.g., eagles, buteos, vultures, harriers, and ospreys) from approaching the rotor swept zone of operating wind turbines, in a manner that could support the U. S. Fish and Wildlife Service embracing the technology as an approved conservation measure. We conducted a pilot study at the Manzana site in the Mojave Desert, where seven DTBird systems were installed to support this research and we variably gathered data over two annual periods in 2017 and 2018. We then expanded the study with support from the U. S. Department of Energy to augment some analyses of the Manzana data and extend the investigation to a second site located in a very different landscape setting (a temperate grassland ridgeline above the Columbia River) at the Goodnoe Hills, where we again collected data across two annual periods from 2021-2023.

False negatives are defined as flights of targeted birds (or UAV surrogates in this study) that pass within detection range of a DTBird system but are not detected. Their quantification supports both understanding the flight conditions under which detections occur—or conversely, relevant flights are missed (false negatives)—and forms the basis for quantifying the probability of detection. We used randomized flights of unmanned aerial vehicles (UAVs) designed to mimic the general size, weight, and coloration of golden eagles to quantify the probability of detection at both sites.

False positives are defined as DTBird detection events that are triggered by nontarget birds, bats, or other inanimate objects. Because the DTBird system does not automatically distinguish different kinds of targets (e.g., birds versus aircraft), false positive detections commonly occur and comprise two primary forms: true false positives (TFPs) representing non-avian factors such as aircraft, insects, spinning turbine blades, and high-contrast sky conditions that sometimes trigger false detections (called sky artifacts); and nontarget avian false positives (NTAFPs) representing detections of bats and birds other than focal—for this study—large raptors (i.e., defined here as eagles, vultures, buteos, and ospreys). Excessive deterrent signaling caused by false positives could reduce the long-term effectiveness of the technology by contributing to negative habituation of target bird species, and result in excessive disturbance of nontarget wildlife and/or human neighbors. To investigate false positives, we used event data recorded in the online digital analysis platform (DAP) maintained by Liquen for all DTBird installations.

Our objectives for the investigations summarized herein were as follows:

- 1) Use the results of randomized UAV flights to quantify the probability of DTBird detecting eagle-sized birds within an estimated (calibrated) 240-meter-radius maximum detection envelope for golden eagles, and model the probability of detection (the converse of false negatives) in relation to various positioning covariates to help understand overall detection dynamics and compare results for the two study sites.
- 2) Summarize and compare the proportional representations of different sources of TFPs and NTAFPs at the two study sites, limited to evaluating relevant detections that triggered deterrents.
- 3) Estimate the average daily per-turbine TFP and NTAFP deterrent-triggering and signal duration rates at the two study sites.
- 4) Analyze variation in daily, turbine-specific TFP and NTAFP detection totals at the two study sites across standardized 28-day sampling periods and calendar months to discern patterns that could help inform improving the DTBird detection filtering algorithms to reduce false positives.
- 5) Compare the false negative and false positive proportions and detection rates at the two study sites in relation to established quantitative performance targets derived from the Manzana pilot study as a basis for determining if performance of the DTBird systems at Goodnoe Hills improved upon performance of the Manzana systems.

The established performance targets stipulated that (a) the overall TFP deterrent-trigger rate should not exceed 1.6–2.8 triggers/turbine/day; (b) no more than 36% of all relevant and classified detections recorded by the DTBird systems should result from TFPs; and (c) the overall, estimated false negative proportion should be no greater than 27–47% of the relevant flight transects used to quantify the probability of detection.

The TFP deterrent-triggering rates and proportions of detection events resulting from TFPs that we documented during Goodnoe Hills Year 1 generally ranged much higher than the established performance targets. However, once Liquen was authorized to make additional adjustments to the DTBird false positive filtering algorithms part way through Year 2 (which they typically do over the first 6–8 weeks following declaring the systems fully "commissioned"), both metrics for Goodnoe Hills dropped below the performance targets and were lower than at Manzana, suggesting improvement in the filtering algorithms.

Collectively, the results of this multi-site investigation suggested the following relative to false positives:

- DTBird systems should not be considered fully commissioned and maximally effective until Liquen
  completes fine-tuning to minimize false positives caused by spinning blades and other factors
  without all deterrents muted during this phase.
- The Goodnoe Hills Year 2 post-adjustments results suggested that Liquen should continue to prioritize additional improvements to the DTBird filtering algorithms to further reduce the potential for especially blade-related, insect, and sky-artifact TFPs.

- The prevalence of different sources of TFPs (i.e., aircraft, insects, and sky artifacts, in particular) may vary considerably in different facility areas and seasonally, potentially offering opportunities for further site-specific tailoring of the DTBird false-positive filtering algorithms.
- NTAFPs represent a complicated management issue, in that protecting all native bird species from
  unnecessary human-caused mortality is a worthy objective, but excessive deterrent triggering by
  nontarget birds could lead to deleterious negative habituation among target birds. Developing and
  implementing an AI system capable of distinguishing species and fine-tailoring the deterrent triggers
  is a logical solution to reduce NTAFPs.

Based on the Manzana pilot study, a performance standard for the probability of detection of 63% (or 37% for false negatives) was established to evaluate the comparative performance of DTBird systems installed at Goodnoe Hills. A generalized linear mixed modeling (GLMM) analysis relating the probability of detection to various predictors indicated similar patterns at the two study sites. Tailored to represent detection probabilities limited to the projected 240-meter-radius detection envelope for golden eagles, the models confirmed a nominally higher detection probability at Manzana (66%) than at Goodnoe Hills (64%), with both estimates exceeding the established performance standard. This outcome suggests consistent performance of the primary detection functions of the DTBird systems at both sites.

The GLMM analysis also provided insight concerning factors that influence DTBird's detection performance. Specifically, the probability of detection increased through the day, likely related to the relative influence of solar position and intensity. More importantly, the probability of detection was highest when the target flew at moderate distances from the turbine (i.e., average flight distances of 80–160 m) through the midsection of the camera viewshed (i.e., viewing angles from camera up to UAV of 25–40°). These results are perhaps not surprising in suggesting the highest detection rates occur in the middle of the camera viewsheds, but here it is important to note that poorer detection low and close or high and close to a turbine can result in little time for the deterrents to trigger and discourage continued closer passage before a bird enters the collision risk zone.

#### **Table of Contents**

Section 1.0 Introduction	1
Section 2.0 Methods	3
2.1 DTBird System Operation	4
2.2 Sampling and Classification of Detected Targets for False Positives Assessment	6
2.3 Analysis of False Positive Detection and Deterrent-Triggering Rates	8
2.4 Analysis of Probability of Detection/False Negatives Based on UAV Flight Trials	9
Section 3.0 Results	11
3.1 DTBird Event Classifications	11
3.1.1 True False Positives	12
3.1.2 Nontarget Avian False Positives	15
3.2 False Positive Deterrent Triggering Rates and Durations	15
3.2.1 Statistical Models	17
3.3 Probability of Detection/False Negatives	21
Section 4.0 Discussion	25
4.1 False Positives	25
4.2 Probability of Detection and False Negatives	27
Section 5.0 References	
Appendix A. Summary Classifications of DTBird Detection Events that Triggered Deterrents at the Manzana Wind Power Project as Large Raptors, True (Non-avian) False Positive (TFPs), and Nontarget Avian False Positives (NTAFPs) by Turbine and 28-day Cycle Sampling Periods Between January 1 and October 31, 2017	31
Appendix B. Summary Classifications of DTBird Detection Events that Triggered Deterrents at the Goodnoe Hills Wind Farm as Large Raptors, True (Non-avian) False Positive (TFPs), and Nontarget Avian False Positives (NTAFPs) by Turbine and 28-day Cycles Sampling Periods Between September 1, 2021 and August 2, 2023	35
Appendix C. Model Selection to Illustrate Relationships Predicting the Probability of DTBird  Detection with Selected Model Highlighted in Green and Null Model in Gray	47
Appendix D. Model Coefficients, Odds Ratio Estimates, and Diagnostic Metrics for Final Model Selected to Illustrate Relationships Predicting the Probability of DTBird Detection	48

#### **Figures**

Figure 1.	Layout of the Manzana Wind Power Project in southern California showing locations of installed DTBird systems.	3
Figure 2.	Layout of the Goodnoe Hills Wind Farm in south-central Washington showing locations of installed DTBird systems.	4
Figure 3.	Rates of True False Positives Caused by Insects that Triggered DTBird Deterrents by Month at the Manzana Wind Power Project in California (January – October 2017) at the Goodnoe Hills Wind Farm in Washington (September–August 2021–2022 and 2022–2023)	14
Figure 4.	Rates of True False Positives Caused by Sky Artifacts that Triggered DTBird  Deterrents by Month at the Manzana Wind Power Project in California (January– October 2017) and at the Goodnoe Hills Wind Farm in Washington (September– August 2021–2022 and 2022–2023)	14
Figure 5.	Predicted Average Daily Per Turbine True False Positive (TFP) DTBird Deterrent- Triggering Rates Across 28-day Sampling Periods During Study Years 1 and 2 at the Goodnoe Hills Wind Farm in Washington. Nonoverlapping Confidence Intervals Indicate Significant Pairwise Comparisons.	19
Figure 6.	Predicted Average Daily Per Turbine True False Positive (TFP) DTBird Deterrent- Triggering Rates Across 12 28-day Sampling Periods (Variable Calendar Periods) at the Manzana Wind Power Project in California and During Study Year 2 at the Goodnoe Hills Wind Farm in Washington. Nonoverlapping Confidence Intervals Indicate Significant Pairwise Comparisons.	19
Figure 7.	Predicted Average Daily Nontarget Avian False Positive (NTAFP) DTBird Deterrent- Triggering Rates Across 11 Months During Study Years 1 and 2 at the Goodnoe Hills Wind Farm in Washington. Nonoverlapping Confidence Intervals Indicate Significant Pairwise Comparisons.	20
Figure 8.	Predicted Average Daily Nontarget Avian False Positive (NTAFP) DTBird Deterrent- Triggering Rates Across Nine Common Sampling Months at the Manzana Wind Power Project in California and During Study Year 2 at the Goodnoe Hills Wind Farm in Washington. Nonoverlapping Confidence Intervals Indicate Significant Pairwise Comparisons.	21
Figure 9.	Modeled Linear Relationship Between Predicted DTBird Detection Probabilities for Individual UAV Flight Transects and Hour of the Day	23
Figure 10.	Modeled Third-Order Relationship Between Predicted DTBird Detection Probabilities for Individual UAV Flight Transects and the Minimum Line-of-Sight Distance to the DTBird Camera	23

Figure 11.	Modeled Second-Order Relationship Between Predicted DTBird Detection	
	Probabilities for Individual UAV Flight Transects and the Average Vertical Angle from	
	the DTBird Camera	24
Tables		
Table 1.	DTBird Detection Events that Triggered Deterrents Classified as Large Raptors, True False Positives (TFPs), and Nontarget Avian False Positives (NTAFPs) at the Manzana Wind Power Project in California and Goodnoe Hills Wind Farm in Washington	11
Table 2.	Numbers and Percentages by Type of True False Positive (TFP) DTBird Detections that Triggered a Deterrent Signal at the Manzana Wind Power Project in California and Goodnoe Hills Wind Farm in Washington	13
Table 3.	Numbers and Percentages of Nontarget Avian False Positive (NTAFP) DTBird  Detections at the Manzana Wind Power Project in California and Goodnoe Hills Wind  Farm in Washington	16
Table 4.	Overall Durations and Average Per Turbine Duration Rates for DTBird Deterrent Signals Triggered by True False Positives (TFPs) and Nontarget Avian False Positives (NTAFP) at the Manzana Wind Power Project in California and Goodnoe Hills Wind Farm in Washington	17
Table 5.	Numbers of turbine-specific days from which samples were drawn for investigating temporal differences in DTBird false-positive detection rates between sampling years at the Goodnoe Hills Wind Farm in Washington	18
Table 6.	Numbers of UAV flight transects by sampled turbine analyzed to quantify and investigate variation in the probability of DTBird detecting an eagle-like UAV at the Manzana Wind Power Project in California and Goodnoe Hills Wind Farm in Washington	22
List of F	Preparers	
Jeff P. Smi	th, Ph.D., Associate Wildlife Ecologist—Project Manager	
Scott B. To	errill, Ph.D., Principal, Wildlife Ecology—Principal-in-Charge	
Sophie Ber	rnstein, M.S., Wildlife & Quantitative Ecologist	
John Roma	ansic, Ph.D., Wildlife & Quantitative Ecologist	
Stephanie	Schneider, M.S., Wildlife & Quantitative Ecologist	
Alex Henr	y, B.S., Field Biologist	
Cooper Sn	nith, B.S., Field Biologist	
Zach Ham	pson, B.S., Field Biologist	
Cassandra	Butler B.S. Field Biologist	

#### **Section 1.0 Introduction**

DTBird® (Liquen Consultoría Ambiental, S.L., Madrid, Spain) is an automated detection and audio deterrent system designed to discourage birds from entering the rotor swept zone of spinning wind turbines (see <a href="https://dtbird.com">https://dtbird.com</a>). In this report, we present integrated results from research conducted at two commercial wind energy facilities in California (Manzana Wind Power Project operated by Avangrid Renewables) and Washington (Goodnoe Hills Wind Farm operated by PacifiCorp) designed to evaluate the prevalence of false negatives and false positives at the two study sites. These assessments constitute two facets of a broader research agenda focused on evaluating the effectiveness of DTBird in detecting and discouraging golden eagles (Aquila chrysaetos) and other large soaring raptors (e.g., eagles, buteos, vultures, harriers, and ospreys) from approaching the rotor swept zone of operating wind turbines, in a manner that could support the U. S. Fish and Wildlife Service embracing the technology as an approved conservation measure (H. T. Harvey & Associates 2018, 2019a).

False negatives are defined as flights of targeted birds (or UAV surrogates in this study) that pass within detection range of a DTBird system but are not detected. Their quantification supports both understanding the flight conditions under which detections occur, or conversely relevant flights are missed (false negatives), and forms the basis for quantifying the probability of detection.

False positives are defined as DTBird detection events that are triggered by nontarget birds, bats, or other inanimate objects. Because the DTBird system does not automatically distinguish different kinds of targets (e.g., birds versus aircraft), false-positive detections commonly occur and comprise two primary forms: true false positives (TFPs) representing non-avian factors such as aircraft, insects, spinning turbine blades, and high-contrast sky conditions that sometimes trigger false detections (called sky artifacts); and nontarget avian false positives (NTAFPs) representing detections of non-focal bird species (in this case birds other than eagles and other large soaring raptors). Excessive deterrent signaling caused by false positives could reduce the long-term effectiveness of the technology by contributing to negative habituation of target bird species, and result in excessive disturbance of nontarget wildlife and/or human neighbors. High false positive rates could also lead to turbine curtailment and loss of power generation in situations where the DTBird systems are operated with an optional automated control-stop module (not evaluated in as part of this research).

We previously presented site-specific analyses of false positives and the probability of detection/false negatives for the two study sites in H. T. Harvey & Associates (2018, 2019b, 2022a, 2022b). In this report, we present integrated analyses combining insight from the two study sites on these two topics. Our specific objectives for this investigation were as follows:

1) Use the results of randomized flights of unmanned aerial vehicles (UAVs) designed to mimic golden eagles conducted at both study sites to quantify the probability of DTBird detecting eagle-sized birds—the converse being the probability of false negatives—within an estimated (calibrated) 240-meter-radius maximum detection envelope for birds the size of golden eagles, and model the

- probability of detection in relation to various positioning covariates to help understand overall detection dynamics and compare results for the two study sites.
- 2) Summarize and compare the proportional representations of different sources of TFPs and NTAFPs at the two study sites (based on documented DTBird detections of *in situ* objects/birds), limited to evaluating detections that triggered deterrents.
- 3) Estimate the average daily per-turbine TFP and NTAFP deterrent-triggering and signal duration rates at the two study sites.
- 4) Analyze variation in daily, turbine-specific TFP and NTAFP detection rates at the two study sites across standardized 28-day (28d) sampling periods and calendar months to discern patterns that could help inform improving the DTBird detection filtering algorithms to reduce false positives.
- 5) Compare the false negative and false positive detection rates and proportions at the two study sites in relation to quantitative performance targets established based primarily on the initial Manzana pilot study (H. T. Harvey & Associates 2018) to provide a basis for determining if performance of the DTBird systems at the Goodnoe Hills study site improved upon performance of the systems evaluated at the Manzana site (H. T. Harvey & Associates 2019a).

The specifications promulgated by DTBird Team (2017) specified that DTBird systems comparable to those installed at the Manzana and Goodnoe Hills sites should be expected to result in a yearly average TFP deterrent trigger rate of 0.2–4.0 events/turbine/day, amounting to a total duration of 0.1–2.5 minutes/turbine/day. The performance targets established for the Goodnoe Hills study stipulated that (a) the overall TFP deterrent-trigger rate should not exceed 1.6–2.8 triggers/turbine/day; (b) no more than 36% of all classified detections recorded by the DTBird systems should result from TFPs; and (c) the overall, estimated false negative proportion should be no greater than 27–47% of the relevant UAV flight transects used to quantify the probability of detection.

#### Section 2.0 Methods

The Manzana Wind Project has been in operation since 2012 and comprises 126 1.5 MW GE 1.5-77 wind turbines, with a hub height of 65 meters and a rotor-swept diameter of 82.5 meters, located in the southwestern foothills of the Tehachapi Mountains of southern California in northwestern Antelope Valley, which constitutes the westernmost extension of the Mojave Desert (Figure 1). The landscape is a gradually sloping alluvial fan incised by dry desert washes. The northwestern sector of the facility features more complex foothill topography adjacent to a primary riparian drainage, and the topography grades downslope to the southeast into a more-uniform plain. The desert scrub and woodland vegetation is typical of the upper Mojave Desert region. Seven DTBird systems were strategically installed here to support this research (Figure 1; H. T. Harvey & Associates 2018).

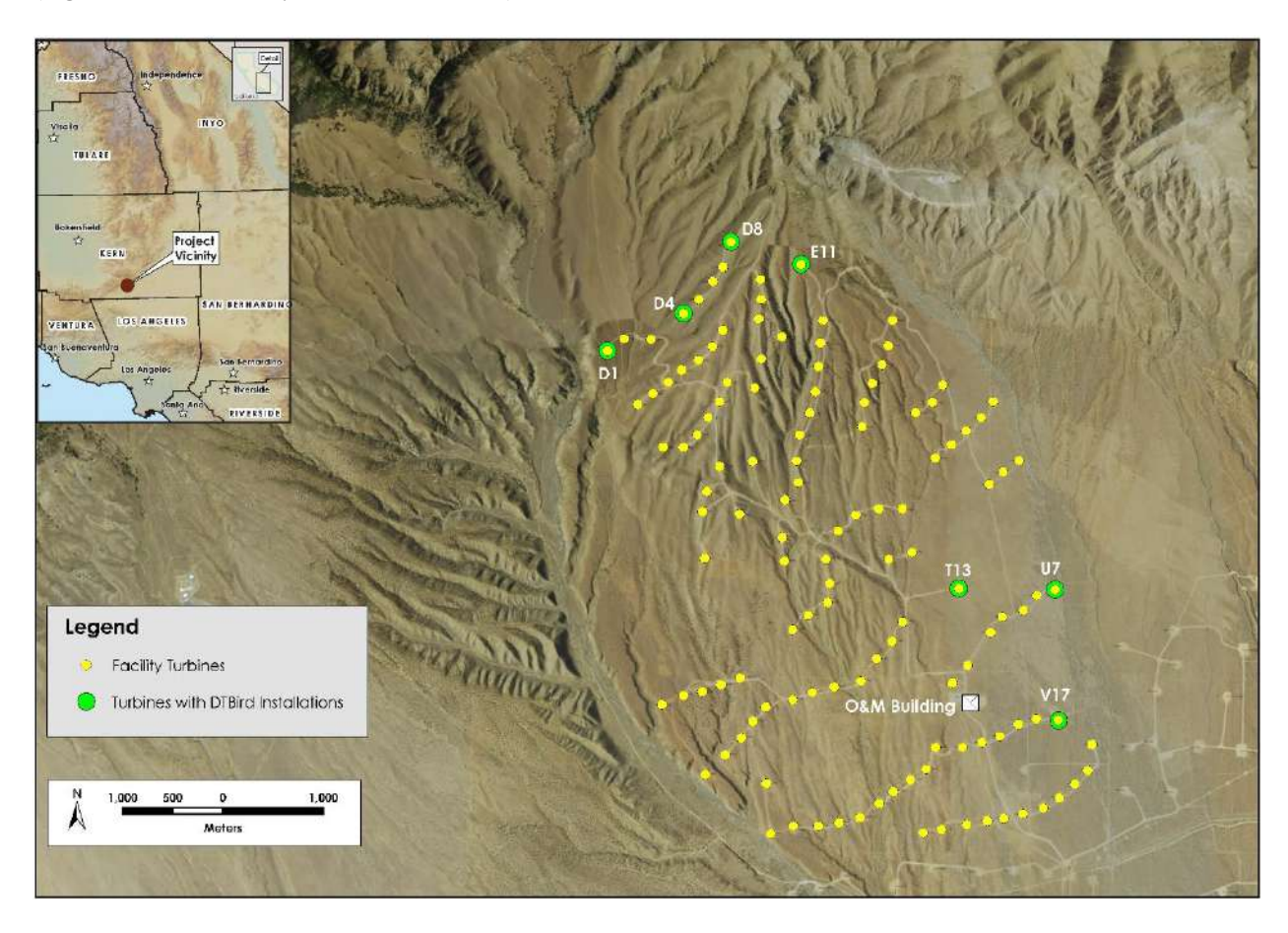


Figure 1. Layout of the Manzana Wind Power Project in southern California showing locations of installed DTBird systems.

The Goodnoe Hills Wind Farm has been in operation since 2008 and currently comprises 47 2.2 MW Vestas V110 Mark C and B wind turbines, with a hub height of 87 meters and a rotor-swept diameter of 110 meters located in south-central Washington atop an east-west ridgeline flanking the Columbia River approximately 3–6 km away (Figure 2). The topography descends steeply south of the ridgeline approximately 610 meters to

the Columbia River and more gradually to the north approximately 500 meters down into Rock Creek Canyon and associated riparian corridors. The project area is dominated by a mosaic of grazed grassland and shrubsteppe, with inclusions of ponderosa pine (*Pinus ponderosa*) and Oregon white oak (*Quercus garryana*) woodlands on the ridge's north-facing slopes. Fourteen DTBird systems were installed around the perimeter of this facility to support this research; however, the extent of effective operation varied among the installed systems during the 2-year study at this site (H. T. Harvey & Associates 2023a).

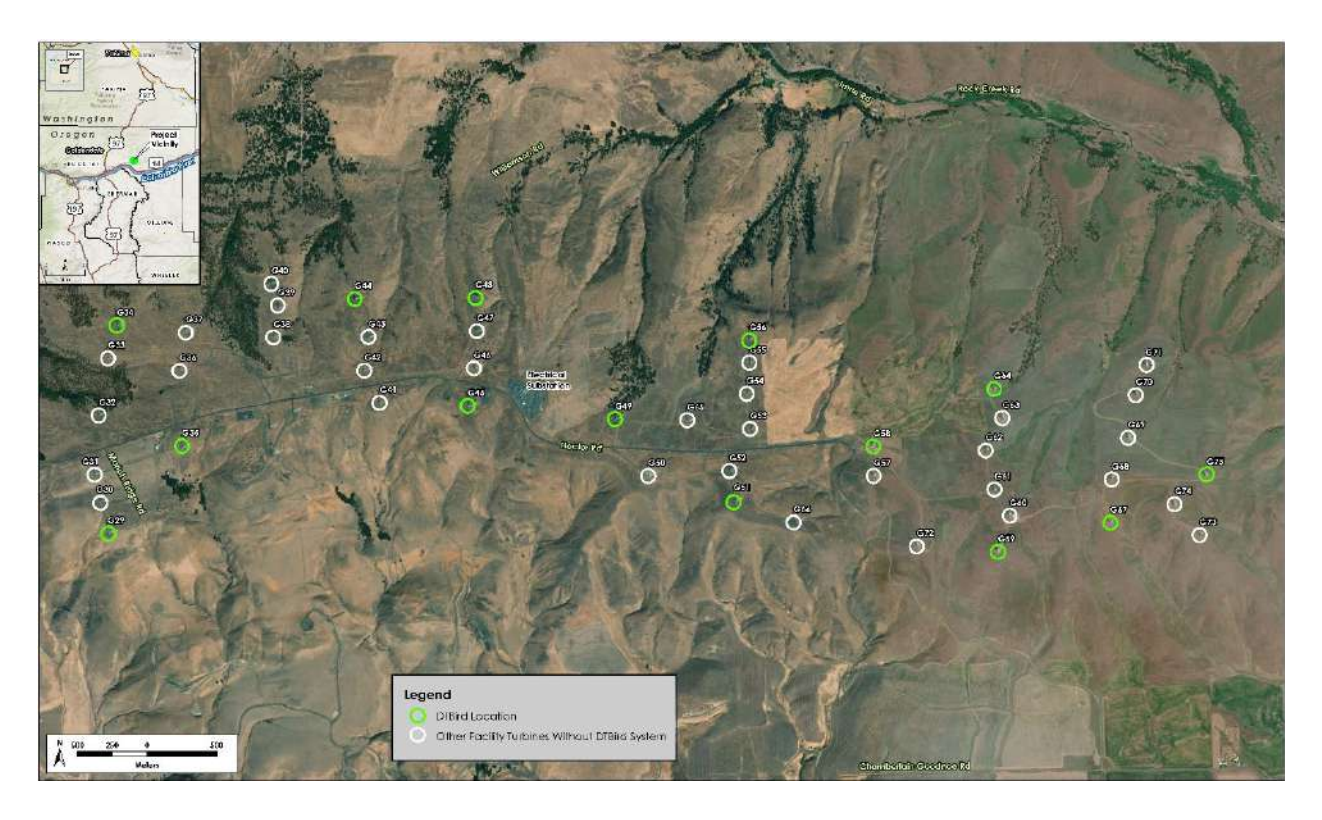


Figure 2. Layout of the Goodnoe Hills Wind Farm in south-central Washington showing locations of installed DTBird systems.

#### 2.1 DTBird System Operation

A detailed description of the general DTBird system set-up and operations relevant to both study sites can be found in H. T. Harvey & Associates (2018). Detailed overviews of the systems and operational parameters at the Manzana and Goodnoe Hills study sites can be found in H. T. Harvey & Associates (2018) and H. T. Harvey & Associates (2019a, 2022a), respectively. The equipment setup at the two sites was the same except that the Goodnoe Hills installations included a second ring of four broadcast speakers installed on the turbine towers just below hub height. This modification was implemented to account for taller turbines at the Goodnoe Hills and thereby help to ensure effective deterrent broadcasting throughout a larger overall detection envelope and collision risk zone (H. T. Harvey & Associates 2019a).

When a DTBird system first detects a targeted object, it creates a new event record in the online digital analysis platform (DAP) database Liquen maintains to store detection records and extracted video clips for all

DTBird installations. The DAP records a timestamp for each initial detection event along with other limited data. If a targeted object subsequently or simultaneously triggers one or both of two deterrent signals (early warning or a more raucous dissuasion signal if a target approaches closer to the turbine) information is added to the same DAP event record to document the unique timestamps and signal durations for each deterrenttriggering event. Each event record has video clips attached to it representing the four cameras, which the system extracts to begin 10 seconds before targeting began and continue for 30 seconds after the last targeted object exits the detection envelope. There must be no objects targeted for at least 26 seconds before a given DTBird system can initiate a new detection event record. If a system targets multiple objects concurrently during the same event period, timestamps are recorded only for the first detection, warning-trigger, and dissuasion-trigger events, and those respective events may not be triggered by the same object. In these cases, sometimes it can be difficult to determine exactly which bird or object was responsible for the timestamped events. Technicians must screen all relevant DAP records and videos to classify and enumerate the detected objects, which can include birds of all types and sizes as well as myriad other animate and inanimate flying objects, and to identify other sources of false positive detections caused by the detection system perceiving dynamic, high-contrast elements in the viewshed associated with moving turbine blades, clouds, and other turbine equipment as moving objects of interest.

The DTBird detection and targeting systems incorporate algorithms that reduce false positives caused by factors such as commercial aircraft, insects, and the focal turbine's spinning blades. The constant-pace, arrow-straight flights of high-altitude commercial aircraft are relatively easy to filter out and ignore. Many insects can be filtered out based on their rapid wing beats and erratic flights. Once a specific DTBird installation has been operational for period, a filtering "mask" can be developed that defines the rotor swept area each camera sees and thereby helps the system to filter out false triggers caused by the spinning blades.

Before beginning the Manzana pilot study (H. T. Harvey & Associates 2018), we did not understand that Liquen typically continues adjusting the TFP filtering algorithms of the DTBird systems they install for as much as an additional 6–8 weeks after they deem the systems fully operational and "commissioned." Although standard practice, once we learned of this additional post-commissioning adjustment practice, we asked Liquen to cease making any further adjustments to create a stable platform for assessing system performance for the remainder of our research at the Manzana site. That point in time was mid-February 2017, approximately 2 months after the Manzana systems were commissioned, which means Liquen had already completed most of the typical post-commissioning adjustments by that time. The false positive performance standard established to guide expansion of this research to the Goodnoe Hills was set based on results derived under this Manzana setup history.

When the Goodnoe Hills systems were setup, we initially requested, once Liquen deemed a given system "fully commissioned", that they make no further algorithm adjustments to establish a consistent and stable platform for our subsequent evaluations. However, a preliminary analysis of the observed false positive rate recorded under this scenario during the first 6.5 months of DTBird operation at the Goodnoe Hills revealed an excessively high rate that greatly exceeded the relevant performance standard for the project (H. T. Harvey & Associates 2022a). As a result, a proposal was made to the DOE to alter the setup during Year 2 of the overall Goodnoe Hills field study by allowing Liquen to make whatever further adjustments they could to

minimize the overall false positive rate. It was agreed that doing so would provide a better basis for comparing DTBird's false positive performance at the two study sites using data collected subsequently at the Goodnoe Hills. Those further adjustments were completed in January 2023.

### 2.2 Sampling and Classification of Detected Targets for False Positives Assessment

We present Manzana results based on data collected from January through October 2017 (excludes initial partial month of data from December 2016; H. T. Harvey & Associates 2019b), and Goodnoe Hills results based on data collected from September 2021 through July 2023 (H. T. Harvey & Associates 2022a, augmented with more recent data). For each DTBird installation, we randomly selected 10 days per sequential 28-day operational period as our sampling framework. We limited the selections to days when a given turbine and the associated DTBird system were operating at least mostly as expected, with the blades spinning and deterrents triggering when targets were registered to have crossed calibrated distance ranges. For both sites, we excluded from the sample selections all turbine-specific days where and when we conducted UAV flight trials (H. T. Harvey & Associates 2023b, and see Section 2.4). On those days, our flight-trial activities undoubtedly influenced the otherwise typical patterns of bird activity around the focal turbines, biasing any other activity observations from those specific days.

Once the arrays of turbine-specific sampling days were selected, technicians reviewed the DAP records and videos from those days to classify the targets associated with all detection events recorded while the turbine blades were spinning. Then we focused this multi-site analysis on all such detection events for which the classified target was a TFP or NTAFP that triggered a deterrent signal. False positive detections that do not trigger an audio deterrent may result in excessively cluttered detection databases, which can hamper efficient evaluations of system operation, but they do not run the risk of excessively disturbing nontarget wildlife, wind technicians, and proximate human neighbors or contributing to negative habituation among target species of interest (H. T. Harvey & Associates 2018, 2019b, 2023b). Accordingly, for this multi-site assessment we focused exclusively on false positives that triggered deterrent signals.

The technicians classified the targets associated with selected detection events into a broad range of bird species, species groups, and general size categories (species-level identifications were difficult due to low-resolution video records), as well as a range of TFP subcategories. Classification subcategories we lumped together to assess overall TFP detection rates and proportions included several varieties of aircraft (i.e., airplane, helicopter, UAV [excluding our research UAVs], paraglider, and parachute), turbine blades (focal or neighboring turbine), insects, snow, rain, sky artifacts, equipment (i.e., sky artifacts triggered at edges of non-blade turbine features), debris (i.e., floating balloons, paper, plastic bags, etc.), and software/video failures (i.e., poor quality videos preclude target identification). We defined NTAFPs as birds other than large soaring raptors, including abundant common ravens, occasional distinctive falcons (Falco spp.) and accipiters (Accipiter spp.), and other species ranging from small passerines to large geese, cranes, and pelicans (plus a few crepuscular bats). Typical large soaring raptors at both study sites were golden eagles, turkey vultures (Cathartes aura), red-tailed hawks (Buteo jamaicensis), and northern harriers (Circus budsonicus). Less common

species at both sites were osprey (*Pandion haliaetus*), Swainson's hawk (*B. swainsoni*; migration and summer only), and ferruginous hawk (*B. regalis*; migration and winter only). Other relevant species unique to each site were abundant rough-legged hawks (*B. lagopus*) and less common bald eagles (*Haliaetus leucocephalus*) during migration/winter at Goodnoe Hills, and rare sitings of California condors (*Gymnogyps californicus*) at Manzana.

The generally poor resolution of the extracted video clips stored in the DAP precluded confidently identifying large proportions of the detected avian targets beyond coarse-scale size/group categories (H. T. Harvey & Associates 2018, 2019b, 2022a, 2023a). Despite intensive QA/QC by the Project Manager/senior avian-raptor expert, nearly 800 Goodnoe Hills records and more than 1200 Manzana records relevant to evaluations of false positives remained classified only as unidentified "big size bird", "unknown medium/large raptor", or "unknown bird", with each classification potentially including some unconfirmed large soaring raptors. To bolster the overall comparative estimates of TFP and NTAFP rates and proportions, we manually classified all unidentified big size birds and unknown birds as either large raptors, medium/large raptors, or NTAFPs based on (a) carefully evaluating representations of other confirmed raptor, raven, and general NTAFP identifications at a given focal turbine on relevant days, (b) considering the general relative abundance of large raptors and ravens at the focal turbine, and (c) making logical assignments based on those considerations. Similarly, we reclassified some records the technicians originally classified as unknown medium/large raptors as large raptors or NTAFPs based on other proximate records identified to species or those two groups.

Partial and complete operational malfunctions of the DTBird systems—caused by several factors—were common at both sites, which led to a variety of sampling imbalances through time and among the different DTBird installations. Operational issues were particularly prevalent at one of the seven Manzana installations (Turbine V17, Figure 1; and see H. T. Harvey & Associates 2018, 2019b). At the Goodnoe Hills, operational constraints and issues were comparatively rife throughout the study period there. The following constraints were most notable during the 23-month period of record considered in this report:

- System challenges resulted in no useful data being collected at 3 of 14 installations (G29, G51, and G56; see Figure 2) during Year 1 (H. T. Harvey & Associates 2022a, 2023a, 2023b).
- The installation at turbine G56 was not fully commissioned until the second 28d Cycle of Year 2.
- The installation at turbine G48 failed and remained inoperable from mid-November 2022 through early March 2023.
- No useful data were collected at turbine G59 from December 2022 through early April 2023 and at turbine G64 during the month of December 2022.
- The Bonneville Power Administration shut off power to the entire facility from May 1–24, and most of the DTBird systems were not successfully rendered fully operational again until June 6, 2023.
- The installation at turbine G51 was nonfunctional after early July 2023.
- The installation at turbine G67 was largely nonfunctional from early June through early July 2023.
- Most of the installations were largely nonfunctional during the latter half of July 2023.

Given the scale of operational challenges at the Goodnoe Hills, in particular, and the fact that we were not specifically interested in evaluating variation among individual turbines for the assessments herein, we included in our analyses all available and useful data from selected sampling days that met the necessary turbine-DTBird operational criteria for inclusion, as described above. Then we standardized the dependent variables for analysis as the daily counts of TFPs and NTAFPs at each turbine on selected sampling days with relevant records (see Appendixes A and B for summaries of the records used for analysis), and we included *Turbine ID* as a random effect in the statistical models we developed for analyzing variability among the sites and through time (Section 2.3). This approach and the robustness of modern analytical models to sampling imbalances and modest violations of distributional assumptions (Schielzeth et al. 2020) helped to reduce potential biases caused by unequal sampling among the sites and DTBird installations.

## 2.3 Analysis of False Positive Detection and Deterrent-Triggering Rates

We used R 4.3.2 (R Core Development Team, Vienna, Austria) to develop generalized linear mixed models (GLMMs) illustrating variation in TFP and NTAFP rates at the two study sites. We developed independent analyses for TFPs and NTAFPs, focusing on four model constructs for TFPs and two model constructs for NTAFPs. Given the additional false-positive filtering adjustments made during Year 2 of the Goodnoe Hills study, our first analytical objective was to compare TFP and NTAFP rates at the Goodnoe Hills across comparable periods of Year 1 and Year 2. Then we analyzed differences between the two study sites by comparing results from the Manzana site against results from only a comparable period of Year 2 at the Goodnoe Hills. For both sets of comparisons, we analyzed two models with the following variable structures:

#### Goodnoe Hills Year 1 versus Year 2

```
TFPs / Turbine / Day \sim (1 \mid Turbine ID) + (1 \mid 28d Cycle : Date) + Year + 28d Cycle + Year * 28d Cycle 
NTAFPs / Turbine / Day <math>\sim (1 \mid Turbine ID) + (1 \mid Month : Date) + Year + Month + Year * Month
```

#### Manzana versus Goodnoe Hills Year 2

```
TFPs / Turbine / Day \sim (1 \mid Turbine \mid ID) + (1 \mid 28d \mid Cycle : Date) + Site + 28d \mid Cycle + Site * 28d \mid Cycle 
NTAFPs / Turbine / Day \sim (1 \mid Turbine \mid ID) + (1 \mid Month : Date) + Site + Month + Site * Month
```

We included *Turbine ID* as a random effect in all models to account for uncontrolled variation resulting from the unique spatial and temporal influences of individual turbine locations and to avoid pseudoreplication, and we treated *Date* as a random categorical factor nested within *28d Cycle* or *Month* to account for the influence of variable sampling days and avoid pseudoreplication. We examined the models with *28d Cycle* and *Month* as alternative temporal predictors to address different interests in examining patterns of variation though time. Specifically, we used *28d Cycle* to evaluate the influences of operational duration on TFP rates, and we used *Month* to evaluate the seasonal influences of specific times of year on the prevalence of NTAFPs (including natural factors that vary seasonal, such as precipitation and insects).

We analyzed these data using negative binomial GLMMs, which account for typical overdispersion of count-based data. We used the 'glmmTMB' package in R (Brooks et al. 2017a, b; Magnussen et al. 2022) to generate

the models with a log-link. The negative binomial response distribution ('binom2', with variance =  $\mu[1+\mu/k]$ , where  $\mu$  is the mean and k is the overdispersion parameter) accounted for overdispersion in the data.

We tested for differences in daily counts among 28d Cycles or Months using chi-squared maximum likelihood-ratio tests to evaluate the significance of the fixed factors in the models. To obtain estimated means for daily turbine-specific TFP and NTAFP counts based on the selected final models, we used the 'ggpredict' function ('ggeffects' package; Lüdecke et al. 2022). We identified differences among means using planned post-hoc comparisons following Tukey's Honestly Significant Differences test (Tukey 1949) to maintain a family-wise alpha of 0.05. The planned comparisons were limited to pairwise comparisons among 28d Cycles or Months within Years or Sites.

## 2.4 Analysis of Probability of Detection/False Negatives Based on UAV Flight Trials

We used UAVs designed to mimic golden eagles to evaluate performance characteristics of the DTBird detection systems at both study sites (H. T. Harvey & Associates 2023b). Information presented in H. T. Harvey & Associates (2018) for the Manzana site and in H. T. Harvey & Associates (2022b) for the Goodnoe Hills site included initial site-specific analyses relating the probability of detecting an eagle-like UAV—converse of the probability of false negatives—to several temporal and position metrics of interest. Herein, we advance those assessments by integrating data from the two study sites in a combined analysis, and generate a combined estimate of the probability of detection for the DTBird systems installed at the two sites.

To generate estimates of the probability of detecting an eagle-like UAV, we matched DAP detection event records in space and time (resolved to 1-second resolution) with the UAV tracking records to classify each independent UAV flight transect as Detected or Not Detected by the relevant DTBird system. We then calculated the proportions of flight transects detected and not detected at each turbine where we conducted flight trials. The grand-average of the proportions detected then represented the overall estimate of the probability of detecting an eagle-like UAV that passed within the expected 240-meter maximum detection range of the calibrated DTBird systems at each study site, and the converse represented the false negative rate (i.e., the percentage of flights that passed within detection range but were not detected by the DTBird systems).

To generate insight about patterns of variability in the probability of detection, we used ArcGIS tools to calculate the horizontal direction, vertical viewing angle, and line-of-sight (LoS) distance from the detection camera to each individual GPS point along a given UAV flight path, and we used circular statistics to calculate the average *Exposure Direction* (horizontal direction) for each flight transect (Zar 1998). Then we conducted a logistic regression analysis (Systat 13.2.01; Systat Software, Inc., San Jose, CA) with Detected or Not Detected as the binary response variable and several potential predictors considered in the models for evaluation. The relevant predictors were:

• Site (Manzana or Goodnoe Hills)

- Hour of the Day (e.g., 0900 or 1500 H Pacific Standard Time, using the majority value if the flight segment overlapped two hourly periods)
- Detection Angle (°; average vertical angle from camera to UAV)
- LoS Distance (minimum line-of-sight distance from camera to UAV)
- Exposure Direction (average horizontal angle from turbine to position of UAV, transformed to two orthogonal vectors: sine(Exposure Direction) representing a west [negatives values] to east [positive values] vector and cosine(Exposure Direction) representing a south [negatives values] to north [positive values] vector).

Given expectations of non-linear relationships from prior site-specific analyses, we considered second-order polynomial terms in the models for *Hour of the Day* and *Detection Angle*, and third-order polynomial terms for *LoS Distance*. We used Akaike's Information Criterion (AIC) scores, individual parameter tests, log-likelihood ratio chi-square tests, and Nagelkerke pseudo-R<sup>2</sup> values to identify the top predictive model given the predictors considered and evaluate the relative influences of various predictors on the probabilities of detection. The logistic GLMMs resulted in predictions of the ln(odds of a response). We used a standard formula (100\*exp[ln[odds]]/[1+exp[ln[odds]]]) to transform the log-odds estimates to probabilities of response (0 to 1 translated to percentages) for the purpose of describing and graphically displaying relationships (Hosmer and Lemeshow 1989).

We also note here that Nagelkerke pseudo- $R^2$  values do not correlate with typical coefficients of determination  $R^2$  values for non-GLMM models reflecting the proportion of explained variance. Instead, although not well documented in published literature, a typical rule of thumb for interpreting Nagelkerke pseudo- $R^2$  values is that values  $\leq 2$  indicate a weak relationship, values between 0.2 and 0.4 indicate a moderate relationship, and values  $\geq 4$  indicate a strong relationship (Shah 2023).

#### Section 3.0 Results

#### 3.1 DTBird Event Classifications

The 10-month, seven-turbine dataset analyzed from the Manzana site to derive results for this multi-site assessment involved 3,051 detections that triggered one or both deterrents (i.e., warning and/or dissuasion signals). With unknown big birds, unknown medium/large raptors, and unknown birds proportionately allocated where appropriate to the large raptors and NTAFP groups as described in Section 2.2, the Manzana records included 789 detections classified as large soaring raptors, 917 detections classified as TFPs, and 1,212 detections classified as NTAFPs (Table 1). The analyzed 11-turbine dataset from Year 1 at the Goodnoe Hills involved 11,265 detections that triggered deterrents, including 1,529 classified as relevant raptors, 5,744 as TFPs, and 3,955 as NTAFPs. The analyzed intermittently 14-turbine dataset from Year 2 at the Goodnoe Hills involved 8,075 detections that triggered deterrents, including 1,673 classified as relevant raptors, 3,441 as TFPs, and 2,958 as NTAFPs.

At Manzana, NTAFPs caused an estimated 40% of all deterrent triggers, TFPs caused 30%, large raptors caused 26%, and birds that remained classified as unknown medium/large raptors caused 4%. Particularly high raven activity at one DTBird turbine contributed to complaints from a residence approximately 500 meters away from that turbine (H. T. Harvey & Associates 2019b). At Goodnoe Hills, adjusted NTAFPs caused a similar 36% of all deterrent triggers, whereas TFPs caused a higher 48% and large raptors caused a lower 17% of the total. Confirmed common ravens caused 24% of all false-positive deterrent triggers at Goodnoe Hills and 15% at Manzana.

Table 1. DTBird Detection Events that Triggered Deterrents Classified as Large Raptors, True False Positives (TFPs), and Nontarget Avian False Positives (NTAFPs) at the Manzana Wind Power Project in California and Goodnoe Hills Wind Farm in Washington

				Large R	aptors <sup>2</sup>	TFP	<b>s</b> <sup>3</sup>	NTAFPs <sup>4</sup>		
Site	Number of Operational DTBird Systesms	Period of Record	Total Detection Events <sup>1</sup>	Number of Detection Events		Number of Detection Events		Number of Detection Events		
Manzana	7	Jan-Oct 2017	3,051	789	1.1	917	1.3	1,212	1.7	
Goodnoe Hills Year 1	11	Sep 2021- Aug 2022	11,260	1,529	1.3	5,744	4.9	3,955	3.3	
Goodnoe Hills Year 2	14	Sep 2022- Jul 2023	8,075	1,673	1.5	3,441	3.0	2,958	2.6	
Total	Max 21	_	22,386	3,991	1.3	10,102	3.3	8,125	2.7	

Includes unidentified medium/large raptors that we did not reclassify as Large Raptors or NTAFPs and were excluded from analyses.

Restricted to large soaring species; i.e., eagles, vultures, buteos, harriers, and ospreys.

<sup>3</sup> Includes events triggered by inanimate objects, insects, and software/video interpretation errors and failures.

<sup>4</sup> Includes events triggered by birds other than large soaring raptors and unknown medium/large raptors.

#### 3.1.1 True False Positives

At Goodnoe Hills, the additional false-positive filtering adjustments made in January 2023 reduced the overall rate of TFP deterrent triggers from approximately 529 to 71 per month across all sampled turbines (87% reduction). Substantial proportional reductions in the monthly TFP deterrent triggering rates included those caused by insects (97%), sky artifacts (94%), floating debris (93%), other turbine equipment features (91%), spinning turbine blades (88%), precipitation (67%), and software/video issues (39%). Note, however, that unequal seasonal sampling and variation also could have affected the outcomes for insects, sky artifacts, floating debris, and precipitation. In addition, modifications of the absolute numbers substantially altered the proportional contributions of different types of TFPs observed at Goodnoe Hills in only a few cases. The proportion of blade-related TFPs declined only slightly from 32% of all TFP deterrent triggers in Year 1 to 28% post-adjustments in Year 2. The proportion of insect-related TFPs declined more substantially from 28% in Year 1 to 9% post-adjustments in Year 2, and the proportion of TFPs caused by aircraft increased from 11% in Year 1 to 30% post-adjustments in Year 2, and the proportion of TFPs caused by software failures increased from 4% in Year 1 to 18% post-adjustments in Year 2.

The range of TFP source types was similar but the percentage contributions of different sources varied at the two study sites (Table 2). Before the false-positive filtering was adjusted at the Goodnoe Hills study, turbine blades (30–32% of TFPs) and insects (28–48%) variably ranked as the most and second-most common sources of TFPs, with TFPs caused by aircraft (6–11%) and sky artifacts (9–23%) variably ranked as the third and fourth most common sources. At Manzana by contrast, aircraft caused a majority of the TFPs (60%), sky artifacts caused the second highest proportion (25%), and insects caused a notably lower, third highest proportion (5%). The only other instance where another source caused more than 5% of the TFPs recorded during one of the four site-sampling periods involved software failures during the Goodnoe Hills Year 2 post-adjustments period (18% of TFPs in that period).

The proportion of TFPs caused by insects showed distinctly different patterns both between years at Goodnoe Hills and between the two sites (Figure 3). At Manzana, insect TFPs were generally much less prevalent than at Goodnoe Hills and occurred mostly in early to mid-summer. During Goodnoe Hills Year 1, insect TFPs started out high in the fall, were largely absent during winter, began to ramp up in spring, and peaked in summer. In contrast, during Goodnoe Hills Year 2, insect TFPs were very high initially during fall (expanding the summer peak from Year 1), dropped off and again were rare through winter, but unlike during Year 1, remained low and comparable to the Manzana rates after that.

The prevalence of TFPs caused by sky artifacts showed very different patterns across 28d Cycles in Years 1 and 2 at Goodnoe Hills, whereas the patterns were much more similar for Manzana and Goodnoe Hills Year 2 (Figure 4). After the fifth cycles, sky artifact TFPs dropped off markedly and remained low at both the Manzana site and at Goodnoe Hills during Year 2. Note that, while this drop-off marked the time when further changes were made in the false positive filtering algorithms at Goodnoe Hills, it did not correspond to any such change at Manzana. After this point, though showing comparable rates and variation through the first 4–5 cycles, the rate of sky artifact TFPs increased markedly during Goodnoe Hills Year 1 and remained

Table 2. Numbers and Percentages by Type of True False Positive (TFP) DTBird Detections that Triggered a Deterrent Signal at the Manzana Wind Power Project in California and Goodnoe Hills Wind Farm in Washington.

				Numl	oers of	TFPs			Percentages Within Site-Sampling Periods						riods
	TFP Cause		Goodnoe Hills <sup>2</sup>						Goodnoe Hills <sup>2</sup>						
TFP Class		Manzana <sup>1</sup>	Year 1	Year 2a	Year 2b	Year 2 Total	Two Year Total	Combined Grand Total	Manzana	Year 1	Year 2a	Year 2b	Year 2 Total	Two Year Total	Combined Grand Total
Artificial	Blades – Focal Turbine	21	1817	854	130	984	2801	2822	2.2	31.6	28.6	28.4	28.6	30.5	27.8
	Blades – Other Turbine	0	1	33		33	34	34	0.0	0.0	1.1	0.0	1.0	0.4	0.3
	Airplane	507	586	161	103	264	850	1357	53.3	10.2	5.4	22.5	7.7	9.2	13.4
	Helicopter	64	46	11	33	44	90	154	6.7	8.0	0.4	7.2	1.3	1.0	1.5
	UAV	2	1			0	1	3	0.2	0.0	0.0	0.0	0.0	0.0	0.0
	Paraglider	0			3	3	3	3	0.0	0.0	0.0	0.7	0.1	0.0	0.0
	Parachute	0	3	1		1	4	4	0.0	0.1	0.0	0.0	0.0	0.0	0.0
	Debris	3	31	4	1	5	36	39	0.3	0.5	0.1	0.2	0.1	0.4	0.4
	Turbine Equipment	1	14	14	1	15	29	30	0.1	0.2	0.5	0.2	0.4	0.3	0.3
	Subtotal	598	2499	1078	271	1349	3848	4446	62.8	43.5	36.1	59.2	39.2	41.9	43.8
Natural	Insects	51	1593	1428	41	1469	3062	3113	5.4	27.7	47.9	9.0	42.7	33.3	30.7
	Falling Ice	0	41	50	7	57	98	98	0.0	0.7	1.7	1.5	1.7	1.1	1.0
	Rain	4	59	15	2	17	76	80	0.4	1.0	0.5	0.4	0.5	0.8	0.8
	Snow	0	10	12	15	27	37	37	0.0	0.2	0.4	3.3	0.8	0.4	0.4
	Subtotal	55	1703	1505	65	1570	3273	3328	5.8	29.6	50.5	14.2	45.6	35.6	32.8
Software/Video	Functional Failure	13	216	122	81	203	419	432	1.4	3.8	4.1	17.7	5.9	4.6	4.3
Failure	Sky Artifacts	251	1326	278	41	319	1645	1896	26.4	23.1	9.3	9.0	9.3	17.9	18.7
	Undetermined <sup>3</sup>	35	6	0	0	0	6	41	3.7	0.1	0.0	0.0	0	0.1	0.4
	Subtotal	299	1548	400	122	522	2070	2369	31.4	26.9	13.4	26.6	15.2	22.5	23.4
Total		952	5750	2983	458	3441	9191	10143	_	_		_	_	_	_

<sup>1</sup> Data were variably collected at seven DTBird installations operated from January through October 2017.

<sup>&</sup>lt;sup>2</sup> Data were variably collected at 14 DTBird installations. Year 1 = September 2021 through August 2022. Year 2a = September 2022 through January 2023 before false positive filters were adjusted. Year 2b = February through July 2023 after false positive filters were adjusted.

<sup>&</sup>lt;sup>3</sup> Cases eliminated from analytical consideration.

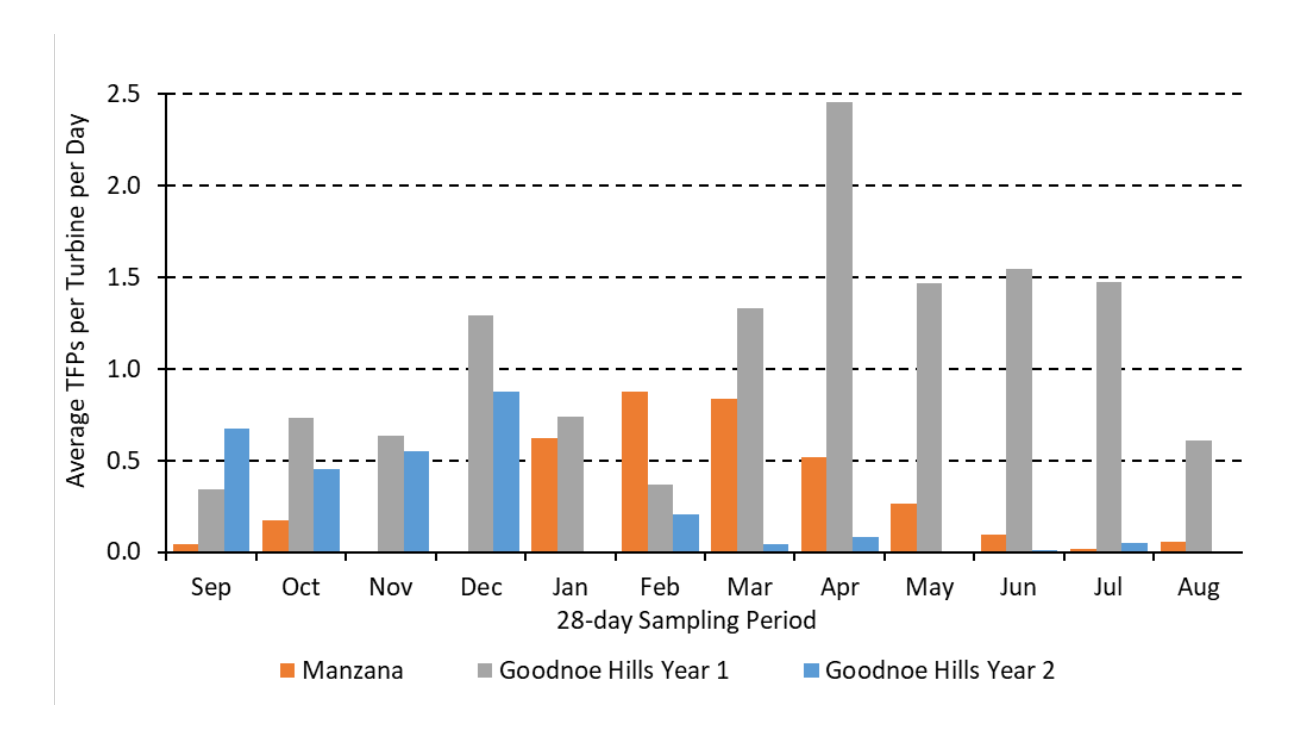


Figure 3. Rates of True False Positives Caused by Insects that Triggered DTBird Deterrents by Month at the Manzana Wind Power Project in California (January – October 2017) at the Goodnoe Hills Wind Farm in Washington (September–August 2021–2022 and 2022–2023).

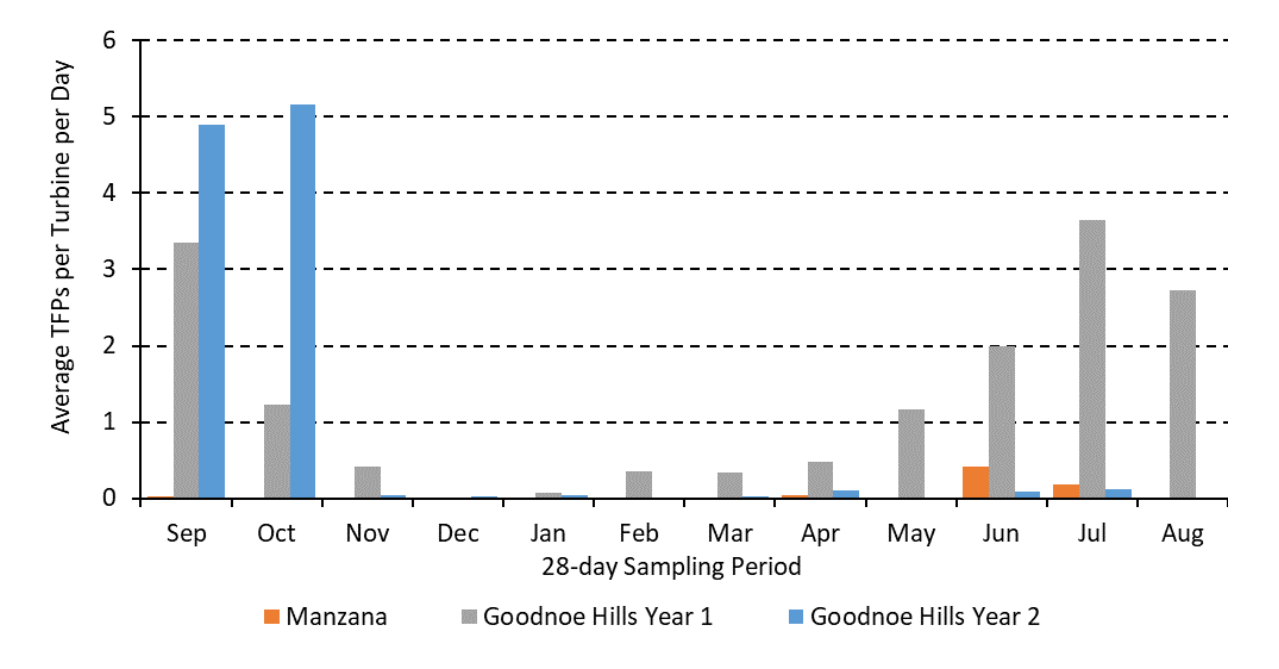


Figure 4. Rates of True False Positives Caused by Sky Artifacts that Triggered DTBird Deterrents by Month at the Manzana Wind Power Project in California (January–October 2017) and at the Goodnoe Hills Wind Farm in Washington (September–August 2021–2022 and 2022–2023).

high through the 12<sup>th</sup> cycle, before dropping back down again to a moderate level during the 13<sup>th</sup> cycle (Figure 4, noting that for Goodnoe Hills the indicated patterns across months are essentially the same as for 28d Cycles, whereas 28d Cycle 1 was in January at Manzana). Considering the patterns in relation to calendar months further suggested that seasonal variation in the relative prevalence of sky artifact TFPs also might have contributed to the observed patterns. Though temporal mismatches in the site-specific datasets confound seasonal comparisons, it appeared that sky artifact TFPs were most common at Manzana in late winter early spring and dropped off during summer, whereas the Goodnoe Hills Year 1 data suggested comparatively high rates across the year and an extended period of peak activity from spring through summer (Figure 4).

### 3.1.2 Nontarget Avian False Positives

The range of general categories of NTAFP sources was similar at the two study sites. The only material difference in the proportional representations was that the percentage of confirmed common ravens was lower at Manzana (28% of classified NTAFPs) than during either sampling year at the Goodnoe Hills (39–42%), whereas the proportion of unidentified big birds that we ultimately classified as NTAFPs was higher at Manzana (57%) than it was during both years at Goodnoe Hills (40–45%) (Table 3).

## 3.2 False Positive Deterrent Triggering Rates and Durations

The overall average large-raptor deterrent triggering rates were relatively consistent across the three primary site-sampling periods, ranging from 1.3–1.5 detections with deterrent triggers/turbine/day (Table 1). The overall average TFP deterrent triggering rates were more variable, ranging from a low of 1.3 detections with deterrent triggers/turbine/day at Manzana to a high of 4.9 detections with deterrent triggers/turbine/day during Year 1 at the Goodnoe Hills; the Year 2 TFP deterrent triggering rate at the Goodnoe Hills was midday between the other two estimates. The same general pattern of differences was evident among the NTAFP deterrent triggering rates (Table 1).

Standardized for variable sampling intensity, the overall average TFP-caused warning signal durations on turbine-days when deterrents were triggered averaged 17.3 seconds/turbine/day at the Manzana site and a significantly higher 26.2 seconds/turbine/day at the Goodnoe Hills site (Table 4). The average warning signal duration rate at the Goodnoe Hills declined from 27.0 seconds/turbine/day during Year 1 down to 23.4 seconds/turbine/day during the Year 2 post-adjustments period, but still remained notably longer than at Manzana. In contrast, the average duration rates for dissuasion signals rose slightly at Goodnoe Hills between Year 1 (30.7 seconds/turbine/day) and the Year 2 post-adjustments period (33.6 seconds/turbine/day), but in this case the higher Year 2 post-adjustments rate more closely matched the Manzana rate (33.5 seconds/turbine/day).

Similar patterns of variation were evident in the overall average NTAFP-caused deterrent signal duration rates (Table 4), except differences among the Goodnoe Hills sampling periods and between the two study sites were less pronounced, and the duration rates declined slightly for both warning and dissuasion signals between Year 1 and the post-adjustments Year 2 period at the Goodnoe Hills.

Table 3. Numbers and Percentages of Nontarget Avian False Positive (NTAFP) DTBird Detections at the Manzana Wind Power Project in California and Goodnoe Hills Wind Farm in Washington

			Numb	ers of N	NTAFPs			Manzana Year Year Year Year Year Year 1 2a 2b 2 Total Total  1 2 1 3 2 2 28 41 39 42 40 41					ods	
			Go	odnoe	Hills <sup>2</sup>		C			Go	odnoe	Hills		C l- !l
Source	Manzana <sup>1</sup>	Year 1	Year 2a	Year 2b	Year 2 Total	Two Year Total	Combined Grand Total	Manzana	Year 1				Year	- Combined Grand Total
Raptors <sup>3</sup>	14	124	26	54	80	204	218	1	2	1	3	2	2	2
Common Ravens	453	2680	1034	865	1899	4579	5032	28	41	39	42	40	41	39
Unidentified Big Birds <sup>4</sup>	944	2794	1067	916	1983	4777	5721	57	43	40	45	42	42	44
Other Birds	235	925	534	223	757	1682	1917	14	14	20	11	15	15	15
Total	1646	6523	2661	2058	4719	11242	12888	-	_	_	-	_	_	

<sup>&</sup>lt;sup>1</sup> Data were variably collected at seven DTBird installations operated from January through October 2017.

<sup>&</sup>lt;sup>2</sup> Data were variably collected at 14 DTBird installations. Year 1 = September 2021 through August 2022. Year 2a = September 2022 through January 2023 before false positive filters were adjusted. Year 2b = February through July 2023 after false positive filters were adjusted.

<sup>3</sup> Includes raptors confirmed or suspected to be other than focal large soaring species (i.e., species other than eagles, vultures, buteos, harriers, and ospreys).

<sup>4</sup> Includes large birds that could not be confidently distinguished as ravens or large raptors, portions of which were classified as NTAFPs for analytical summary purposes (see text).

Table 4. Overall Durations and Average Per Turbine Duration Rates for DTBird Deterrent Signals
Triggered by True False Positives (TFPs) and Nontarget Avian False Positives (NTAFP) at
the Manzana Wind Power Project in California and Goodnoe Hills Wind Farm in
Washington

		,	Warning Sig	ınals	D	issuasion Si	gnals
Site	Sampling Period	Number of Triggers	Total Duration (minutes)	Average Duration/ Turbine/Day (seconds)	Number of Triggers	Total Duration (minutes)	Average Duration/ Turbine/Day (seconds)
TFPs							
Manzana	10 months	487	294	17.3	662	370	33.5
Goodnoe Hills	Year 1	654	217	27.0	4820	2465	30.7
	Year 2 – 4.5 months pre- adjustments	493	78	26.5	2551	1361	32.0
	Year 2 – 6.5 months post- adjustments	199	589	23.4	685	383	33.6
NTAFPs							
Manzana	10 months	979	364	22.3	458	223	29.1
Goodnoe Hills	Year 1	2510	1097	26.2	173.5	960	33.2
	Year 2 – pre	1138	484	25.5	797	438	33.0
-	Year 2 – post	1083	458	25.4	602	321	32.0

#### 3.2.1 Statistical Models

With the analysis limited to comparing results across 12 common 28d Cycles, the numbers of days from which samples were drawn to compose the GLMM relating daily turbine-specific counts of TFPs that triggered deterrents to Year and 28d Cycle at the Goodnoe Hills varied from 10-119 per turbine across 11 sampled turbines in Year 1, and from 57-97 per turbine across 14 sampled turbines in Year 2 (Table 5). For the analysis comparing Goodnoe Hills results by Year and Month, we excluded May from the comparison due to an absence of data from that month in Year 2. For this reason, the sample sizes used to compare Year 1 and Year 2 by Month at the Goodnoe Hills were slightly lower for Year 1 than in the 28d-Cycle analysis (Table 5). The GLMM relating daily turbine-specific TFP counts to Year and 28d Cycle revealed a highly significant main effect for Year (Wald  $\gamma^2$ , P < 0.0001), a non-significant main effect for 28d Cycle (P = 0.98), and a highly significant interaction term (P < 0.0001). Nakagawa's marginal pseudo-R<sup>2</sup> for the model was 0.288, indicating that the fixed effects in the model provided moderate explanatory power (Nakagawa and Schielzeth 2013). Given the significant interaction, we conducted planned post-hoc comparisons to identify significant pairwise differences between Years within 28d Cycles and among 28d Cycles within Years. These comparisons confirmed the substantial shift in TFP prevalence after the additional filtering adjustments were made during the fifth 28d Cycle of Year 2 (Figure 5). Before that, the TFP rates did not differ markedly during corresponding 28d Cycles of the two sampling years. After that, the TFP rates remained significantly lower in Year 2 than in Year

1 during all subsequent 28d Cycles. Further, the post-adjustments Year 2 rates remained consistently low post-adjustments, whereas the corresponding Year 1 rates rose steadily after the sixth cycle to the highest rate for the year during the twelfth cycle.

Table 5. Numbers of turbine-specific days from which samples were drawn for investigating temporal differences in DTBird false-positive detection rates between sampling years at the Goodnoe Hills Wind Farm in Washington.

		lysis by 28d Cy mmon Cycles 1			nalysis by Mon Nonths Except	
Turbine	Year 1	Year 2	Total	Year 1	Year 2	Total
G29	-	95	95	-	95	95
G34	98	91	189	104	91	195
G35	89	87	176	88	87	175
G44	107	79	186	103	79	182
G45	108	87	195	103	87	190
G48	112	57	169	110	57	167
G49	105	90	195	101	90	191
G51	-	80	80	-	80	80
G56	-	70	70	_	70	70
G58	117	97	214	115	97	212
G59	104	57	161	106	57	163
G64	119	91	210	118	91	209
G67	112	86	198	111	86	197
G75	10	75	85	10	75	85
Total	1,081	1,142	2,223	1,069	1,142	2,211

The GLMM relating daily turbine-specific counts of TFPs that triggered deterrents to *Site* and *28d Cycles* at the Manzanas and during Goodnoe Hills Year 2 revealed a highly significant main effect for *Site* (Wald  $\chi^2$ , *P* <0.0001), a non-significant main effect for *28d Cycle* (P = 0.92), and a highly significant interaction term (P < 0.0001). Nakagawa's marginal pseudo- $R^2$  for the model was 0.219, indicating the fixed effects provided moderate explanatory power. Planned post-hoc pairwise comparisons confirmed that (a) both sites had relatively elevated TFP rates during the first two *28d Cycles* of the respective sampling periods, (b) the early rates during Goodnoe Hills Year 2 were much higher than during the two corresponding cycles at the Manzanas, and (c) after adjustments were completed during the fifth cycle of Year 2 at the Goodnoe Hills, the TFP deterrent-triggering rates followed similar patterns at the two sites, remained low and did not vary significantly across subsequent sampling cycles, and often were lower at the Goodnoe Hills post-adjustments than at the Manzanas (Figure 6).

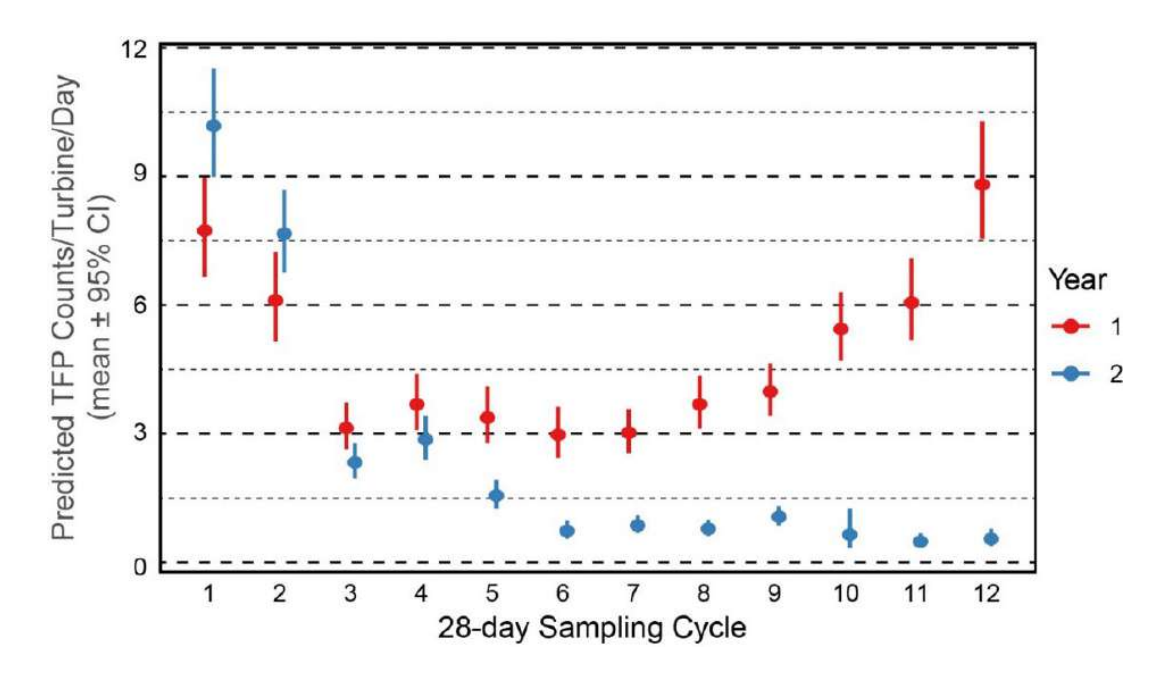


Figure 5. Predicted Average Daily Per Turbine True False Positive (TFP) DTBird Deterrent-Triggering Rates Across 28-day Sampling Periods During Study Years 1 and 2 at the Goodnoe Hills Wind Farm in Washington. Nonoverlapping Confidence Intervals Indicate Significant Pairwise Comparisons.

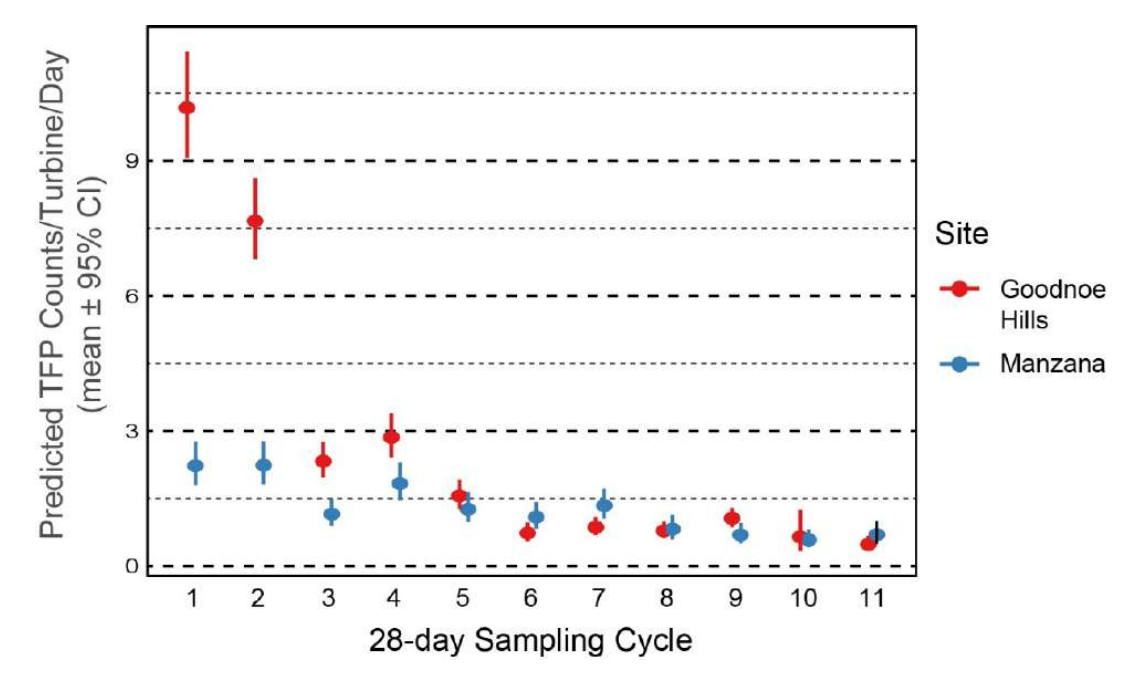


Figure 6. Predicted Average Daily Per Turbine True False Positive (TFP) DTBird DeterrentTriggering Rates Across 12 28-day Sampling Periods (Variable Calendar Periods) at the
Manzana Wind Power Project in California and During Study Year 2 at the Goodnoe
Hills Wind Farm in Washington. Nonoverlapping Confidence Intervals Indicate
Significant Pairwise Comparisons.

The GLMM relating daily turbine-specific counts of NTAFPs that triggered deterrents to *Year* and *Month* at the Goodnoe Hills revealed a highly significant main effect for *Year* (Wald  $\chi^2$ , P < 0.0001), a non-significant main effect for *28d Cycle* (P = 0.99), and a highly significant interaction term (P < 0.0001). Nakagawa's marginal pseudo- $R^2$  for the model was 0.085, indicating the fixed effects provided marginal explanatory power. Unlike the TFP results, no dramatic shift in NTAFP prevalence occurred post-adjustments at the Goodnoe Hills; however, the post-adjustment rates in Year 2 (after January) did generally remain significantly lower than during all corresponding months in Year 1 (Figure 7).

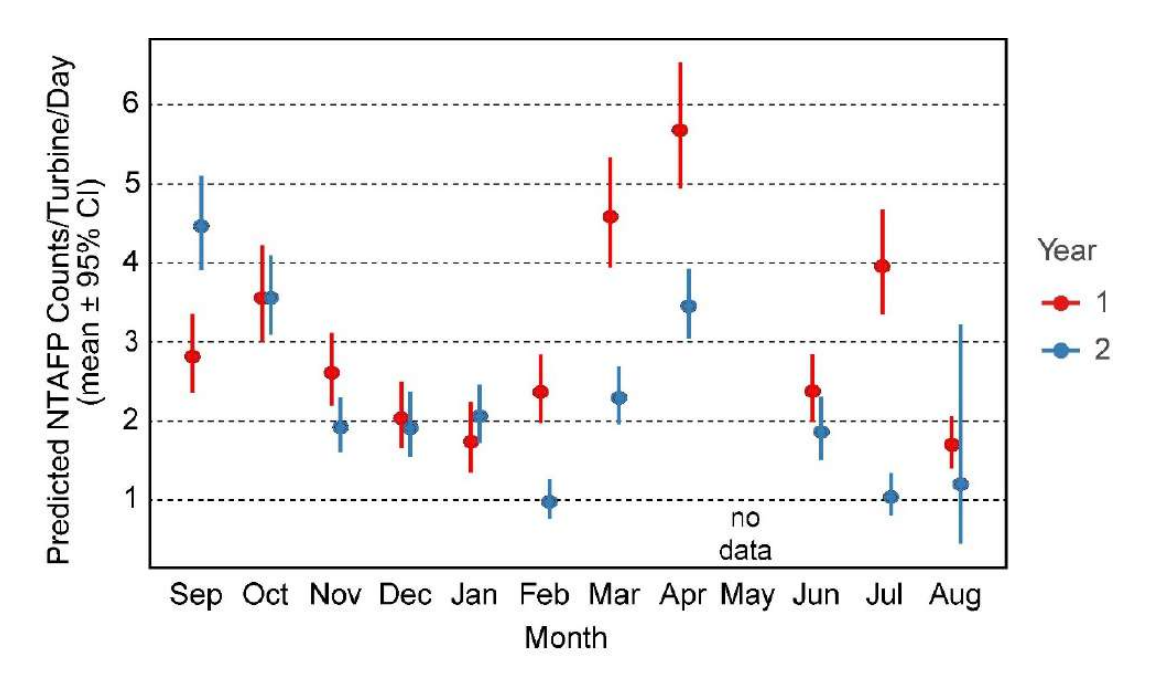


Figure 7. Predicted Average Daily Nontarget Avian False Positive (NTAFP) DTBird Deterrent-Triggering Rates Across 11 Months During Study Years 1 and 2 at the Goodnoe Hills Wind Farm in Washington. Nonoverlapping Confidence Intervals Indicate Significant Pairwise Comparisons.

The GLMM relating daily turbine-specific counts of NTAFPs that triggered deterrents to *Site* and *Month* at Manzana and at the Goodnoe Hills during sampling Year 2 revealed a non-significant main effect for *Site* (Wald  $\chi^2$ , P = 0.23), a non-significant main effect for *28d Cycle* (P = 0.98), and a highly significant interaction term (P < 0.0001). Nakagawa's marginal pseudo-R<sup>2</sup> for the model was 0.129, indicating the fixed effects provided marginal explanatory power. Across the nine relevant calendar months, the two sites showed similarities towards higher NTAFP prevalence in spring, declining into mid-summer, then increasing some again in fall (Figure 8). The only substantive difference in pattern was that NTAFP prevalence was notably elevated at Goodnoe Hills during September and October compared to Manzana, suggesting higher fall migratory activity of nontarget birds at Goodnoe Hills.

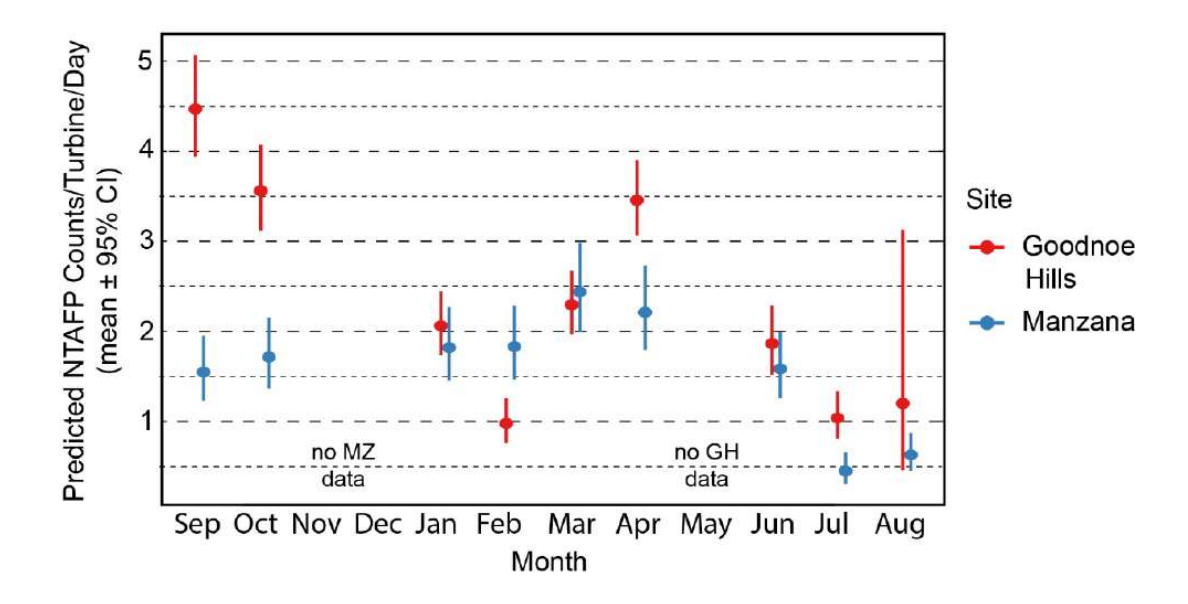


Figure 8. Predicted Average Daily Nontarget Avian False Positive (NTAFP) DTBird Deterrent-Triggering Rates Across Nine Common Sampling Months at the Manzana Wind Power Project in California and During Study Year 2 at the Goodnoe Hills Wind Farm in Washington. Nonoverlapping Confidence Intervals Indicate Significant Pairwise Comparisons.

## 3.3 Probability of Detection/False Negatives

The sample sizes of independent site- and turbine-specific UAV flight transects that formed the basis for quantifying and investigating variation in the probability of detection ranged from 144–221 samples per turbine at the Manzana site and 54–131 samples per turbine at the Goodnoe Hills site (Table 6). At the Manzana site, DTBird detected 798 of 1,279 (62%) UAV flight transects, with the detected proportions ranging from 47–75% across seven sampled turbines. At Goodnoe Hills, DTBird detected 310 of 481 (64%) UAV flight transects, with the detected proportions ranging from 56–80% across five sampled turbines (Table 6).

The final model derived to illustrate the influence of spatial and temporal predictors on the probability of detection based on UAV flight trials had the following form:

 $ln(Odds of Detection) \sim Site + Hour of the Day + LoS Distance + LoS Distance^2 + LoS Distance^3 + Detection Angle + Detection Angle^2$ 

The log-likelihood ratio goodness-of-fit test comparing the selected model and null model indicated a highly significant fit ( $\chi^2$  =476.7, df = 7, P < 0.001) and the Nagelkerke Psuedo-R<sup>2</sup> for the model was 0.324, indicating a moderate relationship. Comparisons with other candidate models are illustrated in Appendix C, and coefficients, parameter tests, and diagnostics for the selected model are presented in Appendix D.

Table 6. Numbers of UAV flight transects by sampled turbine analyzed to quantify and investigate variation in the probability of DTBird detecting an eagle-like UAV at the Manzana Wind Power Project in California and Goodnoe Hills Wind Farm in Washington

Site	Turbine	Detected	Not Detected	Total	% Detected
Manzana	D01	80	64	144	56
	D04	129	62	191	68
	D08	106	65	171	62
	E11	143	54	197	73
	T13	116	38	154	75
	U7	130	91	221	59
	V17	94	107	201	47
Subtotal		798	481	1,279	62
Goodnoe Hills	G34	65	16	81	80
	G44	81	50	131	62
	G58	69	36	105	66
	G64	33	21	54	61
	G75	62	48	110	56
Subtotal		310	171	481	64
Total		1,108	652	1,760	63

The selected model indicated that the probability of detection:

- Averaged higher at Goodnoe Hills than at Manzana (discussed further below).
- Increased as the day progressed, from an average of approximately 57% during the 06:00 H to 75% during the 20:00 H (Figure 9).
- Was highest (estimated average ~75%) when the LoS Distance to a flight track was 50–75 meters
  from the cameras; decreased slightly at closer distances; and decreased at greater distances down to
  an estimated average of approximately 50% at the 240 meter expected (calibrated) maximum
  detection distance for targets the size of golden eagles, but remained at an estimated 30% as far out
  as 380 meters from the cameras (Figure 10).
- Was highest (estimated mean ~65%) when the Average Detection Angle from the camera to a flight track was moderate (approximately 20–30° above horizontal from the camera) and decreased on average by 25–35% at minimum lower and maximum higher observed angles (Figure 11).

Based on the model output and the range of flights considered in formulating that model, the overall average probability of detecting an eagle-like UAV at the two study sites was  $63 \pm 1.1\%$  (95% CI). However, as the basis for the predictive model, we included a broad range of flights with LoS Distances extending out as far

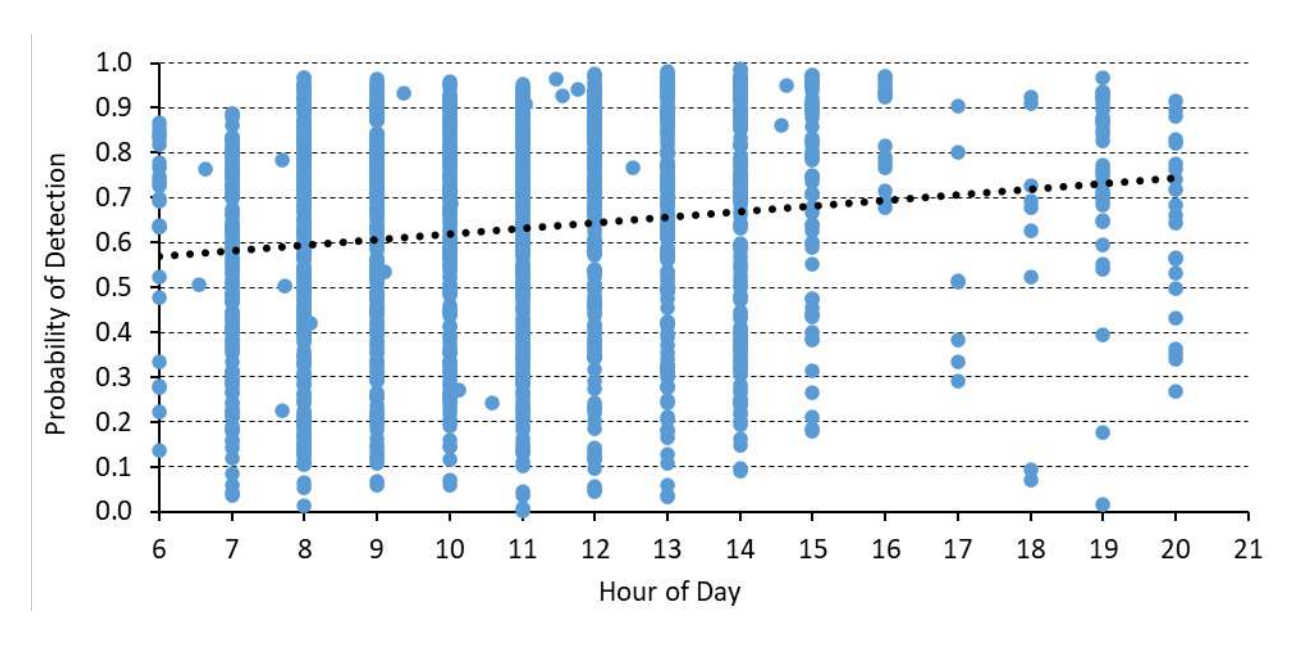


Figure 9. Modeled Linear Relationship Between Predicted DTBird Detection Probabilities for Individual UAV Flight Transects and Hour of the Day.

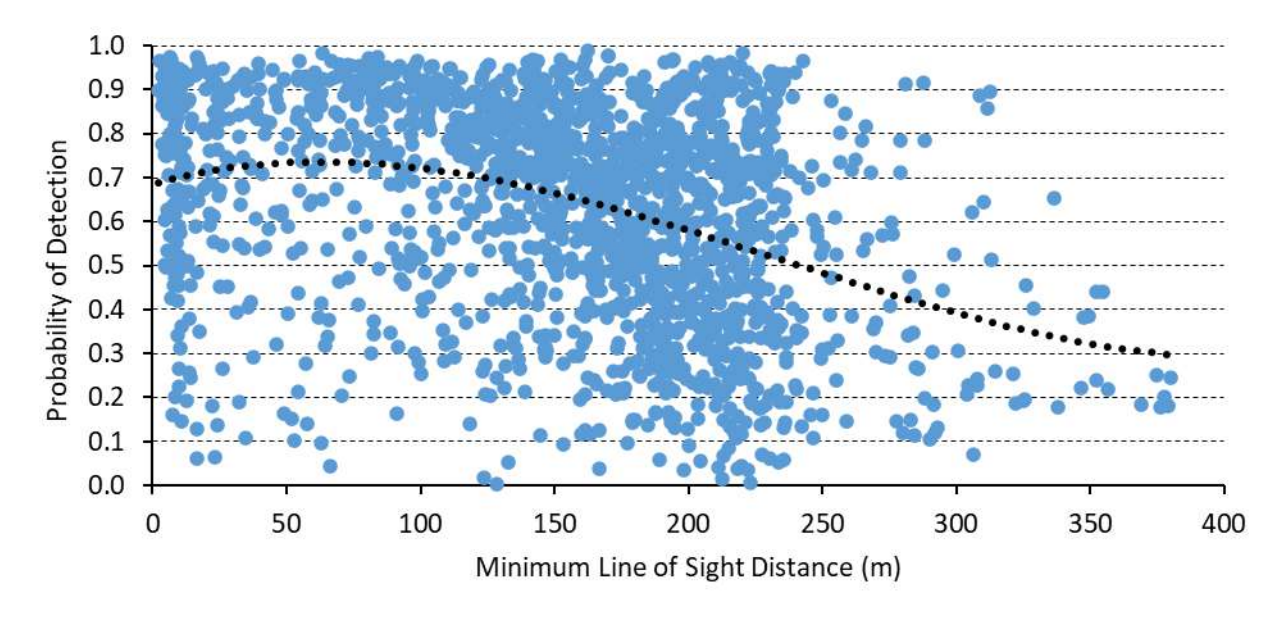


Figure 10. Modeled Third-Order Relationship Between Predicted DTBird Detection Probabilities for Individual UAV Flight Transects and the Minimum Line-of-Sight Distance to the DTBird Camera.

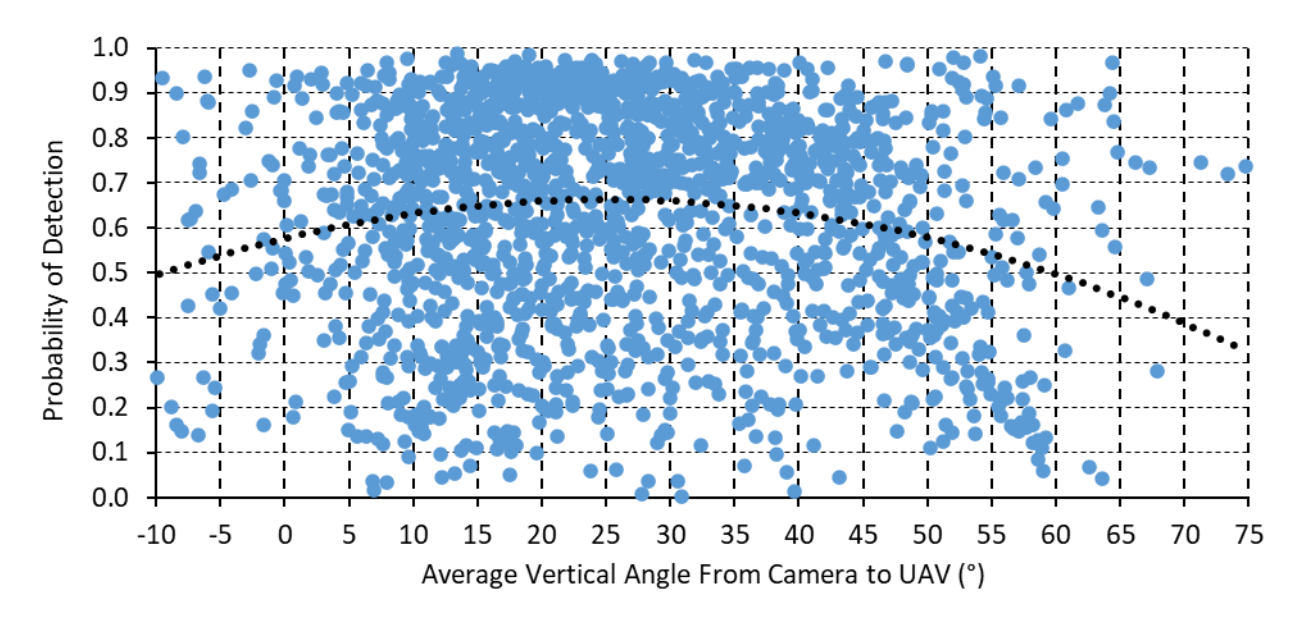


Figure 11. Modeled Second-Order Relationship Between Predicted DTBird Detection Probabilities for Individual UAV Flight Transects and the Average Vertical Angle from the DTBird Camera.

as 380 meters, including DTBird detection distances of up to 375 meters. The intent was to maximize good model fit by including useful data that extended spatially beyond the focal, calibrated maximum detection distance of 240 meters. For the purpose of comparing the estimated overall probability of detection (or conversely false negatives) against the performance standard established for this project (63%), a fairer metric is the probability of detecting an eagle-like UAV that flies within 240 meters or less of the cameras. Based on model output and this restriction, the relevant detection probabilities were  $66 \pm 1.3\%$  (95% CI) at Manzana,  $64 \pm 1.9\%$  at Goodnoe Hills, and  $65 \pm 1.1\%$  overall. Note that these indicators suggest that the probability of detection was slightly higher at the Manzana site, whereas the modeled full dataset suggested the opposite (Table 6), clearly emphasizing that any difference between the two sites was at best marginal.

Flipped about to focus on false negatives, these results suggest that the probability of DTBird missing a detectable flight was overall <20% when the LoS Distance to the flight was between approximately 30–120 meters, <30% at distances of <20 meters and between 120–160 meters from the cameras, and exceeded 50% only beyond 200 meters. Otherwise, flights were missed more often at the Goodnoe Hills, during morning light, and at both low and high detection angles.

## Section 4.0 Discussion

#### 4.1 False Positives

The specifications promulgated by Liquen (2017) specified that DTBird systems comparable to those installed at Manzana and Goodnoe Hills should be expected to result in a yearly average TFP deterrent trigger rate of 0.2–4.0 events/turbine/day, amounting to a total duration of 0.1–2.5 minutes/turbine/day. With seven turbines evaluated across 10 months, estimates from the Manzana study fell within these ranges: averages of 1.2–1.8 TFP deterrent triggers/turbine/day among the seven turbines (H. T. Harvey & Associates 2019b) and an overall average rate derived from the integrated analysis presented herein of 1.3 TFP detections with deterrent triggers/turbine/day. Similarly, the TFP deterrent emittance rate (warning and dissuasion signals combined) was estimated to average 0.6–0.9 minutes/turbine/day among the seven installations, and the overall average rate derived from the integrated analysis presented herein was 0.8 minutes/turbine/day. Results from the Manzana study and other prior studies of DTBird technology (May et al. 2012, Aschwanden et al. 2015) formed the basis for the performance targets specified for the Goodnoe Hills study (H. T. Harvey & Associates 2019a): maximum of 1.6–2.8 TFP deterrent triggers/turbine/day, and no more than 36% of all relevant detection events resulting from TFPs.

The overall-average TFP deterrent-triggering event rate at Goodnoe Hills across 23 months of sampling was 3.9 TFP deterrent triggers/turbine/day, which substantially exceeded the established performance target. However, after Liquen made additional adjustments to reduce the false positive rate in January 2023, the rate for the subsequent 7 months dropped to an average of 0.8 TFP deterrent triggers/turbine/day, well below the performance target. Similarly, although TFPs resulted in more than 50% of all detections that triggered deterrents before the adjustments were made, the proportion dropped to 25% post-adjustments, again falling below the established performance target. Moreover, in both cases the post-adjustment rates at Goodnoe Hills were lower than at Manzana, suggesting improvement in the filtering algorithms.

Across the periods of record, the overall TFP-caused deterrent signal durations (warning and dissuasion signals combined) on turbine-days when deterrents were triggered averaged 0.84 minutes/turbine/day at Manzana and 0.96 minutes/turbine/day at Goodnoe Hills. Post-adjustments, the combined deterrent signal duration rate at Goodnoe Hills fell only slightly to 0.95 minutes/turbine/day, despite the significant reduction in numbers of TFPs. This suggests that fewer signals averaged longer in duration per trigger after the adjustments, which may indicate that birds exposed to fewer TFP-triggered deterrents may have subsequently lingered more around the turbines with DTBird installations (a possible manifestation of negative habituation to prior excessive TFP signaling). Regardless, all documented signal duration rates fell below Liquen's desired standard of <2.5 minutes/turbine/day.

The results focused on variation in the prevalence of TFPs caused by insects during Goodnoe Hills Year 1 suggested the potential for substantial seasonal variation at this site, with a lesser magnitude of seasonal variation also evident at Manzana (H. T. Harvey & Associates 2019b). However, the comparative results for Goodnoe Hills Year 2 suggested that the additional adjustments Liquen made in 2023 substantially

mitigated/dampened what would otherwise have continued to be a significant source of excessive deterrent signaling during summer/fall at Goodnoe Hills (and perhaps at Manzana had earlier adjustments not been made there).

The notable contrasts in temporal patterns of sky artifact TFPs among years at Goodnoe Hills and between Manzana and Goodnoe Hills likely reflects a combination of factors. First, the documented difference in prevalence in Goodnoe Hills Years 1 and 2, showing a similar pattern as for insect TFPs, suggested that the further adjustments to the false positive filtering algorithms Liquen made in early 2023 probably also reduced the probability of sky artifact TFPs and contributed to the much lower post-adjustments sky artifact TFP rate in Year 2 compared to the corresponding cycles in Year 1. However, examining the patterns in relation to calendar months also suggested the possibility of weather-related differences in the source of TFPs at the two sites. Specifically, sky artifact TFPs were generally common throughout the year at Goodnoe Hills and appeared to be particularly prevalent from spring through mid-summer (in Year 1 when not limited by additional filtering), whereas sky artifact TFPs appeared to be more restricted to late winter/early spring at Manzana. This suggests that the variable climatic regimes of the two study regions also contributed to the differences between the two sites. Specifically, highly dynamic, partly cloudy skies tend to be more restricted to late winter/spring in the relatively xeric environment of the Mojave Desert where the Manzana site lies, whereas variable storminess and cloudy weather are often consistently more prevalent both during snowy winters and extending later in spring and into early summer in the Columbia Gorge region of Washington where the Goodnoe Hills site lies. Sky-artifact TFPs appear to arise more frequently when cloud cover is more prevalent and variable, dynamically producing more high-contrast elements that the DTBird system erroneously interprets as target movement.

Efficiently focusing a deterrent system such as DTBird on specific species of conservation interest is often the primary objective for facility managers. In this context, avoiding unnecessary detections and deterrent signaling caused by non-focal bird species will often be important to minimize risks of negative habituation. At both the Manzana and Goodnoe Hills sites, relatively high proportions of the DTBird detections and deterrent signaling resulted from the activities of nontarget birds, especially common ravens.

Data from the Manzana and Goodnoe Hills study sites were also similar in showing some common seasonal patterns in the prevalence of detections reflecting the activities of NTAFPs, with generally higher activity during spring and fall migration, lowest activity during mid-summer in California, and moderate activity during winter in both areas. Natural seasonal cycles in the distribution and abundance of insects contributing to TFPs and birds contributing to NTAFPs are expected, but may also occur relative to sky artifacts as solar and cloud cover variations greatly influence that source of TFPs. If predictable enough through time, it may be possible to improve the DTBird false-positive filtering algorithms to be more sensitive to these factors and thereby efficiently reduce the overall false positive rate.

Excessive false-positive detections hinder effective use of the DAP system for tracking activity and identifying exposure risk for focal species. Previously we emphasized the burden of sifting through thousands of false positive records that did not trigger deterrents when the study motivation calls for screening such records (H. T. Harvey & Associates 2018, 2019b, 2022a). However, such events did not contribute to potentially limiting DTBird's effectiveness through negative habituation of target raptors. Hence, for

screening Goodnoe Hills Year 2 records and the analyses presented herein, we ignored all such superfluous records, depending on a "rotor state" indicator typically recorded for each record in the DAP as the basis for discerning when the turbine rotor was spinning, the DTBird deterrents were triggering, and the record therefore was a candidate for evaluation. Although this approach greatly reduced the number of records we screened, thousands of potentially deleterious false positive records that triggered deterrents remained, amounting to roughly 2,000 such TFP/NTAFP records in both the Manzana and Goodnoe Hills post-adjustments datasets. More generally, the results of this study and previous studies clearly illustrate that limited AI discernment capabilities combined with audio deterrents may result in significantly variable system effectiveness.

Collectively, the results of this multi-site investigation suggest the following relative to false positives:

- DTBird systems should not be considered fully commissioned and maximally effective until at least 2 months after Liquen declares the systems "commissioned" and they complete fine-tuning to minimize false positives caused by spinning blades and other factors. Most importantly, if the deterrents are allowed to broadcast during the continued adjustments, excessive deterrent triggering from false positives could easily stimulate an initial negative habituation response from resident birds.
- The Goodnoe Hills Year 2 post-adjustment results generally suggested that Liquen should prioritize additional improvements of the DTBird filtering algorithms to further reduce the potential for especially blade-related, insect, and sky-artifact TFPs, which result in substantial clutter within the DAP and unnecessarily trigger an abundance of potentially deleterious deterrent signals.
- NTAFPs represent a complicated management issue, in that protecting all native bird species from unnecessary human-caused mortality is a worthy objective, but excessive deterrent triggering by nontarget birds and other factors could lead to deleterious negative habituation among eagles that occur in the vicinity of wind facilities. Further study would be needed to test this. Developing and implementing an AI system capable of distinguishing species and fine-tailoring the deterrent triggers is the only logical solution to reduce NTAFPs.

## 4.2 Probability of Detection and False Negatives

The probability of detection/false negatives modeling results indicated similar patterns at the two study sites. Our initial comparison of non-modeled rates suggested an exact match of a 63% probability of detection at both sites (H. T. Harvey & Associates 2022b). The refined modeling results presented herein, tailored to represent detection probabilities limited to the projected 240-meter detection envelope for golden eagles, confirmed a nominally higher detection probability at Manzana (66%) than at Goodnoe Hills (64%). In both cases, the estimates exceed the performance standard of 63% established as a basis for evaluating DTBird performance at Goodnoe Hills, though clearly nothing done to potentially improve the detection systems between the Manzana pilot study and the subsequent Goodnoe Hills study led to better performance at

Goodnoe Hills. Instead, this outcome suggests consistent performance of the primary detection functions of the DTBird systems at both sites.

The probability of detection modeling analysis also provided useful perspective concerning factors that influence the overall probability of DTBird detecting an eagle-like UAV if it flies anywhere through the detection envelope projected based on calibration for golden eagles. The limitation of this analysis is that for flights that are not detected (false negatives) there are no reference points to use for precisely characterizing the flight, location, and environmental characteristics at the time of a specific DTBird event to use as covariates. Consequently, we focused attention on discerning the influences of only a select few metrics derived by using GIS tools to calculate selected minimum and averaging position metrics across all points along a given sample flight. Nevertheless, this relatively simple approach illustrated variability in the probability of detection through the day, likely related to the relative influence of solar position and intensity. More importantly, the results emphasized that the probability of detection was highest when the target flew at moderate distances from the turbine (generally high with average flight distances of 80-160 m) through the midsection of the camera viewshed (generally high with viewing angles from camera up to UAV of 25-40°). Conversely, the probability of detection averaged lower when the target flew either closer to or farther away from the camera or primarily within the lower or upper margins of the camera viewshed. These results are perhaps not surprising in suggesting that detection tends to be lower around the margins of the camera viewsheds and higher when a bird is flying at moderate distances from and in the center of a camera viewshed. The latter conditions are exactly when birds approaching a spinning turbine tend to be at greatest risk of entering the RSZ of spinning turbines. However, especially hunting or displaying raptors such as golden eagles often make very dynamic movements that can either rapidly drop them down from up high or pop them up from down low and quickly bring them into the RSZ danger zone at relatively close range. For this reason, poorer detection low and close or high and close to the turbine can result in problematic interactions with little time for the deterrents to trigger and discourage continued closer passage before entering the collision risk zone.

## Section 5.0 References

- Aschwanden, J., S. Wanner, and F. Liechti. 2015. Investigation on the Effectivity of Bat and Bird Detection at a Wind Turbine: Final Report Bird Detection. Prepared for Interwind AG, Swiss Federal Office of Energy, and Federal Office for the Environment. Schweizerische Vogelwarte, Sempach, Switzerland.
- Brooks, M. E., K. Kristensen, K. J. van Benthem, A. Magnusson, C. W. Berg, A. Nielsen, H. J. Skaug, M. Mächler, and B. M. Bolker. 2017a. glmmTMB balances speed and flexibility among packages for zero-inflated generalized linear mixed modeling. The R Journal 9:378–400.
- Brooks, M. E., K. Kristensen, K. J. van Benthem, A. Magnusson, C. W. Berg, A. Nielsen, H. J. Skaug, M. Mächler, and B. M. Bolker. 2017b. Modeling zero-inflated count data with glmmTMB. BioRxiv:132753. <a href="https://www.biorxiv.org/content/biorxiv/early/2017/05/01/132753.full.pdf">https://www.biorxiv.org/content/biorxiv/early/2017/05/01/132753.full.pdf</a>.
- Hosmer, D. W., and S. Lemeshow. 1989. Applied Logistic Regression. John Wiley & Sons, New York, NY, USA.
- H. T. Harvey & Associates. 2018. Evaluating a Commercial-Ready Technology for Raptor Detection and Deterrence at a Wind Energy Facility in California. Research report. Los Gatos, California. Prepared for the American Wind Wildlife Institute, Washington, D.C.
- H. T. Harvey & Associates. 2019a. Evaluating the Effectiveness of a Detection and Deterrent System in Reducing Eagle Fatalities at Operational Wind Facilities. Detailed study plan. Los Gatos, California. Prepared for the American Wind Wildlife Institute, Washington, D.C., in conjunction with U.S. Department of Energy Cooperative Agreement DE-EE0007883.
- H. T. Harvey & Associates. 2019b. Analysis of DTBird False Positive Detections at the Manzana Wind Power Project Through October 2017. Research report. Los Gatos, California. Prepared for the American Wind Wildlife Institute, Washington, D.C.
- H. T. Harvey & Associates. 2022a. Initial Analysis of DTBird False Positive Detections at the Goodnoe Hills Wind Farm, Washington: September 1, 2021 March 15, 2022. Research Report. Los Gatos, CA, USA. Prepared for the Renewable Energy Wildlife Institute, Washington, D.C., USA, in conjunction with U.S. Department of Energy Cooperative Agreement DE-EE0007883.
- H. T. Harvey & Associates. 2022b. Initial Analyses of DTBird Detection and Deterrent-Triggering Response Distances and Probability of Detection at the Goodnoe Hills Wind Farm, Washington. Research Report. Research Report. Los Gatos, CA, USA. Prepared for the Renewable Energy Wildlife Institute, Washington, D.C., USA, in conjunction with U.S. Department of Energy Cooperative Agreement DE-EE0007883.
- H. T. Harvey & Associates. 2023a. Results of Controlled Two-Year Experiment to Evaluate Effectiveness of the DTBird® Automated Detection and Deterrence System in Reducing Collision Risk for Eagles and Other Large Raptors at the Goodnoe Hills Wind Farm, Washington. Los Gatos, CA, USA. Prepared for

- the Renewable Energy Wildlife Institute, Washington, D.C., USA, in conjunction with U.S. Department of Energy Cooperative Agreement DE-EE0007883.
- H. T. Harvey & Associates. 2023b. Analysis of DTBird Detection and Deterrent-Triggering Response Distances at Commercial Wind-Energy Facilities in California and Washington. Los Gatos, CA, USA. Prepared for the Renewable Energy Wildlife Institute, Washington, D.C., USA, in conjunction with U.S. Department of Energy Cooperative Agreement DE-EE0007883.
- H. T. Harvey & Associates. 2023c. Analysis of Behavioral Responses of Eagles and Other Large Raptors to DTBird Audio Deterrents at Commercial Wind-Energy Facilities in California and Washington. Los Gatos, CA, USA. Prepared for the Renewable Energy Wildlife Institute, Washington, D.C., USA, in conjunction with U.S. Department of Energy Cooperative Agreement DE-EE0007883.
- DTBird Team. 2017. DTBird® System Specifications for Wind Turbines. Liquen Consultoría Ambiental, S.L., Madrid, Spain. <a href="https://dtbird.com/images/Downloads/DTBird\_System\_Specifications">https://dtbird.com/images/Downloads/DTBird\_System\_Specifications</a>. \_November\_2017.pdf>.
- Lüdecke, 2022. Package ggeffects: create tidy data frames of marginal effects for 'ggplot' from model outputs. Version 1.1.3. <a href="https://cran.r-project.org/web/packages/ggeffects/index.html">https://cran.r-project.org/web/packages/ggeffects/index.html</a>.
- Magnussen, A., H. J. Skaug, A. Nielsen, C. W. Berg, K. Kristensen, M. Maechler, K. J. van Bentham, N. Sadat, B. M. Bolker, and M. E. Brooks. 2022. Package glmmTMB: generalized linear mixed models using template model builder. <a href="https://CRAN.R-project.org/package=glmmTMB">https://CRAN.R-project.org/package=glmmTMB</a>>.
- May, R., Ø. Hamre, R. Vang, and T. Nygård. 2012. Evaluation of the DTBird Video-System at the Smøla Wind-Power Plant: Detection Capabilities for Capturing Near-Turbine Avian Behaviour. NINA Report 910. Norwegian Institute for Nature Research, Trondheim, Norway.
- Nakagawa, S., and H. Schielzeth. 2013. A general and simple method for obtaining R<sup>2</sup> from generalized linear mixed-effects models. Methods in Ecology and Evolution 4:133–142. https://doi.org/10.1111/j.2041-210x.2012.00261.x.
- Schielzeth, H., N. J. Dingemanse, S. Nakagawa, D. F. Westneat, H. Allegue, C. Teplitsky, D. Réale, N. A. Dochtermann, L. Z. Garamszegi, and Y. G. Araya-Ajoy (2020). Robustness of linear mixed-effects models to violations of distributional assumptions. Methods in Ecology and Evolution 11:1141–1152. https://doi.org/10.1111/2041-210X.13434.
- Tukey, J. 1949. Comparing individual means in the analysis of variance. Biometrics 5:99-114.

Appendix A. Summary Classifications of DTBird Detection Events that Triggered Deterrents at the Manzana Wind Power Project as Large Raptors, True (Non-avian) False Positive (TFPs), and Nontarget Avian False Positives (NTAFPs) by Turbine and 28-day Cycle Sampling Periods Between January 1 and October 31, 2017

					Cla	ssification G	roup					
Turbine	28-day Cycle Sampling Period	Total Classified Events	Unknown Medium/ Large Raptor <sup>1</sup>	Large Raptor <sup>2</sup>	TFP	NTAFP	CORA <sup>3</sup>	Unknown Big Bird <sup>4</sup>	Unknown Bird <sup>5</sup>	Estimated Medium/ Large Raptor	Estimated Large Raptor	Estimated NTAFP
D01	1	74	1	6	26	4	20	15	2	1	9	38
	2	79	3	2	22	1	16	29	6	3	5	49
	3	66	3	8	15	1	15	9	15	3	15	33
	4	66	0	6	8	10	13	26	3	0	13	45
	5	57	2	3	14	7	12	17	2	2	9	32
	6	42	0	4	7	7	13	8	3	0	8	27
	7	37	0	2	9	4	8	7	7	0	6	22
	8	11	0	0	7	0	0	4	0	0	2	2
	9	41	1	5	7	3	9	15	1	1	11	22
	10	102	5	18	4	2	25	40	8	6	42	50
	11	59	7	10	4	2	13	17	6	9	17	29
Su	btotal	634	64	22	123	41	144	187	53	25	137	349
D04	1	40	2	9	14	2	4	6	3	4	11	11
	2	70	1	12	34	0	2	13	8	2	21	13
	3	64	0	9	16	1	9	15	14	0	23	25
	4	52	1	2	25	1	12	7	4	2	6	19
	5	49	0	3	27	1	5	12	1	0	9	13
	6	61	1	7	13	0	10	24	6	1	16	31
	7	41	1	6	9	0	9	16	0	1	12	19
	8	11	0	2	1	2	0	6	0	0	6	4
	9	22	1	3	3	1	4	8	2	1	6	12

					Cla	ssification G	roup					
Turbine	28-day Cycle Sampling Period	Total Classified Events	Unknown Medium/ Large Raptor <sup>1</sup>	Large Raptor <sup>2</sup>	TFP	NTAFP	CORA <sup>3</sup>	Unknown Big Bird <sup>4</sup>	Unknown Bird <sup>5</sup>	Estimated Medium/ Large Raptor	Estimated Large Raptor	Estimated NTAFP
	10	64	5	10	7	5	12	18	7	8	21	28
	11	38	1	0	5	2	7	15	8	1	4	28
Su	ubtotal	512	63	13	154	15	74	140	53	20	135	203
D08	1	62	2	3	21	0	5	29	2	3	13	25
	2	81	6	19	17	1	7	27	4	8	37	19
	3	55	9	4	8	0	8	23	3	15	13	19
	4	39	0	5	11	3	6	14	0	0	12	16
	5	34	0	1	8	1	11	12	1	0	2	24
	6	47	0	4	10	1	10	19	3	0	14	23
	7	28	0	2	10	0	6	9	1	0	6	12
	8	13	0	5	4	1	0	2	1	0	6	3
	9	23	1	3	7	1	3	6	2	2	4	10
	10	38	1	10	2	0	5	18	2	1	19	16
	11	30	2	4	7	1	1	8	7	2	14	7
St	ubtotal	450	60	21	105	9	62	167	26	31	140	174
E11	1	50	0	0	38	0	3	3	6	0	2	10
	2	36	0	4	17	1	3	7	4	0	8	11
	3	49	0	5	18	3	7	13	3	0	13	18
	4	42	3	4	18	0	3	11	3	5	7	12
	5	52	0	12	5	4	4	17	10	0	23	24
	6	52	0	9	18	2	3	16	4	0	17	17
	7	35	0	0	32	0	0	2	1	0	1	2
	8	12	0	1	9	0	0	2	0	0	2	1
	9	18	0	1	11	1	1	2	2	0	1	6
	10	25	3	2	6	0	6	8	0	4	4	11
	11	21	6	3	0	0	1	8	3	6	12	3
Su	ubtotal	392	41	12	172	11	31	89	36	15	90	115
T13	1	45	1	2	23	1	5	11	2	2	8	12
	2	37	0	3	22	0	3	8	1	0	5	10
	3	63	0	14	11	0	16	21	1	0	24	28

<b>Turbine</b>	28-day Cycle Sampling Period	Total Classified Events	Unknown Medium/ Large Raptor <sup>1</sup>	Large Raptor <sup>2</sup>	TFP	NTAFP	CORA <sup>3</sup>	Unknown Big Bird <sup>4</sup>	Unknown Bird <sup>5</sup>	Estimated Medium/ Large Raptor	Estimated Large Raptor	Estimated NTAFP
	4	108	1	30	5	2	17	53	0	1	66	36
	5	61	0	11	8	3	10	28	1	0	25	28
	6	32	2	4	5	5	1	14	1	2	11	14
	7	16	0	1	12	1	0	2	0	0	2	2
	8	15	0	2	11	2	0	0	0	0	2	2
	9	11	1	1	4	0	1	4	0	2	2	3
	10	30	3	4	5	3	2	13	0	3	10	12
	11	16	2	0	7	0	1	5	1	4	0	5
Sul	btotal	434	72	10	113	17	56	159	7	14	155	152
J07	1	35	0	3	13	0	5	11	3	0	10	12
	2	45	0	4	22	0	7	10	2	0	10	15
	3	35	0	6	3	2	9	12	3	0	8	19
	4	74	3	7	28	0	10	23	3	5	13	22
	5	29	0	2	13	1	5	8	0	0	19	12
	6	43	2	7	11	3	5	12	3	2	4	20
	7	15	0	0	10	1	0	4	0	0	10	3
	8	9	0	1	7	0	1	0	0	0	2	1
	9	17	2	2	6	0	3	4	0	2	1	5
	10	16	2	3	5	1	3	2	0	2	4	4
	11	18	0	0	9	1	0	5	3	0	5	8
Sul	btotal	336	35	9	127	9	48	91	17	11	77	121
/17	1	25	0	2	12	1	2	7	1	0	4	9
	2	34	1	4	16	0	5	6	2	1	8	9
	3	40	0	6	11	0	9	12	2	0	12	17
	4	50	6	2	26	1	3	8	4	8	3	13
	5	31	1	3	7	0	7	9	4	1	5	18
	6	35	3	0	10	1	6	11	4	3	2	20
	7	14	0	1	12	0	0	1	0	0	1	1
	8	10	0	1	7	0	1	1	0	0	1	2
	9	19	1	5	7	0	1	4	1	1	9	2

					Cla	ssification G	roup					
Turbine	28-day Cycle Sampling Period	Total Classified Events	Unknown Medium/ Large Raptor <sup>1</sup>	Large Raptor <sup>2</sup>	TFP	NTAFP	CORA <sup>3</sup>	Unknown Big Bird <sup>4</sup>	Unknown Bird <sup>5</sup>	Estimated Medium/ Large Raptor	Estimated Large Raptor	Estimated NTAFP
	10	23	3	2	10	0	3	5	0	3	5	5
	11	12	0	2	5	0	0	3	2	0	5	2
Su	btotal	293	28	15	123	3	37	67	20	17	55	98
Grand Tot	al	3,051	363	102	917	105	452	900	212	133	789	1,212

<sup>1</sup> Unidentified raptors that could have been one of the smaller "large soaring raptors" below, some of which were reclassified as Large Raptors or NTAFPs based on confirmed representation of those groups on each turbine-day.

<sup>&</sup>lt;sup>2</sup> Confirmed or strongly suspected large to very large soaring species including eagles, vultures, buteos, harriers, and ospreys.

<sup>&</sup>lt;sup>3</sup> Common raven (Corvus corax).

<sup>&</sup>lt;sup>4</sup> Large birds that could not be reliably distinguished as common ravens or large raptors.

<sup>&</sup>lt;sup>5</sup> Estimates derived by strategically assigning all Unknown Big Birds and Unknown Birds, and some Unknown Medium/Large Raptors, to these categories for summary purposes and producing more robust estimates of NTAFP event rates.

Appendix B. Summary Classifications of DTBird Detection Events that Triggered Deterrents at the Goodnoe Hills Wind Farm as Large Raptors, True (Non-avian) False Positive (TFPs), and Nontarget Avian False Positives (NTAFPs) by Turbine and 28-day Cycles Sampling Periods Between September 1, 2021 and August 2, 2023

						Clas	sification G	roup					
Year <sup>1</sup>	Turbine	28-day Cycle Sampling Period	Total Classified Events	Unknown Medium/ Large Raptor <sup>2</sup>	Large Raptor <sup>3</sup>	TFP	NTAFP	CORA4	Unknown Big Bird <sup>5</sup>	Unknown Bird <sup>6</sup>	Estimated Medium/ Large Raptor	Estimated Large Raptor	l Estimated NTAFP
1	G34	1	211	1	25	145	10	26	4	0	1	27	38
		2	52	0	0	27	6	19	0	0	0	0	25
		3	60	0	10	29	5	13	2	1	0	11	20
		4	43	0	1	30	1	11	0	0	0	1	12
		5	62	0	4	41	2	11	4	0	0	6	15
		6	21	0	5	11	3	2	0	0	0	5	5
		7	68	0	9	30	6	14	9	0	0	10	28
		8	80	1	5	38	8	27	1	0	1	5	36
		9	168	0	9	56	20	79	4	0	0	10	102
		10	118	0	5	56	20	36	1	0	0	6	56
		11	91	0	7	54	10	18	2	0	0	7	30
		12	2	0	0	2	0	0	0	0	0	0	0
		13	155	2	30	89	17	8	9	0	2	34	30
		Subtotal	1131	4	110	808	108	264	36	1	4	122	397
	G35	1	0	0	0	0	0	0	0	0	0	0	0
		2	55	0	3	21	8	23	0	0	0	3	31
		3	76	0	8	48	5	12	3	0	0	9	19
		4	67	0	8	38	5	14	2	0	0	8	21
		5	63	0	5	30	1	24	3	0	0	7	26
		6	51	0	1	42	3	5	0	0	0	1	8
		7	102	0	8	52	12	26	4	0	1	8	41

						Clas	sification G	roup					
Year <sup>1</sup>	Turbine	28-day Cycle Sampling Period	Total Classified Events	Unknown Medium/ Large Raptor <sup>2</sup>	Large Raptor <sup>3</sup>	TFP	NTAFP	CORA4	Unknown Big Bird <sup>5</sup>	Unknown Bird <sup>6</sup>	Estimated Medium/ Large Raptor	Estimated Large Raptor	d Estimated NTAFP
		8	86	0	4	19	19	44	0	0	0	4	63
		9	166	2	6	70	14	66	8	0	2	9	85
		10	128	0	2	85	17	21	3	0	0	2	41
		11	52	0	1	40	3	6	2	0	0	3	9
		12	234	0	6	136	46	46	0	0	0	6	92
		13	108	2	15	53	7	21	10	0	2	20	33
		Subtotal	1188	4	67	634	140	308	35	0	5	80	469
	G44	1	98	0	5	78	2	12	1	0	0	6	14
		2	82	0	3	60	3	16	0	0	0	3	19
		3	21	0	3	8	3	7	0	0	0	3	10
		4	17	0	2	11	0	4	0	0	0	2	4
		5	17	0	1	6	1	6	3	0	0	1	10
		6	9	0	0	7	1	0	1	0	0	0	2
		7	46	2	15	14	5	7	3	0	2	17	13
		8	63	0	8	11	5	38	1	0	0	8	44
		9	71	0	5	20	11	31	4	0	0	6	45
		10	98	0	2	70	5	21	0	0	0	2	26
		11	132	0	8	109	9	4	2	0	0	8	15
		12	100	0	18	66	8	6	2	0	0	20	14
		13	56	0	14	32	7	0	3	0	0	17	7
		Subtotal	810	2	84	492	60	152	20	0	2	93	223
	G45	1	12	0	1	8	0	2	1	0	0	1	3
		2	121	0	1	73	1	44	2	0	0	2	46
		3	73	0	23	19	2	28	1	0	0	23	31
		4	105	0	21	25	2	52	5	0	0	23	57
		5	45	0	7	20	0	18	0	0	0	7	18
		6	85	0	26	24	3	27	5	0	0	30	31
		7	132	0	13	42	2	75	0	0	0	13	77
		8	174	1	4	47	4	117	1	0	1	4	122
		9	238	0	24	63	14	115	22	0	0	32	143

						Cla	ssification G	roup					
Year <sup>1</sup>	Turbine	28-day Cycle Sampling Period	Total Classified Events	Unknown Medium/ Large Raptor <sup>2</sup>	Large Raptor <sup>3</sup>	TFP	NTAFP	CORA4	Unknown Big Bird <sup>5</sup>	Unknown Bird <sup>6</sup>	Estimated Medium/ Large Raptor		t Estimated NTAFP
		10	215	0	9	80	6	115	5	0	0	10	125
		11	97	0	13	50	8	21	5	0	0	16	31
		12	220	2	53	90	4	70	1	0	2	54	74
		13	99	0	27	41	2	24	5	0	0	31	27
		Subtotal	1616	3	222	582	48	708	53	0	3	246	785
	G48	1	81	0	2	68	1	9	1	0	0	2	11
		2	69	0	0	66	1	1	1	0	0	0	3
		3	24	0	0	11	1	10	2	0	0	0	13
		4	35	0	1	28	2	4	0	0	0	1	6
		5	28	0	4	11	1	12	0	0	0	4	13
		6	18	0	5	9	0	3	1	0	0	6	3
		7	95	1	30	30	6	24	3	1	1	31	33
		8	82	0	10	41	7	21	3	0	0	11	30
		9	103	0	5	56	10	27	5	0	0	8	39
		10	89	0	2	44	11	29	3	0	0	4	41
		11	171	0	13	133	6	14	5	0	0	14	24
		12	108	0	30	62	6	6	4	0	0	30	16
		13	61	0	5	44	2	7	3	0	0	7	10
		Subtotal	964	1	107	603	54	167	31	1	1	118	242
	G49	1	163	0	6	110	14	30	3	0	0	7	46
		2	78	0	1	43	6	25	3	0	0	1	34
		3	87	1	14	42	5	25	0	0	1	14	30
		4	31	0	1	11	1	14	4	0	0	2	18
		5	29	0	3	16	2	8	0	0	0	3	10
		6	56	0	13	32	0	9	2	0	0	13	11
		7	50	0	9	20	8	10	3	0	0	10	20
		8	82	0	6	36	13	24	3	0	0	8	38
		9	108	0	4	24	29	45	6	0	0	6	78
		10	75	0	3	32	15	23	2	0	0	3	40
		11	12	0	0	8	0	2	2	0	0	0	4

						Clas	ssification G	roup					
Year <sup>1</sup>	Turbine	28-day Cycle Sampling Period	Total Classified Events	Unknown Medium/ Large Raptor <sup>2</sup>	Large Raptor <sup>3</sup>	TFP	NTAFP	CORA4	Unknown Big Bird <sup>5</sup>	Unknown Bird <sup>6</sup>	Estimated Medium/ Large Raptor	Estimated Large Raptor	d Estimated NTAFP
		12	130	0	30	64	16	10	10	0	0	36	30
		13	68	0	10	41	8	4	5	0	0	13	14
		Subtotal	969	1	100	479	117	229	43	0	1	116	373
	G58	1	99	0	4	74	2	14	5	0	0	5	20
		2	101	0	4	58	4	35	0	0	0	4	39
		3	65	1	16	15	12	18	3	0	1	17	32
		4	64	1	17	26	13	6	1	0	1	18	19
		5	46	0	18	16	10	2	0	0	0	18	12
		6	41	1	15	14	2	7	2	0	1	16	10
		7	63	0	6	18	7	30	2	0	0	7	38
		8	123	0	3	55	8	53	4	0	0	3	65
		9	103	0	2	55	20	19	7	0	0	6	42
		10	116	0	17	57	10	30	2	0	0	19	40
		11	55	0	4	39	7	2	3	0	0	5	11
		12	116	0	30	56	14	10	6	0	0	36	24
		13	73	0	13	46	4	2	8	0	0	20	7
		Subtotal	1065	3	149	529	113	228	43	0	3	174	359
	G59	1	86	0	9	36	4	36	1	0	0	9	41
		2	95	0	8	52	11	20	4	0	0	10	33
		3	96	1	29	45	7	11	3	0	1	32	18
		4	51	0	18	18	8	7	0	0	0	18	15
		5	94	1	30	41	5	10	7	0	1	34	18
		6	45	1	10	23	5	5	1	0	1	11	10
		7	75	0	24	17	4	24	6	0	0	27	31
		8	44	0	3	13	1	25	2	0	0	3	28
		9	56	0	2	17	8	28	1	0	0	2	37
		10	93	0	3	59	7	22	2	0	0	4	30
		11	42	0	3	20	12	4	3	0	0	4	18
		12	132	0	10	82	8	24	8	0	0	14	36
		13	65	0	9	45	4	3	4	0	0	12	8

						Clas	sification G	roup					
Year <sup>1</sup>	Turbine	28-day Cycle Sampling Period	Total Classified Events	Unknown Medium/ Large Raptor <sup>2</sup>	Large Raptor <sup>3</sup>	TFP	NTAFP	CORA4	Unknown Big Bird <sup>5</sup>	Unknown Bird <sup>6</sup>		Estimated Large Raptor	i Estimated NTAFP
		Subtotal	974	3	158	468	84	219	42	0	3	180	323
	G64	1	121	0	4	92	8	16	1	0	0	4	25
		2	89	0	1	52	13	22	1	0	0	1	36
		3	114	0	18	34	28	27	7	0	0	20	60
		4	46	0	3	21	16	6	0	0	0	3	22
		5	60	0	4	28	21	6	1	0	0	4	28
		6	85	1	9	45	19	5	6	0	1	12	27
		7	97	0	11	52	13	21	0	0	0	11	34
		8	139	0	17	65	13	35	9	0	0	22	52
		9	150	0	18	58	18	41	15	0	0	23	69
		10	112	0	11	59	12	24	6	0	0	13	40
		11	86	1	10	57	8	8	2	0	1	11	17
		12	158	2	18	89	30	14	4	1	2	18	49
		13	119	0	15	89	5	4	6	0	0	21	9
		Subtotal	1376	4	139	741	204	229	58	1	4	163	468
	G67	1	144	0	5	88	9	40	2	0	0	5	51
		2	33	0	2	18	2	10	1	0	0	2	13
		3	77	2	20	37	5	10	3	0	2	22	16
		4	167	0	40	105	9	12	1	0	0	41	21
		5	44	0	2	34	3	3	2	0	0	3	7
		6	57	0	12	9	17	16	3	0	0	13	35
		7	75	1	18	30	6	10	10	0	1	25	19
		8	42	0	5	25	3	8	1	0	0	5	12
		9	54	0	6	19	4	22	3	0	0	7	28
		10	79	1	16	39	13	6	4	0	1	19	20
		11	76	0	12	35	20	5	3	1	0	13	28
		12	189	2	48	87	20	20	12	0	2	58	42
		13	75	0	14	42	5	11	3	0	0	16	17
		Subtotal	1112	6	200	568	116	173	48	1	6	229	309
	G75	1	33	0	2	28	2	1	0	0	0	2	3

						Cla	ssification G	roup					
Year <sup>1</sup>	Turbine	28-day Cycle Sampling Period	Total Classified Events	Unknown Medium/ Large Raptor <sup>2</sup>	Large Raptor <sup>3</sup>	TFP	NTAFP	CORA4	Unknown Big Bird <sup>5</sup>	Unknown Bird <sup>6</sup>		Estimated Large Raptor	d Estimated NTAFP
		2	0	0	0	0	0	0	0	0	0	0	0
		3	0	0	0	0	0	0	0	0	0	0	0
		4	0	0	0	0	0	0	0	0	0	0	0
		5	0	0	0	0	0	0	0	0	0	0	0
		6	0	0	0	0	0	0	0	0	0	0	0
		7	0	0	0	0	0	0	0	0	0	0	0
		8	0	0	0	0	0	0	0	0	0	0	0
		9	0	0	0	0	0	0	0	0	0	0	0
		10	0	0	0	0	0	0	0	0	0	0	0
		11	0	0	0	0	0	0	0	0	0	0	0
		12	22	0	4	12	2	2	2	0	0	6	4
		13	0	0	0	0	0	0	0	0	0	0	0
		Subtotal	55	0	6	40	4	3	2	0	0	8	7
Year 1 Tot	al		11260	1342	5744	31	1048	2680	411	4	32	1529	3955
2	G29	1	194	0	15	72	46	61	0	0	0	15	107
		2	158	0	15	67	12	64	0	0	0	15	76
		3	16	0	4	1	2	8	1	0	0	4	11
		4	45	0	8	20	7	10	0	0	0	8	17
		5	75	0	18	7	4	40	6	0	0	21	47
		6	15	0	8	1	1	4	1	0	0	8	6
		7	58	0	10	7	4	33	4	0	0	13	38
		8	149	0	25	9	12	87	16	0	0	29	111
		9	149	0	13	9	17	95	15	0	0	20	120
		10	10	0	3	4	3	0	0	0	0	3	3
		11	95	2	36	7	12	32	6	0	2	36	50
		12	72	0	45	6	10	10	1	0	0	45	21
		Subtotal	1036	2	200	210	130	444	50	0	2	217	607
	G34	1	195	0	10	136	18	30	1	0	0	10	49
		2	129	0	1	84	12	31	1	0	0	1	44
		3	31	0	3	15	0	13	0	0	0	3	13

						Clas	sification G	roup					
Year <sup>1</sup>	Turbine	28-day Cycle Sampling Period	Total Classified Events	Unknown Medium/ Large Raptor <sup>2</sup>	Large Raptor <sup>3</sup>	TFP	NTAFP	CORA4	Unknown Big Bird <sup>5</sup>	Unknown Bird <sup>6</sup>		Estimated Large Raptor	i Estimated NTAFP
		4	64	0	4	44	4	11	1	0	0	4	16
		5	14	0	1	7	1	5	0	0	0	1	6
		6	17	0	1	4	1	11	0	0	0	1	12
		7	28	0	11	5	3	8	1	0	0	12	11
		8	34	0	5	3	3	17	6	0	0	6	25
		9	56	0	9	8	4	29	6	0	0	10	38
		10	4	0	1	2	1	0	0	0	0	1	1
		11	24	0	7	0	1	14	2	0	0	8	16
		12	16	0	11	1	3	1	0	0	0	11	4
		Subtotal	612	0	64	309	51	170	18	0	0	68	235
	G35	1	206	0	13	110	41	42	0	0	0	13	83
		2	138	0	2	64	54	18	0	0	0	2	72
		3	58	0	0	33	3	22	0	0	0	0	25
		4	51	0	1	31	10	9	0	0	0	1	19
		5	45	0	14	9	4	17	1	0	0	14	22
		6	10	0	1	3	0	6	0	0	0	1	6
		7	34	0	6	10	3	13	2	0	0	7	17
		8	40	0	5	2	3	29	1	0	0	5	33
		9	76	0	10	8	9	45	4	0	0	10	58
		10	3	0	1	1	0	1	0	0	0	1	1
		11	40	0	9	2	5	20	4	0	0	10	28
		12	0	0	0	0	0	0	0	0	0	0	0
		Subtotal	701	0	62	273	132	222	12	0	0	64	364
	G44	1	108	0	5	68	8	27	0	0	0	5	35
		2	43	0	0	26	6	10	1	0	0	0	17
		3	34	0	4	5	6	17	2	0	0	4	25
		4	37	0	0	24	3	10	0	0	0	0	13
		5	95	0	24	50	0	20	1	0	0	24	21
		6	16	0	1	6	1	8	0	0	0	1	9
		7	17	0	5	5	0	4	3	0	0	8	4

						Clas	sification G	roup					
∕ear¹	Turbine	28-day Cycle Sampling Period	Total Classified Events	Unknown Medium/ Large Raptor <sup>2</sup>	Large Raptor <sup>3</sup>	TFP	NTAFP	CORA4	Unknown Big Bird <sup>5</sup>	Unknown Bird <sup>6</sup>		Estimated Large Raptor	I Estimated NTAFP
		8	33	0	22	2	1	6	2	0	0	23	8
		9	16	0	4	3	2	6	1	0	0	5	8
		10	1	0	0	0	0	1	0	0	0	0	1
		11	14	0	6	4	1	2	1	0	0	6	4
		12	5	0	3	0	0	1	1	0	0	3	2
		Subtotal	419	0	74	193	28	112	12	0	0	79	147
	G45	1	117	0	12	65	0	40	0	0	0	12	40
		2	60	0	7	36	4	13	0	0	0	7	17
		3	24	0	1	19	0	3	1	0	0	2	3
		4	22	0	5	12	1	4	0	0	0	5	5
		5	18	0	2	8	1	7	0	0	0	2	8
		6	5	0	3	1	0	1	0	0	0	3	1
		7	26	0	8	3	1	9	5	0	0	11	12
		8	72	0	25	5	0	31	11	0	0	31	36
		9	77	0	23	6	0	42	6	0	0	24	47
		10	2	0	0	0	0	2	0	0	0	0	2
		11	29	0	12	4	2	10	1	0	0	12	13
		12	18	0	14	1	0	1	2	0	0	15	2
		Subtotal	470	0	112	160	9	163	26	0	0	124	186
	G48	1	177	0	34	111	8	24	0	0	0	34	32
		2	125	0	2	93	5	25	0	0	0	2	30
		3	70	0	3	34	4	28	1	0	0	3	33
		4	0	0	0	0	0	0	0	0	0	0	0
		5	0	0	0	0	0	0	0	0	0	0	0
		6	0	0	0	0	0	0	0	0	0	0	0
		7	26	0	12	1	1	7	5	0	0	13	12
		8	26	0	5	5	0	12	4	0	0	5	16
		9	31	0	10	6	0	14	1	0	0	11	14
		10	0	0	0	0	0	0	0	0	0	0	0
		11	10	0	5	3	1	1	0	0	0	5	2

						Clas	sification G	roup					
Year <sup>1</sup>	Turbine	28-day Cycle Sampling Period	Total Classified Events	Unknown Medium/ Large Raptor <sup>2</sup>	Large Raptor <sup>3</sup>	TFP	NTAFP	CORA4	Unknown Big Bird <sup>5</sup>	Unknown Bird <sup>6</sup>	-	Estimated Large Raptor	d Estimated NTAFP
		12	8	0	5	1	0	1	1	0	0	5	2
		Subtotal	473	0	76	254	19	112	12	0	0	78	141
	G49	1	127	0	17	57	27	26	0	0	0	17	53
		2	148	0	2	102	12	32	0	0	0	2	44
		3	78	0	10	28	3	36	1	0	0	10	40
		4	20	0	5	7	5	3	0	0	0	5	8
		5	46	0	15	5	5	21	0	0	0	15	26
		6	42	0	15	5	4	18	0	0	0	15	22
		7	38	0	14	3	2	14	5	0	0	17	18
		8	64	0	16	11	6	21	10	0	0	21	32
		9	53	0	19	2	18	10	4	0	0	22	29
		10	12	0	6	0	1	3	2	0	0	7	5
		11	0	0	0	0	0	0	0	0	0	0	0
		12	30	0	17	9	2	1	1	0	0	17	4
		Subtotal	658	0	136	229	85	185	23	0	0	148	281
	G51	1	103	0	5	71	3	21	3	0	0	7	25
		2	130	0	6	100	12	10	2	0	0	8	22
		3	49	0	8	27	4	9	1	0	0	8	14
		4	36	0	4	30	0	2	0	0	0	4	2
		5	33	0	9	14	3	6	1	0	0	9	10
		6	25	0	5	18	1	1	0	0	0	5	2
		7	36	0	6	20	4	5	1	0	0	6	10
		8	33	0	8	12	1	11	1	0	0	8	13
		9	24	0	3	11	8	2	0	0	0	3	10
		10	5	0	2	1	0	1	1	0	0	3	1
		11	23	0	5	8	8	0	2	0	0	6	9
		12	0	0	0	0	0	0	0	0	0	0	0
		Subtotal	497	0	61	312	44	68	12	0	0	67	118
	G56	1	0	0	0	0	0	0	0	0	0	0	0
		2	124	0	14	68	7	30	5	0	0	15	41

						Clas	sification G	roup					
Year <sup>1</sup>	Turbine	28-day Cycle Sampling Period	Total Classified Events	Unknown Medium/ Large Raptor <sup>2</sup>	Large Raptor <sup>3</sup>	TFP	NTAFP	CORA4	Unknown Big Bird <sup>5</sup>	Unknown Bird <sup>6</sup>		Estimated Large Raptor	t Estimated NTAFP
		3	21	0	4	8	2	5	2	0	0	5	8
		4	20	0	1	16	2	1	0	0	0	1	3
		5	27	0	15	0	4	7	1	0	0	16	11
		6	21	0	6	3	1	7	4	0	0	8	10
		7	20	0	4	7	3	3	3	0	0	5	8
		8	32	0	8	10	0	6	8	0	0	12	10
		9	33	0	7	18	1	7	0	0	0	7	8
		10	7	0	4	1	1	1	0	0	0	4	2
		11	24	0	8	2	4	7	3	0	0	11	11
		12	5	0	2	0	2	0	1	0	0	2	3
		Subtotal	334	0	73	133	27	74	27	0	0	86	115
	G58	1	185	0	14	137	18	13	3	0	0	14	34
		2	156	0	15	98	19	21	3	0	0	15	43
		3	45	0	16	13	6	6	4	0	0	18	14
		4	31	0	3	18	3	6	1	0	0	3	10
		5	40	0	13	8	10	7	2	0	0	14	18
		6	30	0	7	13	4	4	2	0	0	9	8
		7	49	0	16	14	12	3	4	0	0	17	18
		8	69	0	38	9	5	10	7	0	0	40	20
		9	48	0	11	18	7	9	3	0	0	13	17
		10	10	0	6	2	0	1	1	0	0	7	1
		11	25	0	11	3	4	6	1	0	0	11	11
		12	18	0	9	5	2	1	1	0	0	9	4
		Subtotal	706	0	159	338	90	87	32	0	0	170	198
	G59	1	184	0	26	119	9	18	12	0	0	30	35
		2	94	0	13	47	5	18	11	0	0	19	28
		3	51	0	12	24	7	3	5	0	0	14	13
		4	32	0	18	12	0	1	1	0	0	18	2
		5	0	0	0	0	0	0	0	0	0	0	0
		6	0	0	0	0	0	0	0	0	0	0	0

						Clas	sification G	roup					
Year <sup>1</sup>	Turbine	28-day Cycle Sampling Period	Total Classified Events	Unknown Medium/ Large Raptor <sup>2</sup>	Large Raptor <sup>3</sup>	TFP	NTAFP	CORA4	Unknown Big Bird <sup>5</sup>	Unknown Bird <sup>6</sup>		Estimated Large Raptor	i Estimated NTAFP
		7	0	0	0	0	0	0	0	0	0	0	0
		8	0	0	0	0	0	0	0	0	0	0	0
		9	65	0	16	25	5	9	10	0	0	22	18
		10	1	0	1	0	0	0	0	0	0	1	0
		11	15	0	4	7	3	1	0	0	0	4	4
		12	26	0	16	4	3	3	0	0	0	16	6
		Subtotal	468	0	106	238	32	53	39	0	0	124	106
	G64	1	179	0	23	119	10	17	10	0	0	27	33
		2	165	0	7	116	28	12	2	0	0	8	41
		3	41	0	15	10	6	7	3	0	0	15	16
		4	36	0	9	11	11	3	2	0	0	11	14
		5	64	0	20	6	10	19	9	0	0	25	33
		6	17	0	6	0	2	8	1	0	0	7	10
		7	17	0	8	2	0	5	2	0	0	8	7
		8	49	0	22	6	4	12	5	0	0	23	20
		9	44	1	13	3	7	17	3	0	1	16	24
		10	2	0	1	0	1	0	0	0	0	1	1
		11	13	0	2	0	6	5	0	0	0	2	11
		12	24	0	5	8	9	2	0	0	0	5	11
		Subtotal	651	1	131	281	94	107	37	0	1	148	221
	G67	1	120	0	11	82	15	9	3	0	0	12	26
		2	104	0	11	73	6	13	1	0	0	12	19
		3	36	0	11	15	4	3	3	0	0	12	9
		4	74	0	38	17	8	8	3	0	0	41	16
		5	75	0	45	13	5	8	4	0	0	46	16
		6	28	0	17	7	2	2	0	0	0	17	4
		7	35	0	17	10	2	5	1	0	0	17	8
		8	41	0	12	11	7	6	5	0	0	13	17
		9	28	0	12	7	3	3	3	0	0	15	6
		10	0	0	0	0	0	0	0	0	0	0	0

						Clas	sification G						
Year <sup>1</sup>	Turbine	28-day Cycle Sampling Period	Total Classified Events	Unknown Medium/ Large Raptor <sup>2</sup>	Large Raptor <sup>3</sup>	TFP	NTAFP	CORA4	Unknown Big Bird <sup>5</sup>	Unknown Bird <sup>6</sup>	Estimated Medium/ Large Raptor		Estimated NTAFP
		11	0	0	0	0	0	0	0	0	0	0	0
		12	11	0	8	1	1	1	0	0	0	8	2
		Subtotal	552	0	182	236	53	58	23	0	0	193	123
<del>-</del>	G75	1	185	0	11	156	11	6	1	0	0	12	17
		2	82	0	2	53	17	8	2	0	0	2	27
		3	27	0	5	15	4	3	0	0	0	5	7
		4	28	0	2	24	1	0	1	0	0	3	1
		5	60	0	27	13	10	7	3	0	0	28	19
		6	21	0	12	2	2	2	3	0	0	14	5
		7	29	0	14	6	2	5	2	0	0	15	8
		8	40	0	20	5	6	7	2	0	0	22	13
		9	22	0	3	1	6	7	5	0	0	4	17
		10	0	0	0	0	0	0	0	0	0	0	0
		11	0	0	0	0	0	0	0	0	0	0	0
		12	4	0	1	0	1	0	2	0	0	2	2
		Subtotal	498	0	97	275	60	45	21	0	0	107	116
Year 2 Total	I		8075	1533	3441	3	854	1900	344	0	3	1673	2958
Grand Total	i		19335	2875	9185	34	1902	4580	755	4	35	3202	6913

Year 2 sampling ultimately continued through a fourteenth 28-day Cycle, but the data for cycles 13 and 14 were not yet fully available for this analysis. In addition, few data were collected for cycle 10 in Year 2, because Bonneville Power Administration cut off all power to the facility for most of May 2023.

<sup>&</sup>lt;sup>2</sup> Unidentified raptors that could have been one of the smaller "large soaring raptors" below, some of which were reclassified as Large Raptors or NTAFPs based on confirmed representation of those groups on each turbine-day.

<sup>3</sup> Confirmed or strongly suspected large to very large soaring species including eagles, vultures, buteos, harriers, and ospreys.

<sup>&</sup>lt;sup>4</sup> Common raven (Corvus corax).

<sup>&</sup>lt;sup>5</sup> Large birds that could not be reliably distinguished as common ravens or large raptors.

<sup>&</sup>lt;sup>6</sup> Estimates derived by strategically assigning all Unknown Big Birds and Unknown Birds, and some Unknown Medium/Large Raptors, to these categories for summary purposes and producing more robust estimates of NTAFP event rates.

# Appendix C. Model Selection to Illustrate Relationships Predicting the Probability of DTBird Detection with Selected Model Highlighted in Green and Null Model in Gray

Madel	AIC	AAIG	Log- Likelihood Ratio Chi-	Nagelkerke
Model Site + Hour + LoS Distance + LosDistance <sup>2</sup> + LosDistance <sup>3</sup> +	AIC	ΔΑΙϹ	Square P	R <sup>2</sup>
Detection Angle + Detection Angle <sup>2</sup>	1859.7	0	<0.001	0.324
Hour + LoS Distance + LosDistance <sup>2</sup> + LosDistance <sup>3</sup> + Detection Angle + Detection Angle <sup>2</sup>	1862.2	2.5	<0.001	0.321
Site + Hour + LoS Distance + Detection Angle + Detection Angle <sup>2</sup>	1864.1	4.4	<0.001	0.319
Site + Hour + Hour <sup>2</sup> + LoS Distance + Detection Angle + Detection Angle <sup>2</sup>	1865.2	5.5	<0.001	0.319
Site + Hour + LoS Distance + LoS Distance <sup>2</sup> + Detection Angle + Detection Angle <sup>2</sup>	1865.4	5.7	<0.001	0.319
Site + Hour + Hour <sup>2</sup> + LoS Distance + LoS Distance <sup>2</sup> + Detection Angle + Detection Angle <sup>2</sup> + cos(Direction)	1868.0	8.3	<0.001	0.320
Site + Hour + Hour <sup>2</sup> + LoS Distance + LoS Distance <sup>2</sup> + Detection Angle + Detection Angle <sup>2</sup>	1868.5	8.8	<0.001	0.320
Full model	1869.9	10.2	<0.001	0.320
Site + Hour + Hour <sup>2</sup> + LoS Distance + LoS Distance <sup>2</sup> + Detection Angle + Detection Angle <sup>2</sup> + sin(Direction)	1870.4	10.7	<0.001	0.320
Site + Hour + LoS Distance + LoS Distance <sup>2</sup> + Detection Angle	2062.9	203	<0.001	0.194
Site + Hour + LoS Distance + Detection Angle	2092.0	232	<0.001	0.173
Site + Hour + Hour <sup>2</sup> + LoS Distance + Detection Angle	2092.9	233	<0.001	0.174
Site + Hour + LoS Distance + Detection Angle + sin(Direction) + cos(Direction)	2095.4	236	<0.001	0.173
LoS Distance + LoS Distance <sup>2</sup>	2139.1	279	<0.001	0.138
LoS Distance	2178.0	318	<0.001	0.109
Detection Angle + Detection Angle <sup>2</sup>	2191.1	331	<0.001	0.101
Hour	2264.6	405	<0.001	0.046
Hour + Hour <sup>2</sup>	2265.1	405	<0.001	0.047
Detection Angle	2322.1	462	0.132	0.002
Null model	2322.4	463	-	-
Site	2323.7	464	0.425	0.000

# Appendix D. Model Coefficients, Odds Ratio Estimates, and Diagnostic Metrics for Final Model Selected to Illustrate Relationships Predicting the Probability of DTBird Detection

0.507 01

#### **Parameter Estimates**

					95%	% CI
Parameter	Estimate	SE	Z	P	Lower	Upper
CONSTANT	-1.886	0.328	-5.76	0.000	-2.528	-1.244
Site_Goodnoe	0.303	0.144	2.11	0.035	0.021	0.585
Hour of Day	0.189	0.023	8.37	0.000	0.145	0.233
Minimum LoS Distance	0.004	0.007	0.65	0.515	-0.009	0.017
MINLoS <sup>2</sup>	0.000	0.000	-2.96	0.003	0.000	0.000
MINLoS <sup>3</sup>	0.000	0.000	2.88	0.004	0.000	0.000
Average Detection Angle	0.177	0.015	11.49	0.000	0.147	0.207
AVGVANG <sup>2</sup>	-0.003	0.000	-11.58	0.000	-0.003	-0.002

#### **Odds Ratio Estimates**

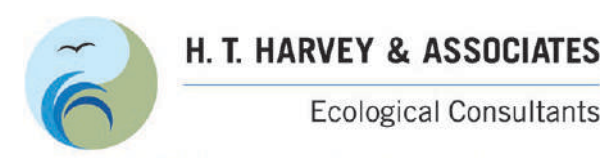
			<u> 757</u>	<u>. Cl</u>
Parameter	Odds Ratio	SE	Lower	Upper
SITE_Goodnoe	1.354	0.195	1.022	1.795
Hour of Day	1.208	0.027	1.156	1.262
Minimum LoS Distance	1.004	0.007	0.991	1.017
MINLoS <sup>2</sup>	1.000	0.000	1.000	1.000
MINLoS <sup>3</sup>	1.000	0.000	1.000	1.000
Average Detection Angle	1.193	0.018	1.158	1.230
AVGVANG <sup>2</sup>	0.997	0.000	0.997	0.998

#### **Overall Model Fit**

Log-Likelihood of Constant Only Model	-1,160.2
Log-Likelihood of Full Model	-921.9
Chi-Square	476.7
df	7
P-value	< 0.001

### **R-Square Measures**

Naglekerke's R-Square 0.324



50 years of field notes, exploration, and excellence

**Research Report** 

Analysis of Behavioral Responses of Eagles and Other Large Raptors to DTBird® Audio Deterrents at Commercial Wind-Energy Facilities in California and Washington

Project #4080-01

Prepared for:

Renewable Energy Wildlife Institute 1990 K Street NW, Suite 620

Washington, D.C. 20006-1189

Prime Contractor: DOE Cooperative Agreement DE-EE0007883

Prepared by:

H. T. Harvey & Associates

Final – May 30, 2024











# **Executive Summary**

DTBird® is an automated detection and audio deterrent system designed to discourage birds from entering the rotor swept zone (RSZ) of spinning wind turbines. As part of a multi-faceted research program conducted in collaboration with the Renewable Energy Wildlife Institute, we previously conducted site-specific analyses of DTBird performance based on seven systems installed and operated for the first time at the Manzana Wind Power Project in southern California, USA. We then expanded the research with funding from the U. S. Department of Energy to include comparative assessments and expanded research involving 14 DTBird systems installed and operated for the first time at the Goodnoe Hills Wind Farm in south-central Washington, USA. The overarching goal of this research is to evaluate the effectiveness of DTBird in detecting and discouraging golden eagles (*Aquila chrysaetos*) and other large raptors from approaching the RSZ of operating wind turbines.

We previously prepared initial site-specific analyses of the behavioral responses of eagles and other large raptors to audio deterrents broadcasted by the DTBird systems operated at the two facilities, one located in a desert/foothills landscape in southern California and the other located on a grassland-dominated ridgetop paralleling the Columbia River in southern Washinton. Herein we present a new integrated analysis of data gathered at the two facilities. Based on results from the Manzana pilot study, a performance metric was established to gauge the comparative effectiveness of the DTBird systems in deterring eagles and other large raptors from entering the RSZ of spinning turbines at the Goodnoe Hills site. The established performance metric stipulated that the Goodnoe Hills DTBird systems should result in ≥50% confirmed effective deterrence for golden eagles. Because it is often difficult to confidently identify the species of birds evident in DTBird videos, this metric was based on combining data for confirmed and probable golden eagles.

The Goodnoe Hills assessment differed in one key manner from the Manzana pilot study, in that the broader experimental research agenda for the expanded study presented the opportunity for conducting a control-treatment evaluation of deterrence responses at the Goodnoe Hills site. The implemented study design supported distinguishing between the deterrence effects of spinning turbines alone versus spinning turbines plus audio deterrents. However, because we were not able to implement a similar control-treatment design at the Manzana facility, we launched the multi-site investigation seeking to achieve the following objectives:

- 1) Use chi-square contingency table analyses with *Site* and categorical *Response* classifications as factors to determine if the apparent responses of eagles and other large raptors to DTBird deterrent signals broadcasted in association with spinning turbine blades differed at the two wind facilities.
- 2) If the probability of effective deterrence in response to the combination of spinning turbine blades and broadcasted deterrents differed significantly at the two facilities:

i

a. Conduct additional logistic generalized linear model (LGLM) analyses to evaluate how various potential predictors influence the probability of effective deterrence at the two sites, limited to the "treatment" data collected at both facilities (i.e., responses to spinning turbines with the deterrents broadcasting).

- b. Conduct no statistical analyses including the "control" data from the Goodnoe Hills site (i.e., responses to spinning turbines with the deterrents muted).
- 3) If the probability of effective deterrence in response to the combination of spinning turbine blades and broadcasted deterrents did not differ significantly at the two facilities, expand the chi-square and LGLM analyses to include the full combination of treatment data from both sites and control data from the Goodnoe Hills, ignoring *Site* but including *Treatment Group* as a predictor.
- 4) Develop estimates of the probability of effective deterrence at the two sites that include consideration of the added benefit the DTBird audio deterrents appear to provide above and beyond the effect of spinning turbines alone.

Results from the Goodnoe Hills site indicated significantly lower probabilities of confirmed effective deterrence responses for golden eagles and all analyzed species groups compared to results from the Manzana facility. Therefore, we did not pursue Objective 3 above and instead focused on evaluating comparative indices from the two sites based only on responses to broadcasted deterrents.

The multi-species and golden eagle LGLM analyses that we conducted based only on responses to broadcasted deterrents at the two study sites further confirmed that the probability of effective deterrence generally was higher at the Manzana site. Reasons for this difference are uncertain, but could reflect the influence of differences in the relative proportions of different species and residents versus transients frequenting the two sites, with variable sensitivities and/or habituation tendencies, and/or factors such as different wind regimes that influence how birds respond to the deterrents. Both the multi-species and golden eagle models also reflected at least marginally significant relationships between the probability of deterrence and wind speed. Increasing wind speeds generally resulted in a higher probability of effective deterrence for larger eagles and vultures, but not for smaller buteos. Possible explanations for this pattern include: (a) faster-spinning turbine blades themselves may act as a greater deterrent to approaching larger birds and more effectively amplify the effect of the audio deterrents; (b) higher wind speeds may generally facilitate greater maneuverability and responsiveness for large soaring raptors that often strongly rely on the energy savings provided by wind-driven (or thermal) lift; and (c) smaller buteos are generally more maneuverable and more easily constrained by strong winds, such that increasing wind speeds may be a detriment rather than a benefit for them in influencing their ability to respond to the deterrents. There was also some indication—albeit statistically nonsignificant—that effective deterrence of golden eagles was actually more likely at the Goodnoe Hills than at the Manzana site at moderate or higher wind speeds. In addition, the multi-species model suggested that eagles tended to be increasingly more responsive to the deterrents than vultures and buteos as wind speeds increased. Regardless, the documented site differences clearly suggest that effectiveness of the DTBird deterrence system may vary significantly depending on the local landscape characteristics and species assemblages.

The probability of effective deterrence tended to be highest for birds we classified as at moderate risk of exposure to turbine collisions, rather than for those we classified as at high risk of exposure. This outcome may reflect that birds at high risk of exposure appear less responsive simply because they have less time and room to respond effectively if not deterred before entering a high-risk zone.

The proportion of confirmed effective responses for golden eagles at the Goodnoe Hills (27%) fell well below the desired performance standard of  $\geq$ 50% effective deterrence. It can be very difficult to identify targeted birds and effectively discern subtle behavioral details in the low-resolution videos saved by the DTBird systems, as well as to measure flight-diversion angles based on two-dimensional renderings of three-dimensional movements. Therefore, rather than focus only on cases we confirmed as effective deterrence events, we advocate for focusing on the combination of responses we classified as confirmed and potentially effective as the focal metric of interest. Quantified in this manner, the proportion of presumed effective responses for golden eagles was 79% at the Manzana site and 61% at the Goodnoe Hills, still a noteworthy difference between the two sites but with both values exceeding the desired  $\geq$ 50% performance standard (as was also the case for other species groups).

At Goodnoe Hills, broadcasted deterrents consistently resulted in at least a doubling of the proportion of cases where an effective or potentially effective response was evident compared to when no signals were actually broadcasting. The patterns of differential responses were similar for all analyzed species and groups. We think it is reasonable to presume that a similar proportional effect of spinning turbines and broadcasted deterrents would apply at the two study sites.

# **Table of Contents**

Executive S	Summary	i
Section 1.	Introduction	1
Section 2.	Methods	3
2.1 S	Study Sites and DTBird Installations	3
	OTBird System Operation	
	Classifying Responses to Deterrents	
2.4 A	Analyses	8
2.4	1.1 Contingency Tables	8
2.4	1.2 Logistic GLMs	8
Section 3.	Results	10
3.1 S	Sampling Results	10
3.2 B	Response to Deterrents	10
3.2	2.1 Contingency Table Analyses	10
3.2	2.2 Logistic GLM Analyses	17
Section 4.	Discussion	24
Section 5.	References	27
Figure 1. Figure 2.	Layout of the Manzana Wind Power Project in southern California showing locations of installed DTBird systems.  Layout of the Goodnoe Hills Wind Farm in south-central Washington showing locations of installed DTBird systems.	
Figure 3.	Depiction of DTBird video camera and broadcast speaker locations on turbines at the Manzana Wind Power Project (left panel, single ring of speakers) and Goodnoe Hills Wind Farm (right panel, two rings of speakers)	5
Figure 4.	Proportional representation of the effectiveness of behavioral responses to broadcasted DTBird audio deterrents (combined responses to warning and dissuasion signals acting alone or in tandem) in reducing collision risk for all large raptors combined by site and classified risk level before deterrent exposure at the Manzana Wind Power Project in California and the Goodnoe Hills Wind Farm in Washington	13
Figure 5.	Proportional representation of the effectiveness of behavioral responses to broadcasted DTBird audio deterrents (combined responses to warning and dissuasion signals acting alone or in tandem) in reducing collision risk for golden eagles by site and classified risk level before deterrent exposure at the Manzana Wind Power Project in California and the Goodnoe Hills Wind Farm in Washington	15
Figure 6.	Proportional representation of the effectiveness of behavioral responses to broadcasted DTBird audio deterrents (combined responses to warning and dissuasion signals acting alone or in tandem) in reducing collision risk for turkey vultures by site and classified risk level before deterrent exposure at the Manzana Wind Power Project in California and the Goodnoe Hills Wind Farm in Washington	16

Figure 7.	Proportional representation of the effectiveness of behavioral responses to broadcasted DTBird audio deterrents (combined responses to warning and dissuasion signals acting alone or in tandem) in reducing collision risk for buteos by site and classified risk level before deterrent exposure at the Manzana Wind Power Project in California and the Goodnoe Hills Wind Farm in Washington	17
Figure 8.	Modeled probability of effective DTBird deterrence for all large raptors combined and golden eagles alone at the two wind facilities evaluated in this study	19
Figure 9.	Modeled probability of effective DTBird deterrence for all large raptors combined and golden eagles alone in relation to classified risk of exposure to turbine collisions at the two wind facilities evaluated in this study	20
Figure 10.	Modeled probability of effective DTBird deterrence for large raptors by species group and in relation to wind speed measured by turbine anemometer at time of events at the two wind facilities evaluated in this study.	21
Figure 11.	Modeled probability of effective DTBird deterrence for golden eagles in relation to wind speed measured by turbine anemometer at time of events at the two wind facilities evaluated in this study, showing results with and without $Site*WindSpeed$ interaction (improves AIC score but nonsignificant $P=0.118$ parameter test)	23
Tables		
Table 1.	DTBird events recorded from January through August 2017 at the Manzana Wind Power Project in California and from September 2021 through August 2022 at the Goodnoe Hills Wind Farm in Washington, which formed the basis for assessing the behavioral responses of eagles and other large raptors to DTBird audio deterrents	10
Table 2.	Classification of the effectiveness of behavioral responses (combined responses to warning and dissuasion signals acting alone or in tandem) in reducing collision risk for all large raptors combined (eagles, vultures, and buteos) at the Manzana Wind Power Project in California and the Goodnoe Hills Wind Farm in Washington	11
Table 3.	Classification of the effectiveness of behavioral responses (combined responses to warning and dissuasion signals acting alone or in tandem) in reducing collision risk for confirmed and probable golden eagles at the Manzana Wind Power Project in California and the Goodnoe Hills Wind Farm in Washington	11
Table 4.	Classification of the effectiveness of behavioral responses (combined responses to warning and dissuasion signals acting alone or in tandem) in reducing collision risk for confirmed and probable turkey vultures at the Manzana Wind Power Project in California and the Goodnoe Hills Wind Farm in Washington	12
Table 5.	Classification of the effectiveness of behavioral responses (combined responses to warning and dissuasion signals acting alone or in tandem) in reducing collision risk for confirmed and probable buteos at the Manzana Wind Power Project in California and the Goodnoe Hills Wind Farm in Washington	12
Table 6.	Classification of the effectiveness of behavioral responses to broadcasted DTBird audio deterrents (combined responses to warning and dissuasion signals acting alone or in tandem) in reducing collision risk for all large raptors combined by site and classified risk level before deterrent exposure at the Manzana Wind Power Project in California and the Goodnoe Hills Wind Farm in Washington	13
Table 7.	Classification of the effectiveness of behavioral responses to broadcasted DTBird audio deterrents (combined responses to warning and dissuasion signals acting alone or in tandem) in reducing collision risk for confirmed and probable golden eagles by site and	

	classified risk level before deterrent exposure at the Manzana Wind Power Project in California and the Goodnoe Hills Wind Farm in Washington	14
Table 8.	Classification of the effectiveness of behavioral responses to broadcasted DTBird audio deterrents (combined responses to warning and dissuasion signals acting alone or in tandem) in reducing collision risk for confirmed and probable turkey vultures by site and classified risk level before deterrent exposure at the Manzana Wind Power Project in California and the Goodnoe Hills Wind Farm in Washington	15
Table 9.	Classification of the effectiveness of behavioral responses to broadcasted DTBird audio deterrents (combined responses to warning and dissuasion signals acting alone or in tandem) in reducing collision risk for confirmed and probable buteos by site and classified risk level before deterrent exposure at the Manzana Wind Power Project in California and the Goodnoe Hills Wind Farm in Washington	16
Table 10.	Percentages of behavioral responses to broadcasted DTBird deterrents (combined responses to warning and dissuasion signals acting alone or in tandem) classified as effective or potentially effective in reducing collision risk for different species groups at the Manzana Wind Power Project in California and the Goodnoe Hills Wind Farm in Washington	17
Table 11.	Comparison of AIC scoring results for top candidates and selected other multi-species logistic GLMs portraying potential relationships between the probability of effective deterrence and various predictors.	18
Table 12.	Parameters of final multi-species logistic GLM selected to represent relationship between the ln(odds of effective deterrence) and various predictors at the Manzana and Goodnoe Hills wind-energy facilities	19
Table 13.	Comparison of AIC scoring results for top candidates and selected other logistic GLMs portraying potential relationships for golden eagles between the ln(odds of effective deterrence) and various predictors.	21
Table 14.	Parameters of final logistic GLM selected to represent relationship between the ln(odds of effective deterrence) for golden eagles and various predictors at the Manzana and Goodnoe Hills wind-energy facilities.	22

# **List of Primary Preparers**

Jeff P. Smith, Ph.D., Associate Wildlife Ecologist—Project Manager

Scott B. Terrill, Ph.D., Principal in Wildlife Ecology and Senior Ornithologist—Principal-in-Charge

John M. Romanisc, Ph.D., Wildlife and Quantitative Ecologist

Stephanie R. Schneider, M.S., Wildlife and Quantitative Ecologist

Alex W. Henry, B.S., Field Biologist

Cooper J. Smith, B.S., Field Biologist

### **Section 1. Introduction**

DTBird® (Liquen Consultoría Ambiental, S.L., Madrid, Spain; hereafter "Liquen") is an automated detection and audio deterrent system designed to discourage birds from entering the rotor swept zone (RSZ) of spinning wind turbines (see <a href="https://dtbird.com">https://dtbird.com</a>). DTBird can also include an automated turbine control-stop module that was not installed as part of the systems evaluated herein. Funded by the American Wind Wildlife Institute (now the Renewable Energy Wildlife Institute [REWI]), H. T. Harvey & Associates (2018) previously analyzed the performance of seven DTBird systems operated for the first time at the Manzana Wind Power Project in southern California. Following this pilot study, we continued the research in collaboration with REWI, funded by the U.S. Department of Energy, by augmenting some of the pilot-study analyses and expanding the investigations to the Goodnoe Hills Wind Farm in south-central Washington (H. T. Harvey & Associates 2019a).

The goal of this research is to quantify the effectiveness of DTBird as a measure to reduce collision risk for golden eagles (*Aquila chrysaetos*) and other large raptors. If found to be effective and accepted by the U.S. Fish and Wildlife Service (USFWS), DTBird could be considered for use by commercial wind energy facilities in conservation plans, as a best management practice under the Bald and Golden Eagle Protection Act (Eagle Act) (16 U.S.C. §668–668c), as a minimization measure for take permits or habitat conservation plans, or as an adaptive management measure.

Previously, we independently presented initial site-specific analyses of the behavioral responses of golden eagles and other large raptors to the audio deterrents broadcasted by DTBird systems installed at the Manzana facility (H. T. Harvey & Associates 2019b) and at the Goodnoe Hills facility (H. T. Harvey & Associates 2023a), based on 1 year of data collected at each site during different periods. We derived the data for these analyses from reviewing detection and tracking videos recorded in the online digital analysis platform (DAP) databases maintained by Liquen for these projects. Herein we present integrated analyses of data from the two sites to generate additional insight about (a) potential variability in how raptors respond to the audio deterrents in different landscape settings, and (b) the combined probability of effective responses to the DTBird deterrents. Together the multiplicative combination of the probability of effective detection (e.g., see H. T. Harvey & Associates 2022b) and the probability of effective deterrence compose the desired quantification of DTBird's ultimate effectiveness in reducing the probability of eagles and other large raptors entering the RSZ of spinning turbines (H. T. Harvey & Associates 2018, 2019a).

Our approved study plan for the overall DOE-supported project established a performance standard for the new Goodnoe Hills project of a ≥50% effective deterrence rate given broadcasted deterrents (H. T. Harvey & Associates 2019a), which was based on 8.5 months of data analyzed as part of our initial Manzana pilot study (H. T. Harvey & Associates 2018). As part of our expanded DOE-sponsored research, we updated the Manzana site-specific analysis based on a full year of data (H. T. Harvey & Associates 2019b). Importantly, the new Goodnoe Hills study afforded a unique opportunity to compose a control-treatment experiment that allowed for distinguishing the effects on the probability of effective deterrence of spinning turbines alone versus spinning turbines acting in combination with the audio deterrents (H. T. Harvey & Associates 2023a). Sharp et al. (2011) previously determined that Bald Eagles (Haliaetus leucocephalus) avoided crossing a ridgeline in Alaska

with a string of wind turbines when the blades were spinning but not when they were still. This experimental scenario was made possible by implementing a larger-scale experimental design at the Goodnoe Hills, which involved a daily rotation schedule whereby on a given day a randomized half of the DTBird systems were operated with the audio deterrents broadcasting and the other half were operated with the audio deterrents triggered only virtually and not actually broadcasting (see H. T. Harvey & Associates 2019a). Implementing an analogous control-treatment design for evaluating responses to the deterrents was not feasible during the Manzana pilot study. Accordingly, to prepare this multi-site assessment we sought to achieve the following objectives:

- 1) Use chi-square contingency table analyses with *Site* and categorical *Response* classifications as factors to determine if the apparent responses of eagles and other large raptors to DTBird deterrent signals broadcasted in association with spinning turbine blades differed at the two wind facilities.
- 2) If the probability of effective deterrence in response to the combination of spinning turbine blades and broadcasted deterrents differs significantly at the two facilities:
  - a. Conduct additional logistic generalized linear model (LGLM) analyses to evaluate how various potential predictors influence the probability of effective deterrence at the two sites, limited to the "treatment" data collected at both facilities (i.e., responses to spinning turbines with the deterrents broadcasting).
  - b. Conduct no statistical analyses including the "control" data from the Goodnoe Hills site (i.e., responses to spinning turbines with the deterrents muted).
- 3) If the probability of effective deterrence in response to the combination of spinning turbine blades and broadcasted deterrents does not differ significantly at the two facilities, expand the chi-square and LGLM analyses to include the full combination of treatment data from both sites and control data from the Goodnoe Hills, ignoring Site but including Treatment Group as a predictor. The objective here would be to enhance the single-site control-treatment analysis presented in H. T. Harvey & Associates (2023a) by substantially bolstering the available sample size of cases in the treatment group.
- 4) Develop estimates of the probability of effective deterrence at the two sites that include consideration of the added benefit the DTBird audio deterrents appear to provide above and beyond the effect of spinning turbines alone. The derivation of such estimates will vary depending on whether option (2) or (3) above proves appropriate to pursue.

### Section 2. Methods

### 2.1 Study Sites and DTBird Installations

The Manzana Wind Project has been in operation since 2012 and comprises 126 1.5 MW GE 1.5-77 wind turbines, with a hub height of 65 meters and a rotor-swept diameter of 82.5 meters, located in the southwestern foothills of the Tehachapi Mountains of southern California in northwestern Antelope Valley, which constitutes the westernmost extension of the Mojave Desert (Figure 1). The landscape is a gradually sloping alluvial fan incised by dry desert washes. The northwestern sector of the facility features more complex foothill topography adjacent to a primary riparian drainage, and the topography grades downslope to the southeast into a more-uniform plain. The desert scrub and woodland vegetation is typical of the upper Mojave Desert region.

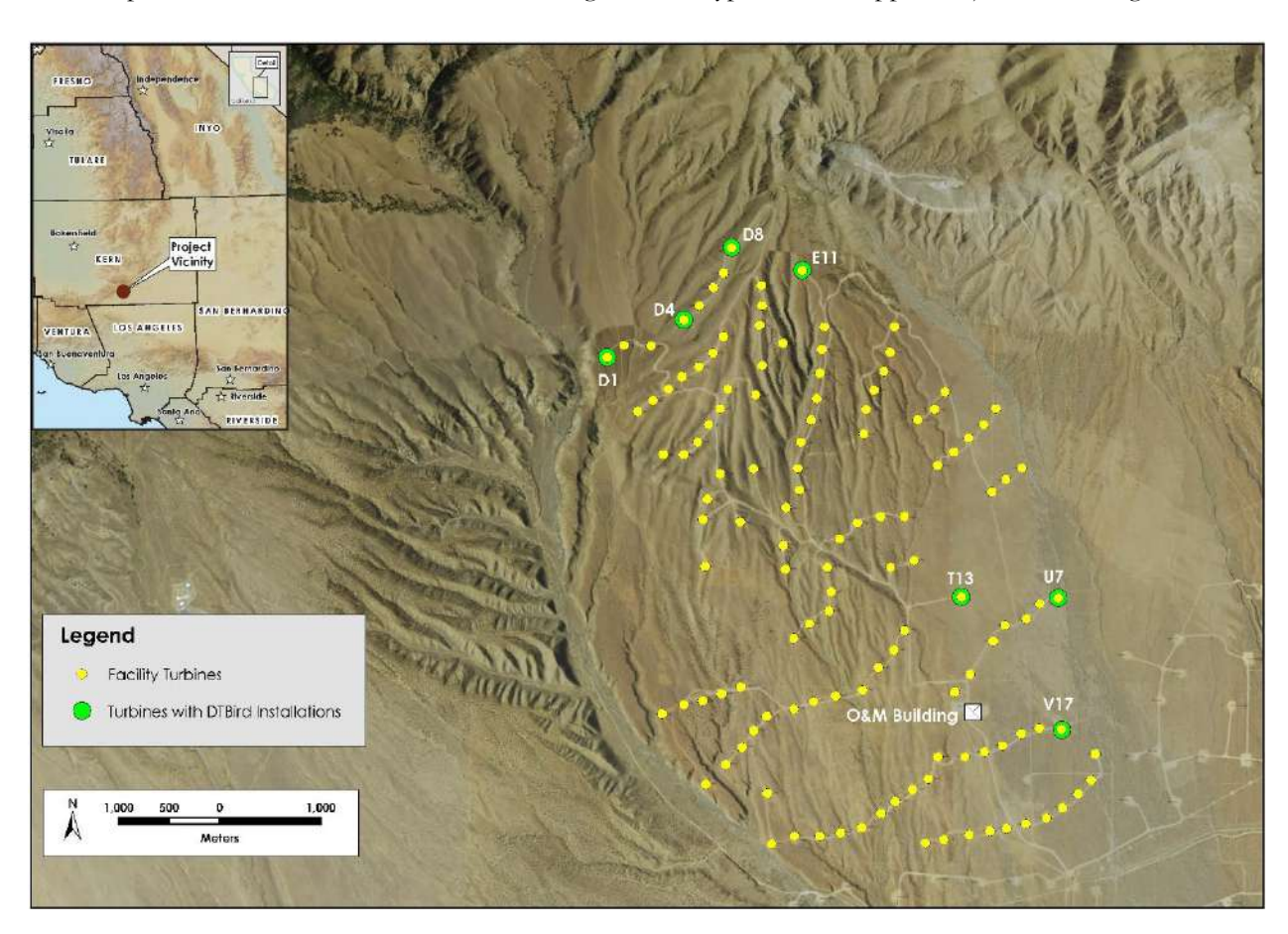


Figure 1. Layout of the Manzana Wind Power Project in southern California showing locations of installed DTBird systems.

The Goodnoe Hills Wind Farm has been in operation since 2008 and currently comprises 47 2.2 MW Vestas V110 Mark C and B wind turbines, with a hub height of 87 meters and a rotor-swept diameter of 110 meters located in south-central Washington atop an east-west ridgeline flanking the Columbia River approximately 3–6 km away (Figure 2). The topography descends steeply south of the ridgeline approximately 610 meters to the Columbia River and more gradually to the north approximately 500 meters down into Rock Creek Canyon and

associated riparian corridors. The project area is dominated by a mosaic of grazed grassland and shrubsteppe, with inclusions of ponderosa pine (*Pinus ponderosa*) and Oregon white oak (*Quercus garryana*) woodlands on the ridge's north-facing slopes. Fourteen DTBird systems were installed at this facility to support this research; however. We spread the installations around the outer perimeter of the overall facility with sufficient spacing to minimize the potential for target raptors to be simultaneously exposed to multiple deterrent signals. Note, however, that only 11 of these DTBird units were sufficiently functional to contribute data for the Year 1 analyses presented here (excludes installations at turbines G29, G51, and G56; Figure 2)

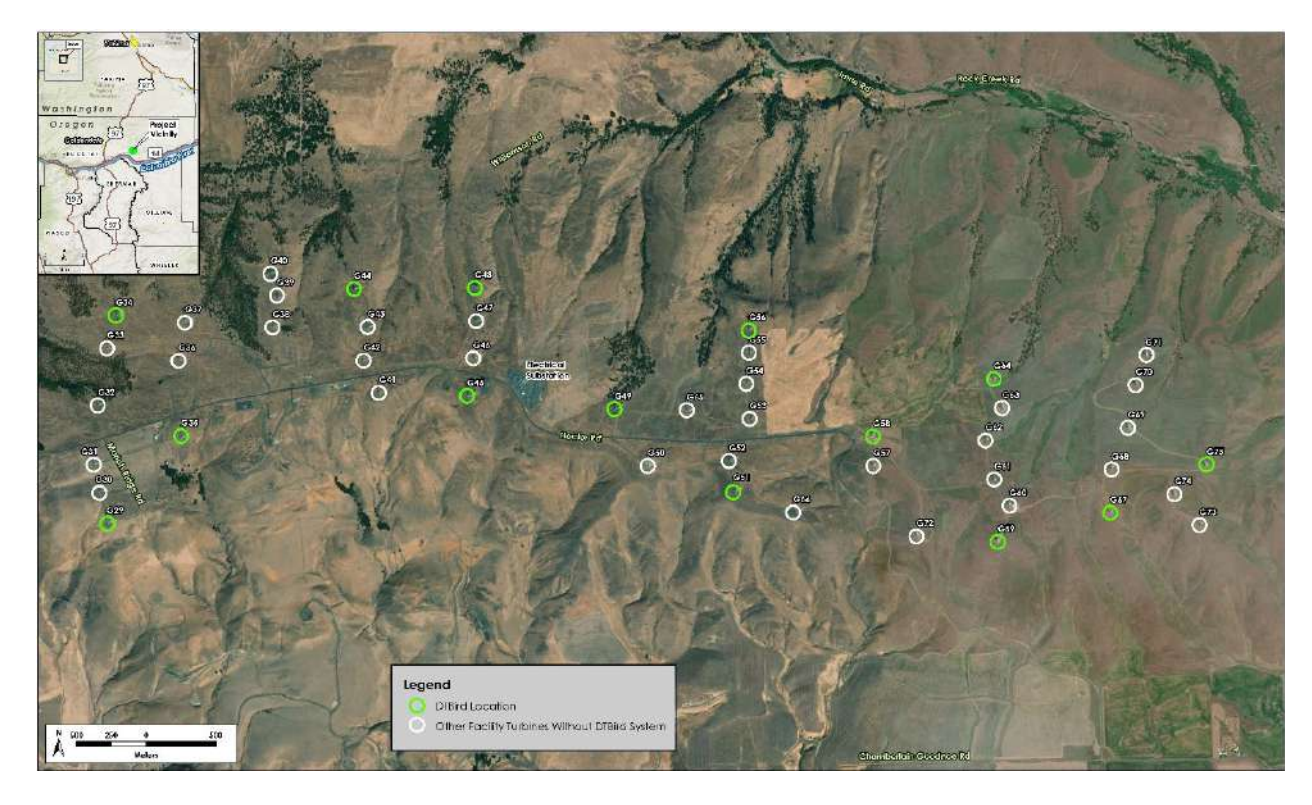


Figure 2. Layout of the Goodnoe Hills Wind Farm in south-central Washington showing locations of installed DTBird systems.

## 2.2 DTBird System Operation

Detailed descriptions of the general DTBird system set-up and operation can be found in H. T. Harvey & Associates (2018). At both study sites, each turbine-specific DTBird monitoring system comprised four video cameras (6-megapixel resolution) installed on the turbine tower approximately 5 meters off the ground, which surveilled the skies throughout daylight hours, and a ring of four broadcast speakers installed on the tower just below the lower RSZ. The only noteworthy difference between the installations at the Manzana and Goodnoe Hills sites was that the latter systems included a second set of deterrent broadcast speakers located on the turbine tower just below hub height (Figure 3). This modification was necessary because the Goodnoe Hills turbines are taller and sweep a greater rotor-swept diameter than the Manzana turbines. Installing a second set of speakers higher up on those towers was expected to help ensure effective deterrent broadcasting throughout a larger overall detection envelope and collision risk zone.

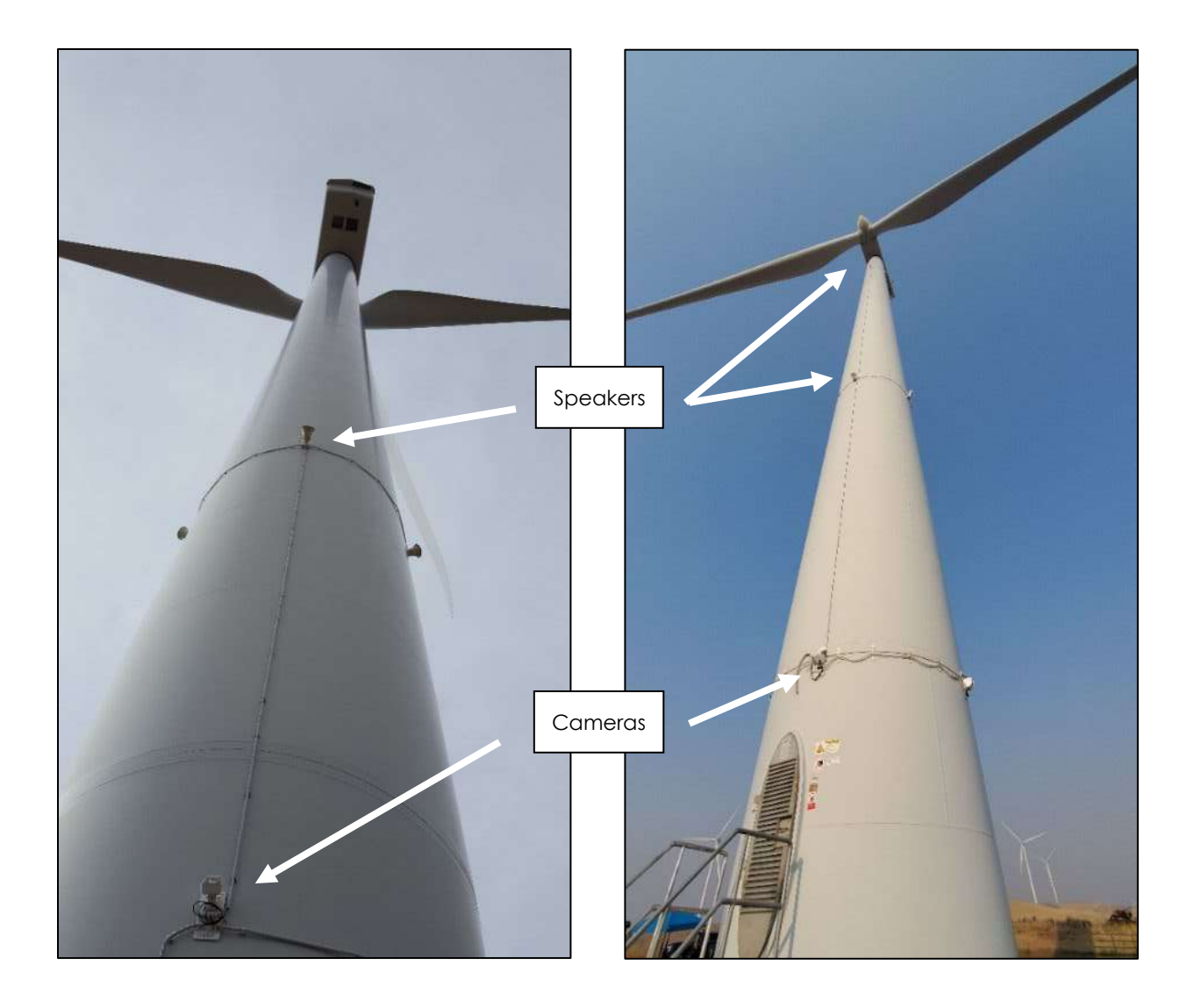


Figure 3. Depiction of DTBird video camera and broadcast speaker locations on turbines at the Manzana Wind Power Project (left panel, single ring of speakers) and Goodnoe Hills Wind Farm (right panel, two rings of speakers).

When a DTBird system first detects a targeted object, it creates a new event record in the DAP and records a timestamp for the initial *detection* event along with other limited data. If a targeted object subsequently or simultaneously triggers one or both of the deterrent signals (early *warning* or a more raucous *dissuasion* signal if a target approaches closer to the turbine) information is added to the same DAP event record to document the unique timestamps and signal durations for each deterrent-triggering event. Each event record has video clips attached to it representing the four cameras, which the system extracts to begin 10 seconds before targeting began and continue for 30 seconds after the last targeted object exits the detection envelope. There must be no objects targeted for at least 26 seconds before a given DTBird system can initiate a new event record. If a system targets multiple objects concurrently during the same event period, timestamps are recorded only for the first detection, warning-trigger, and dissuasion-trigger events, and those respective events may not be

triggered by the same object. In these cases, it can be difficult to determine exactly which bird or object was responsible for the timestamped events.

For the purpose of the overall Goodnoe Hills DTBird performance assessment (H. T. Harvey & Associates 2019a), the DTBird-equipped turbines were operated on a schedule whereby, on a given day, approximately half of the operating units were run with the deterrent signals triggered virtually but not actually broadcasting, while the other half were operating normally with the deterrents broadcasting. The suite of DTBird units operating in each mode varied on a daily basis according to a stratified, randomized schedule that sought to equitably distribute broadcasting and non-broadcasting units across the facility each day. This experimental setup (designed to support another overall project objective) provided an ideal circumstance for composing a control-treatment design for the initial Goodnoe Hills site-specific behavioral analyses previously presented in H. T. Harvey & Associates (2023a). That is, our data-entry technicians reviewed all relevant videos without knowledge of whether or not a given DTBird unit was actually broadcasting the triggered deterrent signals. The motivation for this "deaf" trial assessment acknowledged that approaching birds may divert their flight in response to the presence of spinning blades alone. The implemented control-treatment design provided a means of comparing the patterns of responses with and without the deterrents broadcasting, and thereby isolating responses to the broadcasted deterrents. However, as previously mentioned, implementing an analogous control-treatment setup at the prior Manzana study site was not feasible, which therefore required a stepwise, conditional approach to implementing integrative multi-site analyses based on data collected at both study sites.

# 2.3 Classifying Responses to Deterrents

We developed the Manzana dataset used for evaluating the behavioral responses of raptors to the DTBird deterrents based on 1 yr of data collected from January through December 2017, screening all DTBird detections recorded at the seven DTBird installations that triggered a deterrent signal on a randomized 10 days per 28-day period, and classifying the behavioral responses of all confirmed and probable golden eagles, as well as selections of other observations that we classified as either other confirmed species of large raptors (i.e., bald eagles [Haliaeetus leucocephalus], buteos [Buteo spp.], or turkey vultures [Cathartes aura]) or that we could classify only as unidentified large raptors (H. T. Harvey & Associates 2018). We developed a comparable Goodnoe Hills dataset based on 1 yr of data collected from September 2021 through August 2022, screening all DTBird detections recorded at 11 operable DTBird installations on randomized selections of 10 days per 28-day period during that year (part of the aforementioned larger experimental design), and classifying the behavioral responses of all confirmed/probable golden eagles and other large raptors detected during those periods (H. T. Harvey & Associates 2018). In both cases, our sampling objective was to amass temporally and taxonomically representative datasets sufficient to support robust assessments of the probability of effective deterrence for in situ eagles and other large raptors as a group, reasonable independent assessments for all confirmed/probable golden eagles, all confirmed/probable bald eagles and all confirmed/probable eagles combined at the Goodnoe Hills site (bald eagles were rare at the Manzana site), and representative samples of confirmed/probable turkey vultures and buteos (mostly red-tailed hawks [Buteo jamaicensis] year-round at both sites and rough-legged hawks [B. lagopus] during winter in Washington).

Additional detail about the protocols we followed and the methods we used to evaluate and analyze the responses of *in situ* raptors to the deterrent signals independently at the two study sites are outlined in prior technical reports (H. T. Harvey & Associates 2018, 2023a). In particular, Appendix A in H. T. Harvey & Associates (2018) contains a step-by-step account of the classification process we used to categorize the responses of relevant raptors to the deterrent signals. The process incorporated several subjective and objective criteria for classifying the behavioral response of a given raptor upon exposure to a warning signal and/or dissuasion signal, culminating in a final classification of responses as one of the following:

- *CE: Confirmed effective*, confirmed effective reacted in a way that, based on the change in flight pattern and direction, reduced the risk of collision with the turbine blades
- PE: Potentially effective appeared to react to signal including a flight diversion, but response was not definitive or discernable enough to be confident that the bird was at less risk after signal emission
- N: Not effective reacted to signal (e.g., temporarily altered its flapping rate) but did not alter its flight path away from RSZ
- Z: No response did not visibly react to signal
- U: Unknown/undetermined bird was already moving away from the turbine when the signal was emitted; the video quality or bird image quality was not favorable for determining the 3D reaction of the bird on the 2D video screen; or it simply was not possible to determine with any sense of confidence whether a reaction occurred or not due to other factors.

We excluded from further consideration all cases where we classified a response as "unknown/undetermined." In addition, because the difference between N and Z responses was effectively immaterial for the purpose of analyses represented herein, we generally lumped together those as "I = Ineffective response", which also helped eliminate missing cells in some relevant contingency tables.

Along with evaluating behaviors and flight trajectories to classify a bird's response pattern when it triggered a deterrent signal, we classified the potential *Collision Risk* the bird was facing prior to triggering a deterrent as follows:

- *High* moving toward turbine on a trajectory and at an altitude that could take it near the current RSZ (defined for this purpose as the current, approximate 2D plane of rotation).
- *Medium* moving toward turbine on a trajectory and at an altitude that may take it near the turbine, but likely either below or above the RSZ.
- Low moving tangential to or away from the turbine distant from the RSZ, or at high altitude well above the RSZ.

### 2.4 Analyses

#### 2.4.1 Contingency Tables

To evaluate differences in the categorical responses of raptors to broadcasted deterrent signals at the two study sites, we used 2-way Pearson chi-square analyses performed using the base R package version 4.3.1 (R Core Team 2023). For these analyses, classifications by *Site* (two groups) and *Response* (three groups) categories composed the 2 x 3 contingency tables of interest. If given at least a marginally significant ( $P \le 0.10$ ) overall chi-square test, we proceeded to conduct post-hoc comparisons to further characterize the specific *Response* categories within which notable *Site*-specific differences were apparent. For these tests, we used the second post-hoc comparison approach outlined in McDonald (2014). To evaluate the individual significance of the three contrasts of interest, we compared the resulting P values to Bonferroni-adjusted values of 0.017 for significance at the overall level of  $P \le 0.05$  and 0.033 for marginal significance at the overall level of  $P \le 0.05$  and 0.033 for marginal significance at the overall level of 0.05 <  $P \le 0.10$ .

We prepared these chi-square analyses for all analyzed cases, all confirmed/probable golden eagles, all confirmed/probable turkey vultures, and all confirmed/probable buteos. Further, the datasets included three possible response variables, one pertaining to responses to warning signals alone, one pertaining to responses to dissuasion signals alone, and one including responses to single deterrents or to the combination of both deterrents signaling in sequence, where applicable. Insight about the relative responses of raptors to the warning versus dissuasion signals can be found in previous site-specific reports (H. T. Harvey & Associates 2019b, 2023a); however, for this multi-site analysis we focused only on the combined response data to maximize sample sizes and emphasize the overall effects of the deterrent system. In a few cases, the resulting cell sample sizes were small, but Pearson chi-square tests are known to be robust as long as expected cell frequencies exceed 1.0 (Jeffreys 1939), and our preliminary investigations showed no notable differences in outcome using the alternative Fisher's Exact Test. We did not strive to develop more complicated 3-way chi-square statistical models that included consideration of relative collision risk prior to deterrent triggering as a third predictor (H. T. Harvey & Associates 2018), in part because of sample-size limitations (H. T. Harvey & Associates 2023a). However, we ultimately addressed this important potential influence again using the LGLM approach described next.

#### 2.4.2 Logistic GLMs

As described further in Section 3.2, the initial chi-square analyses indicated that the probability of effective responses to broadcasted deterrents was often lower at the Goodnoe Hills facility than at the Manzana facility. Therefore, pursuing the second phase of Objective 2 rather than Objective 3, as outlined in the Introduction, was warranted. Accordingly, we did not seek to integrate the treatment data from both sites to compare against the control data generated only at the Goodnoe Hills. Instead, we sought to develop further insight about possible drivers of the difference in the probability of effective responses to broadcasted deterrents at the two sites by composing LGLM analyses to evaluate the influences of several potential predictors. These analyses were necessarily limited to cases involving responses to broadcasted deterrents. Further, we collapsed the Response variable from four to two categories to compose a binary response variable for the LGLM analysis: 1

= probable effective response (CE + PE classifications as described above) and 0 = no effective response (I = N + Z classifications). We prepared two analyses—one based on the multi-species dataset and one limited to probable golden eagles—and focused only on the combined deterrence response classifications. For the multi-species analysis, we included a *Species Group* variable in the model to highlight potential differences among the three primary species groups: eagles, vultures, and buteos. To facilitate evaluation of *Species Group* as a predictor, we reduced the dataset to only those cases that we could confidently identify as belonging to one of these three groups. The initial full model for the multi-species analysis was as follows:

ln(Odds of effective deterrence) ~ *Site* (Manzana CA or Goodnoe WA) + *Species Group* (Eagle, Vulture, or Buteo) + *Preexposure Risk* (risk of exposure to turbine before deterrence: low, medium, or high) + *Wind Speed* (meters/second; measured by turbine anemometer) + all possible 2-way interactions

The initial full model for golden eagles was the same except for excluding the *Species Group* variable. We implemented the LGLM analyses using the 'glm' function in R (R Core Team 2023). To settle on final models, we used likelihood ratio tests for individual parameters and compared Akaike Information Criterion (AIC) scores for all possible candidate models reflected in the full model statements to identify the most parsimonious combinations of predictors (Burnham and Anderson 2010). In considering the merits of different candidate models, we also used diagnostic residual plots to evaluate conformity to the assumptions of LGLMs, plots of model residuals versus leverage and Cook's distance to identify potential outliers, and McFadden's pseudo-R<sup>2</sup> to assess the explanatory power of models (McFadden 1974, Friendly and Meyer 2016).

The LGLM resulted in predictions of the ln(odds of effective deterrence). We used a standard formula (100\*exp[ln[odds]]/[1+exp[ln[odds]]]) to transform the log-odds estimates to probabilities of response (0 to 1 translated to percentages) for the purpose of describing and graphically displaying relationships (Hosmer and Lemeshow 1989).

### Section 3. Results

### 3.1 Sampling Results

Table 1 summarizes the classified large-raptor deterrence events from the two study sites that we analyzed for this assessment.

Table 1. DTBird events recorded from January through August 2017 at the Manzana Wind Power Project in California and from September 2021 through August 2022 at the Goodnoe Hills Wind Farm in Washington, which formed the basis for assessing the behavioral responses of eagles and other large raptors to DTBird audio deterrents.

	Manzana	Goodno	e Hills	
Species <sup>1</sup>	Deterrents Broadcasting	Deterrents Broadcasting	Deterrents Muted	Total
Golden Eagle	80	33	45	158
Bald Eagle	1	14	25	40
Unknown Eagle	0	11	9	20
Turkey Vulture	21	52	54	127
Buteo <sup>2</sup>	122	52	55	229
Golden Eagle or Vulture	39	7	3	49
Golden Eagle or Buteo	7	3	6	16
Unknown Eagle/Vulture	11	34	49	94
Unknown Eagle/Buteo	0	16	22	38
Total	281	222	268	771

Classifications represent all cases where we either confirmed or strongly suspected ("probable") involvement of the relevant species or species group.

# 3.2 Response to Deterrents

#### 3.2.1 Contingency Table Analyses

Given many cases where we could not confidently classify the species of raptor detected and tracked by the DTBird systems (e.g., see H. T. Harvey & Associates 2019b, 2022a, 2022b, 2023a), we began our assessment by examining the deterrent response patterns reflected in all 503 of the selected cases involving large raptors exposed to broadcasted deterrents at the two study sites (Table 1). Overall, we classified 73% of the Manzana cases and 63% of the Goodnoe Hills cases as either confirmed or potentially effective responses (Table 2). The chi-square analysis of this dataset indicated a marginally significant difference (0.05 <  $P \le 0.10$ ) in the response patterns at the two sites ( $\chi^2 = 5.59$ , df = 2, P = 0.061). Post-hoc comparisons further indicated that the higher proportion of *Confirmed effective* responses approached significance only at the Manzana site (P = 0.076), the proportion of *Potentially effective* responses did not differ at the two sites (P = 0.683), and the proportion of

<sup>&</sup>lt;sup>2</sup> Primarily red-tailed hawks year-round at both sites and rough-legged hawks during winter at the Goodnoe Hills.

Ineffective (I = N + Z) responses was marginally higher at the Goodnoe Hills (P = 0.023 falls below the Bonferroni-corrected significance threshold for maintaining an overall Type II error rate of  $\leq 0.10$ ).

Focused on confirmed/probable golden eagles, the proportion of confirmed/potentially effective responses was again higher at the Manzana site (79%) compared to the Goodnoe Hills (60%) (Table 3), and the overall chi-square analysis again indicated that the pattern of variation among the *Response* classifications was at least marginally different at the two sites ( $\chi^2 = 5.84$ , df = 2, P = 0.054). Post-hoc comparisons further indicated that the proportion of *Confirmed effective* responses was marginally higher at the Manzana site (P = 0.027), the proportion of *Potentially effective* responses did not differ at the two sites (P = 0.629), and the higher proportion of *Ineffective* responses at the Goodnoe Hills approached significance (P = 0.047).

Table 2. Classification of the effectiveness of behavioral responses (combined responses to warning and dissuasion signals acting alone or in tandem) in reducing collision risk for all large raptors combined (eagles, vultures, and buteos) at the Manzana Wind Power Project in California and the Goodnoe Hills Wind Farm in Washington.

Classified	Manzar	ıa	Goodnoe Hills			
Response	Number of Cases	%	Number of Cases	%		
Confirmed Effective (CE)	118	42.0	76	34.2		
Potentially Effective (PE)	87	31.0	69	29.3		
Not Effective (N)	13	4.6	17	7.2		
No Response (Z)	63	22.4	60	29.3		
Total	281	_	222	_		

Note: test of independence with N+Z lumped:  $\chi 2=5.59$ , df=2, P=0.061—indicating the overall pattern of responses was marginally different at the two sites. Bonferroni-corrected post-hoc comparisons confirmed a marginally higher proportion of Potentially effective responses and a marginally lower proportion of Ineffective (N+Z) responses at the Manzana site.

Table 3. Classification of the effectiveness of behavioral responses (combined responses to warning and dissuasion signals acting alone or in tandem) in reducing collision risk for confirmed and probable golden eagles at the Manzana Wind Power Project in California and the Goodnoe Hills Wind Farm in Washington.

Classified	Manzan	ıa	Goodnoe Hills		
Response	Number of Cases	%	Number of Cases	%	
Confirmed Effective (CE)	40	50.0	9	27.3	
Potentially Effective (PE)	23	28.8	11	33.3	
Not Effective (N)	3	3.7	5	15.2	
No Response (Z)	14	17.5	8	24.2	
Total	80	_	33	_	

Note: chi-square test of independence with N + Z lumped:  $\chi^2 = 5.84$ , df = 2, P = 0.054—indicating the overall pattern of responses was marginally different at the two sites. Bonferroni-corrected post-hoc comparisons confirmed a marginally higher proportion of Confirmed effective responses and a marginally lower proportion of Ineffective (N+Z) responses at the Manzana site.

For confirmed/probable turkey vultures, the proportion of confirmed/potentially effective responses was again higher at the Manzana site (81%) compared to the Goodnoe Hills site (61%) (Table 4), and the overall chi-square analysis indicated that the pattern of variation among the *Response* classifications differed at the two sites

( $\chi^2 = 6.20$ , df = 2, P = 0.045). Post-hoc comparisons further indicated that the proportion of *Confirmed effective* responses was higher at the Manzana site (P = 0.015), the proportion of *Potentially effective* responses did not differ at the two sites (P = 0.424), and the higher proportion of I responses at the Goodnoe Hills approached significance (P = 0.069).

Table 4. Classification of the effectiveness of behavioral responses (combined responses to warning and dissuasion signals acting alone or in tandem) in reducing collision risk for confirmed and probable turkey vultures at the Manzana Wind Power Project in California and the Goodnoe Hills Wind Farm in Washington.

Classified	Manzar	ıa	Goodnoe Hills			
Response	Number of Cases	%	Number of Cases	%		
Confirmed Effective (CE)	11	52.4	12	23.1		
Potentially Effective (PE)	6	28.6	20	38.4		
Not Effective (N)	0	0	4	7.7		
No Response (Z)	4	19.0	16	30.8		
Total	21	_	52	_		

Note: Chi-square test of independence with N + Z lumped:  $\chi 2 = 6.20$ , df = 2, P = 0.045—indicating that the overall pattern of responses differed at the two sites. Bonferroni-corrected post-hoc comparisons confirmed a higher proportion of Confirmed effective responses at the Manzana site.

For confirmed/probable buteos, the difference between the overall proportions of confirmed/potentially effective responses was again notably higher at the Manzana site (72%) than at the Goodnoe Hills (56%). The chi-square analysis confirmed a significant difference in pattern at the two sites ( $\chi^2 = 6.31$ , df = 2, P = 0.043; Table 5). Post-hoc comparisons further indicated that the proportion of *Confirmed effective* responses did not differ at the two sites (P = 0.095), but the proportion of *Potentially effective* responses was marginally higher (P = 0.028) and the proportion of I responses was marginally lower (I = 0.035) at the Manzana site.

Table 5. Classification of the effectiveness of behavioral responses (combined responses to warning and dissuasion signals acting alone or in tandem) in reducing collision risk for confirmed and probable buteos at the Manzana Wind Power Project in California and the Goodnoe Hills Wind Farm in Washington.

Classified	Manzan	ıa	Goodnoe Hills		
Response	Number of Cases	%	Number of Cases	%	
Confirmed Effective (CE)	44	36.1	19	36.6	
Potentially Effective (PE)	44	36.0	10	19.2	
Not Effective (N)	8	6.6	5	9.6	
No Response (Z)	26	21.3	18	34.6	
Total	122	_	52	_	

Note: Chi-square test of proportions:  $\chi 2 = 6.31$ , df = 2, P = 0.042—indicating the overall pattern of responses differed at the two sites. Bonferroni-corrected post-hoc comparisons confirmed a marginally higher proportion of Potentially effective responses and a marginally lower proportion of Ineffective (N + Z) responses at the Manzana site.

In relation to collision *Risk*, the raw percentage results for the multi-species Manzana dataset suggested that the proportion of *Confirmed effective* responses to broadcasted deterrents increased from 36% to 49% as the classified level of pre-exposure risk increased from low to high, whereas the proportions of *Potentially effective* and *I* 

responses each decreased by seven percentage points with increasing exposure risk (Table 6, Figure 4). In contrast, the multi-species Goodnoe Hills dataset suggested that the proportions of both *Confirmed effective* and *Potentially effective* responses were highest and the proportion of *I* responses lowest for birds at moderate pre-exposure risk.

Table 6. Classification of the effectiveness of behavioral responses to broadcasted DTBird audio deterrents (combined responses to warning and dissuasion signals acting alone or in tandem) in reducing collision risk for all large raptors combined by site and classified risk level before deterrent exposure at the Manzana Wind Power Project in California and the Goodnoe Hills Wind Farm in Washington.

	Site / Risk Level								
	Manzana					Goodnoe Hills			
Response	Low	Med	High	Total	Low	Med	High	Total	
Confirmed Effective (CE)	42	58	18	118	28	39	9	76	
Potentially Effective (PE)	40	37	10	87	27	31	7	65	
Ineffective $(I = N + Z)$	36	31	9	76	40	29	12	81	
Total Cases	118	126	37	281	95	99	28	222	
% Confirmed Effective	36	46	49	42	29	39	32	34	
% Potentially Effective	34	29	27	31	28	31	25	29	
% Ineffective	31	25	24	27	42	29	43	36	

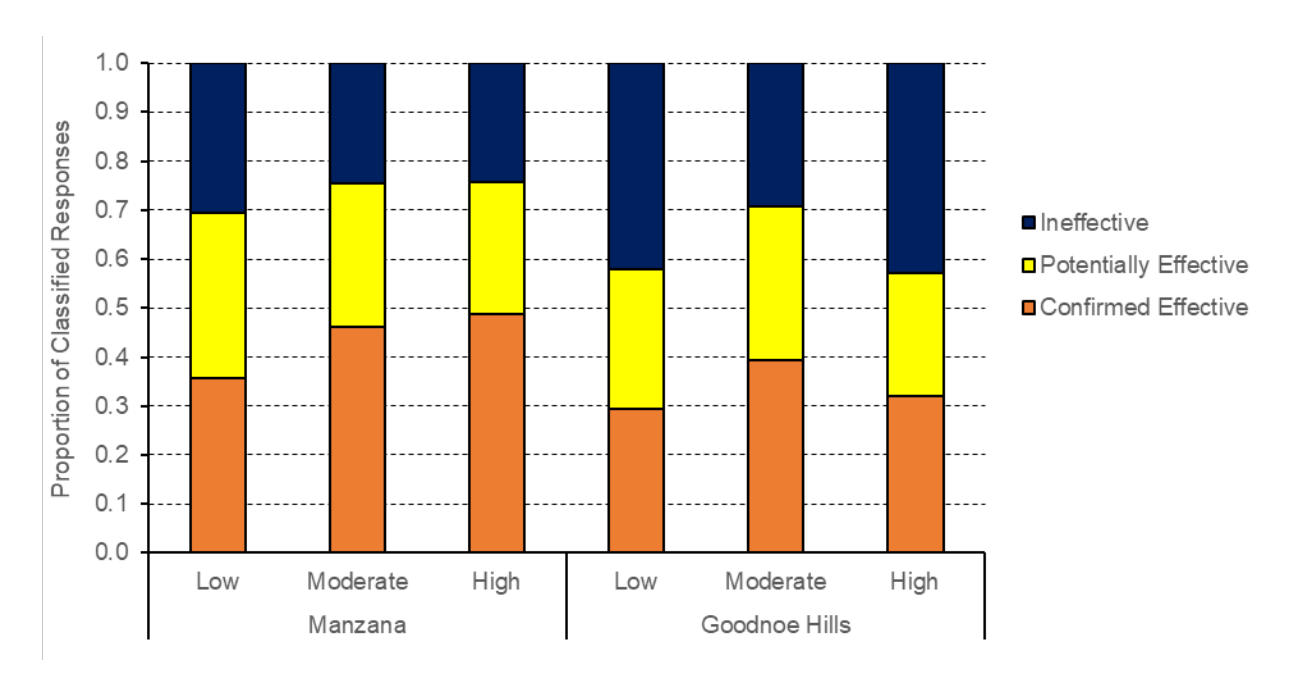


Figure 4. Proportional representation of the effectiveness of behavioral responses to broadcasted DTBird audio deterrents (combined responses to warning and dissuasion signals acting alone or in tandem) in reducing collision risk for all large raptors combined by site and classified risk level before deterrent exposure at the Manzana Wind Power Project in California and the Goodnoe Hills Wind Farm in Washington.

The Response–Risk data for confirmed/probable golden eagles were sparse across many cells of the relevant 3 x 3 contingency tables for both sites, especially the Goodnoe Hills, which may limit the value of generated insight (Table 7). The Manzana data suggested that the proportions of Confirmed effective responses were higher for birds at high (50%) and especially moderate (58%) risk of exposure than for birds at low risk of exposure (40%), and the proportions of I responses were concomitantly lower for birds at moderate to high risk (Figure 5). In contrast, the Goodnoe Hills data showed a modest increasing trend in the proportions of Confirmed effective responses as risk increased (22–33%); however, among birds at moderate risk of exposure, the highest proportion (44%) exhibited relatively subtle Potentially effective responses, and the highest proportions of birds at both low (56%) and high (50%) risk of exposure exhibited no effective responses.

Table 7. Classification of the effectiveness of behavioral responses to broadcasted DTBird audio deterrents (combined responses to warning and dissuasion signals acting alone or in tandem) in reducing collision risk for confirmed and probable golden eagles by site and classified risk level before deterrent exposure at the Manzana Wind Power Project in California and the Goodnoe Hills Wind Farm in Washington.

	Site / Risk Level								
	Manzana					Goodnoe Hills			
Response	Low	Med	High	Total	Low	Med	High	Total	
Confirmed Effective (CE)	12	21	7	40	2	5	2	9	
Potentially Effective (PE)	8	11	4	23	2	8	1	11	
Ineffective $(I = N + Z)$ )	10	4	3	17	5	5	3	13	
Total Cases	30	36	14	80	9	18	6	33	
% Confirmed Effective	40	58	50	50	22	28	33	27	
% Potentially Effective	27	31	29	29	22	44	17	33	
% Ineffective	33	11	21	21	56	28	50	39	

The Manzana sample sizes for confirmed/probable turkey vultures were sparse when broken out into a 3 x 3 Response—Risk table; however, the pattern of sparseness suggested that vultures at moderate to high risk of exposure exhibited a pronounced tendency to respond effectively, whereas birds at low risk of exposure were close to equally likely to exhibit any one of the three responses (Table 8, Figure 6). In contrast, the Goodnoe Hills data suggested that Confirmed effective responses were least likely regardless of the pre-exposure risk level and were proportionately least common among birds at high risk, but no other consistent patterns were evident.

For confirmed/probable buteos, neither of the site-specific datasets exhibited distinctive trends in the response patterns in relation to pre-exposure risk levels (Table 9, Figure 7). At the Manzana site, overall variation across cells of the 3 x 3 Response–Risk table was not pronounced. The highest proportion of birds at high risk (44%) exhibited Confirmed effective responses, whereas marginally highest proportions of the birds at low (40%) and moderate (36%) risk exhibited Potentially effective responses. At the Goodnoe Hills, the proportions of I responses were notably highest for birds at both low and high risk, whereas the proportion of Confirmed effective responses was notably highest for birds at moderate risk.

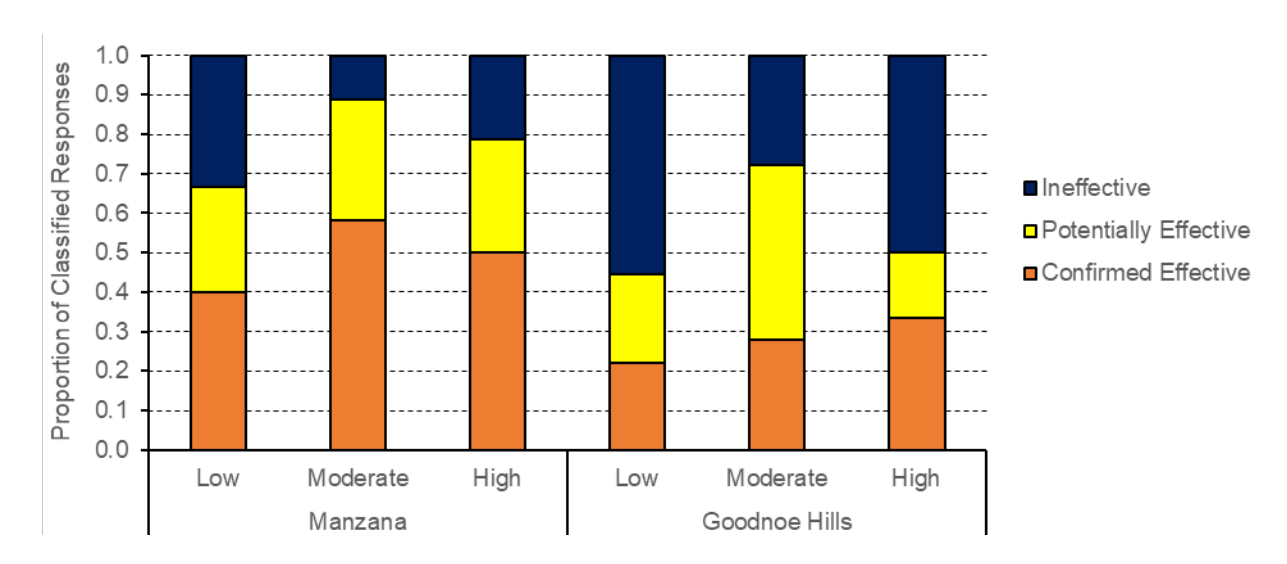


Figure 5. Proportional representation of the effectiveness of behavioral responses to broadcasted DTBird audio deterrents (combined responses to warning and dissuasion signals acting alone or in tandem) in reducing collision risk for golden eagles by site and classified risk level before deterrent exposure at the Manzana Wind Power Project in California and the Goodnoe Hills Wind Farm in Washington.

Table 8. Classification of the effectiveness of behavioral responses to broadcasted DTBird audio deterrents (combined responses to warning and dissuasion signals acting alone or in tandem) in reducing collision risk for confirmed and probable turkey vultures by site and classified risk level before deterrent exposure at the Manzana Wind Power Project in California and the Goodnoe Hills Wind Farm in Washington.

	Site / Risk Level								
	Manzana					Goodnoe Hills			
Response	Low	Med	High	Total	Low	Med	High	Total	
Confirmed Effective (CE)	4	6	1	11	5	5	2	12	
Potentially Effective (PE)	5	0	1	6	9	6	5	20	
Ineffective $(I = N + Z)$	4	0	0	4	7	9	4	20	
Total Cases	13	6	2	21	21	20	11	52	
% Confirmed Effective	31	100	50	52	24	25	18	23	
% Potentially Effective	38	0	50	29	43	30	45	38	
% Ineffective	31	0	0	19	33	45	36	38	

The performance standard of ≥50% successful or effective deterrence for golden eagles established based on the initial Manzana pilot study (H. T. Harvey & Associates 2018) was further corroborated for that site by the initial 53% estimate derived from the subsequent expansion of that site-specific assessment to include a full year of data (H. T. Harvey & Associates 2019b). Further minor adjustments to the relevant dataset in preparation for the multi-site evaluation presented herein modified that estimate to 50% *Confirmed effective* responses, with another 29% *Potentially effective* responses, yielding a total estimated probable effectiveness of 79% for golden eagles (Table 10). In comparison, the Goodnoe Hills results indicated a lower 27% confirmed

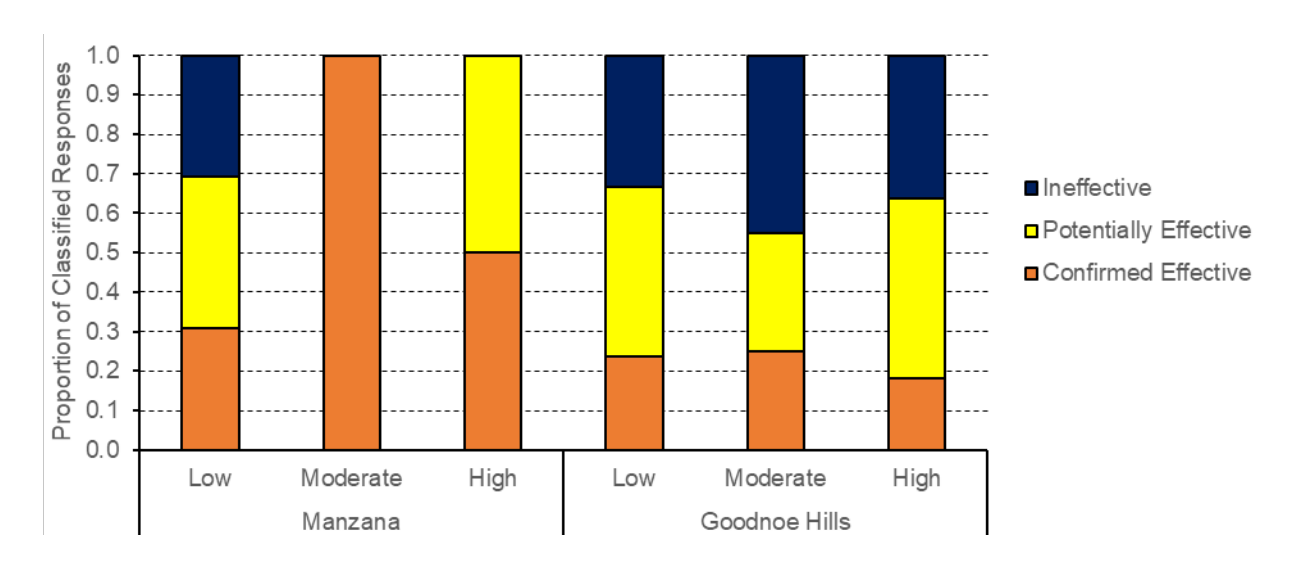


Figure 6. Proportional representation of the effectiveness of behavioral responses to broadcasted DTBird audio deterrents (combined responses to warning and dissuasion signals acting alone or in tandem) in reducing collision risk for turkey vultures by site and classified risk level before deterrent exposure at the Manzana Wind Power Project in California and the Goodnoe Hills Wind Farm in Washington.

Table 9. Classification of the effectiveness of behavioral responses to broadcasted DTBird audio deterrents (combined responses to warning and dissuasion signals acting alone or in tandem) in reducing collision risk for confirmed and probable buteos by site and classified risk level before deterrent exposure at the Manzana Wind Power Project in California and the Goodnoe Hills Wind Farm in Washington.

	Site / Risk Level								
	Manzana					Goodnoe Hills			
Response	Low	Med	High	Total	Low	Med	High	Total	
Confirmed Effective (CE)	15	21	8	44	8	9	2	19	
Potentially Effective (PE)	17	22	5	44	2	7	1	10	
Ineffective $(I = N + Z)$	11	18	5	34	16	4	3	23	
Total Cases	43	61	18	122	26	20	6	52	
% Confirmed Effective	35	34	44	36	31	45	33	37	
% Potentially Effective	40	36	28	36	8	35	17	19	
% Ineffective	26	30	28	28	62	20	50	44	

effective responses, falling well below the established performance standard; however, the combined estimate of 60% confirmed/probable effective responses, though still notably lower than at the Manzana site, did exceed the 50% performance threshold. Similar patterns were shown for vultures and the multi-species group, except that the proportion of effective responses for the multi-species group fell below the 50% threshold. In contrast, for buteos the proportions of effective responses did not differ at the two sites and were well below the 50% threshold (27–29%); however, the combined proportion of confirmed/probable effective responses was again notably higher at the Manzana site (72%) than at the Goodnoe Hills site (56%) (Table 10).

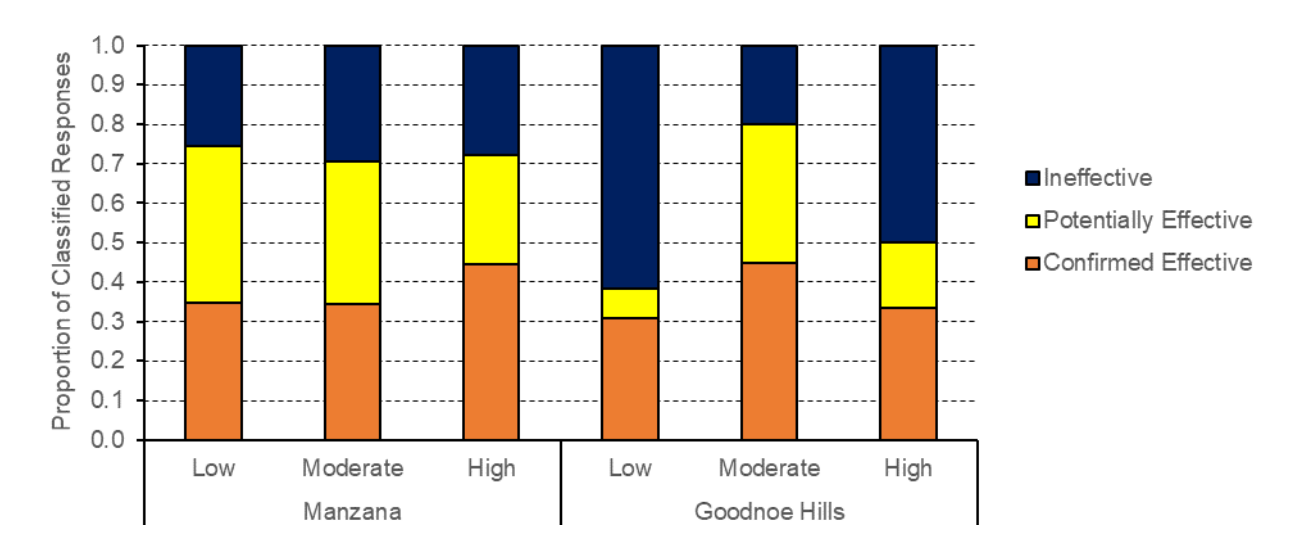


Figure 7. Proportional representation of the effectiveness of behavioral responses to broadcasted DTBird audio deterrents (combined responses to warning and dissuasion signals acting alone or in tandem) in reducing collision risk for buteos by site and classified risk level before deterrent exposure at the Manzana Wind Power Project in California and the Goodnoe Hills Wind Farm in Washington.

Table 10. Percentages of behavioral responses to broadcasted DTBird deterrents (combined responses to warning and dissuasion signals acting alone or in tandem) classified as effective or potentially effective in reducing collision risk for different species groups at the Manzana Wind Power Project in California and the Goodnoe Hills Wind Farm in Washington.

Species Group	Manzana	Goodnoe Hills		
Golden Eagles	50 / 79¹	27 / 60		
Vultures	52 / 81	23 / 61		
Buteos	36 / 72	37 / 56		
All Groups Combined	42 / 73	34 / 63		

First number = % of responses confirmed effective; second number = overall % of confirmed + potentially effective responses.

#### 3.2.2 Logistic GLM Analyses

Given that the initial chi-square analyses pointed to at least marginally significant differences in the deterrence response patterns of golden eagles and other large raptors at the two study sites, we did not consider pursuing Objective 3 as outlined in the Introduction. Instead, we pursued the second element of Objective 2, which entailed preparing LGLM analyses to provide further insight about potential drivers of the evident site-specific differences in the apparent sensitivity of raptors to the broadcasted deterrents.

#### **Multi-species Model**

The LGLM analysis based on the multi-species dataset resulted in the final model listed below (and see Table 11) and the interpretations that follow:

 $\label{eq:log-control} \begin{tabular}{l} Log(Odds of effective deterrence) $\sim$ Site + Species Group + Preexposure Risk + Wind Speed + Species Group $$ Wind Speed $$$ 

Diagnostics for this final model revealed no outliers and residuals consistent with adequate model fit.

Table 11. Comparison of AIC scoring results for top candidates and selected other multi-species logistic GLMs portraying potential relationships between the probability of effective deterrence and various predictors.

Candidate Model <sup>1</sup>	AIC <sup>2</sup>	ΔΑΙC	McFadden's R <sup>2</sup>
Site + Species Group + Preexposure Risk + Wind Speed + Species Group : Wind Speed	465.52	0.00	0.055
Site + Species Group + Preexposure Risk + Wind Speed + Species Group : Wind Speed + Site : Wind Speed	466.44	0.92	0.057
Site + Species Group + Wind Speed + Species Group : Wind Speed	466.87	1.35	0.044
Site	469.29	3.77	0.018
Site + Species Group	470.37	4.85	0.024
Site + Species Group + Preexposure Risk + Wind Speed + Species Group : Preexposure Risk + Species Group : Wind Speed + Site : Wind Speed	470.53	5.01	0.066
Site + Wind Speed	471.16	5.64	0.018
Site + Species Group + Wind Speed	471.92	6.40	0.025
Species Group*Wind Speed	474.30	8.78	0.024
Null model	475.60	10.08	_
Site + Species Group + Preexposure Risk + Wind Speed +Species Group : Site + Species Group : Preexposure Risk + Species Group : Wind Speed +Site : Preexposure Risk + Site : Wind Speed	477.23	11.71	0.068
Site + Species Group + Preexposure Risk + Wind Speed + Species Group : Site + Species Group : Preexposure Risk + Species Group : Wind Speed + Site : Wind Speed	477.33	11.81	0.068
Site + Species Group + Preexposure Risk + Wind Speed + Species Group : Site + Species Group : Preexposure Risk + Species Group : Wind Speed + Site : Preexposure Risk + Site : Wind Speed + Preexposure Risk : Wind Speed	481.22	15.70	0.068

<sup>&</sup>lt;sup>1</sup> Site = Manzana or Goodnoe Hills wind facility. Species Group = eagle, vulture or buteo. Preexposure Risk (of approaching rotor swept area of spinning turbine prior to deterrent triggering) = low, moderate or high. Wind Speed measured at turbine in meters / second.

- *Site* effect (*P* =0.002; Table 12) reflected a higher average probability of effective deterrence at the Manzana site (Figure 8).
- Preexposure Risk was only marginally significant (P = 0.069), but its inclusion reduced the AIC score by 1.35 points (Table 11). Birds facing moderate risk were the most likely to show effective deterrence responses, while birds facing low risk were the least likely to show effective responses; however, none of the pairwise differences were significant on their own, suggesting a gradient of variation rather than a discrete segregation of probability groups (Table 12, Figure 9).

<sup>&</sup>lt;sup>2</sup> Akaike Information Criterion score.

Table 12. Parameters of final multi-species logistic GLM selected to represent relationship between the In(odds of effective deterrence) and various predictors at the Manzana and Goodnoe Hills wind-energy facilities.

Parameter <sup>1</sup>	Estimate	SE	z	Р
Intercept	0.6394	0.5112	1.251	0.211
Site-Manzana	0.7416	0.2439	3.041	0.002
Species Group-Eagle	-0.8740	0.5548	-1.575	0.115
Species Group-Vulture	-0.6512	0.6965	-0.935	0.350
Preexposure Risk-Low	-0.2023	0.3355	-0.603	0.547
Preexposure Risk–Moderate	0.3748	0.3395	1.104	0.270
Wind Speed	-0.0725	0.0508	-1.427	0.153
Species Group-Eagle : Wind Speed	0.2220	0.0858	2.587	0.010
Species Group-Vulture : Wind Speed	0.1562	0.0993	1.574	0.116

Site reference category = Goodnoe Hills. Species Group reference category = buteo. Preexposure Risk reference category = high.

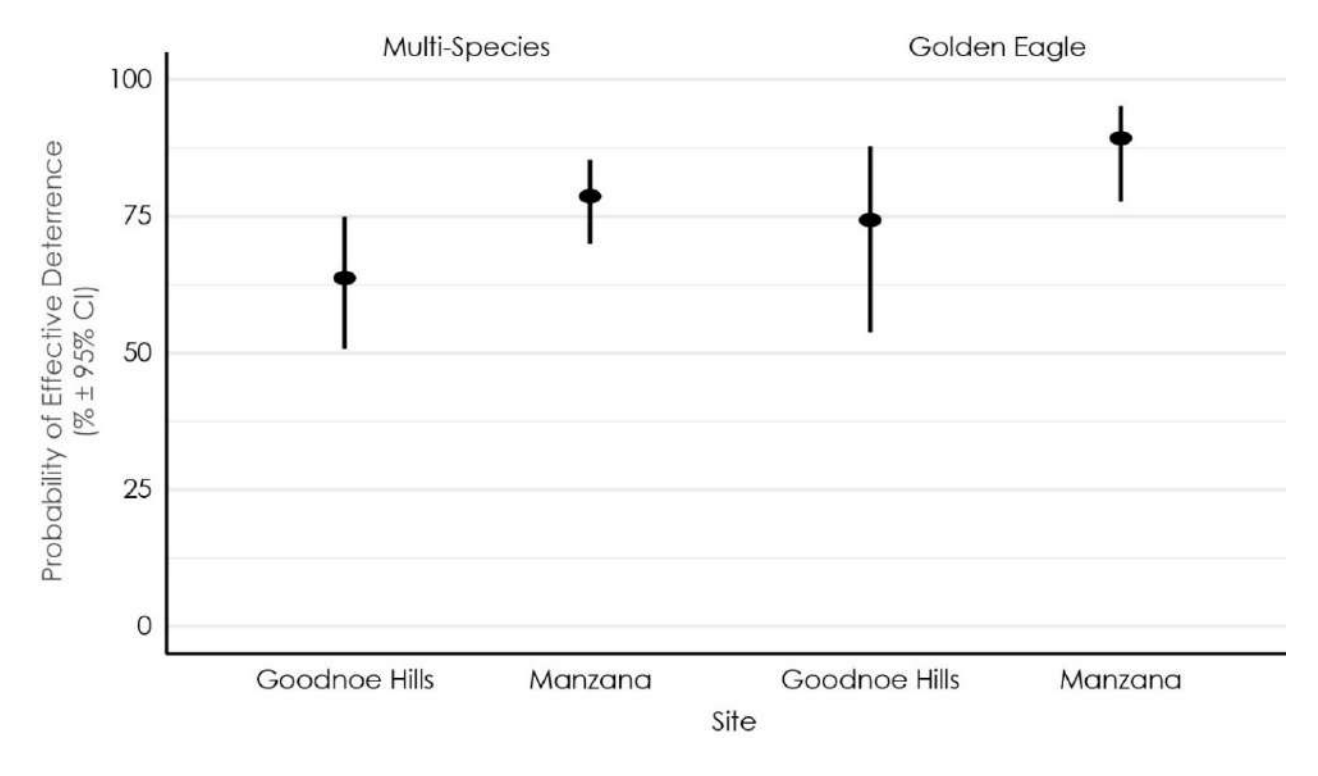


Figure 8. Modeled probability of effective DTBird deterrence for all large raptors combined and golden eagles alone at the two wind facilities evaluated in this study.

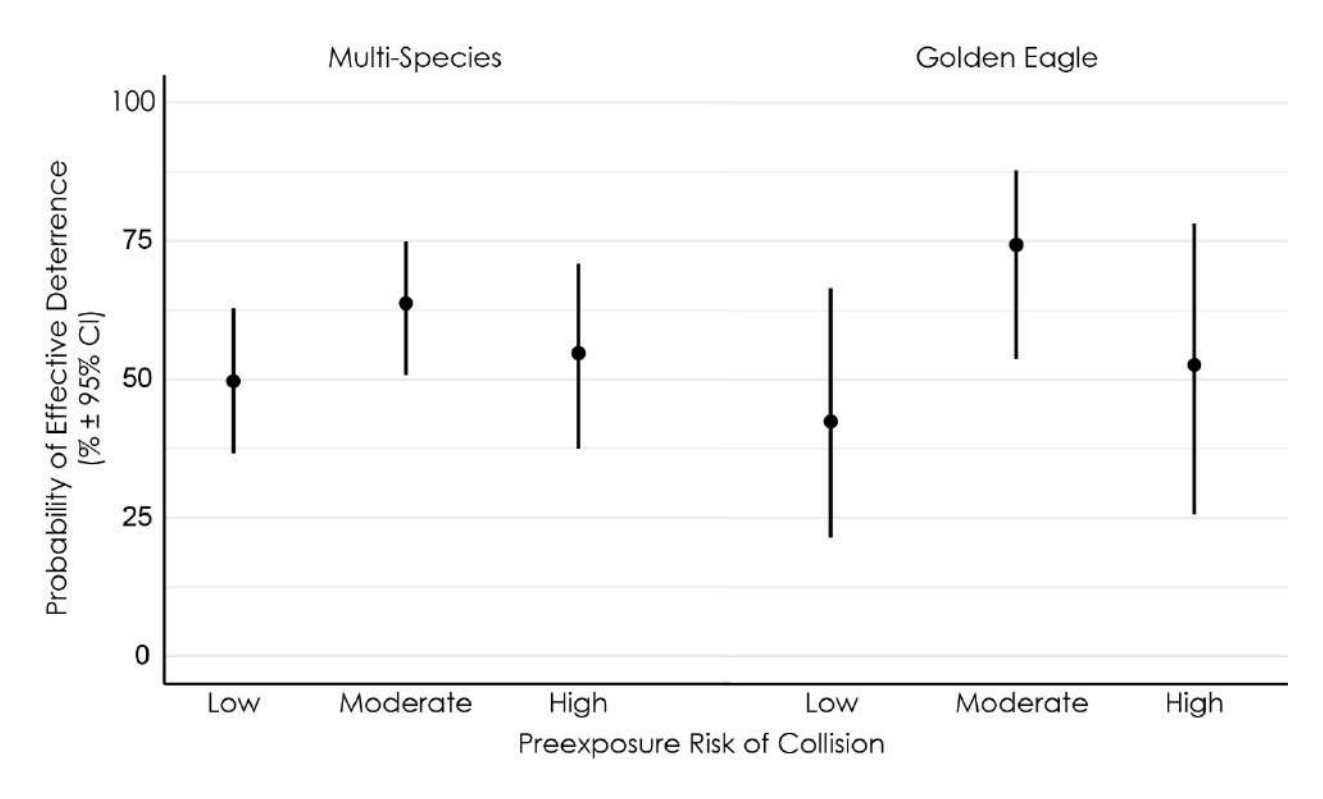


Figure 9. Modeled probability of effective DTBird deterrence for all large raptors combined and golden eagles alone in relation to classified risk of exposure to turbine collisions at the two wind facilities evaluated in this study.

- Species Group and Wind Speed did not contribute significant main effects, but their 2-way interaction was significant (P = 0.019). The Species Group \* Wind Speed interaction reflected the following (Table 12, Figure 10):
  - O At low wind speeds below approximately 4 meters/second (m/s) (just above the turbine cut-in speed of 3 m/s), the probability of effective deterrence was lowest for eagles, slightly higher for vultures, and slightly higher still for buteos, whereas wind speeds above 4 m/s resulted in the opposite pattern.
  - O At wind speeds above approximately 4 m/s, the probability of effective deterrence was:
    - highest for eagles and increased strongly as wind speeds increased
    - second highest for vultures and increased moderately as wind speeds increased
    - lowest for the smaller buteos and decreased moderately as wind speeds increased

#### Golden Eagle Model

The LGLM analysis for golden eagles resulted in the final model listed below (and see Table 13) and the interpretations that follow:

Log(Odds of effective deterrence) ~ Site + Preexposure Risk + Wind Speed

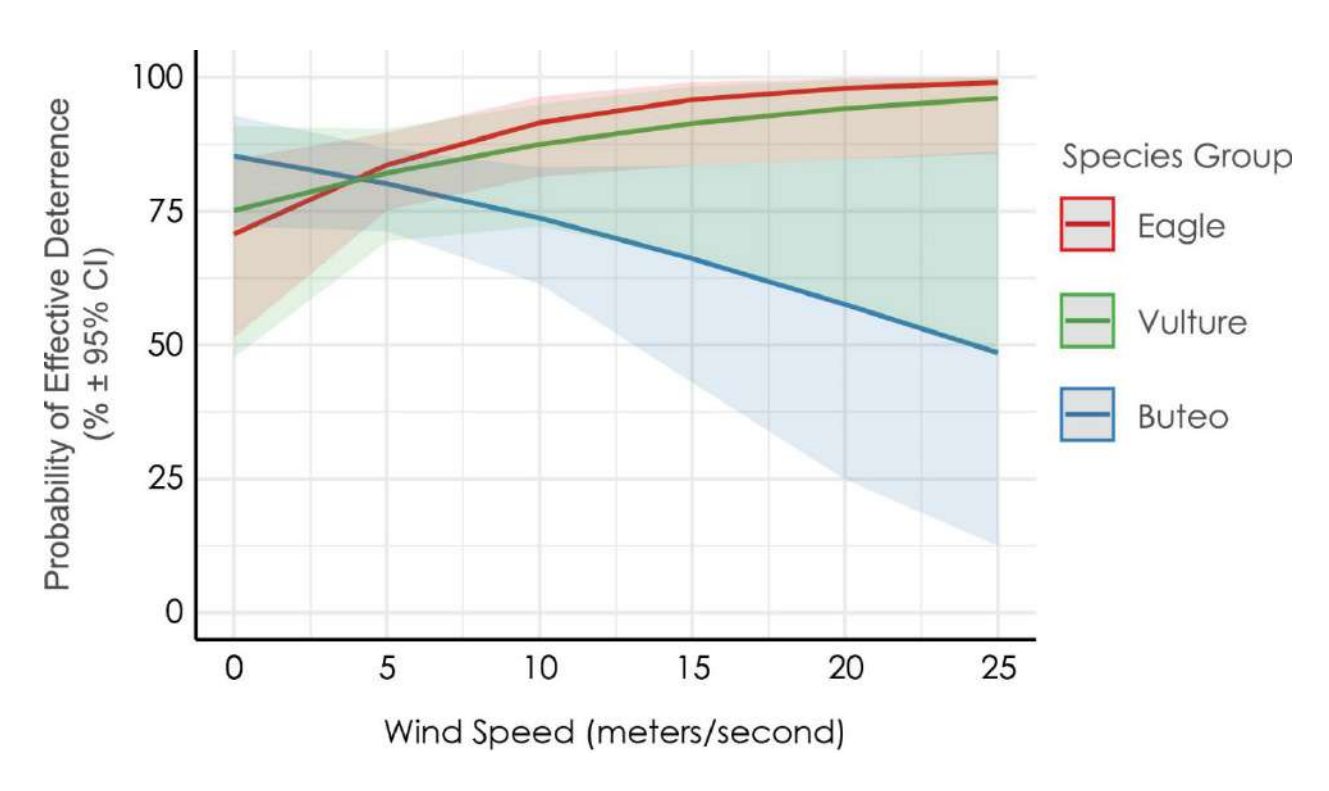


Figure 10. Modeled probability of effective DTBird deterrence for large raptors by species group and in relation to wind speed measured by turbine anemometer at time of events at the two wind facilities evaluated in this study.

Table 13. Comparison of AIC scoring results for top candidates and selected other logistic GLMs portraying potential relationships for golden eagles between the In(odds of effective deterrence) and various predictors.

Candidate Model <sup>1</sup>	AIC <sup>2</sup>	ΔΑΙC	McFadden's R <sup>2</sup>
Site + Preexposure Risk + Wind Speed + Site : Wind Speed	126.23	0.00	0.127
Site + Preexposure Risk + Wind Speed	126.68	0.45	0.108
Site + Preexposure Risk	127.90	1.67	0.083
Site + Wind Speed + Site : Wind Speed	128.64	2.41	0.078
Preexposure Risk + Wind Speed	129.47	3.24	0.071
Site + Preexposure Risk + Wind Speed + Site : Preexposure Risk + Site : Wind Speed	130.12	3.89	0.127
Site	131.01	4.78	0.029
Preexposure Risk	131.06	4.83	0.044
Wind Speed	131.92	5.69	0.022
Preexposure Risk + Wind Speed + Preexposure Risk : Wind Speed	132.51	6.28	0.079
Null model	132.51	6.28	-
Site + Preexposure Risk + Wind Speed + Site : Preexposure Risk + Site : Wind Speed + Preexposure Risk : Wind Speed	132.79	6.56	0.128

<sup>&</sup>lt;sup>1</sup> Site = Manzana or Goodnoe Hills wind facility. Species Group = eagle, vulture or buteo. Preexposure Risk (of approaching rotor swept area of spinning turbine prior to deterrent triggering) = low, moderate or high. Wind Speed measured at turbine in meters / second.

 $<sup>^{2}</sup>$  Akaike Information Criterion score.

Diagnostics for this final model revealed no influential outliers and residuals consistent with adequate model fit.

- *Site* effect (*P* =0.029; Table 14) reflected a higher average probability of effective deterrence at the Manzana site (Figure 8).
- Preexposure Risk effect (P = 0.041) reflected that the probability of effective deterrence was highest for birds at moderate risk, moderate for birds at high risk, and significantly lowest for birds at low risk (Table 14, Figure 9).
- Wind Speed was only marginally significant (P = 0.087; Table 14), but its inclusion reduced the AIC score by 1.2 pts (Table 12) and reflected a positive relationship with the probability of deterrence (Table 14, Figure 10).

Table 14. Parameters of final logistic GLM selected to represent relationship between the In(odds of effective deterrence) for golden eagles and various predictors at the Manzana and Goodnoe Hills wind-energy facilities.

Parameter <sup>1</sup>	Estimate	SE	z	P
Intercept	-0.6933	0.7694	-0.901	0.3675
Site-Manzana	1.0615	0.4867	2.181	0.0292
Preexposure Risk-Low	-0.4103	0.6253	-0.656	0.5118
Preexposure Risk–Moderate	0.9581	0.6470	1.481	0.1386
Wind Speed	0.1612	0.0942	1.711	0.0870

Another model including the *Site* \* *Wind Speed* interaction scored lowest on the AIC scale, but improved the AIC score by only a nominal 0.45 points compared to the second-best model chosen as the final. Further, the parameter-test P value for the interaction (0.118) exceeded even the  $P \le 0.10$  threshold for marginal significance. Nevertheless, the suggested interactive relationship indicated a potentially interesting pattern, whereby (a) the probability of deterrence rose more quickly as wind speed increased at the Goodnoe Hills than at the Manzana site, and (b) as a consequence, was higher at the Manzana site at winds speeds below about 7 m/s, but was higher at the Goodnoe Hills at wind speeds greater than that (Figure 11).

The final model and the model including the *Site* \* *Wind Speed* interaction had a McFadden's pseudo-*R*<sup>2</sup> values of 0.108 and 0.127, respectively, and were the two models with the highest such values (Table 13). The closeness of the pseudo-*R*<sup>2</sup> values of these two models indicates that they have essentially equal ability to explain variation in deterrence probabilities. Both values are between 0.1 and 0.2, indicating "good" predictive value (values of 0.1–0.2 are considered a "good" result, while values of 0.2–0.4 are considered an "excellent" result; McFadden 1974, 1979).

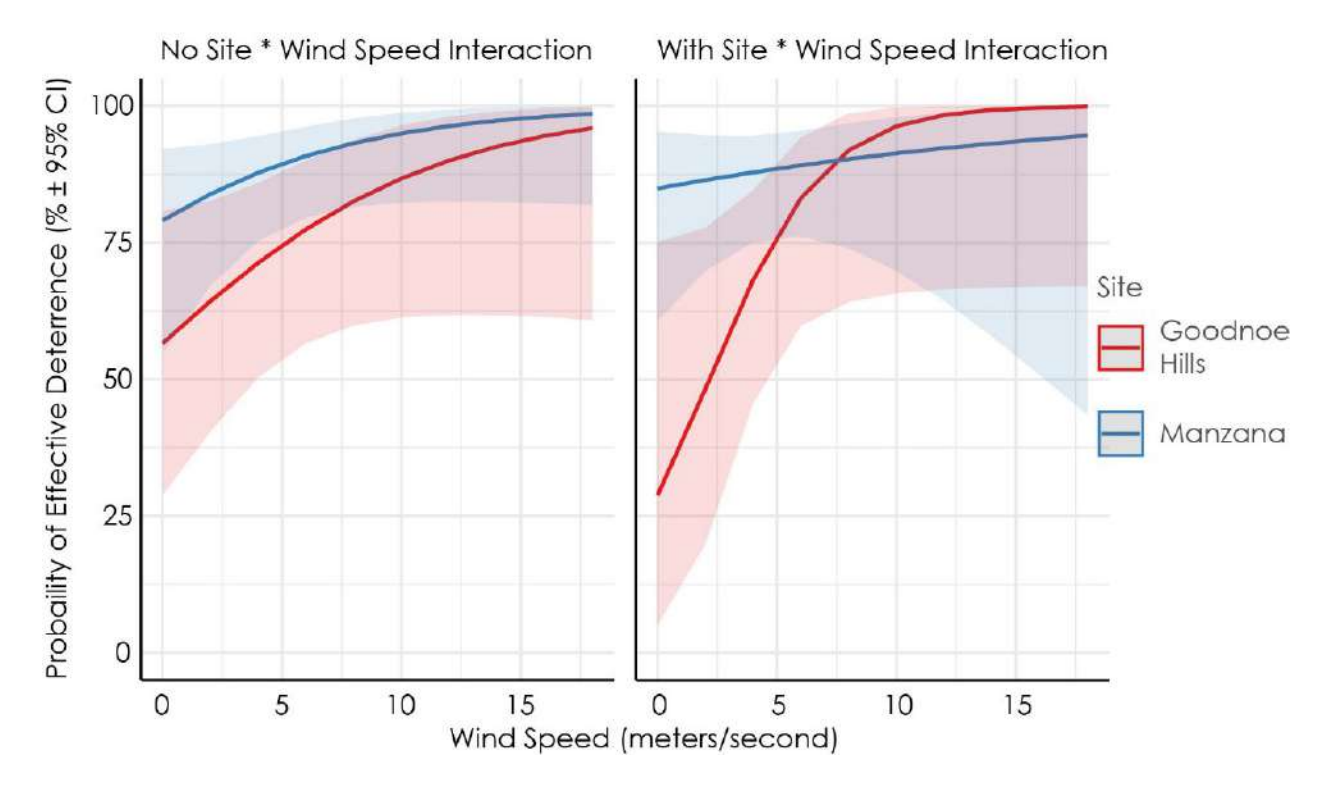


Figure 11. Modeled probability of effective DTBird deterrence for golden eagles in relation to wind speed measured by turbine anemometer at time of events at the two wind facilities evaluated in this study, showing results with and without Site \* Wind Speed interaction (improves AIC score but nonsignificant P = 0.118 parameter test).

### Section 4. Discussion

The results of this integrative analysis of large-raptor behavioral responses to broadcasted DTBird audio deterrents illustrated noteworthy differences in the apparent responsiveness of golden eagles, turkey vultures, and buteos at two wind facilities located in different landscape settings. When exposed to broadcasted deterrents, on average the birds at the Manzana facility in a California foothills/desert landscape appeared to respond more effectively than their counterparts at the Goodnoe Hills facility occupying a ridgetop/grassland landscape bordering the Columbia River in Washington. Reasons for this difference are uncertain, but could reflect the influence of differences in the relative proportions of different species and residents versus transients frequenting the two sites, with variable sensitivities and habituation tendencies. Alternatively, variable wind and climate regimes may have differentially influenced the response behaviors of birds at the two sites by influencing birds' abilities to hear and respond to the deterrents. Wind speeds recorded as part of the records analyzed for this analysis averaged and gusted slightly higher at the Goodnoe Hills (average  $6.3 \pm SD$  of 3.41 m/s, maximum 21.1 m/s) than at the Manzana site (average 5.7 ± 2.79 m/s, maximum 17.0 m/s); however, the modeling results suggested that higher wind speeds tended to increase rather than decrease the probability of effective deterrence. Note, however, that eagles tended to be increasingly more responsive to the deterrents than vultures and buteos as wind speeds increased, and there was some suggestion for golden eagles that the probability of effective deterrence tended to be higher at the Goodnoe Hills than at the Manzana site at moderate and higher wind speeds. These tendencies may have helped to ameliorate the evident site-specific difference in deterrence effectiveness during periods of high wind speeds and power production at the Goodnoe Hills. Regardless, the documented site differences clearly suggest that effectiveness of the DTBird deterrence system may vary significantly depending on the local landscape characteristics and species assemblages.

Both the multi-species and golden eagle models also reflected at least marginally significant relationships between the probability of deterrence and wind speed. Increasing wind speeds generally resulted in a higher probability of effective deterrence for larger eagles and vultures, but not for smaller buteos. We included wind speed as a potential predictor in the LGLMs thinking that higher wind speeds could reduce the probability of effective deterrence by either limiting a bird's ability to hear the deterrents and/or hindering its ability to maneuver effectively in response to the deterrents. The modeling results suggested our hypothesis was incorrect, however, at least for the larger eagles and vultures. One possibility is that faster-spinning turbine blades themselves act as a greater deterrent to approaching larger birds and more effectively amplify the effect of the audio deterrents. It is also possible that higher wind speeds actually facilitate greater maneuverability and responsiveness in many cases for large soaring raptors, which often strongly rely on the energy savings provided by wind-driven (or thermal) lift. In contrast, smaller buteos are generally more maneuverable and more easily constrained by strong winds, such that increasing wind speeds may be a detriment rather than a benefit for them in influencing their ability to respond effectively to the deterrents.

Evidence that the probability of effective deterrence tended to be highest for birds we classified as at moderate risk of exposure to turbine collisions, rather than for those we classified as high risk of exposure, also may relate to birds having enough time and room to maneuver effectively in response to the deterrents. We expected responsiveness to be lower for birds at low risk of exposure, because such birds have little need to divert their

flights to avoid risk. In contrast, birds at high risk of exposure may appear less responsive simply because they have less time and room to respond effectively if not deterred before entering a high-risk zone.

Accurately characterizing the behavioral responses of raptors to the DTBird audio deterrents was greatly confounded by two primary factors: 1) low-resolution video recordings frequently obscured the details of bird behaviors, such as changes in flapping rates, distinct "flinches" and head movements, and subtle flight path alterations; and 2) seeking insight about the degree of response based on evaluating two-dimensional renderings of three-dimensional movement scenarios, especially pertaining to measuring flight diversion angles as a relevant criteria. With this perspective in mind, if eagles and other raptors tended to respond to the deterrents less dramatically, but nonetheless effectively, at the Goodnoe Hills, then the limitations outlined above could have more easily reduced our ability to effectively discern subtler effective responses at the Goodnoe Hills. For this reason, comparing the proportions of only confirmed effective responses at the two sites may be misleading, as opposed to focusing on the combination of effective and potentially effective responses as a better comparative indicator of relative success.

The Goodnoe Hills results clearly did not meet the performance metric established based only on confirmed effective responses from the Manzana study. Further, combining CE and PE responses reduces but does not eliminate the indication of greater deterrence effectiveness at the Manzana facility, but it does result in effectiveness metrics for both sites and all species groups that exceed the ≥50% effectiveness threshold established as performance metric for this DOE-sponsored research project (Table 10). Taking this approach may overestimate DTBird's effectiveness to some degree. We expect, however, that there is a higher likelihood of underestimating the system's effectiveness by limiting the results to confirmed effective responses, because of our limited ability to confidently discern and classify relatively subtle but nonetheless effective behavioral responses.

The control-treatment setup for the Goodnoe Hills study provided further insight about the degree to which responses to spinning turbines and broadcasting audio deterrents contributed to the effectiveness statistics presented herein (H. T. Harvey & Associates 2023a). Based on the comparative control-treatment results and for all analyzed groups and species, broadcasted deterrents consistently resulted in at least a doubling of the proportion of cases where an effective or potentially effective response was evident. Further, results for all four analyzed species groups consistently indicated that confirmed effective responses were more common when the deterrent signals were broadcasting, and that birds exhibiting no apparent response at the time a deterrent was triggered were always significantly more common when the deterrents were triggered only virtually. Although we had no ability to conduct a similar control-treatment evaluation at the Manzana site to provide comparatively robust insight, we think it is reasonable to presume that a similar proportional effect of spinning turbines and broadcasted deterrents would apply at the two sites. At both sites, the visual effects of spinning turbines should be similar, and higher average wind speeds should have similar effects on sound hearing/transmission and bird maneuverability at both sites.

In summary, the results of this investigation pointed to noteworthy differences in the apparent effectiveness of the DTBird deterrence system in different landscape settings, for undetermined reasons but with species and wind-regime differences potentially important. Although the results from the Goodnoe Hills site in Washington clearly demonstrated a lower level of confirmed effective deterrence than the results from the Manzana site in

California, which fell well below the ≥50% effective deterrence performance standard, we advocate that our combination of confirmed and potentially effective deterrence responses provides the best indicator of likely effectiveness at the two sites. In this light, the probability of effective deterrence given broadcasted deterrents exceeded the established performance standard for golden eagles at both the Manzana (79%) and Goodnoe Hills (61%) sites, with similar results obtained for the multi-species group and vultures and buteos as independent comparative groups.

### Section 5. References

- Burnham, K. P., and D. R. Anderson. 2010. Model Selection and Multimodel Inference: A Practical Information-Theoretic Approach. Second Edition. Springer, New York, New York, USA.
- Friendly, M., and D. Meyer. 2016. Discrete Data Analysis with R: Visualization and Modeling Techniques for Categorical and Count Data. CRC Press, New York, New York, USA.
- Hosmer, D. W., and S. Lemeshow. 1989. Applied Logistic Regression. John Wiley & Sons, New York, NY, USA
- H. T. Harvey & Associates. 2018. Evaluating a Commercial-Ready Technology for Raptor Detection and Deterrence at a Wind Energy Facility in California. Research Report. Los Gatos, CA, USA. Prepared for the American Wind Wildlife Institute, Washington, D.C., USA.
- H. T. Harvey & Associates. 2019a. Evaluating the Effectiveness of a Detection and Deterrent System in Reducing Eagle Fatalities at Operational Wind Facilities: Detailed Study Plan. Los Gatos, CA, USA. Prepared for the American Wind Wildlife Institute, Washington, D.C., USA, in conjunction with U.S. Department of Energy Cooperative Agreement DE-EE0007883.
- H. T. Harvey & Associates. 2019b. Analysis of DTBird False Positive Detections at the Manzana Wind Power Project Through October 2017. Research Report. Los Gatos, CA, USA. Prepared for the American Wind Wildlife Institute, Washington, D.C., USA, in conjunction with U.S. Department of Energy Cooperative Agreement DE-EE0007883.
- H. T. Harvey & Associates. 2022a. Initial Analysis of DTBird False Positive Detections at the Goodnoe Hills Wind Farm, Washington: September 1, 2021 March 15, 2022. Research Report. Los Gatos, CA, USA. Prepared for the Renewable Energy Wildlife Institute, Washington, D.C., USA, in conjunction with U.S. Department of Energy Cooperative Agreement DE-EE0007883.
- H. T. Harvey & Associates. 2022b. Initial Analyses of DTBird Detection and Deterrent-Triggering Response Distances and Probability of Detection at the Goodnoe Hills Wind Farm, Washington. Research Report. Los Gatos, CA, USA. Prepared for the Renewable Energy Wildlife Institute, Washington, D.C., USA, in conjunction with U.S. Department of Energy Cooperative Agreement DE-EE0007883.
- H. T. Harvey & Associates. 2023a. Analysis of the Behavioral Responses of Eagles to DTBird® Audio Deterrents at a Commercial Wind-Energy Facility in Washington. Research Report. Los Gatos, CA, USA. Prepared for the Renewable Energy Wildlife Institute, Washington, D.C., USA, in conjunction with U.S. Department of Energy Cooperative Agreement DE-EE0007883.
- Jeffreys, H., 1939. Theory of Probability. Oxford University Press, Oxford, UK.
- McDonald, J. H. 2014. Chi-square test of independence. In Handbook of Biological Statistics. Third edition. Sparky House Publishing, Baltimore, Maryland, USA. <a href="http://www.biostathandbook.com/chiind.html">http://www.biostathandbook.com/chiind.html</a>. Accessed September 2023.

- McFadden, D. 1974. Conditional logit analysis of qualitative choice behavior. Pages 105–142 in P. Zarembka, editor, Frontiers in Econometrics. Academic Press, New York, USA and London, UK.
- R Core Team. 2023. R: A language and environment for statistical computing. R Foundation for Statistical Computing, Vienna, Austria. <a href="https://www.R-project.org/">https://www.R-project.org/</a>.
- Sharp, L., R. Friedel, K. Kosciuch, C. Herrmann, T. Allison, and R. MacIntosh. 2011. Pre- and post-construction monitoring of Bald Eagle use at the Pillar Mountain Wind Project, Kodiak, Alaska, 2007–2011. Oral presentation. National Wind Coordinating Collaborative Research Webinar, 31 October 2011.

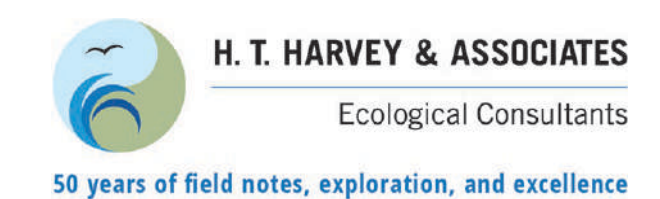












# **Research Report**

Estimates of Collision Risk Reduction for Eagles in Response to Operation of DTBird® Automated Detection and Deterrence Systems at Two Operational Wind Energy Facilities

Project #4080-01

Prepared for:

Renewable Energy Wildlife Institute 1990 K Street NW, Suite 620 Washington, D.C. 20006-1189

Prime Contractor: DOE Cooperative Agreement DE-EE0007883

Prepared by:

H. T. Harvey & Associates

Final - May 30, 2024

## **Table of Contents**

Section 1.0	Introduction	1
Section 2.0	Summary of Relevant Findings from Prior Assessments	3
2.1	Probability of Detection	3
2.2	Probability of Effective Deterrence	4
2.3	Activity Rates of Eagles at Installations with Broadcasted Versus Muted Audio Deterrents	6
Section 3.0	Estimates of Collision Risk Reduction	8
Section 4.0	References	.11

# **List of Preparers**

Jeff P. Smith, Ph.D., Associate Wildlife Ecologist—Project Manager

Scott B. Terrill, Ph.D., Principal, Wildlife Ecology—Principal-in-Charge

#### **Section 1.0 Introduction**

DTBird® (Liquen Consultoría Ambiental, S.L., Madrid, Spain; hereafter Liquen) is an automated detection and audio deterrent system designed to discourage birds from entering the rotor swept zone (RSZ) of spinning wind turbines (see https://dtbird.com). The research results presented herein represent the culmination of a multi-faceted, multi-year evaluation of the DTBird system conducted in collaboration with the Renewable Wildlife Energy Institute (REWI) at two commercial wind-energy facilities located in different landscapes: the Manzana Wind Power Project in a desert foothills environment of southern California and the Goodnoe Hills Wind Farm in a grassland ridgeline environment above the Columbia River in south-central Washington (H. T. Harvey & Associates 2018, 2019a). The overarching goal of this research has been to evaluate the effectiveness of DTBird in detecting and discouraging especially golden eagles (*Aquila chrysaetos*), but also bald eagles (*Haliaeetus leucocephalus*) and other large soaring raptors from approaching the rotor swept zone (RSZ) of operating wind turbines.

Herein we present a synthesis of results presented in several preceding technical reports that together provide insight about the overall effectiveness of DTBird in reducing the risk of eagles entering the RSZ of operational turbines at the two facilities. The overall study was based on seven DTBird installations operated at the Manzana facility for 2 years and 14 installations operated at the Goodnoe Hills facility for 25 months. The Goodnoe Hills research uniquely incorporated a control-treatment experiment that afforded opportunities for distinguishing between the effects of spinning turbines alone (control group) versus spinning turbines plus DTBird deterrents (treatment group) in discouraging eagles from approaching the RSZ of turbines. Preceding analyses and technical reports from which we draw insight for this overarching synthesis include the following:

- 1) Multi-site assessment of the probability of DTBird detecting eagles based on using unmanned aerial vehicles (UAVs) as eagle surrogates (H. T. Harvey & Associates 2023a, 2023b).
- 2) Initial assessment of the probability of DTBird audio deterrents eliciting positive behavioral responses from eagles at the Goodnoe Hills facility, including unique insight about the synergistic deterrence effects of spinning turbines and audio deterrents (H. T. Harvey & Associates 2023c).
- 3) Multi-site assessment of the probability of DTBird audio deterrents eliciting positive behavioral responses from eagles (H. T. Harvey & Associates 2023d).
- 4) Results of 2-year control-treatment experiment at the Goodnoe Hills facility used to quantify the effects of DTBird operation and audio deterrents on the activity rates of eagles near DTBird-equipped turbines (H. T. Harvey & Associates 2023e).

Additional preceding reports that provide further background information about the setup and operation of the relevant DTBird installations, site-specific data collection and analysis procedures, and initial site-specific analyses and results from the two study sites can be found in H. T. Harvey & Associates (2018, 2019a, 2022a,

2022b). We do not reiterate herein detailed descriptions of the study sites, DTBird setups, and our research methodologies.

Herin, we use data generated by the two-site DTBird evaluations and the controlled experiment at Goodnoe Hills to quantify DTBird's effect on golden eagle collision risk. We initially intended to translate our results to applying the Bayesian collision risk model (CRM) recommended by the U.S. Fish and Wildlife Service (2013; and see New et al. 2015), using eagle flight times recorded by DTBird at control and treatment turbines as a proxy for eagle activity. However, we found comparisons of proportional responses to be most germane, because any estimates we could generate portraying absolute reductions in the number of eagles killed per year would be site specific, whereas proportional estimates have the potential to be applied across sites based on site-specific fatality projections.

# Section 2.0 Summary of Relevant Findings from Prior Assessments

#### 2.1 Probability of Detection

At both study sites, we used foam-bodied, fixed-wing UAVs of a similar size and mass and painted to resemble golden eagles to evaluate the detection characteristics of the installed DTBird systems. We conducted flight trials at each site over variable periods involving primarily preplanned, automated flight sequences conducted at selected DTBird installations. We designed the flight sequences based on stratified random sampling designs that effectively sampled the expected detection envelopes by running multiple series of mostly linear transects that traversed the envelopes at various altitudes, orientations, trajectories, and flight speeds. The UAVs were equipped with high spatial and temporal resolution GPS tracking capabilities that enabled precise temporal matching with DTBird detection and deterrent-triggering records (1-second resolution), which in turn allowed for high-precision spatial mapping of DTBird's detection and deterrent-triggering responses. The UAV avionics also output abundant metrics that enabled evaluation of the DTBird responses in relation to variables such as wind speed and UAV flight speed, trajectory, and pitching and rolling (reflective of relative surface exposure to cameras).

To estimate the probability of DTBird detecting an eagle-like UAV (or conversely the probability of *false negatives*), we segregated the flight-trial data into independent flight segments and determined which flight segments DTBird detected. Independent flight segments represented individual flights that began beyond the expected maximum detection range, traversed the detection envelope, continued beyond the expected maximum detection range, and did not reenter the detection envelope for at least 30 seconds to allow for a new DTBird detection event record to be initiated. We then developed GLMs to evaluate the influences of various predictors on the probability of detection, including study site, hour of the day, minimum line-of-sight flight distance from camera, vertical detection angle from camera, and orthogonal vectors representing east—west and north-south horizontal exposure directions from camera.

The probability of detection modeling results indicated similar patterns at the two study sites. The overall modeled probability of detection was nominally higher at Manzana (66%) than at Goodnoe Hills (64%), in both cases exceeding the performance metric for the DOE-sponsored study of 63% established as a basis for evaluating DTBird performance at Goodnoe Hills. These results indicate that any changes made to the detection system between the Manzana pilot study and the subsequent Goodnoe Hills study did not lead to better performance at Goodnoe Hills. Instead, this outcome indicated consistent performance of the primary detection functions of the DTBird systems at both sites. The modeling results also illustrated variability in the probability of detection through the day, likely related to the relative influence of solar position and intensity (ranging from averages of 57% in the morning up to 75% in the evening), as well as noteworthy spatial variation.

Most importantly, the probability of detection was highest when the target flew at moderate distances from the turbine (i.e., generally ≥70% with minimum LoS distances of approximately 20–120 meters and >60% out to the expected initial dissuasion-trigger zone at 170 meters) through the midsection of the camera viewshed (generally high with viewing angles from camera up to UAV of 25–40°). These are the circumstances when birds are often at greatest risk of entering the RSZ of spinning turbines; however, especially hunting or displaying raptors such as golden eagles often make very dynamic movements that can either rapidly drop them down from up high or pop them up from down low and quickly bring them into the RSZ danger zone at relatively close range. For this reason, poorer detection low and close or high and close to the turbine can result in problematic interactions with little time for the deterrents to trigger and discourage continued closer passage before a bird enters the collision risk zone. Accordingly, although quantifying the overall probability of detection as DTBird's ability to detect an eagle-like UAV anywhere within the expected (calibrated) 240-m maximum detection range for golden eagles may underestimate to some degree DTBird's true effectiveness in helping to keep eagles from approaching the RSZ of operational turbines, focusing only on detection probabilities given optimal conditions for detection in the core risk zone has a similar potential to overestimate DTBird's true effectiveness.

#### 2.2 Probability of Effective Deterrence

We quantified the probability of effective deterrence at the two study sites by reviewing tracking videos recorded by the DTBird detection systems and evaluating and classifying the apparent behavioral responses of *in situ* eagles to the audio deterrents. Technicians compared flight behaviors and directions immediately before and after a given bird triggered a deterrent signal and, based on cues such as changes in flight style (e.g., variable flapping rates and shifts from circling/soaring to powered directional flight) and direction (notably away from the turbine, if relevant), classified the degree to which the apparent response appeared to reduce the probability of the bird entering the RSZ of the relevant turbine (i.e., effective, potentially effective, not effective, or no response).

Having set up a unique 2-year control-treatment experiment at the Goodnoe Hills, with some DTBird installations broadcasting deterrents and others with deterrents muted on any given day, we were also able to compose a "deaf" trials study to evaluate behavioral responses at this site. Specifically, the technicians assigned to screening videos and classifying responses 1) were always unaware of which turbines were operating in control versus treatment mode on a given day, and 2) conducted all such screening while deaf to the deterrent sounds recorded as part of the video clips. Having technicians unaware of whether or not they were classifying responses to broadcasted or muted deterrents supported analytically distinguishing between the influence of spinning turbines alone versus spinning turbines plus audio deterrents at the Goodnoe Hills. Such an analysis was not possible for the Manzana site because the DTBird units there were operated normally throughout that 2-year study period.

Focused only on detection events for which we recorded behavioral responses to broadcasted deterrents, the proportion of confirmed effective responses for golden eagles at the Goodnoe Hills (27%) fell well below the performance standard of  $\geq$ 50% effective deterrence established to judge the effectiveness of DTBird at this

site. That performance standard was based on an initial value demonstrated for the Manzana site (53%). However, it can be very difficult to identify targeted birds and effectively discern subtle behavioral details in the low-resolution videos saved by the DTBird systems. Given the poor quality of videos that DTBird uses, we took a conservative approach to classifying behavioral responses, meaning that we categorized responses based on the degree to which we could discern a behavior as effectively reducing risk for the eagle. Partially in order to maintain a sufficient sample size for analysis, we chose to consider effectiveness estimates that included both confirmed effective and potentially effective deterrence responses to evaluate the potential for DTBird deterrents to reduce the risk of eagles and other large raptors entering the RSZ of spinning turbines at the two study sites. This may overestimate DTBird's effectiveness to some degree. However, it is just as likely, if not more likely, limiting the results to confirmed effective responses would have underestimated the rate at which DTBird effectively reduced risk for eagles, because of our limited ability to confidently discern and classify relatively subtle but nonetheless effective behavioral responses. All further results summarized below are based on statistics representing the combination of confirmed effective (CE) and potentially effective (CE) responses as the basis for estimating the probability of effective deterrence.

Quantified in this manner, for golden eagles the proportion of presumed effective (CE + PE) behavioral responses to the combination of spinning blades and audio deterrents was a higher 79% at the Manzana site compared to 60% at the Goodnoe Hills, still a noteworthy difference between the two sites but with both values exceeding the desired ≥50% performance standard. In addition, though not strongly significant patterns, the Manzana dataset indicated that the proportion of confirmed effective responses increased from 39% to 49% as the relative risk of collision exposure increased from low to high (classified based on apparent flight position, speed, and direction), whereas the Goodnoe Hills dataset also indicated the lowest proportion of effective responses among birds at low risk of exposure (29%), but the highest proportion among birds at moderate risk of exposure (39%).

The unique control-treatment setup at the Goodnoe Hills provided further insight about the behavioral effects of the deterrent signals independent of the potential inherent deterrence effects of spinning turbines (including visual and aural effects). The logistic GLMMs we constructed for this purpose with *Treatment Group* (i.e., deterrents broadcasting or not) as a primary predictor indicated that broadcasted deterrents significantly increased the probability of presumed effective deterrence for golden eagles alone from 38% (95% CI: 18–44%) to 68% (CI 47–89%) in response to warning signals and from 23% (CI 8–28%) to 53% (CI 30–75%) in response to dissuasion signals. When examined alone, bald eagles appeared to show greater sensitivity to broadcasted signals (89–100% presumed effective responses) than golden eagles; however, these species-specific assessments were based on relatively limited samples, potentially confounding such indicators. An analysis based on data for both species combined yielded similar insight as the golden eagle model; i.e., a significant increase in presumed effective deterrence from 36% (CI 21–41%) at control turbines to 74% (CI 59–90%) at treatment turbines in response to warning signals and from 21% (CI 10–25%) to 61% (CI 44–77%) in response to dissuasion signals. In summary, the results of these analyses consistently indicated that operation of the DTBird audio deterrents contributed between a near-doubling and near-tripling of the likelihood of presumed effective deterrence responses from eagles at the Goodnoe Hills, which amounted to

effective deterrence beyond the influence of spinning turbines alone of an additional 30% of the golden eagles and 40% of all golden and bald eagles combined.

### 2.3 Activity Rates of Eagles at Installations with Broadcasted Versus Muted Audio Deterrents

The 2-year controlled experiment at the Goodnoe Hills involved daily, randomized rotations whereby on a given day approximately 50% of the DTBird-equipped turbines were operating in control mode with the audio deterrents muted but triggering virtually and 50% were operated in treatment mode with the audio deterrents broadcasting normally. We then quantified the probability of an eagle triggering a dissuasion signal and the average dwell times of eagles detected at turbines operating in control versus treatment mode over the 25-month study period. Dissuasion signals are the more raucous of two potential DTBird audio deterrent signals, triggered at closer distances than initial warning signals. The dwell times of detected eagles were approximated by the lengths of the videos recorded by the DTBird detection systems to represent a given targeting/tracking event. We developed appropriate generalized linear mixed models (GLMMs) for the two dependent variables, with Treatment Group as a primary predictor of interest and including other independent variables that influenced the outcomes. We developed independent predictive models for confirmed and probable golden eagles alone, and for all confirmed and probable golden and bald eagles combined.

The dissuasion-trigger model for golden eagles alone indicated a 29% reduction in the probability of triggering a dissuasion signal at DTBird turbines operating in treatment mode, consistent with our research hypothesis that the probability of dissuasion triggers should be lower at turbines where the DTBird deterrents were broadcasting. However, that difference did not emerge as statistically significant in the presence of other influential predictors such as monitoring Year (46% decrease in the probability of dissuasion triggers in Year 2), Time of Day (positive relationship), and Wind Speed (negative relationship). The more-robust dissuasiontrigger model for all eagles combined also failed to reveal a significant overall treatment effect (as well as any species effect), but did reveal some insightful interactive relationships between Treatment Group and other predictors, namely Cloud Cover and the number of false positives triggering deterrents on a given day (FPs per Day). When cloud cover was present, the probability of dissuasion triggers was slightly lower at treatment turbines, consistent with the research hypothesis; however, when fair skies prevailed the probability of dissuasion triggers was anomalously and substantially higher at treatment turbines, contrary to the research hypothesis. At installations operating in treatment mode, the probability of dissuasion triggers decreased as FPs per Day increased. This result indicates that the added deterrent broadcasting caused by false positives helped to deter eagles from closely approaching the RSZ of relevant turbines. In contrast, at installations operating in control mode, the probability of focal eagles/raptors virtually triggering a dissuasion signal increased concomitantly with increasing false positive detections that virtually triggered deterrents. These results suggest that both non-target birds (e.g., especially common ravens [Corvus corax]) and focal eagles/raptors more often entered the detection zone and triggered deterrents—hence were at greater risk of entering the RSZ—around turbines where DTBird installations were operating with the deterrents muted.

Much stronger overall *Treatment Group* effects emerged when we modeled dwell time as the dependent variable, and the indicators were consistent with our research hypothesis that the average dwell time of eagles should be lower at treatment turbines where the deterrents are broadcasting. The more-robust dwell-time models also emphasized both some common and novel influences of other evaluated covariates compared to the dissuasion-trigger models. For golden eagles alone, the final model indicated a significant 27% overall reduction in average dwell time at treatment turbines (from approximately 25 to 19 seconds per event, with the estimated difference curiously similar to the magnitude of effect for dissuasion triggers, albeit nonsignificant in that case), but an interactive relationship with *FPs per Day* further indicated that the more false positives contributed to deterrent broadcasting at treatment turbines, the less likely were eagles to dwell in the vicinity of those turbines (effect not shown at control turbines).

The combined-eagles dwell time modelling again confirmed no species effect with data for golden and bald eagles combined. Otherwise, the outcomes of this modeling effort yielded similar insights as for predicting the dwell time of golden eagles alone. Most germane was a comparable and significant estimated overall reduction (24%) in the average dwell time of eagles at treatment turbines, with the average dwell time reduced from approximately 26 to 17 seconds per event.

Although not reflected in demonstrable *Treatment Group* effects as described above, the dissuasion-trigger model for golden eagles alone and the dwell-time models for both golden eagles and all eagles combined indicated increasing avoidance of DTBird turbines by eagles as the study progressed. For golden eagles alone, the probability of triggering a dissuasion signal declined by an estimated 46% in Year 2 compared to Year 1, and the average dwell time across the facility decreased significantly in relation to the progression of 28-day sampling cycles. Given that these trends did not emerge differentially around treatment and control turbines, the overall pattern may provide evidence of positive habituation through time among resident and seasonally resident eagles. Here it is important to note, however, that this unanticipated, potential habituation pattern could have been accentuated by two factors that resulted in an atypically high deterrent triggering rate across most of the study (H. T. Harvey & Associates 2023a).

#### Section 3.0 Estimates of Collision Risk Reduction

Our first approach to estimating the overall effectiveness of DTBird in reducing the risk of eagles entering the RSZ of spinning turbines involves the product of the estimated overall probability of detection from the UAV flight trials and the estimated probability of presumed effective deterrence from the behavioral analysis. For golden eagles alone, the results suggested variable performance at the two study sites as follows:

Manzana: 66% probability of detection x 79% probability of effective deterrence = 52% probability of reducing risk of entering RSZ of spinning turbines

Goodnoe Hills: 64% probability of detection x 60% probability of effective deterrence = 38% probability of reducing risk of entering RSZ of spinning turbines

Data for all eagles combined from the Goodnoe Hills (bald eagles rarely occur at the Manzana site) indicated similar results as for golden eagles alone, except that limited data suggested the probability of effective deterrence was higher for bald eagles than for golden eagles.

The Goodnoe Hills control-treatment experimental setup allowed for confirming that the addition of DTBird audio deterrents significantly increased the probability of effective deterrence compared to spinning turbines alone (deterrent signals muted). The difference amounted to a 1.8–2.3-fold (depending on signal type) increase in effective deterrence beyond the influence of spinning turbines for golden eagles alone, and a 2.1–2.9-fold increase for all golden and bald eagles combined, with bald eagles appearing more sensitive to the audio deterrents than golden eagles. We have no basis for comparison at the Manzana facility, but we suspect similar proportional effects would be evident there, perhaps heightened somewhat by evidence of greater overall deterrence effectiveness at that site.

Recalculating the estimates of DTBird's overall detection and deterrence effectiveness for golden eagles alone based on the added benefits estimate from the Goodnoe Hills results in the following modifications:

Manzana: 66% probability of detection x 40% probability of added effective deterrence = 24% probability of reducing risk of entering RSZ of spinning turbines

Goodnoe Hills: 64% probability of detection x 30% probability of effective deterrence = 19% probability of reducing risk of entering RSZ of spinning turbines

If we further narrow the focus to evaluating DTBird's effectiveness in detecting eagles (or UAV surrogates) and deterring eagles that were flying in core exposure locations (i.e., primary dissuasion-trigger risk zone within approximately 170 meters or less of the relevant turbines) and that we classified for behavioral analysis as at moderate to high risk of exposure to the RSZ of spinning turbines, the estimates of effectiveness across the two study sites increase markedly as follows:

Effectiveness of Spinning Turbines + Deterrents: 68% probability of detection x 80% probability of effective deterrence = 54% probability of reducing risk of entering RSZ of spinning turbines

Added Effectiveness of Deterrents: 68% probability of detection x 44% probability of effective deterrence = 30% probability of reducing risk of entering RSZ of spinning turbines

By eliminating from the equation eagles that were at low risk of approaching the RSZ of turbines and whose behavior was less likely to be influenced by either the spinning turbines or triggered audio deterrents, these heightened estimates of effectiveness are more likely to represent the true proportional benefits of the DTBird systems in reducing the risk of golden eagles entering the RSZ of focal turbines at the two study sites.

Our second approach to quantifying DTBird's overall effectiveness stems from the 2-year controlled experiment comparing eagle activity rates at DTBird installations operating in control mode with deterrents muted and in treatment mode with deterrents broadcasting normally. For golden eagles alone, the dissuasion-trigger and dwell-time models indicated similar reductions (27–29%) in indicative activity rates at turbines with the audio deterrents broadcasting compared to turbines with the audio deterrents muted. Assuming activity rates are positively correlated with the potential for collision risk, these percentage estimates of reduced activity levels in the vicinity of treatment turbines should represent roughly comparable estimates of DTBird's deterrence and collision-risk reduction benefits as those derived from our first estimation approach. Assuming this is true, the proportional estimates of collision-risk reduction from DTBird for golden eagles derived from the various estimation approaches were notably similar (19%, 27%, and 29%). Together these results suggest that, for golden eagles that fly anywhere within the calibrated maximum detection range for the species, operation of the DTBird automated detection and audio deterrence system can be expected to reduce the probability of approaching the RSZ of spinning turbines by 20–30%. Again we note, however, that further narrowing the focus to eagles (or surrogates) whose flight patterns exposed them to relatively high risk of entering the RSZ of turbines elevated the estimate of core effectiveness by at least 11%.

Properly scaled and tailored to the unique "survey" effort represented by the automated DTBird monitoring (not an easy task in this case due to highly variable turbine-specific sampling over 25 months), the dwell time data potentially could be translated to a surrogate for the pre-construction "eagle activity minutes" metrics used to project fatality rates at wind-energy facilities using the Bayesian collision risk model developed by the U.S. Fish & Wildlife Service (2013) and partners (New et al. 2015). If so, one could then theoretically compare independently projected post-construction fatality estimates tailored to the Goodnoe Hills based on dwell-time activity levels at control turbines versus treatment turbines to derive a quantitative estimate of projected fatality reduction from operation of DTBird at that facility. However, the magnitude of such a comparison (i.e., a reduced number of fatalities/year) could not be directly extrapolated to other facilities with different collision-risk infrastructure and eagle activity rates and behaviors. Instead, our perspective is that proportional/percentage estimates of effectiveness can be more easily tailored to projecting the magnitude of DTBird's beneficial effects in reducing collision risk at different facilities once initial pre-construction fatality projections tailored to the specific site are developed using the USFWS Bayesian risk model.

We designed this study to yield overarching insight about DTBird's effectiveness by sampling across an array of turbine-specific installations at two study sites, but with no expectation of producing facility-level estimates of effectiveness based on evaluating the influences of specific spatial arrays and densities of DTBird installations. As a result, the estimates of effects summarized herein should be thought of only as indicators

of how individual DTBird systems can be expected to influence activity around the specific turbine on which a given system is installed. The estimated proportional effects can certainly be extrapolated across multiple turbines within a facility to develop a sense of the potential aggregate effects of installing multiple DTBird systems, but cannot be used to infer potential interactive benefits that could accrue from having multiple installations arrayed in particular configurations. Further, the comparative result we derived from the two study sites—one in a desert foothills landscape and one in temperate grassland ridgeline landscape—clearly indicated that DTBird's overall effectiveness may vary in different landscape/climatic settings with different resident and transient eagle populations and variable false-positive deterrent-triggering rates that may influence the eagle responses.

#### **Section 4.0 References**

- H. T. Harvey & Associates. 2018. Evaluating a Commercial-Ready Technology for Raptor Detection and Deterrence at a Wind Energy Facility in California. Research report. Los Gatos, California. Prepared for the American Wind Wildlife Institute, Washington, D.C.
- H. T. Harvey & Associates. 2019a. Evaluating the Effectiveness of a Detection and Deterrent System in Reducing Eagle Fatalities at Operational Wind Facilities: Detailed Study Plan. Los Gatos, California. Prepared for the American Wind Wildlife Institute, Washington, D.C., in conjunction with U.S. Department of Energy Cooperative Agreement DE-EE0007883.
- H. T. Harvey & Associates. 2019b. Analysis of DTBird False Positive Detections at the Manzana Wind Power Project Through October 2017. Research Report. Los Gatos, California. Prepared for the American Wind Wildlife Institute, Washington, D.C., in conjunction with U.S. Department of Energy Cooperative Agreement DE-EE0007883.
- H. T. Harvey & Associates. 2022a. Initial Analyses of DTBird Detection and Deterrent-Triggering Response Distances and Probability of Detection at the Goodnoe Hills Wind Farm, Washington. Research Report. Research Report. Los Gatos, CA, USA. Prepared for the Renewable Energy Wildlife Institute, Washington, D.C., USA, in conjunction with U.S. Department of Energy Cooperative Agreement DE-EE0007883.
- H. T. Harvey & Associates. 2022b. Initial Analysis of DTBird False Positive Detections at the Goodnoe Hills Wind Farm, Washington: September 1, 2021 March 15, 2022. Research Report. Draft August 25, 2022. Los Gatos, California. Prepared for the Renewable Energy Wildlife Institute, Washington, D.C., in conjunction with U.S. Department of Energy Cooperative Agreement DE-EE0007883.
- H. T. Harvey & Associates. 2023a. Analysis of DTBird False Negatives and False Positives at Commercial Wind-Energy Facilities in California and Washington. Research Report. DOE Review Draft November 29, 2023. Los Gatos, California. Prepared for the Renewable Energy Wildlife Institute, Washington, D.C., in conjunction with U.S. Department of Energy Cooperative Agreement DE-EE0007883.
- H. T. Harvey & Associates. 2023b. Analysis of DTBird Detection and Deterrent-Triggering Response Distances at Commercial Wind-Energy Facilities in California and Washington. Research Report. Los Gatos, CA, USA. Prepared for the Renewable Energy Wildlife Institute, Washington, D.C., USA, in conjunction with U.S. Department of Energy Cooperative Agreement DE-EE0007883.
- H. T. Harvey & Associates. 2023c. Analysis of the Behavioral Responses of Eagles to DTBird Audio Deterrents at a Commercial Wind-Energy Facility in Washington. Prepared for the Renewable Energy Wildlife Institute, Washington, D.C., USA, in conjunction with U.S. Department of Energy Cooperative Agreement DE-EE0007883.
- H. T. Harvey & Associates. 2023d. Analysis of Behavioral Responses of Eagles and Other Large Raptors to DTBird Audio Deterrents at Commercial Wind-Energy Facilities in California and Washington. Los

- Gatos, CA, USA. Prepared for the Renewable Energy Wildlife Institute, Washington, D.C., USA, in conjunction with U.S. Department of Energy Cooperative Agreement DE-EE0007883.
- H. T. Harvey & Associates. 2023e. Results of Controlled Two-Year Experiment to Evaluate Effectiveness of the DTBird® Automated Detection and Deterrence System in Reducing Collision Risk for Eagles and Other Large Raptors at the Goodnoe Hills Wind Farm, Washington. Research Report. Los Gatos, CA, USA. Prepared for the Renewable Energy Wildlife Institute, Washington, D.C., USA, in conjunction with U.S. Department of Energy Cooperative Agreement DE-EE0007883.
- New, L., E. Bjere, B. Millsap, M. C. Otto, and M. C. Runge. 2015. A Collision Risk Model to Predict Avian Fatalities at Wind Facilities: An Example Using Golden Eagles, *Aquila chrysaetos*. PLoS ONE 10(7): e0130978. doi:10.1371/journal.pone.0130978.
- U.S. Fish and Wildlife Service. 2013. Eagle Conservation Plan Guidance Module 1 Land-based Wind Energy, Technical Appendix D. Version 2. Division of Migratory Bird Management, Washington, D.C., USA. <a href="https://www.fws.gov/guidance/sites/guidance/files/documents/eagleconservationplanguidance.pdf">https://www.fws.gov/guidance/sites/guidance/files/documents/eagleconservationplanguidance.pdf</a>.



DTBird®V4D8

## DTBIRD SYSTEM COST ANALYSIS: GOODNOE HILLS SITE (USA)

**GOODNOE HILLS WIND FARM** 

Ref.: RC\_OF\_CO\_2024\_025\_(EN)\_rev1



#### **DOCUMENT MANAGEMENT**

CLASSIFICATION	DOCUMENT TYPE	STATE
Public	Technical	☐ Draft
☐ Internal	Presentation	☐ In revision
Restricted	Report	Living document
	Other:	

#### **REVISION HISTORY**

DATE	REV.	AUTHOR(S)	DESCRIPTION
08/03/2024 08/03/2024	RC_OF_CO_2024_ 025_(EN)_rev1	Milagros Bonacchi (A) Agustín Riopérez (R)	Proposal writing Revision

Project ID: Not applicable

DOE Award Number: #DE-EE0007883

The following report is prepared for Renewable Energy Wildlife Institute Prepared by Liquen Consultoría Ambiental S.L. on March 8th, 2024.



#### **INDEX:**

1.	EXECUTIVE SUMMARY	4
2. C	OST OF INSTRUMENTATION	5
3. D	ATA MANAGEMENT	7
	ATA ANALYSIS	
	EPLOYMENT	
	ETRIEVAL	
	PERATION	



#### 1. EXECUTIVE SUMMARY

This executive summary provides an evaluation of the overall costs to install, operate, and maintain the DTBird systems at a site.

16 DTBirdV4D8 units were manufactured in 2019 and delivered to Goodnoe Hills wind farm by the end of the year. 14 units operated under the evaluation and experimental design from August 2021 to September 2023.

Below we have provided the actuals for the installation, operation, and maintenance/service of DTBirdV4D8 units in Table 1:

Table 1. Actual Cost(s) to Install, Operate, and Maintain the DTBird system (2016-2024)

Project Cost(s)	Amount (USD)	Unitary cost for the 14 units (USD)
ACTUAL DTBIRD PURCHASE COST FOR 14 UNITS	\$208.619,64	\$14.901,40
SHIPPING DTBIRDV4D8 UNITS TO GOODNOE HILLS SITE AND US CUSTOMS *	\$17.114,49	\$1.069,66
INSTALLATION COSTS (TRAVEL & SALARIES COSTS) – OCT 26 <sup>TH</sup> TO NOV 3 <sup>RD</sup> 2019	\$10.659,23	\$761,37
YEAR 1: TOTAL YEARLY SERVICE 13 DTBirdV4D8 (12 months) including technician travelling costs to repair multiple maintenance issues - August 2021 till July 2022	\$42.997,43	\$3.071,25
YEAR 2: TOTAL YEARLY SERVICE 14 DTBirdV4D8 (12 months) – August 2022 till September 2023	\$35.199,41	\$2.514,24
TOTAL 14 SYSTEMS + 24 MONTHS OF SERVICE	\$327.278,51	\$23.377,04
*16 units were delivered to the site		

When including the overall cost of LIQUEN´s Internal Services and R&D Department, the standard DTBirdV4D8 model sale cost (cameras model Falco and Larus software) is around \$18K - \$22K, and the yearly service sale cost around \$2K - \$3K. There are other project specific indirect costs for installation (around 4K\$-6K\$ per unit) and onsite maintenance (around 0.6 K\$-2K \$ per unit and year).



#### 2. COST OF INSTRUMENTATION

For the Purchase of the equipment including the manufacturing and shipping, the economic difference between the planned vs actual costs is \$2.923,70. So the real invoiced value is 1,21% below the planned cost.

For the Installation costs of the equipment, the economic difference between the planned vs actual costs is \$13.243,43. So the real invoiced value is 55,40% below the planned cost.

For the technical service costs, the planned number of months it was meant to run was 14. However, the project due to the onset of Covid 19 and technical difficulties in the system commissioning the project timeline was extended. The economic difference between the planned vs actual costs is \$10.549,58. So the real invoiced value is 19,70% below the planned cost for the first year of technical service.

As for the second year of technical service, the real invoiced value was also below the original planned cost. The economic difference between the planned vs actual costs is \$18.347,60 with a 34,26% below the planned cost for the second year of the technical service.

If we proceeded to do a simulation having had all original 16 units operating at the site including a trip from LIQUEN HQ to the site for maintenance repairs, the technical service costs would still be 20,97% below the planned original costs.

The following, Table 2 below accounts for the purchase, manufacturing, delivery, and installation of 16 DTBirdV4D8 units in USD dollars to fulfill with the scope of bird monitoring and mortality mitigation in the Wind Farm Goodnoe Hills, located in Washington (USA).

Table 2: Planned Costs vs Actual Costs

Cost of Instrumentation	Planned Costs (USD)	Cost of Instrumentation	Actual Costs (USD)
Total Unitary Cost per DTBirdV4 Detection Module	\$10.479,39	10.479,39 Hardware Procurement Of 16 DTBird V4D8 Units	
Total Unitary Cost per DTBirdD8 Collision Avoidance Module	\$3.661,63	Manufacturing Hours Of 16 DTBirdV4D8 Units	\$55.554,59
Total Unitary Cost per DTBird V4D8 Unit Delivery	\$943,11	Shipping Of 16 DTBirdV4D8 units to Goodnoe Hills Site and US Customs	\$17.114,49
Total Unitary Cost	\$15.084,13	Total Unitary Cost	\$14.901,40
Total Cost For 16 Units	\$241.346,14	<b>241.346,14</b> Total Cost For 16 Units	
Total Travelling + Installation Coordination and Final Check by DTBird	\$23.902,66	Installation Costs (Travel & Salaries Costs) – Oct 26 <sup>th</sup> to Nov 3 <sup>rd</sup> 2019	\$10.659,23
Total Yearly Service 16 DTBirdV4D8 (12 Months)	\$53.547,01	Total Yearly Service 13 DTBirdV4D8 (12 Months)	\$42.997,43
Total Yearly Service 16 DTBirdV4D8 (12 Months)	\$53.547,01	Total Yearly Service 14 DTBirdV4D8 (12 Months)	\$35.199,41
TOTAL Yearly Service for 2 years	\$107.094,01	TOTAL Yearly Service for 2 years	\$78.196,84

Per the purchase and service agreement for the DTBird units in place between Liquen and REWI, Liquen covered the sale, delivery, and commissioning costs for 2 out of 16 DTBirdV4D8 units delivered to and installed at Goodnoe Hills Wind Farm. These units were manufactured and delivered to the site



but unable to be used due to equipment malfunctions. Components of these units were utilized to resolve equipment malfunctions with other units. The cost share amount reflects the anticipated total of \$30,168.27 while the actual sale, delivery, and commissioning costs of these two units was \$29,802.81.

In terms of Project Participation Labor, Liquen covered \$365.19 of their associated labor costs to participate in the project, as incurred from January through July 2022.

Table 3 below accounts for the addition of Liquen's project cost share of 2 units.

Table 3: Project Cost Share Costs

Project Share Costs	Actual Costs (USD)
Project Cost Share of 2 Units: Purchase	\$29.802,81
Project Cost Share of 2 Units: Participation Labor	\$365,19
TOTAL	\$30,168.27



#### 3. DATA MANAGEMENT

Data management included online project team meetings and coordination with REWI and other project partners, invoicing preparation to REWI, and improvements to the false positive filters by the IT team. Given additional purchase of equipment and the need to calibrate and configure the equipment hardware prior to shipping and once installed onsite, this has also been included in the labor hours. Other related areas of data management include the storage of videos and data in a Tier 4 server for the duration of the project. As well as the cost employed by DTBird O&M technicians to oversee the correct functioning of the systems. Below are the labor costs covered by LIQUEN personnel.

Table 4: Liquen Personnel Costs

Liquen Project Coordination Meetings  Offer preparation and contracts signature (Supervision)  Offer preparation and contracts signature (writing)  Offer preparation and contracts signature (Administration)  Technical information exchange  Coordination and Hardware acquisition  Assembling of DTBird cabinet  Assembling Aluminum plates, cameras outdoors cabling  Packaging  Delivery control  Software installation + configuration  Operational test-quality assurance  Adjusting Detection module  Bird flight review. DTBird adjustments  Installation report, Commissioning report, quality check  Metal plates with speakers  Horizontal cabling  Vertical cabling
Offer preparation and contracts signature (Supervision) Offer preparation and contracts signature (writing) Offer preparation and contracts signature (Administration) Technical information exchange Coordination and Hardware acquisition Assembling of DTBird cabinet Assembling Aluminum plates, cameras outdoors cabling Packaging Delivery control Software installation + configuration Operational test-quality assurance Adjusting Detection module Bird flight review. DTBird adjustments Installation report, Commissioning report, quality check Metal plates with speakers Horizontal cabling Vertical cabling Vertical cabling
Offer preparation and contracts signature (Administration) Technical information exchange Coordination and Hardware acquisition Assembling of DTBird cabinet Assembling Aluminum plates, cameras outdoors cabling Packaging Delivery control Software installation + configuration Operational test-quality assurance Adjusting Detection module Bird flight review. DTBird adjustments Installation report, Commissioning report, quality check Metal plates with speakers Horizontal cabling Vertical cabling
Technical information exchange Coordination and Hardware acquisition Assembling of DTBird cabinet Assembling Aluminum plates, cameras outdoors cabling Packaging Delivery control Software installation + configuration Operational test-quality assurance Adjusting Detection module Bird flight review. DTBird adjustments Installation report, Commissioning report, quality check Metal plates with speakers Horizontal cabling Vertical cabling
Coordination and Hardware acquisition Assembling of DTBird cabinet Assembling Aluminum plates, cameras outdoors cabling Packaging Delivery control Software installation + configuration Operational test-quality assurance Adjusting Detection module Bird flight review. DTBird adjustments Installation report, Commissioning report, quality check Metal plates with speakers Horizontal cabling Vertical cabling
Assembling of DTBird cabinet  Assembling Aluminum plates, cameras outdoors cabling Packaging Delivery control Software installation + configuration Operational test-quality assurance Adjusting Detection module Bird flight review. DTBird adjustments Installation report, Commissioning report, quality check  Metal plates with speakers Horizontal cabling Vertical cabling
Assembling Aluminum plates, cameras outdoors cabling Packaging Delivery control Software installation + configuration Operational test-quality assurance Adjusting Detection module Bird flight review. DTBird adjustments Installation report, Commissioning report, quality check Metal plates with speakers Horizontal cabling Vertical cabling
Packaging Delivery control Software installation + configuration Operational test-quality assurance Adjusting Detection module Bird flight review. DTBird adjustments Installation report, Commissioning report, quality check  Metal plates with speakers Horizontal cabling Vertical cabling
Delivery control Software installation + configuration Operational test-quality assurance Adjusting Detection module Bird flight review. DTBird adjustments Installation report, Commissioning report, quality check Metal plates with speakers Horizontal cabling Vertical cabling
Software installation + configuration Operational test-quality assurance Adjusting Detection module Bird flight review. DTBird adjustments Installation report, Commissioning report, quality check Metal plates with speakers Horizontal cabling
Operational test-quality assurance Adjusting Detection module Bird flight review. DTBird adjustments Installation report, Commissioning report, quality check Metal plates with speakers Horizontal cabling
Adjusting Detection module Bird flight review. DTBird adjustments Installation report, Commissioning report, quality check  Metal plates with speakers Horizontal cabling
Bird flight review. DTBird adjustments Installation report, Commissioning report, quality check  Metal plates with speakers Horizontal cabling
Installation report, Commissioning report, quality check  Metal plates with speakers  Horizontal cabling  Vertical cabling
Metal plates with speakers Horizontal cabling
Horizontal cabling
Vertical cabling
Packaging \$6.342,2
Operational test-quality assurance
Installation report, Commissioning report, quality check
YEAR 1 Software licenses, Detection and Data Analysis Platform
(subcontractor detection software licenses, recovery of investment in
current detection software subcontractor and DTBird technicians; Data
Analysis platform software development and maintenance) \$16.045,9
YEAR 1 Annual technical service Detection and Collision Avoidance (13
units) 249 Spanish working days. DTBird DAP flight reviewer. \$2.978,7
YEAR 1 Annual technical service Detection and Collision Avoidance (13
units) 249 Spanish working days. DTBird O&M technicians \$8.037,8
YEAR 1Remote Technical assistance onsite maintenance Detection and
Collision Avoidance (13 units) x interventions and hours. DTBird O&M
technicians \$1.914,4
YEAR 1 2-year video and data storage Tier 4 server (13 units) \$1.434,1
YEAR 2 Software licenses, Detection and Data Analysis Platform
(subcontractor detection software licenses, recovery of investment in
current detection software subcontractor and DTBird technicians; Data
Analysis platform software development and maintenance) \$13.369,8
YEAR 2 Annual technical service Detection and Collision Avoidance (14
units) 249 Spanish working days. DTBird DAP flight reviewer. \$3.054,7
YEAR 2 Annual technical service Detection and Collision Avoidance (14
units) 249 Spanish working days. DTBird O&M technicians \$8.955,9

DTBIRD SYSTEM COST ANALYSIS: GOODNOE HILLS SITE (USA)



YEAR 2 2-year video and data storage Tier 4 server (14 units)	\$1.470,68
TOTAL	\$96.060.83



#### 4. DATA ANALYSIS

No data analysis was required for the bird flight recordings performed by LIQUEN outside of standard operation control of the systems from the Data Analysis Platform(DAP) and the O&M perspective. These two items are mentioned in the Data Management & Operation epigraphs.

Additionally, the Technical Area had to develop a way to automate the turning on and off of the Collision Avoidance Module according to the Sound Deterrence Turbine Rotation Schedule prepared by project partner HTH. This labor afterwards involved the regular deployment of cycles, changing it from one WTG to another. This task was carried out by O&M Technicians.

During the period of June till end of September 2023 due to a malfunction in the reception of WTG signals by the DTBird systems after a month-long power outage in May at the Wind Farm, LIQUEN underwent the task of matching Data Analysis Platform (DAP) datasets with Pacificorp's turbine rotor readings. These readings went from June till September. It was done to facilitate the scientific analysis of the data by project partner HTH. A software script was developed by the LIQUEN Technical Area to expedite the matching and aid in finalizing the data analysis on time. As a project contribution by LIQUEN, the time/cost spent on this task was not invoiced to REWI.

Table 5: Estimated Additional Liquen Personnel Costs

Estimated Additional Liquen Personnel Costs	Actual Costs (USD)
Estimated cost of sound deterrence automation by the Technical Area: 4hrs including indirect costs.	\$219,94
Estimated cost of sound deterrence rotation schedule application & operational checks by O&M Technicians: 2hrs including indirect costs.	\$753,56
Estimated cost of software script creation and deployment by the Technical Area: 22hrs including indirect costs.	\$1.209,69
TOTAL	\$2.183,19



#### 5. DEPLOYMENT

In terms of delivery and shipping of the units to the US, the planned shipping costs (including indirect cost) of the 16 units is detailed below. Customs Tax at destination is not accounted for. The actual shipping costs (including indirect cost) of the 16 units is detailed below whereas in this case, customs tax at destinations is accounted for.

Table 6: Costs of Shipping Planned vs Actual Costs

Costs of Deployment	Planned Costs (USD)	Costs of Deployment	Actual Costs (USD)
Delivery 16 DTBirdV4D8	\$15.089,80	Shipping of 6 Wooden Packages and 14 Packages with Customs Tax at Destination	\$17.114,49
UNITARY COST PER DTBirdV4D8 UNIT DELIVERY	\$943,11	UNITARY COST PER DTBIRDV4D8 UNIT DELIVERY	\$1.000,63
TOTAL	\$15.089,80	TOTAL	\$17.114,49

During the planning of the DTBird project, it was to be arranged for two DTBird technicians to travel to the Goodnoe Hills site and remain there for a week or 7 working days to train the installation team onsite, organize materials, and start installation and connection. Following this, they would return to Spain and one DTBird technician would return to the site the last week installation for four working days to confirm a cooperative connection and assess the status of all 16 DTBird Units.

During the project, two DTBird technicians were sent to aid in the installation of the DTBird systems at the Goodnoe Hills site, however a technician did not make return travel. Instead, PacifiCorp and their subcontractor finalized the installation of all systems in 2 phases.

The costs for the travel of the two DTBird technicians from October 26<sup>th</sup> – November 3<sup>rd</sup>, 2019, are detailed below.

Table 7 Costs of Installation Planned vs Actual costs:

Costs of Installation	Planned Costs (USD)	Costs of Installation	Actual Costs (USD)	
Travelling to the wind farm for installation (2 technicians)	\$23.902,66	Travelling to the wind farm for installation (2 technicians) with salary costs	\$10.659,23	
TOTAL	\$23.902,66	TOTAL	\$10.659,23	

DTBIRD SYSTEM COST ANALYSIS: GOODNOE HILLS SITE (USA)



#### 6. RETRIEVAL

On the Purchase Contract of the units, it is mentioned the following clause  $n^{\circ}$  32: In case that DTBird units finish the service, the customer is the responsible to dismantle all the equipment and treat the disposals generated according with the country's regulations. The DTBird team will provide uninstallation instructions and will be available in remote for any query during the performance of the work.

Below is provided the estimated costs for deinstallation of 14 DTBird units, including 2 US based rope technicians to deinstall cameras & speakers at height. We estimate 1.600 USD per system.



#### 7. OPERATION

Over the course of the project 2 units were eliminated from the project due to a combination of technical and economic reasons.

During Year 1, only 13 units were operational since the 14th one was pending to be commissioned by the end of the Year 1 experiment period.

Year 1 actual costs were below the planned costs, despite including the travelling costs of 1 DTBird technician onto the Goodnoe Hills site for maintenance purposes. When comparing them with Year 2's actual costs, these are also below the planned costs although these may appear as extra costs at first.

Liquen trained Titley Scientific technician Mark Eubanks included in some project emails, but he eventually left the company. Due to the lack of a new US based technician to take over Liquen ended providing the service from Spain. It's worth noting that there was no scheduled remote maintenance intervention performed with the presence of a LIQUEN technician during Year 2. All issues were resolved via email during Spanish working days and business hours.

Table 8 Yearly Service Costs Planned vs Actual Costs

Yearly Service Costs	Planned Costs (USD)	Yearly Service Costs Year 1	Actual Costs (USD)	Yearly Service Costs Year 2	Actual Costs (USD)
Unitary cost per year of service (16 DTBirdV4D8 units)	\$2.974,83	Unitary Cost Per Year of Service (13 DTBirdV4D8 units) including technician travelling costs	\$3.307,49	Unitary Cost Per Year of Service (14 DTBirdV4D8 units)	\$2.514,24
Unitary Cost 14 Months of Service (16 DTBirdV4D8 units)	\$3.904,47	Unitary Cost 12 Months of Service (13 DTBirdV4D8 units) including technician travelling costs	\$292,87	Unitary Cost 12 Months of Service (14 DTBirdV4D8 units)	\$209,52
TOTAL COST 14 MONTHS OF SERVICE (16 DTBirdV4D8 units)	\$62.471,51	TOTAL YEARLY SERVICE 13 DTBirdV4D8 (12 months) including technician travelling costs to repair multiple maintenance issues	\$42.997,43	TOTAL YEARLY SERVICE 14 DTBirdV4D8 (12 months) – August 2022 till September 2023	\$35.199,41



#### 8. MAINTENANCE

Over the course of the project, onsite maintenance & replacement of broken parts was executed by Pacificorp technicians and their Electrical Subcontractor.

Below in Table 9 are the mandatory spare parts sent in accordance with the Yearly Technical Service.

Table 9: Detailed System Maintenance Actual Costs

Detailed Costs Year 1	Actual Costs (USD)	Detailed Costs Year 2	Actual Costs (USD)
Yearly replacement of lens cover (13 units) 2 replacements/year	\$3.212,39	Yearly replacement of lens cover (14 units) 2 replacements/year	\$3.595,01
2 Deliveries of replacement camera lenses/year	\$245,15	1 Delivery of replacement camera lenses/year includes real costs and customs	\$382,17
Yearly replacement of lens cover (Unit GH56) 2 replacements/year	\$247,11	Delivery of 2 boxes of Spare Parts sent back to Madrid, Spain - September 2022	\$616,05
TOTAL	\$3.704,65	TOTAL	\$4.593,23





Avda. de la Democracia nº 7, OFICINA. 28031 Madrid - Spain Tfno. +34 91 344 90 86 • CIF: ES-B83521732 info@dtbird.com - www.dtbird.com

#### LIQUEN CONSULTORÍA AMBIENTAL S.L

Liquen Consultoría Ambiental, S.L. Avda. de la Democracia nº 7, N 406 28031 Madrid (Spain) VAT Nº: ES-B-83521732 T: 00 34 91 344 90 86 info@dtbird.com - www.dtbird.com